Déformation d'un continent au-dessus d'une dorsale océanique active en subduction

Bruno Scalabrino

UNIVERSITE MONTPELLIER II
SCIENCES ET TECHNIQUES DU LANGUEDOC

T H E S E

pour obtenir le grade de

DOCTEUR DE L'UNIVERSITE MONTPELLIER II

Discipline : Sciences de la Terre et de l'Univers
Ecole Doctorale : SIBAGHE (Systèmes Intégrés en Biologie, Agronomie, Géosciences, Hydrosciences, Environnement)

présentée et soutenue publiquement par

Bruno SCALABRINO

Le 3 Novembre 2009

Déformation d'un continent au-dessus d'une dorsale océanique active en subduction.

La transversale du point triple du Chili, Patagonie Centrale (Chili-Argentine).

JURY

Rolando Armijo	**Directeur de Recherche**	**IPGP**	**Rapporteur**
Nicolas Arnaud	**Directeur de Recherche**	**GM**	**Invité**
Michel De Saint-Blanquat	**Chargé de Recherche**	**LMTG**	**Examinateur**
Yves Lagabrielle	**Directeur de Recherche**	**GM**	**Directeur de thèse**
Serge Lallemand	**Directeur de Recherche**	**GM**	**Examinateur**
Jacques Malavieille	**Directeur de Recherche**	**GM**	**Directeur de thèse**
Othmar Muntener	**Professeur**	**Lausanne**	**Rapporteur**
Jean-François Ritz	**Chargé de Recherche**	**GM**	**Invité**

Remerciements

Décembre 2006, arrivée à Coihaique, capitale de la région d'Aysen, Patagonie Centrale, mon rêve se réalise : Découvrir les Andes et la Patagonie. Cette aventure andine qui débuta en Master 1 s'est concrétisée au cours de ces 3 ans de thèse et restera gravée à jamais dans mes pensées.

Je tiens d'abord à remercier les rapporteurs de thèse, Othmar Muntener et Rolando Armijo qui ont pris le temps de juger ce travail et d'apporter de nombreuses discussions afin de le rendre encore meilleur. Un grand merci également à Serge Lallemand, Michel de Saint-Blanquat pour avoir accepter d'examiner cette thèse.

Je remercie ensuite avec un grand 'MERCI' mes directeurs de thèse Yves Lagabrielle et Jacques Malavieille pour leur disponibilité, leur bonne humeur, leur rigueur scientifique et leurs capacités à transmettre les compétences scientifiques indispensables à la réalisation de ce travail. Ces compétences transmises me suivront inévitablement tout au long de ma vie…Je les remercie également pour l'ambiance magnifique ayant régnée au cours de différentes missions de terrain, loin de tout, au bord d'un glacier sous les notes d'un Charrango ou d'une flute, ou au bord du lac Général Carrera lors de quelques parties de pêche à la truite.

Je tiens également à remercier Jeff Ritz pour sa bonne humeur et son expertise en géomorphologie transmise en partie au cours d'une mission de terrain en février 2009, au niveau de la meseta del lago Buenos Aires (dont certains endroits ressemblaient à Mars !!). Le steak de 500 gr à 'Viva el Viento' à los Antiguos après une semaine de riz restera un très bon souvenir !! (mon estomac s'en souvient encore !).

Je remercie ensuite toutes les personnes qui ont participé à ce travail au cours de ces 3 années de thèse à savoir Stéphane Dominguez, Nicolas Arnaud, Daniel Melnick, Christelle Guivel, Bernard Célérier, Andréa Tommasi, Diane Arcay… Et sans oublier los amigos Chilenos y Argentinos, Manuel Suarez, Eduardo Rossello, Diego Morata, Felipe Espinoza, Gisel Peri et Leonardo Zuniga Diaz alias 'Pituso'. Je remercie également Aude de la Rupelle et Emmanuelle Boutonnet qui grâce à leurs travaux de M2 ont apporté de nouvelles données indispensables à ce travail. Je leur souhaite bonne chance pour leur thèse. Un grand merci aussi à tous les membres d'ECOS et plus particulièrement Chantal de Verneuil.

Je n'oublierai pas tous les participants du Trek Patagonia en février 2008. Un grand merci à Helmut Echlter sans qui cette aventure dans les parties reculées du Campo Hielo Norte n'aurait été possible. Merci donc à Daniel, Viki, Julius et à toute l'équipe des guides chiliens nous ayant accompagné. *Fuerza Patagonia, Viva Patagonia* !!!!

Que dire du laboratoire Géosciences Montpellier… tout simplement merveilleux !!! Merci à toutes les secrétaires du labo Natahlie Mouly, Marie-France Roch, Céline Fabrégat, Bernadette Marie et José Ramos, pour leur aide, leur professionnalisme et leur bonne humeur quotidienne. Merci également à Anne Delplanque pour ces diverses interventions sur Illustrator et son aide non négligeable à la réalisation de posters.

Ayant été moniteur au cours de ma thèse, je remercie les membres de l'équipe enseignante de Géosciences Montpellier à savoir Henri de la Boisse, Suzanne Raynaud, Jean-Emmanuel Hurtrez, et Alain Vauchez. Un grand merci également à tous les étudiants de L1, L2, L3, et de M1 qui ont du me supporter en cours !!

Une grande partie de ma formation en géologie s'est effectuée à Montpellier et je tiens à remercier tous mes professeurs : André Leyreloup, Jean-Marie Dautria, Jean-Michel Liotard, Michel Condomines, Laurent Dézileau, Michel Séranne, Michel Lopez, Marc Daignières, Roger Bayer, Serge Lallemand, Yves Lagabrielle, Jacques Malavieille, Hervé Philip, Andréa Tommasi, Alain Vauchez, Philippe Laurent.

Comment ne pas penser à tous les potes de galère et de fiesta du laboratoire….impossible !!!! Une ambiance incroyable qui, je pense, ne se retrouvera nulle part ailleurs. Tout d'abord merci à mon colloc de bureau Flo pour cette ambiance de fou pendant 3 ans.…Hamtouk !!! Puis merci à Pierre, que j'ai supporté pendant 6 ans à Montpellier !! Je n'oublierai pas également Lyde (Mister after party at home !!), Matt, Micky, Vince, Fabien, Riccardo, Karen, Tom, Mag, Titou, Rémi, Simon (Mr Rooney), Charlotte, Vaness, Thomas, Véro, Marion, Andy, Clémence et bien d'autres. Et Mr Mitchou avec qui j'ai passé des moments complètements fous !!! Merci à tous !!!!!!!!!!

Ces 6 années à Montpellier m'ont permis de découvrir de nouvelles personnes mais je tiens à remercier tous mes potos de chez moi à savoir Kali, Toun, Titi, Doudou, Coni, Raph, Youf… Vous êtes énormes !!!

Bien entendu la famille à jouer un grand rôle dans toute cette histoire. Un grand merci à mon père, ma mère, Bernard, Christian, Marianne, Annie, Maguin….Et pour finir un énorme MERCI à ma petite Maelle pour sa compréhension, son aide et sa patience dans les moments les plus rudes. MERCI ma puce.

Table des matières

Introduction 1

- Subduction de dorsale sous la Patagonie et Problématique 3
- Démarche et déroulement des campagnes de terrain 4
- Plan de la thèse 6

I. Formation des fenêtres asthénosphériques (slab-window) et exemples de chaînes de subduction anciennes et actuelles 9

- Introduction 11

I.1. Le concept de fenêtre asthénosphérique (slab-window) : une approche théorique 12

I.1.1. Définition de la fenêtre asthénosphérique 13

I.1.2. Géométrie de la fenêtre asthénosphérique 14

I.1.3. Effets thermiques et dynamique mantellique lors de la subduction d'une dorsale active et de la formation d'une fenêtre asthénosphérique 19

I.1.3.1. Considérations thermiques liées à la subduction d'une dorsale 19

I.1.3.2. Dynamique mantellique en relation avec le développement d'une fenêtre asthénosphérique 23

I.2. Les exemples mondiaux d'interactions dorsale/chaînes de subduction 25

I.2.1. Le Japon 27

I.2.2. L'Alaska et l'arc des Aléoutiennes 31

I.2.3. La Colombie Britannique 33

I.2.4. La Californie et la Basse Californie 36

I.2.5. L'Amérique Centrale et le point triple du Panama 40

I.2.6. La Péninsule Ouest Antarctique 41

I.2.7. Le bassin de Woodlark 42

I.2.8. La subduction de Sunda-Java 43

I.2.9. La subduction de la dorsale du Chili 45

II. Subduction de la dorsale active du Chili. Contexte géodynamique général : Les Andes et la Cordillère de Patagonie 47

II.1. Géodynamique et segmentation morphostructurale des Andes 49

II.1.1. Les Andes septentrionales 50

II.1.2. Les Andes centrales 52

II.1.2.1. Les Andes centrales du nord 54

II.1.2.2. Les Andes centrales 55

II.1.2.3. Les Andes centrales du sud 58

II.1.3. Les Andes méridionales 60

II.1.3.1. La Patagonie du nord 61

II.1.3.2. La Patagonie australe 63

II.1.4. Les processus contrôlant l'orogénèse andine 65

II.2. La Patagonie Centrale et la subduction de la dorsale active du Chili 69

II.2.1. La Patagonie Centrale entre le Paléozoïque et l'Eocène 69

II.2.1.1. Le Paléozoïque 69

II.2.1.2. Le Mésozoïque 70

II.2.1.3. Du Paléocène à l'Eocène 71

II.2.2. La Patagonie Centrale depuis l'Oligocène 72

II.2.2.1. Subduction de la dorsale active du Chili et développement de la fenêtre asthénosphérique sous la Patagonie 72

II.2.2.2. Evolution tectonique et magmatique de la Patagonie Centrale depuis l'Oligocène 75

Article 1 : ***Subduction of an Active Spreading Ridge beneath southern South America : A review of the Cenozoic record from the Andean Foreland, Central Patagonia (46°S-47°S).*** 77

III. Evolution morphotectonique Néogène de la Patagonie Centrale (46°S-47°S). Apports du magmatisme au front de la Cordillère 99

III.1. Evolution morphotectonique Néogène de la Patagonie Centrale (46°S-47°S). 103

<u>Article 2 :</u> A morphotectonic analysis of Central Patagonian Cordillera. Negative inversion of the Andean belt over a buried spreading center ? 105

III.2. Apports de la géochronologie et tectonique extensive de la Patagonie Centrale orientale 161

<u>Article 3 :</u> Pliocene extensional tectonics in the Eastern Central Patagonian Cordillera : geochronological and new fiels evidence 163

IV. Morphologie glaciaire et tectonique extensive. La Patagonie Centrale (45°S-47°S) au Plio-Quaternaire et développement de la fenêtre asthénosphérique 175

IV.1. Les glaciations Mio-Pliocène et évolution morphotectonique de la Patagonie centrale orientale, mesetas del Lago Buenos Aires et Guenguel 179

<u>Article 4 :</u> Mio-Pilocene glaciations of Central Patagonia : New evidence and tectonic implications 181

IV.2. Morphologie glaciaire et tectonique extensive : Bordure nord-ouest de la meseta del Lago Buenos Aires 219

<u>Article 5 :</u> When a subducting spreading ridge triggers relief inversion in Central Patagonia : Evidence from glacial morphology 221

IV.3. Evolution morphotectonique de la région de Coihaique (Aysen) ; Influence de la subduction de la dorsale du Chili au nord du point triple du Chili 239

<u>Article 6 :</u> Oligocene to recent morphostructural évolution of the Coihaique area (Aysen région), Central Patagonia : Tectonic events at the tip of a propagating slab window. 241

V. Conclusion générale et perspectives. Un modèle d'évolution des chaînes Circum-Pacifique lors de la subduction d'une dorsale active 279

V.1. Conclusion : Réponse de la Cordillère de Patagonie Centrale à la subduction de la dorsale du Chili 281

V.2. Perspectives concernant le chantier Patagonie 285

V.3. Subduction de dorsale active et chaînes de type 'andin' : vers un modèle à l'échelle du Pacifique 286

Annexes 293

Melnick et al., 2009. Neotectonics along the eastern flank of the Northern Patagonian Icefield, southern Chile : Cachet and Exploradores fault zones. 295

Boutonnet et al., accepté. Subduction of the South Chile active spreading ridge : A 17 Ma to 3 Ma magmatic record in Central Patagonia (western esdge of the meseta del Lago Buenos Aires, Argentina). 301

Références 361

Introduction

• Subduction de dorsale sous la Patagonie et Problématique

L'évolution des chaînes de subduction est étroitement reliée aux caractéristiques de la lithosphère océanique en subduction. En effet, le couplage interplaque, la vitesse de convergence, et son obliquité par rapport à la fosse, vont conditionner le régime tectonique et la déformation de la plaque chevauchante. De plus, des anomalies topographiques ou structurales présentes sur la plaque océanique en subduction (volcans sous-marins, plateaux océaniques, rides asismiques et dorsales actives), vont modifier localement le couplage interplaque, influençant ainsi l'état de contraintes de la plaque supérieure.

La Cordillère des Andes, qui s'étend sur plus de 8000 km de long depuis le Vénézuela jusqu'à la Terre de Feu, constitue un exemple majeur de chaîne de montagnes interagissant avec la subduction d'anomalies topographiques et structurales (Figure 1A). Dans ce travail, nous analysons l'impact de la subduction de la dorsale active du Chili sur la déformation et la morphologie de la plaque supérieure. Vers 46°S de latitude, un axe d'accrétion séparant les plaques Nazca et Antarctique, passe en subduction sous le continent sud-américain. Actuellement, cette configuration est unique au monde et de ce fait, la Patagonie Centrale (45°S-48°S) constitue un laboratoire à terre propice à l'étude des interactions entre les lithosphères océaniques et continentales lors de la subduction d'une dorsale active. Les nombreuses études menées conjointement par des équipes françaises (Montpellier, Brest), chiliennes et argentines depuis ces 15 dernières années ont révélé qu'à la latitude du point triple actuel, l'évolution tectonique et magmatique de la cordillère patagonienne est étroitement liée à la migration vers le nord de la dorsale active du Chili sous le continent. En effet, Lagabrielle et al (2000 et 2004) ont montré qu'entre l'Oligocène et le Miocène moyen (15-14 Ma), la surrection de la cordillère patagonienne était due à l'augmentation du couplage à l'interface des plaques en relation avec l'approche de la dorsale vers la fosse chilienne. Ces travaux ont également permis de soulever des problèmes tels que la position anormale de magmatisme alcalin en domaine 'arrière-arc', et la présence de dépressions transverses et internes affectant la cordillère patagonienne. Depuis la fin du Miocène, la subduction oblique de la dorsale du Chili a induit la formation d'une fenêtre asthénosphérique ('*slab-window*') sous la plaque supérieure. De ce fait, la Patagonie Centrale est un objet particulièrement intéressant pour étudier les effets de certains processus profonds, en relation avec le développement d'une fenêtre asthénosphérique, sur l'évolution tectonomagmatique et morphologique d'une chaine de subduction.

Le travail présenté dans cette thèse fait suite aux études géologiques préliminaires réalisées au niveau de la transversale du point triple du Chili dans le cadre des programmes (ECOS…) mis en place sous la responsabilité de Y. Lagabrielle et de M. Suarez et D. Morata au Chili et de E. Rossello en Argentine, avec le soutien des programmes Dyeti et Reliefs de l'INSU. L'objectif principal de cette thèse est de comprendre l'évolution tectonique et morphologique de cette portion de Cordillère, dans une période comprise entre la fin du Miocène et le Quaternaire, période durant laquelle se développe la fenêtre asthénosphérique sous la Patagonie Centrale. En effet, les caractéristiques des événements tectoniques et morphologiques responsables de la topographie très particulière de cette chaîne posent des questions : Quel est le régime tectonique global de la cordillère patagonienne à la latitude du point triple ? Où et comment se localise la déformation responsable de la topographie générale particulière de la Cordillère ? Quel est l'âge de la déformation et quelle est son amplitude? Le régime tectonique post-Miocène-Pliocène est-il en relation avec le développement de la fenêtre asthénosphérique sous la plaque chevauchante ? La fenêtre asthénosphérique a-t-elle des conséquences géologiques au nord du point triple du Chili ?

- **Démarche et déroulement des campagnes de terrain**

Afin de répondre à ces questions fondamentales permettant de contraindre l'évolution d'une chaîne de subduction actuelle interagissant avec une dorsale active en subduction, j'ai choisi une approche pluridisciplinaire, intégrant à la fois, la géologie régionale et structurale, la microtectonique et la géomorphologie réalisée lors de plusieurs missions de terrain (4 mois et demi sur 3 ans). Ce travail de terrain a été couplé à l'analyse et l'interprétation de diverses données d'imagerie et données topographiques (MNT). L'ensemble de ces travaux a été réalisé au niveau de secteurs clés de la cordillère patagonienne pouvant permettre de répondre, suivant les cas, aux différentes questions posées suivantes :

i) Dans la partie interne de la Cordillère. La première partie de la mission de terrain en 2006 (1 mois) m'a permis de me familiariser avec l'objet de l'étude et de débuter une étude structurale et morphologique de la région du lac Général Carrera-Buenos Aires (Figure 1B) (LGCBA, 2ème plus grand lac d'Amérique du Sud, profondeur maximale -380 mètres), en compagnie de Y. Lagabrielle, J. Malavielle, J.F. Ritz, M. Suarez, N. Arnaud, C. Guivel, et complétée fin 2007. Fin 2006-début 2007 (3 semaines), j'ai réalisé avec l'aide technique de Leonardo Zuñiga Díaz, une étude structurale des bordures Nord et Est de la dépression du lac Lapparent, 50 km au nord du LGCBA, apportant des informations complémentaires sur la structure de la cordillère.

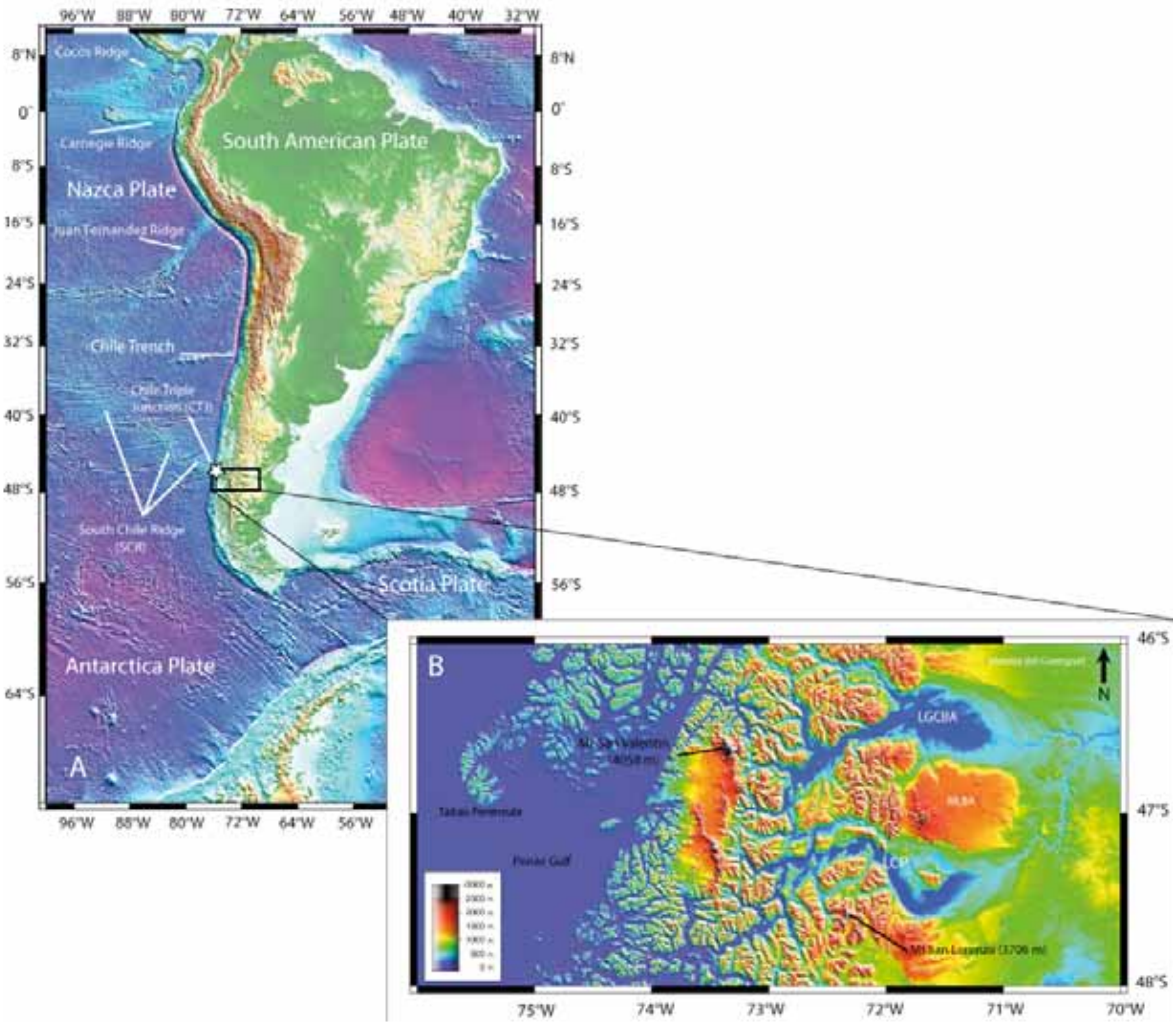

Figure 1 : A : Modèle numérique de terrain de l'Amérique du Sud et de la Péninsule Ouest Antarctique (DEM SRTM-90m). Les anomalies topographiques et structurales des plaques océaniques en subduction sous le continent sud-américain sont représentées. L'étoile blanche correspond au point triple du Chili localisé à la latitude de 46°S. B : Modèle numérique de terrain de la Patagonie Centrale à la latitude du point triple du Chili (DEM SRTM-90m). Nous remarquons que cette région est caractérisée par une topographie très particulière où à l'ouest et à l'est des hauts reliefs dominent des dépressions transverses et internes à la chaine. LGCBA : Lac General Carrera-Buenos Aires ; LCP : Lac Cochrane-Pueyerredon ; MLBA : Meseta del Lago Buenos Aires.

ii) Au niveau du front morphotectonique et du bassin d'avant-pays (partie Est de la chaine) (figure 1-B), dont les derniers événements compressifs ont été datés à environ 15 Ma (Lagabrielle et al., 2004). Afin d'expliquer les anomalies topographiques de cette région, l'hypothèse d'une inversion négative du front chevauchant avait été émise lors d'une précédente mission de terrain réalisée par notre équipe. Au cours de la première mission de 2007, une campagne d'échantillonnage de produits magmatiques a été réalisée dans cette zone. De plus, j'ai pu compléter l'analyse structurale et morphologique de ce secteur au cours d'une mission de terrain fin 2007 dont j'ai assumé l'organisation en collaboration avec de Michel de Saint-Blanquat et Alejandro Sanchez.

iii) Au niveau de la bordure ouest de la meseta del Lago Buenos Aires (Figure 1-B). Ce plateau est constitué de laves OIB datées entre 12 Ma et 3 Ma (Gorring et al., 1997 ; Guivel et al., 2006) dans lesquelles sont intercalés des tills datés entre 7 Ma et 3 Ma (Lagabrielle et al., accepté). Cette séquence volcanique localisée à quelques kilomètres du front morphotectonique, recouvre les molasses d'avant pays. Ce plateau, en position topographique inversée, est caractérisé par la présence de marqueurs morphologiques glaciaires déconnectés de tout réseau glaciaire provenant de l'ouest. Dans ce secteur j'ai pu réalisé, en compagnie de Jean-François Ritz, une étude morphologique et structurale détaillée couplée à un échantillonnage de basaltes lors d'une mission de terrain en 2009 (3 semaines).

iv) Au niveau de la partie ouest de la Cordillère, à quelques kilomètres du Campo Hielo Norte (point culminant Mont San Valentin, 4058 m, Figure 1-B). Une expédition réalisée début 2008 (2 semaines) en collaboration avec une équipe allemande (GFZ Potsdam : D. Melnick, V. Georgieva, Julius Munoz) a eu pour but une reconnaissance générale du secteur. Une étude morpho-structurale a été réalisée, accompagnée d'un échantillonnage de granites (traces de fission et U-Th/He sur apatite). Cette partie du travail sera exposée sous la forme d'un abstract dans la partie Annexe.

v) Enfin, à environ 100 km au nord du point triple du Chili. Au niveau de la transversale de Coihaique, j'ai pu effectuer début 2008 (3 semaines), une étude morphotectonique, complétant ainsi les données structurales et morphologiques de cette partie de la Patagonie.

• Plan de la thèse

Ce travail est présenté sous la forme de 5 chapitres rédigés en français (chapitre I, première partie du chapitre 2 et une partie de la conclusion) et d'articles publiés, acceptés, en révisions ou soumis (chapitres II, III, IV, et fin de la conclusion).

Le chapitre 1 intitulé '***Formation des fenêtres asthénosphériques (slab-window) et exemples de chaînes de subduction anciennes et actuelles***' présente les mécanismes de formation d'une fenêtre asthénosphérique lors de la subduction d'une dorsale active et passe en revue les exemples anciens et modernes de chaines de montagnes interagissant avec une 'subduction chaude'.

Le chapitre 2 '***Subduction de dorsale active du Chili. Contexte géodynamique général : Les Andes et la Cordillère de Patagonie***' se compose d'une introduction générale sur les Andes suivie par la présentation du contexte particulier du point triple du Chili. Ensuite, nous présentons l'histoire pré-subduction de dorsale de la Patagonie Centrale entre le Jurassique et l'Oligocène. Enfin, les manifestations majeures de la migration de la subduction de la dorsale du Chili sur l'ensemble de la Patagonie entre l'Oligocène et le Pliocène sont exposées sous la forme d'un article publié en 2009 à *International Journal of Earth Sciences, spécial volume, Subduction Zones Dynamics* (Scalabrino et al., 2009).

Le chapitre 3 '***Evolution morphotectonique de la Patagonie Centrale (46°-47°S) au Néogène*** est rédigé sous la forme de plusieurs articles soumis et publiés. Cette partie décrit l'évolution tectonique, morphologique et magmatique de la Patagonie Centrale à la latitude du point triple et ceci lors de la période post-subduction de dorsale (entre 15 Ma et l'actuel). La première sous partie correspond à un article soumis à *Tectonics* (Scalabrino et al.,) portant sur l'analyse structurale et morphologique détaillée de la Cordillère. Je propose une carte morphologique, une carte structurale et enfin un modèle d'évolution de la chaîne depuis l'Oligocène à l'actuel. La seconde partie quand à elle, est consacrée à un travail structural et à un ensemble de datations réalisées à l'est du front morphotectonique et dont les résultats et interprétations ont été publiés en 2007 dans *Terra Nova* (Lagabrielle et al., co-auteur).

Le chapitre 4 ' ***La morphologie glaciaire : un marqueur de la tectonique extensive plio-quaternaire en relation avec l'évolution de la fenêtre asthénosphérique***' est également présenté sous la forme de plusieurs articles soumis ou en cours de révision. Ici, l'aspect morphologie glaciaire est le fil conducteur du chapitre afin de contraindre de façon précise l'âge et l'amplitude des événements tectoniques qui ont suivi la subduction de dorsale. Une première partie porte sur l'histoire tectonique et glaciaire fin Miocène-Pliocène de la cordillère patagonienne, au niveau de la meseta del Lago Buenos Aires. Ce travail fait l'objet d'un article accepté à *Andean Geology, spécial volume Patagonia* (Lagabrielle et al., 2nd auteur). La deuxième partie porte sur l'étude des nouvelles observations morphologiques et structurales de la bordure NW de la meseta del Lago Buenos Aires recueillies lors de la mission de 2009. L'ensemble des résultats est présenté dans un article soumis à *Geology*

(Scalabrino et al.,). Enfin, la troisième partie présente l'analyse morphostructurale de la région de Coihaique, située à une centaine de kilomètres au nord du point triple. Ici, nous discutons l'impact possible de la subduction de la dorsale du Chili sur l'évolution tectonique et morphologique de la cordillère au nord du point triple actuel. Les résultats sont soumis dans un article à *Andean Geology, spécial volume Patagonia* (Scalabrino et al.,).

Enfin, le dernier chapitre intitulé '***Conclusion générale et perspectives. Un modèle d'évolution des chaînes circum-Pacifique lors de la subduction d'une dorsale active***' est une synthèse reprenant les implications géodynamiques de l'étude structurale et morphologique de la cordillère patagonienne centrale lors de la subduction de la dorsale active du Chili et du développement d'une fenêtre asthénosphérique depuis le Pliocène. Cette partie sera également composée de la présentation d'un modèle d'évolution globale des chaînes de montagne de type 'andin' circum-Pacifique depuis un stade pré-subduction à un stade post-subduction de dorsale.

Chapitre I :

Formation des fenêtres asthénosphériques (slab-window) et exemples de chaînes de subduction anciennes et actuelles.

Introduction

Au niveau des zones de subduction océanique les plus courantes, la lithosphère océanique épaisse et relativement froide plonge sous la lithosphère continentale. L'état thermique d'une zone de subduction dite 'mature' est représenté sur la Figure I.1.a, où l'on note la forte déflection des isothermes. Ainsi, ces zones de subduction caractérisent des régions anormalement froides de la Terre. Lors de la subduction d'une dorsale active, dont la majorité des exemples est réparti autour du Pacifique, l'état thermique sous le continent est fortement perturbé. La lithosphère océanique approchant la fosse, est fine et chaude et sa subduction va, au cours du temps, induire des modifications importantes sur la structure thermique générale de la subduction (Figure. I.1.b). Les conséquences de ces perturbations thermiques sur la dynamique du manteau, sur les interactions asthénosphère/lithosphère et sur l'évolution de la plaque chevauchante sont nombreuses Elles font l'objet de ce chapitre.

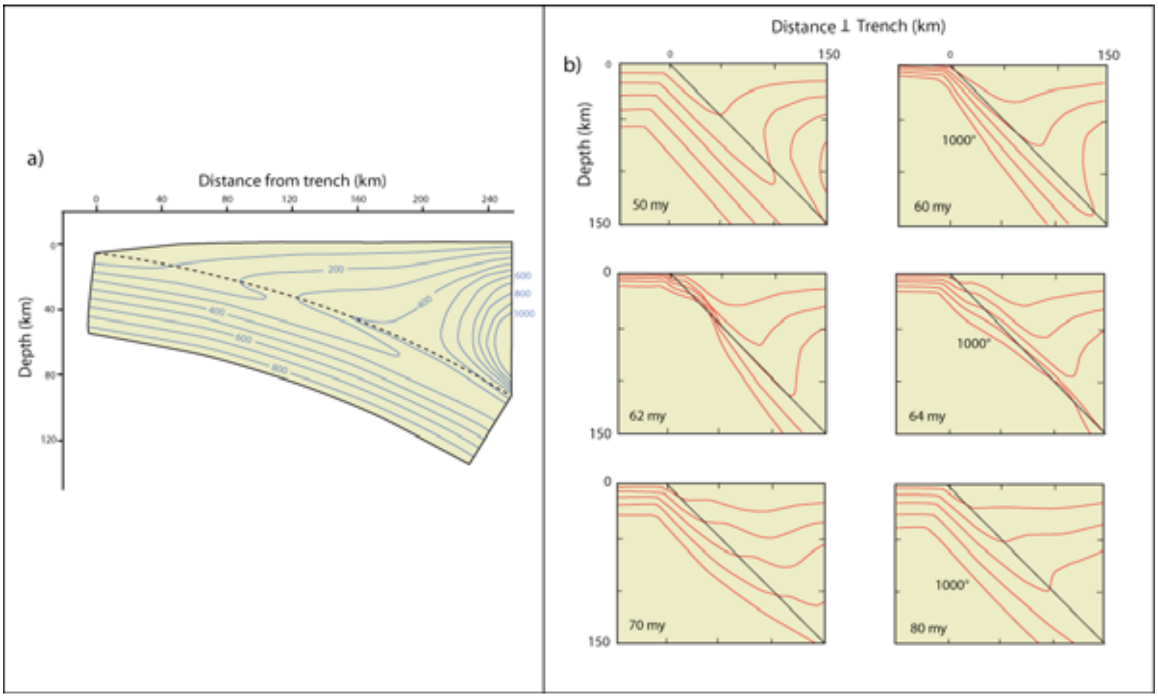

Figure I.1 : Comparaison de la structure thermique d'une zone de subduction normale a- ayant atteint son état mature (Van den Beukel et Wortel, 1988) avec b- celui d'une zone de subduction perturbée par le passage d'une dorsale (DeLong et al., 1979).

Dans ce chapitre, le problème d'interactions dorsale/fosse sera abordé, en introduisant la notion de fenêtre asthénosphérique (slab-window), suivie par les exemples mondiaux de chaînes de subduction ayant interagi avec des dorsales en subduction. Dans une première partie, nous présentons une approche géométrique et thermique de la fenêtre asthénosphérique lorsque deux plaques océaniques divergentes passent en subduction. Dans un second temps, nous résumerons les différentes interactions dorsale/fosse à travers le monde en insistant particulièrement sur l'évolution tectonique de la plaque supérieure.

I.1. Le concept de fenêtre asthénosphérique (slab-window) : une approche théorique.

La lithosphère océanique est créée à l'axe des dorsales et est recyclée au niveau des zones de subduction. L'ensemble de ces processus s'effectue généralement dans le même bassin océanique (comme par exemple dans le bassin Pacifique). La formation de plaques océaniques est un processus symétrique par rapport à la frontière divergente, tandis que la subduction de dorsale peut se produire obliquement par rapport à la frontière divergente induisant ainsi un recyclage asymétrique du bassin océanique. La subduction d'une dorsale active se traduit par l'existence d'un point triple à la jonction entre 3 plaques différentes.

La configuration de ce point triple peut être de différentes natures suivant la configuration de la subduction : Ride-Ride-Fosse (RRF), dans le cas où l'axe de la dorsale subducte, Transformante-Fosse-Fosse (TFF), lorsqu'une faille transformante passe en subduction, Transformante-Transformante-Fosse (TTF) et Ride-Transformante-Fosse (RTF). De ce fait, l'interaction du point triple avec la marge convergente peut conduire à deux situations :

- dans certains cas, la subduction est interrompue. Elle est suivie par la cessation de l'accrétion océanique à l'axe de la dorsale et est accompagnée par la fragmentation de la plaque océanique en microplaques. Ce cas a été suggéré pendant le Tertiaire, lorsque la dorsale Est-Pacifique a approché la marge nord-américaine (Menard, 1978 ; Dixon and Farrar, 1980 ; Riddihough, 1984 ; Atwater and Severinghaus, 1989 ; Farrar and Dixon, 1993). Ces hypothèses, à l'époque, ne tenaient pas compte du concept de formation d'une fenêtre asthénosphérique lors de la subduction d'une dorsale.

- plus couramment, la dorsale passe en subduction. Les bordures de plaques nouvellement formées à l'axe vont subduire, puis s'écarter en suivant le mouvement inexorable des plaques, créant ainsi un espace favorable à la remontée d'asthénosphère chaude sous la plaque supérieure (on parlera ici de subduction 'chaude'). Ce phénomène conduit à l'ouverture du slab : on parle alors de fenêtre asthénosphérique ou slab-window (Dickinson and Snyder, 1979 ; Thorkelson and Taylor, 1989).

I.1.1. Définition de la fenêtre asthénosphérique.

Le concept de fenêtre asthénosphérique se développant sous une plaque continentale a été introduit pour la première fois par Dickinson and Snyder (1979) dans la cordillère nord-américaine lors du développement de la faille de San Andréas et de la subduction des plaques Farallon et Pacifique. Leurs travaux proposaient qu'après l'interaction dorsale/fosse, une région adjacente à la faille était dépourvue de lithosphère océanique plongeante. De plus, afin d'expliquer certaines caractéristiques magmatiques et tectoniques de la plaque chevauchante, les auteurs avaient émis l'hypothèse de flux asthénosphériques chaud sous la plaque nord-américaine.

Généralement, avant la subduction de la dorsale, la frontière divergente est le lieu d'accrétion océanique par accroissement de surface lithosphérique. Une fois la dorsale enfouie sous la plaque supérieure, l'asthénosphère remontée par convection à l'aplomb de l'axe ne va pas se refroidir et la production de lithosphère océanique cesse. La fenêtre asthénosphérique correspond donc à un domaine à fort gradient de température .La subduction d'une dorsale active peut être vue comme étant le remplacement d'une subduction 'froide' par une subduction 'chaude' (Figure. I.2).

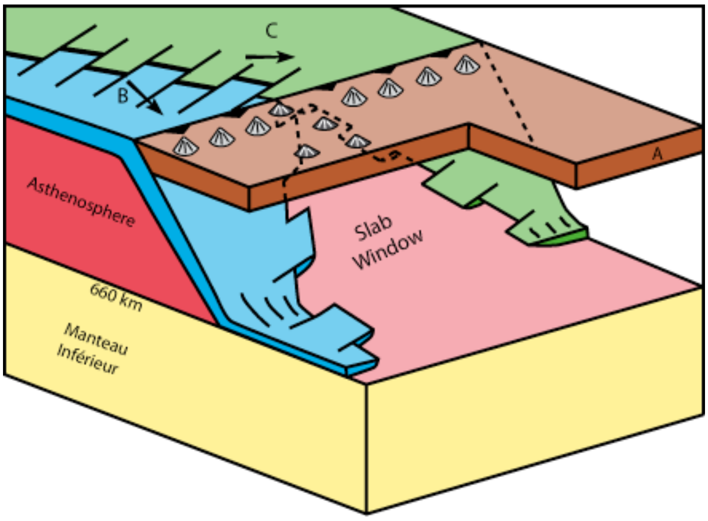

Figure I.2 : Schéma classique d'une fenêtre asthénosphérique s'ouvrant lors de la subduction d'une dorsale active (Thorkelson et al., 1996).

I.1.2. Géométrie de la fenêtre asthénosphérique.

Lors de leurs travaux, Dickinson and Snyder (1979) ont proposé, pour le cas du développement de la faille de San Andréas, qu'une zone dépourvue de lithosphère plongeante était présente sous le continent nord-américain. Afin de délimiter géométriquement cette zone, plusieurs hypothèses avaient été proposées : (1) le mouvement divergent à l'axe de la dorsale est toujours symétrique et perpendiculaire à celui-ci ; (2) les mouvements relatifs des plaques sont parallèles aux failles transformantes et (3) la lithosphère océanique jeune et chaude continue de subduire. Il en résulte que la fenêtre asthénosphérique prédite a une forme triangulaire dont l'amplitude évolue avec le temps (Figure. I.3).

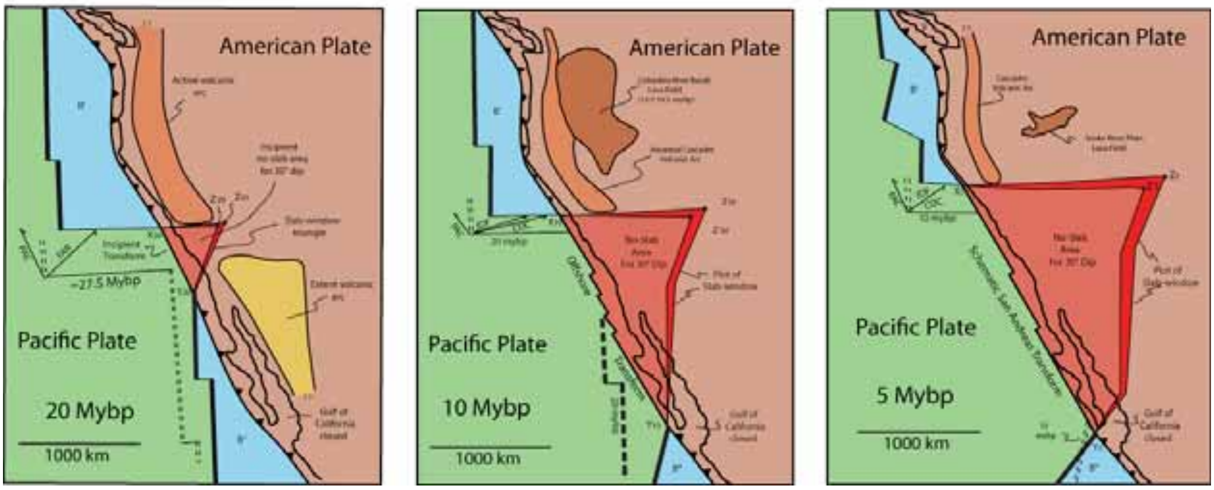

Figure I.3 : Reconstitutions géométriques et cinématiques de l'évolution de la fenêtre asthénosphérique sous le contient nord-américain entre 20 et 5 Ma (Dickinson et Snyder, 1979).

Plus récemment, Thorkelson (1996) a proposé plusieurs modèles de développement et d'évolution de fenêtres asthénosphériques. Afin de créer un espace entre les deux plaques océaniques, dont les bordures sont parallèles aux mouvements entre le point triple et les plaques plongeantes, il suppose (1) que la subduction des 2 plaques continue et (2) que l'accrétion lithosphérique à l'axe cesse. Suivant ces conditions, la forme de la fenêtre asthénosphérique va être dépendante de trois facteurs principaux (Dickinson and Snyder, 1979 ; Thorkelson and Taylor, 1989) : (1) les vitesses de convergence, (2) la configuration pré-subduction axes d'accrétion/failles transformantes et (3) les angles de subduction des plaques océaniques.

Les figures I.4, I.5 et I.6 illustrent la forme théorique de la fenêtre asthénosphérique obtenue dans le cas d'une subduction horizontale et orthogonale, montrant l'importance des trois principaux facteurs. La figure I.4 présente la forme de la fenêtre obtenue dans le cas d'une subduction d'un axe d'accrétion orthogonal à la fosse (Thorkelson, 1996). Ici, les paramètres majeurs sont les vitesses de convergence des plaques océaniques C et B par rapport à la plaque chevauchante supposée fixe A.

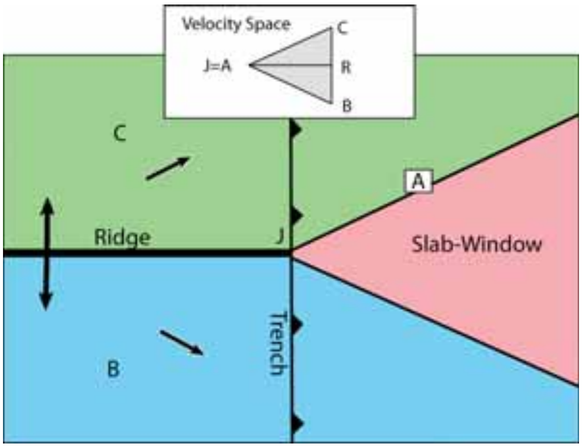

Figure I.4 : Construction d'une fenêtre entre 2 plaques océaniques en subduction dans le cas d'une interaction dorsale/fosse perpendiculaire à la marge. La forme de la fenêtre est contrôlée par les vecteurs entre le point triple et les plaques subduites (vecteurs JC et JB) (Thorkelson, 1996).

Dans le cas d'une subduction plate, les bordures de la fenêtre asthénosphérique sont parallèles aux vecteurs entre le point triple et les plaques subduite (JB et JC, Figure. I-4). Le point triple ne migrant pas (schéma des vecteurs vitesses, A=J, Figure. I.4), les bordures de la fenêtre sont parallèles aux vecteurs de convergences, suivant les vecteurs AB et AC (schéma des vecteurs vitesse, Figure. I-4). Il en résulte une fenêtre triangulaire sous la plaque supérieure et dont la taille augmentera avec le temps. La figure I.5 présente la géométrie de la fenêtre asthénosphérique induite par la subduction orthogonale et horizontale de segments d'accrétion séparés par des failles transformantes. Ici, les paramètres majeurs sont bien les vitesses de convergence et la configuration pré-subduction du système divergent en subduction.

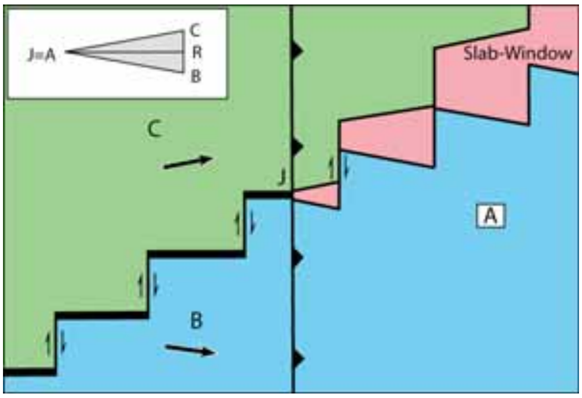

Figure I.5 : Construction d'une fenêtre entre 2 plaques océaniques en subduction dans le cas d'une interaction dorsale/fosse perpendiculaire à la marge. La subduction de plusieurs segments et failles transformantes induira la forme de la fenêtre composite (Thorkelson, 1996).

Dans ce cas, le jeu des failles transformantes induira la formation d'une fenêtre pour chaque segment subduit, qui au cours du temps évoluera en une fenêtre composite (Thorkelson, 1996). Enfin, la figure I.6 présente l'influence de l'angle de plongement des plaques océaniques sur la projection en surface de la fenêtre. Ici, la subduction horizontale est limitée à un seul axe d'accrétion. Nous remarquons que le pendage de plongement des plaques modifie considérablement la trace en surface de la fenêtre. En effet, plus le pendage est élevé plus la taille de la fenêtre prédite sera grande (Thorkelson, 1996).

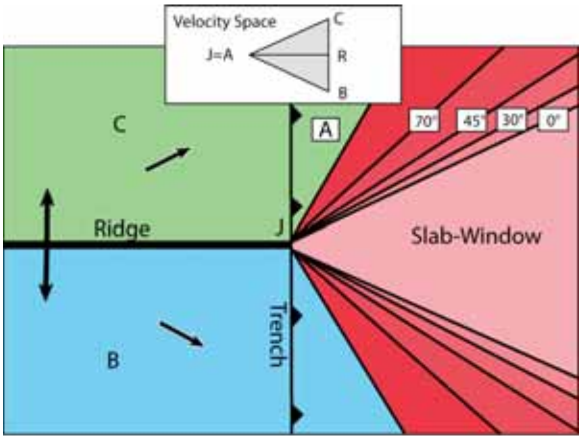

Figure I.5 : Effets de l'angle de subduction sur la géométrie en surface de la fenêtre. Projection en surface des bordures de la fenêtre pour des angles de 0 à 70°. Plus l'angle est important, plus la géométrie de la fenêtre est modifiée (Thorkelson, 1996).

Les figures I.7, I.8 et I.9 illustrent la forme de la fenêtre asthénosphérique lors d'une subduction horizontale et oblique. Le cas traité ici correspond à la configuration de la dorsale du Chili passant en subduction sous la plaque sud-américaine (notre sujet d'étude) et illustré dans la thèse de C. Guivel (1999). La figure I.7 montre le cas simple d'un segment de dorsale oblique de 15° par rapport à la marge avec une migration du point triple vers le nord (J0, J1, J2, Figure. I.7) au fur et à mesure que le segment passe en subduction (cas du point triple du Chili). Cette figure montre que la forme triangulaire de la fenêtre est contrôlée par les vecteurs entre le point triple et les plaques subduites (vecteurs JB et JC, Figure I.7).

La figure I.8 met en avant l'importance de la configuration pré-subduction du système dorsale/faille transformante sur la géométrie de la fenêtre. La forme de la fenêtre devient composite lors de la subduction de plusieurs segments et failles transformantes de longueurs inégales. De plus, la migration du point triple varie en fonction de la structure subduite. En effet lors du passage d'un axe d'accrétion, le point triple migre vers le nord tandis que la subduction d'une faille transformante induira la migration du point triple vers le sud (Cande et Leslie, 1986 ; Cande et al., 1987 ; Guivel, 1999). Notons également que la longueur de l'axe en subduction a une répercussion directe sur la surface de la plaque supérieure affectée par la migration du point triple. Enfin, la figure I.9 illustre la variabilité de la trace en surface de la forme de la fenêtre suivant différents angles de pendage des plaques océaniques en subduction. Plus il sera élevé, plus la forme de la fenêtre en surface sera grande.

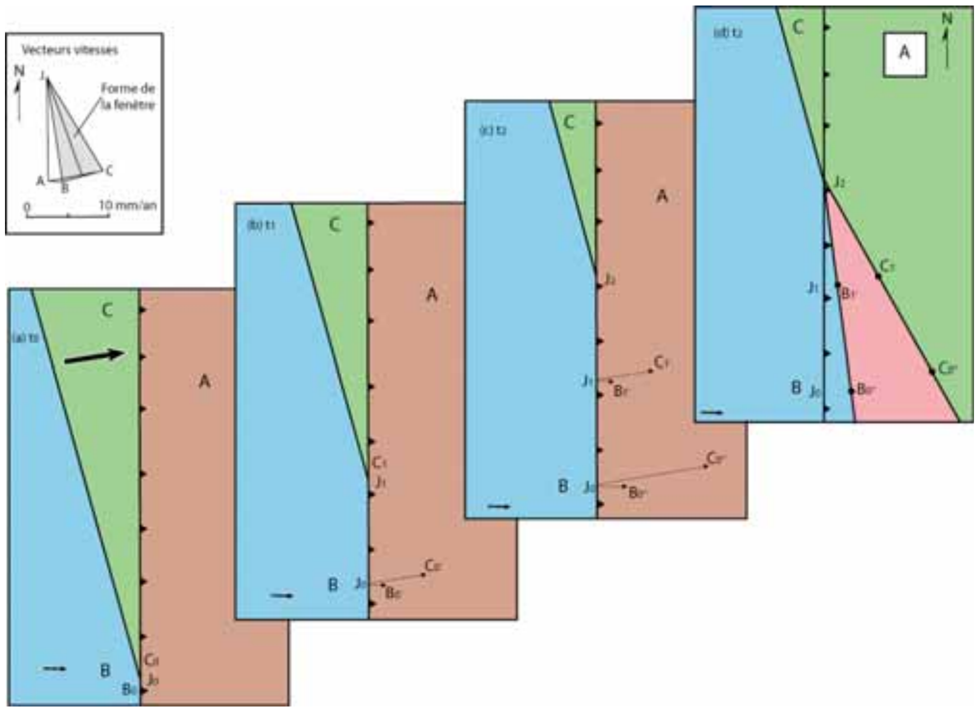

Figure I.7 : Construction d'une fenêtre asthénosphérique entre 2 plaques océaniques en subduction dans le cas d'une interaction dorsale/fosse oblique de 15° (cas de la dorsale du Chili). Les vecteurs vitesses correspondent à la migration du point triple du point A au point J à 160 mm/an, et à la vitesse de convergence entre les plaques A et B de 20 mm/an et entre A et C de 84 mm/an. Ces paramètres correspondent à l'exemple du point triple du Chili (A=plaque Amérique du Sud, B= plaque Antarctique, C= plaque Nazca) (d'après Guivel, 1999).

La représentation de la forme de la fenêtre asthénosphérique présentée ci dessus est essentiellement géométrique et ne tient pas compte de divers paramètres pouvant la modifier. En effet, la taille et la forme de celle-ci sont influencées par : (1) l'érosion thermique (McKenzie, 1969 ; Severinghaus and Atwater, 1990 ; Kay et al., 1993 ; Thorkelson and Breitsprecher, 2005) affectant les bordures de la fenêtre et tendant à l'élargir ; (2) les forces de volume (spherical shell strain) (Yamaoka and Fukao ; 1986), qui augmente avec la profondeur, contrebalançant l'érosion thermique ; (3) les variations latérales de pendage des plaques océaniques (Dickinson and Snyder, 1979 ; Cross and Pilger, 1982 ; Thorkelson and Taylor, 1989) ; et (4) les forces de slab-pull tendant à élargir la fenêtre.

Dans le cas de la subduction de la dorsale du Chili, la forme de la fenêtre asthénosphérique composite a été reconstituée par plusieurs auteurs (Forsythe et al., 1987 ;

Gorring et al., 1997 ; Lagabrielle et al., 2004), et récemment actualisée par Breitsprecher and Thorkelson (2009) comme nous le verrons dans la suite de ce travail.

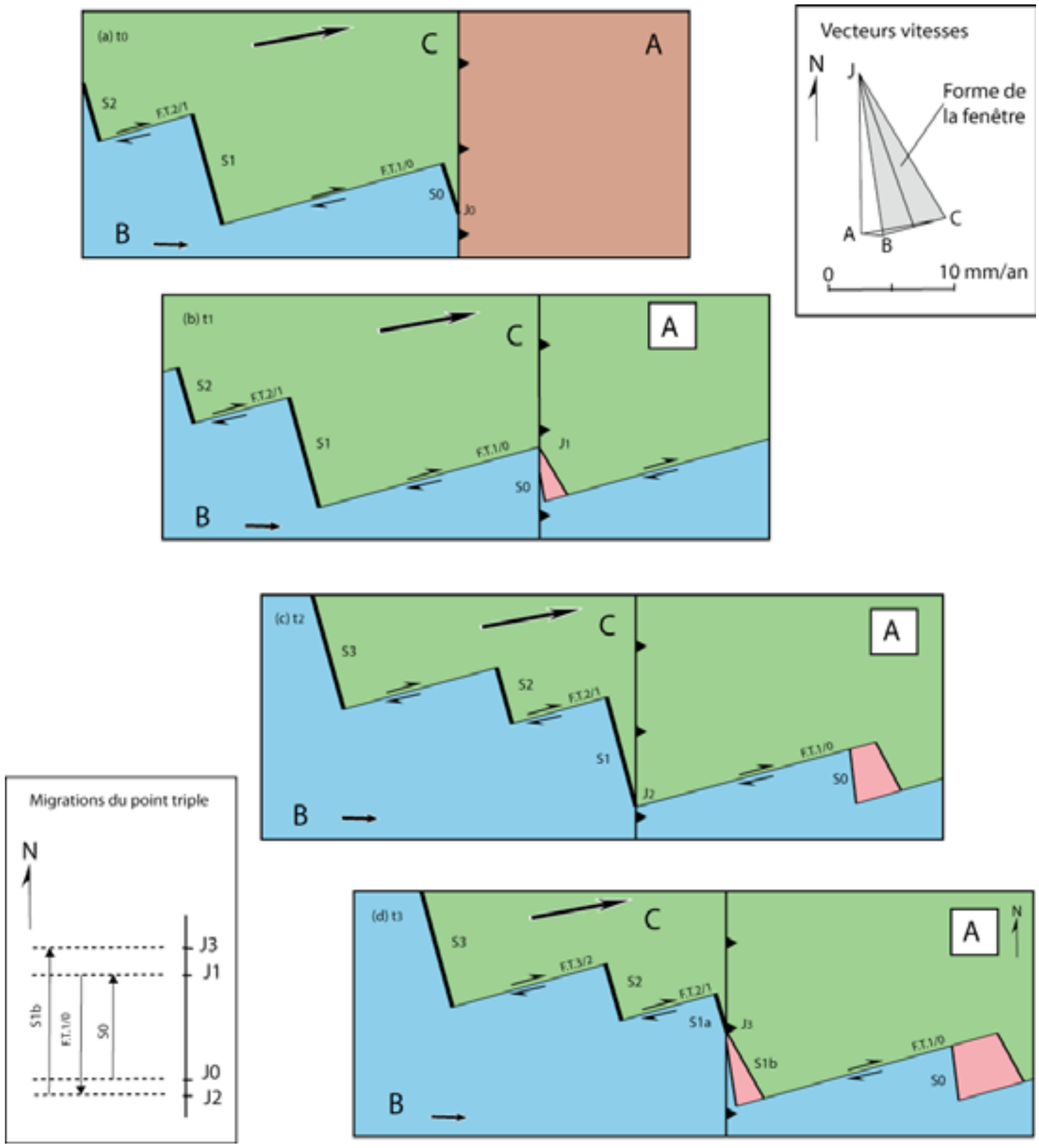

Figure I.8 : Construction d'une fenêtre entre 2 plaques océaniques divergentes en subduction. Les diagrammes (a) à (d) montrent l'évolution de la forme de la fenêtre qui devient composite lors de la subduction de plusieurs segments et failles transformantes de longueurs inégales. L'encadré en haut à droite indique le système de vitesse entre les plaques A, B et C et la forme de la fenêtre. L'encadré en bas à gauche donne le sens de migration du point triple en fonction de la subduction d'un segment (migration vers le nord) ou de la subduction d'une faille transformante (migration vers le sud). (a) temps t_0, le segment S_0 entre en subduction. (b), temps t_1, une fenêtre triangulaire se développe suite à la subduction du segment S_0. Les bordures de la fenêtre sont parallèles aux vecteurs JB et JC du diagramme de vitesse. (c), temps t_2, la faille transformante entre les segments S_1 et S_0 (F.T.1/0) est passée en subduction et la fenêtre du segment S_0 s'est agrandie adoptant une forme trapézoïdale. (d) au temps t_3, une partie du segment S_1 (S_{1b}) est entré en subduction alors que la fenêtre S_0 évolue toujours (d'après Guivel, 1999).

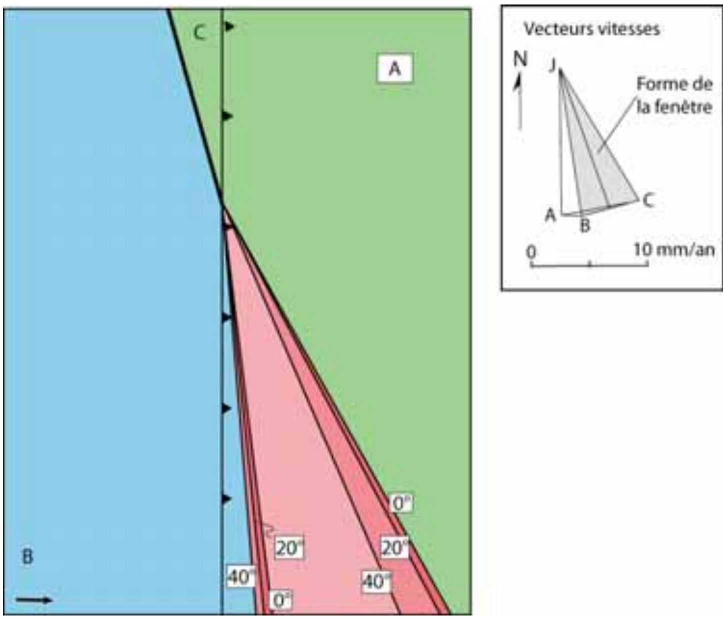

Figure I.9 : Effets de l'angle de plongement des plaques océaniques sur la géométrie en surface de la fenêtre. Projection en surface des bordures de la fenêtre pour des angles de 20 et 40° (Guivel, 1999).

I.1.3. Effets thermiques et dynamique mantellique lors de la subduction d'une dorsale active et de la formation d'une fenêtre asthénosphérique.

I.1.3.1. Considérations thermiques liées à la subduction d'une dorsale active

Lors de la subduction 'normale' d'une lithosphère océanique, le panneau plongeant est froid et se déshydrate au fur et à mesure de son enfouissement. De ce fait, le coin de manteau asthénosphérique sous –continental ('supra-slab') est refroidi par transfert de chaleur vers la plaque océanique (McKenzie, 1969) et à la fois hydraté par les fluides relâchés lors du métamorphisme prograde de la plaque plongeante (Gill, 1981 ; Peacock, 1993). Au contraire, l'asthénosphère située sous la plaque océanique en subduction (sub-slab) ne va pas subir de perturbations, restant ainsi chaude et sèche. Dans le cas d'un contexte de subduction de dorsale active, induisant le développement d'une fenêtre asthénosphérique sous la plaque chevauchante, la structure thermique de la zone de subduction sera fortement modifiée. En effet, l'asthénosphère chaude 'sub-slab' est directement en contact avec l'asthénosphère 'supra-slab' et la lithosphère continentale, entrainant des transferts de chaleur vers ces deux domaines (Figure. I.10). Il en résulte ainsi une inversion complète du régime thermique de la zone de subduction.

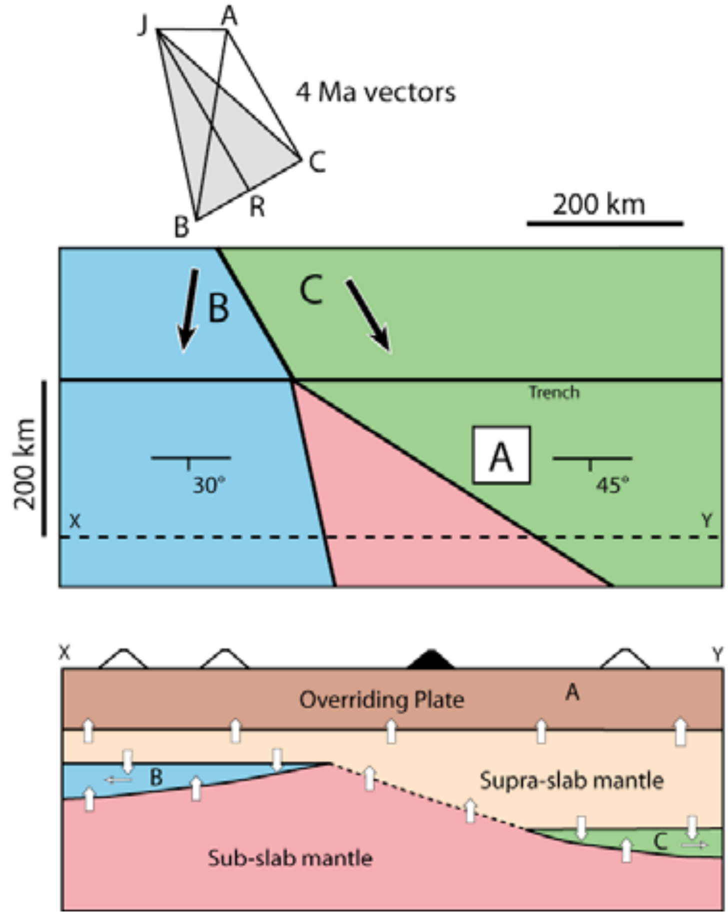

Figure I.10 : Fenêtre asthénosphérique vue en plan et en coupe entre 2 plaques océaniques divergentes ayant 2 pendages différents. Les transferts possibles (flèches blanches) entre les différents domaines sont : asthénosphère sous-océanique ('sub-slab'), asthénosphère sous-continentale ('supra-slab') et lithosphères océaniques et continentales (Thorkelson, 1996).

De plus, au-dessus de la fenêtre asthénosphérique, l'hydratation de est stoppée et la température va augmenter. De telles anomalies thermiques peuvent être mise en évidence par l'imagerie tomographique et par la géophysique. Les hétérogénéités latérales de densité devraient être reflétées par des hétérogénéités latérales de vitesses observables par la tomographie sismique. A l'échelle de la Terre, les travaux de Debayle (2005) mettent en évidence qu'entre 100 km et 300 km de profondeur, des anomalies thermiques anormalement chaudes sont présentes au Japon, en Alaska, au niveau du continent nord-américain, à l'extrémité sud de l'Amérique du Sud et en Antarctique (Figure. I.11). Ces anomalies étant probablement liées à la présence de fenêtres asthénosphériques.

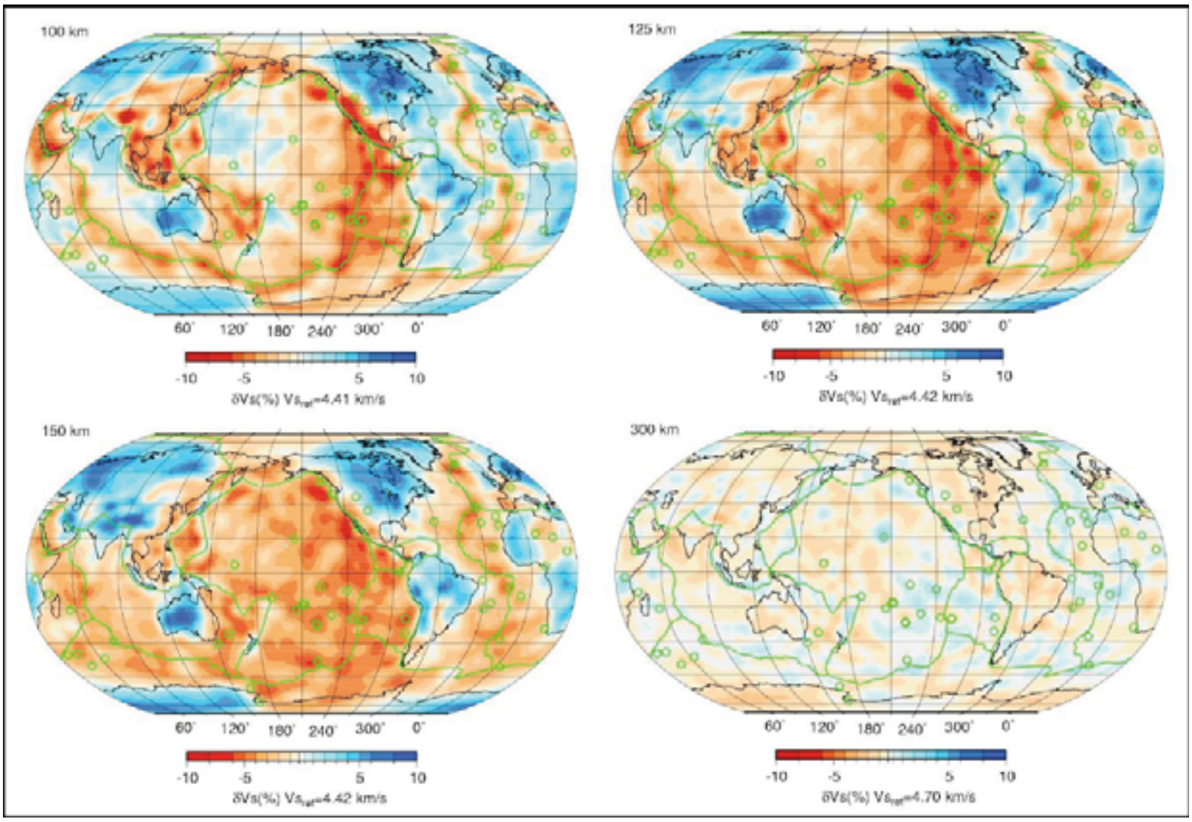

Figure I.11 : Coupes de tomographie sismique à 100, 125, 150 et 300 km de profondeur montrant les domaines chauds (couleur rouge) à travers les cordillères circum-Pacifique, dont les anomalies thermiques sont probablement associées à la formation de fenêtres asthénosphériques (Debayle et al., 2005).

A une échelle plus locale, Heintz et al (2005) montrent, par tomographie sismique, que le sud de l'Amérique du Sud est caractérisée par un ralentissement des vitesses sismiques (Vs) de l'ordre de 6 à 8 % caractérisant un manteau anormalement chaud sous le continent (Figure. I.12). Cette anomalie thermique est directement liée à la fenêtre asthénosphérique présente sous la plaque chevauchante. D'autres données géophysiques, telles que les mesures de flux de chaleur en surface, permettent de contraindre ces anomalies thermiques en profondeur. C'est le cas pour la région des cordillères nord-américaines (valeurs supérieures à 100 mW/m2, Sass et al., 1994), le Japon (Horai and Uyeda, 1963) et pour le sud de l'Amérique du Sud (valeurs supérieures à 160 mW/m2, Hamza and Munoz, 1996). Basé sur les données de flux de chaleur en surface, Artemieva (2006) propose un modèle thermique de la lithosphère continentale mettant en évidence la température de la lithosphère à 50 km de profondeur (Figure. I.13). Dans ce modèle, nous remarquons que les régions circum-Pacifique telles que le Japon, les cordillères américaines, le sud de l'Amérique du Sud et l'Antarctique présentent des anomalies de températures majeures (entre 700°C et 900°C à 50 km de profondeur) pouvant être associées aux fenêtres asthénosphériques. Ces anomalies thermiques persistent pendant plusieurs millions d'années (Groome et Thorkelson, 2009).

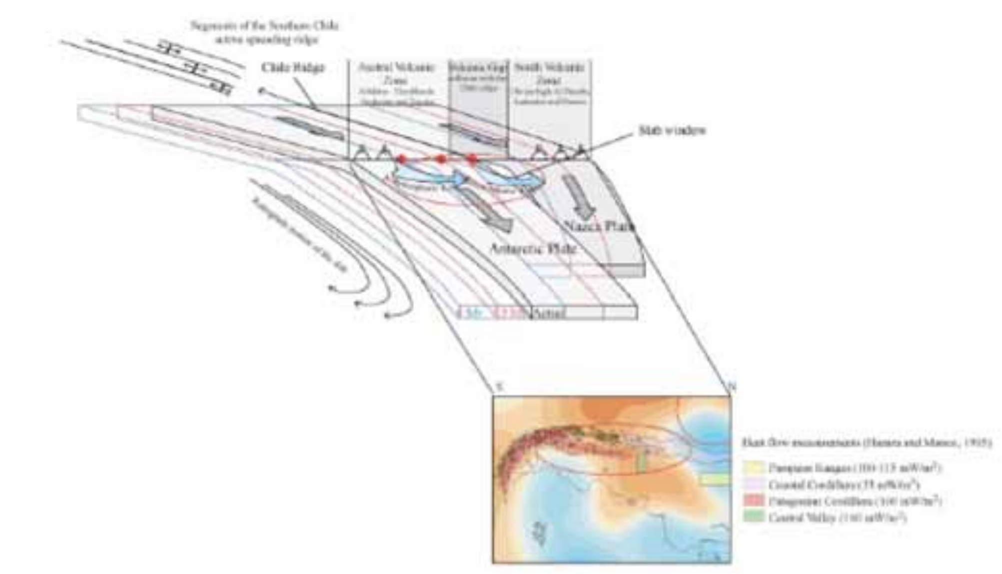

Figure I.12 : Bloc diagramme 3D illustrant la migration du point triple du Chili le long de la marge sud-américaine. . L'ensemble de la Patagonie est caractérisée par des flux de chaleur anormalement élevés (mesures réalisées par Hamza et Munoz, 1996) (d'après Heintz et al., 2005). Nous remarquons que dans leur modèle, les auteurs ne suggèrent pas la présence d'une fenêtre asthénosphérique permettant la remontée de matériel chaud, mais plutôt une déchirure du slab, le rendant ainsi limité dans l'interprétation géodynamiques des résultats.

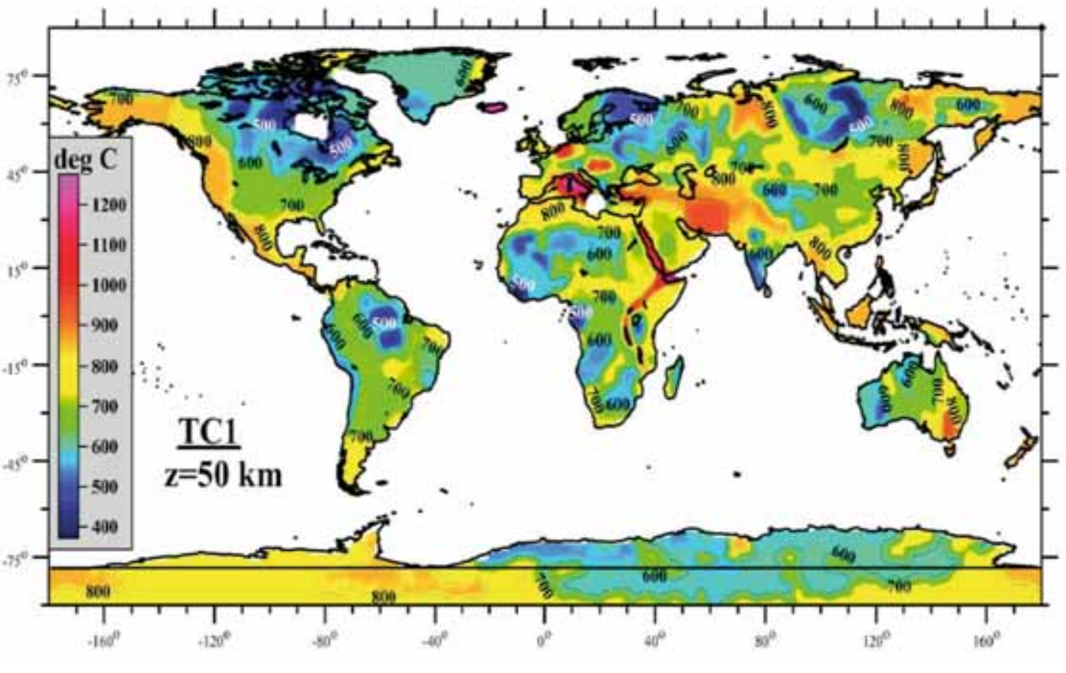

Figure I.13 : Carte de l'état thermique de la lithosphère continentale à 50 km de profondeur (Artemieva et al., 2006). Les régions situées entre le Japon et l'Antarctique présentent des lithosphères continentales anormalement chaudes à 50 km de profondeur.

I.1.3.2. Dynamique mantellique en relation avec le développement d'une fenêtre asthénosphérique

Dans le contexte de la subduction d'une plaque océanique sous une plaque continentale, la dynamique du manteau et de l'ensemble de la région est caractérisée par différents courants asthénosphériques plus ou moins complexes. La déformation du manteau s'accompagne d'une orientation préférentielle de réseau de l'olivine. L'axe cristallographique le log duquel la propagation des ondes sismiques est la plus rapide est orienté dans la direction de l'écoulement. Ainsi, les données d'anisotropie sismique obtenues à partir des directions rapides de polarisation des ondes permettent de déterminer les écoulements de manteau dans ce type de contexte. De nombreuses études ont montré différents types de convection au niveau des zones de subductions 'normales' et caractérisés par des courants de plusieurs types: (1) perpendiculaires à la fosse, telles que les subductions d'Izu-Bonin (Fouch et al., 1996), et des Mariannes (Fouch et al., 1998) ; (2) parallèles à la fosse, comme au niveau des subductions en Nouvelle-Zélande (Audoine et al., 2000), et aux Aléoutiennes (Yang et al., 1995 ; Savage, 1999) ; (3) plus complexes comme au Japon (Okada et al., 1995 ; Hiramatsu et al., 1998 ; Nakajima and Hasegawa, 2004), en Alaska (Wiemer et al., 1999), au Kamchatka (Levin et al., 2002) et en Amérique du sud (Silver and Russo, 1994 ; Polet et al., 2000, Helffrich et al., 2002), impliquant quelquefois des courants de part et d' autres des bordures de la plaque plongeantes (Figure. I.14) (Silver et Russo, 1994 ; Peyton et al., 2001 ; Long et Silver, 2008).

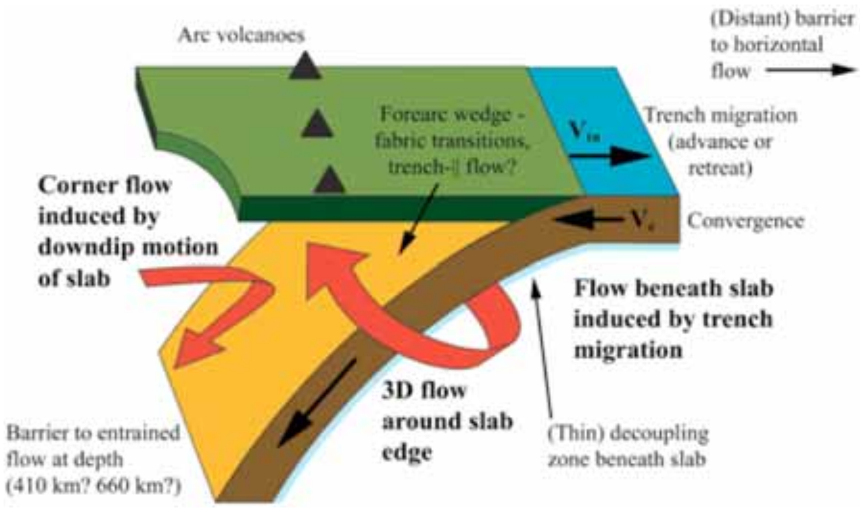

Figure I.14 : Schéma simplifié des principaux courants mantelliques au niveau d'une zone de subduction illustrant les complexités 2D et 3D de la circulation de manteau sous la plaque supérieure et au voisinage de la plaque plongeante (d'après Long et Silver, 2008)

Le développement d'une fenêtre asthénosphérique, considérée comme un gap dans le panneau plongeant, induit des perturbations majeures dans la dynamique du manteau sous la plaque supérieure. L'hypothèse de courants asthénosphériques profonds ascendants, passant à travers cette fenêtre, a été proposée pour la première fois par Uyeda et Miyashiro (1974) et Marshak et Karig (1977) afin d'expliquer des anomalies volcaniques de la plaque chevauchante. Cette hypothèse a été ensuite reprise par Dickinson and Snyder (1979), suggérant l'implication de courants asthénosphériques ascendants dans l'évolution tectono-magmatique des cordillères nord-américaines. Les données d'anisotropie sismique appuient ces hypothèses. En effet, Murdie et Russo, (1999) et Zandt et Humphreys, (2008) évoquent de fortes perturbations dans l'écoulement du manteau au niveau des fenêtres asthénosphériques situées au sud de l'Amérique du Sud et sur la partie ouest de l'Amérique du Nord respectivement. Les auteurs proposent que la remontée de matériel asthénosphérique chaud à travers cette ouverture modifie la convection sous la plaque supérieure, sur une surface plus ou moins grande suivant la taille de la fenêtre. Les répercussions sur la plaque supérieure vont être majeures. Tout d'abord, l'effet de chalumeau thermique ou '*blow torch*' introduit par DeLong et al., (1979), est responsable d'un métamorphisme BP-HT et d'un magmatisme varié et particulier proche de la fosse (de type MORB, basaltes alcalins et calco-alcalins, granites d'anatexie, adakites…), observés au niveau de différents avant-arcs à travers les chaînes circum-Pacifique: (1) au Japon (Hibbard et Karig, 1990 ; Kiminami et al., 1994 ; Kinoshita, 2002) ; (2) en Alaska et dans les Aléoutiennes (Moore et al., 1983 ; Sisson et Palvis, 1993 ; Bradley et al., 1995, 2003 ; Palvis et Sisson, 1995 ; Sisson et al., 2003 ; Bowman et al., 2003 ; Kusky et al., 2003 ; Groome et al., 2003, Haeussler et al., 2003, Cole et al., 2006 ; Cole et Stewart, 2009) ; (3) en Colombie Britannique (Allan et al., 1993 ; Hole et al., 1991 ; Madsen et Thorkelson, 2006) ; (4) en Californie (Johnson et O'Neil, 1984 ; Fox et al., 1985 ; Cole et Basu, 1995 ; Breitsprecher et al., 2003 ; Cole et Stewart, 2009) ; (5) en Basse Californie (Maury et al., 1996 ; Bourgois et Michaud, 2002 ; Michaud et al., 2006) ; (6) en Amérique Centrale (Johnston et Thorkelson, 1997) ; (7) au niveau de la Péninsule Antarctique (Hole et Larter, 1993) ; (8) dans le bassin de Woodlark (Johnson et al., 1987) ; (9) au niveau du point triple du Chili (Figure. I.15) (Forsythe et al., 1985a,b ; Kaeding et al., 1990 ; Forsythe et Prior, 1992 ; Lagabrielle et al., 1994, 2000 ; Bourgois et al., 1993,1996 ; Guivel et al., 1999, 2003). Les répercussions sur la plaque supérieure sont également importantes au niveau des régions loin de la fosse. En effet, l'ascension de matériel chaud à travers la fenêtre asthénosphérique va induire une interruption du volcanisme calco-alcalin d'arc et remplacé par un magmatisme anormal de type tholéiitique et alcalin de grande ampleur (Forsythe et al., 1986 ; Kay et al., 1993 ; Hole et Larter, 1993 ; Gorring et al., 1997 ; D'Orazio et al., 2001 ; Gorring et Kay, 2001 ; Guivel et al., 2003, 2006 ; Lagabrielle et al., 2004 ; Espinoza et al., 2005, 2008).

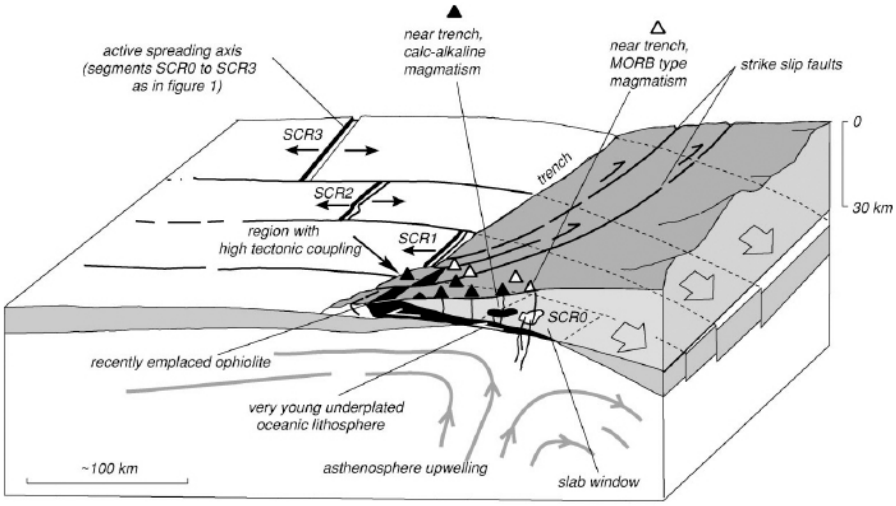

Figure I.15 : Bloc diagramme basé sur la région du point triple du Chili illustrant les effets tectonomagmatiques majeurs en relation avec la subduction d'une dorsale active sous une marge continentale (d'après Lagabrielle et al., 2000).

Du point de vue de la déformation de la plaque supérieure, des perturbations du régime tectonique sont attendues, se caractérisant généralement par des phases d'uplift, et par des phases tectoniques compressives à décrochantes et extensives (Dickinson et Snyder, 1979 ; Tamaki, 1985 ; Farrar and Dixon, 1985 ; Babcock et al., 1992 ; Roeske et al., 1995 ; Rahl et al., 2002 ; Lagabrielle et al., 2004).

L'évolution tectonique de la plaque supérieure et le magmatisme (en partie) seront traités plus en détail dans la suite de ce chapitre au niveau d'anciens exemples d'intéractions dorsale/chaîne de subduction, et dans la suite de ce manuscrit pour ce qui concerne l'exemple actuel de la subduction de la dorsale du Chili.

I.2. Les exemples mondiaux d'interactions dorsale/chaînes de subduction.

Lors de l'évolution des bassins océaniques, les interactions de dorsales actives avec les marges en convergence sont inévitables. L'analyse de la bathymétrie actuelle du bassin Pacifique (Figure. I.16) montre très clairement les interactions actuelles dorsales/zones de subduction :

- au niveau de la Colombie Britannique (NW des Etats-Unis, Canada), où la dorsale Explorer, séparant la plaque océanique Pacifique de la microplaque Explorer, entre en subduction sous la marge canadienne (type RRF) (au nord de l'île de Vancouver) (Hyndman and Lewis, 1999 ; Madsen, 2006).

- le long de la Californie et du Mexique où trois points triples sont connus. Le point triple de Mendecino (TTF) s'est initié à l'Oligocène (Atwater and Stock, 1998) lors de la collision de la dorsale Farallon-Pacifique avec la marge américaine. La configuration dorsale/fosse et la migration du point triple vers le nord auraient induit la formation de la faille de San Andreas (Dickinson et Snyder, 1979). Le point triple de Rivera (RTF), correspond à l'intersection de la plaque Pacifique et de la micro-plaque Rivera avec la plaque Amérique du Nord. Sa formation, à environ 5 Ma, est reliée à l'individualisation de la micro-plaque de Rivera (Bourgois et Michaux, 2002). Ce point triple est caractérisé par une forte instabilité et une migration vers le sud (Johnson et O'Neil, 1984 ; Cole and Basu, 1995; Bourgois et Michaud, 2002). Enfin, le point triple du Mexique (RTF ?), dont la migration vers le sud depuis 12 Ma (Bourgois et Michaud, 2002) correspond à la collision de la dorsale Est-Pacifique avec la marge mexicaine. Sa localisation actuelle, peu contrainte vu l'instabilité du point triple, se situe au sud de la Basse-Californie.

- au niveau de l'Amérique Centrale (au large du Costa-Rica), la faille décrochante de Panama, appartenant au système d'accrétion Cocos-Nazca, passe en subduction (Johnston et Thorkelson, 1997). Dans cette région, l'instabilité et la complexité du point triple de Panama (TFF) rendent l'étude des interactions dorsale/zone de subduction très difficile.

- au sud de l'Amérique du sud, où la dorsale du Chili, passe en subduction sous la marge sud-américaine depuis 15 Ma (Forsythe and Nelson, 1985 ; Cande et Leslie, 1986). Le point triple du Chili (RRF), correspondant à l'intersection des plaques Nazca et Antarctique avec la plaque sud-américaine, a migré vers le nord afin d'atteindre sa position actuelle à la latitude de 46°S. Les différentes caractéristiques de ce contexte unique de segments de dorsale subducté sous une marge continentale seront traitées dans la suite de cette thèse.

- le long de la Péninsule ouest Antarctique où l'interaction de la dorsale Phoenix-Antarctique avec la marge Antarctique se produit entre la fin de l'Oligocène et le Pliocène (Barker et al., 1984 ; Larter and Barker, 1991 ; Eagles et al., 2005 ; Lagabrielle et al., 2009).

- dans la partie ouest du bassin Pacifique, où la dorsale de Woodlark passe en subduction sous un système de micro-plaques océaniques (Nouvelle Bretagne et Salomon du Sud) (Johnson et al., 1987).

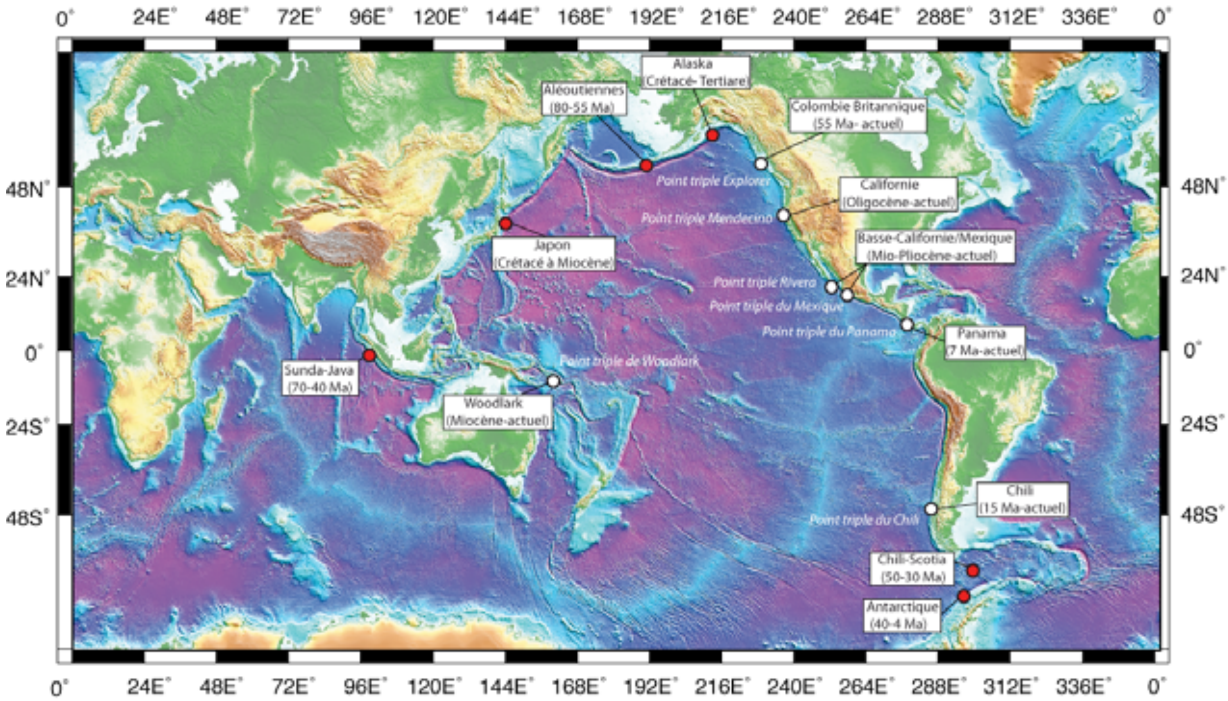

Figure I.16 : Carte topographique et bathymétrique centrée sur le bassin Pacifique illustrant les interactions Dorsale/Fosse passées (point rouge) et actuelles (point blanc). La topographie provient des données GTOPO30 EROS (USGS) et la bathymétrie de Smith et Sandwell (1997).

Les exemples anciens d'interactions entre des dorsales et des chaînes de subduction sont nombreux et divers. La majorité des exemples Cénozoïque étudiés depuis environ 40 ans est répartie autour du Pacifique. Des exemples plus anciens ont été étudiés en Ibérie et au Canada où l'implication de subductions de dorsales au Phanérozoïque a été invoquée (e.g Kusky and Polat, 1999 ; Castro et al., 1996, 1999). Les reconstitutions cinématiques des différentes plaques composant le bassin Pacifique indiquent une multitude d'interactions dorsale/chaînes de subduction depuis environ 140 Ma (Muller et al., 2008), en particulier au niveau des Cordillères nord-américaine, de l'Alaska et du Japon.

I.2.1. Le Japon

Depuis environ 100 Ma, le Japon a connu une série de subductions de dorsales actives dont les principales répercussions ont été étudiées au niveau du prisme d'accrétion Crétacé-

Miocène de Shimanto. La présence de basaltes de type MORB, de laves OIB, de ceintures adakitiques et andésitiques et de roches métamorphiques HT-BP au niveau du prisme de Shimanto impliquent la présence de fenêtres asthénosphériques sous le Japon depuis le Crétacé jusqu'au Miocène (Hibbard et Karig, 1990a ; Osozawa, 1992 ; Iwamori , 2000 ; Kinoshita, 2002). La corrélation entre la localisation de ces séries magmatiques et leur âge de mise en place à permis à Osozowa (1992) de proposer une première reconstitution cinématique basée sur la migration de points triples le long de la marge japonaise (Figure. I.17). L'auteur fait intervenir deux subductions de dorsales orthogonales à environ 50 Ma. La première correspond à la dorsale Kula-Nouvelle Guinée du Nord et caractérisée par une migration vers le nord-est. La seconde séparant la plaque Pacifique de la plaque Nouvelle Guinée du Nord, va migrer vers le sud-ouest.

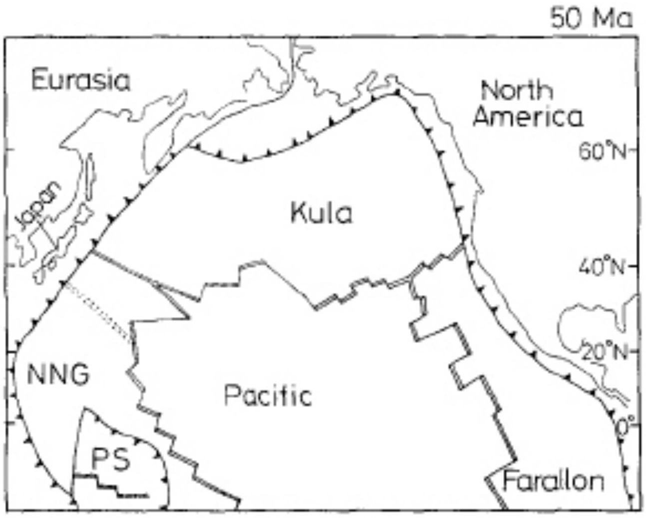

Figure I.17 : Configuration des plaques du Pacifique Nord et position des points triples au niveau du Japon à 50 Ma, basée sur la migration des points triples marqués par la mise en place des basaltes (Osozawa, 1992).

Des reconstitutions cinématiques plus récentes invoquent une configuration différente de celle proposée par Osozowa (1992). En effet, Muller et al., (2008) proposent qu'à environ 55 Ma, un système d'accrétion long de plusieurs milliers de kilomètres et parallèle à la fosse passe en subduction depuis la Chine du Sud jusqu'à la Corée du Nord. Cette configuration implique le développement d'une fenêtre majeure sous l'Asie de l'est à cette époque (Figure. I.18).

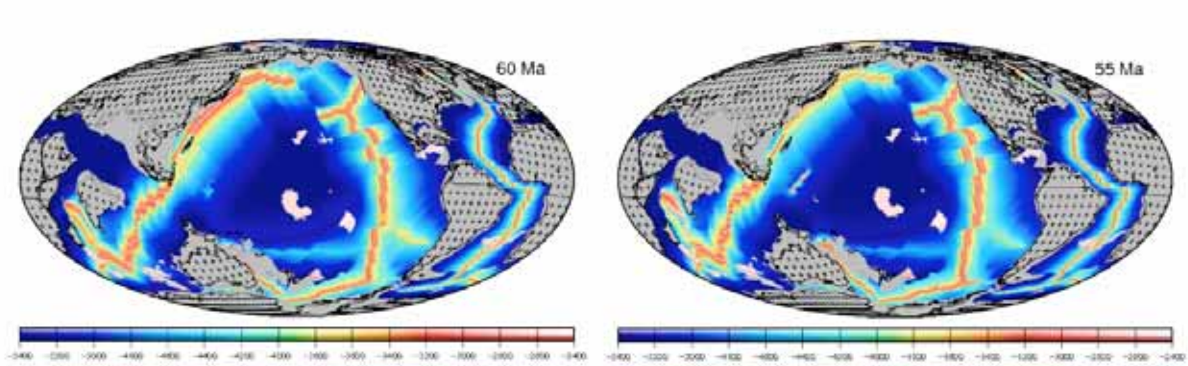

Figure I.18 : Reconstitutions cinématiques des plaques du bassin Pacifique entre 60 et 55 Ma, illustrant la subduction d'un système divergent long de plusieurs milliers de kilomètres sous l'Asie de l'est (d'après Muller et al., 2008).

A l'Oligocène, la région Est du Japon est marquée par la formation du bassin arrière-arc de Shikoku en relation avec la subduction vers le sud-ouest de la plaque Pacifique. L'ouverture de ce bassin arrière-arc se localise principalement au niveau de l'axe d'accrétion de Shikoku dont l'activité a été datée entre 26 et 15 Ma (Hibbard et Karig, 1990a ; Hibbard et Karig, 1990b). Le type et les conséquences de l'interaction de ce bassin arrière-arc avec la marge japonaise ne sont pas encore bien contraints. Toutefois, certains auteurs proposent que la subduction de l'axe d'accrétion de Shikoku vers le nord est responsable d'un uplift important, d'un magmatisme anormal et de changements tectoniques majeurs au niveau de l'avant-arc à environ 15 Ma (Hibbard et Karig, 1990 a,b). Pendant cette même période, l'ouest du Japon connaît une phase d'extension majeure responsable de l'ouverture du bassin arrière-arc de la mer du Japon. Celaya et McCabe (1987) proposent que cette ouverture arrière-arc débute au milieu du Tertiaire suivie au Miocène par une phase d'extension importante responsable des bassins de Yamato et Tsushima. L'accrétion océanique se terminant vers 12 Ma. Les causes de cette extension arrière-arc à l'ouest du Japon sont multiples et discutées à l'heure actuelle. Toutefois certains auteurs proposent, comme Underwood et al., (1993), que l'ouverture de ce bassin serait reliée à la subduction de l'axe d'accrétion de Shikoku. Toutefois, Yamamoto et Hoang, (2009) montrent qu'au début de l'ouverture du bassin du Japon, le point triple formé par cette dorsale avec la marge coulissante japonaise est situé 500 km au sud du Japon (Figure. I.19). A cette époque, le Japon est essentiellement contrôlé par la dynamique de la subduction de la plaque Pacifique.

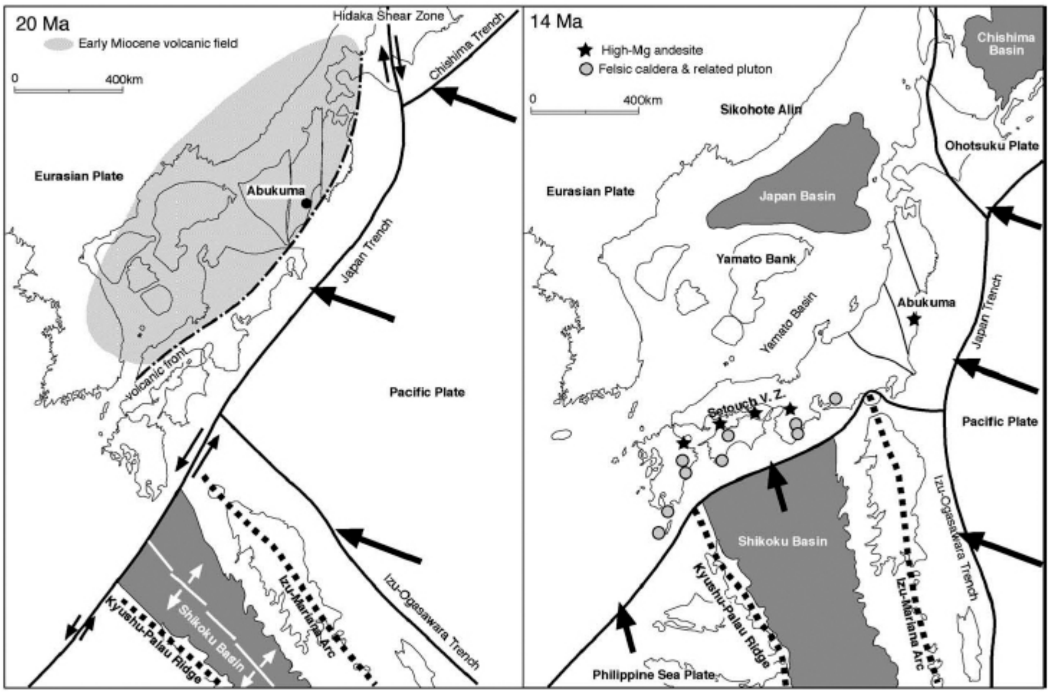

Figure I.19 : Reconstructions cinématiques du bassin de la mer du Japon et du sud est du Japon à 20 Ma et 14 Ma (les flèches indiquent le mouvement des plaques). 1) à 20 Ma, l'ouverture des bassins de Shikoku et de la mer du Japon se poursuivent, tandis que l'axe d'accrétion de Shikoku migre vers le nord-est. 2) à 14 Ma, le Japon et la mer du Japon sont à la jonction de plusieurs complexités géodynamiques perturbant la dynamique mantellique sous cette région (d'après Yamamoto et Hoang, 2009).

A environ 15 Ma, l'axe de la dorsale de Shikoku est en subduction sous la marge japonaise induisant les perturbations géologiques de l'avant-arc précédemment décrites. A cette époque, les régions du Japon et de la mer du Japon sont à la frontière entre plusieurs complexités géodynamiques (Figure. I.19) telles que : (1) la subduction orthogonale de la dorsale de Shikoku, et du développemnt d'une fenêtre asthénosphérique associée (2) la subduction vers l'ouest de la plaque Pacifique (roll-back ?) sous le nord du Japon (3) la subduction vers l'ouest de la plaque Pacifique sous la plaque Philippine portant le bassin-arrière-arc de Shikoku. Cette dernière impliquant la formation d'un point triple particulier avec la fosse japonaise de type Foss-Fosse-Fosse. Ces trois contextes induisent inévitablement des perturbations dans la dynamique du manteau. Finalement, Yamamoto et Hoang, 2009 proposent que l'évolution du bassin arrière-arc de la mer du Japon est liée à un manteau asthénosphérique anormalement chaud, combinaison de plusieurs processus géodynamiques majeurs affectant cette région, dont une fenêtre asthénosphérique.

I.2.2. L'Alaska et l'arc des Aléoutiennes

L'arc des Aléoutiennes et l'Alaska ont été le site de nombreuses subductions de dorsales depuis le Crétacé (Sisson et Palvis, 1993 ; Sisson et al., 2003 ; Muller et al., 2008). Entre environ 80 Ma et 55 Ma, la dorsale séparant la plaque Kula de la plaque Ressurection a migré vers l'est (Madsen et al., 2006 ; Cole and Stewart, 2009) afin d'atteindre la région de Sanak-Baranof induisant le plutonisme Eocène observé au niveau de ces îles (Figure. I.20) (Marshak et Karig, 1977 ; Bol et al., 1992 ; Bradley et al., 2003 ; Cole and Stewart, 2009).

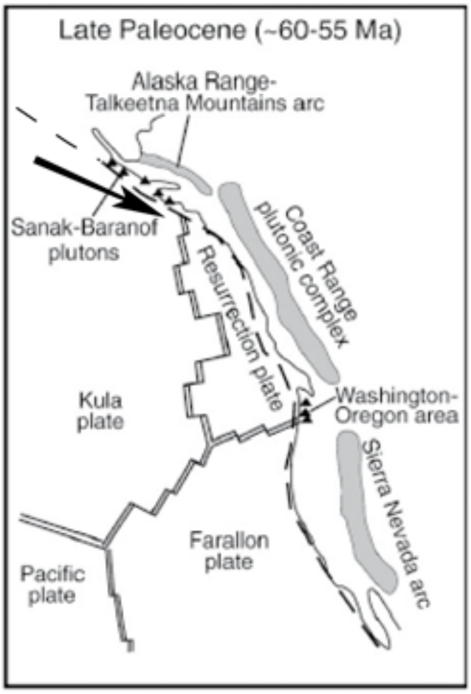

Figure I.20 : Reconstitution cinématique des plaques Kula, Ressurection, Farallon et Pacifique par rapport à la marge nord américaine il y a environ 60 Ma. La dorsale Kula/Ressurection débute sa subduction sous la marge des Aléoutiennes à environ 80 Ma et migre vers le sud est, afin d'atteindre le sud de la région Sanak-Baranof vers 55 Ma. La migration du point triple est indiquée par la flèche noire. Les provinces magmatiques avant-arc et arrière –arc sont également représentées (d'après Cole and Stewart, 2009).

Les études menées au niveau de l'avant-arc accrété à la marge montre une relation temporelle et spatiale entre le magmatisme anormal, le métamorphisme HT-BP et un régime extensif avec le développement d'une fenêtre asthénosphérique sous l'Alaska au Cénozoïque (e.g. Sisson et Palvis, 1993 ; Kusky et al., 2003 ; Bradley et al., 2003 ; Madsen et al., 2006 ; Cole et Stewart, 2009). En ce qui concerne les parties internes de la chaîne, les analyses structurales sont limitées du fait qu'une grande partie de ces régions sont recouvertes par les glaciers. Toutefois, Bradley et al (2003) suggèrent un régime extensif associé à un magmatisme arrière-arc à l'aplomb de la fenêtre asthénosphérique (Figure. I.21).

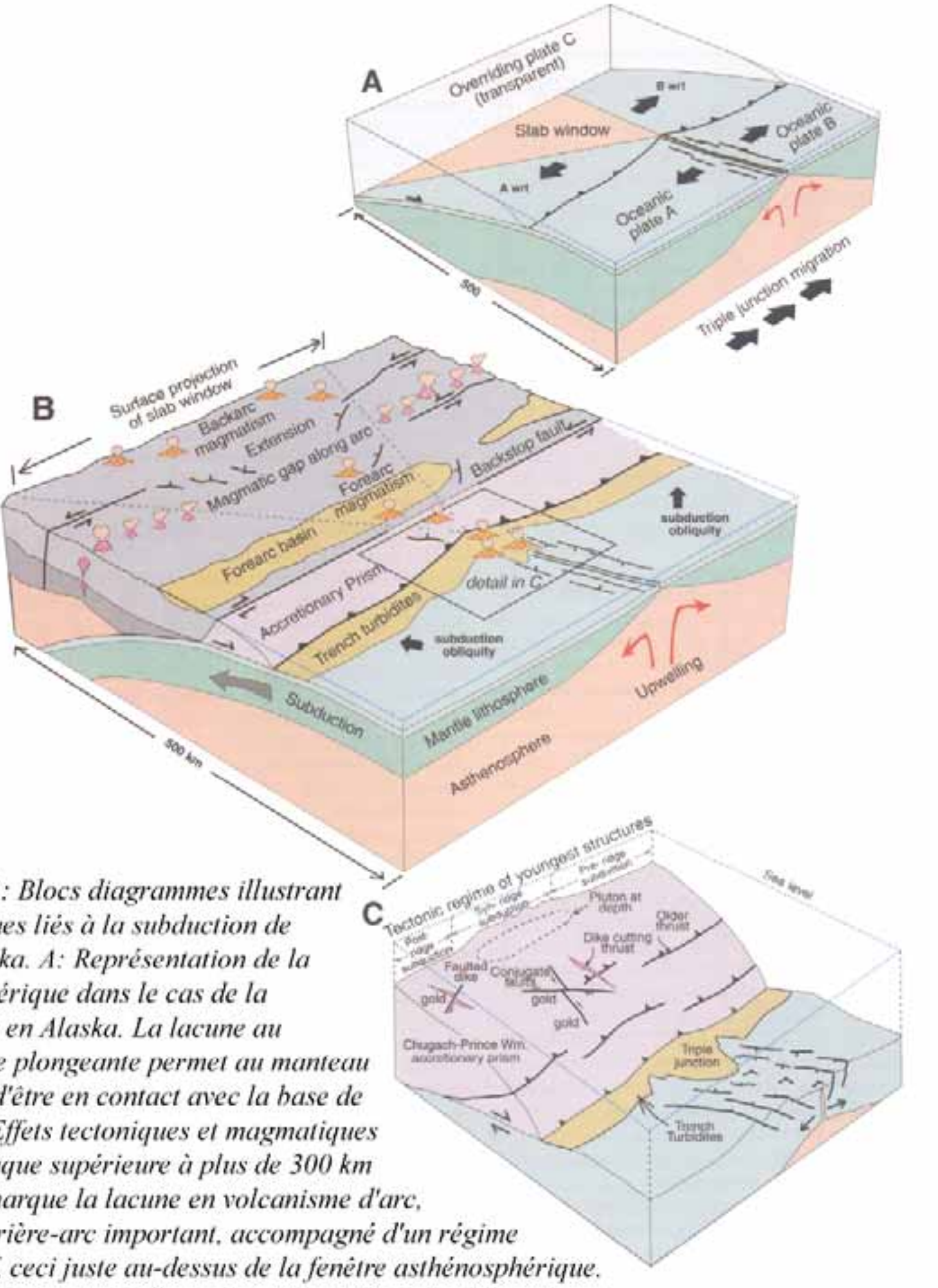

Figure I.21: Blocs diagrammes illustrant les effets géologiques liés à la subduction de dorsale sous l'Alaska. A: Représentation de la fenêtre asthénosphérique dans le cas de la subduction Eocène en Alaska. La lacune au niveau de la plaque plongeante permet au manteau asthénosphérique d'être en contact avec la base de la lithosphère. B: Effets tectoniques et magmatiques au niveau de la plaque supérieure à plus de 300 km de la fosse. On remarque la lacune en volcanisme d'arc, un magmatisme arrière-arc important, accompagné d'un régime tectonique extensif, ceci juste au-dessus de la fenêtre asthénosphérique. C: Effets tectoniques et magmatiques observés au niveau de l'avant-arc, à proximité de l'intearction dorsale active/fosse (d'après Bradley et al. 2003).

L'exemple des Aléoutiennes est très intéressant car il présente, quelques centaines de kilomètres au nord de la fosse, un bassin arrière-arc occupé par la mer de Béring. Le début de l'extension responsable de ce bassin arrière-arc est mal contraint. Cependant, Cooper et al., (1992) suggèrent que les premiers stades d'accrétion océanique s'initient au début de l'Eocène (environ 55 Ma). Les causes géodynamiques de cette extension ne sont pas connues. Toutefois, l'hypothèse d'un roll-back du slab Kula peut être envisagée induisant un régime extensif et un volcanisme arrière-arc au niveau de la plaque supérieure. L'hypothèse d'une fenêtre asthénosphérique est également envisageable. En effet, entre 80 et 60 Ma, la dorsale Kula-Ressurection passe en subduction sous cette région, induisant la formation d'une fenêtre permettant ainsi au manteau asthénosphérique d'interagir avec la lithosphère continentale. De ce fait, les premiers stades d'extension, de type rifting continental, pourraient être mis en relation avec la subduction de la dorsale Kula-Ressurection. La présence de manteau chaud à 100 km de profondeur, observé par tomographie sismique, entre l'arc des aléoutiennes et la mer de Béring plaide en faveur d'une fenêtre asthénosphérique de grande ampleur sous cette région (Levin et al., 2005). Finalement, l'interaction de ces deux phénomènes pourrait induire l'extension polyphasée et le magmatisme alcalin à tholéiitique du domaine arrière-arc des Aléoutiennes.

I.2.3. La Colombie Britannique

Située le long de la marge ouest canadienne, la Colombie Britannique a été sujette à de nombreuses interactions de dorsales en subduction au cours du Cénozoïque. Les reconstitutions cinématiques des plaques Kula, Ressurection, Eshima, Farallon et Pacifique depuis 55 Ma montrent clairement que cette région a été affectée par au moins 5 dorsales (Madsen et al., 2006). A 55 Ma, la dorsale Kula/Ressurection continue sa migration vers l'est pour atteindre l'extrémité ouest du Canada, tandis que la dorsale séparant la plaque Ressurection de la plaque Farallon, plus au sud, migre vers le nord en direction de Vancouver Island (Figue. I.22). Deux fenêtres asthénosphériques composites se développent sous ses régions (Figure. I.22a,). A 39 Ma, pas moins de 4 fenêtres asthénosphériques entre le nord-ouest du Canada et les Cascades (Figure. I.22.b) sont présentes sous la plaque nord-américaine (Kula-Eshamy, Kula-Ressurection, Ressurection-Farallon, Kula-Farallon). Entre l'Oligocène et l'actuel, la subduction de ces dorsales va induire la formation d'une fenêtre asthénosphérique composite de taille importante affectant une majeure partie de l'ouest Canadien (Figure. I.22c). Les répercutions sur l'évolution tectonomagmatique de ces régions vont être importantes. Plusieurs pulses magmatiques alcalins à tholéiitiques, construisant les grandes provinces magmatiques nord américaines, ont été daté entre 60 Ma et l'actuel (Figure. I.23) (e.g. Dickinson et Snyder, 1979 ; Breitsprecher et al., 2003 ; Madsen et al., 2006 ; Cole and Stewart, 2009).

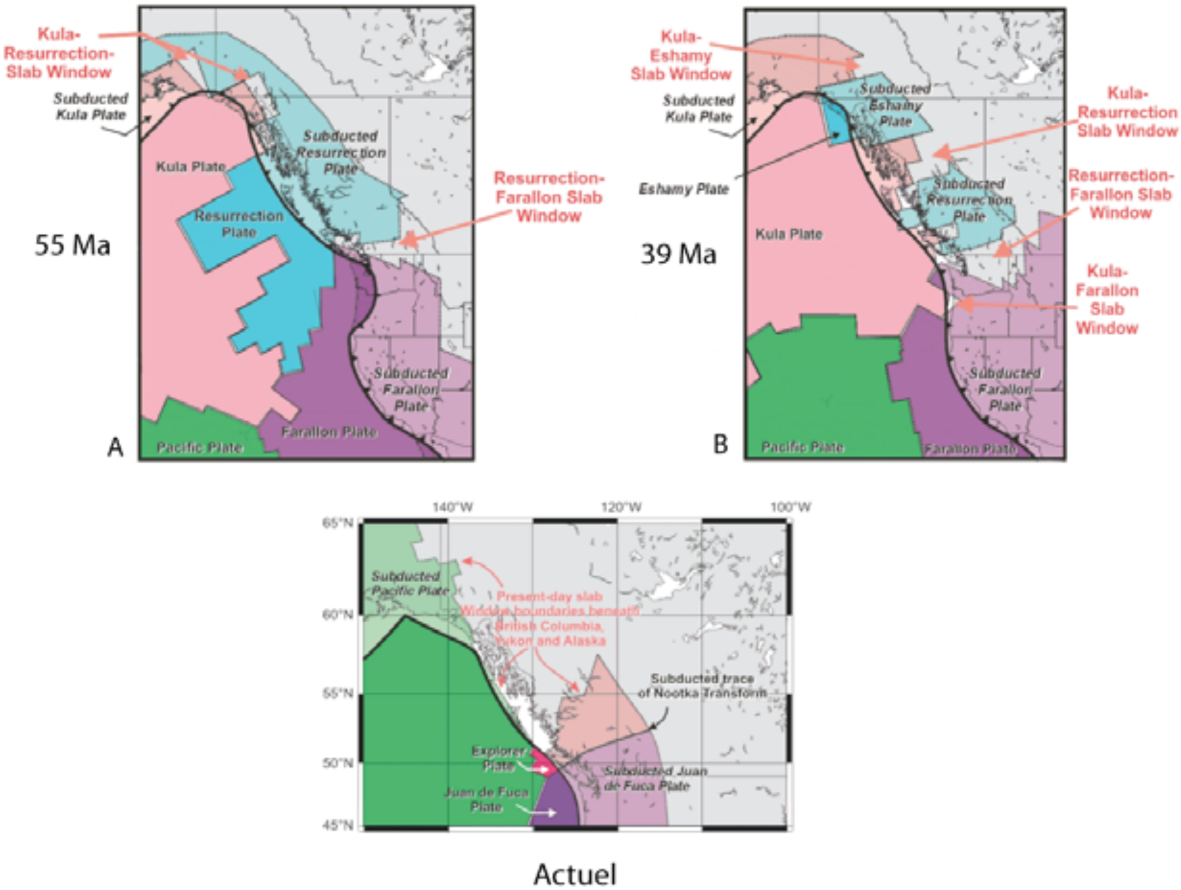

Figure I.22 : Modèle cinématique des plaques constituant le bassin nord-Pacifique, et représentation des fenêtres asthénosphériques successives se développant entre 55 Ma et l'actuel entre l'Alaska et la Colombie Britannique (d'après Madsen et al., 2006). A : à 55 Ma, les dorsales Kula-Ressurection et Ressurection-Farallon intersectent la marge nord-américaine, suivie par le développement de 3 fenêtres asthénosphériques composites. Ces fenêtres seront responsables du magmatisme anormal observé à cette époque entre l'Alaska et l'Orégon. B : La fragmentation de la plaque Ressurection en 2 plaques, Eshamy au nord et Ressurection au sud (à environ 47 Ma) induit la subduction d'une nouvelle dorsale (Eshamy/Ressurection). A 39 Ma, la région nord-américaine est affectée par une multitude de fenêtres asthénosphériques, permettant à du manteau asthénosphérique d'être en contact avec la lithosphère sus-jacente. C : Cette évolution continue jusqu'à l'actuel où la marge américaine est caractérisée par la migration du point triple Explorer. Nous remarquons que l'ensemble du grand nord américain est caractérisé par une lacune de lithosphère océanique subductée. Cette région est marquée par la présence de manteau chaud directement sous la lithosphère continentale (Frederiksen et al., 1998) . Les répercutions sur la plaque supérieure vont être un magmatisme alcalin et tholéiitique important associé à un régime extensif plus ou moins important suivant les régions.

Simultanément, le régime tectonique est perturbé suivant une transition d'un régime compressif à un régime extensif. Le régime extensif est responsable de la formation de dépressions, de pull-aparts, et du développement de Metamorphic Core Complex en Colombie Britannique, au niveau de l'île de Vancouver, dans le Yukon et dans les états de

Washington, d’Orégon et d’Idaho (Figure. I.23) (Coney et al., 1987 ; Wernicke et al., 1987 ; O’Neill et al., 1988 ; Parrish et al., 1988 ; Edwards et Russel, 1999 ; Rahl et al., 2002 ; Madsen et al., 2006). Cette activité tectonomagmatique semble être directement reliée à la remontée de manteau asthénosphérique chaud perturbant la lithosphère continentale sus-jacente (e.g. Hole et al., 1991 ; Madsen et al., 2006 ; Cole and Stewart, 2009). La trace actuelle de la fenêtre asthénosphérique prédite par Madsen et al., (2006) est limitée au nord par la plaque Pacifique et au sud par les plaques Explorer et Juan de Fuca. Ces dernières, en subduction depuis 40 Ma sous l’état de Washington et 20 Ma sous l’île de Vancouver, sont responsables de la subduction des Cascades. Quant à elle, l’anomalie thermique actuelle sous le nord Canada a été mise en évidence par la tomographique sismique (e.g. Frederiksen et al., 1998).

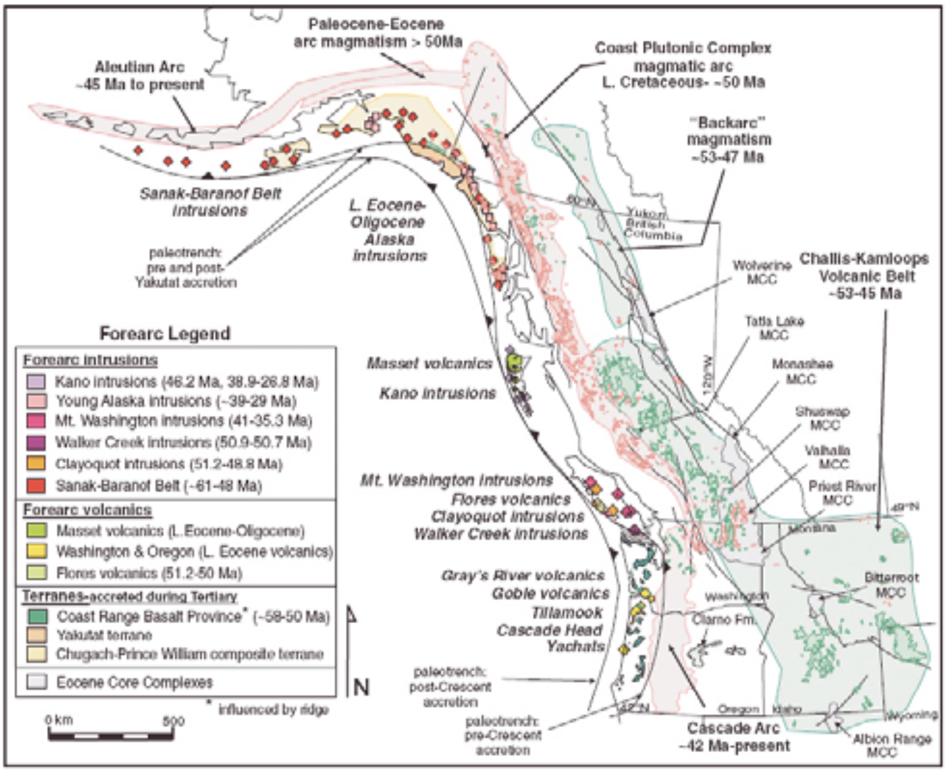

Figure I.23 : Carte simplifiée illustrant le magmatisme d’avant-arc, d’arc et d’arrière-arc entre le Paléogène et l’Oligocène au niveau de la côte nord-ouest nord américaine. Le magmatisme d’arc est représenté en rose et le magmatisme d’arrière-arc en vert clair. Les objets magmatiques de petite taille sont repésentés par des diamants. Cette figure montre également la présence de Metamorphic Core Complex développés au cours de l’Eocène (MCC-Metamorphic Core Complex, gris clair). Les failles majeures sont représentées par un trait noir (d’après Madsen et al., 2006).

I.2.4. La Californie et La Basse Californie

Les premiers travaux impliquant la subduction de dorsale active sous la Californie ont montré qu'au cours de l'Oligocène, l'interaction de la dorsale Farallon-Pacifique avec la marge américaine avait induit la formation de la faille de San Andreas (Dickinson et Snyder, 1979). Leurs travaux proposent qu'après l'interaction Dorsale/Fosse, une région adjacente à la faille était dépourvue de lithosphère océanique plongeante (Figure. I.3). Actuellement, le point triple de Mendecino (TTF) séparant les plaques Juan de Fuca et Pacifique de la plaque nord-américaine se situe à 40°N et se connecte au sud à la faille de San Andreas. L'évolution magmatique, entre 100 et 600 km à l'intérieur de la plaque nord-américaine est variée et complexe (Figure. I.24). Par exemple, elle est caractérisée par un magmatisme précoce calco-alcalin au niveau de l'arc de la Sierra Nevada, passant à un magmatisme tholéiitique à alcalin lors de la subduction de segments de dorsale (Cole et Basu, 1995). Au centre de la Californie, les régions de Santa Maria et des Coast Ranges sont caractérisées par un volcanisme bimodal, daté à 19 Ma, et mis en place lors de la subduction d'un ou plusieurs segments de la dorsale Est-Pacifique pendant cette période (Cole et Basu, 1995).

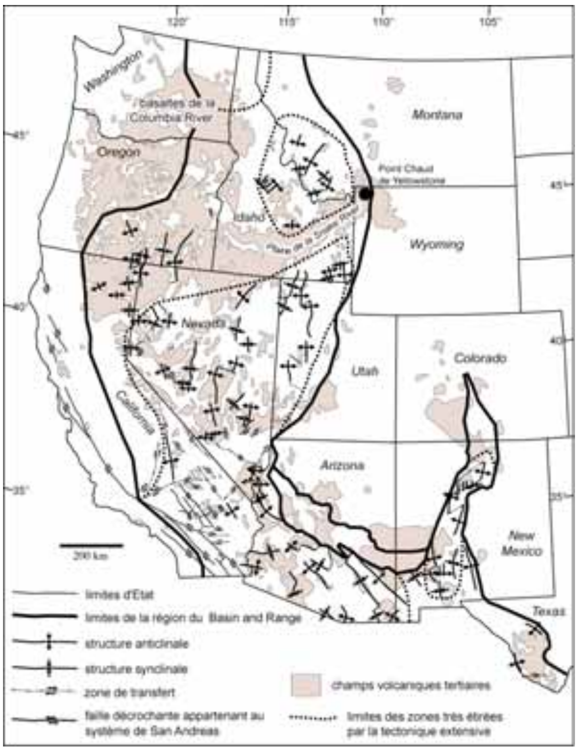

Figure I.24 : Carte simplifiée illustrant les grandes provinces magmatiques Oligocène à actuelle de l'ouest américain. La structure simplifiée et les domaines du Basin and Range et des zones fortement affectées par l'extension sont également représentées (trait noir épais continu et discontinu respectivement).

D’un point de vue tectonique, après une phase compressive responsable de la chaîne des Laramides, plusieurs phases d’extension affectent la plaque supérieure (Wernicke et al., 1987 ; Coney et al., 1987 ; Malavieille, 1987 ; Lerch et al., 2008). La première phase d’extension, datée entre le Paléocène et le Miocène moyen va être responsable de l’extension post-orogénique des Laramides dont les témoins les plus frappant correspondent à la dénudation des Metamorphic Core Complex et à l’extension arrière-arc responsable des premiers stades du Rio Grande Rift (Figure. I.25) (Malavieille et al., 1987 ; Wernicke et al., 1987 ; Thorkelson et al., 2002). Cette phase est reliée, suivant certains auteurs, au roll-back de la plaque Farallon en subduction. La deuxième phase, datée entre le Miocène et l’actuel, affecte le nord du Basin and Range et serait reliée à la migration vers le nord du point triple de Mendocino (Thorkelson et al., 2002). Enfin la troisième phase, induirait entre la fin du Miocène et l’actuel, une extension crustale de la partie sud du Basin and Range et du Rio Grande Rift et de l’uplift du plateau du Colorado (Figure. I.25).

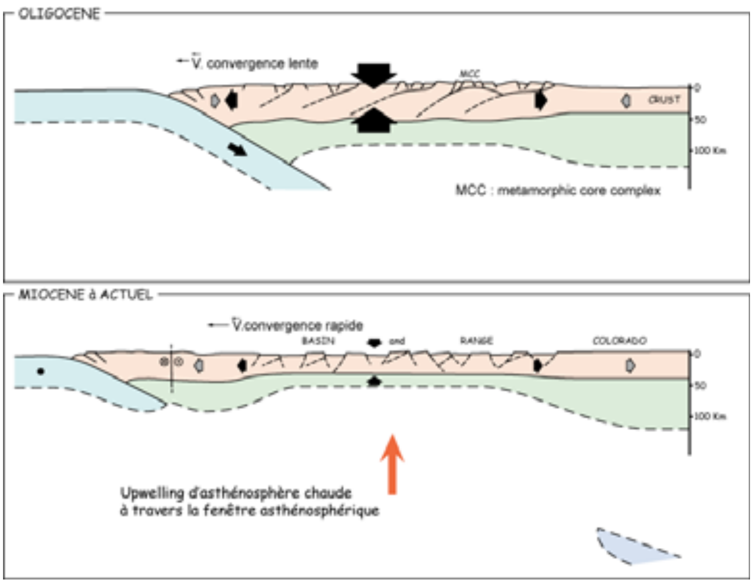

Figure I.25 : Evolution tectonique depuis l’Oligocène à l’actuel de la région du Basin and Range. A l’Oligocène, l’extension induit le développement et la dénudation de Metamorphic Core complex (MCC) repris ensuite par une extension crustale de plus faible ampleur entre le Miocène et l’actuel. La remontée de matériel chaud à travers 2 fenêtres asthénosphériques (Mendecino et Rivera) serait responsable des derniers stades d’extension observées (modifiée d’après Malavielle, 1987).

Thorkelson et al., (2002) met en relation cette dernière phase avec la migration vers le sud du point triple de Rivera et de la fenêtre asthénosphérique associée ; modèle également proposé par Dickinson et Snyder en 1979. Ce point triple très instable, s’est formé il y a environ 5 Ma lors de l'individualisation de la micro-plaque de Rivera par rapport à la plaque Pacifique (Bourgois et Michaud, 2002). Il est clair que la région ouest américaine est constituée de domaines magmato-tectoniques complexes et variés impliquant plusieurs causes géodynamiques. Toutefois, la présence de manteau asthénosphérique chaud sous la plaque supérieure est invoquée pour chacun des exemples (Parsons et al., 1994 ; Liu and Shen, 1998 ; Sass et al., 1999 ; Moucha et al., 2006). De ce fait, l'influence des subductions de dorsales actives depuis l'Oligocène dans cette région est importante même si d'autres facteurs géodynamiques entrent en compte.

Au sud de la Californie, la région de la Basse-Californie a été sujette à la migration vers le sud du point triple du Mexique depuis environ 12 Ma (Figure. I.26) (Bourgois et Michaud, 2002). Le point triple du Mexique correspond à la collision de la dorsale Est-Pacifique avec la marge continentale mexicaine (Figure. I.26). Dans ce cas, Michaud et al., (2006) proposent que la subduction est interrompue à environ 10 Ma, et que l'accrétion à l'axe de la dorsale cesse à environ 7-8 Ma

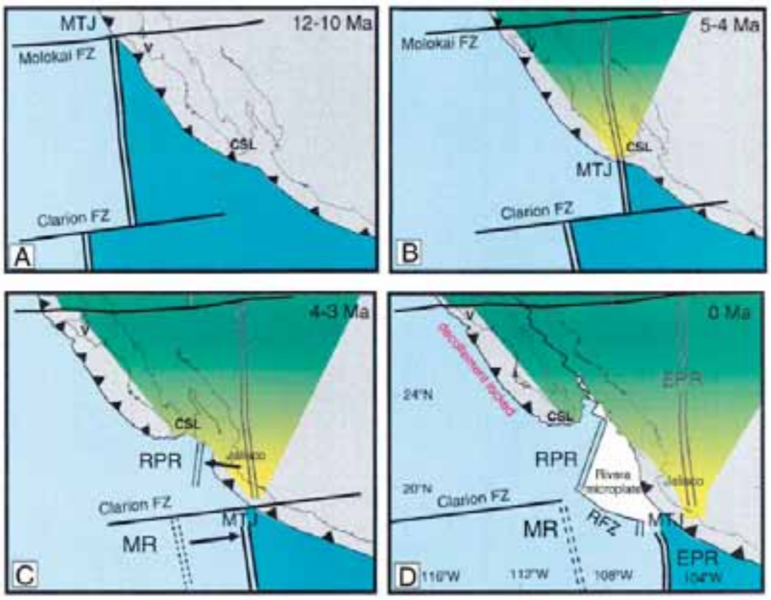

Figure I.26 : Evolution de la configuration des plaques tectoniques au large du Mexique entre 12 Ma et l'actuel. A partir de 4 Ma, la fragmentation de la plaque Pacifique en une nouvelle plaque, la plaque Rivera, va induire la formation d'un point triple se connectant au sud du système de rifting du Golfe de Californie (d'après Bourgois et Michaux, 2002).

Toutefois, les auteurs proposent que l'interaction de la dorsale avec la marge a induit un détachement du panneau plongeant parallèlement à la fosse. L'évolution tectonique de la plaque supérieure est assez complexe. Le rifting continental à l'accrétion océanique observé dans le Golfe de Californie a débuté entre 30 Ma et 20 Ma avec une phase majeure d'extension entre 12 et 6 Ma (Stock et Hodges, 1989). Ce système de rift oblique se connecte au nord à la faille de San Andreas et au sud au point triple de Rivera. Différents modèles ont été proposés afin d'expliquer ce rifting, comme par exemple : (1) des interactions entre les points triples du Mexique et Rivera et leurs fenêtres asthénosphériques associées (Figure. I.27) (e.g. Dickinson et Snyder, 1979 ; Bourgois et Michaud, 2002 ; Michaud et al., 2006) et (2) à un saut de dorsale vers l'est lors de la migration des points triples (Miller, 2002). Le magmatisme dans cette région évolue à partir de 12 Ma. La présence de bajaite indique une interaction majeure avec une croûte océanique très jeune en subduction et dont la signature est proche des adakites (Maury et al., 1996). De plus, cette région est caractérisée par plusieurs pulses magmatiques entre 6 et 3 Ma dont la signature alcaline suggère une source profonde et une relation majeure avec l'extension crustale (Stock et al., 2007).

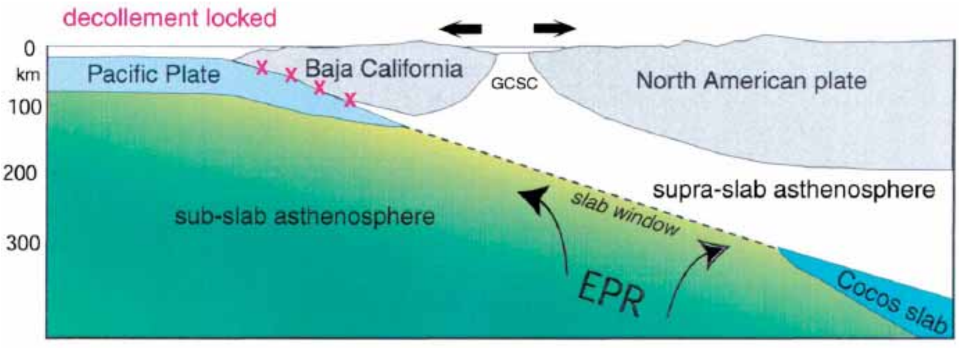

Figure I.27 : Coupe lithosphérique simplifiée de la fenêtre asthénosphérique du Mexique au sud du Golfe de Californie (d'après Bourgois et Michaud, 2002).

A l'est du Golfe du Mexique, la région des Sierras de Madre et de la Mesa Central est caractérisée par plusieurs périodes d'activités magmatiques (Ferrari et al., 2006): (1) à l'Eocène où des andésites et des rhyolites constituent une large province magmatique, (2) entre 32-28 Ma et 24-20 Ma où deux événements siliceux sont responsables de grands épanchements ignimbritiques, (3) après 20 Ma, par une phase de volcanisme transitionnel constituant les provinces basaltiques du sud ouest des Etats-Unis, et (4) entre la fin du Miocène et le Pléistocène, où le volcanisme post-subduction de type alcalin sera dominant. Ces périodes magmatiques sont, à partir de 30 Ma, couplées à des phases d'extension majeures (Ferrari et al., 2006). L'extension débute à l'Oligocène dans les parties est de la chaîne et est contrôlée par des failles à fort pendage. L'extension migre au cours du temps vers l'ouest, et son amplification induit la dénudation de metamorphic core complexes. A la fin du Miocène, l'extension atteint les régions adjacentes au Golfe de Californie. D'un point de vue géodynamique, les répercussions tectono-magmatiques complexes, sont pour les premiers stades, reliées au roll-back de la plaque Farallon (Ferrari et al., 2006 ; Tristan-Gonzalez et al., 2009). L'hypothèse d'un détachement du slab, induisant la présence de manteau chaud sous la plaque supérieure, et lié à la collision de la dorsale Est-Pacifique avec la marge pourrait être responsable des derniers événements tectono-magmatiques enregistrés dans cette région (Storey et al., 1989 ;Ferrari et al., 2006 ; Michaud et al., 2006).

I.2.5. L'Amérique Centrale et le point triple du Panama

Le point triple du Panama correspond à l'intersection des plaques Cocos, Nazca et Caraïbes. La configuration actuelle du point triple est de type RFF (Johnston et Thorkelson, 1997). La dorsale Cocos-Nazca entre en subduction sous le Panama entre 7 et 2 Ma conduisant au développement d'une fenêtre asthénosphérique sous le Panama (Figure. I.28) (Johnston et Thorkelson, 1997). Cette section d'Amérique Centrale est caractérisée par la présence d'andésite, et d'adakites provenant de la fusion de plaques océaniques jeunes et chaudes. De plus, certaines laves du Costa Rica attesteraient de la contamination de type point chaud, dont la source proviendrait de la migration d'asthénosphère enrichie provenant du point chaud des Galapagos, via la fenêtre asthénosphérique (Johnston et Thorkelson, 1997).

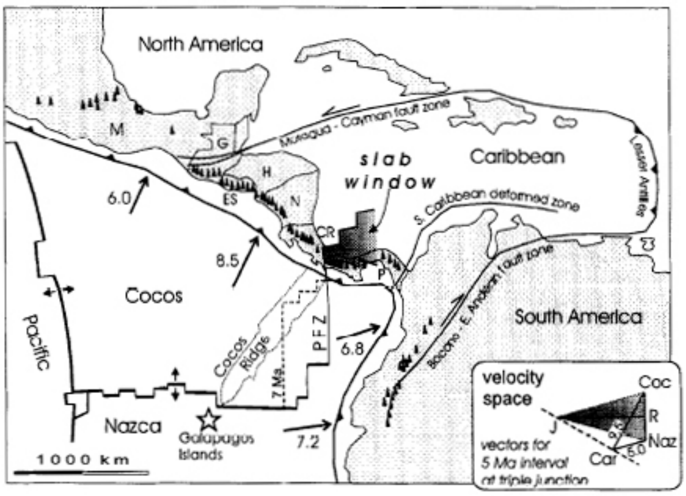

Figure I.28 : Contexte géodynamique de l'Amérique Centrale illustrant la localisation de la fenêtre asthénosphérique qui s'est développée suite à l'interaction du système d'accrétion Cocos-Nazca avec la fosse panaméenne (Johnston et Thorkelson, 1997).

Cette fenêtre explique également l'absence de séismes sous cette région. Au niveau de l'évolution tectonique, l'influence de l'ouverture de la mer des Caraïbes en relation avec la subduction des Caraïbes à l'est est majeure. Aucune donnée ne permet de mettre en relation l'évolution structurale de la plaque supérieure avec la présence de la fenêtre asthénosphérique Cocos-Nazca.

I.2.6. La Péninsule Ouest Antarctique

La Péninsule Antarctique a connu de nombreuses interactions de dorsales actives en subduction (Hole et al., 1991). A l'Eocène, la dorsale séparant la plaque Farallon de la plaque Phoenix a migré vers le sud le long de la marge chilienne pour atteindre à environ 30 Ma la latitude de l'actuelle mer de Scotia. Cette dorsale entre en collision avec la fosse chilienne-antarctique orthogonalement, induisant la formation d'une fenêtre asthénosphérique. Lagabrielle et al., (2009) proposent que cette subduction serait en partie responsable de l'ouverture de la mer de Scotia à partir de 30 Ma. Simultanément, la dorsale séparant la plaque Antarctique de la plaque Phoenix (ou Aluk) subduit sous la marge ouest antarctique (Figure. I. 29).

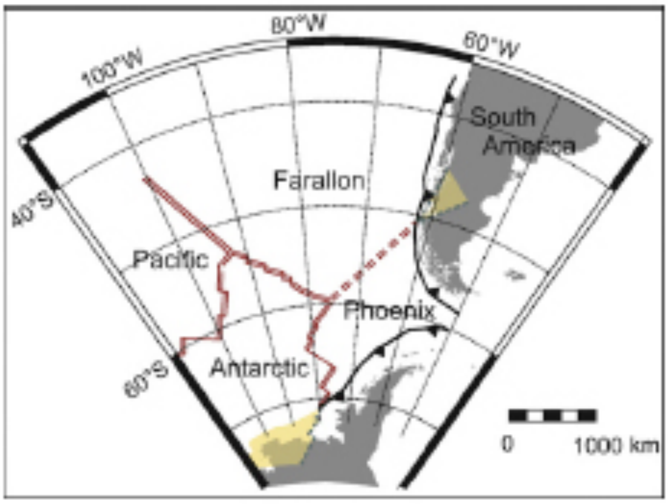

Figure I.29 : Configuration possible des dorsales en subduction sous l'Amérique du Le bassin de Woodlark Phoenix sous la palque Amérique du Sud est contrainte par les données géochimiques d'Espinoza et al., (2005). La fenêtre asthénosphérique migre vers le nord-est jusqu'à 4 Ma (d'après Breitsprecher et Thorkelson, 2008)

Le point triple ainsi formé avec la plaque continentale Antarctique, migre vers le nord-est depuis environ 40 Ma, entrainant un arrêt progressif de la subduction du sud vers le nord. La subduction de la dorsale s'est arrêtée il y a environ 4 Ma au niveau de l'extrémité nord de la péninsule. Les axes d'accrétion sont quasi parallèles à la fosse antarctique induisant ainsi, lors de leur passage sous la marge, une fenêtre asthénosphérique composite (Breitsprecher et

Thorkelson, 2009). A 7 Ma, le volcanisme générale de la péninsule passe d'une signature calco-alcaline à une signature purement alcaline dans une zone située à 200 km de la fosse (Hole, 1988 ; Hole and Larter, 1993 ; Garret and Storey, 1987). L'évolution tectonique depuis la fin du Miocène montre que la Péninsule ouest Antarctique a subi une phase importante d'extension caractérisée par une série de horsts et de grabens et associée au volcanisme alcalin (Figure. I.30) (Baker et al., 1977 ; Saunders et Tarney, 1982 ; Garret et Storey, 1987). L'implication d'une activité asthénosphérique induisant des remontées de manteau chaud à travers la fenêtre asthénosphérique Antarctique/Phoenix semble être responsable de l'activité tectono-magmatique Mio-Pliocène de cette portion de l'Antarctique (Garret and Storey, 1987).

Figure I.30 : Carte des linéaments tectoniques crustaux de la Péninsule Ouest Antarctique, interprétée à partir d'analyses d'images satelittes couplées à des données géophysiques (Garret et Storey, 1987).

I.2.7. Le bassin de Woodlark

Le bassin de Woodlark est situé dans la partie sud-ouest du bassin Pacifique. Il est bordé au nord-est par l'arc des îles Salomon, au nord ouest par la ride de Woodlark et au sud-est par la ride et la fosse de Pocklington (Figure. I.31). La ride de Simbo, correspondant à une faille transformante du système d'accrétion du bassin de Woodlark, entre en collision avec la marge formant ainsi un point triple entre les plaques Pacifique, Salomon et Indo-Australienne. A l'est de la ride de Simbo, la ride de Ghizo serait un axe d'accrétion en subduction (Figure. I. 31).

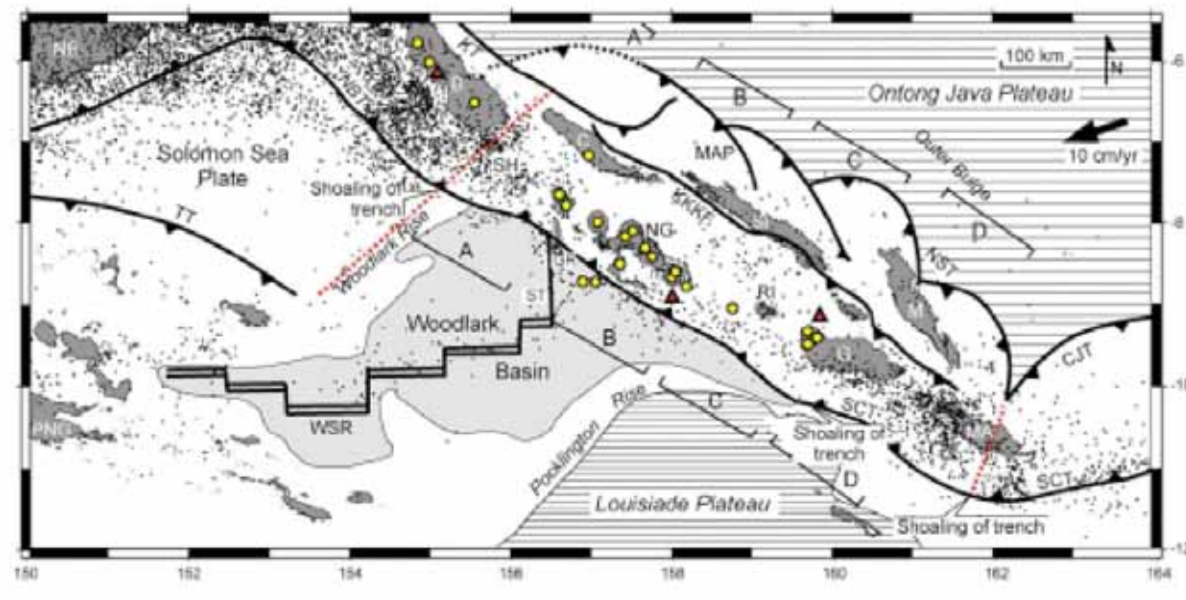

Figure I.31 : Schéma structural simplifié du bassin de Woodlark et de la partie sud-ouest du plateau d'Ontong-Java. A noter la double polarité de la subduction entre les îles Salomon. Les parties émergées sont représentées en gris foncé, le bassin de Woodlark en gris clair et le plateau d'Ontong Java par des traits horizontaux. Les points jaunes indiaquent la position de volcans Plio-Pléistocène et les triangles rouges des volcans dont l'activité est connue historiquement (d'après Mann et Taira, 2004).

La manifestation la plus remarquable de l'interaction entre cet axe et le domaine avant-arc est l'activité volcanique intense formant les îles de Nouvelle-Géorgie. Ces îles sont caractérisées par des laves tholéiitiques, calco-alcalines, alcalines et des MORB. Cette région du bassin ouest Pacifique subit au cours de la fin du Miocène la collision du plateau d'Ontong Java, provoquant l'inversion de polarité de la subduction (Figure. I.31) (e.g . Mann et Taira, 2004). Cette collision majeure entraine une réorganisation importante du régime tectonique de la plaque supérieure, accentuant ainsi la complexité de ce système.

I.2.8. La subduction de Sunda-Java

L'exemple de la subduction de Sunda-Java, impliquant la subduction d'une dorsale active et du développement d'une fenêtre asthénosphérique sous les îles indonésiennes a été mis en évidence par Whittaker et al., (2007) (fig II.32).

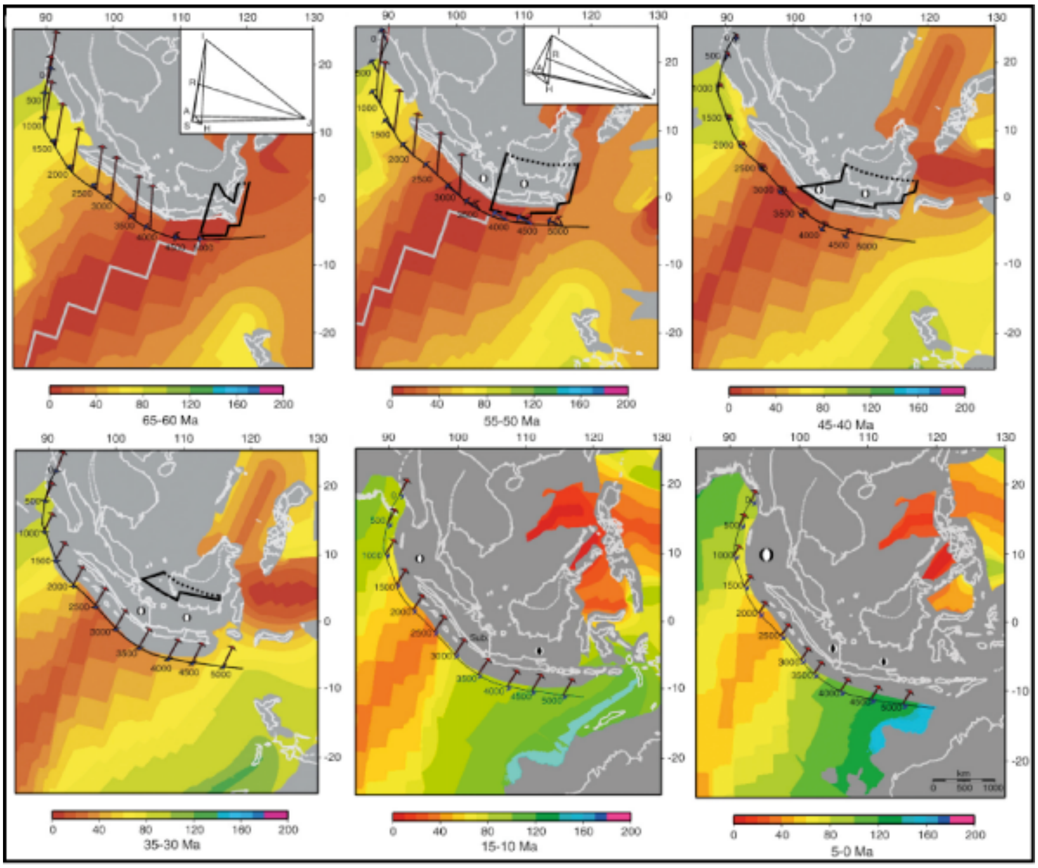

Figure I.32 : Reconstitution cinématique (mouvements absolus) des plaques Sundaland (plaque supérieure) et Indo-Australienne (en subduction) entre 60 ma et l'actuel. La position de la fenêtre asthénosphérique prédite est représentée en trait noir gras. Les mécanismes au foyer indiquent le régime tectonique de la plaque supérieure (d'après Whittaker et al., 2007).

A partir de leurs reconstitutions cinématiques, les auteurs ont montré qu'entre 70 et 40 Ma, l'intersection d'une dorsale avec la marge indonésienne avait abouti à la formation d'un point triple migrant vers le nord-ouest. Cette migration est accompagnée par le développement d'une fenêtre asthénosphérique qui, entre 70 et 40 Ma, a migré vers le nord ouest (Figure. I.32). La superficie de cette fenêtre est importante et la trace prédite par les auteurs s'étend sur plus de 1000 km de la fosse. Ce gap dans la plaque plongeante va être responsable de la remontée de matériel chaud sous la lithosphère indonésienne. Suivant Whittaker et al., (2007), les perturbations mantelliques induiraient le volcanisme particulier daté entre 80 et 40 Ma le long de cette marge, et l'extension arrière-arc du bassin de Java et de l'accrétion océanique du détroit de Makassar entre 60 et 45 Ma (Figure. I.32).

I.2.9. La subduction de la dorsale du Chili

A l'Eocène, la marge sud-chilienne est marquée par la migration vers le sud du point triple formé par les plaques Farallon-Phoenix et sud-américaine (Figure. I.19). Dans la région du lac Général Carrera-Buenos Aires (46°S de latitude), des laves alcalines datées à environ 40 Ma constituant la base d'un plateau volcanique (Meseta Chile Chico) semblent être liées à la subduction de cette dorsale (Espinoza, et al., 2005). La dorsale Farallon/Phoenix, comme nous l'avons vu dans la section II.2.6, a migré jusqu'à la pointe sud de l'Amérique du Sud. A 30 Ma et pendant plusieurs millions d'années, elle passera en subduction sous la future mer de Scotia.

Depuis 15 Ma, la subduction de la dorsale active du Chili est caractérisée par l'enfouissement de plusieurs segments d'accrétion induisant dans la formation d'une fenêtre asthénosphérique de grande ampleur (fig. I.33). Les paramètres cinématiques de cette subduction de dorsale sont bien contraints (Cande et Leslie, 1986 ; Cande et al., 1987). Au nord du point triple du Chili, formé par l'intersection des plaques Nazca, Antarctique et Amérique du sud, la plaque Nazca subduite à la vitesse de 84 mm/an (Cande et Leslie, 1986 ; DeMets et al., 1990). Au sud du point triple, la plaque Antarctique s'enfonce sous la marge sud-américaine à la vitesse de 20 mm/an (Cande et Leslie, 1986 ; DeMets et al., 1990). L'orientation de la dorsale par rapport à la fosse est d'environ 15°, ce qui induit depuis 15 Ma une migration du point triple vers le nord. De ce fait, la fenêtre asthénosphérique associée a affecté toute l'extrémité sud du continent sud américain depuis la Terre de Feu jusqu'à sa position actuelle de 46°S de latitude. Plusieurs particularités dans l'évolution géologique du sud de l'Amérique du Sud sont liées à la subduction de la dorsale du Chili : (1) la surrection rapide puis la subsidence du domaine avant-arc (Bourgois et al., 1992), (2) la mise en place d'un magmatisme avant-arc observé au niveau de la Péninsule de Taitao (Bourgois et al., 1992 ; Guivel et al., 1999 ; Lagabrielle et al., 2000) et associé à l'obduction des ophiolites de Taitao (Lagabrielle et al., 1994), (3) un arrêt du magmatisme d'arc entre 47°S et 49°S (Stern et Kilian, 1996), (4) la mise en place de larges plateaux volcaniques intraplaques à 400 km de la fosse et liés à la subduction de la dorsale du Chili (Ramos et Kay, 1992 ; Gorring et al., 1997 ; Gorring et al., 2003 ; Guivel et al., 2006), (5) une évolution tectonique caractérisée avant la subduction de la dorsale, entre 30 et 15 Ma, par une phase de compression responsable de la surrection de la Patagonie Centrale (Thomson et al., 2001 ; Lagabrielle et al., 2004 ; Blisniuk et al., 2005 ; Guillaume, 2009). L'évolution post-15 Ma étant le sujet de cette thèse, nous y reviendrons dans les chapitres suivants.

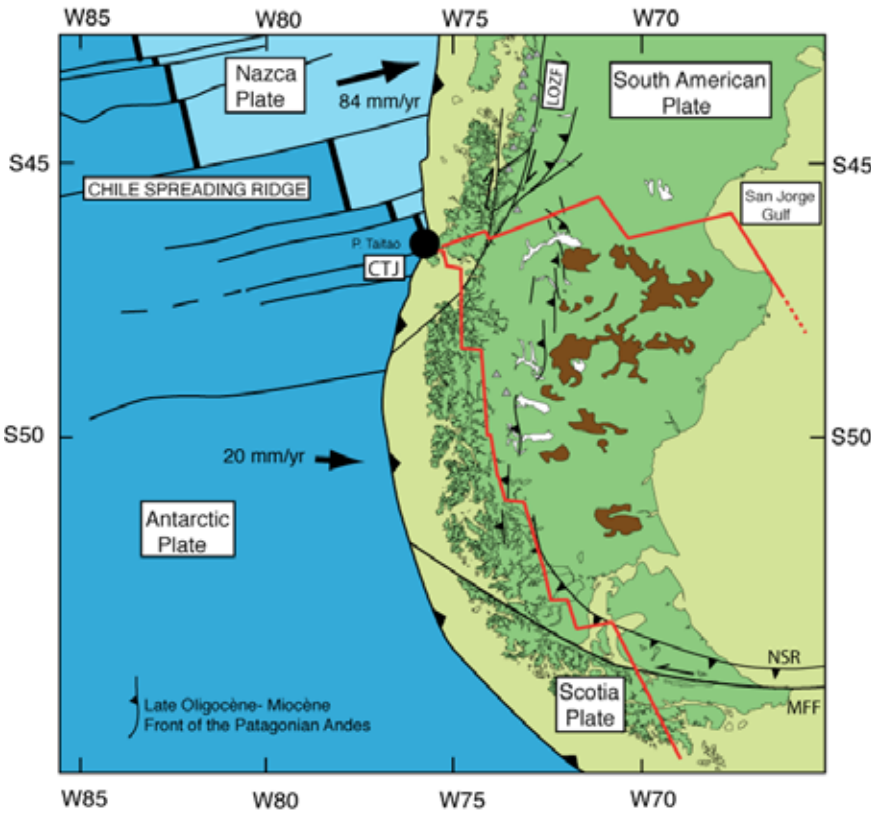

Figure I.33 : Contexte géodynamique de la subduction de la dorsale active du Chili sous la plaque sud-américaine. La position de la fenêtre asthénosphérique sous la Patagonie est représentée en rouge (position prédite par Breitsprecher et Thorkelson, 2008). Les plateaux basaltiques sont représentés en marron. Convergence des plaques océaniques Nazca et Antarctique par rapport à la plaque sud-américaine supposée fixe d'après DeMets et al., 2000.

Chapitre II :

Subduction de la dorsale active du Chili.

Contexte géodynamique général :

Les Andes

et

la Cordillère de Patagonie

II.1. Géodynamique et segmentation morphostructurale des Andes

La Cordillère des Andes est la plus longue chaîne de montagnes actuelle, s'étendant sur plus de 8000 km le long de la bordure occidentale du continent sud-américain et culminant localement à plus de 7000 mètres d'altitude (Aconcagua, Chili). Elle constitue l'exemple type de chaîne de montagnes non-collisionelle, formée le long d'une marge active par la subduction de plusieurs plaques (Nazca et Antarctique) sous la plaque sud-américaine (Figure. II.1). Cette subduction est probablement en place depuis le Jurassique mais les principaux traits morphostructuraux actuels des Andes ont été acquis au cours de l'Oligocène (Isacks, 1988 ; Sempere et al., 1990 ; Allmendinger et al., 1997 ; Lamb et al., 1997 ; Charrier et al., 2002). A cette époque, la convergence entre les plaques accélère et devient plus orthogonale en relation avec la fragmentation de la plaque Farallon en deux plaques distinctes, la plaque Nazca et la plaque Cocos (Pardo-Casas et Molnar, 1987 ; Somoza et al., 1998 ; Londsale, 2005).

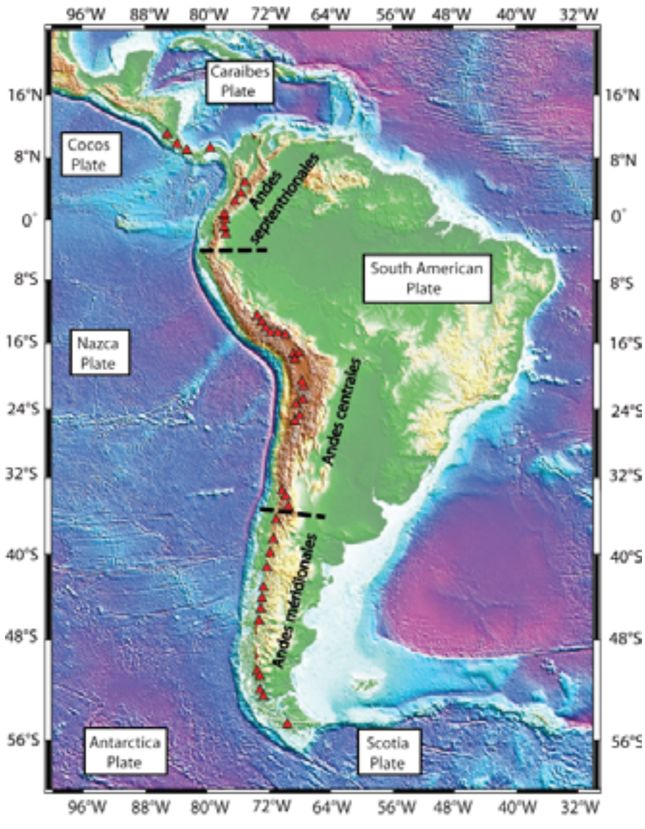

Figure II.1 : Modèle numérique de terrain illustrant la segmentation morphostructurale de la Cordillère des Andes. Les pointillés noirs représentent la séparation des différents domaines (Jordan et al., 1983). Les triangles rouges représentent le volcanisme d'arc actif. La topographie provient des données GTOPO30 (EROS data Center-USGS) et la bathymétrie de Smith and Sandwell (1997).

La Cordillère des Andes est subdivisée en trois grands domaines morphostructuraux (Figure. II.1) définis par Jordan et al., (1983) sur la base de particularités tectoniques et volcaniques représentées sur la figure II.2. Les domaines morphostructuraux sont : lesAndes septentrionales, les Andes centrales et les Andes méridionales. Géographiquement, le volcanisme d'arc actif est observé au sein de quatre zones (Thorpe et al., 1981) (Figure. II.2B): la Zone Volcanique du Nord (ZVN) entre 5°N et 2°S, la Zone Volcanique Centrale (ZVC) entre 16°S et 28°S, la Zone Volcanique du Sud (ZVS) entre 35°S et 46°S et enfin la Zone Volcanique Australe (ZVA) située au sud de 48°S. Leurs principales caractéristiques sont décrites dans les paragraphes suivants.

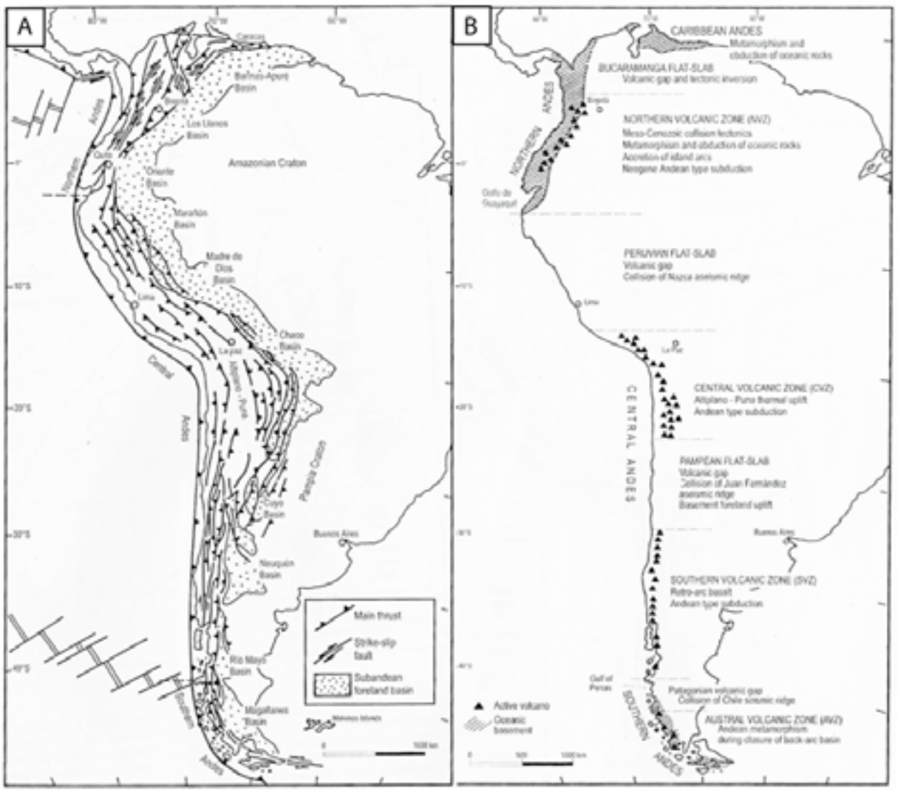

Figure II.2 : A : Caractéristiques structurales majeures de la Cordillère des Andes illustrant également les chevauchements frontaux de la partie orientale de la chaîne. Les parties nord et extrémité sud des Andes sont contrôlées principalement par des décrochements (d'après Ramos, 2000). B : Illustration de la segmentation des provinces volcaniques le long de la Cordillère des Andes et des processus géodynamiques et tectoniques contrôlant ces différents domaines (d'après Ramos, 2000).

II.1.1. Les Andes septentrionales

Les Andes septentrionales s'étendent depuis le Vénézuela à 12°N de latitude jusqu'à la frontière Équateur-Pérou à 4°S de latitude (Golfe de Guayaquil). Dans cette région, la chaîne est caractérisée par une largeur n'excédant pas 500 km. Entre le Mésozoïque et le début du Cénozoïque, les régions des Caraïbes, de la Colombie et de l'Équateur ont été le site de nombreuses accrétions tectoniques de domaines océaniques le long de la proto-marge nord andine induisant des déformations de grande ampleur et un métamorphisme important local le long de décrochements (e.g. Restrepo et Toussaint, 1973 ; Bourgois et al., 1985 ; Mégard, 1987 ; Jaillard et al., 1995 ; Lapierre et al., 1999). Sur plus de 1500 km de long, cette région est caractérisée par la présence de ceintures d'ophiolites et de schistes bleus, témoins de ces diverses collisions. A la fin du Cénozoïque, cette partie des Andes connaît une réorganisation structurale importante. En effet, l'évolution de l'extrémité nord des Andes septentrionales est contrôlée par l'interaction de la plaque Caraïbes avec la plaque sud-américaine et par la subduction plate de Bucaramanga, induisant une inversion tectonique de failles normales préexistantes, suivie par un régime transpressif actuellement actif le long du Vénézuela (Schubert et Vivas, 1993 ; Colleta et al., 1997). La subduction plate de Bucaramanga a également comme conséquence un arrêt du volcanisme d'arc à la fin du Cénozoique au nord de la latitude 5°N (Pennington, 1981 ; Méndez-Fajuri, 1989).

A la suite d'une longue période d'accrétion de domaines océaniques le long de la marge ouest andine, la Colombie et l'Équateur connaissent au cours du Miocène une subduction de type andin. Un magmatisme d'arc se met en place le long de la marge subissant une migration vers l'est au cours du Pliocène (Northern Volcanic Zone, NVZ, Figure II.2B) (Figure. II.3) (e.g. Toussaint et Restrepo, 1982).

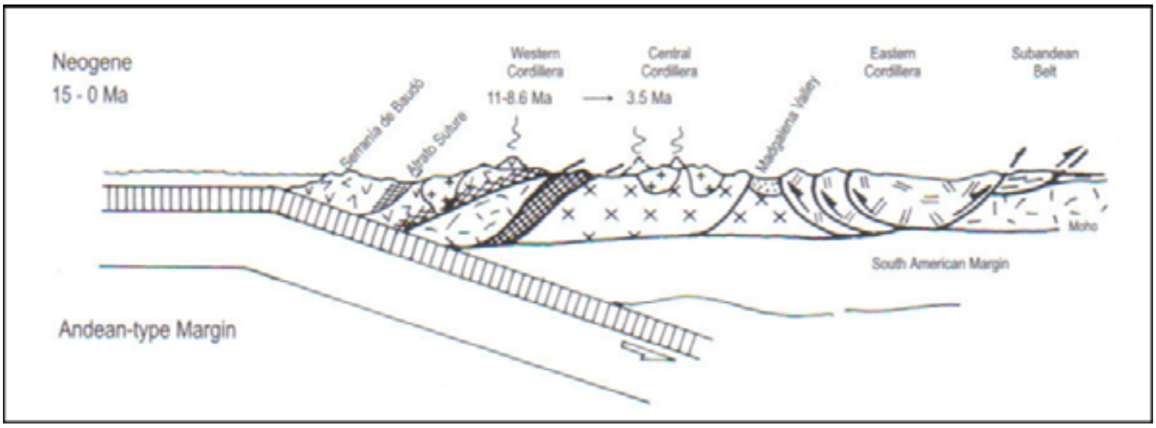

Figure II.3 : Coupe lithosphérique schématique de la Colombie occidentale entre le Miocène et l'actuel illustrant le style structural de cette portion des Andes. Nous remarquons la présence, en noir, d'un domaine correspondant à l'accrétion d'unités océaniques au cours du Jurassique et caractérisé par la présence d'ophiolites et de schistes bleus. Cette figure illustre également la migration du front volcanique vers l'est en relation avec la diminution du pendage de la plaque plongeante. Celle-ci induisant une phase compressive active dans la partie sub-andine de la chaîne (d'après Ramos, 2000).

L'ouverture du Golfe de Guayaquil au cours du Miocène est caractérisée par de nombreux décrochements induisant la formation de bassins en pull-apart (Jaillard et al., 1999). L'initiation de la subduction de la ride de Carnegie sous la marge nord andine à la fin du Miocène a pour conséquence l'inversion de ces bassins (Daly, 1989). Il en résulte également une surrection importante de la région de l'ordre de 0,7 mm/an depuis environ 8-9 Ma, soit plus de 6 km d'uplift et caractérisé par un régime compressif actif à l'aplomb de la ride (Figure. II.4) (Steinmann et al., 1999 ; Gutscher et al., 1999 ; Pedoja et al., 2006), tandis que la migration vers le nord du bloc nord andin induit une extension active importante au niveau du Golfe de Guayaquil (e.g. Witt et al., 2006).

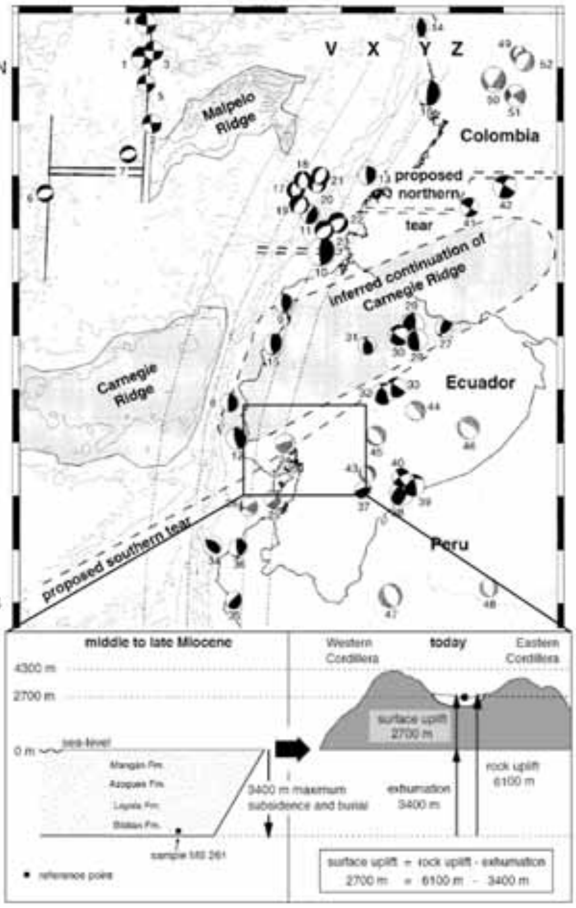

Figure II.4 : Interaction de la ride asismique de Carnegie avec la marge équatorienne. La position de la ride subduite est également représentée. De plus, cette figure illustre la sismicité associée à cette subduction. Nous remarquons que le régime général est de type compressif à décrochant sauf au nord de l'Equateur où un régime extensif est présent (Gutscher et al., 1999). L'encadré noir correspond à la localisation de la zone d'étude de Steinmann et al, (1999). Les auteurs proposent, à partir d'études basées sur la thermochronologie basse-température (traces de fission sur apatites), un uplift d'environ 6 km depuis la fin du Miocène.

II.1.2. Les Andes centrales

Les Andes centrales sont localisées entre le Golfe de Guayaquil (4°N de latitude) et 35°S de latitude. Cette portion des Andes, non affectée par l'accrétion de terrains allochtones, est en grande partie contrôlée par la subduction de la plaque Nazca. Elle a été marquée par différents styles tectoniques avant le début de la subduction de type andin. En effet, au début du Mésozoïque, l'ensemble de la marge est affecté par une extension importante reliée à l'éclatement de la Pangée, suivie par des phases de compression et d'extension à la fin du Mésozoïque en relation avec la subduction de la plaque Nazca.

Les Andes centrales sont caractérisées par une géométrie arquée où localement la largeur de la chaîne atteint plus de 800 km (Bolivie) (Figure. II.5). Ce segment présente également l'un des plus haut plateau du monde, le haut plateau de l'Altiplano-Puna dont l'altitude moyenne est de l'ordre de 4000 mètres, entourés de sommets à plus de 6000 mètres d'altitude (Figure. II.5). Les Andes centrales sont divisées en sous domaines, les Andes centrales du nord (4°N-14°S), les Andes centrales s.s. (14°S-27°S) et les Andes centrales du sud (27°S-35°S) dont les principales caractéristiques sont les suivantes.

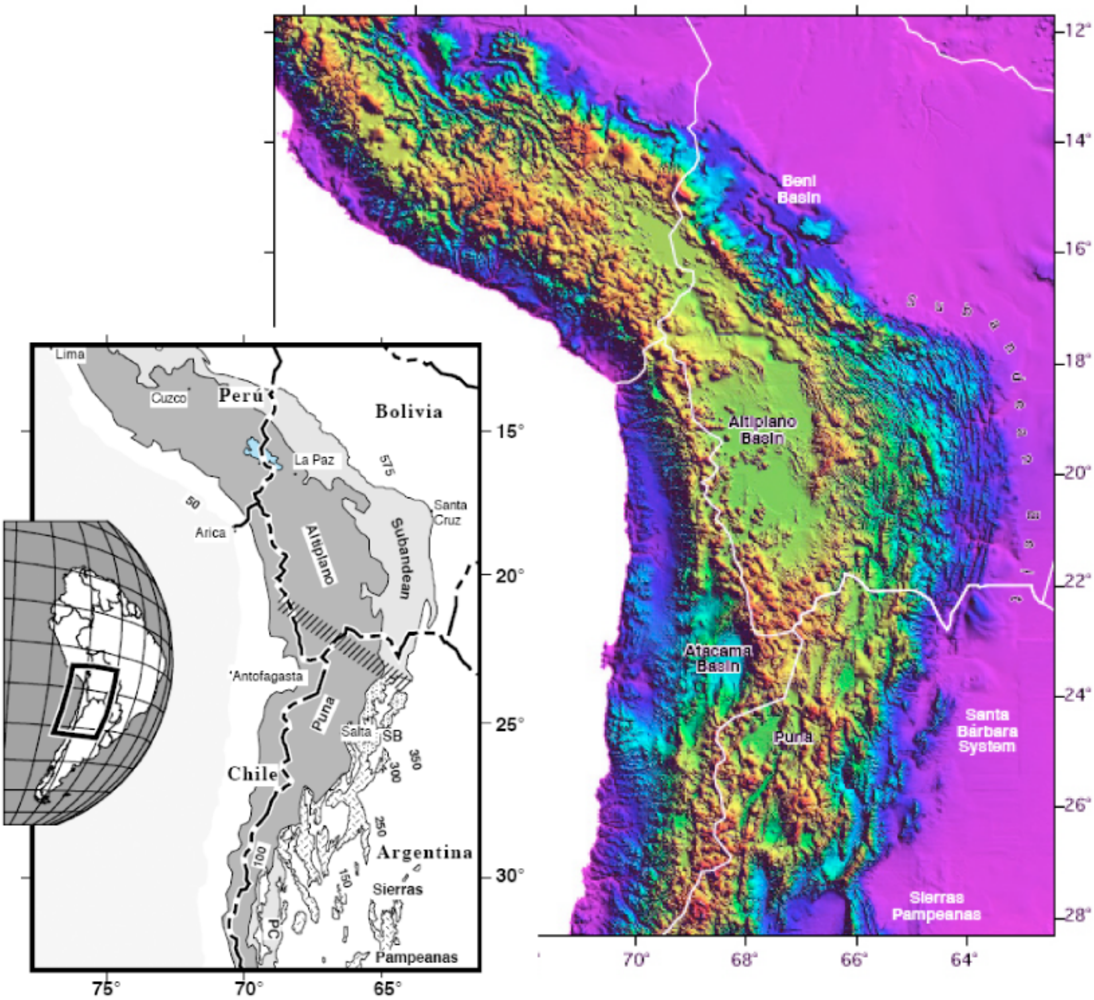

Figure II.5 : Modèle numérique de terrain montrantt le segment des Andes Centrales et plus particulièrement de la région des hauts plateaux de l'Altiplano-Puna, culminant à environ 4000 mètres d'altitude. Les sommets en rouge correspondent à des reliefs dépassant 5000 mètres d'altitude (d'après Allmendinger et al., 1997).

II.1.2.1. Les Andes centrales du nord

Les Andes centrales du nord sont comprises entre le sud de l'Équateur et le Pérou. Mégard (1987) a proposé que cette portion des Andes centrales résulte d'une forte extension au cours du Jurassique puis de phases compressives caractérisées par des inversions tectoniques le long de failles à fort pendage enregistrées entre la fin du Crétacé et le Miocène. La phase Péruvienne à la fin du Crétacé est responsable de la surrection de la Cordillère Ouest (Vicente et al., 1990), la phase Inca entre l'Eocène et l'Oligocène a pour principale conséquence la surrection majeure des Andes péruviennes (Vicente et al., 1979) et la phase Quechua au Miocène induit la surrection et la déformation de la Cordillère Est et du bassin d'avant-pays. Ces 3 phases majeures sont synchrones d'une accélération de la vitesse de convergence des plaques en présence (Amérique du Sud, Farallon, puis Nazca et Cocos) (Pardo-Casas et Molnar, 1987 ; Somoza, 1998). On ne note également une diminution du pendage de la plaque Nazca induisant également une migration du magmatisme d'arc vers l'est (Pilger, 1984). Durant la dernière période de compression au Miocène, la Cordillère ouest péruvienne est marquée par un contexte de subduction plate (Figure. II.6), suivie à la fin du Miocène par la subduction de la ride asismique de Nazca (Sébrier et Soler, 1991). Simultanément, la haute Cordillère de l'Ouest est affectée par la mise en place du batholite de la Cordillère Blanche (13-3 Ma) dont l'exhumation débute à environ 5 Ma (Garver et al., 2003). Cette exhumation rapide s'accompagne d'une forte extension contrôlée par une faille de détachement majeure entre le Pliocène et l'Actuel (e.g. Deverchère, 1988 ; Garver et al., 2003). Tandis qu'à l'est, le domaine plissé de l'avant pays péruvien est en compression. Cette phase d'extension locale est mise en relation avec une instabilité gravitaire liée à la surrection régionale de la haute Cordillère de l'Ouest (Garver et al., 2003).

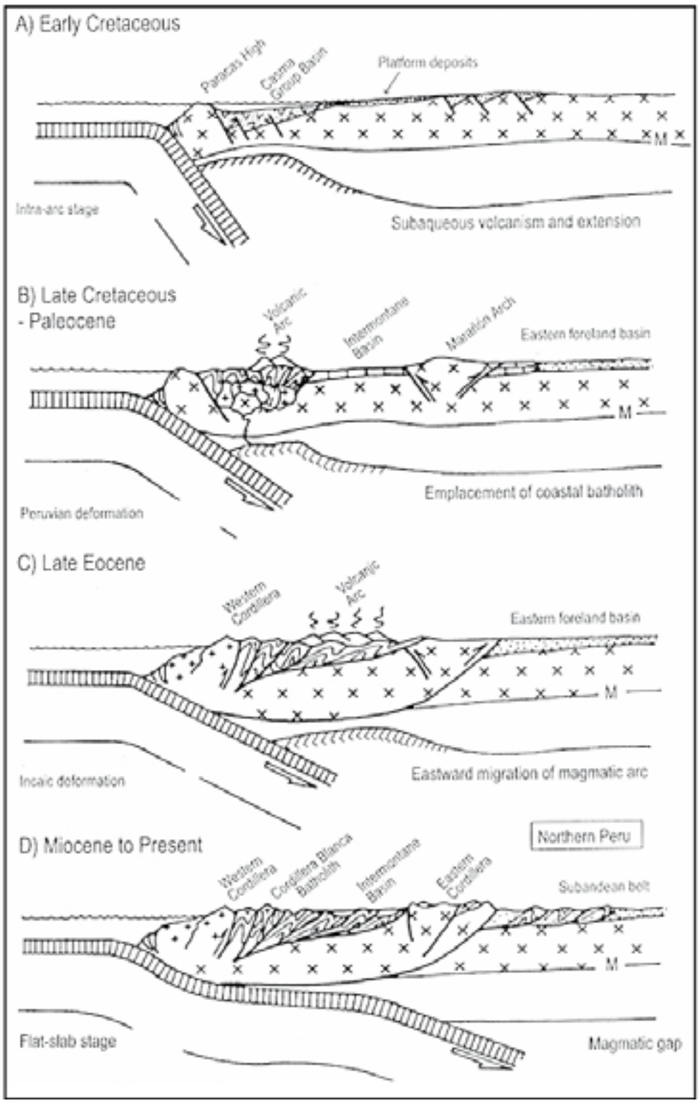

Figure II.6 : Evolution tectonique des Andes centrales du Nord depuis un stade d'extension arrière-arc au début du Crétacé à un stade de régime compressif au cours du Cénozoïque. Nous remarquons au niveau du stade D) que l'extension importante de la Cordillère Blanche n'est pas mentionnée (d'après Ramos, 2000).

II.1.2.2. Les Andes centrales

Les Andes centrales s.s. comprennent le sud du Pérou, la Bolivie, le nord du Chili et le nord-ouest de l'Argentine. Cette partie des Andes centrales est divisée d'ouest en est en sous domaines : la Cordillère Occidentale, la Cordillère Blanche uniquement présente au nord, les hauts plateaux andins de l'Altiplano et de la Puna, la Cordillère Orientale et le domaine Sub-andin (Figure. II.7) (Jordan et al., 1983).

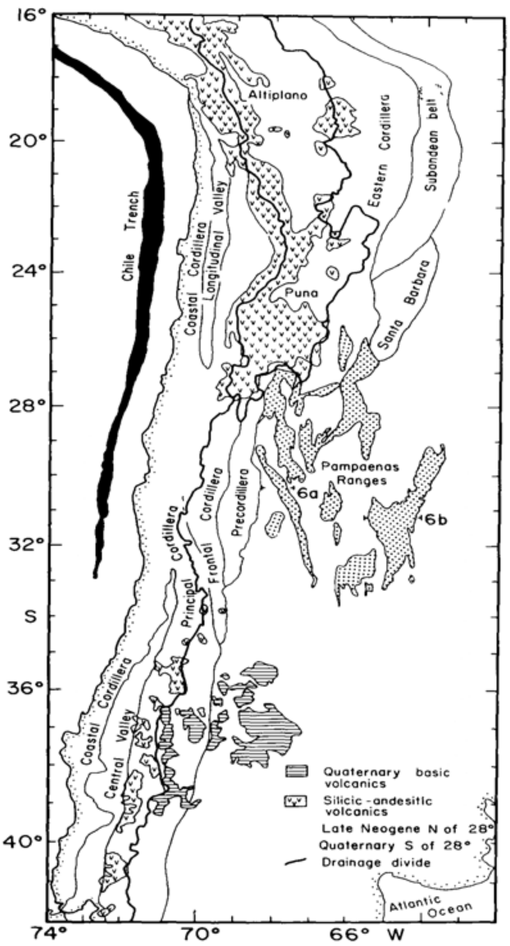

Figure II.7 : Carte des provinces tectoniques et localisation des séries volcaniques récentes des Andes centrales entre la Bolivie, le Chili et l'Argentine (latitudes 16°S et 40°S). Cette carte illustre également le partage des eaux contrôlé par les hauts plateaux de l'Altiplano-Puna (trait noir gras). La limite pacifique correspond à la ligne de crête andine de la frontière ouest des hauts plateaux, tandis que la limite Atlantique correspond à la bordure est des hauts plateaux (d'après Jordan et al., 1983)

Ce segment, comme celui situé plus au nord, est caractérisé par une forte extension au Mésozoïque où un bassin-arrière arc important se développe entre 21°S et 27°S de latitude (Mpodozis et Ramos, 1990). A cette même époque, la forte obliquité de la plaque océanique en subduction par rapport à la marge andine induit le développement du système décrochant d'Atacama, contrôlant l'emplacement du batholite côtier entre le Jurassique et le crétacé le long de la Cordillère côtière (Naranjo et al., 1984). A la fin du Crétacé, ce système est tectoniquement inversé lors de la phase de compression précédemment décrite le long du Pérou (phase péruvienne) (Mpodozis et Ramos, 1990). En ce qui concerne les régions de l'Altiplano et de la Puna, une phase d'extension au cours du Crétacé moyen (Albien) induit la formation de grabens (Salfity, 1994). Ces bassins seront inversés à partir de 25 Ma lors de la phase de compression majeure Quechua (Sempere et al., 1990 ; Allmendinger et al., 1997). Cette phase est synchrone de la fragmentation de la plaque Farallon en 2 plaques, la plaque Cocos et la plaque Nazca, de l'augmentation de la vitesse de convergence de la plaque Nazca par rapport à la marge andine et de la diminution du pendage du slab (Pardo-Casas et Molnar, 1987 ; Somoza, 1998).

Les hauts plateaux de l'Altiplano et de la Puna sont présents sur plus de 1800 km de long, 400 km de large à une altitude moyenne de plus de 3500 mètres d'altitude (Figure II.5). Ils sont situés dans la partie la plus large de la chaîne, dont les parties occidentales et orientales sont contrôlées par un système de chevauchements opposés, caractéristiques d'une structure en pop-up. La surrection de ces plateaux débute à 25 Ma pour l'Altiplano et 15 Ma pour le plateau de la Puna (phase Quechua) (Allmendinger et al., 1997). Ils connaissent une deuxième phase de surrection majeure entre 12-6 Ma et 1-2 Ma respectivement (Allmendinger et al., 1997 ; Coutand et al., 2006 ; Mortimer et al., 2006 ; Strecker et al., 2007) avec des taux de surrection de l'ordre de 0,2 à 0,3 mm/an (Grégory-Wodzicki, 2000) et un raccourcissement maximal de 320 km (Kley et al., 1999). Les causes de la surrection de ces hauts plateaux sont encore débattues mais certains auteurs proposent une combinaison entre un raccourcissement horizontal important accompagné d'environ 20 à 30% de sous-placage magmatique (e.g. Allmendinger et al., 1997). Ces deux processus induisent un épaississement crustal très significatif pour une chaîne de subduction, dont les valeurs varient entre 70 km à 80 km d'épaisseur (Zandt et al., 1994 ; Beck et al., 1996). Plus récemment, Garzione et al., (2006) proposent qu'un processus de délamination lithosphérique soit responsable des derniers stades de surrection des hauts plateaux andins. Pendant la surrection de l'Altiplano, la déformation compressive migre vers l'est depuis la Cordillère Orientale vers le système sub-andin où une proto-chaîne se met en place (Figure II.8). Celle-ci est accompagnée par la subduction continentale vers l'ouest du bouclier brésilien débutant au Miocène et dont les effets sont majeurs sur la surrection de la chaîne occidentale (Figure II.8). En ce qui concerne le volcanisme, cette région est caractérisée par un arc magmatique large depuis le Néogène lié à des variations de pendage du slab (Central Volcanic Zone, CVZ, Figure II.2). Par exemple, entre 17 et 12 Ma, des marques de volcanisme calco-alcalin sont observées à l'est de l'Altiplano associées à une diminution du pendage de la plaque Nazca en subduction (Kay et al., 1999).Tandis qu'entre 12 et 3 Ma, d'importants épanchements ignimbritiques sont observés. Leur migration vers l'ouest indique une augmentation légère du pendage de la subduction (Kay et al., 1999).

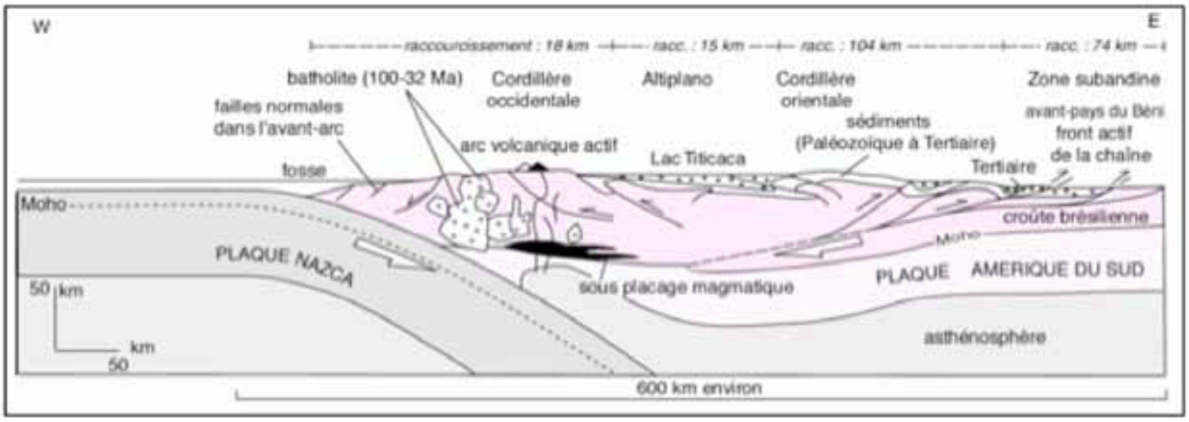

Figure II.8 : Coupe lithosphérique de la subduction andine au niveau de la transversale des Andes Centrales (latitude des hauts plateaux boliviens). Cette figure illustre le contrôle de la surrection des hauts plateaux par le raccourcissement et par le sous-placage magmatique. Nous remarquons également la propagation de la déformation de la déformation compressive vers l'est caractérisée par une série de chevauchements (tectonique de type thin-skinned) affectant la zone sub-andine (extrait d'Elément de Géologie, 13ème édition, Lagabrielle, Pomerol, Renard, Edition Dunod)..

L'évolution tectonique récente de cette portion majeure des Andes centrales est caractérisée par la propagation vers l'est de la déformation au niveau du bassin d'avant-pays du système sub-andin et par la réactivation hors-séquence des chevauchements de l'Altiplano-Puna et de la Cordillère Orientale (Ramos, 2000). Actuellement, les bordures nord et sud des hauts plateaux andins sont affectées par une tectonique extensive (e.g. Sébrier et al., 1985 ; Allmendinger et al., 1997). Ce système évoque la possibilité d'un fluage crustal vers le nord et le sud sous le segment central (e.g. Gerbault et al., 2002) Il est à noter également que la formation de ces hauts plateaux a une influence majeure sur le climat de cette portion des Andes, induisant une organisation asymétrique W-E des précipitations (Strecker et al., 2007).

II.1.2.3. Les Andes centrales du sud

Les Andes centrales du sud s'étendent entre 27°S et 35°s de latitude entre le Chili et l'Argentine. Ce segment est constitué d'ouest en est de : la Cordillère Côtière, la Dépression Centrale, la Cordillère Principale, la Cordillère Frontale , le bassin d'avant pays et localement les Sierras Pampeanas (Figure. II.7) (Jordan et al., 1983). Comme observé précédemment au niveau des segments morphostructuraux situés plus au nord, les Andes centrales du sud ont connu une phase d'extension majeure au début du Mésozoïque, caractérisée par l'ouverture d'un bassin marginal à environ 300 km de la fosse. Ce bassin a été progressivement rempli par des séquences volcano-clastiques (Charrier, 1984). L'extension mésozoïque est contrôlée par des failles normales à faible pendage à l'ouest du domaine (27°S, Mpodozis et Allmendinger, 1993) tandis que la partie est de la chaîne montre des failles normales à fort pendage. L'extension se termine au Crétacé en relation avec une réorganisation des plaques en présence (Mpodozis et Ramos, 1990). L'arc magmatique est présent entre le Jurassique et le Paléogène. De nombreux auteurs ont montré que l'érosion tectonique de la marge andine est responsable de la migration vers l'est du front magmatique (Ramos, 1988 ; Stern, 1991). Au niveau de la Cordillère Principale située au centre du Chili, une phase d'extension datée entre 36 Ma et la fin de l'Oligocène est responsable de la formation de bassins. Cette extension est reliée par Charrier et al., (2002) à un taux de convergence de la plaque Nazca assez faible. Ces bassins extensifs sont ensuite inversés à partir de 21 Ma, en relation avec une phase de déformation compressive liée à l'augmentation du taux de convergence de la plaque Nazca (Charrier et al., 2002). Pendant cette période, une transgression marine majeure, la transgression Paranense, envahit une majeure partie du bassin flexural andin du côté amazonien dont plusieurs témoins sont observables en Argentine, dans la Cordillère Principale et également en Bolivie avec des épaisseurs de sédiments dépassant 4000 mètres (e.g. Ramos 2000). Simultanément, le volcanisme d'arc migre rapidement vers l'est, en relation avec une diminution du pendage de la plaque plongeante (Jordan et al., 1983). L'entrée en subduction de la ride asismique Juan Fernandez à partir de 15 Ma induit également des perturbations dans le régime tectono-magmatique de la plaque supérieure. En effet, sur la transversale de Santiago du Chili, une phase de surrection rapide de la Cordillère côtière a été datée entre 10.5 Ma et 4.6- 2 Ma et directement mis en relation avec la subduction plate de la plaque Nazca et de la subduction de la ride de Juan Fernandez (Farias et al., 2008). Cette subduction provoque également un arrêt du volcanisme d'arc entre 7 et 4 Ma puis une migration importante vers l'est de l'arc magmatique actif Quaternaire dont les principaux volcans sont situés à plus de 700 km de la fosse (Kay et al., 1991). Elle est également responsable d'une forte activité sismique au niveau de la Pré-Cordillère andine et des Sierras Pampeanas (Figure II.9), où une surrection majeure est observée depuis 3 Ma (Zapata et Allmendinger, 1996 ; Giambiagi et al., 2003). L'origine de la vallée Centrale pose des problèmes structuraux. En effet, des observations récentes de sismicité et de tectonique permettent d'avancer qu'une faille inverse à pendage est contrôle les reliefs de cette région (Farias et al., 2008 ; Armijo et al., soumis). Finalement, les Andes centrales du sud se caractérisent globalement par un raccourcissement total de l'ordre de 140 à 160 km (Introcaso et al., 1992) et dont le style tectonique est contrôlé par à une déformation composite dominée par un type thick-skinned, caractérisée par l'inversion de failles normales préexistantes depuis l'Oligocène (Godoy et al., 1999 ; Charrier et al., 2002).

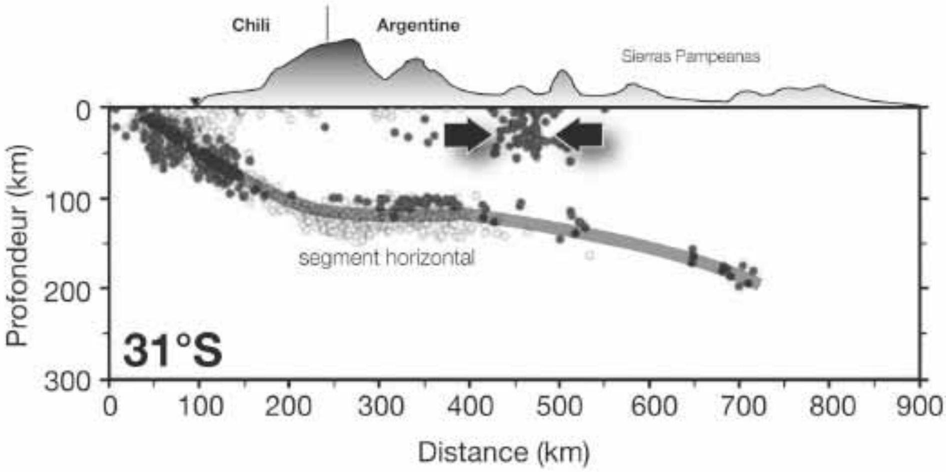

Figure II.9 : Coupe verticale de la sismicité enregistrée sur un profil localisé à la latitude de 31°S (d'après Pardo et al., 2002). Suite à la subduction de la ride Juan Fernandez, le slab a tendance à s'horizontaliser. A l'avant de ce segment plat se développe une forte sismicité crustale, témoignant de la transmission des contraintes vers l'avant-pays au niveau des Sierra Pampeanas, impliquant le socle dans les chevauchements (cas de tectonique de type thick-skinned).

II.1.3. Les Andes méridionales

Les Andes méridionales ou Cordillère de Patagonie se situent entre 35°S et 55°S de latitude (latitude de la Terre de Feu) (Figure II.10). La morphologie de ce segment des Andes est très différente des précédents segments. En effet, la topographie générale décroit progressivement du nord vers le sud depuis des sommets à environ 3500 mètres d'altitude jusqu'à des reliefs de faible altitude (en moyenne environ 1000 mètres) ponctués de quelques hauts sommets (Mt San Valentin, 4058 m ; Mt San Lorenzo, 3608 m ; Fitz Roy, 3405m). La morphologie de la marge est très morcelée contrairement aux segments situés plus au nord. Cette caractéristique est observée depuis le nord de l'île de Chiloé jusqu'à la Terre de Feu (Figure II. 10). Les différentes unités morphostructurales sont les suivantes. Entre 35°S et 42°S et d'ouest en est, la cordillère se divise en une Cordillère Côtière, une Dépression Centrale, une Cordillère Principale une zone Sub-Andine et localement le plateau de Somuncara. Au sud du point triple du Chili, localisé à 46°12'S, la Cordillère est carcatérisée par la Cordillère de Patagonie (massifs Northern and Southern Ice Cap), le massif de Deseado à l'est et la Cordillère de Darwin au sud dont l'orientation générale est NO-SE (Figure II.10).

La segmentation ouest-est dans cette partie des Andes méridionales n'est pas présente. Une des particularités majeure de ce segment situé entre le point triple du Chili et la Terre de feu est la présence de dépressions transverses à la chaîne, occupées actuellement par des lacs post-glaciaires.

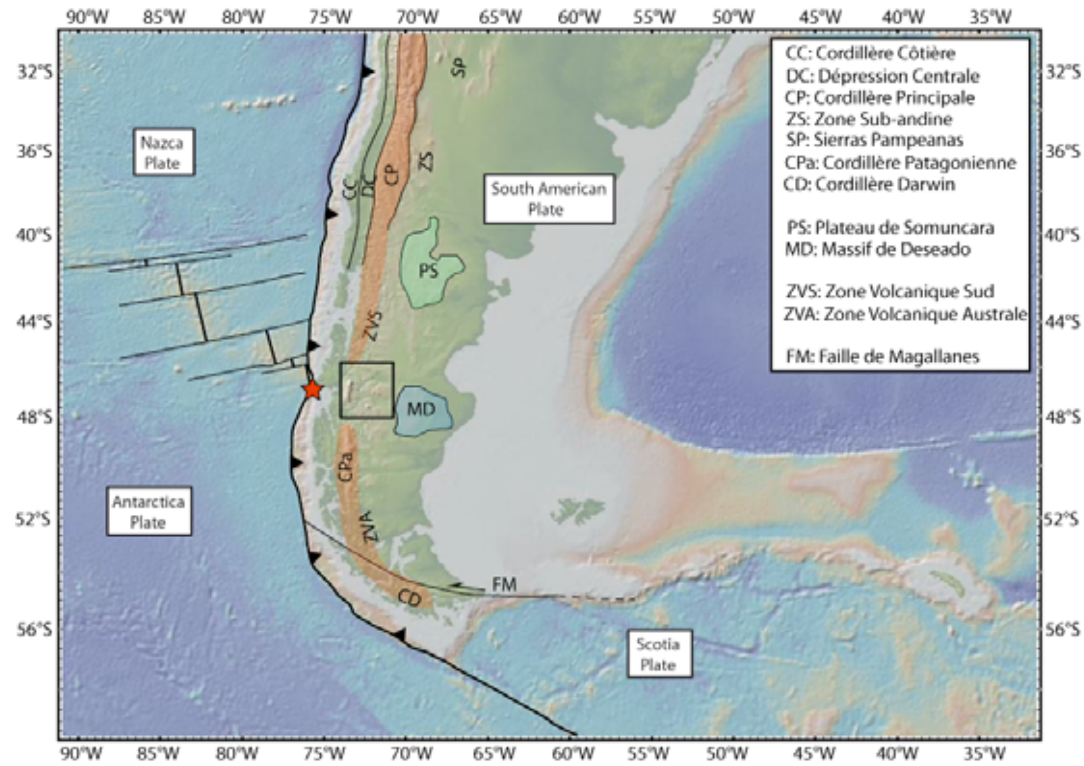

Figure II.10 : Unités morphostructurales des Andes méridionales. Les principales provinces volcaniques sont représentées en orange. Nous remarquons qu'à la latitude du point du Chili, une lacune en volcanisme d'arc est présente, en relation avec la subduction de la dorsale du Chili. L'encadré noir correspond à notre zone d'étude, décrite dans la suite de cette thèse.

Dans cette partie, nous nous intéressons aux segments situés entre 35°S et 45°S et entre 50°S et 55°S de latitude. L'évolution tectono-magmatique de la Patagonie Centrale (45°S-48°S), qui fait l'objet de ce mémoire, est abordée avec plus de détail dans la partie II.2 de ce chapitre.

II.1.3.1. La Patagonie du nord

La Patagonie du nord est située entre les latitudes 35°S et 45°S Cette région a connu au cours du Mésozoïque une phase d'extension majeure, comparable à celle décrite au niveau des segments situés plus au nord. Cette phase d'extension est suivie au Crétacé supérieur par une phase de raccourcissement très bien observée au niveau de la Cordillère Principale, caractérisée par l'inversion de failles normales mésozoïques (e.g. Cobbold et Rossello, 2003 ; Ramos et Folguera, 2005). Plus à l'est, au niveau du bassin de Neuquén, la déformation du socle et de la couverture sédimentaire accommode l'essentiel des 45 à 55 km de raccourcissement enregistrés dans cette région entre le Crétacé supérieur et l'Eocène (Introcaso et al., 1992 ; Ramos, 1999 ; Cobbold et Rossello, 2003). A cette époque, l'arc magmatique migre vers l'est en direction du bassin d'avant-pays (Ramos et Folguera, 2005). Entre l'Oligocène et le Miocène inférieur, la marge andine se caractérise par une extension générale (Munoz et al., 2000). Cette dernière démontrée plus au nord par Charrier et al. (2002) a été le sujet de nombreux travaux entre 36°S et 39°S par Jordan et al. (2001), Ramos et Folguera (2005) et Burns et al. (2006) et à la latitude de 41°S par Munoz et al. (2000). En ce qui concerne le magmatisme, cette époque est caractérisée par une activité importante et par une migration de l'arc volcanique principal en direction de la fosse (Ramos et Folguera, 2005). Au Miocène moyen, une seconde phase de raccourcissement, identique à celle des parties septentrionales, nommée phase Quechua, induit l'inversion des bassins extensifs préexistants. Comme nous l'avons vu au niveau des Andes centrales du Sud, cette phase de raccourcissement est datée entre 21 et 16 Ma (Charrier et al., 2002) tandis qu'au niveau du bassin de Neuquén le raccourcissement débute à environ 12 Ma (Folguera et al., 2006). Durant cette période, le magmatisme d'arc migre de nouveau vers l'est, à plus de 500 km de la fosse (Kay, 2002). Entre le Pliocène et le Quaternaire, le régime tectonique des Andes de Neuquén est sujet à controverse. En effet, certains auteurs proposent que suivant la phase de compression Quechua, une phase extensive débuterait à partir de 5 Ma (Folguera et al., 2006). A l'inverse, Cobbold et Rossello (2003) et Galland et al. (2007) proposent, à partir d'analyses structurales et morphologiques, que la phase compressive se poursuit entre le Pliocène et l'actuel (Figure. II-11), situation comparable à celle décrite plus au nord au niveau des Andes centrales du sud (Zapata et Allmendinger, 1996 ; Giambiagi et al., 2003).

Entre 39°S et 46°S, la marge chilienne est affectée sur plus de 1000 km de long par un système de failles décrochantes dextres, appelé Zone de Faille de Liquine-Ofqui (ZFLO). Ce système de failles actives depuis le Cénozoïque accommode l'obliquité de la convergence de la plaque Nazca par rapport à la plaque Amérique du Sud (Hervé, 1994 ; Cembrano et al., 1996, 2002 ; Rosenau et al., 2006). L'accommodation de la convergence par la ZFLO induit très peu de raccourcissement dans la partie arrière-arc de cette région (Figure. II.11). En effet, Martinez et al., (1997) proposent seulement 20 à 40 km de raccourcissement depuis le Cénozoïque à 40°S de latitude..

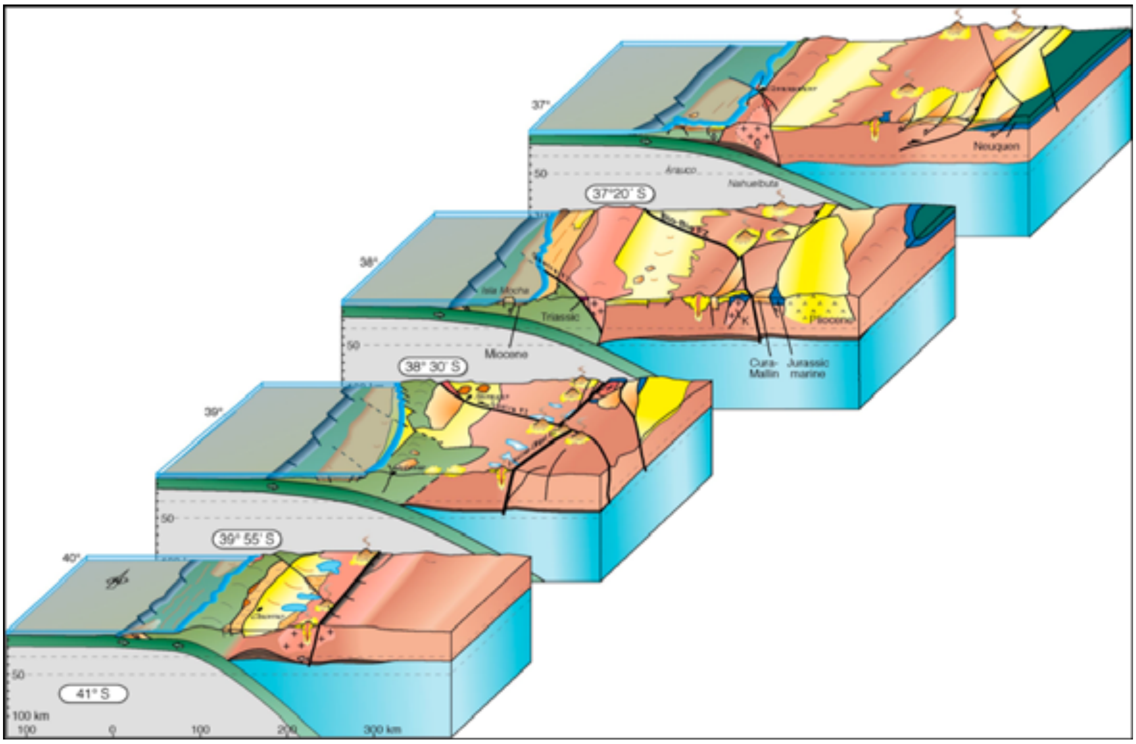

Figure II.11 : Blocs 3D schématiques illustrant le style tectonique actuel de la Cordillère patagonienne du nord entre les latitudes 37°S et 41°S. A 37°S de latitude, le bassin de Neuquén est caractérisé par une série de chevauchements à vergence est, tandis que plus au sud, la majorité du raccourcissement est accommodé le long de grands décrochements lithosphériques tels que la zone de failles Liquine-Ofqui (d'après Echlter, séminaire Géosciences Montpellier, 2006).

II.1.3.2. La Patagonie australe

Les Andes méridionales australes sont situées entre 50°S et 55°S de latitude. La forme incurvée de cette portion des Andes diffère de l'ensemble de l'orogène andin. Les principales unités géologiques correspondent à un socle métamorphique Paléozoïque à degré de métamorphisme variable, à des unités volcaniques siliceuses datées entre le Jurassique moyen et la fin Jurassique, à un batholite côtier Méso-Cénozoïque, à une séquence ophiolitique comprise entre le Jurassique et le Crétacé inférieur (ceintures des Rocas Verdes), à une séquence sédimentaire Cénozoique correspondant au bassin de Magellan dont l'épaisseur des sédiments dépasse localement 8000 mètres suivie par des unités volcaniques Cénozoïques. L'évolution tectonique de cette région est caractérisée par plusieurs phases de déformations majeures. Entre le Trias et le début du Crétacé, une extension importante est responsable d'un volcanisme siliceux de grande ampleur accompagné par le rifting de l'ensemble de la marge de la Terre de Feu, aboutissant à la formation de croûte océanique (Dalziel et al., 1974 ; Dalziel, 1981, Dalziel and Forsythe, 1985 ; Cunningham, 1993). A la fin du Crétacé, le régime tectonique devient compressif, transition sensiblement reliée à un pic de convergence à 100 Ma. Il en résulte la fermeture et l'inversion du bassin des Rocas Verdes (Dalziel et al., 1974). Simultanément, la Cordillère de Darwin et la Cordillère patagonienne subissent une phase de surrection majeure (Dalziel, 1985 ; Cunningham, 1993). A cette époque, la chaîne de Magellan et le bassin d'avant-pays de Magellan (ou bassin Austral) se développent (Ramos, 1989 ; Kraemer et Riccardi, 1997 ; Coutand et al., 1999). Au cours du Paléogène, le régime compressif à transpressif se poursuit depuis la cordillère jusqu'au bassin d'avant-pays où plus de 5000 mètres d'épaisseur de sédiments se déposent (Biddle et al., 1986). La propagation de la déformation vers l'est se poursuit jusqu'au Pliocène (Diraison et al., 1997). Enfin, au cours du Tertiaire, une série de grabens perpendiculaires à la chaîne se développe sur l'ensemble de la région (Diraison et al., 1997). L'âge exact de ce rifting transverse n'est pas contraint actuellement. L'extrémité sud de la Patagonie est également caractérisée par l'interruption du front tectonique par une série de failles normales contrôlant la marge passive nord de la mer de Scotia (Lagabrielle et al., 2009).

Cette région est également caractérisée par une série d'intrusions Miocène localisée entre 48°S et 55°S, le long d'un linéament nord-sud (Zone Volcanique Sud et Zone Volcanique Australe) (Halpern, 1973 ; Michael, 1984 ; Michel et al., 2008). Ces plutons sont caractérises par des signatures différentes comprises entre des complexes acides à mafiques et à des adakites. Les intrusions acides à mafiques correspondent du sud au nord : (1) Au complexe du Torres del Paine (51°S de latitude) dont l'âge de mise en place dans les séries Crétacé est daté entre 12.50 ± 0.02 Ma et 12.59 ± 0.02 Ma (Michel et al., 2006). Ce complexe constitué de diorites et de gabbros (Baumgartner et al., 2006 ; Leuthold et al., 2007) s'est mis en place dans un contexte transpressif et transtensionel (Altenberger et al., 2003). (2) Au Cerro Moyano et Cerro Elefante (51°S de latitude) dont les diorites les constituants sont datées à 16 ± 1 Ma (Ramos et al., 2004). (3) Au massif du Fitz Roy (environ 49°S) daté à 18 ± 3 ma (Nullo et al., 1978). Les corrélations spatiales et temporelles de l'emplacement de ces intrusions par rapport à la subduction de la dorsale du Chili débutant à 18 Ma montrent que ces plutons sont plus vieux que le début de la subduction (Sanchez et al., 2008). Mais cette corrélation n'est pas valide pour le complexe du Torres del Paine dont l'âge de mise en place est relativement corrélé avec la collision d'un segment avec la fosse chilienne (segment SCR-

1). En ce qui concerne les plutons adakitiques, ils sont représentés par le Mt Chalten (49°S, 14.50 ± 0.55 Ma), par le Mt puesto Nuevo (48°50'S, 13.12 ± 0.55 Ma) et par le massif du Cerro Pampa (48°S, 11.36 ± 0.55) (Kay et al., 1993 ; Ramos et al., 2004). Ces auteurs proposent que leur formation est liée à la fusion de la croûte océanique jeune et chaude de la plaque Nazca, avant l'entrée en subduction de la dorsale du Chili.

A travers ce résumé de la segmentation morphostructurale et des événements tectono-magmatiques ayant affectés la Cordillère des Andes depuis le Mésozoïque, nous remarquons que l'évolution de cette chaîne est complexe et est marquée par des phases d'extensions et de compressions, d'arrêts et/ou de migration du volcanisme. De plus, la topographie le long de la Cordillère des Andes est très variables depuis le nord des Andes jusqu'à la Terre de Feu où des reliefs à plus de 6000 mètres d'altitude, dominant la partie centrale des Andes, contrastent avec les faibles reliefs du sud de l'Amérique du Sud.

II.1.4. Processus contrôlant l'orogénèse andine

La déformation de la plaque supérieure au-dessus d'une zone de subduction résulte de plusieurs facteurs :

1) Intuitivement, le couplage à l'interface des deux plaques est un paramètre important. En effet la transmission des contraintes de la plaque plongeante vers la plaque supérieure est dépendante de la pression fluide à l'interface des deux plaques (Lamb et Davies, 2003). De ce fait, la contrainte cisaillante à l'interface des deux plaques dépendra de la présence ou non de sédiments à la fosse. Plus la quantité de sédiments est importante plus la contrainte cisaillante est faible. Lamb et Davies (2003) ont suggéré que l'évolution de l'orogénèse andine était contrôlée par les processus de sédimentation et d'érosion, dépendant eux-mêmes du climat. Un climat humide favorisera l'érosion du relief, dont les produits de l'érosion se déposeront dans les bassins sédimentaires de part et d'autre de la chaîne. Ainsi, l'accumulation de sédiments dans la fosse induira une lubrification à l'interface des plaques provoquant une diminution de la friction et par conséquent une diminution du raccourcissement de la plaque supérieure (Lamb et Davies, 2003). De ce fait, nous voyons que la tectonique peut-être contrôlée par le climat mais l'inverse est également possible. En effet, la création d'une barrière orogénique induira des perturbations majeures au niveau du climat le long d'un orogène. L'exemple des Andes étant l'un des exemples les plus

remarquables vu sa disposition nord-sud créant une asymétrie majeure dans les précipitations (Montgomery et al., 2001 ; Strecker et al., 2007).

2) La vitesse absolue des plaques et notamment celle de la plaque chevauchante est également un des paramètres important contrôlant la tectogénèse. Il a été montré qu'une bonne corrélation existe entre la vitesse absolue de la plaque supérieure (référentiel lié aux points chauds) et sa déformation (Silver et al., 1998 ; Heuret et Lallemand, 2005). Dans le cas d'un mouvement absolu vers l'océan, la plaque chevauchante enregistrera un raccourcissement tandis que si le mouvement absolu de la plaque supérieure est dans la direction opposée, cette dernière se caractérisera par un régime extensif (Figure. II.12). En ce qui concerne la vitesse absolue de la plaque Amérique du Sud en direction de l'ouest, celle ci a très peu varié depuis le Crétacé supérieur (2 à 3 cm/an, Silver et al., 1998). Ce concept est appliqué dans 75% des cas selon Heuret et Lallemand, (2005). Ils interprètent ces résultats comme la conséquence de l'ancrage des slabs dans le manteau inférieur, s'opposant au déplacement des zones de subduction. Ce concept est uniquement applicable dans le cas de subduction relativement ancienne où le slab atteint le manteau inférieur. Dans le cas de la subduction d'une lithosphère océanique jeune ce modèle n'est plus valable.

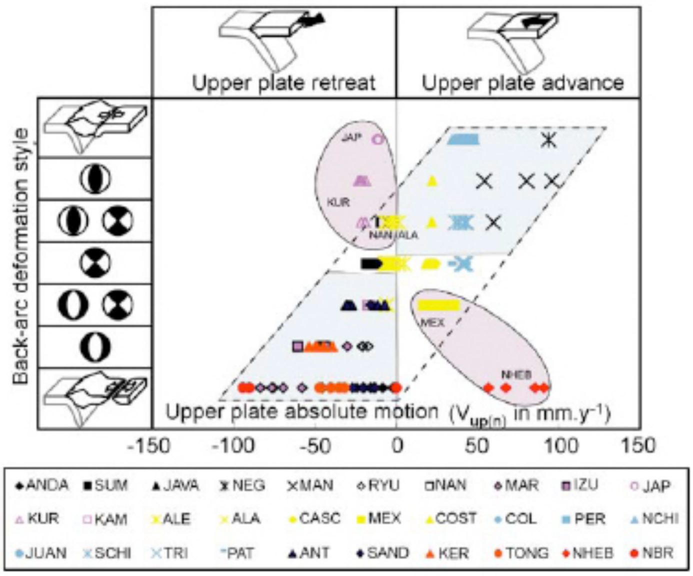

Figure II.12 : Diagramme illustrant la déformation arrière-arc en fonction du mouvement absolu de la plaque supérieure ($V_{up(n)}$). La zone bleue correspond au domaine où la déformation arrière-arc est cohérente avec le mouvement absolu de la plaque chevauchante. Les zones rouges correspondent aux convergences qui ne vérifient pas cette *relation. Nous remarquons que lorsque la plaque supérieure avance, la déformation est de type compressif (d'après Heuret et Lallemand, 2005)*

La déformation de la plaque supérieure est également fonction du retrait de la fosse (Schellart, 2008). Plus une fosse se retire rapidement plus l'extension enregistrée par la plaque supérieure est importante. Dans le cas d'un retrait lent voir nul, la plaque supérieure enregistre un raccourcissement, cas observé lors de l'avancée de la plaque chevauchante vers l'océan. Dans le cas des Andes la vitesse absolue de la plaque Amérique du Sud en direction de l'ouest, est de l'ordre de 2 à 3 cm/an (Silver et al., 1998). Différents pics de vitesse de convergence de la plaque en subduction ont été enregistrés. Un premier pic à 100 Ma est relié à l'ouverture du segment équatorial de l'océan Atlantique, un second pic au cours de l'Eocène (55 Ma) et un dernier pic à 25 Ma lié à la rupture de la plaque Farallon (Pardo-Casas et Molnar, 1987 ; Londsale, 2005). La vitesse de convergence a varié entre 10 et 15 cm/an pendant les pics de convergence pour diminuer à 7 cm/an au cours du Paléocène et de l'Oligocène. Le dernier pic à 25 Ma est bien corrélé avec la dernière phase de déformation majeure enregistrée sur la plaque supérieure (e.g. Allmendinger et al., 1997 ; Sempere et al., 1990 ; Charrier et al., 2002). Ce concept est valable dans le cas d'une subduction d'une plaque relativement mature. En effet dans l'exemple d'une subduction de lithosphère jeune et chaude induisant une diminution du pendage du slab et une diminution du taux de convergence (Cross and Pilger, 1982 ; Larter and Barker, 1991 ; Cloos, 1993), le retrait de la fosse pourra être plus ou moins élevé provoquant ainsi un régime extensif au niveau de la plaque supérieure.

3) La présence d'anomalies topographiques (volcans sous-marins, rides asismiques, plateaux océaniques) en subduction joue un rôle majeur sur l'évolution de la plaque supérieure. Ces anomalies modifient de manière plus ou moins localisée le couplage à l'interface des deux plaques et de ce fait le régime de contraintes de la plaque supérieure. Dans le cas des Andes, plusieurs rides asismiques sont en subduction, du nord au sud : la ride Carnegie (2°N), la ride de Nazca (15°S), la ride d'Iquique (22°S) et la ride Juan Fernandez (33°S) (Figure. II.13). Nous avons pu voir précédemment que leur subduction coïncide avec une horizontalisation du slab générant une migration de la déformation vers l'avant-pays, un arrêt du volcanisme et un soulèvement de l'avant-arc.

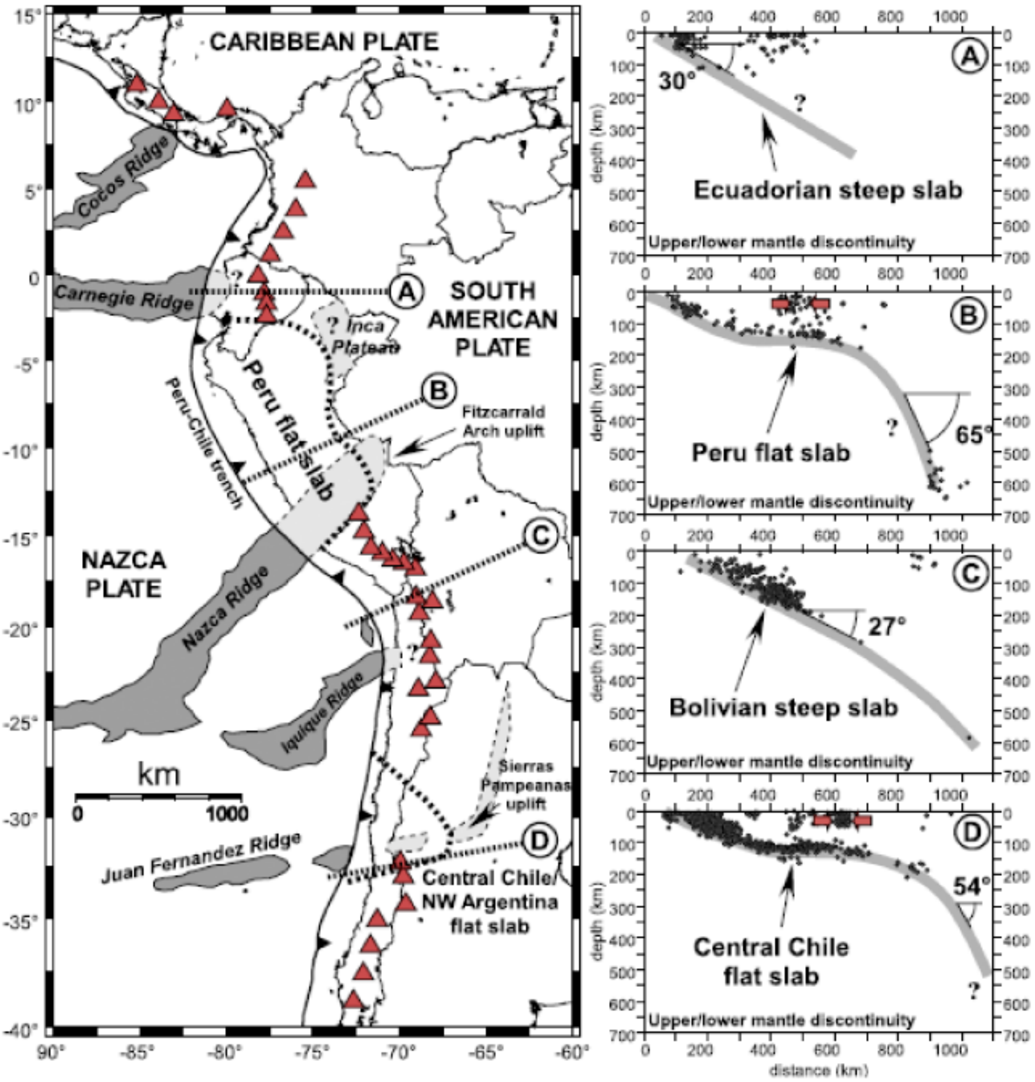

Figure II.13 : Illustration des interactions rides asismiques/fosse le long de la marge andine entre 10°N et 40°S de latitude. La localisation et la longueur prédite de ride subduite sont représentées en gris pour chaque anomalie subduite. Les triangles rouges correspondent au volcanisme d'arc andésitique actif (Gutscher et al., 2000). On a également représenté 4 profils illustrant les variations du style de subduction en relation avec des anomalies de la plaque plongeante (A : Equateur, B : Pérou, C : Bolivie, D : Chili). Nous remarquons que dans les cas de subduction de rides asismiques (profils B et D), la subduction s'horizontalise et la plaque supérieure enregistre une déformation compressive au niveau de l'avant-pays. Les flèches rouges indiquent le maximum de raccourcissement au niveau de la plaque supérieure (d'après Espurt et al., 2008).

4) La rhéologie de la plaque supérieure intervient également dans le style et dans la localisation de la déformation. En effet, l'épaisseur et la composition de la lithosphère chevauchante et son héritage structural gouvernent sa capacité à se déformer (e.g. Burov et Diament, 1996).

Il est évident que la subduction d'une dorsale active, accompagnée par le développement d'une fenêtre asthénosphérique induit des modifications majeures dans les conditions imposées par le matériel situé sous la plaque supérieure. Nous avons pu voir à travers le Chapitre I que l'ensemble des exemples de chaînes de subduction circum-Pacifique ayant interagi avec une subduction 'chaude' a connu des perturbations géologiques majeures comme l'arrêt du volcanisme d'arc, la surrection momentanée de l'avant-arc, des transitions d'un régime compressif à un régime extensif de plus ou moins grande amplitude et un magmatisme arrière-arc important.

De ce fait, les Andes de Patagonie Centrale constitue un objet unique afin d'étudier l'évolution d'une chaîne de subduction lors de l'interaction actuelle d'une dorsale active avec un continent.

II.2. La Patagonie Centrale et la subduction de la dorsale active du Chili

Cette partie est consacrée à l'évolution depuis le Paléozoïque de la Patagonie Centrale entre 45°S et 47°S de latitude. L'histoire pré-Cambrienne et Cambrienne n'étant pas directement dans le propos de cette thèse, nous ne présenterons pas l'évolution de la chaîne pendant cette période. Toutefois, certains grands traits de cette évolution ont été abordés par de nombreux auteurs tels que Hervé, (2000) ; Ramos, (2002) ; Pankhurst et al. (2000) ; Pankhurst et al. (2006).

II.2.1. La Patagonie Centrale entre le Paléozoïque et l'Eocène

II.2.1.1. Le Paléozoïque

Les roches les plus anciennes présentes dans cette région et plus particulièrement dans la partie occidentale de la Cordillère (ouest et sud du Lac Général-Carrera-Buenos Aires) correspondent à des roches métamorphiques d'âge dévono-carbonifère. Ces roches correspondent à des métapélites, des marbres, des métaconglomérats et des métabasites définissant le Complexe Métamorphique Oriental Andin (Hervé, 1993) au Chili et la Formation Rio Lacteo en Argentine. Les protolithes sont supposés être des sédiments clastiques et des roches volcaniques ayant enregistrées une période de déformation majeure et un métamorphisme MP-MT lors de leur accrétion reliée à une subduction ancienne le long de la proto marge du Gondwana (Hervé et al., 1998 ; Ramos, 1989 ; Bell et Suarez, 2000).

II.2.1.2. Le Mésozoïque

Le Jurassique supérieur et le Crétacé inférieur sont caractérisés par une phase de volcanisme acide de type calco-alcalin en relation avec les processus de subduction (Suarez et De la Cruz, 2000). Cette unité volcanique nommée Groupe Ibanez au Chili et Complexe El Quemado en Argentine, discordante sur le socle Paléozoïque (Niemeyer et al., 1984, De la Cruz et al., 2005, 2006), est constituée de rhyolites, de dacites, d'andésites et de basaltes, et localement pour les parties les plus récentes de séries sédimentaires détritiques (Bruce, 2001 ; De la Cruz et al., 2003, 2004, De la Cruz et al., 2006 ; Suarez et al., 2009). Cette unité caractérise une série d'événements explosifs de grande ampleur (Province de Chon Aike), se mettant en place pendant une phase d'extension majeure affectant l'ensemble de la plaque sud-américaine associée à l'ouverture de l'océan Atlantique (Figure. II.14). La partie ouest de la chaîne est caractérisée par la présence du Batholite Patagonien, longeant la marge chilienne entre 42°S et 55°S. Ce complexe d'une longueur de plus de 1000 km sur plus de 200 km de large est associé à la subduction le long de la marge active sud-américaine, et dont l'âge des différents corps intrusifs varie depuis le Jurassique supérieur jusqu'au Pliocène (Halpern, 1973 ; Bruce, 2001 ; Hervé et al., 1984 ; Pankhurst et al., 1999 ; Suarez et De la Cruz, 2001 ; Hervé et al., 2007). Dans la région du lac Général Carrera-Buenos Aires (46°S de latitude), la formation Ibanez est recouverte en discordance par les formations sédimentaires marines du Groupe Coihaique, déposées dans les bassins arrière-arcs extensifs du bassin Austral (Biddle et al., 1986). Ce groupe caractérise une transgression majeure dont les principales unités correspondent à la formation Toqui constituée de calcaire et de grès (De la Cruz et al., 2003 ; Suarez et De la Cruz, 1994). La formation Katterfeld (Fm. Rio Mayer en Argentine) est constituée de grès et de marnes fossilifères, déposées sur la formation Toqui (De la Cruz et al., 2003). Enfin, la dernière formation du Groupe Coihaique est la formation Apeleg constitué principalement de grès (Fm. Rio Belgrano en Argentine). La phase de compression à environ 100 Ma, responsable de la fermeture du bassin marginal de Rocas Verdes dans le sud des Andes, a sans doute été enregistrée dans cette région, se caractérisant par une légère inversion de ces bassins arrière-arcs. A environ 45°S de latitude, le Groupe Divisadero recouvre en discordance les formations volcanique du Groupe Ibanez. Ces formations volcanoclastiques d'une épaisseur de plus de 2000 mètres se sont déposées ntre le Crétacé inférieur et le Crétacé supérieur (Suarez et De la Cruz, 2000 ; Parada et al., 2001).

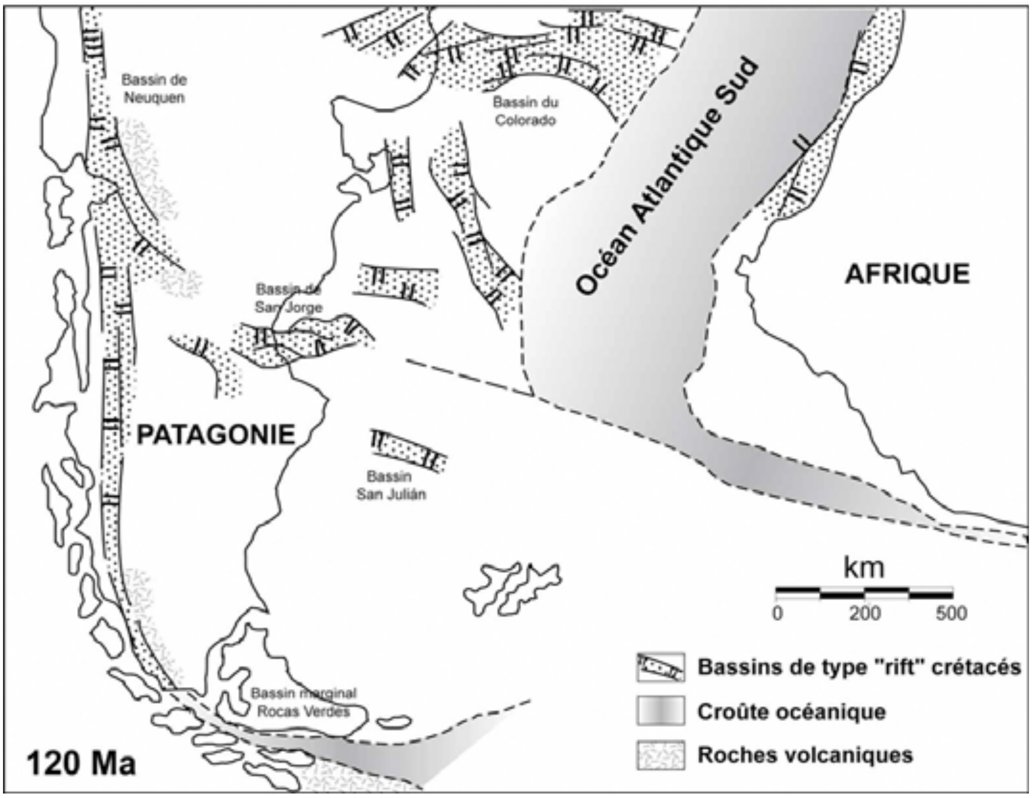

Figure II.14 : Reconstitution paléogéographique des Andes méridionales et de l'Océan Atlantique Sud au Crétacé inférieur. A cette époque, de grandes structures extensives et leurs bassins associés se développent (Ramos, 2000). A l'extrémité sud de l'Amérique du Sud, l'extension plus importante induit la formation de croûte océanique au niveau du bassin marginal de Rocas Verdes, qui sera fermé au Crétacé supérieur au cours d'une phase de compression majeure (Dalziel et al., 1974 ; Diraison et al., 2000) (figure extraite de Guillaume, 2009).

II.2.1.3. Du Paléocène à l'Eocène

La période du Paléocène et l'Eocène inférieur, est caractérisée par une phase de compression, la phase Inca, dont les témoins sédimentaires sont très bien observés dans les Andes centrales et dans les Andes de Patagonie du sud à environ 50°S. Au niveau de la Patagonie Centrale, les dépôts syn-orogéniques léhèrement discordants sont très peu développés et correspondent à la formation Ligurio Marquez (Suarez et al., 2000). La région de Patagonie Centrale est caractérisée à l'Eocène par la mise en place de basaltes alcalins à signature OIB, correspondant aux basaltes Posadas, formant la base de la meseta de Chile Chico (48.6 ± 1.8 Ma, Espinoza, 2003 ; bordure sud du lac Général Carrera-Buenos Aires). Leur genèse est mise en relation avec la subduction de la dorsale Farallon/Aluk durant l'Eocène induisant la formation d'une fenêtre asthénosphérique sous la plaque supérieure

II.2.2. La Patagonie Centrale depuis l'Oligocène

II.2.2.1. Subduction de la dorsale du Chili et développement de la fenêtre asthénosphérique sous la Patagonie

Au cours de l'Oligocène, la cinématique des plaques est marquée par la rupture de la plaque Farallon à environ 25 Ma, formant les plaques Cocos et Nazca (Londsale, 2005). Cette période est également marquée par une augmentation de la convergence entre la plaque Nazca, nouvellement formée, et la plaque Amérique du Sud (Pardo-Casas et Molnar, 1987) ainsi que par le changement dans la direction de la convergence entre ces plaques devenant plus orthogonale (Cande et Leslie, 1986).

Au niveau de la Patagonie, la dorsale active du Chili migre vers l'est en direction de la marge chilienne. Les reconstitutions cinématiques utilisées ici sont celles réalisées par Aude de la Rupelle (mémoire M2, 2007 et co-signataire de l'article présenté ci-dessous) et par Breitsprecher et Thorkelson (2008) rendant compte de la migration du point triple du Chili depuis 18 Ma, époque où la dorsale du Chili commence à subduire sous la plaque sud-américaine, et illustrant de façon précise l'évolution du développement de la fenêtre asthénosphérique sous la plaque supérieure (Figure. II.15). A partir de 18 Ma, la dorsale du Chili entre en subduction sous la plaque sud-américaine. Le point triple formé par les plaques Nazca, Antarctique et Amérique du Sud, migre vers le nord. A 16 Ma, une quadruple jonction, situation inédite et transitoire, se développe à environ 50°S de latitude (Breitsprecher et Thorkelson, 2009). Le point triple du Chili migre vers le nord jusqu'à sa position actuelle à 46°12'S de latitude, tandis que la dorsale séparant les plaques Antarctique et Phoenix migre vers le nord-est le long de la marge Antarctique (Figure. II.15).

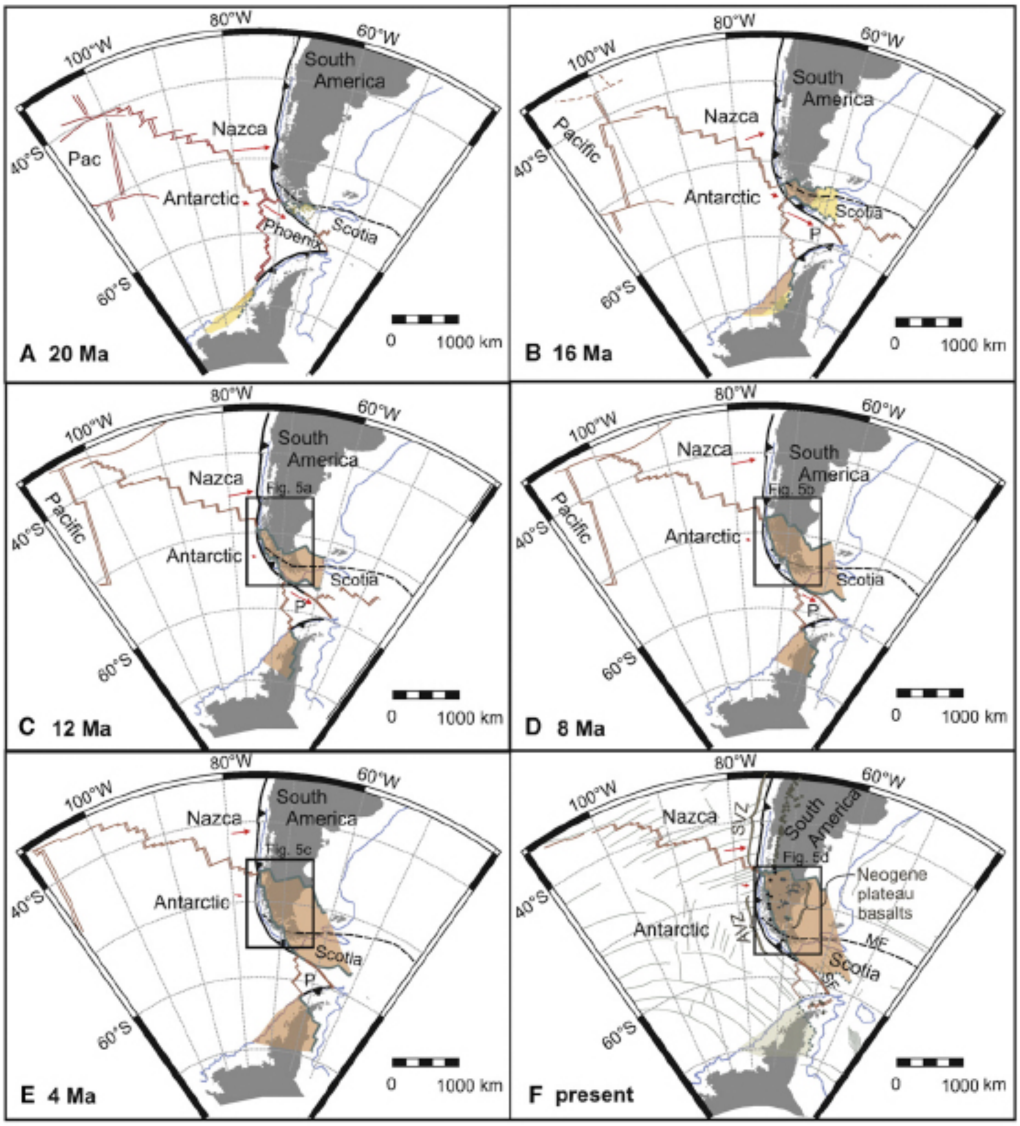

Figure II.15 : Reconstitutions cinématiques du sud-est pacifique entre les Andes méridionales et l'Antarctique depuis l'Eocène à l'actuel (Breitsprecher et Thorkelson, 2009). Les subductions de la dorsale du Chili sous la Patagonie et de la dorsale Farallon/Antarctique sous la Péninsule ouest Antarctique conduisent à l'ouverture de fenêtres asthénosphériques (représentées ici en orange) migrant vers le nord et le nord-est respectivement.

La subduction de la dorsale du Chili sous la plaque Amérique du Sud induit la formation d'une fenêtre asthénosphérique (Figure. II.16). Au nord du point triple, la vitesse de convergence de la plaque Nazca par rapport à la plaque sud-américaine supposée fixe est de 8 cm/an (DeMets et al., 1990) suivant une direction oblique par rapport à la fosse. Au sud du point triple, la plaque Antarctique est caractérisée par une direction orthogonale par rapport à la fosse et une vitesse de convergence de l'ordre de 2 cm/an (DeMets et al., 1990). De ce fait, la Patagonie Centrale à la latitude du point triple actuel, correspond actuellement à une frontière en surface entre deux styles de subduction différente. Le développement de la fenêtre asthénosphérique sous la Patagonie a été largement discuté dans plusieurs articles (e.g. Lagabrielle et al., 2004 ; Guivel et al., 2006) est illustré récemment par Breitsprecher et Thorkelson, (2009). Nous remarquons que la taille de celle ci augmente avec une amplification de sa surface vers le nord-est au cours du temps (Figure. II.16). Cette fenêtre est actuellement présente sous la Patagonie depuis la latitude de 45°S jusqu'à la Terre de Feu. De plus, le développement de cette fenêtre induisant un gap dans la plaque plongeante permet la remontée de matériel asthénosphérique sous la lithosphère continentale, depuis environ 3 Ma (Figure. II.16).

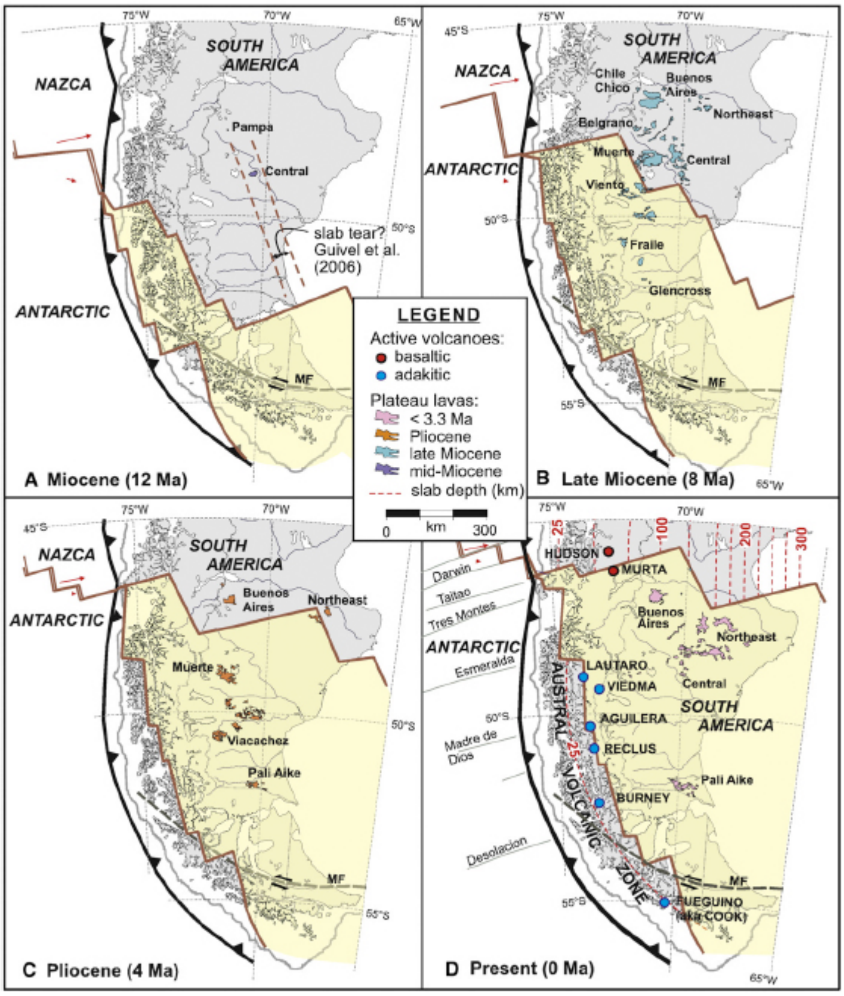

Figure II.16 : Reconstitution de la localisation prédite de la fenêtre asthénosphérique (en jaune) sous le continent sud-américain entre le Miocène et l'actuel (d'après Breitsprecher et Thorkelson, 2009). Les flèches rouges indiquent le mouvement des plaques Nazca et Antarctique par rapport à la plaque supérieure supposée fixe. La profondeur du slab est indiquée sur la figure D par des pointillés rouges. Le volcanisme d'arc actif est matérialisé par des points rouges (au nord du point triple) et bleus (au sud du point triple). Nous remarquons qu'entre 4 Ma et l'actuel, la fenêtre se développe sous la région du lac Général Carrera-Buenos Aires.

La compilation de tous les âges obtenus en Patagonie sur les laves alcalines Tertiaires par Guivel et al, (2006) a fait apparaître une contradiction majeure dans les premiers raisonnements reliant l'ouverture de la fenêtre asthénosphérique et la remontée de manteau asthénosphérique à travers l'ouverture ainsi créée dans le slab. En effet, les séries volcaniques constituants la base des mesetas de la Muerte (48°30'S), Belgrano (47°30'S) et del Lago Buenos Aires (47°S) et datées à environ 14-12 Ma, prédatent l'entrée en subduction de la dorsale du Chili à ces latitudes. En effet, comme nous pouvons le voir sur la figure II.16C, à 12 Ma, la fenêtre asthénosphérique est localisée le long de la marge chilienne à plus de 300 km au sud des plateaux basaltiques. De ce fait, les coulées principales constituant les mesetas ne peuvent pas être reliées au développement de la fenêtre asthénosphérique et de la remontée de manteau à travers cette ouverture. Guivel et al, (2006) proposent un modèle de déchirure du slab (slab-tear) en avant de la dorsale subduite afin d'expliquer ce magmatisme précoce,hypothèse également présentée dans l'article ci-dessous. C'est la raison pour laquelle, Breitsprecher et Thorkelson, (2009) évoque sur leur figure l'hypothèse du slab-tear à 12 Ma.

Nous remarquons également que la bordure ouest de la fenêtre correspond à l'arc magmatique (Zone Volcanique Sud et Zone Volcanique Australe), dont plusieurs volcans sont de type adakitique, tandis que la position de la bordure orientale n'est contraire que géométriquement. En effet, les effets d'érosion thermique et de slab-pull lié à la subduction de la plaque Nazca et tendant à élargir la fenêtre ne sont pas pris en compte. Ceci suggère que la position de la bordure orientale de la fenêtre pourrait se situé plus vers le nord-est.

II.2.2.2. Evolution tectonique et magmatique de la Patagonie Centrale depuis l'Oligocène

Cette partie fait l'objet d'un article publié en 2009 dans la revue International Journal of Earth Sciences, volume spécial Subduction Zone Dynamics, proposant un bilan des principales caractéristiques tectoniques, sédimentaires et magmatiques de la Patagonie Centrale depuis l'Oligocène, lors d'une évolution d'un contexte pré-subduction de dorsale à un contexte subduction de dorsale et développement d'une fenêtre asthénosphérique.

Subduction of an Active Spreading Ridge beneath southern South America :

A review of the Cenozoic Geological record from the Andean Foreland,

Central Patagonia (46°S-47°S)

Bruno Scalabrino[1], Yves Lagabrielle[1], Aude de la Rupelle[1], Jacques Malavieille[1], Mireille Polvé[2,] Felipe Espinoza[3], Diego Morata[3] , Manuel Suarez[4].

1) CNRS-UMR 5243 Géosciences Montpellier, Université Montpellier 2, CC 60, Place Eugène Bataillon, Montpellier Cedex5, 34095, France.

2) OMP, Université Paul Sabatier, Toulouse, France.

3) Departamento de Geología, Universidad de Chile, Casilla 13518, Correo 21, Santiago, Chile.

4) Servicio Nacional de Geología y Minería, Avenida Santa María 0104, Santiago, Chile.

Subduction of an Active Spreading Ridge Beneath Southern South America: A Review of the Cenozoic Geological Records from the Andean Foreland, Central Patagonia (46–47°S)

Bruno Scalabrino, Yves Lagabrielle, Aude de la Rupelle,
Jacques Malavieille, Mireille Polvé, Felipe Espinoza,
Diego Morata and Manuel Suarez

Abstract The Chile-Argentina Patagonian Cordillera is a natural laboratory to study the interactions between oceanic and continental lithosphere during the subduction of an active spreading ridge beneath a continent. Subduction of the South Chile spreading ridge, which separates the Nazca plate from the Antarctic plate, started around 15–14 Ma at the southern tip of Patagonia. Presently, the southernmost segment of the Chile Ridge enters the Peru-Chile trench at 46°S, at the site of the Chile Triple Junction (CTJ). We review the main events which occurred on land in the CTJ region (46–47°S), related with processes of ridge subduction. We summarize tectonic, sedimentary, and magmatic features in a 30 Ma-to Present chronological table. A pre-ridge subduction stage, from 30 to 15 Ma, is characterized by the onset and growth of Patagonian relief and by a shift from marine to continental detrital sedimentation in the foreland at 20–22 Ma. The change from pre-ridge subduction to ridge subduction is marked on land by a transition from calc-alkaline to alkaline volcanism, at 14–12 Ma, and by the onset of eruption of very large flood basalt provinces (future volcanic plateaus) following rapid erosion of the eastern foreland belt. Post-plateau basaltic volcanism (<4 Ma) is coeval with a period of tectonic and morphological rejuvenation during which the eastern foreland of the Cordillera has been affected by extensional/transtensional tectonics. We place these events in the framework of a tectonomagmatic model involving the opening of slab windows due to both slab tear and ridge axis subduction.

Keywords Central Patagonia • South Chile Ridge • Subduction • Cenozoic • Geological records • Compressional to extensional tectonics • Geodynamic model

B. Scalabrino
CNRS-UMR 5243 Géosciences Montpellier, Université Montpellier 2, CC 60, Place Eugène Bataillon, Montpellier Cedex 5 34095, France, scalabrino@gm.univ-montp2.fr

S. Lallemand and F. Funiciello (eds.), *Subduction Zone Geodynamics*,
DOI 10.1007/978-3-540-87974-9, © Springer-Verlag Berlin Heidelberg 2009

1 Introduction

During the Cenozoic, the Patagonian Cordillera, which forms the southern segment of the Andes, north of the Andes of Tierra del Fuego, was built coevally with the subduction of the southern part of the Farallon-Nazca plate followed by subduction of the southern part of the Chile Spreading Ridge, which separates the Nazca plate from the Antarctic plate. The South Chile Ridge entered the south Chile trench, bounding the South American plate, at around 15 Ma at the southern tip of Patagonia. The Chile Triple Junction (CTJ), now located at 46°12′S, is the point where the Nazca, Antarctic, and South American plates meet (Fig. 1). The subduction of successive spreading segments of the South Chile Ridge led to the opening of a slab

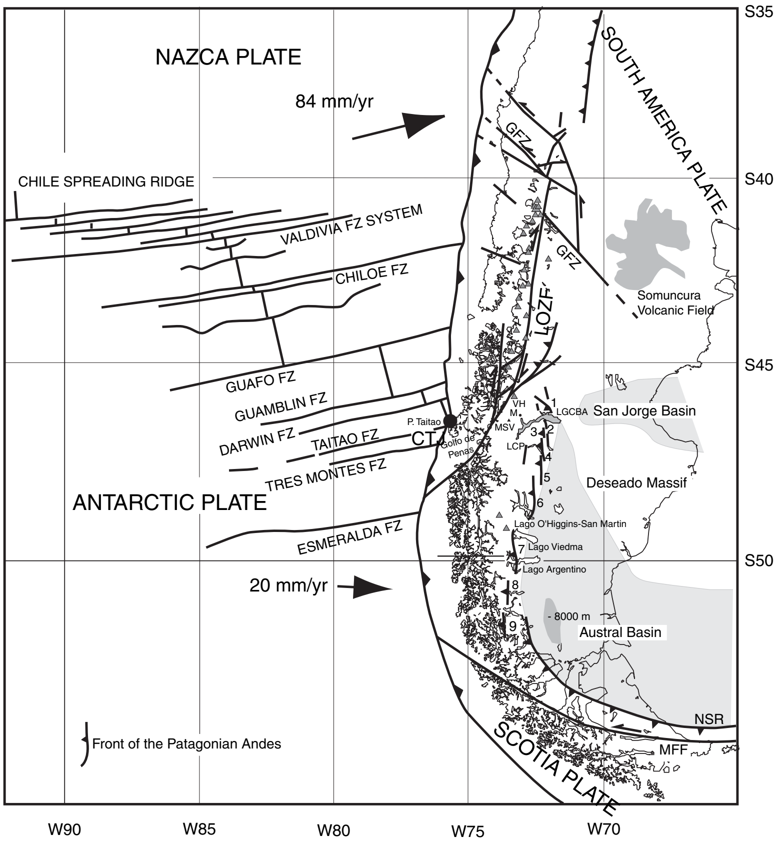

Fig. 1 Plate tectonic setting of southern South America between 35 and 55°S and main features of the subducting South Chile Ridge, including transform fault zones (*FZ*) and active spreading segments (*thick black lines*) (adapted from Tebbens et al., 1997; Ramos, 1989; DeMets et al., 1990; Cembrano et al., 1996; Guivel et al., 1999). Tectonic data are compiled after: Ramos, 1989; Tebbens et al., 1997; Cembrano et al., 1996, 2002; Coutand et al., 1999; Diraison et al., 2000; Melnick et al., 2002; Lagabrielle et al., 2004 and Ghiglione and Ramos, 2005). Location of Somuncura volcanic field is after De Ignacio et al. (2001). The segments of the tectonic front of the Cordillera south of the latitude of the Chile Triple Junction are labelled *1–9*: (*1*) Balmaceda-Portezuelo segment; (*2*) Chile Chico segment; (*3*) Las Horquetas segment; (*4*) Paso Roballos segment; (*5*) Lago Posadas segment; (*6*) Lago San Martin segment; (*7*) Lago Viedma segment; (*8*) Paine segment; and (*9*) Cordillera Riesco segment. *CTJ* Chile Triple Junction, *LGCBA* Lake General Carrera Buenos Aires, *LCP* Lake Cochrane-Pueyrredon, *MSV* Monte San Valentin, *VH* Volcan Hudson, *M* Murta basalts, *LOZF* Liquine Ofqui Fault Zone, *GTZ* Gastre Fault Zone, *MFF* Magallanes-Fagnano Fault, *NSR* western tip of the North Scotia Ridge, corresponding to the North Scotia orogenic front

window beneath the South American upper plate, triggering large scale changes in the rheology of the lithosphere due to dynamic upwelling of hot mantle beneath the entire region (Lagabrielle et al., 2004). A similar situation is reported for the Antarctic Peninsula and the western Scotia Sea, where active ridge segments have been subducting coevally (Garret and Storey, 1987).

The Patagonian Cordillera is almost topographically continuous from 54°S to 40°S. However, between 45°S and 47°S, at the latitude of the CTJ in Central Patagonia, it is characterized by several topographic anomalies. This unusual region includes both the highest mountains (Monte San Valentin, 4058 m a.s.l.) and a series of internal deep transverse incisions occupied by large post-glacial lakes (Fig. 1) (Lake General Carrera Buenos Aires: LGCBA; Lake Cochrane Pueyrredon: LCP; Lake Lapparent). The bottom of the largest lakes lie well below sea level, with lakeshores close to +200 m. Therefore, the axial region of the Central Patagonia Cordillera has an average low elevation, rather than showing the highest peaks, as along the Central and Northern Andes, and in most mountain belts worldwide. It has been suggested that these internal belt basins have tectonically controlled edges, although evidence of recent deformation is scarce due to the strong imprint of glacial processes during landscape evolution (Lagabrielle et al., 2004, 2007; Scalabrino et al., 2007). Such peculiar depressions are locally associated with very recent basaltic volcanism implying a MORB-like source from a buried spreading centre at depth (e.g., Guivel et al., 2006).

It has been suggested that the evolution of the Southern Andes contains a succession of events related to the various steps of subduction of the South Chile Ridge. The aim of this article is first to provide a synthesis of available plate kinematic models of the region (Sect. 2), and second to summarize the history of the Patagonian Cordillera at the latitude of the CTJ (46–47°S) since 30 Ma, based on regional geological records (Sect. 3). This history can be divided into two main periods: a pre-ridge subduction stage of "normal subduction" (30–15 Ma), and a ridge subduction stage involving opening of slab windows, due to both slab tear and ridge axis subduction (15 Ma-Present). This two-period history is in turn divided into a six-stage model, as proposed in the last section.

2 Subduction of Active Ridges and Plate Kinematics of the South American-Antarctica Junction Since 60 Ma: A Synthesis of Available Models

North of the CTJ, the present-day relative motion vector between the Nazca and the South American plates is oriented N80 (Gripp and Gordon, 1990; DeMets et al., 1990) with a magnitude of 84 mm/year (Fig. 1). Oblique subduction has led to tectonic partitioning in the Cordillera, and a part of the convergence is now accommodated along the Liquine-Ofqui fault zone north of the CTJ (Hervé, 1994; Cembrano et al., 1996, 2002; Roseneau et al., 2006) (Fig. 1). South of the CTJ, the current convergence rate between the Antarctic and the South American plates is 20 mm/year, in an E-W direction (Gripp and Gordon, 1990; DeMets et al., 1990) (Fig. 1).

The Patagonian and Antarctic Peninsulas have undergone a long history of ridge subduction throughout the Cenozoic. Figure 2 shows a series of cartoons based on a compilation of various reconstructions gathered from the literature, highlighting the changes in plate configuration of the Antarctica-Patagonia junction region since 60 Ma. This figure shows for the first time on a large scale all the active spreading centres that existed in the area including both the Pacific and the Atlantic sides of South America, and the successive key steps of the evolution this domain.

In the early Cenozoic, the South American and Antarctic plates were welded, constituting a single large continental plate. The Phoenix oceanic plate was subducting beneath this large plate at a rate of about 102 mm/a (McCarron and Larter, 1998) (Fig. 2). The Antarctica-Phoenix active spreading center was subducting under the western Antarctica Peninsula (Ramos, 2005; Eagles, 2003; Eagles et al., 2005).

Around 50 Ma, subduction of the Farallon-Phoenix spreading center under the South America plate began in the N20° direction (Pardo-Casas and Molnar, 1987). This ridge progressively migrated southward along the South American trench, leading to the opening of a first slab window below the continent, as recorded by the alkaline Eocene plateau basalts of Central Patagonia (Ramos and Kay, 1992; Espinoza et al., 2005). This stage was also characterized by the onset of the dislocation of the South American and Antarctic plates south of the future Tierra del Fuego. The relative motion between South America

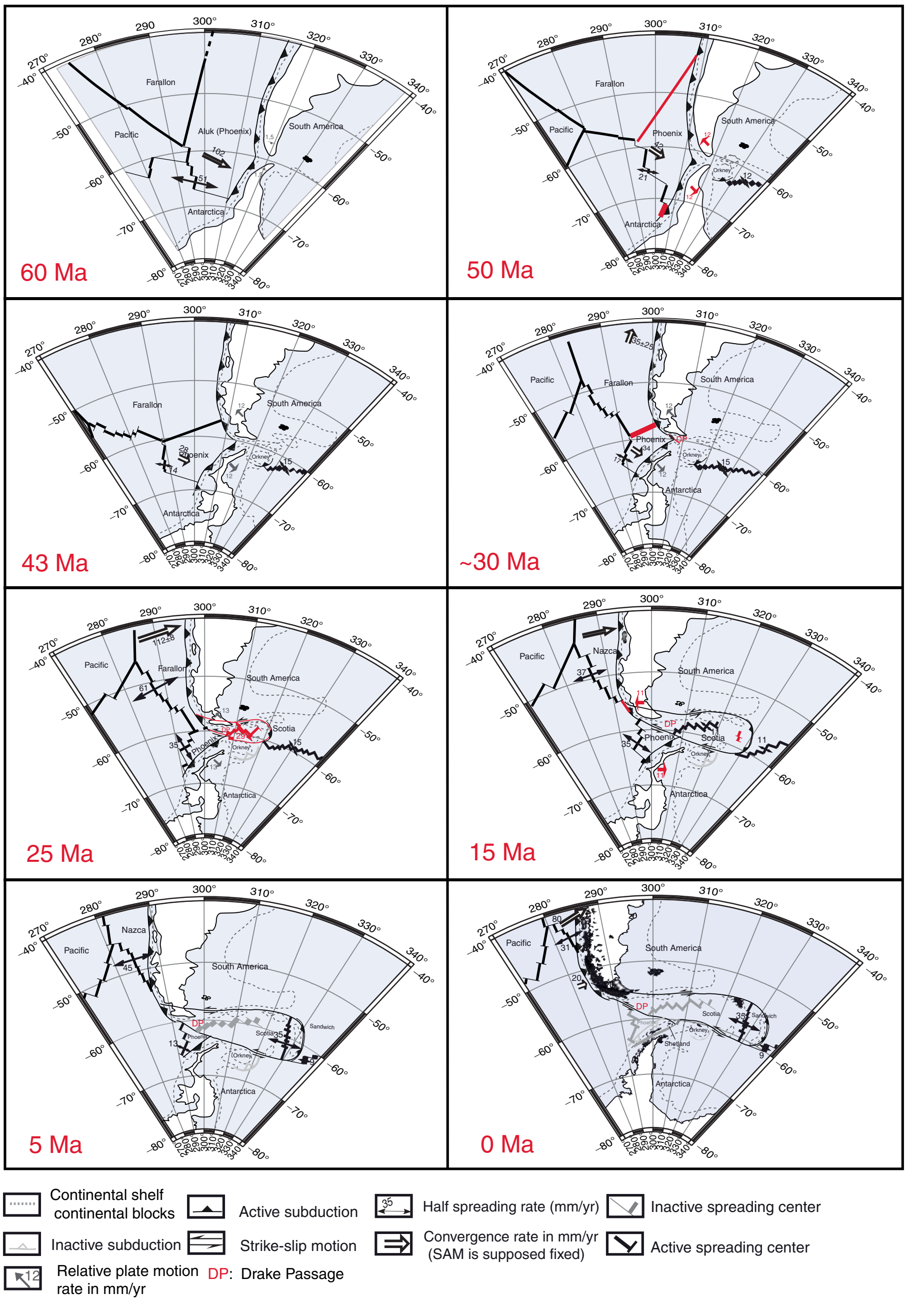

Fig. 2 Simplified kinematic reconstructions of the junction between the South American and Antarctic Peninsulas since 60 Ma, emphasizing the relationships between the subductions of numerous active spreading ridges, the migrations of several triple junctions and the onset of oceanic spreading within the Scotia Sea region. These reconstructions are based on a compilation of plate kinematic models available for the region. The South American plate is considered fixed

and Antarctica increased from 3 to 24 km/Ma, and was oriented WNW-ESE (Livermore et al., 2005), causing small continental blocks to detach from the continental shelf near the South American and Antarctic peninsula junction (Fig. 2). A decrease in the Phoenix plate convergence rate to 42 mm/a occurred as a segment of the Phoenix-Antarctic active spreading center approached the Antarctic trench (McCarron and Larter, 1998).

Around 43 Ma, dislocation between South America and Antarctica continued. The Farallon-Phoenix spreading center was still subducting beneath the South American plate and migrating southwards. The Phoenix plate was converging on the Antarctic Peninsula at a rate of 28 mm/a (McCarron and Larter, 1998) (Fig. 2).

The Oligocene was characterized by the onset of oceanic spreading in the Scotia Sea, along the West Scotia spreading center (oldest anomalies at 30 Ma; e.g., Eagles et al., 2003, 2005; Lawver and Gahagan, 2003; Livermore et al., 2005, 2007) (Fig. 2). A significant change in the convergence rate and direction of the Nazca (ex-Farallon plate) plate with respect to South America occurred in this period: the earlier rate of 35 ± 25 mm/a at 40 Ma increased to 112 ± 8 mm/a at 25 Ma (Pardo-Casas and Molnar, 1987), and the plate underwent clockwise rotation of about 70°, with a new convergence direction of N90° (Pardo-Casas and Molnar, 1987). These changes led the South Chile Ridge to lie near the Chile trench, in a slightly oblique position. The Farallon-Phoenix-South American triple junction reached Tierra del Fuego in the Early Oligocene; this event was followed by the cessation of Phoenix-Farallon spreading center activity (Fig. 2).

The subduction of southern segments of the South Chile Ridge at 15–14, 14–13, 12, 6, 3, and 0.3 Ma (Herron et al., 1981; Cande and Leslie, 1986; Cande et al., 1987; Nelson et al., 1994; Tebbens and Cande, 1997; Tebbens et al., 1997) progressively buried at depth, led to the opening of a large slab window beneath Patagonia (Fig. 4) (Ramos and Kay, 1992; Gorring et al., 1997; Gorring and Kay, 2001).

This complex evolution, which implies the subduction of various spreading ridges since 60 Ma, obviously had a significant effect on various characteristics of the mantle convecting beneath this region. Disruption of the Antarctic-Patagonian connection and rapid seafloor spreading in the Scotia region may be viewed as consequences of this evolution. The successive migration of two spreading centers beneath southern South America also left a clear volcanic mark along the Patagonian Cordillera, including a very large gap in Cenozoic typical calc-alkaline products, the development of basaltic plateau basalts (50 Ma to Present), and the occurrence of a volcanic arc of adakitic edifices outlining the Antarctic edge of the current slab window (Hole and Larter, 1993; Stern and Kilian, 1996; Stern, 2004; D'Orazio et al., 2005) (Fig. 4).

3 Subduction of the South Chile Ridge: Geological Records from the Patagonian Cordillera

Since the Late Paleozoic, the western margin of South America has been characterized by eastward subduction of oceanic crust (Bell and Suarez, 2000). As a consequence, Jurassic subduction-related acidic volcanics and volcanosedimentary rocks of the Ibañez Group unconformably overlie the Paleozoic basement rocks. The western part of the Patagonian belt is characterized by exposures of Patagonian Batholith calc-alkaline granitoids, which were emplaced over a continuum subduction environment from the Late Jurassic to the Cretaceous (Pankhurst et al., 2000; Suarez and de la Cruz, 2001) and were exhumed during the Cenozoic (Thomson et al., 2001).

In the following section, we detail the major sedimentary, magmatic and tectonic features of the Central Patagonian Cordillera, focusing particularly on the internal part and eastern side of the belt. These features represent geologic records related to pre-ridge subduction to ridge subduction stages of the Cordillera, over the period 30–0 Ma.

3.1 Sedimentary Records from the Central Patagonian Cordillera

South of 45°S, Cenozoic sedimentation is represented by foreland molasse deposits and internal inverted basins that are roughly the same age along strike (Fig. 3). All records from regions north of the Tierra del Fuego are consistent with a major constriction of the Cordillera before Chile Ridge subduction, that is 30–14 Ma (Marenssi et al., 2003; Lagabrielle et al., 2004). Three main steps in the development of the Cenozoic clastic sequences can be described.

In a first step, Patagonia experienced generalized regression that initiated during the Late Eocene-Early Oligocene, related to the onset of uplift due to first compressional events in the Cordillera. The maximum of this phase, characterized by the deposition of clastic continental sequences in the proto-Cordillera, occurred around 30 Ma. Such a clastic sequence is clearly observed in the internal part of the Central Patagonian belt, south of Lake General Carrera Buenos Aires, in the tectonically inverted Cosmelli basin

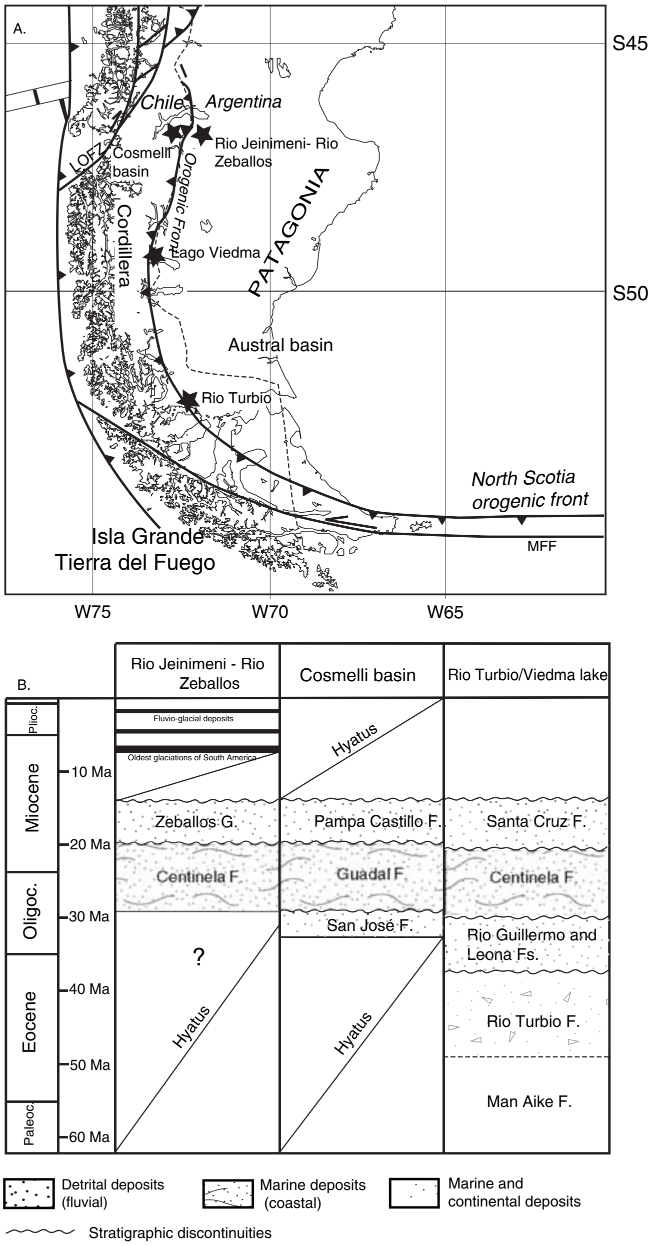

Fig. 3 **(a)** Simplified map of Central and Southern Patagonia showing key-localities (black stars) used to synthesize the main sedimentary records discussed in the text. MFF: Magallanes-Fagnano Fault. **(b)** Simplified stratigraphic sections of some key-localities located in Figure A. The orogenic front between central Patagonia and Tierra del Fuego is also shown

(Flint et al., 1994) where it corresponds to the San José Formation (Fig. 3).

In a second step, an important transgressive phase occurred during the Late Oligocene and Early Miocene (29–20 Ma), in which all of southern Patagonia was invaded by the *Patagoniano Sea*, including regions now located in the core of the belt, close to the Pacific coast. This stage of relative high sea-level is typically recorded by the Centinela Formation (Fig. 3), characterized by fossiliferous, shallow-water, coastal sediments, well exposed in the foothills region of Patagonia (Santa Cruz Province). It is best explained by foreland basin subsidence due to flexural response to crustal thickening in the western Cordillera. In the Cosmelli basin, this marine sequence corresponds to the Guadal Formation deposited from Late Oligocene to Early Miocene (Fig. 3), and overlies the San José Formation (Flint et al., 1994). The Guadal Formation often shows contractional syn-sedimentary deformation, such as internal thrusts and duplex systems.

In a third step, continuous shortening and uplift of the Cordillera led to a shift from shallow marine to renewed continental fluvial conditions, still recording an important outflow of detrital sediments. These voluminous erosional products now form the well-known Santa Cruz Formation of the Patagonian foothills of Argentina (Fig. 3). An equivalent of the Santa Cruz Formation, the Pampa Castillo Formation (Fig. 3), is exposed in the Cosmelli basin and includes terrestrial sandstones, claystones, and minor conglomerates. The transition from the Guadal to the Pampa Castillo Formation marks the withdrawal of the middle Cenozoic Patagonia seaway after it reached its maximum northward and westward extents (Flynn et al., 2002). At the latitude of the CTJ, the morphotectonic front of the belt exposes continental beds of the Rio Zeballos Group, which correspond to the Santa Cruz Formation (Fig. 3). In the Rio Jeinimeni-Rio Zeballos valleys, the Rio Zeballos Group stratigraphically overlies the Centinela Formation. This consists of a 1500 m thick sequence of fluvial sandstones, siltstones, and conglomerates that record rapid erosion of uplifted relief (Escosteguy et al., 2002). At Cerro Zeballos, at the head of Rio Zeballos, these sandstones are capped by lava flows dated to 16 and 14 Ma (Espinoza et al., 2006). South of the Lake General Carrera Buenos Aires, the sub-horizontal basal flows of the volcanic meseta Lago Buenos Aires, dated around 12 Ma (Guivel et al., 2006), rest unconformably over these deposits, confirming that erosion and compressional tectonics ceased completely between 14 and 12 Ma (Lagabrielle et al., 2004).

South of Lake General Carrera Buenos Aires, in the Lake Cochrane-Pueyrredon region, the continental deposits of the Santa Cruz Formation are represented by clastic fluvial deposits dominated by sand-, silt- and claystone beds locally with conglomerates, resting on the Centinela Formation (Fig. 3). The age of the Santa Cruz Formation in this region has been constrained to be between 22 and 14 Ma by tuffaceous deposits (Blisniuk et al., 2005).

The overall stratigraphy of the Cenozoic detrital formations exposed in Central Patagonia is very close to the successions exposed in more southern Patagonian regions. South of 50°S, in the southwestern corner of the Santa Cruz province, the Rio Turbio Formation of Middle Eocene age comprises marine and terrestrial sandstones and conglomerates. It is followed by the Rio Guillermo and Rio Leona fluvial deposits (Upper Eocene-Lower Oligocene), equivalent to the San Jose Formation (Fig. 3). These continental sequences are unconformably overlain by the marine Centinela Formation. Isotopic dating of oysters and Ar/Ar data yield ages between 27 and 20 Ma for the Centinela Formation (Parras et al., 2004; Guerstein et al., 2004), thus dating the major Cenozoic transgression in all Patagonia. A similar succession is found in the Viedma Lake region (Marenssi et al., 2003) (Fig. 3).

The Patagonian Cordillera is also characterized by a complex succession of Upper Miocene to Quaternary glacial deposits (Fig. 3). Some of these, dated between 7 and 3 Ma, are still preserved as tills interbedded within lava flow successions of Meseta Lago Buenos Aires or close to it (Mercer and Sutter, 1982; Lagabrielle et al., 2007). A complete review of such deposits is beyond the scope of this paper.

3.2 Volcanic and Plutonic Records of the Central Patagonian Belt

The volcanic-plutonic history of the Patagonian Cordillera at the latitude of the CTJ is characterized by successive magmatic events related to the successive subduction of two active spreading ridges, the Farallon-Phoenix (Aluk) ridge and the Chile Spreading Ridge.

South of the Lake General Carrera Buenos Aires, the Meseta Chile Chico (2160 m a.s.l, Fig. 4) exposes a Cenozoic succession unconformably overlying the Jurassic volcanic rocks of the Ibanez Group (Suarez and de la Cruz, 2000; Suarez et al., 2000a, b). This succession, 1000 m thick, consists of: a) Late Paleocene-Eocene basalts with alkaline and sub-alkaline tholeiite affinities (OIB signature, Espinoza, 2003) dated to 57–34 Ma (Charrier et al., 1979; Petford et al., 1996; Flynn et al., 2002); these overlie late Paleocene-Lower Eocene fluvial deposits and are related to a slab window that opened during the older Farallon-Aluk ridge subduction (Espinoza, 2003); and b) Late Miocene to Pliocene basalts overlying Late Oligocene-Early Miocene marine sediments of the Guadal Formation. These basaltic flows are 400 m thick and have alkaline and sub-alkaline affinities; they give K/Ar ages ranging between 4. ± 0.8 and 9.8 ± 0.1 Ma (Espinoza et al.,

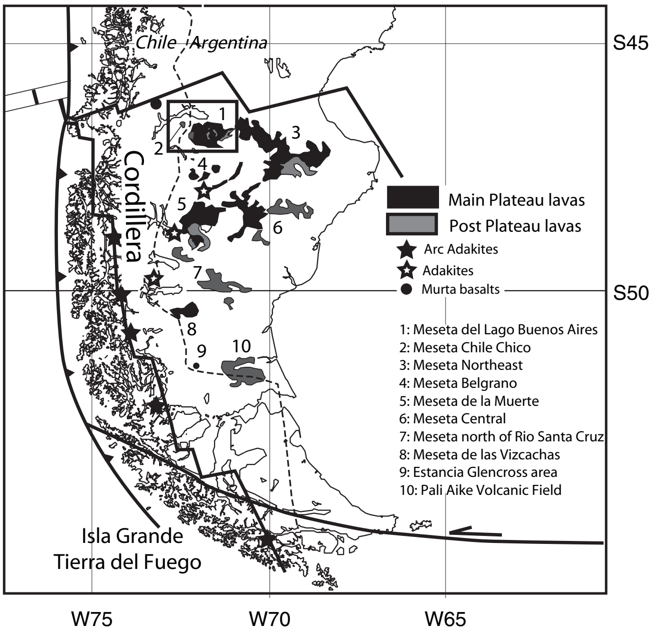

Fig. 4 Simplified map of Central and Southern Patagonia showing the distribution of Cenozoic Patagonian lavas: Main Plateau (black) and Post Plateau lavas (grey). The map also shows the location of the Patagonian adakites (*black and white stars*) and the Murta Quaternary basalts (*black circle*). The predicted extent of the Patagonian slab window is represented by black lines (after Breitsprecher and Thorkelson, submitted). *MFF* Magallanes-Fagnano Fault. The black frame delineates the area of Fig. 5

2003) (Figs. 5a, b). These are related to the subduction of the South Chile Ridge and were probably connected to lava flows of the Meseta Lago Buenos Aires, located some km to the southeast. The youngest flows of Meseta Chile Chico correlate with basaltic flows exposed on the poorly known Avellanos paleo-surface, which dominates the northern side of Lake General Carrera Buenos Aires (Lagabrielle et al., 2007).

At the morphotectonic front of the Central Patagonian belt, a basaltic flood volcanism event post-dates a period of intense peneplanation of the tectonic front (Lagabrielle et al., 2004). The remnants of these flows now form large basaltic plateaus or mesetas that morphologically dominate the eastern pampa region. The largest plateau in Central Patagonia is the flat-topped Meseta del Lago Buenos Aires (MLBA; Figs. 4–5), mainly formed by a first-stage OIB-like basaltic magmatism dated from 12.4 to 5 Ma (Main-Plateau basalts, Gorring et al., 1997; Guivel et al., 2006). Sporadic volcanic activity occurred later, as shown by numerous scoria cones, maars and lava flows younger that 5 Ma emplaced over the Miocene basalts (Post-Plateau basalts; Gorring et al., 2003; Brown et al., 2004; Guivel et al., 2006, Fig. 5b). Flows are interbedded with fluvial deposits and glacial sediments, confirming that basalts were emplaced along a main drainage area that is now topographically inverted. This later volcanism event is thought to be the expression of opening of a slab window due to the presence of subducted segments below them (Gorring et al., 2003). However, discrepancies between the ages of the oldest flows (around 12 Ma) and the date of the onset of migration of the subducted segment of the South Chile Ridge at the latitude of the Meseta Lago Buenos Aires led some authors to propose a model involving slab tear within the Nazca plate prior to ridge subduction (Guivel et al., 2006).

More recently, the northern side of Lake General Carrera Buenos Aires was marked by the emplacement of the Murta Quaternary E-MORB type basalts (Fig. 4). The source of these basalts has clear affinities with oceanic mantle (Demant et al., 1998; Guivel et al., 2006), confirming the presence of an opened slab window below the region. Only a few km to the NW of the Murta basalts, the Cerro Hudson active arc-volcano is the southernmost volcano of the South Volcanic Zone and represents the limit of the volcanic arc gap (Stern and Kilian, 1996; Stern, 2004). Due to the presence of relatively primitive basaltic magmas forming the lower part of this edifice, this volcano has also been interpreted as a consequence of opening of a slab window related to the subduction of a young segment of the South Chile Ridge (Gutiérrez et al., 2005).

Numerous examples of large volcanic fields related to slab window development are also observed south of the latitude of the CTJ. First, immediately south of

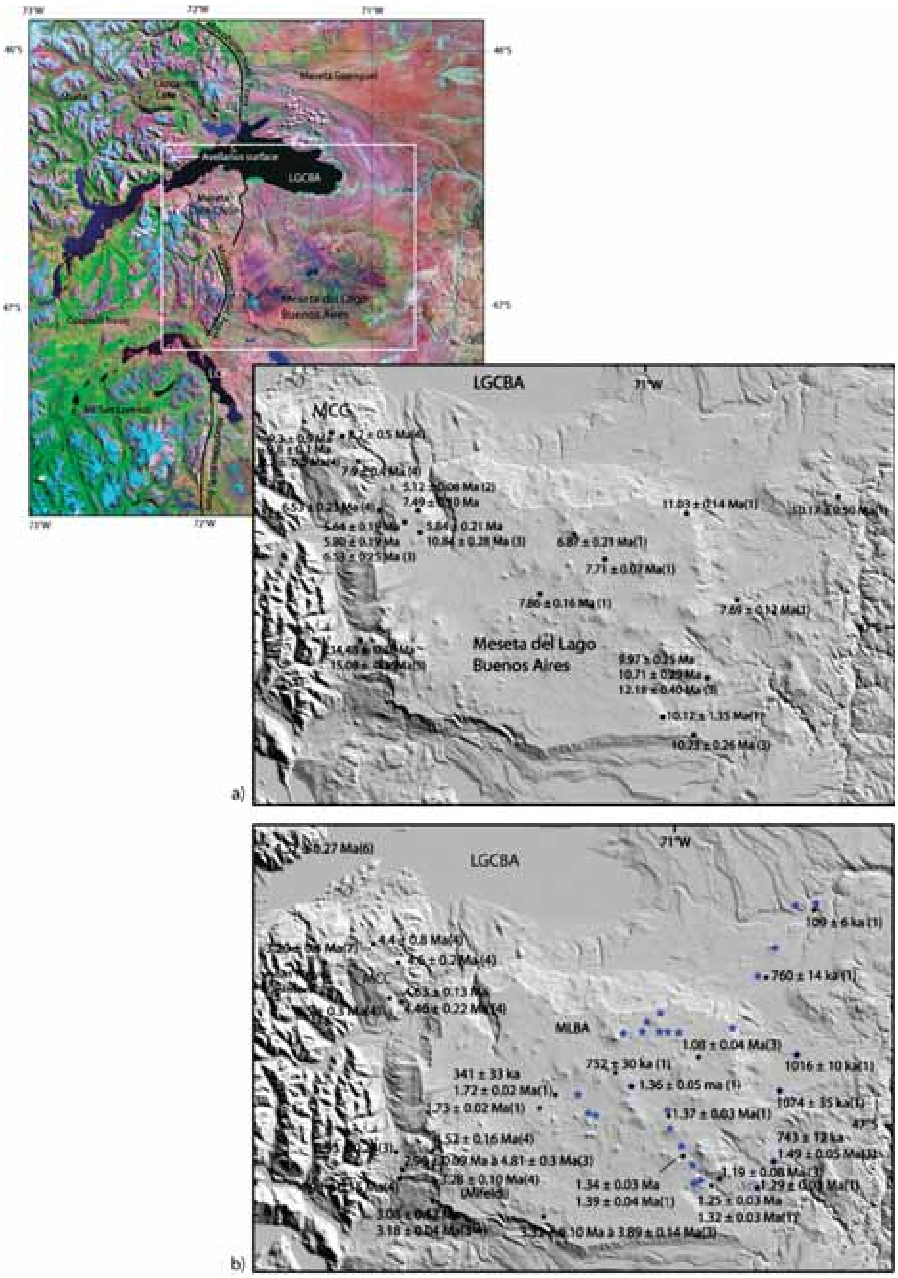

Fig. 5 Landsat 7 image of the internal part of Central Patagonia at the latitude of the Chile Triple Junction (see location in Fig. 4) and a compilation of published ages of volcanic rocks shown on a DEM of the Meseta del Lago Buenos Aires region (after Scalabrino et al., in preparation). Main Plateau **(a)** and Post Plateau **(b)** volcanics are shown separately. Black dots in Figure (a) correspond to dated samples. The origin of data is marked as numbers in brackets after each age, as follows: (1) Brown et al., 2004; (2) Mercer and Sutter, 1982; (3) Guivel et al., 2006; (4) Espinoza et al., 2005; (5) Espinoza, 2003; (6) Pelleter, 2003; (7) Suarez et al., 2000b. Grey stars in Figure (b) are the locations of the Pliocene-Pleistocene Post-Plateau lavas studied by Gorring et al., (1997). LGCBA Lake General Carrera Buenos Aires, MLBA Meseta del Lago Buenos Aires, MCC Meseta Chile Chico

the Meseta Lago Buenos Aires, around 48–49°S, four plateau lavas are present: Meseta Northeast, Meseta Central, Meseta de la Muerte, and Meseta Belgrano (Fig. 4). These all exhibit a typical bi-modal succession, including: a) Late Miocene to Early Pliocene tholeiitic voluminous main plateau sequences with whole rock Ar/Ar ages ranging from 13.88 ± 0.32 to 4.99 ± 0.11 Ma (Gorring et al., 1997), and b) Latest Miocene to Plio-Pleistocene alkaline minor post-plateau lava sequences dated from 6.22 ± 0.09 to 1.96 ± 0.16 Ma (Gorring et al., 1997). D'Orazio et al. (2000, 2001, 2005) found similar plateau lavas sequences exposed between 50°S and 52°S (Fig. 4). The tholeiitic main plateau lavas are located close to the Estancia Glencross (at around 52°S) and exhibit ages between 9.02 ± 1.03 and 7.34 ± 1.01 Ma, while alkaline post-plateau lavas of the Camusu Aike Volcanic Field located on the northern side of Glencross meseta give Ar/Ar ages between 2.95 ± 0.06 and 2.51 ± 0.09 Ma. Further south, in the Pali Aike volcanic field, alkaline to sub-alkaline basalts give Ar/Ar ages of 3.78 ± 0.17–0.17 Ma (Mercer, 1976; Linares and Gonzalez, 1990; Meglioli, 1992; Singer et al., 1997; Corbella, 1999). It has been suggested that these southernmost Patagonian mesetas are related to the recent widening of the slab window beneath the South American plate (D'Orazio et al., 2000, 2001, 2005).

Various plutonic bodies also characterize the internal Patagonian belt near 47°S. First, a Tertiary pluton crops out at the summit of the Monte San Lorenzo, forming the second highest peak in Patagonia (3706 m a.s.l), which yields biotite K/Ar ages of 6.6 ± 0.4 Ma (Welkner, 1999; Suarez and de la Cruz, 2000). On the southern coast of the LGCBA, a young pluton crops out in the Paso Las Llaves, which gives biotite Ar/Ar dates of 9.6 ± 0.5 and 9.6 ± 0.4 Ma (Petford and Turner, 1996), a Rb/Sr isochron of 10.3 ± 0.4 Ma (Pankhurst et al., 2000), a biotite K/Ar age of 10 ± 1.1 Ma (Suarez and de la Cruz, 2000) and a zircon fission track date of 9.7 ± 0.4 Ma (Thomson et al., 2001). The Las Nieves plutonic body crops out close to the Meseta Chile Chico (Fig. 5b), and gives a biotite K/Ar age of 3.2 ± 0.4 Ma (Suarez et al., 2000a, b) and an apatite fission track date of 4.3 ± 0.7 Ma (Morata et al., 2002). Recently, a small alkaline body exposed on the western side of the meseta del Lago Buenos Aires, the Mifeldi pluton, gave a whole rock K/Ar age of 3.28 ± 0.1 Ma (Espinoza et al., 2005) (Fig. 5b). These Pliocene plutons have been interpreted as the result of a thermal anomaly linked to slab window development. Fast exhumation of the Mifeldi pluton may be a consequence of tectonic activity and rapid erosion of an important lineament running along the Patagonia front, the Rio Zeballos fault zone (Lagabrielle et al., 2004, 2007).

3.3 Tectonic Records from the Central Patagonian Cordillera

From the CTJ to north of the Tierra del Fuego, the morphotectonic segments of the Patagonian Cordillera are 20–100 km long and more often show right lateral offset (Ramos, 1989; Coutand et al., 1999; Diraison et al., 2000; Thomson et al., 2001; Lagabrielle et al., 2004) (Figs. 1–6). As reported above, it has been suggested that the first stage of constriction of Central Patagonia started close to the Eocene-Oligocene boundary (32–24 Ma) (e.g., Marenssi et al., 2003). To the south, in Southern Patagonia or in the Fuegian Andes, the tectonic history of the belt is different because of the presence of an old back-arc basin with a mafic sea-floor (Rocas Verdes basin) (Dalziel, 1981; Ramos 1989, 2005; Ghiglione and Ramos, 2005). The Southern Andean foothills correspond to a thin-skinned fold and thrust belt built up from the Late Cretaceous (closure of Rocas Verdes basin) (Dalziel, 1981) to the Late Miocene (Kraemer et al., 1998; Coutand et al., 1999). Later, this portion of the Patagonian belt was affected by a major Neogene extensional phase affecting the Magallanes foreland, giving rise to graben systems (Diraison et al., 1997) (Fig. 6).

At the latitude of the CTJ, the eastern orogenic front is marked by a topographic jump of several hundred meters, due to an easterly vergent thrust system, juxtaposing internal Paleozoic and Mesozoic units of the main Cordillera over the Mesozoic-Cenozoic foreland deposits to the east (Ray, 1996; Suarez and de la Cruz, 2000; Lagabrielle et al., 2004). This compressive stage started at around 32 Ma, as shown by contractional syn-sedimentary deformation recorded by the fluvial deposits of the San Jose and Rio Leona Formations (Upper Eocene-Late Oligocene) and by marine sediments of the Guadal and Centinela Formations (Lower Oligocene-Early Miocene). As reported earlier, the change from continental to marine depositional environment is related to foreland basin subsidence due to flexural response to crustal thickening in the western

Cordillera. The ages of main uplift and exhumation of the central Patagonian Andes are confirmed by apatite and zircon fission track ages that show accelerated denudation between 30 and 12–8 Ma and up to 200 km eastward migration of the locus of maximum denudation during this period (Thomson et al., 2001). The age of the frontal thrust is now well constrained by calc-alkaline flows dated at 16–14 Ma that conformably overlie the eroded upper beds of the Zeballos Group (Espinoza et al., 2006). Therefore, it appears that compressional tectonics ceased in Central Patagonia at around 14 Ma, which is the time when the South Chile Ridge entered the Chile trench.

During the Latest Miocene-Pliocene, the eastern foreland of the Patagonian Cordillera experienced an episode of relief inversion, revealed by the presence of relict planar surfaces capping the flat-topped mesetas (Avellanos surface, meseta Chile Chico, meseta Lago Buenos Aires, meseta del Guenguel). Before this event, the overall topography was smoother and not so deeply incised as the present-day (Lagabrielle et al., 2004). The transverse incisions of the General Carrera Buenos Aires and Cochrane-Pueyrredon lakes, the N-S oriented valleys paralleling the front of the Cordillera (Rio Jeinimeni and Rio Ghio valleys), and the tectonically-controlled depressed area in the core of the belt did not exist before 5–4 Ma (Lagabrielle et al., 2004; Scalabrino et al., 2007) (Fig. 6). An extensional or transtensional tectonic event occurred after 5 Ma, reactivating ENE and NNW-trending lineaments (Lagabrielle et al., 2007; Scalabrino et al., 2007). Faults are well-observed west and south of meseta Lago Buenos Aires (Fig. 6) as well as on the edges of the Cenozoic inverted pop-down Cosmelli basin. These faults have a complex polyphase history and can be interpreted as back-arc extensional fault that controlled the Cretaceous basins, were slightly inverted during the Late Oligocene-Middle Miocene compressional stage, and have been partially reactivated with a normal to strike-slip component since 5 Ma (Scalabrino et al., 2007). However, since Patagonia was covered by thick ice sheets during the Pliocene-Quaternary glacial periods, the most obvious marks of recent tectonic activity have been erased by widespread glacial erosion. This explains why little evidence of recent active tectonics has been observed to date. The extensional regime that caused local to regional collapse of the belt and relief inversion in Central Patagonia was induced by possible weakening of the South American lithosphere in response to the presence of hot mantle at depth related to opening of a slab window (Lagabrielle et al., 2004, 2007). Such an extensional pattern related to a subducted ridge at depth was also shown by Garret and Storey (1987) in the Antarctic Peninsula.

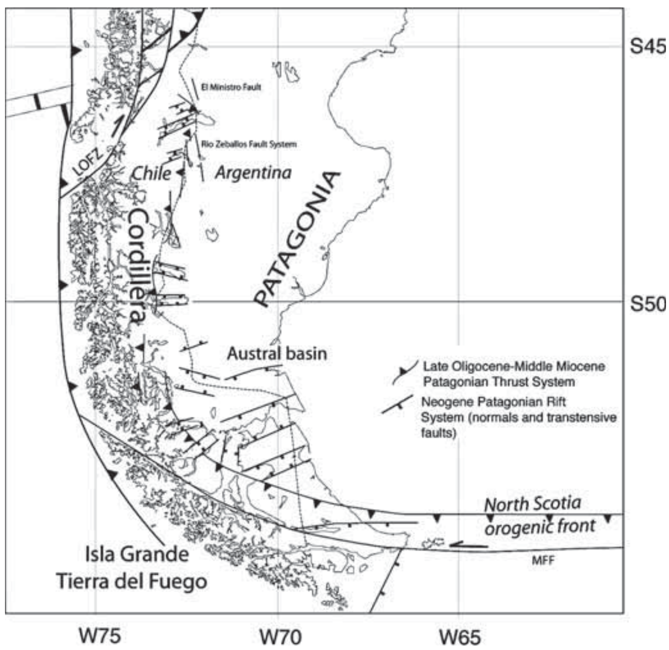

Fig. 6 Simplified structural map of Central and Southern Patagonia showing the main neotectonic features. Segments of the now inactive thrust system are represented by *grey lines*, while Neogene rift systems and extensional areas are marked by *black lines*. Data are compiled after: Ramos, 1989; Coutand et al., 1999; Diraison et al., 2000; Lagabrielle et al., 2004, 2007; Ghiglione and Ramos, 2005 and Scalabrino et al., in preparation *MFF* Magallanes-Fagnano Fault, *LOFZ* Liquine Ofqui Fault Zone

4 Subduction of the South Chile Ridge and Its Impact on the Patagonian Cordillera at the CTJ Latitude: A Six-stage Evolution

In this section, we summarize the onland effects of the subduction of successive segments of the South Chile Ridge in a chronological table for the period 30 Ma to Present (Fig. 7). This table includes tectonic, sedimentological, and magmatic features and is based on data collected over more than 10 years by our group, together with data from other workers.

- First stage (before 30 Ma): This represents the pre-ridge subduction stage. The convergence of the Nazca (ex-Farallon) plate is nearly frontal relative to the Chile trench. A shallow sea with cool water is locally present at the site of the current Patagonian Cordillera. During this period of "normal subduction," no significant magmatic and tectonic activity is observed, probably because of the remnant of a wide slab window due to southward migration of the Phoenix-Farallon spreading ridge before 30 Ma (Figs. 7–8).
- Second stage (around 25 Ma): The Patagonian Cordillera experiences onset of compressional deformation (syn-sedimentary deformation of upper marine sequences – Guadal formation, Fig. 7). This may be due to the increase of the Nazca convergence rate (35–112 mm/year; Pardo-Casas and Molnar, 1987), and the approach of the South Chile Ridge positive bathymetric high, causing increased tectonic coupling between the Nazca and South American plates.
- Third stage (20–15 Ma): A long segment of the South Chile Ridge is very close to the Chile trench (Figs. 7–8). An increase in tectonic coupling causes uplift and compression in the internal Cordillera. During this period, sedimentation shifts from marine to continental deposits (Upper Guadal and Galera formations, fluvial humid to arid, Fig. 7) and easterly vergent frontal thrust systems bring external units over molasse deposits.
- Fourth stage (16–14 Ma): The tip of a segment of the South Chile Ridge enters the Chile trench at around 55°S. In the Patagonian Cordillera, compression resumes and a major phase of erosion results in the rapid peneplanation of a wide frontal part belt on its eastern side (Fig. 7). Very scarce calc-alkaline volcanic lavas erupt (Cerro Zeballos) with a transition to the first alkaline flows that are emplaced on the eastern side of the Cordillera, over the eroded surface.

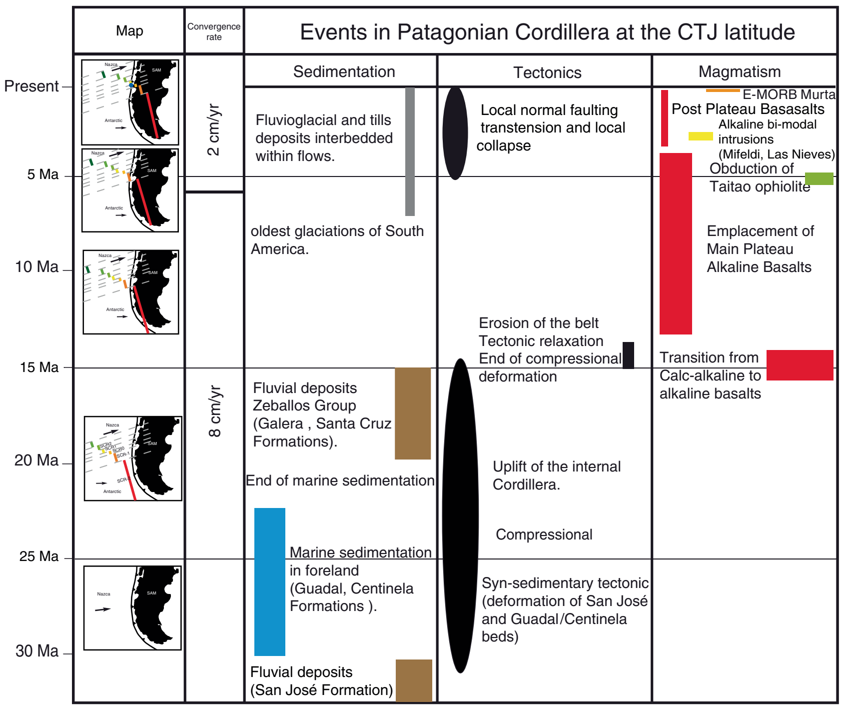

Fig. 7 Chronological table including the main sedimentary, tectonic and magmatic events of the Patagonian Cordillera at the latitude of the CTJ, from 30 to 0 Ma, in relation to the plate tectonic settings (left column)

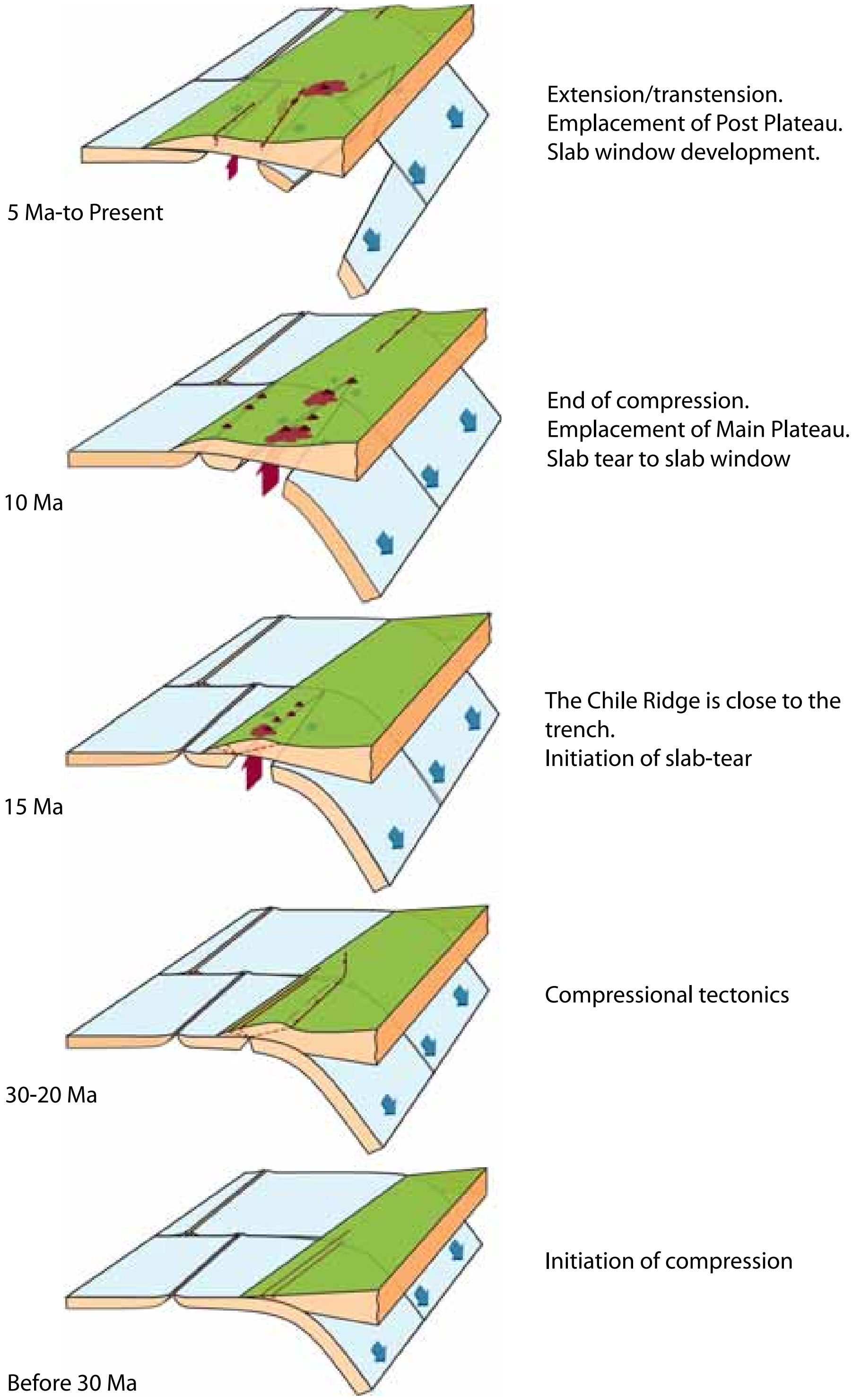

Fig. 8 Simplified geodynamical models showing the six main stages of the evolution of the Patagonian Cordillera, including opening of a slab-tear-related to true slab window during the subduction of the active Chile spreading ridge

– Fifth stage (15 to 5–4 Ma): On the Pacific side of the belt, the coastal domain is dominated by the obduction of the Taitao ophiolite units related to the collision of a segment of the South Chile Ridge (Lagabrielle et al., 2000, Anma et al., 2006). The eastern Patagonian Cordillera records the main magmatic activity, characterized by the emplacement of the largest alkaline plateau basalts (Meseta del Lago Buenos Aires; Meseta Chile Chico, Figs. 7–8). This event is likely linked to the development of a tear in the Nazca slab (Fig. 8), which is a consequence of an increase in tectonic coupling during the ridge-trench collision (Guivel et al., 2006) that occurred before the opening of the "normal" slab window. The main plateau flows are interbedded with fluvioglacial materials, showing that glaciers were flowing on an eastward paleoslope that is now highly dissected and topographically inverted. During this period, no significant tectonic activity is known in the Cordillera domain.
– Sixth stage (5–4 Ma to Present): The main plateau basalt volcanism ceases with a change to post-plateau volcanic activity. This volcanic change is followed by the emplacement of alkaline plutonic bodies in the western flank of the meseta Lago Buenos Aires, and locally in the internal belt (Fig. 7). The consequences of a transtensional/extensional phase are local collapse of the belt and the development of deep depressions in the axial part of the belt. We suggest that the tectono-magmatic activity recorded from 5 to 4 Ma to Present is closely linked to the development of an asthenospheric slab window beneath the study area (Fig. 8). Emplacement of the Murta basalts in the bottoms of Quaternary glacial valleys confirms that a hot "oceanic" mantle is present beneath the axis of the Patagonian belt at the latitude of the CTJ.

5 Discussion and Conclusions

Subduction of active spreading ridges occurs at relatively few locations along present-day active margins worldwide. However, due to plate motions and migrations of triple junctions, interaction between subducting ridges and continents has drastically modified long portions of the circum-Pacific margin during the Cretaceous and Tertiary. Modern triple junctions that include a ridge along the Pacific margin are of three types: (1) ridge-trench-trench (RTT): British Columbia, Woodlark, Antarctica and Chile Triple Junctions, (2) ridge-trench-transform (RTTr): Rivera Triple Junction, and (3) trench-transform-transform (TTT): Mendocino and Panama Triple Junctions.

Studies of ancient systems that may expose mid-crustal rocks provide important perspectives on the long-term temporal evolution of a ridge subduction event. However, it is necessary to investigate modern examples of ridge subduction because robust links can be established between magmato-tectonic manifestations at the surface and well-constrained locations of slab windows at depth. In the case of the Chile triple junction, the entire region of the Patagonia-Antarctic connection is characterized by a strong thermal anomaly due to successive subduction of various spreading ridges, as summarized by our reconstructions in Fig. 2. Global models show that a thin lithosphere is present beneath southern South America and Antarctica (Artemieva, 2006) and that a region of abnormal heat flow is present in the Patagonia-Antarctic connection (Shapiro and Ritzwoller, 2004). The development of a slab window beneath all of Patagonia is proven or suggested by a number of geophysical data, including a gap in seismic activity along the Chile trench south of 46°S, a region of abnormally hot mantle revealed by seismic tomography (Heintz et al., 2005) and abnormal terrestrial heat flow values along the Patagonian Andes (Hamza and Munoz, 1996). Figure 9 compiles data showing the extent of the thermal anomaly at the scale of the Antarctic-Patagonian region.

Geological records from ancient triple junctions implying ridge subduction, such as Alaska and Japan during the Late Cretaceous and Tertiary, show that the various components of subduction have changed through time. Therefore, long term variations in the configurations of subduction parameters are expected in these complex tectonic settings. Table 1 gives a summary of the major geological features linked to the subduction of active spreading ridges beneath Alaska, Northern and Central America, Chile, Antarctica, Woodlark and Japan. This table summarizes data collected from review articles related to these type-localities. It shows that triple junction areas are first characterized by rapid shifts in kinematics inducing temporal and spatial variations in the structural history of the upper plate. The most common magmatic impacts of ridge subduction include a gap in normal orogenic volcanism, and back-arc magmatism with an alkalic signature. Such features are well expressed in southern Chile, where correlations can be

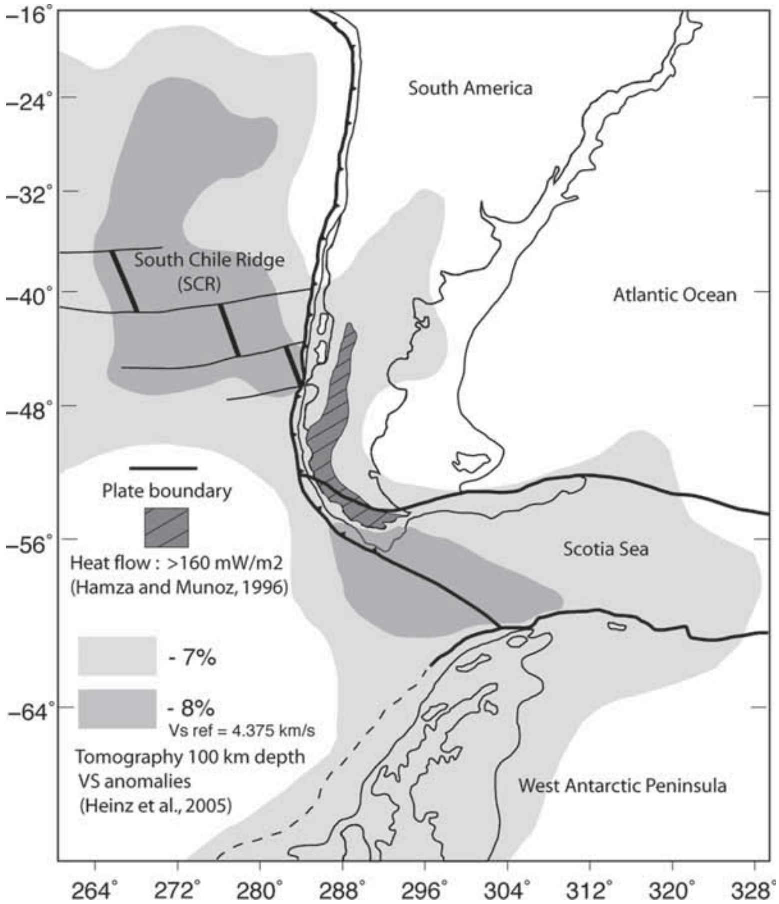

Fig. 9 Compilation map of SV wave heterogeneity at 100 km (red regions, after Heintz et al., 2005) and heat flow measurements in Central and Southern Patagonia (dashed region, after Hamza and Munoz, 1996)

Table 1 Summary of geological and geophysical impacts of Cretaceous to Present ridge subductions in the Circum-Pacific area

Geological processes	Characteristics	Some examples
Tectonics	Rapid shifts in kinematics in one region Temporal and spatial variations in structural history Extensional tectonism	Alaska and Northern America (Bradley et al. 2003). Antarctica Peninsula (Garret and Storey, 1987) South Chile (Lagabrielle et al. 2004, 2007; Scalabrino et al. this paper)
Magmatism	Abnormal near-trench volcanism Gap in normal arc magmatism Back-arc magmatism with alkalic signature localized N-MORB basaltic volcanism	Alaska and Northern America (Kusky et al. 2003; Sisson and Palvis, 1993; Sisson et al., 2003) California (Thorkelson et al., 1990; Cole and Basu, 1992, 1995) Woodlark (Johnson et al., 1987) Antarctica Peninsula (Hole and Larter, 1993) Japan (Hibbard and Karig, 1990, Maeda and Kagami, 1983) South Chile (Lagabrielle et al., 1994; Gorring et al., 1997; Guivel, 1999; Guivel et al., 2006, Espinoza et al., 2005, 2006)

(continued)

Table 1 (continued)

Geological processes	Characteristics	Some examples
Metamorphism	Low pressure/high temperature metamorphism Buchan series metamorphism	Japan (Osaozawa, 1992) Alaska and Northern Cordillera (Bowman et al., 2003; Zumsteg et al., 2003) South Chile (Bell and Suarez, 2000)
Others	Punctuated periods of tectonic erosion during ridge interactions Regional gold deposits Accretion of forearc ophiolites Strong gravimetry anomalies on the upper plate Seismic gap and abnormal hot mantle at depth	South Chile (Behrmann et al., 1994) Alaska (Haeussler et al., 1995, 2003) Chile (Lagabrielle et al., 2000; Anma et al., 2006) Alaska (Nelson and Forsythe, 1989; Kusky and Young, 1999) South Chile (Murdie et al., 2000) Japan (Sakagushi, 1996) South Chile (Hamza and Munoz, 1996; Murdie et al., 2000; Heintz et al., 2005; Artemieva, 2006) and Antarctica (Shapiro and Ritzwoller, 2004)

established between the migration of the Chile triple junction along the trench since 15 Myr, the age of the alkalic magmatism, and the timing of deformational events. Our review of records from the central Patagonian foreland helps better constrain the consequences of the subduction of an active ridge on the geological evolution of the upper plate. Five features can be outlined:

1. During the Cenozoic, the Central Patagonia region shows a simple correlation of sedimentary and tectonic events. Cenozoic sedimentation can be simply explained by foreland subsidence followed by contractional tectonics and uplift of the belt during the pre-ridge subduction stage.
2. In Southern and Central Patagonia, compressional tectonics ceased around 14 Ma, when the active Chile ridge entered the Chile trench. This tectonic relaxation may have been induced by a drastic decrease in the tectonic coupling at the trench, inducing weakening of the horizontal forces that maintained active shortening.
3. The spatial and temporal distribution of Cenozoic Patagonian basaltic plateaus (main-plateau basalts) cannot be simply explained by slab window development beneath the South American plate. A slab tear model ahead of subducted spreading ridge segments has been proposed by Guivel et al. (2006), but alternative models may imply return of asthenospheric mantle flow such as that described for the Somuncura volcanic field in Northern Patagonia (41°S) (De Ignacio et al., 2001).
4. The limits of the slab window below Patagonia can be followed by the presence of the adakitic belt on the western side (e.g., Stern, 2004) and the basaltic mesetas on the eastern side. Recent extensional and transtensional tectonics in Central and Southern Patagonia record important changes in lithosphere rheology that occurred after subduction of the Chile Ridge. The areas where this new tectonic regime develops are likely to delineate the central region of the slab-window opened at depth; the same is true for the Pali-Aike field in southernmost Patagonia (Stern et al., 1990).
5. The Central Patagonia Cordillera is characterized by anomalous topography and the occurrence of several tectonically-controlled transverse depressions bounded by regions of high elevation, which is opposite of what is expected for an orogenic belt in a classical subduction context. This facet warrants further development, in particular because it is not clear whether a phase of doming existed before local collapse of transverse depressions. This is important as doming may be the only topographic consequence of slab window opening. However, previous studies in the Antarctica Peninsula and Alaska have reported extensional tectonics in the upper plate following ridge subduction (Garret and Storey, 1987; Bradley et al., 2003). Therefore, Central Patagonia should remain a suitable location to study the balance between coupling at the trench and vertical forces due to abnormal mantle at depth in controlling the topography of subduction-related mountain belts.

Acknowledgements This research was funded by grants from the Chilean-French ECOS-CONICYT program (project C05U01) and CNRS-INSU DyETI (France) program. We thank R. Stern and C. Faccenna for constructive and helpful reviews.

References

Anma, R., Armstrong, R., Danhara, T., Orihashi, Y., Iwano, H., 2006. Zircon sensitive high mass-resolution U-Pb and fission-track ages for gabbros and sheeted dykes of the Taitao ophiolite, Southern Chile, and their tectonic implications. Island Arc 15, 130–142.

Artemieva, I.M., 2006. Global 1°×1° therma model TC1 for the continental lithosphere: Implications for the lithosphere secular evolution. Tectonophysics 416, 245–277.

Bangs, N.L., Cande, S.C., Lewis, S.D., Miller, J.J., 1992. Structural framework of the Chile margin at the Chile Ridge collision zone. Proceedings of Ocean Drilling Program Initial Report 141, 11–21.

Bell, M., Suarez, M., 2000. The Rio Lacteo Formation of southern Chile. Late Paleozoic orogeny in the Andes of the southernmost South America. Journal of South American Earth Sciences 13, 133–145.

Behrmann, J.H., Leslie, S.D., Cande, S.C., 1994. ODP Leg 141 scientific party. Tectonics and geology of spreading ridge subduction at the Chile Triple Junction: a synthesis of results from Leg 141 of the Ocean Drilling Program. Geol. Rundsch, 83, 832–853.

Blisniuk, P.M., Stern, L.A., Chamberlain, C.P., Idleman, B., and Zeitler, P.K., 2005. Climatic and ecologic changes during Miocene surface uplift in the Southern Patagonian Andes. Earth Planet Sciences Letters, 230, 125–142.

Bowman, J.R., Sisson, V.B., Valley, J.W., Pavlis, T.L., 2003. Oxygen isotope constraints on fluid infiltration associated with high-temperature-low-pressure metamorphism (Chugach metamorphic complex) within the Eocene southern Alaska forearc. In Sisson, V.B., Roeske, S.M., and Palvis, T.L., eds., Geology of a transpressional orogen developed during ridge-trench interaction along the North pacific margin: Boulder, Colorado, Geological Society of America Special paper 371, p. 237–253.

Bradley, D., Kusky, T., Haeussler, P., Goldfard, R., Miller, M., Dumoulin, J., Nelson, S.W., and Karl, S., 2003. Geologic signature of early Tertiary ridge subduction in Alaska. In Sisson, V.B., Roeske, S.M., and Palvis, T.L., eds., Geology of a transpressional orogen developed during ridge-trench interaction along the North pacific margin: Boulder, Colorado, Geological Society of America Special paper 371, p. 19–49.

Brown, L.L., Singer, B.S., Gorring, M.L., 2004. Paleomagnetism and $^{40}Ar/^{39}Ar$ chronology of lavas from Meseta del Lago Buenos Aires, Patagonia. Geochem. Geophys. Geosyst. 5 (1), Q01H04. Doi:10.1029/2003GC000526.

Cande, S.C., Leslie, R.B., 1986. Late Cenozoic tectonics of the Southern Chile Trench. Journal of Geophysical Reseach 91, 471–496.

Cande, S.C., Leslie, R.B., Parra, J.C., Hobart, M., 1987. Interaction between the Chile ridge and the Chile trench: geophysical and geothermal evidence. Journal of Geophysical Research 92, 495–520.

Cembrano, J., Hervé, F., Lavenu, A., 1996. The Liquine-Ofqui fault zone: A long-lived intra-arc fault system in Southern Chile. Tectonophysics 259, 207–224.

Cembrano, J., Lavenu, A., Reynolds, P., Arancibia, G., Lopez, G., Sanhueza, A., 2002. Late Cenozoic transpressional ductile deformation north of Nazca-South America-Antarctica triple junction. Tectonophysics 354, 289–314.

Charrier, R., Linares, E., Niemeyer, H., Skarmeta, J., 1979. K-Ar ages of basalt flows of the Meseta Buenos Aires in the southern Chile and their relation to the Southeast Pacific triple junction. Geology 7, 436–439.

Cole, R.B., and Basu, A.R., 1992. Middle Tertiary volcanism during ridge-trench interactions in Western California. Science, 258: 793–796.

Cole, R.B., and Basu, A.R., 1995. Nd-Sr geochemistry and tectonics of ridge subduction and middle Cenozoic volcanism in Western California. Geological Society of America Bulletin, 18, 167–179.

Corbella, H., 1999. Dataciones radiometricas en Pali Aike, patagonia Austral In: XIV Congreso Geologico Argentino, Actas, II, 265–268.

Coutand, I., Diraison, M., Cobbold, P.R., Gapais, D., Rossello, E., 1999. Structure and kinematic of a foothills transect, Lago Viedma, southern Andes (49°30'S). Journal of South American Earth Sciences (Oxford) 12, 1–15.

Dalziel, I.W., 1981. Back-arc extension in the southern Andes: areview and critical reappraisal. Phil. Trans. R. Soc. Lond. A300, 319–335.

Demant, A., Belmar, M., Hervé, F., Pankhurst, R.J., Suarez, M., 1998. Pétrologie et géochimie des basaltes de Murta: une éruption sous-glaciaire dans les Andes patagoniennes (46°S). Relation avec la subduction de la ride du Chili. C. R. Acad Sci., Paris 327, 795–801.

DeMets, C., Gordon, A.E., Aegus, D.F., Stein, S., 1990. Current plate motions. Geophysical Journal International 101, 425–478.

Diraison, M., Cobbold, P.R., Gapais, D., Rossello, E.A., 1997. Magellan strait: Part of a Neogene rift system. Geology 25, 703–706.

Diraison, M., Cobbold, P.R., Gapais, D., Rossello, E.A., Le Corre, C., 2000. Cenozoic crustal thickening, wrenching and rifting in the foothills of the southernmost Andes. Tectonophysics 316, issue 1-2, 91–119.

De Ignacio, C., Lopez, I., Oyarzun, R., Marquez, A., 2001. The Northern Patagonia Somuncura plateau basalts: a product of slab-induced, shallow asthenospheric upwelling? Terra Nova, 13, 117–121, 2001.

D'Orazio, M., Agostini, S., Mazzarini, F., Innocenti, F., Manetti, P., Haller, M., Lahsen, A., 2000. The Pali Aike Volcanic Field. Patagonia: slab-window magmatism near the tip of South America. Tectonophysics 321, 407–427.

D'Orazio, M., Agostini, S., Innocenti, F., Haller, M., Manetti, P., Mazzarini, F., 2001. Slab-window-related magmatism from southernmost South America: The Late Miocene mafic volcanics from the Estancia Glencross area (~52°S Argentina-Chile). Lithos 57, 67–89.

D'Orazio, M., Innocenti, F., Manetti, P., Haller, M.J., Di Vincenzo, G., Tonarini, S., 2005. The Late Pliocene mafic lavas from the Camusù Aike volcanic field (~50°S,

Argentina): Evidence for geochemical variability in slab window magmatism. Journal of South American Earth Sciences 18, 107–124.
Eagles, G., 2003. Plate tectonics of the Antarctic-Phoenix plate system since 15 Ma. Earth and Planetary Science Letters, 88, 289–307.
Eagles, G., Livermore, R.A., Fairhead, J.D., Morris, P., 2005. Tectonic evolution of the west Scotia Sea. Journal of Geophysical Research, 11, B02401.
Escosteguy, L., Dal Molin, C., Franchi, M., Geuna, S., Lapido, O., 2002. Estratigrafia de la cuenca de los rios el Zeballos y Jeinimeni, noroeste de la Provincia de Santa Cruz. Actas del XV Congresso Geologico Argentino. El Calafate.
Espinoza, F., 2003. Petrologia y geoquimica de los basaltos cenozoicos de la meseta de Chile Chico, 46°35'S-46°47'S- 71°46'-72°02'W XI region de Aysen, Chile. Unpublished MSc thesis, Universidad de Chile, Santiago, Chile. 220 pp.
Espinoza, F., Morata, D., Pelleter, E., Maury, R.C., Suarez, M., Lagabrielle, Y., Polvé, M., Bellon, H., Cotten, J., de la Cruz, R., Guivel, C., 2005. Petrogenesis of the Eocene and Mio-Pliocene alkaline basaltic magmatism in Meseta Chile Chico, Southern Patagonia, Chile: evidence for the participation of two slab windows. Lithos 82 (3–4), 315–343.
Espinoza, F., Morata, D., Polvé, M., Maury, R.C., Cotten, J., Bellon, H., Guivel, C., Lagabrielle, Y., Suárez, M., and Rosselló, E., 2006. Mio-Pliocene magmatic variability in the central Patagonia back-arc region (47.5ªS). Backbone of the Americas – Patagonia to Alaska. Geological Society of America, Mendoza (Argentina), 3–7 Abril, CD-rom.
Flint, F.F., Prior, D.J., Agar, S.M., Turner, P., 1994. Stratigraphic and structural evolution of the tertiary Cosmelli basin and its relationships to the Chile Triple Junction. Journal of Geological society of London 151, 251–268.
Flynn, J.J., Novacek, M.J., Dodson, H.E., Frassinetti, D., McKenna, M.C., Norell, M.A., Sears, K.E., Swisher, C.C. III, Wyss, A.R., 2002. A new fossil mammal assemblage from the southern Chilean Andes: Implications for geology, geochronology and tectonics. Journal of Southern American Earth Sciences 15, 285–302.
Garret, S.W., Storey, B.C., 1987. Lithospheric extension on the Antarctica Peninsula during Cenozoic subduction. In Extension in the basin and Range Province and East Pacific Margin, Geological Society, London, Special Publications, v. 28, pp. 419–431.
Ghiglione, M.C., Ramos, V.A., 2005. Progression of deformation and sedimentation in the southernmost Andes. Tectonophysics 405, 25–46.
Gorring, M., Kay, S., 2001. Mantle processes and sources of Neogene slab window magmas from Southern Patagonia, Argentina. Journal of Petrology 42, 1067–1094.
Gorring, M., Kay, S., Zeitler, P., Ramos, V., Rubiolo, D., Fernandez, M., Panza, J., 1997. Neogene Patagonian plateau lavas: continental magmas associated with ridge collision at the Chile Triple Junction. Tectonics 16, 1–17.
Gorring, M., Singer, B., Gowers, J., Kay, S., 2003. Plio-Pleistocene basalts from the Meseta del Lago Buenos Aires, Argentina: evidence for asthenosphere-lithosphere interactions during slab-window magmatism. Chemical Geology 193, 213–235.
Gripp, A.E., Gordon, R.G., 1990. Current plate velocities relative to the hotspots incorporating the NUVEL-1 global plate motion model. Geophysical Research Letters 17, 1109–1112.
Guerstein, G.R., Guler, M.V., and Casadio, S., 2004. Polynostratigraphy and paleoenvironments across the Oligocene-Miocene boundary within the Centinela Formation, southwestern Argentina. Geological Society, London, Special Publications, 230, 325–343.
Guivel, C., Lagabrielle, Y., Bourgois, J., Maury, R.C., Fourcade, S., Martin, H., Arnaud, N., 1999. New geochemical constraints for the origin of ridge-subduction-related plutonic and volcanic suites from the Chile Triple Junction (Taitao Peninsula and site 862, LEG ODP141 on the Taitao Ridge). Tectonophysics 311, 83–111.
Guivel, C., Morata, D., Pelleter, E., Espinoza, F., Maury, R.C., Lagabrielle, Y., Polvé, M., Bellon, H., Cotten, J., Benoit, M., Suarez, M., de la Cruz, R., 2006. Miocene to Late Quaternary Patagonian basalts (46°-47°S): Geochronometric and geochemical evidence for slab tearing due to active spreading ride subduction. Journal of Volcanology and Geothermal Research 149, 346–370.
Gutiérrez, F., Gioncada, A., Gonzalez Ferran, O., Lahsen, A., Mazzuoli, R., 2005. The Hudson volcano and surrounding monogenetic centres (Chilean Patagonia): An example of volcanism associated with ridge-trench collision environment. Journal of Volcanology and Geothermal Research 145, pp. 207–233.
Haeussler, P.J., Bradley, D., Goldfarb, R., Snee, L., Taylor, C., 1995. Link between ridge subduction and gold mineralization in southern Alaska. Geology 23 (11), 995–998.
Haeussler, P.J., Dwight, C., Bradley, D., Goldfarb, R.J., 2003. Brittle deformation along the Gulf of Alaska margin in response to Paleocene-Eocene triple junction migration. In Sisson, V.B., Roeske, S.M., and Palvis, T.L., eds., Geology of a transpressional orogen developed during ridge-trench interaction along the North pacific margin: Boulder, Colorado, Geological Society of America Special paper 371, pp. 119–141.
Hamza, V.M., Munoz, M., 1996. Heat flow map of South America. Geothermics 25(6), 599–646.
Heintz, M., Debayle, E., Vauchez, A., 2005. Upper mantle structure of the South America continent and neighboring oceans from surface wave tomography. Tectonophysics 406, 115–139.
Herron, E.M., Cande, S.C., Hall, B.R., 1981. An active spreading center collides with a subduction zone; a geophysical survey of the Chile margin triple junction. Memoir-Geological Society of America 154, 683–701.
Hervé, F., 1994. The Southern Andes between 39°S and 44°S latitude: the geological signature of a transpressive tectonic regime related to a magmatic arc. In: Reutter, K-J., Scheuber, E., Wigger, P.J., eds., Tectonics of the Southern central Andes. Springer, Berlin, pp. 243–248.
Hibbard, J.P., Karig, D.E., 1990. Structural and magmatic responses to spreading ridge subduction: an example from southwest Japan. Tectonics 9 (2), 207–230.
Hole, M.J., Larter, R.D., 1993. Trench-proximal volcanism following ridge crest-trench collision along the Antarctic Peninsula. Tectonics 12, 897–901.

Johnson, R.W., Jaques, A.L., Langmuir, C.H., Perfit, M.R., Dunkley, P.N., Chappell, B.W., Taylor, S.R., 1987. Ridge subduction and forearc volcanism: petrology and geochemistry of rocks dredged from the western Solomon arc and Woodlark basin. 155–226.

Kraemer, P.E., 2003.Orogenic shortening and the origin of the Patagonian orocline (56° S.lat). Journal of South American Earth Sciences 15, 731–748.

Kusky, T.M., Young, C.P., 1999. Emplacement of the ressurection Peninsula ophiolite in the southernalaska forearc during a ridge-trench encounter. Journal of Geophysical Research, vol. 104, NoB12, p. 29.025–29.054.

Kusky, T.M., Bradley, D., Donley, D.T., Rowley, D., Haeussler, P., 2003. Controls on intrusion of near-trench magmas of the Sanak-Baranof Belt, Alaska, during Paleogene ridge subduction, and consequences for forearc evolution. In Sisson, V.B., Roeske, S.M., and Palvis, T.L., eds., Geology of a transpressional orogen developed during ridge-trench interaction along the North pacific margin: Boulder, Colorado, Geological Society of America Special paper 371, p. 269–292.

Lagabrielle, Y., LeMoigne, J., Maury, R.C., Cotton, J., Bourgois, J., 1994. Volcanic record of the subduction of an active spreading ridge, Taitao peninsula (southern Chile). Geology 22, 515–518.

Lagabrielle, Y., Guivel, C., Maury, R.C., Bourgois, Y., Fourcade, S., Martin, H., 2000. Magmatic-tectonic effects of high thermal regime at the site of active spreading ridge subduction: the Chile Triple Junction model. Tectonophysics 326 (3–4), 215–228.

Lagabrielle, Y., Suarez, M., Rossello, E.A., Hérail, G., Martinod, J., Régnier, M., de la Cruz, R., 2004. Neogene to Quaternary tectonic evolution of the Patagonian Andes at the latitude of the Chile Triple Junction. Tectonophysics 385, 211–241.

Lagabrielle, Y., Suarez, M., Malavieille, J., Morata, D., Espinoza, F., Maury, R.C., Scalabrino, B., Barbero, L., de la Cruz, R., Rossello, E., Bellon, H., 2007. Pliocene extensional tectonics in Eastern Central Patagonian Cordillera: geochronological constraints and new field evidence. Terra Nova in press.

Lawver, L.A., Gahagan, L.M., 2003. Evolution of Cenozoic seaways in the circum-Antarctic region. Palaeogeography, Palaeoclimatology, Palaeoecology 198, 11–37.

Linares, E., Gonzalez, R., 1990. Catalogo de edades radimetricas de la Republica argentina: 1957–1987, Publicaciones Especiales de la Asociacion Geologica Argentina, serie B, vol. 19, 628 pp.

Livermore, R., Nankivell, A., Eagles, G., Morris, P., 2005. Paleogene opening of Drake Passage. Earth and Planetary Science Letters, 236, 459–470.

Livermore, R., Hillenbrand, C.D., Meredith, M., Eagles, G., 2007. Drake Passage and Cenozoic climate: An open and shut case? Geochemistry, Geophysics, Geosystems 8, 1. Q01005, doi:10,1029/2005GC001224.

Maeda, J., and Kagami, H., 1996 Interaction of a spreading ridge and an accretionary prism: implications for MORB magmatism in the Hidaka magmatic zone, Hokkaido, Japan. Geology 24 (1), 31–34.

Marenssi, S.A., Casadio, S., Santillana, S.N., 2003. Estratigrafia y sedimentologia de las unidades del Cretacico superior-Paleogeno aflorantes en la margen sureste del lago Viedma, provincia de Santa Cruz, Argentina. Revista de la Asociacion Geologica Argentina 58 (3), 403–416.

McCarron, J.J., Larter, D.D., 1998. Late cretaceous to Early Tertiary Subduction history of the Antarctic Peninsula. Journal of Geological Society, London 155, 255–268.

Meglioli, A., 1992. Glacial geology and geochronology of southernmost patagonia and Tierra del Fuego, Argentina and Chile. Ph.D. dissertation. Leigh University, Bethlehem, PA, USA.

Mercer, J.H., 1976. Glacial history of southernmost South America. Quat. Res. 6, 125–166.

Melnick, D., Folguera, A., Roseneau, M., Echtler, H., Potent, S., 2002. Tectonics from the northern segment of the Liquine-Ofqui fault system (37°S-39°S), Patagonian Andes, paper presented at Fifth International Symposium of Andean Geodynamics, IRD, Toulouse, France.

Mercer, J.H., Sutter, J.F., 1982. Late Miocene-Earliest Pliocene Glaciation in Southern Argentina: implications for global ice-sheet history. Paleogeography, Paleoclimatology, Paleoecology 38, 185–206.

Morata, D., Barbero, L., Suarez, M., de la Cruz, R., 2002. Early Pliocene magmatism and high exhumation rates in the Patagonian Cordillera (46°40'S): K-Ar, and fission track data. ISAG.

Murdie, R., Styles, P., Prior, D.J., Daniel, A.J., 2000. A new gravity map of southern Chile and its preliminary interpretation. Revista Geologica de Chile 27 (1), 49–63.

Nelson, E.P., Forsythe, R.F., 1989. Ridge collision at convergent margins: implications for Archean and post Archean crustal growth. Tectonophysics 161, 307–315.

Nelson, E., Forsythe, R., Diemer, J., Allen, M., Urbina, O., 1994. Taitao ophiolite: a ridge collision ophiolite in the forearc of the southern Chile (46°S). Revista Geologica de Chile 20(2), 137–165.

Osazawa, A., 1992. Double ridge subduction recorded in the Shimanto accretionary complex, Japan, and plate reconstruction. Geology 20, 939–942.

Pankhurst, R.J., Riley, T.R., Fanning, C.M., Kelley, S.P., 2000. Episodic silicic = volcanism in Patagonian and Antarctic Peninsula: chronology of magmatism associated with break-up of Gondwana. Journal of Petrology 41, 605–625.

Parras, A., Casadio, S., Feldmann, R., Griffin, M., Schweitzer, C.E., 2004. Age and paleogeography of the marine transgression at the Paleogene-Neogene boundary in Patagonia, southern Argentina. Denver Annual Meeting, Geological Society of America Abstracts with programs 16(5), 364.

Pardo-Casas, F., Molnar, P., 1987. Relative motion of the Nazca (Farallon) and South America plates since Late Cretaceous time. Tectonics 6(3), 233–248.

Pelleter, E., 2003. Diversité géochimique et géochronologique des basaltes de la région du lac Général Carrera-Buenos Aires: nouvelles contraintes sur la subduction de la dorsale du Chili. Unpublished DEA Thesis; Université de Bretagne Occidentale, Brest, France.

Petford, N., Cheadle, M., Barreiro, B., 1996. Age and origin of southern flood basalts, Chile Chico region (46°45'S). Third International Symposium on Andean Geology (ISAG), St. Malo, France, 629–632 (extended abstract).

Petford, N., Turner, P., 1996. Reconnaissance 40Ar/39Ar age and paleomagnetic study of igneous rocks around Coyhaique,

S. Chile. Third International Symposium on Andean Geology (ISAG), St. Malo, France, 625–627.
Ramos, V.A., 1989. Andean foothills structures in the northern Magallanes Basin, Argentina. American Association of Petroleum Geologist Bulletin 73, 887–903.
Ramos, V.A., 2005. Ridge collision and topography: foreland deformation in the Patagonian Andes. Tectonophysics 399, 73–86.
Ramos, V., Kay, S.M., 1992. Southern Patagonian plateau basalts and deformation: backarc testimony of ridge collision. Tectonophysics 205, 261–282.
Ray, F.M., 1996. Stratigraphical and structural evolution of Tertiary backarc basins in Southern Chile. University of Liverpool, England, 208 pp; Unpublished Thesis.
Roseneau, M., Melnick, D., Echtler, H., 2006. Kinematic constraints on intra-arc shear and strain partitioning in the southern Andes between 38°S and 42°S latitude. Tectonics vol. 25, TC4013, doi:10.1029/2005TC001943.
Sakagushi, A., 1996. High paleogeothermal gradient with ridge subduction beneath the cretaceous Shimanto accretionary prism, southwest Japan. Geology 24(9), 795–798.
Scalabrino, B., Lagabrielle, Y., Malavieille, J., Dominguez, S., Morata, D., Espinoza, F., Suarez, M., Rossello, E., 2007. Impact of spreading ridge subduction on the morphotectonic evolution of the Patagonian Cordillera since 15 Ma (latitude of the Chile Triple Junction, CTJ). Poster, GEOSUR 2007 International Geological Congress on the Southern hemisphere, Santiago, Chile.
Shapiro, N.M., Ritzwoller, M.H., 2004. Inferring surface heat flux distributions guided by a global seismic model: particular application to Antarctica. Earth and Planetary Earth Letters 223, 213–224.
Singer, B.S., Ton-That, T., Vincze, T., Rabassa, J., Roig, C., Brunstad, K., 1997. Timescale of late Cenozoic climate change in the southern hemisphere from 40Ar/39Ar dating of patagonia lavas. Terra Abs., Eur. Union Geosci. 9(9), 65–66.
Sisson, V.B., and Palvis, T.L., 1993. Geologic consequences of plate reorganization: an example from the Eocene southern Alaska forearc. Geology 21, 913–916.
Sisson, V.B., Poole, A.R., Harris, N.R., Cooper Burner, H., Palvis, T.L., Copeland, P., Donelick, R.A., and McLelland, W.C., 2003. Geochemical and geochronologic constraints for genesis of a tonalite-trondhjemite suite and associated mafic intrusive rocks in the eastern Chugach Mountains, Alaska: a record of ridge-transform subduction. In Sisson, V.B., Roeske, S.M., and Palvis, T.L., eds., Geology of a transpressional orogen developed during ridge-trench interaction along the North pacific margin: Boulder, Colorado, Geological Society of America Special paper 371, p. 293–326.
Stern, C.R., 2004. Active Andean volcanism: its geological and tectonic setting. Revista Geologica de Chile, vol. 31, no. 2, pp. 161–206.
Stern, C.R., Kilian, R., 1996. Role of the subducted slab, mantle wedge and continental crust in the generation of adakites from the Andean Austral Volcanic Zone. Contributions to Mineralogy and Petrology 123, 263–281.
Stern, C.R., Zartman, F.A., Futa, K., Zartman, R.E., Peng, Z., Kyser, T.K., 1990. Trace-element and Sr, Nd, Pb, and O isotopic composition of Pliocene and Quaternary alkali basalts of the Patagonian Plateau lavas of the Southernmost South America. Contributions to Mineralogy and Petrology 104, 294–308.
Stern, C.R., Kilian, R., 1996. Role of the subducted slab, mantle wedge and continental crust in the generation of adakites from the Andean Austral Volcanic Zone. Contributions to Mineralogy and Petrology 123, 263–281.
Suarez, M., de la Cruz, R., 2001. Jurassic to Miocene K-Ar dates from eastern central Patagonian Cordillera plutons, Chile (45°-48°S). Geological Magazine 138(1), 53–66.
Suarez, M., de la Cruz, R., 2000. Tectonics in the eastern central Patagonian Cordillera (45°30'-47°30'S). Journal of the Geological Society (London) 157, 995–1001.
Suarez, M., de la Cruz, R., Troncoso, A., 2000a. Tropical/subtropical Upper Paleocene-Lower Eocene fluviatil deposits in eastern Patagonia, Chile (46°45'S). Journal of South American Earth Sciences 13, 527–536.
Suarez, M., de la Cruz, R., Bell, C.M., 2000b. Timing and origin of deformation along the Patagonian fold and thrust belt. Geological Magazine 137, 345–353.
Tebbens, S.F., Cande, S.C., 1997. Southeast Pacific tectonic evolution from the early Oligocene to Present. Journal of Geophysical Research 102, 12061–12084.
Tebbens, S.F., Cande, S.C., Kpovacs, L., Parra, J.C., Labrecque, J.L., Vergara, H., 1997. The Chile Ridge: a tectonic framework. Journal of Geophysical Research 102, 12035–12059.
Thomson, S.N., Hervé, F., Brix, M., and Stockhert, B., 2001. The Mesozoic-Cenozoic denudation history of the southern Chilean Andes and its correlation to different subduction processes. Tectonics 20, 693–711.
Thorkelson, D.J., 1990. Tectonic and magmatic aspects of slab window, Geological Association of Canada Program and Abstract, 15, A105.
Welkner, D., 1999. Geologia del area del Cerro de San Lorenzo: cordillera patagonica oriental, XI region de Aysen, Chile (47°25'-47°50'S). Memoria Titulo Departemento de Geologia. Universitad de Chile. Unpublished.
Zumsteg, C.L., Himmelberg, G.R., Karl, S.M., Hauessler, P.J., 2003. Metamorphism within the Chugach accretionary complex on southern Baranof Island, southeastern Alaska. In Sisson, V.B., Roeske, S.M., and Palvis, T.L., eds., Geology of a transpressional orogen developed during ridge-trench interaction along the North pacific margin: Boulder, Colorado, Geological Society of America Special paper 371, p. 253–269.

Chapitre III :

Evolution morphotectonique de la Patagonie Centrale (46°S-47°S) au Néogène.

Apports de la connaissance du magmatisme au front de la Cordillère

L'étude de l'évolution morphotectonique de la Patagonie Centrale (46°S-47°S) entre le Miocène et le Quaternaire est présentée sous la forme d'un article, complétée par l'apport des résultats sur le magmatisme Néogène du front de la Cordillère faisant l'objet de deux articles dont je ne suis pas auteur principal.

Le premier article présente un modèle d'évolution morphotectonique, à l'échelle crustale, de la Cordillère de Patagonie Centrale entre la fin de l'Oligocène et l'actuel, en relation avec la subduction de la dorsale active du Chili et du développement d'une fenêtre asthénosphérique sous la plaque supérieure à partir du Pliocène. Il s'appuie sur l'analyse de la topographie actuelle et sur l'évolution géologique de la chaîne. Dans un premier temps, nous analysons la morphologie particulière actuelle de la Patagonie Centrale. Cette analyse porte sur le domaine de la Cordillère caractérisé par la présence de dépressions transverses et internes et sur le domaine de l'avant-pays marqué par une série de plateaux en position de relief inversé (mesetas). L'étude morphologique s'est également concentrée sur l'origine et l'évolution de surfaces d'érosion présentes dans la partie interne de la Cordillère de Patagonie Centrale. En nous appuyant dans un second temps sur une étude structurale détaillée au niveau des dépressions transverses (lac Général Carrera-Buenos Aires et lac Cochrane-Pueyrredon), de la dépression interne du lac Lapparent, et du front morphotectonique de la Cordillère, nous discutons l'influence de la tectonique et des mouvements verticaux sur la morphologie actuelle de la chaîne.

Finalement, nous concluons sur la topographie générale très particulière de la Cordillère de Patagonie Centrale, caractérisée par une partie centrale de faible altitude dominée de part et d'autre par des hauts reliefs ainsi que par la présence de dépressions transverses et internes équivalents de petits rifts. Nous discutons l'influence de la subduction de la dorsale active du Chili et du développement de la fenêtre asthénosphérique sur cette région à partir du Pliocène. Cet article montre ainsi pour la première fois en détail l'effet du régime tectonique extensif et l'inversion tectonique négative sur la topographie de la Cordillère en réponse à la présence de manteau chaud en lien et place d'un slab 'froid'.

L'article suivant concerne l'apport de l'étude du magmatisme Néogène au niveau du front de la Cordillère sur l'évolution morphotectonique de cette portion des Andes. Cet article comprend une compilation d'âges des laves au niveau de la meseta del Lago Buenos Aires permettant de discuter l'évolution tectono-magmatique de la zone située entre le front morphotectonique et la meseta et sur sa signification. Il est suggéré que cette portion de la Cordillère est sujette à une extension contrôlée par des failles normales dont le jeu débute entre 5 et 4 Ma affectant la bordure ouest de la meseta del Lago Buenos Aires. Cette tectonique extensive est également observée à l'intérieur de la chaîne où des coulées basaltiques datées entre 5-4 Ma et situées aujourd'hui à environ 2000 mètres de part et d'autre du lac Général Carrera-Buenos Aires sont déconnectées en raison des dépressions.

III.1. Evolution morphotectonique Néogène de la Patagonie Centrale (46°S-47°S).

A morphotectonic analysis of Central Patagonian Cordillera.

Negative inversion of the Andean belt over a buried spreading center?

Scalabrino, B[1] ; Lagabrielle, Y[1] ; Malavieille, J[1] ; Dominguez, S[1]. ; Melnick, D[2]., Espinoza, F[3]., Suarez, M[4] and Rossello E[5].

[1] *Université Montpellier 2, INSU-CNRS, Laboratoire Géosciences Montpellier, place E. Bataillon, 34095 Montpellier Cedex5, France.*

[2] *Institut fur Geowissenschaften, Universitat Potsdam, 14415 Potsdam, Germany.*

[3] *Departamento de Geología, Universidad de Chile, Casilla 13518, Correo 21, Santiago, Chile.*

[4] *Servicio Nacional de Geología y Minería, Avenida Santa María 0104, Santiago, Chile.*

[5] *CONICET and Universidad de Buenos Aires, Departamento de Ciencias Geológicas, 1428 Buenos Aires, Argentina.*

A morphotectonic analysis of Central Patagonian Cordillera.

Negative inversion of the Andean belt over a buried spreading center?

by :

Scalabrino, B[1] ; Lagabrielle, Y[1] ; Malavieille, J[1] ; Dominguez, S[1]. ; Melnick, D[2]., Espinoza, F[3]., Suarez, M[4] and Rossello E[5].

[1] *Université Montpellier 2, INSU-CNRS, Laboratoire Géosciences Montpellier, place E. Bataillon, 34095 Montpellier Cedex5, France.*

[2] *Institut fur Geowissenschaften, Universitat Potsdam, 14415 Potsdam, Germany.*

[3] *Departamento de Geología, Universidad de Chile, Casilla 13518, Correo 21, Santiago, Chile.*

[4] *Servicio Nacional de Geología y Minería, Avenida Santa María 0104, Santiago, Chile.*

[5] *CONICET and Universidad de Buenos Aires, Departamento de Ciencias Geológicas, 1428 Buenos Aires, Argentina.*

Tectonics, submitted 22th January 2009 ; accepted with minor revisions 12th August 2009

Corresponding author :

Bruno Scalabrino

Université Montpellier 2, INSU-CNRS, Laboratoire Géosciences Montpellier, place E. Bataillon, 34095 Montpellier Cedex5, France.

bruno.scalabrino@gm.univ-montp2.fr

Abstract

We use DEMs and satellite imagery data completed with field observations to develop an integrated morphotectonic analysis of the anomalous topography of the Central Cordillera of Patagonia between 46°S and 48°S, in a region overlying subducted segments of the Chile Spreading Ridge. This region shows a number of peculiar features, not expected in a 'normal' subduction-related belt located away from a buried spreading center. First, it is characterized by overall short wavelength topography and highly contrasted reliefs, typical of deeply incised young mountain belts, but surprisingly, also by an average very low elevation of ca. 900 m. Second, the Cordillera lacks central high reliefs; instead, there is a central, depressed domain with average low slope gradients including the deepest point of the study area (300 m below sea level in the bottom of Lake General Carrera-Buenos Aires). This depressed area is flanked by western and eastern regions of higher elevation having opposite general slope dips. To the east, the Central Patagonian Cordillera is now separated from the flat plains of the Pampean domain (representing its former piedmont) and several elevated basaltic plateaus (mesetas), by N160-N180 trending morphotectonic corridors and the western border scarps of the mesetas. These scarps correspond to neotectonic features controlled by recent vertical faults, mostly active after 3 Ma. Remnants of a former peneplain, the Avellanos surface, are widespread within the entire Cordilleran region. From geological evidence, this peneplain formed between 15 and 4 Ma and was connected originally with the mesetas domain, now is dissected by these corridors. It is shown that a negative inversion related to extensional and strike-slip faulting occurred in the frontal region of the Cordillera at 3 Ma synchronously with the emplacement of magmatic products. Timing of the extensional deformation in Central Patagonia is concomitant with the migration at depth of different segments of the South Chile Ridge, which entered the trench at 6 and 3 Ma, respectively; and the consequent opening of a slab window allows asthenospheric hot mantle to reach lithospheric regions. Finally, migration of segments of the Chile Spreading Ridge since 6 Ma triggered regional uplift of the Cordillera followed by limited extension in relation with increased thermal weakening of the crust.

1. Introduction

Interaction of oceanic and continental lithospheres at active margins usually results in the contraction of the overriding continent and in the building of a linear mountain belt. Anomalies in the evolution of such subduction-related belts along a given margin may develop due to heterogeneities within the down-going oceanic lithosphere. All along the East-Pacific area, active oceanic spreading ridges represent first-order heterogeneities which may enter the trenches, thus affecting significantly the margins of continental upper plate. It is now demonstrated that subduction of an active spreading center leads to the opening of a slab window, triggering in turn drastic changes in the mantle dynamics beneath the orogenic wedge (Thorkelson, 1990, 1996; Breitsprecher and Thorkelson, 2008), and causing visible effects in crustal deformation and surface morphology. Studies of ancient systems implying subduction of spreading ridges have provided important perspectives on the long-term temporal evolution of a ridge subduction event, mostly through the records from mid-crustal rocks. These studies often document overall post-orogenic extension, localized tectonic negative inversion and partial collapse of the subduction-belt such as in the Northern American Cordillera, in Alaska (Dickinson and Snyder, 1979; Thorkelson et al., 1990; Sisson and Palvis, 1993; Bradley et al., 2003), and in the Antarctica Peninsula (Garret et al., 1987). Geological investigations in subduction belt experiencing current spreading ridge subduction are now needed. Indeed, only in such situations, robust links can be established between geological events at the surface and well-constrained locations of slab windows at depth. For these reasons, the Chilean-Argentinian Central Patagonian Cordillera is a unique natural laboratory to study the consequences of the subduction of an active spreading ridge beneath a continent. Southern Patagonia has been first concerned by the "normal" subduction of the Farallon-Nazca plate followed, after 15 Ma, by the subduction of the active axis of the South Chile Spreading Ridge (Cande and Leslie, 1986, Cande et al., 1987, Bangs et al., 1992). Magmatic evidence confirming the development of a slab window beneath Patagonia have been reported from investigations within the post-15 Ma volcanic fields across entire southern South America (Ramos and Kay, 1992; Gorring et al., 1997; Gorring and Kay, 2001; Espinoza et al., 2005; Guivel et al., 2006; Lagabrielle et al., 2007), but only few morphotectonic studies have been conducted in these regions until now (Lagabrielle et al., 2004; 2007).

In this paper we present the results of an integrated study of the morphological and tectonic evolution of a portion of the Central Patagonian belt lying above the current location of subducted segments of the South Chile Spreading Ridge, between 46°S and 48°S. This study is based on original field data enriched with DEMs and satellite imagery from selected key-areas surrounding the Lake General Carrera-Buenos Aires, a major geomorphological feature of this region. Topographic and morphotectonic data show that the study area is composed of an assemblage of various domains exhibiting contrasted tectonic evolutions in relation with Mio-Pliocene vertical displacements.

2. A review of the geological evolution of Central Patagonia : relations with the subduction of the Chile Spreading Ridge

The Central Patagonian Cordillera, is a linear mountain range, oriented approximately north-south and extending between 45°S and 48°S, which constitutes the northern continuation of the Southern Patagonian Cordillera described by Ramos (1989), Coutand et al. (1999) Diraison et al. (2000). It is 200 km in width at the latitude of the CTJ and shows a segmented pattern, consisting of four en échelon ranges, trending N160-170 and limited by frontal thrusts (Lagabrielle et al., 2004). In this first section we provide a review of the basic events that punctuated the geological evolution of Central Patagonia, with emphasize on the influences of the Chile Spreading Ridge.

2.1. Plate configuration and subduction of the Chile Spreading Ridge.

The Nazca and Antarctic plates, separated by the active South Chile Spreading Ridge (SCR) both enter the southern Chile-Peru trench and are presently subducting beneath the South America plate. The Chile Triple Junction (CTJ), the point where the South America, Nazca and Antarctic plates meet, is now located at 46° 12’ S, in front of the Taitao Peninsula, the westernmost point of the Chilean coast (Fig.1-2). After the collision of the SCR with the southern tip of South America at ca. 15 Ma (Cande and Leslie, 1986), the Chile Triple Junction migrated northward along the South American margin to its present-day position. Hence, north of the CTJ, the current relative motion vector between the Nazca and South America plates is oriented N80 with a magnitude of 84 mm/yr (Pardo-Casas and Molnar, 1987; Gripp and Gordon, 1990; De Mets et al., 1990), whereas south of the CTJ, current convergence between the Antarctic and South American plates occurs at a rate of 20 mm/yr, in an E-W direction (Fig. 2) (Gripp and Gordon, 1990; De Mets et al., 1990). (Fig. 2). Oblique subduction has led to strain partitioning in the Cordillera involving complex deformation. North of the CTJ, part of the convergence is accommodated along the Liquiñe-Ofqui Zone (LOFZ), a long-lived, right-lateral, lithospheric scale fault system active since the Tertiary (Hervé, 1994; Cembrano et al., 1993, 1996, 2002). The subduction of successive segments of the SCR at ca. 15 Ma, 6 Ma, 3 Ma and 0.3 Ma (Herron et al., 1981; Cande and Leslie., 1986; Cande et al., 1987; Nelson et al., 1994; Bangs and Cande, 1997; Tebbens and Cande., 1997; Tebbens et al., 1997) led to the progressive opening of the slab window beneath Patagonia (Fig. 2) (Ramos and Kay, 1992; Gorring et al., 1997; Gorring and Kay, 2001; Lagabrielle et al., 2004; Breitsprecher and Thorkelson, 2008 ; Scalabrino et al., in press).

2.2 Geological evolution of Central Patagonia

The neotectonics features described in this paper develop mostly from structures inherited from a rather long tectonic evolution. Since the Late Paleozoic, the western margin of South America has been affected by the eastward subduction of oceanic lithosphere (e.g. Bell and Suárez, 2000). Jurassic subduction-related acidic volcanics and volcanosedimentary rocks of the Ibañez Group unconformably overlie the Paleozoic basement rocks (Fig. 3) (Niemeyer et al., 1984; Charrier et al., 1979; Suárez et al. 1996; De La Cruz et al. 2003, 2004, 2005). The western part of the Patagonian belt is also characterized by exposures of calc-alkaline granitoids forming the Patagonian Batholith, which were emplaced over a continuum subduction environment from the Late Jurassic to the Miocene (Pankhurst et al., 1999; Suárez and De la Cruz, 2001). In the core of the belt, marine Cretaceous sediments are restricted to isolated sedimentary basins. South of 45°S, the Cenozoic sedimentation recorded the uplift of the Cordillera. Syn-orogenic clastic deposits (molasse) accumulated in foreland basins that are roughly of the same age all along strike, as well as within one internal basin, the Cosmelli Basin, located immediately south of Lake General-Carrera Buenos Aires (Flint et al., 1994) (Fig. 3). The foreland sedimentation changed from marine conditions during the Middle Oligocene-Early Miocene to continental conditions during the Early Middle Miocene (Fig. 3). The continental molasse locally more than 1000 m thick, consists of fluvial clastic deposits that recorded climate changes from humid to arid due to rain shadow effect of orogeny (Blisniuk et al., 2005). Between 45°S and 49°S, it ranges in age from 22-23 Ma to 16-15 Ma (Frassinetti and Covasevich, 1999; Flynn et al. 2002; Blisniuk et al., 2005). Since the entire orogeny-related molasse succession was deposited during the Late Oligocene to the Middle Miocene (30-15 Ma), it is noteworthy that main uplift of the Cordillera occurred prior to 15 Ma, that is prior to the subduction of the SCR (Lagabrielle et al., 2004; Scalabrino et al., in press).

Calc-alkaline to transitional flows dated at 16-14 Ma unconformably overlie the upper beds of the continental molasse south of Lake General Carrera-Buenos Aires in the Paso Roballos area (Espinoza et al., 2006; submitted; Boutonnet et al., submitted). This short-lived volcanic episode was followed by a magmatic event of regional importance during which large basaltic flows were emplaced over an erosional surface that truncates the tectonic front (Lagabrielle et al., 2004). The main period of basalt flooding (main-plateau basalts), lasted from 12 to 3 Ma and eruptions occurred mostly along the former tectonic front of the Cordillera. Large remnants of the 12 Ma - 3 Ma flows now form basaltic plateaus such as the Meseta del Lago Buenos Aires that dominates morphologically the eastern pampean region, and the Meseta Chile Chico lying inside the Cordillera, immedialety adjacent to the morphotectonic front. The main-plateau period was followed by more sporadic magmatic events between 3 Ma and some ka (post-plateau basalts) leaving numerous cones, flows and maars on the top surface of the Meseta del Lago Buenos Aires. Lava flows of the main-plateau sequence at Meseta del Lago Buenos Aires are interbedded with fluvio-glacial and glacial polymictic conglomerates (Mercer and Sutter, 1982; Espinoza et al., 2005; Lagabrielle et al., 2007; Lagabrielle et al., submitted). A significant portion of these deposits are granitoid clasts, indicating that during the Late Miocene, some sediments travelled more than 100 km from their source in the western Cordillera, along a main drainage axis now morphologically inverted, forming the top surface of the meseta del Lago Buenos Aires (Mercer and Sutter, 1982**,** Lagabrielle et al., submitted).

Various plutons have been emplaced and rapidly exhumed during the Tertiary in Central Patagonia, indicating important vertical displacements. Plutonic rocks exposed at the summit of Monte San Lorenzo (3706 m a.s.l) yielded biotite K-Ar ages of 6.6 ± 0.5 and 6.4 ± 0.4 Ma (Welkner, 1999; Suarez and De La Cruz, 2001). A young pluton at Paso Las Llaves, on the southern coast of the lake General Carrera-Buenos Aires, has given ages ranging from 10 Ma to 9.7 Ma (Petford and Turner, 1996, Pankhurst et al., 1999; Suarez and De La Cruz, 2001; Thomson et al., 2001). Late Miocene plutonic bodies exposed close to the morphotectonic front at Paso Roballos have given ages around 10 Ma (Ramos,1989). A small pluton exposed south of lake General Carrera-Buenos Aires (Las Nieves pluton) yieldied an age of 3.2 ± 0.4 Ma (Suarez et al., 2000; Morata et al., 2002). Several felsic subvolcanic bodies, mostly shallow level plugs, dykes and laccoliths, are exposed along the southwestern border of the Meseta del Lago Buenos Aires, west of Monte Zeballos. They are intrusive into the main-plateau basaltic pile of the meseta or into the molasse. $^{40}Ar/^{39}Ar$ and whole-rock K-Ar ages dates indicate ages of emplacement between 3.98 and 3.08 Ma, synchronously with that of the more mafic, post-plateau basaltic sequence (Brown et al., 2004 ; Espinoza et al., 2007 ; Boutonnet et al., submitted).

Petrogenetic studies of the Pliocene to Quaternary post-plateau mafic lavas indicate that they were generated from an asthenospheric source and then ascended through a completely opened slab window under the Lago General Carrera-Buenos Aires region (Gorring et al., 2003). A more recent chronological and petrogenetic study of the Miocene main-plateau basalts by Guivel et al. (2006) has shown that the spatial distribution and time span of this OIB-like basaltic magmatism are also explained by a model involving the development of a former asthenospheric window, in relation with a tear in the downgoing Nazca slab. Post-3 Ma evolution of the western border of the Meseta del Lago Buenos Aires has been related to the presence of anomalous mantle lying at depth, due to the presence of subducted segments of the Chile Spreading Ridge (Lagabrielle et al., 2007).

2.3 An updated geological cross-section of Central Patagonia

The structural style of the Central Patagonian Cordillera at the latitude of the Chile Triple Junction is illustrated by the W-E trending, updated cross section presented in Fig. 3b. The section is constructed using data gathered from former studies (De La Cruz et al., 2003; 2004; 2005; Lagabrielle et al., 2004) merged with results of recent structural field works in this region. It confirms that the Cordillera experienced little amount of shortening, in accordance with geophysical informations suggesting that crustal thickness here does not exceed 40 km (Introcaso et al., 1996; Tassara et al., 2003). The western part of the section includes the Taitao ophiolite, accreted as a consequence of the collision of the South Chile Ridge with the trench (Lagabrielle et al., 2000; Veloso et al., 2005). The Patagonian domain comprised between the summits of the Northern Ice Cap and the Meseta del Lago Buenos Aires exhibits a thick-skinned tectonic style controlled only by few steeply dipping reverse faults (fig. 3b). These faults are probably reactivated, older normal faults related to the Gondwana break-up that controlled the geometry of the former Cretaceous marine basins (e.g. Folguera et al., 2004). The current morphotectonic front corresponds to a main fault system that thrust Jurassic units over the Late Oligocene-Miocene foreland molasse. However, reverse fault are still observed in the Pampa region east of the front, 450 km far from the trench, suggesting that the contractional strain at the converging margin was distributed over a wide area into the continent. The Tertiary sedimentary Cosmelli basin lies in the central part of the Cordillera domain. It is limited by steeply dipping faults related to the Late Oligocene-Miocene compressionnal event. As discussed in this paper, these reverse faults have probably been reactivated as normal faults due to further extension in the axial domain. To the east, lava flows forming the basaltic plateaus (e.g. Meseta del Lago Buenos Aires) were emplaced over a 15-12 Ma old peneplain that truncates the compressional structures of the eastern part of the former Cordillera. This clearly confirms that compression in the Central Patagonian Cordillera ceased after 15 Ma (Lagabrielle et al., 2004; Scalabrino et al., in press).

3. Geomorphology of Central Patagonia

In the following section, we describe the most peculiar morphological features of the Central Patagonian Cordillera based on the analysis of a digital elevation model (DEM SRTM-90 m) in an area of 200 x 200 km between latitudes S46° and S48°, from which we extracted topographic profiles and a map of slope gradients (fig. 5).

3.1 General characteristics

As shown on the calculated profile of the mean topography shown in figure 6, the average elevation of the Cordilleran domain is about 900 m and is characterized by an overall short wavelength topography. Mean elevation of the peaks is around 2000 m and the valleys show low elevations, some of them lying at sea level. The Monte San Valentin, in the western part of the Cordillera, is the highest summit with an elevation of 4058 m (Fig. 4). The Central Patagonian Cordillera is flanked to the west by a low-elevated domain limited by the active Liquiñe-Ofqui fault zone that separates the Taitao Peninsula from the continent and representing an extremely sharp boundary between the highest reliefs of the region and the

actively subsiding area of the Penas Gulf. To the east, the Central Patagonian Cordillera is flanked by the Pampean domain (extending up to the Atlantic coast), characterized by wide areas of homogeneous topography including flat plains and several mesetas (Figs. 4-5). Figure 6 compiles a series of W-E trending topographic sections of the Central Patagonian Cordillera between 46°S and 48°S. All profiles show similar peculiar patterns with two opposite, eastern and western regions of relatively high elevation, braketing an axial region of lower elevation. This axial depressed region is also characterized by average low slope gradients as shown in figure 5 and discussed in the following sub-section 3.4. It occurs surprinsingly in a position where higher reliefs should be expected in the case of a normal subduction belt. Both flanking regions of higher elevation are characterized by top surfaces having opposite and low gradient slopes. The western region includes the high reliefs of the Northern Ice Cap. The eastern region comprises the morphotectonic front of the Cordillera and remarkable flat surfaces gently dipping to the east, corresponding to the mesetas.
The mesetas are currently separated from the remaining Cordillera to the west by a succession of N160-N180 trending morphological corridors, delineating the morphotectonic front and corresponding to neotectonic features controlled by recent vertical faults, as described in sub-section 3.5.

3.2. The mesetas : remnants of pearched surface.

East of the morphotectonic front, the morphology is characterized by a succession of plateaus of sedimentary and/or volcanic composition. The largest plateau (80 km wide in an W-E direction, ~6000 km^2) is the flat-topped meseta del Lago Buenos Aires (Fig. 3-5-6-7), formed by middle Miocene-Pliocene OIB-like basalts interbedded with late Miocene-Pliocene fluvio-glacial deposits. Its elevation ranges from 2700 m (Monte Zeballos) to 1100 m in the eastern side. The second most important plateau is the flat Meseta del Guenguel, located north of the Lake General-Carrera Buenos Aires (Fig. 6). It is a depositional surface, composed of late Oligocene-middle Miocene syn-orogenic sediments, locally overlain by younger coarse fluvio-glacial deposits. Its elevation varies from 1200 to 500 m.a.s.l. from west to east. Both mesetas show a gentle slope dipping to the east, having very low slope gradient (< 10%) (Fig. 3-5) and exhibit a well-developed eastward dendritic relict stream network also indicating an eastward dipping paleoslope, as shown on figure 7. These plateaus are now disconnected from the rest of the Cordillera by NW-SE oriented depressions forming narrow corridors paralleling the border of the Cordillera as discussed in section 3.5 (Figs. 3-6-7). Former tributaries of the ancient fluvial network are abruptly cut by landslides actively scrapping the edges of mesetas (Fig. 7), thus confirming recent relief inversion of these plateaus.

3.3 Relictual peneplains pearched inside the Cordillera

A striking feature of the morphology of the Central Patagonian Cordillera is the occurrence of isolated pearched, low relief surfaces. These landscapes are portions of smoothed morphology, representing relicts of a former peneplain characterized by very low slope gradients (< 5%), lying 2000 m above sea level in average (Fig. 8). They contrast with the surrounding jagged relief of peaks and transverse depressions. Using GIS methods, we mapped these high-elevated surfaces within the main Cordillera. (Fig. 5). Most of them are located north of the Lake General Carrera-Buenos Aires. The most striking surface fragment, named the Avellanos relict surface by Lagabrielle et al. (2004), is observed west of the City of Puerto Ibáñez and dominates the northern border of the Lake General Carrera-Buenos Aires (Fig. 7-8). It is a 30 km long, 20 km wide, NE oriented elongated continuous surface. Its western side is notably horizontal along more than 10 km, paralleling the northern edge of the lake, with an average elevation of 2000 m.a.s.l. To the east, the Avellanos surface lowers progressively towards the Puerto Ibáñez-Chile Chico fault zone, reaching an elevation below 300 m.a.s.l., south of Puerto Ibáñez. Observation of satellite images clearly indicates that the flat, highest portion of the Avellanos surface is continuous with the lowered eastern portion. North of the Avellanos surface, several remnants of the corresponding former surface can be observed (fig. 7). The largest one is 20 km long and forms the plateau that dominates the southern edge of Lake Lapparent. It is composed of two narrow surfaces joining to their western edge and culminating at an average elevation of 1500 m.a.s.l. Other remnants cap the reliefs forming the western and eastern edge of the Lapparent basin. The first one corresponds to three NE trending, parallel segments, almost 10 km long, with an elevation varying from 1400 m to 1600 m.a.s.l. (Fig. 7) and the second one, which is also the easternmost surface in the study area, is located between the Lake Lapparent and the morphotectonic front. It is 5-7 km long, with an elevation of 1500 m.a.s.l.

As shown in figure 8, the Avellanos surface clearly cuts the gently folded strata of the Ibáñez Formation. This indicates an erosional origin for this surface which developed at least since the middle Miocene, after 15 Ma, as it was probably achieved at the end of the main contractional tectonic phase which affected Central Patagonia. A flat-lying, 10 m thick transitional basaltic flow was sampled on the top surface of the Avellanos peneplain, yielding a whole-rock K/Ar age of 4.57 ± 0.27 Ma (Pelleter, 2003). This flow correlates with the transitional basaltic flows emplaced on top of the Meseta Chile Chico on the opposite, southern side of the Lake General Carrera-Buenos Aires, which were dated at 4.4 ± 0.8 Ma (Espinoza *et al*., 2005; Lagabrielle *et al*., 2007).

3.4 Depressions opening inside the Central Patagonian Cordillera

Surprisingly, at the latitude of the Chile Triple Junction, the Patagonian Cordillera lowers drastically and a shallow passage at an average elevation of 200 m opens between the Pacific and the Atlantic Oceans (Fig. 3). There, the axial portion of the Cordillera is characterized by the presence of deeply incised, transverse depressions. Two of them are now occupied by large post-glacial lakes, the Lake General Carrera-Buenos Aires in the center, and the Lake Cochrane-Pueyrredón to the south (Fig. 3). The deepest points of Lakes General Carrera-Buenos Aires and Cochrane-Pueyrredón lie at 380 m and 200 m below sea level, respectively (Murdie et al., 1999). During the Plio-Quaternary glacial stages, these transverse depressions were occupied by glaciers flowing eastward, so that a series of well-developed moraines accumulated on the pampa regions of Argentina, forming large amphitheaters, outlining the maximum extension of the glaciers (Fig. 3-5).

The Lake General Carrera-Buenos Aires depression consists of three segments. The deepest segment, to the west trends N50 and includes a north-south trending appendix with shallow water (Bahia Murta, 100 m depth maximum). The central segment is about 580 m maximum deep and trends N60. Both western and central segments exhibit rectilinear outline and sharp edges suggesting tectonically controlled borders (Lagabrielle *et al*., 2004, Scalabrino et al., in press). The eastern segment expands out of the Cordillera in an E-W direction and separates the Meseta del Guenguel to the north from the Meseta del Lago Buenos Aires to the south.

The Lake Cochrane-Pueyrredón depression has topographic characteristics similar to that of the Lake General Carrera-Buenos Aires. It forms a transverse corridor at low elevation, including a narrow and deep western segment trending N50 (220 m b.s.l. Murdie et al., 1999) and an eastern segment with shallow waters, trending N140. The western segment parallels regional lineaments, suggesting tectonically-controlled borders (Fig. 9). The eastern segment cross-cuts the tectonic front of the Cordillera in the area of the Vacas and Yole frontal thrust (Ramos, 1989).

Beside these two major narrow transverse depressions, the internal Cordillera is characterized by the presence of a number of larger depressed areas and smaller basins. By contrast to the entire Cordillera, which is characterized by high slope gradients (>20%) resulting from intensive glacial and fluvial erosion, these internal depressed areas have smoothed topography and gentle slopes, as evidenced on the slope gradient digital map of figure 5. The largest depressed area occupies the axial part of the Cordillera. It is a major morphological feature, well observed on the compilation of topographic profiles of figure 6. It has a V-shaped outline, pointing to the north and extending from the northern tip of the Lake General Carrera-Buenos Aires to the northern shore of Lake Cochrane-Pueyrredón (Figs. 5-6-7). In this triangular area, the slopes are lower than 15%. Mean elevations are low, ranging from 1200 m.a.s.m. maximum, to 380 m.b.s.l minimum, corresponding to the deepest point of the Lake General Carrera-Buenos Aires. The topography is characterized by several steps delimited by linear features oriented N10, N60 and N160, isolating sub-domains, with differencial mean low elevation. The central sub-domain has also a V-shaped outline and extends south of Lake General Carrera-Buenos Aires, including the region of the Cosmelli basin. Its floor exposes Paleozoic metamorphic basement, Jurassic volcanic rocks and the molasse deposits of the Cosmelli basin of late Oligocene-Middle Miocene age. The summital surface of the central portion of the Cosmelli basin, is not horizontal and lowers gently from south (1500 m) to north (300 m), where it reaches the southern shore of the Lake General Carrera-Buenos Aires (Fig. 3).

The western branch of the Cochrane-Pueyrredón depression connects to a region of relatively low-relief and very low elevation named the Tamango basin (Fig. 5). This region has a losangic shape and is delineated by N10, N45 and N160 lineaments (Fig. 9) which affect Paleozoic metamorphic rocks and Mesozoic formations.

An additional remarkable topography anomaly of the Central Patagonian Cordillera is the rhomboidal basin of Lake Lapparent, lying north of the lake General Carrera-Buenos Aires at an average elevation of 500 m (Figs. 3-6-7). This depression, whose contours might recall that of pull-apart basins, is 40 km long and 20 km wide. It sharply opens inside the high-elevated system of peneplain remnants described above. Tectonic lineaments abruptly limit the depression from the Cordillera reliefs. Slopes inside the depression are lower than 10% with minimal values in the northeastern and eastern corners of the depression.

3.5. The N160 tectonic corridors.

The eastern orogenic front is marked by a topographic jump of several hundreds meters, due to the easterly-vergent thrust system, juxtaposing Paleozoic and Mesozoic units of the main Cordillera, over the Mesozoic-Cenozoic foreland deposits to the east. In the study area four segments of the orogenic front have been distinguished from north to south : the Portezuelo Segment, the Chile Chico Segment, the Las Horquetas Segment and the Paso Roballos Segment (Lagabrielle et al., 2004). The Chile Chico Segment connects to a marked tectonic lineament oriented N160-N170 observed in topography, air photos and satellite images across the Lake General Carrera-Buenos Aires that extends northwest of Puerto Ibáñez, named the Puerto Ibáñez-Chile Chico fault zone. The northern portion of this fault system forms the eastern boundary of the Lake Lapparent depression. A major lineament oriented N160-170, paralleling the Paso Roballos segment separates the Cenozoic formations of meseta del Lago Buenos Aires from the rest of the Cordillera (figure 5).

4. Tectonic contribution to the present-day morphology

The morphology of the Central Patagonian Cordillera at the latitude of the Chile Triple Junction exhibits a complex pattern including peaks and narrow valleys at an average low regional elevation of 900 m, defining a short wavelength topography with mean amplitude of 2000 m. This topography is interrupted by narrow and deep corridors and by flat floored depressions. The region is also characterized by the presence of remnants of former flat surfaces forming large mesetas outside the Cordillera or found as relicts capping reliefs inside the Cordillera itself. In this section, we discuss the tectonic significance of the sharp boundaries of the depressed areas and of the N160 trending corridors on the basis of : (1) the interpretation of combined DEM and satellite images of tectonic lineaments, and (2) field tectonic analysis.

4.1 Analysis of tectonic lineaments

Lineaments are natural simple or composite-pattern linear or curvilinear features discernible on the Earth’s surface. In the geologic sense, these features may depict crustal structure or may represent zones of structural weakness. Lineaments of a mountain belt are commonly interpreted as tectonic features, even if glacial and fluvial erosion increase them. The fault distribution derived from the Landsat ETM+7 and DEM SRTM-90 m analysis is shown in Fig. 9. A total of 250 lineaments were observed, concentrated in the eastern part of the belt. Fault extraction from the Landsat and DEM maps provides similar identification and distribution. Faults are usually rectilinear and 5 to 50 km long. Their distribution in a rose-diagram shows two dominant groups close to N45-60 and N160-170 directions. The first group corresponds to features controlling the internal depressions of Lake Lapparent, the western branch of Lake General Carrera-Buenos Aires, the northern part of the Lake Cochrane-Pueyrredón area (Fig. 9). The second group is mainly developed along the tectonic front and at the oblique corridors (Fig. 9). It is noteworthy that these two dominant orientations parallel the directions of the fracture zones and spreading axis of the subducting south Chile Spreading Ridge.

4.2 Tectonic origin of the intra-Cordillera depressions

4.2.1. Lake General Carrera-Buenos Aires depression

Previous work by Lagabrielle et al. (2004) and (2007) already suggested that the depression of Lake General Carrera-Buenos Aires has a tectonic origin, although glacial erosion probably increased to some extent the width and depth of this main morphological corridor. Indeed, the abrupt margins of the central segment of Lake General Carrera-Buenos Aires parallel the N50-60 and N90 trending faults well-observed in the surrounding terranes on both satellites and DEM's images (Fig. 9). Numerous highly dipping faults are well exposed along the southern margin of the lake, forming the N90-trending 40 km-long Pampa La Perra fault zone (Fig. 10) (Lagabrielle et al., 2004). This important tectonic boundary consists of a succession of en échelon, N50-N60-oriented fault segments, some kms long each, defining three north-facing main steps inducing progressive lowering northward. Field observations and fault analysis confirm that these fault segments have normal and transtensional throws, consistent with the tectonic subsidence of the lake basement (Lagabrielle et al., 2004). Local throw along one single fault may reach 10 m as observed within a fault zone well exposed along Rio el Bano (Fig. 10).

The Pampa La Perra fault zone controls the present-day topography of the south margin of the lake. This topography strongly contrasts with the aspect of the northern margin, consisting of one single south-facing scarp. Therefore, as illustrated by the north-south cross section shown in figure 10, the overall topography of the Lake General Carrera-Buenos Aires depression is typically asymmetrical, a character which is also found in other depressions of Central Patagonia, as shown in the following sub-sections. Such morphological asymmetry cannot be explained easily by pure glacial processes.
In the surroundings of the north-south appendix of Lake General Carrera-Buenos Aires (Bahia Murta), rocks of the metamorphic basement and of the overlying Ibáñez Formation are affected by N160-trending faults, paralleling the shores of the lake. This pattern contrasts with the fault distribution controlling the central segment (Fig. 9), which suggests also a strong tectonic control on the depression here.

On the opposite side of the Lake General Carrera-Buenos Aires, east of Guadal, the Tertiary Cosmelli molasse basin is more than 20 km long (Fig 9). As illustrated by cross-section in figure 3, the Cosmelli basin is interpreted as a pop-down basin, deformed as an open synclinal, controlled by thrust faults of Oligocene-Middle Miocene age. The Cosmelli basin is only present on the southern side of the lake, and does not show any equivalent on the northern side, where only basement rocks are exposed, but where thrusts can be traced in the continuation of the thrusts bounding the basin. This observation demonstrates that the Lake General Carrera-Buenos Aires depression corresponds to a major, N40 trending tectonic boundary, along which significant post-Late Miocene-Pliocene vertical displacements have occurred. It implies relative uplift of the northern shore of the Lake and a regional northwards tilt of its southern border during the Plio-Pleistocene. This regional tilt is also demonstrated by the geometry of the molasse sequences in the Cosmelli basin itself. The sandstones beds of the marine and continental molasse (Guadal and Santa Cruz-Galera Fms respectively) are continuously exposed along both edges of the basin. The upper beds of the Guadal Fm. are a well-defined stratigraphic marker, originally horizontal. Elevation of the Guadal-Santa Cruz Fms limit decreases progressively from ca. 1000 m a.s.l. in the south to ca. 300 m a.s.l. in the north, close to the southern shore of Lake General Carrera-Buenos Aires (Flint et al. 1994; Ray, 1996; De La Cruz et al. 2005), confirming long wavelength deformation of the crust adjacent to the Lake General Carrera-Buenos Aires fault system.

Finally, two important features have to be stressed here : (1) The preservation of the molasse deposits at low elevation implies that this region has experienced very little, post-Miocene fluvio-glacial erosion with respect to the surrounding areas. (2) The general tilt of the Cosmelli basin implies post-sedimentary differential vertical displacements, consistent with a tectonic subsidence with maximum values close to the axis of Lake General Carrera-Buenos Aires.

Few kilometers east of Cosmelli basin, the 10 Ma-old plutonic body of Paso Las Llaves is cross-cut by several normal and strike-slip faults varying from N50 to N130 in direction. Several faults parallel the southern edge of the depression in this area**.** Exposure of this pluton here demonstrates the post-10 Ma age of the Lake General Carrera-Buenos Aires depression. Faulting in turn demonstrates a post-10 Ma tectonic activity, involving mostly transtensional displacements consistent with a tectonic control of this depression (Lagabrielle et al., 2004). Additional fault data have been obtained along the Austral Road, east of Paso Las Llaves, where the Ibanez Formation which forms the southern edge of the lake is affected by N30 to N100 and N160 normal to strike-slip trending faults which bearing striaes having pitches ranging from 45° to 85°, confirming transtensional to extensional deformation in this region.

4.2.2. Cochrane-Pueyrredón Lake area and the Tamango basin.

The Cochrane-Pueyrredón Lake consists of the juxtaposition of N40-50 and N140-160 trending portions, indicating also a morphological control by the two sets of faulting directions determined by the extraction of tectonic lineaments. The first set has similar orientation to the fault system which controls the central segment of Lake General-Carrera Buenos Aires depression. The second one parallel the group of faults mainly developed along the tectonic front and within the oblique corridors (Fig. 9).

The eastern border of the Tamango basin is controlled by a 40 km long, N10 trending fault, corresponding to a major fault system named the Tamango Fault Zone (De La Cruz et al., 2004) (Fig. 11). At Cerro Tamango, 10 km north of the city of Cochrane, faulting of Mesozoic formations against the Paleozoic basement is observed. Here, the Tamango Fault Zone consists of a main N10 fault, and of numerous highly-dipping N150 and N40 trending minor normal faults (Fig. 11). Cretaceous marine sediments (Toqui and Apeleg Fms), together with Jurassic volcanic rocks are down-faulted with respect to the Paleozoic basement (Fig. 9-11). Therefore, the Tamango Fault Zone likely represents the eastern margin of a recent narrow hemi-graben. Remnants of the mesozoic cover are only preserved in the northeast corner of the Tamango basin, suggesting regional tilting to the northeast of the depression floor, in a way similar to tilting observed south of the Lake General Carrera-Buenos Aires depression.

North of the western branch of the Lake Cochrane-Pueyrredón, several N40-65, N90 and N150 trending highly-dipping faults delineate depressed areas, which are separated by the E-W trending, 1500 m high, Cordón Chacabuco ranges. These mountains represent a horst with respect to the flanking parallel basins (Fig. 9).

4.2.3. Lake Lapparent area.

Recent field data obtained in the Lake Lapparent depression yield crucial informations on the role played by Neogene normal faulting events in the morphological evolution of the Central Patagonia. This basin is a sharply defined rhomboidal topographic low resembling pull-apart grabens, with an area of ca. 800 km^2 (Figs. 3-9-12). The Lake Lapparent is 20 km long and occupies the southern part of the basin; it has a linear outline suggesting again a strong tectonic control of the depression. The average depth of the depression's floor is 500 m a.s.l., and peaks dominating the basin have a mean elevation of 1500 m, with a maximum of 2318 m at Cerro Castillo. Only Mesozoic volcanic rocks of the Ibáñez Formation are exposed in this area (Niemeyer, 1975; Bruce, 2001).

As observed on Landsat and DEM's maps, the Lapparent basin is bounded by N10, N45 and N160 linear features that define scarps locally 1500 m high (Fig. 12). The eastern limit of the Lapparent depression is delineated by a series of N160 oriented faults belonging to the northern end of the Puerto Ibáñez-Chile Chico tectonic corridor. On the opposite side, the basin is limited by a major N170 trending fault zone. To the south, the basin is outlined by the narrow E-W Lake Lapparent, flanking a zone of relatively high elevation toped by remnants of the Miocene-Pliocene peneplain (see section 3). Figure 13 compiles a series of parallel N-S oriented topographic profiles across the Lake Lapparent region, extracted from the DEM database. As illustrated by profiles 1, 2 and 3, the topography of the region also exhibits an asymmetrical character. To the north, the continuous reliefs of the main Cordillera are sharply cut along the northern boundary of the basin, while the southern border exhibits a smoother topography with moderate to low-reliefs, consisting in a succession of north-facing scarps. These scarps connect progressively the southern, high-elevated regions of the border of the basin to the floor of the depression, a flat area gently dipping to the north.

The morphology of the northern flank of the Lapparent basin is dominated by the existence of a series of triangular facets trending N65 to N130, suggesting recent uplift of the Cerro Castillo area (Fig.9-13-14). Field observations confirm the presence of important tectonic displacements along this boundary. In the NE corner of the depression, the contact between fossiliferous marine Cretaceous sediments (Apeleg Formation) with Jurassic volcanic rocks found at the same elevation, is a major normal fault (Fig. 14). This fault zone is well-exposed and shows a 3 m thick, sub-vertical gouge with poorly-preserved high-dip striaes indicating normal displacement. The marine beds of the Apeleg Fm. are dipping to the north, indicating block tilting in relation with normal displacement along this fault. Numerous evidence of normal faulting consistent with a recent subsidence of the basin are found within the entire Lake Lapparent area. To the south, the Lake occupies an incised valley controlled by N110 trending faults (Fig. 14), and normal faults were analyzed in the eastern part of the basin, along the Rio Ibanez gorges (Lagabrielle et al., 2004). On the western side of the basin, relicts of the Late Miocene-Pliocene erosional surface are affected by N45-trending normal faults which separate tilted blocks (Fig. 14). These faults connect to the N160 trending lineament forming the western tectonic limit of the basin. On its eastern side, N120 to N160 trending sinistral strike-slip and N10 to N120 oriented normal faults belonging to the Puerto Ibáñez-Chile Chico fault zone, cross-cut the Jurassic volcanic rocks. Inside the basin, the glacially-polished volcanic rocks (roches moutonnées) are affected by numerous N20 to N160 fractures and faults.

4.3. Faulting along the N160 oriented corridors: geometrical and chronological constraints from the Rio Zeballos fault zone

As expected in the case of a well developed compressional orogenic system, the eastern front of the Cordillera is marked by a topographic jump, facing to the east, of several hundreds meters, corresponding to the frontal thrusts. However, the frontal region of Central Patagonia displays an unusual character, due to the presence of N180 to N160 oriented linear depressions developed at the foot of a series of west-facing scarps. Due to these depressions, there is a noticeable disconnection between the Cordillera and its former piemont. The N180 to N160 oriented linear depressions correspond to tectonic lineaments well observed in satellite images : the Puerto Ibáñez-Chile Chico fault zone and the Rio Zeballos fault zone. We concentrate here on the latter fault zone exposing a series of recent magmatic rocks allowing precise dating of the tectonic events which strongly modified the morphology of the frontal region during Plio-Quaternay times.

The Río Zeballos corridor extends east of the morphotectonic front and delineates the western border scarp of the meseta del Lago Buenos Aires. It corresponds to a major fault zone, the Río Zeballos Fault Zone, oriented N160-170, which cross-cuts the Late Miocene-Pliocene lava flows of the Meseta del Lago Buenos Aires and the underlying Río Zeballos Group synorogenic sediments (Lagabrielle et al., 2004; 2007) (Fig. 15). Previous works in this region have provided good evidence of post-Pliocene tectonic disruption along this fault zone as follows. (1) Close to Rio Jeinimeni, a 6 Ma basaltic dyke is offset by N150 to N160 sinistral strike-slip faults (Pelleter, 2003; Lagabrielle et al., 2004). (2) Along the Leonera river, a complex of N170 to N50 steeply-dipping normal and reverse faults (defining flower structures) cross-cuts the Late Miocene molasse deposits (Lagabrielle et al., 2004). (3) Along the Alto Rio Ghio, conjugate normal faults cross-cut 5 Ma dykes and control the development of a paleovalley infilled with lavas dated from 7 to 3 Ma (Lagabrielle et al., 2007; Boutonnet et al., submitted). (4) Plutonic felsic bobies dated around 3 Ma are aligned along the N160 trending western scarp of meseta del Lago Buenos Aires (Espinoza et al., 2007).

Updated structural map and cross-sections of this key-area, based on new field data, are presented in figure 15. Frontal tectonics is marked by easterly verging faults that thrust the Jurassic volcanics of the main Cordillera over either remnants of Cretaceous sedimentary basin or Miocene molasse deposits. The Jurassic beds are locally verticalized due to this compressional deformation. Marks of post-compressional deformation are only observed locally, due to frequent covering by quaternary deposits and recent landslides. Normal faults cross-cutting the beds of the Río Zeballos Group are observed in the Portezuelo area. South of the Portezuelo, on the westside of Río Ghio, plutonic bodies of Middle Miocene age (Cerro Indio and Cerro Negro, dated at ca. 12 Ma; Ramos, 2002) are affected by easterly high dipping N160-trending normal faults, showing well-preserved striaes having pitches ranging from 70° to 85°. In addition, the beds of the molasse outcropping all along the border of the meseta del Lago Buenos Aires are systematically affected by a N160 vertical schistosity. This is well observed at Cerro Zeballos.

Despite a reduce number of exposures demonstrating meso-scale faulting, there are geomorphological and geological evidence indicating that this corridor represents a region of major disruption of the previous front of the Cordillera. The lava flows and interbedded tills dated between 5 Ma and 3 Ma and forming the summital beds of the meseta del Lago Buenos Aires at an elevation of 2000-2500 m are also exposed in the Portezuelo area and in the Rio Ghio valley, 700 m below. This demonstrates the relative uplift of the border of the meseta by at least 700 m. This relative uplift is corroborated by the presence of relict of calc-alkaline to transitional flows dated at 16-14 Ma, unconformably overlying the upper beds of the Zeballos Group exposed at Cerro Zeballos summit. These lavas represent the base of the meseta and are found here at an elevation of 1970 m, about ten meters beneath the basal levels of the main meseta immediately to the east (Fig. 15). The most important evidence come from several felsic subvolcanic bodies (Mifeldi pluton, Cerro Lapiz, Pico Rojo) aligned along the N160-170 direction which have been emplaced within the Zeballos Fault Zone between 4 and 3 Ma (Brown et al., 2004 ; Espinoza et al., 2007 ; Boutonnet et al., submitted). Exposure of these bodies indicates that a major tectonic disruption occurred along the Zeballos Fault Zone at 3 Ma or immediately after, causing the relative uplift of the western border of the meseta with respect to the Cordillera.

5. Discussion-Conclusion

5.1. Central Patagonian Cordillera : an unusual regional morphotectonic pattern

This compilation of morphological and tectonic data concerns a portion of the Patagonian Cordillera located at the latitude of the Chile Triple Junction, that is in a region characterized by the occurrence of subducted segments of the Chile Spreading Ridge at depth. A number of striking characters can be extracted from our analysis. Some of them are not encountered in “normal” subduction ranges, i.e. in orogens which are not affected by the subduction of an active spreading ridge.

(i) The Central Patagonian Cordillera is characterized by an overall short wavelength topography and highly contrasted reliefs, typical of deeply incised young mountain belts, but also by an average very low elevation of only ca. 900 m.

(ii) The morphology strongly differs from that of the northernmost Andes. It shows a central, depressed domain, with lowest elevation reaching 300 m below sea level flanked by western and eastern regions of higher elevation having opposite general slope dips. The axial depressed region is also characterized by average low slope gradients and occurs in a position where higher reliefs should be expected in the case of a normal subduction belt.

(iii) Remnants of a former peneplain, the Avellanos surface, locally of erosional origin are widespread within the entire region. Some of these remnants are lying at 2000 m elevation. From geological evidence this peneplain formed between 15 and 4 Ma over the entire region and connected formelly with the meseta domain.

(iv) To the east, the Central Patagonian Cordillera is now separated from the Pampean domain of flat plains and elevated mesetas, representing its former piemont, by N160-N180 trending morphological corridors and west facing scarps. These scarps correspond to neotectonic features controlled by recent vertical faults, mostly active after 3 Ma.

In the core of the Cordillera, 200 km long fault-controlled, linear depressions correspond to asymmetrical tectonic basins. These depression are now occupied by Quaternary glacier valleys and have developed after 10 Ma, cross-cutting the entire belt. This left a main morphological imprint at the scale of entire southern South America. Indeed, at the latitude of the Chile Triple Junction, there is a connection between the Atlantic and Pacific oceans at an elevation of only 200 m. Beside these linear depressions, the Cordillera is cut by polygonal depressions of lesser extent, some of them displaying features typical of tectonically controlled basins such as the Lake Lapparent depression.

5.2. Negative inversion of the frontal thrusts and disruption of the Avellanos surface

Our analysis suggests a former connection between the depositional surface forming the summital regions of the mesetas and the remnants of the Avellanos peneplanation surface exposed in the core of the Cordillera. Interbedding of tills including clasts of the Patagonian batholith and lava flows of the meseta del Lago buenos Aires (Mercer and Sutter, 1982; Lagabrielle et al., 2007) demonstrates such continuity. As reported in detail in upper sections, the age of the upper beds of the molasse, the age of lavas locally capping the Avellanos surface, and the age of the basal flows of the meseta del Lago Buenos Aires strongly constrain the age of the regional Patagonian peneplain between 15 Ma and 4.5 Ma.

Geological and geomorphological features reported in upper sections collectively demonstrate that a major neotectonic event occurred around 3 Ma corresponding to : (1) the tectonic disruption of the former low-relief Avellanos surface along faults oriented N40 to N70 and N160, inside the Cordillera, and (2) the relative uplift of the Cordillera piemont along the N160-N180 trending corridors, in the frontal region. Onset of the erosional dissection of the Avellanos surface and of the borders of the elevating mesetas started at that time, but evidence of normal faulting around 6 Ma have been reported in the Rio Zeballos area (Lagabrielle et al., 2007).

We finally enhance that a negative inversion of the frontal region of the Cordillera occurred at 3 Ma. Vertical offset probably did not exceed 1000 m maximum as observed in the Monte Zeballos region. This represents relatively reduce amount of displacement, but it is enough to significantly impact the regional landscape, inducing the cuesta-like reliefs corresponding to the western edges of the successive mesetas. Such relatively low displacement cannot lead to the neoformation of young, crustal-scale faults, and we infer that the frontal thrusts of the Cordillera have been reactived as normal faults during this period. It is noteworthy that these thrusts are most probably themselves inverted normal faults, inherited from the mid-cretaceous extensional phase which affected South America in relation with the opening of the South Atlantic (Folguera et al., 2004). This scenario has been retained as the main hypothesis in the evolutionary model proposed in figure 17. The occurrence of local, abundant 3 Ma old magmatic products strongly suggests a rooting of these faults deep into the crust, as expected for major tectonic boundaries active since Mesozoic times.

Tectonic inversion in the frontal region due to normal faulting was coeval with collapse of distributed basins inside the Cordillera, and with regional tilt of crustal blocks separated by normal faults. The Lapparent basin is one of the best examples of intra-Cordilleran tectonic depressions. It displays a number of important characteristics: (1) the outlines of the basin are very sharp and linear, (2) triangular facets occur on its northern border, (3) tilted floor to the north indicates flexural deformation linked with normal faulting evoking roll-over style of deformation over a main normal fault. Asymmetrical morphology is also reported from the study of the western and central segments of the Lago General Carrera-Buenos Aires and of the Tamango basin.

Finally, the post-3Ma brittle deformation involves differential tilting of an assemblage of crustal blocks having typical sizes of 20-30 km. This pattern is the key to describe the morphotectonic evolution of Central Patagonia. This tectonic style accounts well for the progressive lowering of the Avellanos peneplain surface towards the east (Fig. 16). Similarly, flexure-driven, eastward tilting of main crustal blocks main explain the regional eastward slope of the meseta del Lago Buenos Aires and meseta del Guenguel.

5.3. Origin and significance of the Avellanos surface

The origin of the high-elevated peneplain of the Central Patagonian Cordillera is an important issue that implies further studies and more detailed investigations and dating. However, in a preliminary approach this surface can be viewed as the consequence of one of two opposite peneplanation processes. The first model derives from the classical view of mountain chains peneplanation by long-term erosion that smoothes relief and progressively lowers elevation of the entire belt near sea-level, as described by Davis (1889). According to this model, observations of remnants of peneplain lying at 2000 m would implie that the entire Central Patagonian Cordillera was capped by a low-elevation surface which has been uplifted to 2000 m during the Pliocene. The second model implies processes of peneplanation at high elevation, resulting from the rise of the base level as described by Babault et al. (2005) in the case of Pyrenean belt. According to this model, high-elevation peneplanation of the Patagonian Cordillera might have started during its tectonic uplift, under the condition that the foreland molasse basins became closed, thus cutting the links with the global marine base level. This might have occurred around 22 Ma during the transition from the marine to the continental molasses. This hypothesis can explain the high-elevated position of remnants of peneplains at 2000 m and the occurrence of fluvio-glacial deposits since 7 Ma in the piemont region, implying elevated reliefs of the Cordillera at that time (Lagabrielle et al., submitted and references herein).

Whatever peneplanation model is retained, it is noteworthy that during the Late Miocene-Pliocene, the morphology of the Patagonian Cordillera was totally different from the current one. The depressions of lakes General Carrera-Buenos Aires and Cochrane-Puyerredon did not exist. Glaciers and rivers were flowing to the east producing a regional surface erasing the reliefs and depositing the upper sequences of the molasse basins. The region was characterized by a continuous slope connecting the high reliefs of the central Cordillera to these now elevated fluvio-glacial depocenters.

5.4. Links with the subduction of the Chile Spreading Ridge

The timing of the extensional deformation deduced from this work is synchronous with the migration at depth of segments of the South Chile Ridge which entered the trench around 6 and 3 Ma, resulting in the opening of an asthenosphere window beneath Central Patagonia (Lagabrielle et al., 2004; Breitsprecher and Thorkelson, 2008, and references therein). The opening of asthenospheric slab-windows allows hot mantle to reach lithospheric regions. This model was proposed by Murdie et al. (2000) in the case of Central Patagonia in order to explain the large negative Bouguer anomaly reaching -160 mgal measured in the central part of the study area. This is also consistent with local features such as the high heat flow values mesuread from bottom sediments of the Lake General Carrera-Buenos Aires (Murdie *et al*., 1999) and the eruption of the Murta basalts with oceanic mantle affinity during the Quaternary, in a valley close to the Lake Lapparent depression (Demant *et al*., 1998; Guivel et al., 2006). The presence of abnormal hot manle at depth is confirmed by evidence at a regional-scale including : 1) low Vs velocities at 100 km depth revealed by seismic tomography (Heintz et al., 2005), and 2) abnormal terrestrial high heat flow values at around 160 mW/m^2 along the Patagonian Cordillera (Hamza and Munoz, 1996), 3) high heat flow values , 4) thin lithosphere less than 100 km (Artemieva et al., 2006)

The tectonic events described in this work occurred synchronously with magmatic activity in Central Patagonia. We have evidenced a clear relationship between the negative inversion of the frontal region and the emplacement of felsic and basic magmas around 3 Ma along the Cordillera front, preferentially in the Rio Zeballos region but also within the Cordillera itself. This magmatic activity has been regarded as the consequence of a thermal anomaly linked to the presence of hot mantle beneath the South America plate, replacing a “normal”, colder slab (Morata et al., 2002; Guivel et al., 2006; Espinoza et al. 2007; Lagabrielle et al. 2007).

Progressive replacement of cold lithosphere by hot mantle may drive overall uplift followed by regional collapse due to weakening of the base of the mountain belt. Uplift of the entire Cordillera occurred first as a consequence of crustal shortening during a long period of “normal subduction” starting around 30 Ma, prior to the collision with the South Chile Ridge at 15 Ma in Southern Patagonia. Compression resumed in Central Patagonia around 15 Ma. The Avellanos surface was progressively established on the piemont of this Cordillera. We do not have any informations allowing to depict the original overall shape of this surface in the period 15 Ma-3 Ma. We may suspect that it connected to higher reliefs to the west, which are now eroded or collapsed. A possible evolution is that the migration of a segment of the Chile Spreading Ridge at 6 Ma triggerred regional uplift of the Cordillera, causing or increasing the doming of the Avellanos surface. In a second stage, around 3 Ma, when a second segment of the Chile Spreading Ridge entered the trench, this dome has been dissected and interrupted by a series of tectonically-controlled depressions in relation with increased weakening of the crust. This hypothesis accounts well for the current morphology of the Central Cordillera, characterized by a central depressed region. This peculiar pattern shows striking affinities with rift topographies having uplifted shoulders and an internal depression controlled by linear faults. Typical rift morphology is also reported farther south in Patagonia were extension has been shown to be still active (Diraison et al., 1997).

Acknowledgements

This work is part of PhD thesis of BS. Field work for the french team (YL, JM, BS) was made possible through grants from the ECOS-Sud program and from the CNRS-INSU Dyeti and Reliefs programs.

References

Artemieva, I.M., 2006. Global 1°x1° thermal model TC1 for the continental lithosphere: implications for lithosphere secular evolution.*Tectonophysics*, 416, 245-277.

Babault, J., Van Den Driessche, J., Bonnet, S., Castelltort, S., Crave, A., 2005. Origin of the hightly elevated Pyrenean peneplain. Tectonics, vol. 24, TC2010, doi:10.1029/2004TC001697.

Bangs, N.L., Cande, S.C., Lewis, S.D., Miller, J.J., 1992. Structural framework of the Chile margin at the Chile Ridge collision zone. Proc. Ocean Drilling Program. Initial report 141, 11-21.

Bell, M., Suarez, M., 2000. The Rio Lacteo Formation of southern Chile. Late Paleozoic orogeny in the Andes of the southernmost South America. Journal of South American Earth Sciences 13, 133-145.

Blisniuk, P.M., Stern, L.A., Chamberlain, P., Idleman, B., Zeitler, P.K., 2005. Climatic and ecologic changes during Miocene surface uplift in the Southern Patagonian Andes. Earth and Planetary Science Letters 230, 125-142.

Boutonnet, E., Arnaud, N., Guivel., C., Lagabrielle, Y., Scalabrino, B. Magmatic evolution of the Patagonian tectonic front : new chronological constraints from the Western edge of Meseta del Lago Buenos Aires, Argentina. Submitted to Lithos.

Bradley, D., Kusky, T., Haeussler, P., Goldfard, R., Miller, M., Dumoulin, J., Nelson, S.W., and Karl, S., 2003. Geologic signature of early Tertiary ridge subduction in Alaska. In Sisson, V.B., Roeske, S.M., and Palvis, T.L., eds., Geology of a transpressional orogen developed during ridge-trench interaction along the North pacific margin: Boulder, Colorado, Geological Society of America Special paper 371, p. 19-49.

Breitsprecher, K. and Thorkelson, D.J., 2008. Neogene kinematic evolution of the Nazca–Antarctic–Phoenix slab windows beneath Patagonia and the Antarctic Peninsula. Tectonophysics. doi: 10.1016/j.tecto.2008.02.013

Brown, L.L., Singer, B.S., Gorring, M.L., 2004. Paleomagnetism and $^{40}Ar/^{39}Ar$ chronology of lavas from Meseta del Lago Buenos Aires, Patagonia. Geoch. Geophys. Geosyst. 5 (1), Q01H04. Doi :10.1029/2003GC000526.

Bruce, Z.R.V., 2001. Mesozoic Geology of the Puerto Ingeniero Ibanez area, 46° South, Chilean Patagonia. PhD Thesis, unpublished, University of Canterbury.

Cande, S.C., Leslie, R.B., 1986. Late Cenozoic tectonics of the Southern Chile Trench. J. Geophys. Res. 91, 471-496.

Cande, S.C., Leslie, R.B., Parra, J.C., Hobart, M., 1987. Interaction between the Chile ridge and the Chile trench : geophysical and geothermal evidence. J. Geophys. Res. 92, 495-520.

Cembrano, J., Hervé, F., 1993. The Liquine-Ofqui fault zone : A major Cenozoic strike-slip duplex in Southern Andes. Second International Symposium on Andean Geodynamics, Oxford (UK), extended abstract, ORSTOM editions.

Cembrano, J., Hervé, F., Lavenu, A., 1996. The Liquine-Ofqui fault zone : A long-lived intra-arc fault system in Southern Chile. Tectonophysics 259, 207-224.

Cembrano, J., Lavenu, A., Reynolds, P., Arancibia, G., Lopez, G., Sanueza, A., 2002. Late Cenozoic transpressional ductile deformation north of the Nazca-Sout America-Antarctica triple junction. Tectonophysics 354, 289-314.

Charrier, R., Linares, E., Niemeyer, H., Skarmeta, J., 1979. K-Ar ages of basalt flows of the Meseta Buenos Aires in southern Chile and their relation to the southeast Pacific triple junction. Geology 7, 436-439.

Coutand, I., Diraison, M., Cobbold, P.R., Gapais, D., Rossello,E.A., Miller, M., 1999. Structure and kinematics of a foothills transect, Lago Viedma, Southern Andes (49°30'S). Journal of South America Earth Sciences (Oxford) 12, 1-15.

Davis, W.M., 1889. The geographical cycle. Geogr. J., 14, 481-504.

De La Cruz, R. and Suárez, M., 2005. Geología del área Puerto Guadal-Puerto Sánchez, Región Aisén del General Carlos Ibáñez del Campo, Escala 1:100.000. *Servicio Nacional de Geología y Minería, Serie Geología Básica, Carta Geológica de Chile.* Santiago, Chile.

De La Cruz, R., Suárez, M., Morata, D., Espinoza, F. and Troncoso, A., 2003. El Cenozoico del Lago General Carrera, Aysén, Chile (46º30'-47º15'S): estratigrafía y tectónica. *In Congreso Geológico Chileno No. 10,* Concepción.

De La Cruz, R., Welkner, D., Suárez, M. and Quiroz, D., 2004. Geología del área oriental de las hojas Cochrane y Villa O'Higgins, Región Aisén del General Carlos Ibáñez del Campo, escala 1:250.000. *Servicio Nacional de Geología y Minería, Serie Geología Básica, Carta Geológica de Chile,* 85. Santiago, Chile.

Demant, A., Belmar, M., Hervé, F., Pankhurst, R.J., Suarez, M., 1998. Pétrologie et géochimie des basaltes de Murta : une éruption sous-glaciaire dans les Andes patagoniennes (46°S). Relation avec la subduction de la ride du Chili. C. R. Acad Sci., Paris 327, 795-801.

DeMets, C., Gordon, R.G., Argus, D.F., Stein, S., 1990. Current plate motions. Geophys. J. Int. 101, 425-478.

Dickinson, W.R., and Snyder, W.S. 1979. Geometry of subducted slab related to the San Andreas transform. Journal of Geology, v.87, p.609-627.

Diraison, M., Cobbold, P.R., Gapais, D., Rossello, E.A., 1997. Magellan strait : Part of a Neogene rift system. Geology 25, 703-706.

Diraison, M., Cobbold, P.R., Gapais, D., Rossello, E.A., Le Corre, C., 2000. Cenozoic crustal thickening, wrenching and rifting in the foothills of the southernmost Andes. Tectonophysics 316, 91-119.

Espinoza, F., Morata, D., Pelleter, E., Maury, R.C., Suarez, M., Lagabrielle, Y., Polvé, M., Bellon, H., Cotten, J., de la Cruz, R., Guivel, C., 2005. Petrogenesis of the Eocene and Mio-Pliocene alkaline basaltic magmatism in Meseta Chile Chico, Southern Patagonia, Chile : evidence for the participation of two slab windows. Lithos 82 (3-4), 315-343.

Espinoza, F., Morata, D., Polvé, M., Lagabrielle, Y., Maury, R. C., Guivel, C., Cotten, J., Bellon, H., Suárez, M. 2007. Bimodal back-arc alkaline magmatism after ridge subduction: Pliocene felsic rocks from Central Patagonia (47ºS). *Lithos*, vol. 101 (1-2), pp. 191-217.

Espinoza, F., Morata, D., Polvé, M., Lagabrielle, Y., Maury, R. C., De la Rupelle, A., Guivel, C., Cotten, J., Bellon, H., Suárez, M. Calc-alkaline back-arc volcanism in Central

Patagonia (47ºS): petrogenesis and implications for Miocene mantle-slab dynamics. Submitted to *Revista Geológica de Chile*.

Espinoza, F., Morata, D., Polvé, M., Maury, R., Cotten, J., Bellon, H., Guivel, C., Lagabrielle, Y., Suarez, M., and Rossello, E. 2006. Mio-Pliocene magmatic variability in the Central Patagonia Back-Arc region (47º5'S). *In Backbone of the Americas*, Mendoza, Argentina. 4-12, 57.

Flint, F.F., Prior, D.J., Agar, S.M., Turner, P., 1994. Stratigraphic and structural evolution of the tertiary Cosmelli basin and its relationships to the Chile Triple Junction. Journal of Geological society of London 151, 251-268.

Flynn, J.J., Novacek, M.J., Dodson, H.E., Frassinetti, D., McKenna, M.C., Norell, M.A., Sears, K.E., Swisher III, C.C., Wyss, A.R., 2002. A new fossil mammal assemblage from the Southern Chilean Andes : implications for geology, geochronology and tectonics. Journal of South American Earth Sciences 15, 285-302.

Folguera, A., Ramos, V.A., Hermanns, R., Naranjo, J., 2004. Neotectonics in the foothills of the southernmost central Andes (37°–38°S): evidence of strike-slip displacement along the Antiñir-Copahue fault zone. Tectonics, vol. 23 (TC 5008), pp. 23.

Frassinetti, D., Covacevich, V., 1999. Fauna de invertebrados fosiles marinos de la Formacionn Guadal en Pampa Castillo, sur del lago General Carrera, Aysen, Chile. Boletin, vol. 51. Servicio Nacional de Geologia y Mineria, Chile. 96 pp.

Garret, S.W., Storey, B.C., 1987. Lithospheric extension on the Antarctica Peninsula during Cenozoic subduction. In Extension in the basin and Range Province and East Pacific Margin, Geological Society, London, Special Publications, v. 28, pp. 419-431.

Gorring, M., Kay, S., 2001. Mantle processes and sources of Neogene slab window magmas from Southern Patagonia, Argentina. J. Petrol. 42, 1067-1094.

Gorring, M., Kay, S., Zeitler, P., Ramos, V., Rubiolo, D., Fernandez, M., Panza, J., 1997. Neogene Patagonian plateau lavas : continental magmas associated with ridge collision at the Chile Triple Junction. Tectonics 16, 1-17.

Gorring, M., Singer, B., Gowers, J., Kay, S., 2003. Plio-Pleistocene basalts from the Meseta del Lago Buenos Aires, Argentina : evidence for asthenosphere-lithosphere interactions during slab-window magmatism. Chem. Geol. 193, 213-235.

Gripp, A.E., Gordon, R.G., 1990. Current plate velocities relative to the hotspots incorporating the NUVEL-1 global plate motion model. Geophysical Research Letters 17, 1109-1112.

Guivel, C., Morata, D., Pelleter, E., Espinoza, F., Maury, R.C., Lagabrielle, Y., Polvé, M., Bellon, H., Cotten, J., Benoit, M., Suarez, M., de la Cruz, R., 2006. Miocene to Late Quaternary Patagonian basalts (46°-47°S) : Geochronometric and geochemical evidence for slab tearing due to active spreading ride subduction. Journal of Volcanology and Geothermal research 149, 346-370.

Hamza, V.M., Munoz, M., 1996. Heat flow map of South America. Geothermics 25(6), 599-646.

Heintz M., Debayle, E., Vauchez. A., 2005. Upper mantle structure of the South America continent and neighboring oceans from surface wave tomography. Tectonophysics, 406, 115-139.

Herron, E.M., Cande, S.C., Hall. B.R., 1981. An active spreading center collides with a subduction zone ; geophysical survey of the Chile margin triple junction. Memoir-Geological Society of America 154, 683-701.

Hervé, F., 1993. Paleozoic metamorphic complexes in the Andes of Aysen, Southern Chile (West of Occidentalia). Proceedings of the First Circum Pacific and Circum Atlantic Terrane Conference, Guanajato, Mexico, pp. 64-65.

Hervé, F., 1994. The Southern Andes between 39°S and 44°S latitude : the geological signature of a transpressive tectonic regime related to a magmatic arc. In : Reutter, K-J., Scheuber, E., Wigger, P.J., (Eds), Tectonics of the Southern central Andes. Springer, Berlin, pp.243-248.

Howard, 1967. A.D. Howard, Drainage analysis in geologic interpretation: a summation. *Am. Assoc. Pet. Geol. Bull.* **51** (1967), pp. 2246–2259.

Introcaso, A., Pacino, M.C., Guspi, F., 1996. The Argentina- Chile Andes. Crustal thickness, isostasy, shortening and anomaly prediction from gravity studies. Third ISAG, St Malo (France).

Lagabrielle, Y., Guivel, C., Maury, R.C., Bourgois, Y., Fourcade, S., Martin, H., 2000. Magmatic-tectonic effects of high thermal regime at the site of active spreading ridge subduction : the Chile Triple Junction model. Tectonophysics 326 (3-4), 215-228.

Lagabrielle, Y., Suarez, M., Rossello, E.A., Hérail, G., Martinod, J., Régnier, M., de la Cruz, R., 2004. Neogene to Quaternary tectonic evolution of the Patagonian Andes at the latitude of the Chile Triple Junction. Tectonophysics 385, 211-241.

Lagabrielle, Y., Suarez, M., Malavieille, J., Morata, D., Espinoza, F., Maury, R., Scalabrino, B., de la Cruz, R., Rossello, E., Barbero, L., Bellon, H., 2007. Pliocene extensional tectonics in Eastern Central Patagonian Cordillera : geochronological constraints and new field evidence. Terra Nova.

Lagabrielle, Y., Scalabrino, B., Suarez, M., Ritz, J.F. Mio-Pliocene glaciations of Central Patagonia: New evidence and tectonic implications. Submitted to Andean Geology.

Mercer, J.H., Sutter, J.F., 1982. Late Miocene-Earliest Pliocene Glaciation in Southern Argentina : implications for global ice-sheet history. Paleogeography, Paleoclimatology, Paleoecology 38, 185-206.

Morata, D., Barbero, L., Suarez, M., de la Cruz, R., 2002. Early Pliocene magmatism and high exhumation rates in the Patagonian Cordillera (46°40'S) : K-Ar, and fission track data. ISAG.

Murdie, R., Styles, P., Prior, D.J., Daniel, A.J., 2000. A new gravity map of Southern Chile and its preliminary interpretation. Revista Geologica de Chile 27 (1), 49-63.

Murdie, R.E., Pugh, D.T., Styles, P., 1999. A lightweight, portable, digital probe for measuring the thermal gradient in shallow water sediments, with examples from patagonia. Geo-Marine Letters 18, 315-320.

Nelson, E., Forsythe, R., Diemer, J., Allen, M., Urbina, O., 1993. Taitao ophiolite : a ridge collision ophiolite in the forearc of the southern Chile (46°S). Revista Geologica de Chile 20(2), 137-165.

Niemeyer, H., Skarmeta, J., Fuenzalida, R and Espinosa, W. 1984. Hojas Peninsula de Taitao y Puerto Aisen, Region de Aisen del General Carlos Ibanez del Campo. Carta Geologica de Chile, 60-61, 1:500.000. Sevicio Nacional de geololgia y Mineria, Chile

Pankhurst, R.J., Weaver, S.D., Hervé, F., Larrondo, P., 1999. Mesozoic-Cenozoic evolution of the North Patagonian Batholith in Aysen, southern Chile. Journal of the Geological Society (London), 156.

Pardo-Casas, F., Molnar, P., 1987. Relative motion of the Nazca (Farallon) and South America plates since Late Cretaceous time. Tectonics 6 no 3, 233-248.

Pelleter, E.W., 2003. Diversité géochimique et géochronologique des basaltes de la région du lac General Carrera Buenos Aires : nouvelles contraintes sur la subduction de la dorsale active du Chili. DEA Thesis, Université de Bretagne Occidentale, Brest, France.

Petford, N., Turner, P., 1996. Reconnaissance 40Ar/39Ar age and paleomagnetic study of igneous rocks around Coyhaique, S. Chile. Third International Symposium on Andean Geology (ISAG), St. Malo, France, 625-627.

Ramos, V., Kay, S.M., 1992. Southern Patagonian plateau basalts and déformation : backarc testimony of ridge collision. Tectonophysics 205, 261-282.

Ramos, V.A., 1989. Andean foothills structures in the northern Magallanes Basin, Argentina. American Association of Petroleum Geologist Bulletin 73, 887-903.

Ramos, V.A., 2002. El magmatismo neógeno de la Cordillera Patagónica. In: M.J. Haller (Ed.): Geología y Recursos Naturales de Santa Cruz. Relatorio del XV Congreso Geológico Argentino. El Calafate, I-13:187-199. Buenos Aires..

Ray, F.M., 1996. Stratigraphical and structural evolution of Tertiary backarc basins in Southern Chile (44°S-47°S). University of Liverpool, England, 208 pp. Unpublished PhD Thesis.

Scalabrino, B., Lagabrielle, Y., de la Rupelle, A., Malavieille, J., Polvé, M., Espinoza, F., Morata, D., Suarez, M. Subduction of an active spreading ridge beneath Southern South America : A review of the Cenozoic geological records from the Andean foreland, Central Patagonia (46-47°S). IJES, special volume, In press.

Singer, B.S., Ackert, R.P., Guillou, H., 2004. $^{40}Ar/^{39}Ar$ and K/Ar chronology of Pleistocene glaciations in Patagonia. Geological Society of America 116, no. 3/4, 434-450.

Sisson, V.B., and Palvis, T.L., 1993. Geologic consequences of plate reorganization: An example from the Eocene southern Alaska forearc. Geology, v.21, p.913-916.

Smith W.H.F and Sandwell D.T., 1997. Seafloor topography from satellite altimetry and strip depth soundings, Science.

Suarez, M., de la Cruz, R., 2000. Tectonics in the eastern central Patagonian Cordillera (45°30'-47°30'S). Journal of the Geological Society (London) 157, 995-1001.

Suarez, M., de la Cruz, R., 2001. Jurassic to Miocene K-Ar dates from eastern central Patagonian Cordillera plutons, Chile (45°-48°S). Geological Magazine 138 (1), 53-66.

Tassara A., Yanez, G., 2003. Relacion entre el espesor elastico de la litosfera y la segmentacion tectonica del margen andino (15°-47°S). Revista Geologica de Chile, vol 30, no.2, p. 159-186.

Tebbens, S.F., Cande, S.C., 1997. Southeast Pacific tectonic evolution from the early Oligocene to Present. Journal of Geophysical Research 102, 12061-12084.

Tebbens, S.F., Cande, S.C., Kpovacs, L., Parra, J.C., Labrecque, J.L., Vergara, H., 1997. The Chile Ridge : A tectonic framework. Journal of Geophysical Research 102, 12035-12059.

Thomson, S.N., Hervé, F., Stockhert, B., 2001. Mesozoic-Cenozoic denudation history of the patagonian Andes (Southern Chile) and its correlation to different subduction processes. Tectonics 20, 693-711.

Thorkelson, D.J., 1990. Tectonic and magmatic aspects of slab window, Geol. Assoc. Can. Progr. Abstr., 15, A105.

Thorkelson D.J.; 1996. Subduction of diverging plates and the principles of slab window formation, *Tectonophysics* **255**, pp. 47–63.

Veloso, E,A,E., Anma, R., Yamazaki, T., 2005. Tectonic rotations during the Chile Ridge collision and obduction of the taitao ophiolite (Southern Chile). Island Arc, v. 14, p. 599-615.

Welkner, G., 1999. Geologia del area del Cerro San Lorenzo cordillera patagonica oriental, XI region de Aysen Chile (47°25'-47°50'). Memoria Titulo Dep. Geologia Univ. Chile. Unpublished.

Figure Captions

Figure 1. Location of the study area in Central Patagonia Cordillera (frame) and of the Chile Triple Junction (star) on a Global Digital Elevation Model of South America and West Antarctic Peninsula together with the bathymetry of the East Pacific Ocean. Land topography is derived from *GTOPO30 EROS Data Center-USGS* and seafloor bathymetry from Smith and Sandwell (1997).

Figure 2. Simplified map of the Chile Triple Junction (CTJ) region and plate tectonic frame of the subduction of the South Chile Ridge (SCR). Active segments (SCR1 to SCR4) and transform faults zone (FZ) are shown (adapted from Tebbens et al., 1987 ; Ramos, 1989 ; DeMets et al., 1990 ; Cembrano et al., 1996 ; Guivel et al., 1999). Magnetic anomalies of Nazca and Antarctica plates are also shown. Inferred position of the slab window below South American plate is represented a dark gray pattern. LGCBA : Lake General Carrera Buenos Aires ; LCP : Lake Cochrane-Pueyrredon.

Figure 3. a) Simplified geological map of the Central Patagonian Cordillera at the latitude of the Chile Triple Junction. LGCBA: Lake General Carrera-Buenos Aires, LCP: Lake Cochrane-Pueyrredon (A-B, section shown in fig. 3b). b) Schematic lithospheric-scale cross section A-B across Patagonian Cordillera at the latitude of the Chile Triple Junction, inferred from surface geology. Section has no vertical exaggeration. LOFZ : Liquine Ofqui Fault Zone ; MLBA : Meseta del Lago Buenos Aires.

Figure 4. Digital Elevation model (DEM SRTM-90m) and Landsat 7 image of the Central Patagonian Cordillera at the latitude of the Chile Triple Junction. MLBA : Meseta del Lago Buenos Aires ; LGCBA : Lake General Carrera Buenos Aires ; LCP : Lake Cochrane Pueyrredon. Black star represents the deepest part of the Lake General Carrera Buenos Aires at approximatively 380 m.b.s.l (bathymetry from Murdie et al., 1999).

Figure 5. Slope gradient digital map of the Central Patagonian Cordillera at the CTJ latitude. High-elevated low-relief surfaces remnants appear as small areas with a local slope less than 10%. The smooth domain within the Cordillera is characterized by local slopes lower than 10% and corresponds to a depressed area including the Oligocene-Miocene internal basin of Cosmelli and the deep floor of the Lake General Carrera-Buenos Aires.

Figure 6. a) Numerical W-E trending topographic sections of the Central Patagonian Cordillera between 46°S and 48°S. b) Swath profile along the Patagonian Cordillera between 46°S and 48°S showing maximal and minimal elevations of the belt. The calculated mean elevation averaged over the study area is shown by the black line inside the grey domain.

Figure 7. Geomorphological map of the Central Patagonian Cordillera showing the main features discussed in text, including : relict Miocene-Pliocene surfaces and internal depressions inside the Cordillera and mesetas lying east of the morphotectonic front.

Figure 8. a) and b) Two panoramic views of the Avellanos surface capping the reliefs of the northern side of the Lake General Carrera Buenos Aires, taken from 2 localities on the opposite side of the lake (see figure. 4 for location). Photograph in (b) illustrates the erosional character of the Avellanos surface cutting the folded stratas of the Ibanez Formation. c) interpretation of b).

Figure 9. a) Structural and geological map of the Central Patagonian Cordillera at the latitude of the Chile Triple Junction extracted from field observations, DEMs and satellite images (Landsat 7 and Spot 5). The map shows the main tectonic features discussed in text. Rose diagram in b) is constructed from a compilation of all the features shown in map a).

Figure 10. The Lake General Carrera Buenos Aires depression. a) NW-SE oriented topographic profile across the central segment of the lake. b) Schematic interpretation of the central segment of the lake illustrating the asymmetrical character of this depression. c)

Interpreted Spot 5 image showing the southern edge of the central segment of the lake in the area of the Pampa la Perra Fault Zone. d) Photograph of the Rio El Bano conjugate normal faults belonging to the Pampa la Perra fault zone.

Figure 11. Panoramic view and schematic interpretation of the Cerro Tamango Fault Zone on the western border of the Lake Cochrane-Pueyrredon area (see fig. 4 for location).

Figure 12. Numerical N-S trending topographic sections of the Lapparent basin and swath profile showing maximal and minimal surfaces of the Lapparent area. The average elevation is shown by the dark line.

Figure 13. Panoramic view and schematic interpretation of the triangular facets forming the northern border of the Lake Lapparent depression (see fig. 4 for location).

Figure 14. Simplified map and cross section A-B of the Lake Lapparent depression showing the main structural and orographic features. Tectonic features include lineaments observed from satellite images, together with strike-slip and normal faults observed in the field. Cross section A-B has no vertical exaggeration.

Figure 15. Simplified map and cross-section A-B of the southern part of the Rio Zeballos Fault Zone close to the Meseta del Lago Buenos Aires showing the main structural and orographic features. Tectonic features include lineaments observed from satellite images, thrusts faults (after Lagabrielle et al., 2004), strike-slip faults and normal faults. Cross section A-B has no vertical exaggeration. LCP : Lake Cochrane-Pueyrredon ; MLBA : Meseta del Lago Buenos Aires.

Figure 16. a) Two panoramic views showing the Lake Lapparent depression, the meseta del Guenguel and the Avellanos surface. These views are constructed from a DEM drapped with

Landsat 7 images. b) Panoramic photograph of the frontal region of the Central Cordillera taken from a view point at the southern edge of the Lake General Carrera-Buenos Aires, south of Los Antiguos (Argentina). c) Tectonic interpretation of the panorama shown in b).

Figure 17. Late Mesozoic-Cenozoic morphostructural evolution of the Central Patagonian Cordillera at the latitude of the Chile Triple Junction (no vertical exaggeration). This interpretation is based on the hypothesis that the main faults in this region are inherited features which have been inverted few times during this tectonic evolution. This was the case for the frontal thrusts which accomodated extension during the negative inversion of the piemont domain after 3 Ma, as well as for some main faults controlling basins inside the Cordillera.

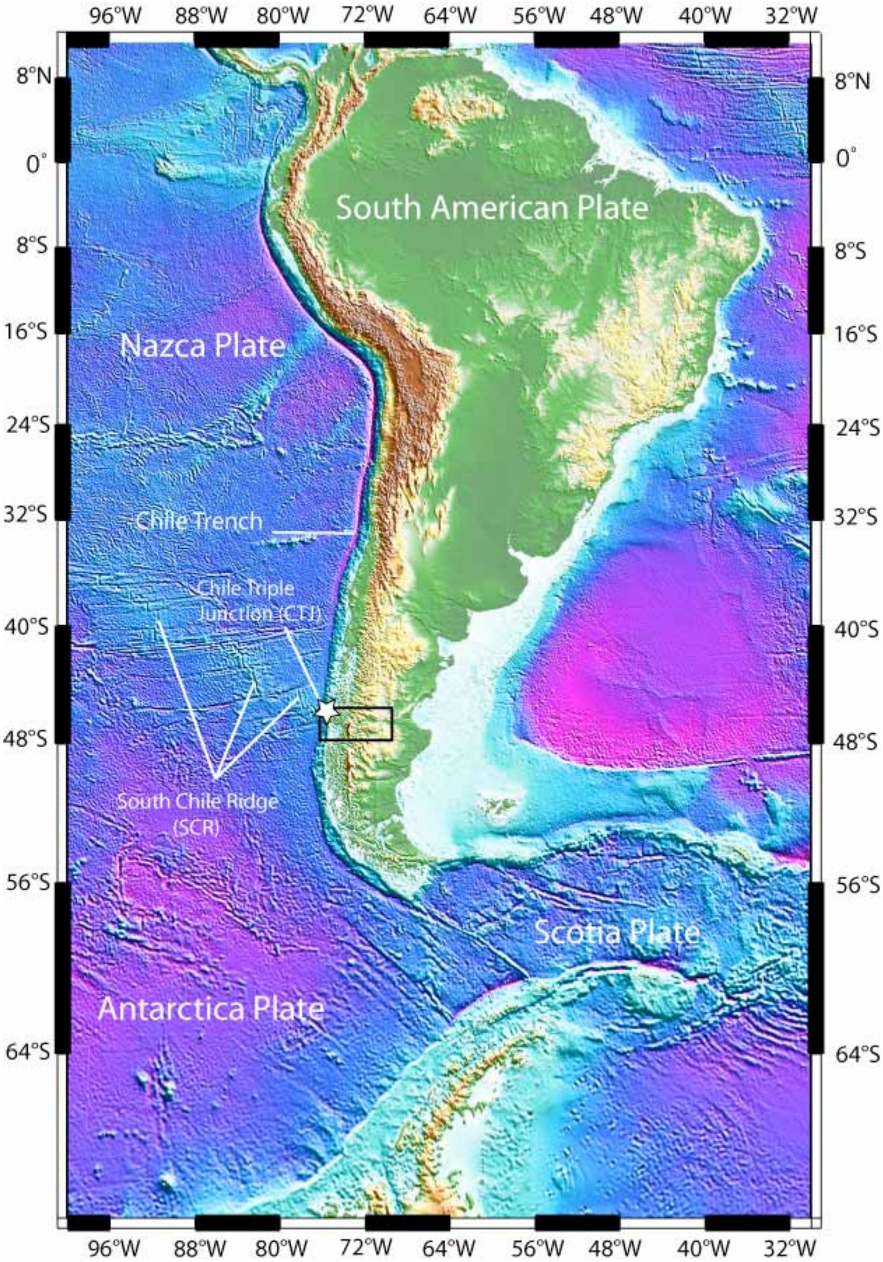
96°W
88°W
80°W
72°W
64°W
56°W
48°W
40°W
32°W
8°N
0°
8°S
16°S
24°S
32°S
40°S
48°S
56°S
64°S
South American Plate
Nazca Plate
Chile Trench
Chile Triple Junction (CTJ)
South Chile Ridge (SCR)
Scotia Plate
Antarctica Plate

Figure 1

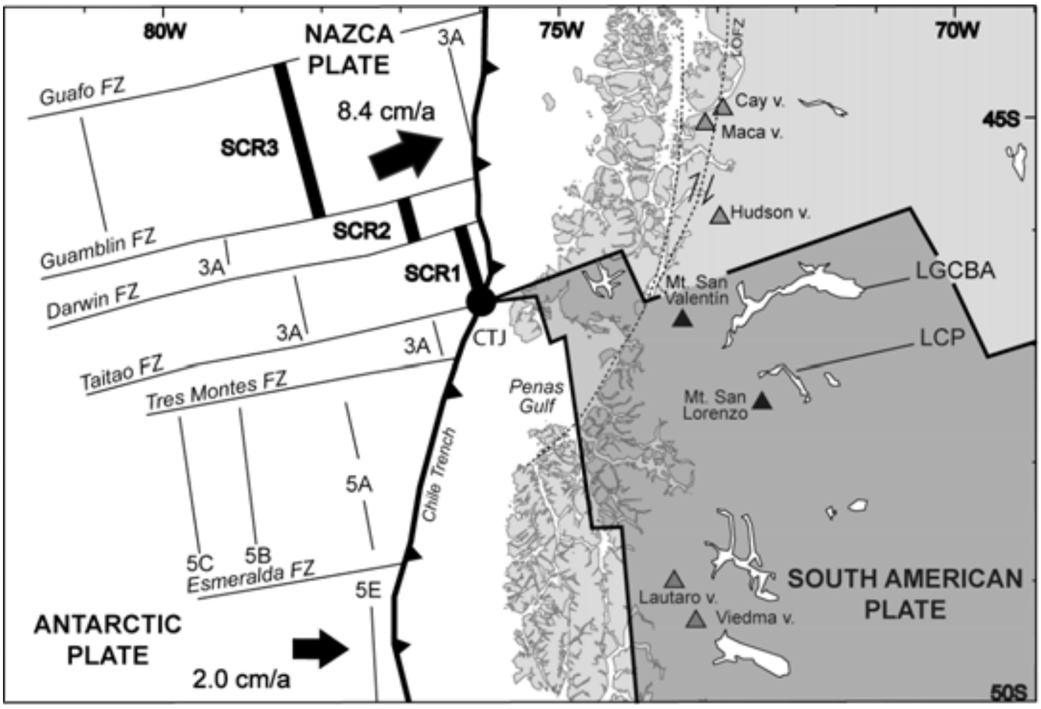
80W
75W
70W
45S
50S
NAZCA PLATE
8.4 cm/a
3A
Guafo FZ
SCR3
SCR2
SCR1
Guamblin FZ
Darwin FZ
3A
CTJ
Taitao FZ
Tres Montes FZ
5A
5C
5B
Esmeralda FZ
5E
Chile Trench
Penas Gulf
ANTARCTIC PLATE
2.0 cm/a
LOFZ
Cay v.
Maca v.
Hudson v.
Mt. San Valentín
LGCBA
LCP
Mt. San Lorenzo
Lautaro v.
Viedma v.
SOUTH AMERICAN PLATE

Figure 2

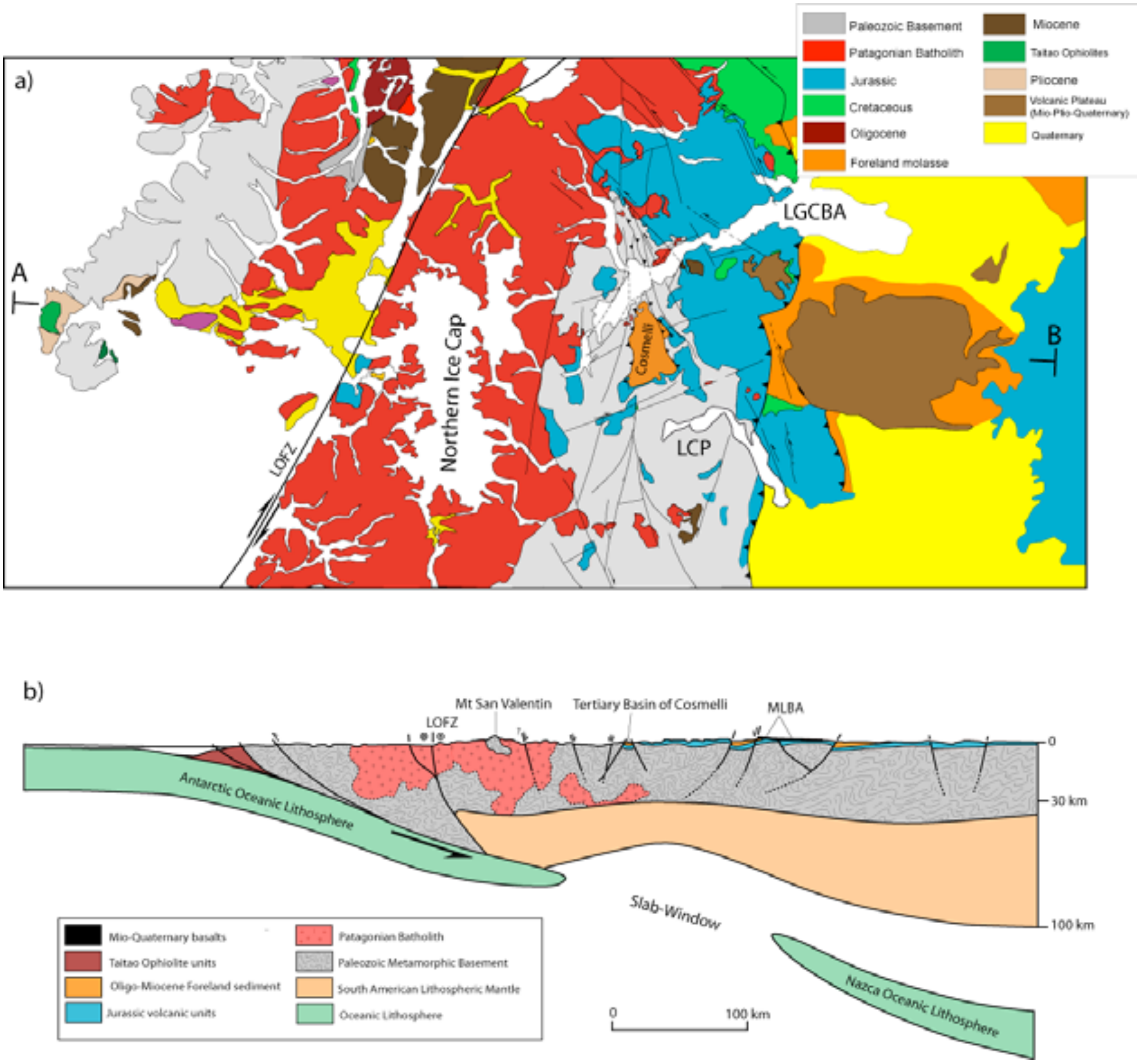

a)
Paleozoic Basement
Patagonian Batholith
Jurassic
Cretaceous
Oligocene
Foreland molasse
Miocene
Taitao Ophiolites
Pliocene
Volcanic Plateau (Mio-Plio-Quaternary)
Quaternary
LGCBA
A
B
Northern Ice Cap
Cosmelli
LCP
LOFZ
b)
Mt San Valentin
Tertiary Basin of Cosmelli
MLBA
LOFZ
0
30 km
100 km
Antarctic Oceanic Lithosphere
Slab-Window
Nazca Oceanic Lithosphere
Mio-Quaternary basalts
Taitao Ophiolite units
Oligo-Miocene Foreland sediment
Jurassic volcanic units
Patagonian Batholith
Paleozoic Metamorphic Basement
South American Lithospheric Mantle
Oceanic Lithosphere
0
100 km

Figure 3

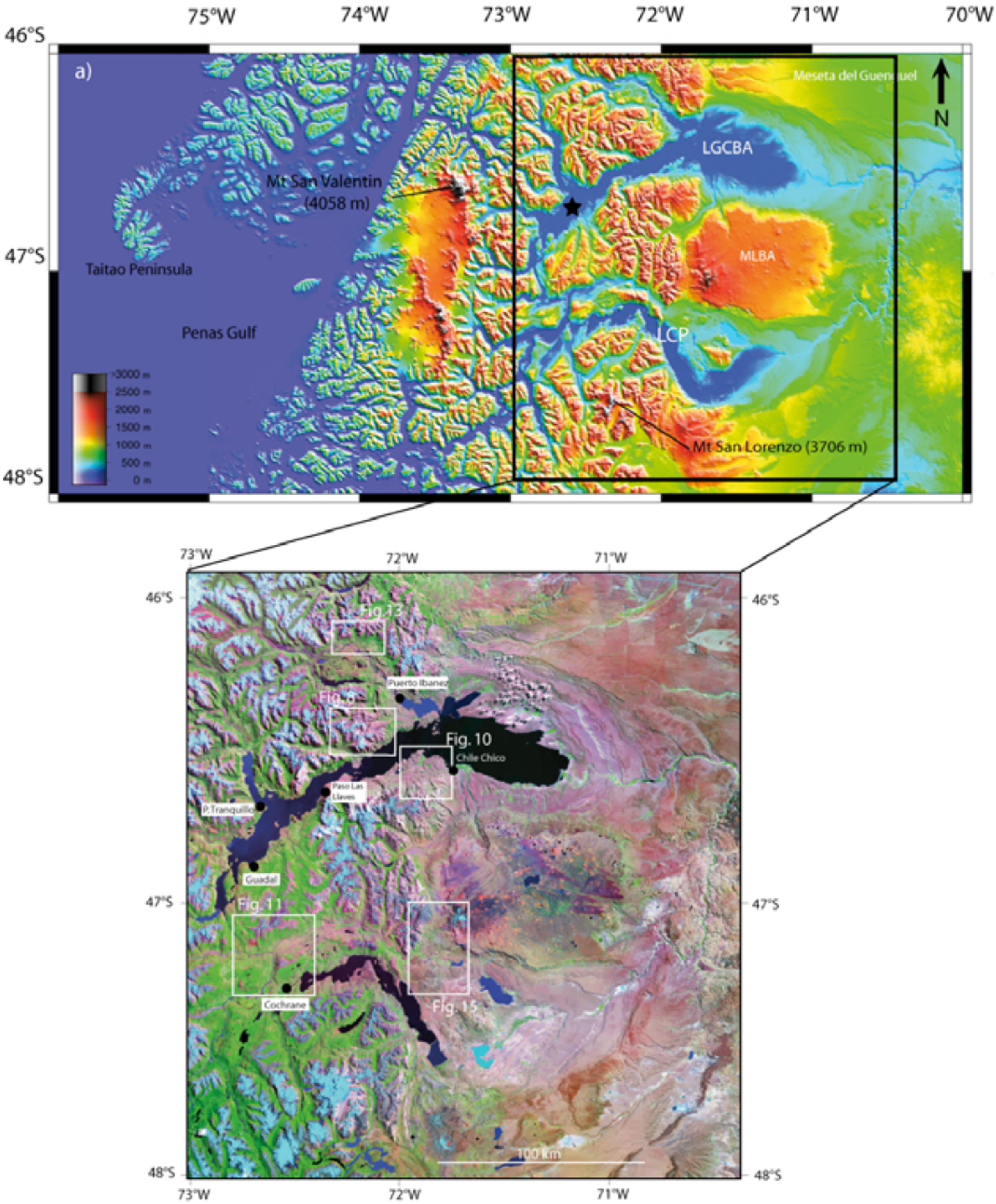
75°W
74°W
73°W
72°W
71°W
70°W
46°S
47°S
48°S
a)
Meseta del Guenguel
N
LGCBA
Mt San Valentin
(4058 m)
Taitao Peninsula
MLBA
Penas Gulf
LCP
>3000 m
2500 m
2000 m
1500 m
1000 m
500 m
0 m
Mt San Lorenzo (3706 m)
Fig.13
Puerto Ibanez
Fig. 8
Fig. 10
Chile Chico
Paso Las Llaves
P. Tranquillo
Guadal
Fig. 11
Cochrane
Fig. 15
100 km

Figure 4

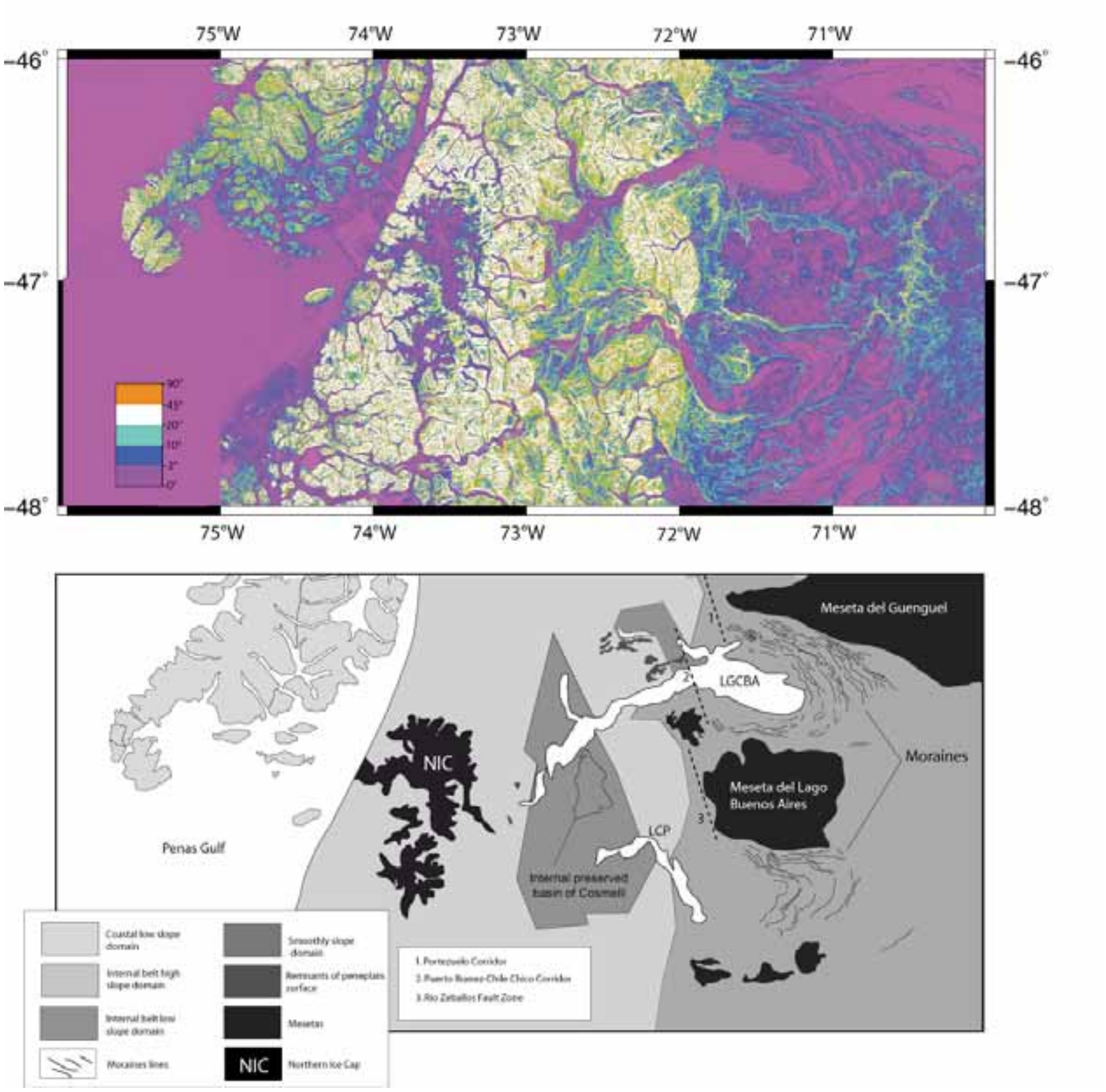
75°W
74°W
73°W
72°W
71°W
-46°
-47°
-48°
90°
45°
20°
10°
3°
0°
Meseta del Guenguel
LGCBA
Moraines
NIC
Meseta del Lago Buenos Aires
LCP
Penas Gulf
Internal preserved basin of Cosmelli
Coastal low slope domain
Internal belt high slope domain
Internal belt low slope domain
Moraines lines
Smoothly slope domain
Remnants of peneplain surface
Mesetas
NIC
Northern Ice Cap
1. Portezuelo Corridor
2. Puerto Ibanez-Chile Chico Corridor
3. Rio Zeballos Fault Zone

Figure 5

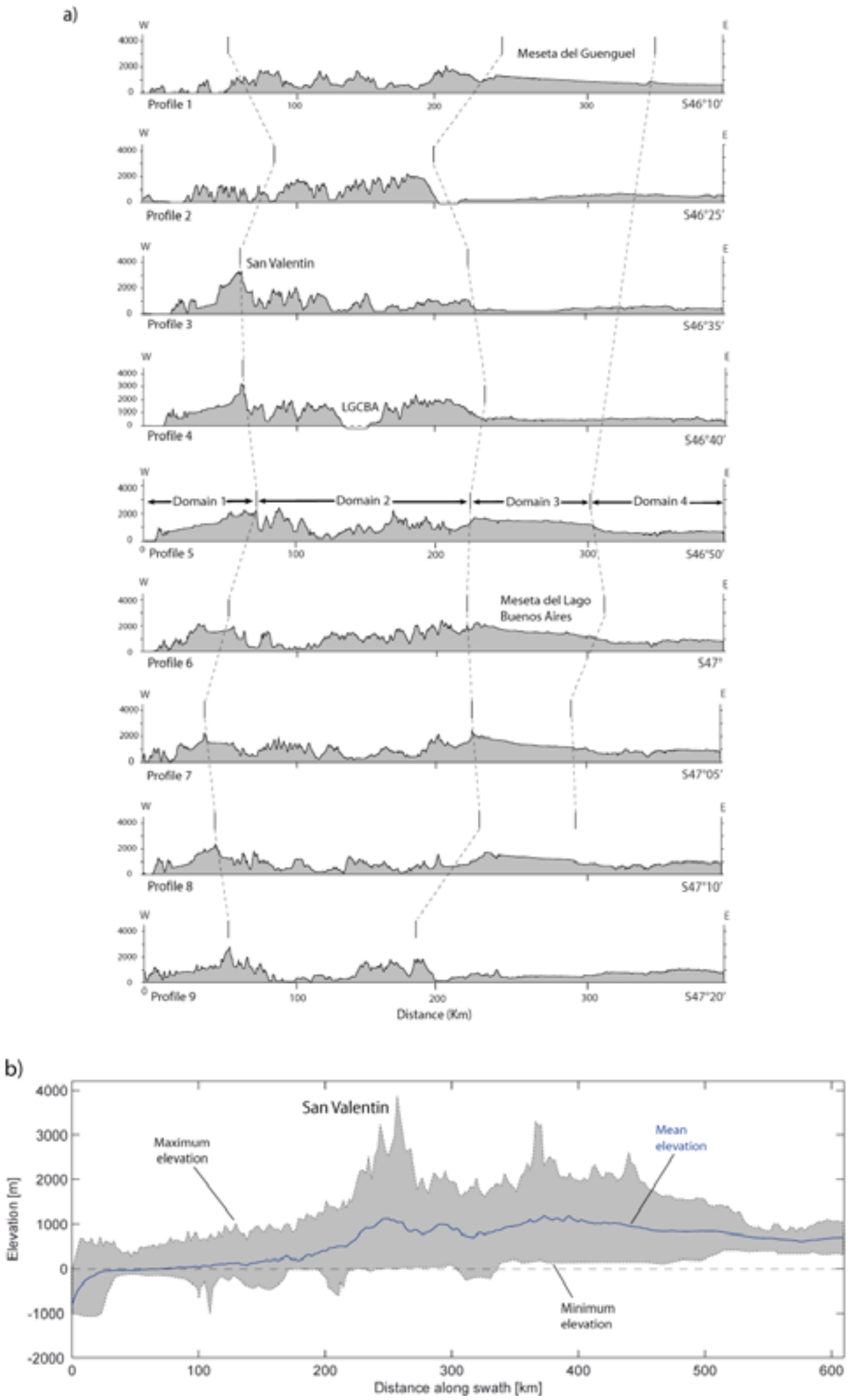

a)
Meseta del Guenguel
Profile 1
S46°10'
Profile 2
S46°25'
San Valentin
Profile 3
S46°35'
LGCBA
Profile 4
S46°40'
Domain 1
Domain 2
Domain 3
Domain 4
Profile 5
S46°50'
Meseta del Lago
Buenos Aires
Profile 6
S47°
Profile 7
S47°05'
Profile 8
S47°10'
Profile 9
S47°20'
Distance (Km)
b)
San Valentin
Maximum
elevation
Mean
elevation
Minimum
elevation
Elevation [m]
Distance along swath [km]

Figure 6

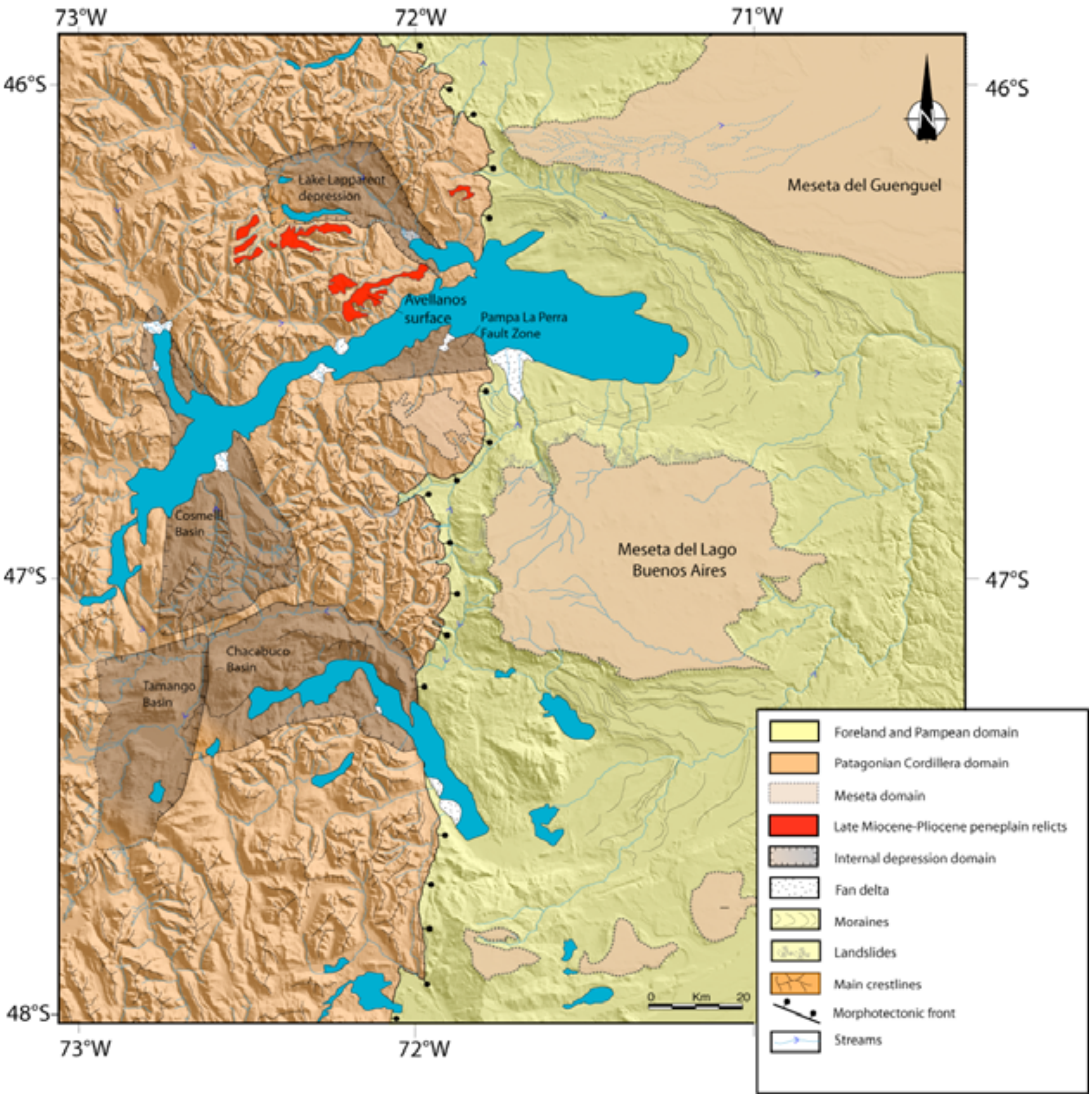

73°W
72°W
71°W
46°S
47°S
48°S
Lake Lapparent depression
Meseta del Guenguel
Avellanos surface
Pampa La Perra Fault Zone
Cosmelli Basin
Meseta del Lago Buenos Aires
Chacabuco Basin
Tamango Basin
0 Km 20
Foreland and Pampean domain
Patagonian Cordillera domain
Meseta domain
Late Miocene-Pliocene peneplain relicts
Internal depression domain
Fan delta
Moraines
Landslides
Main crestlines
Morphotectonic front
Streams

Figure 7

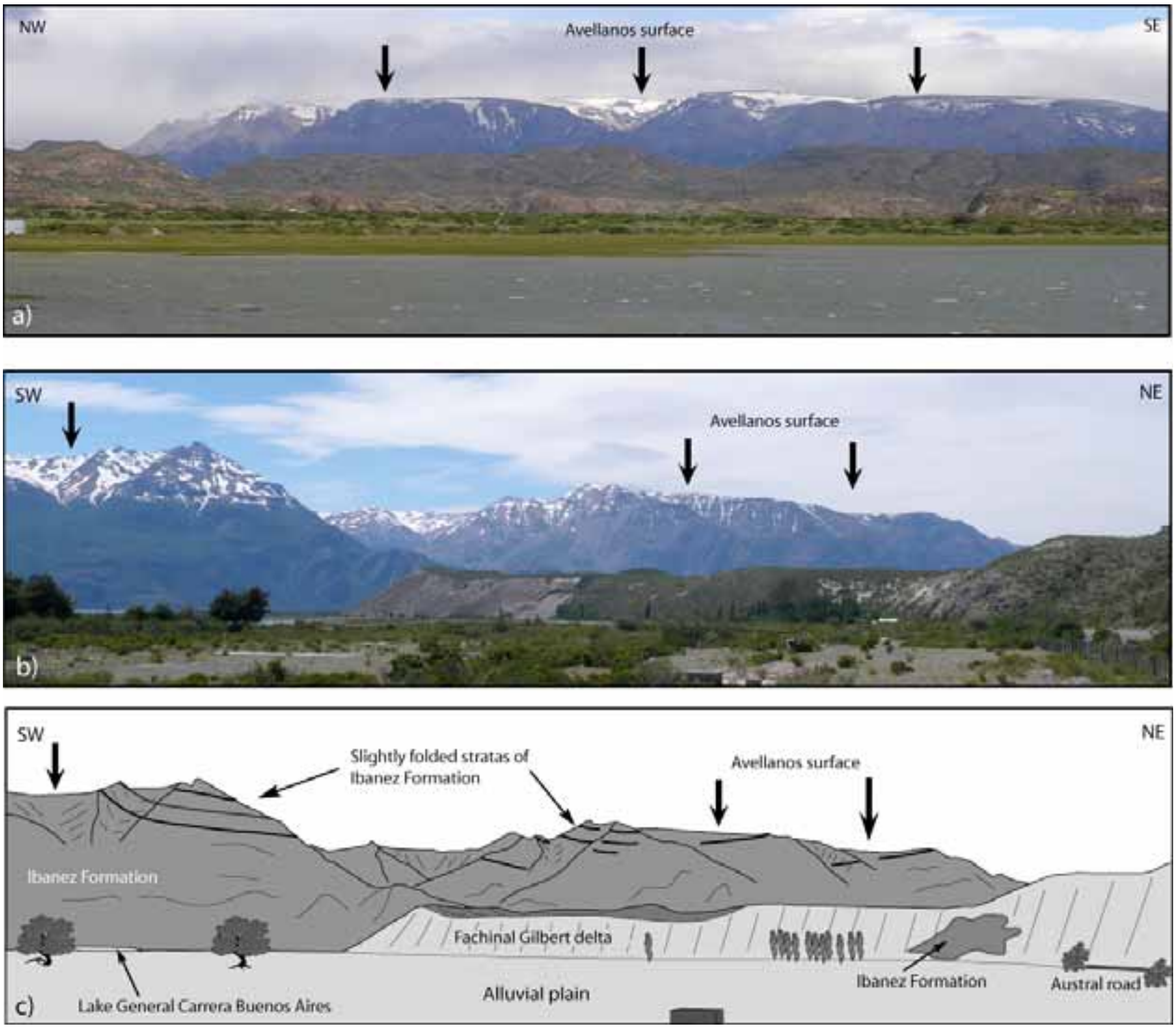
NW
Avellanos surface
SE
a)
SW
NE
Avellanos surface
b)
SW
Slightly folded stratas of
Ibanez Formation
Avellanos surface
NE
Ibanez Formation
Fachinal Gilbert delta
Ibanez Formation
Austral road
Alluvial plain
c)
Lake General Carrera Buenos Aires

Figure 8

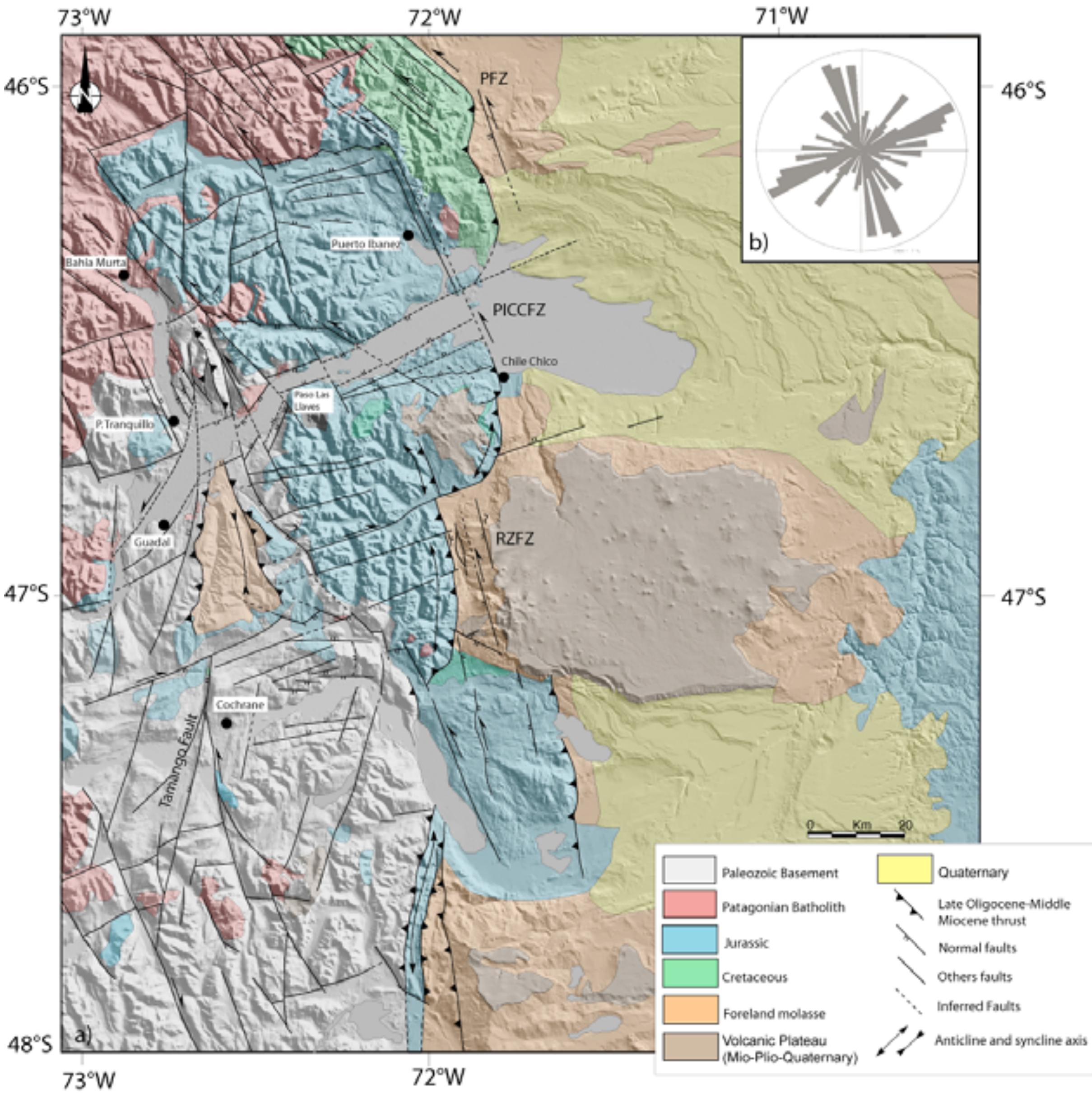

73°W
72°W
71°W
46°S
47°S
48°S
PFZ
PICCFZ
RZFZ
Puerto Ibanez
Bahia Murta
Chile Chico
Paso Las Llaves
P. Tranquillo
Guadal
Cochrane
Tamango Fault
b)
a)
0 Km 20
Paleozoic Basement
Patagonian Batholith
Jurassic
Cretaceous
Foreland molasse
Volcanic Plateau (Mio-Plio-Quaternary)
Quaternary
Late Oligocene-Middle Miocene thrust
Normal faults
Others faults
Inferred Faults
Anticline and syncline axis

Figure 9

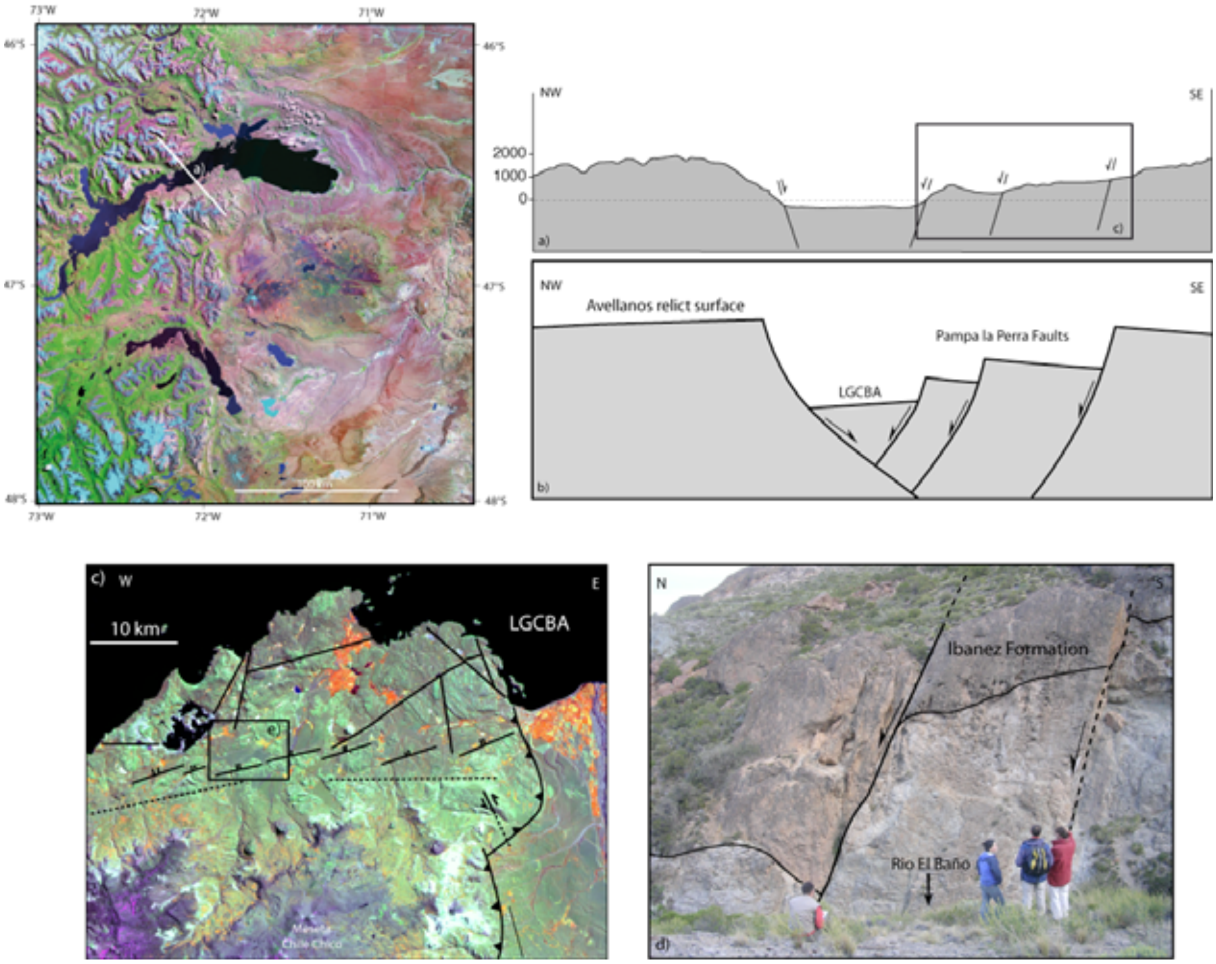

NW
SE
2000
1000
0
a)
c)
NW
SE
Avellanos relict surface
Pampa la Perra Faults
LGCBA
b)
c) W
E
10 km
LGCBA
N
S
Ibanez Formation
Rio El Baño
d)

Figure 10

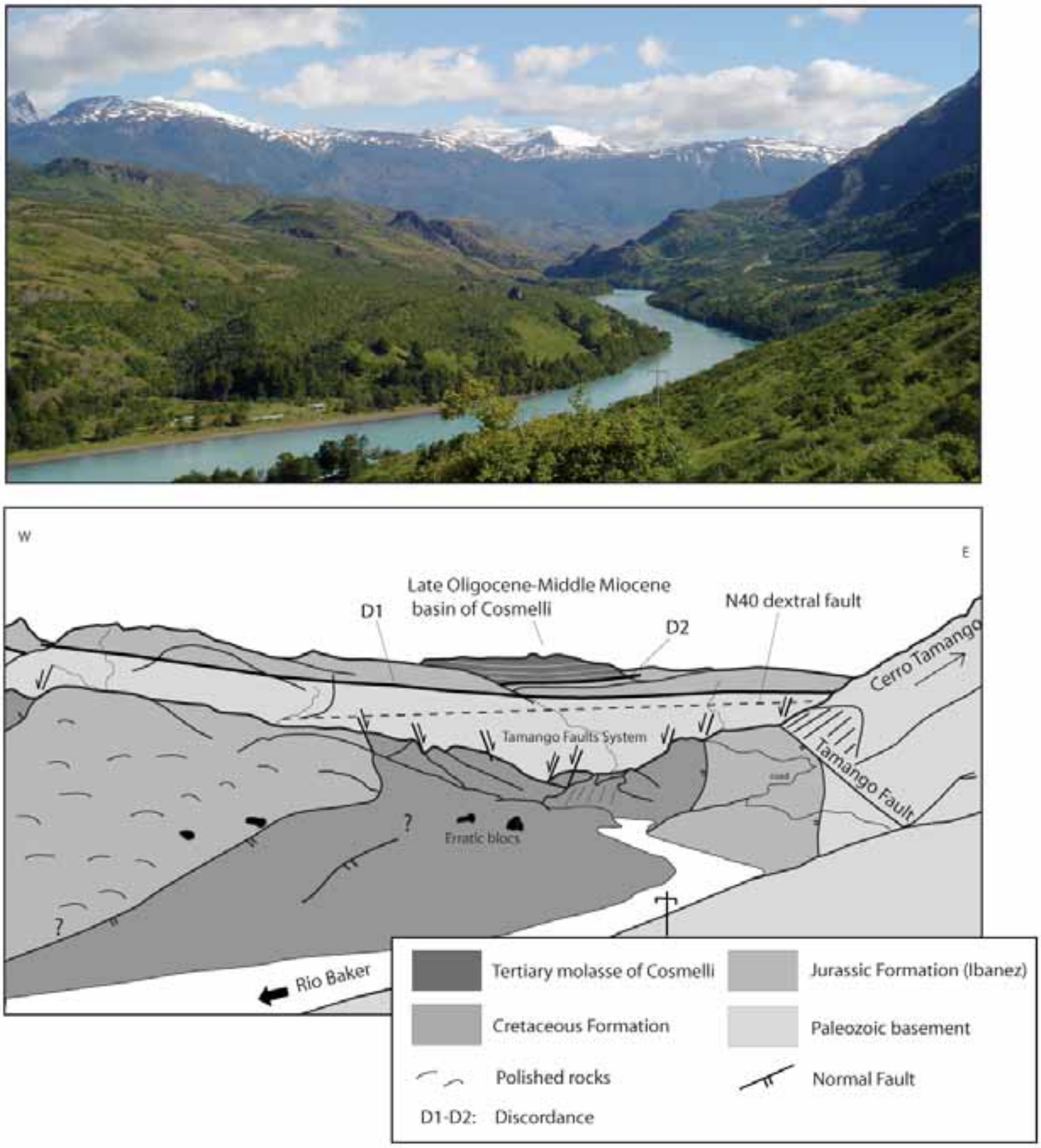

W
E
Late Oligocene-Middle Miocene
basin of Cosmelli
D1
D2
N40 dextral fault
Cerro Tamango
Tamango Faults System
Tamango Fault
Erratic blocs
?
Rio Baker
Tertiary molasse of Cosmelli
Jurassic Formation (Ibanez)
Cretaceous Formation
Paleozoic basement
Polished rocks
Normal Fault
D1-D2: Discordance

Figure 11

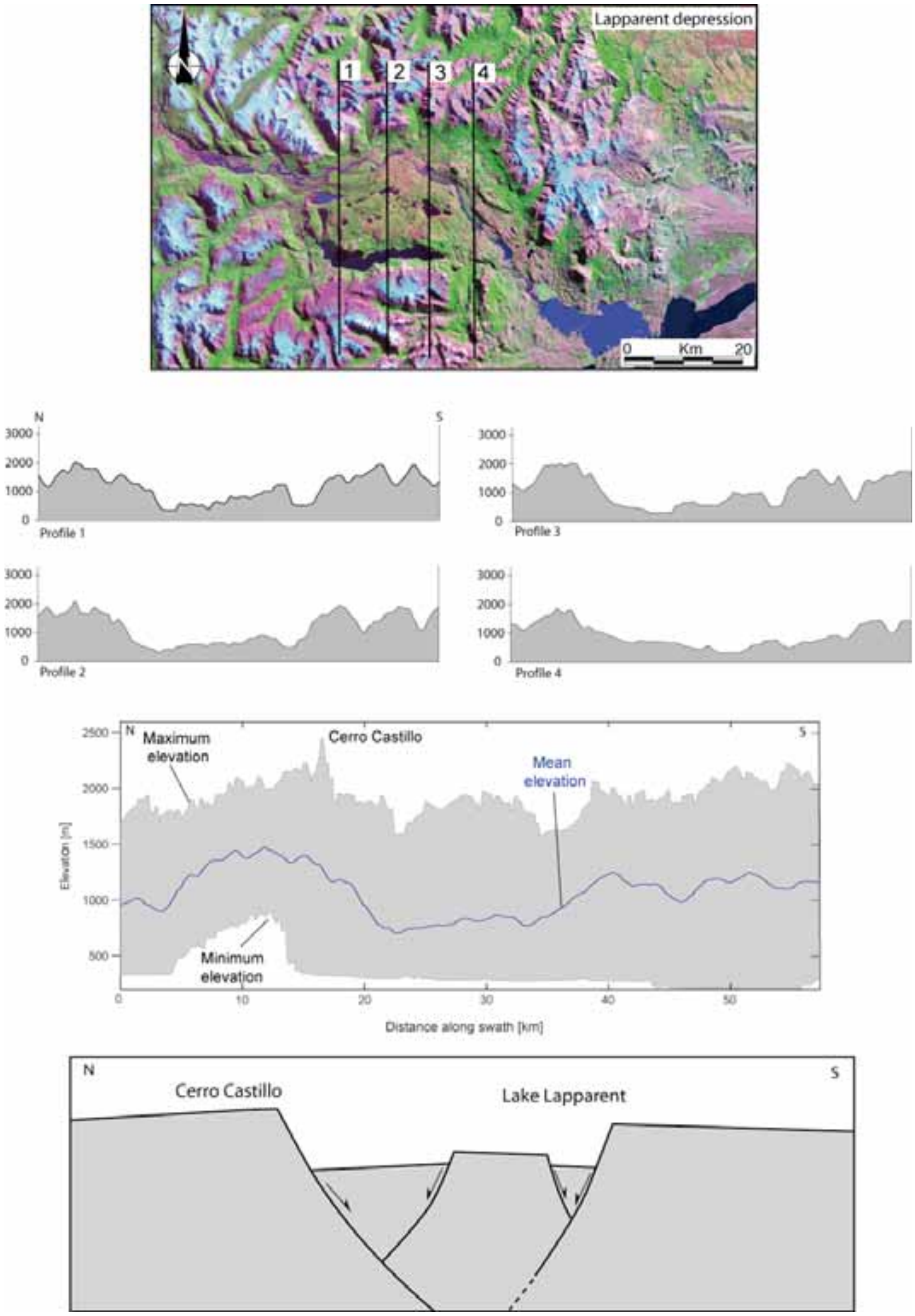

Lapparent depression
1
2
3
4
0
Km
20
N
S
Profile 1
Profile 2
Profile 3
Profile 4
Maximum elevation
Cerro Castillo
Mean elevation
Minimum elevation
Elevation [m]
Distance along swath [km]
Cerro Castillo
Lake Lapparent

Figure 12

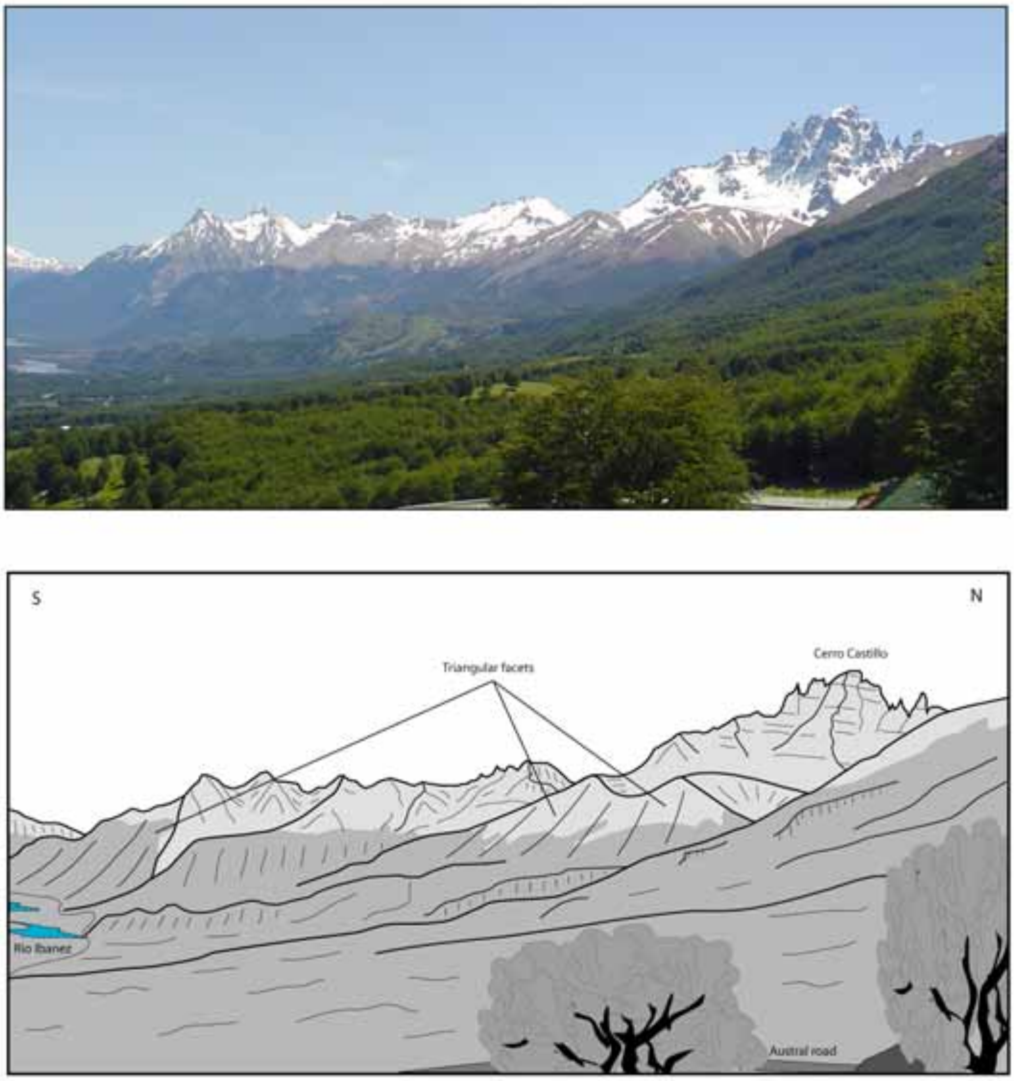
S
N
Triangular facets
Cerro Castillo
Río Ibanez
Austral road

Figure 13

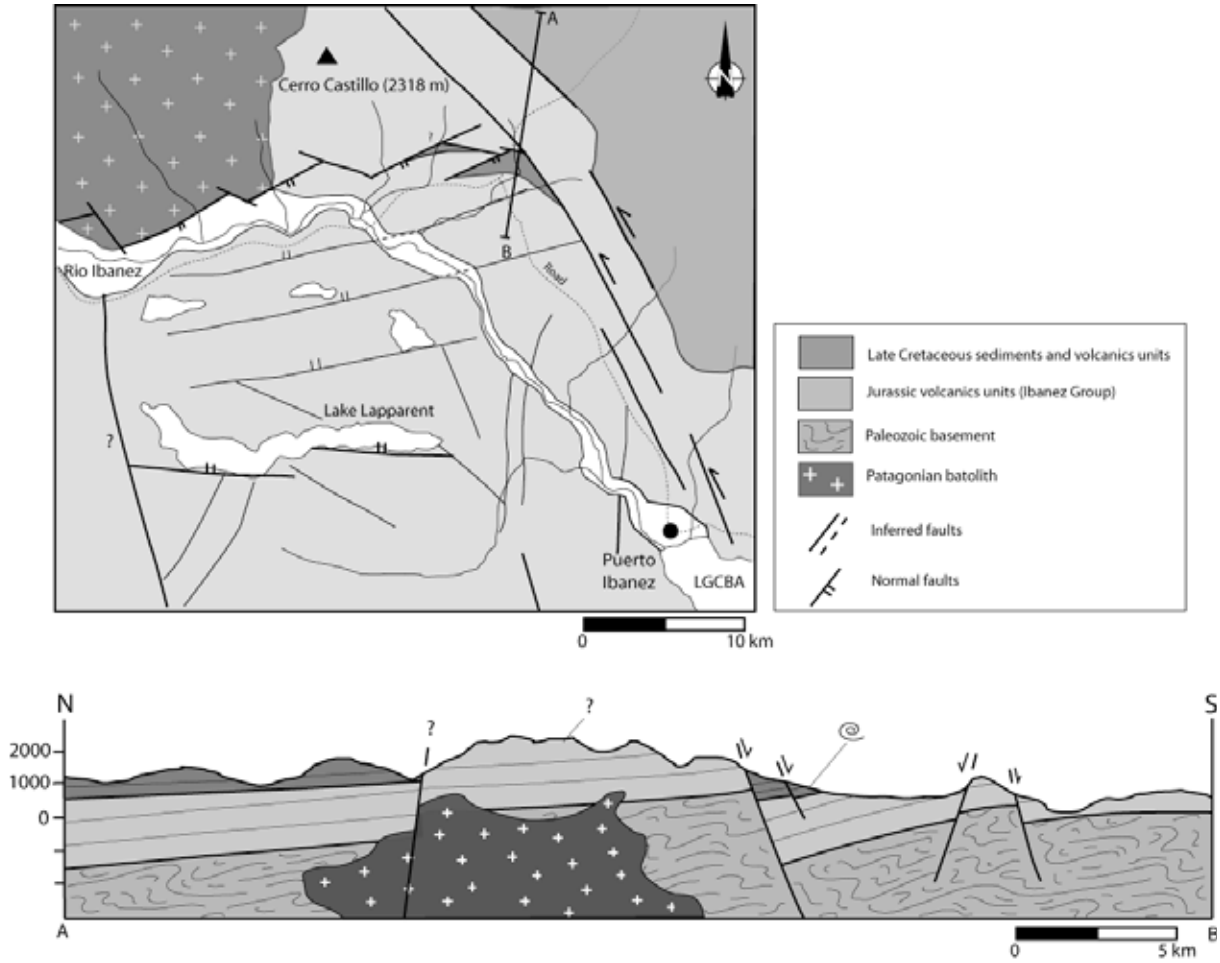
Cerro Castillo (2318 m)
A
B
Rio Ibanez
Road
Lake Lapparent
Puerto Ibanez
LGCBA
?
Late Cretaceous sediments and volcanics units
Jurassic volcanics units (Ibanez Group)
Paleozoic basement
Patagonian batolith
Inferred faults
Normal faults
0
10 km
N
S
2000
1000
0
?
?
A
B
0
5 km

Figure 14

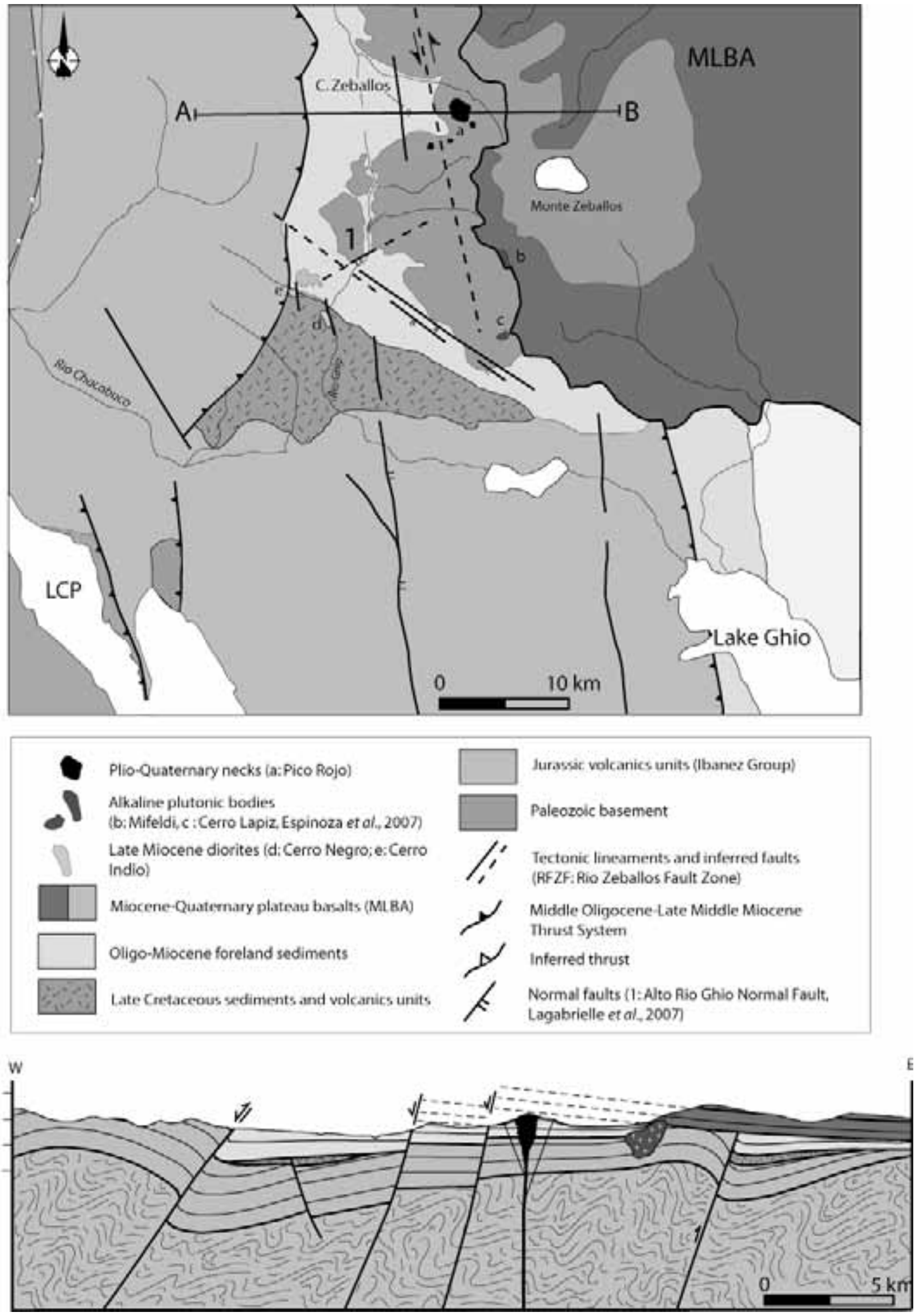
MLBA
C. Zeballos
A
B
Monte Zeballos
Rio Chacabuco
LCP
Lake Ghio
0
10 km
Plio-Quaternary necks (a: Pico Rojo)
Alkaline plutonic bodies (b: Mifeldi, c : Cerro Lapiz, Espinoza et al., 2007)
Late Miocene diorites (d: Cerro Negro; e: Cerro Indio)
Miocene-Quaternary plateau basalts (MLBA)
Oligo-Miocene foreland sediments
Late Cretaceous sediments and volcanics units
Jurassic volcanics units (Ibanez Group)
Paleozoic basement
Tectonic lineaments and inferred faults (RFZF: Rio Zeballos Fault Zone)
Middle Oligocene-Late Middle Miocene Thrust System
Inferred thrust
Normal faults (1: Alto Rio Ghio Normal Fault, Lagabrielle et al., 2007)
W
E
2000
1000
0
0
5 km

Figure 16

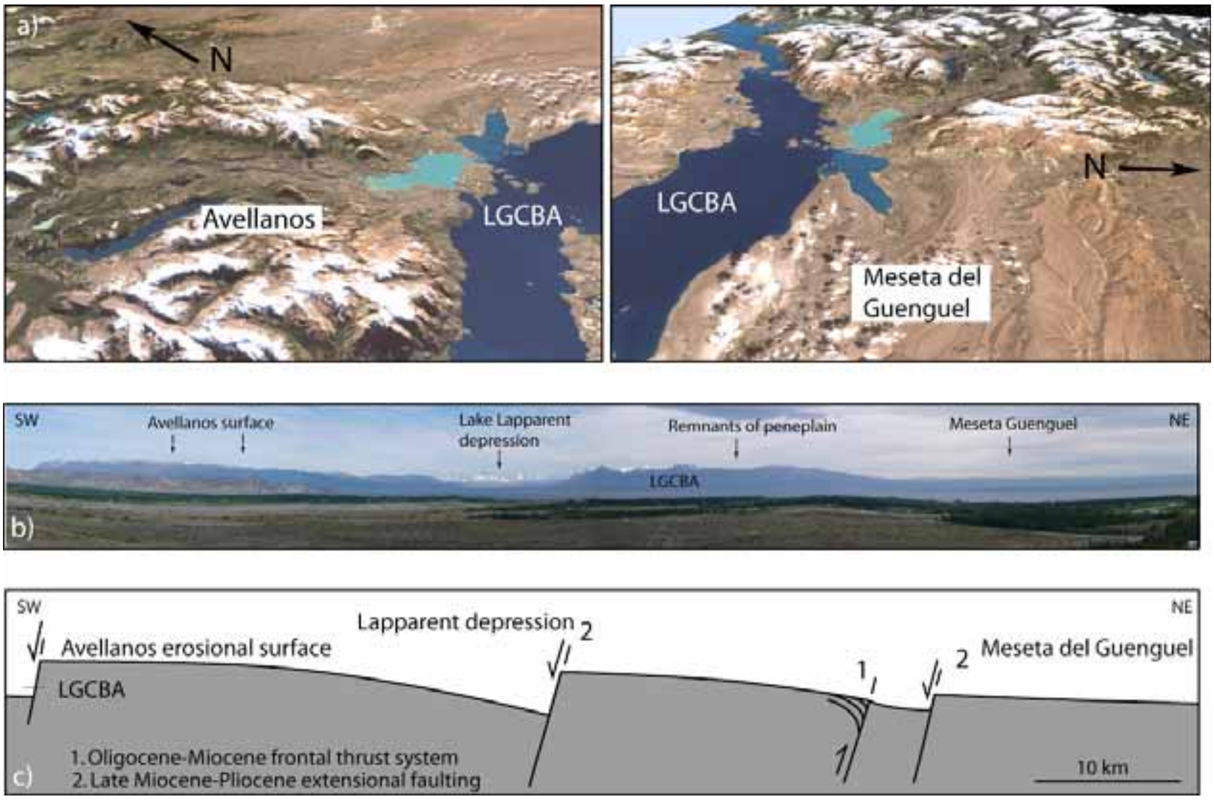
a)
N
Avellanos
LGCBA
LGCBA
N
Meseta del Guenguel
SW
Avellanos surface
Lake Lapparent depression
Remnants of peneplain
Meseta Guenguel
NE
LGCBA
b)
SW
Lapparent depression
2
Avellanos erosional surface
LGCBA
1
2
Meseta del Guenguel
NE
1. Oligocene-Miocene frontal thrust system
2. Late Miocene-Pliocene extensional faulting
10 km
c)

Figure 16

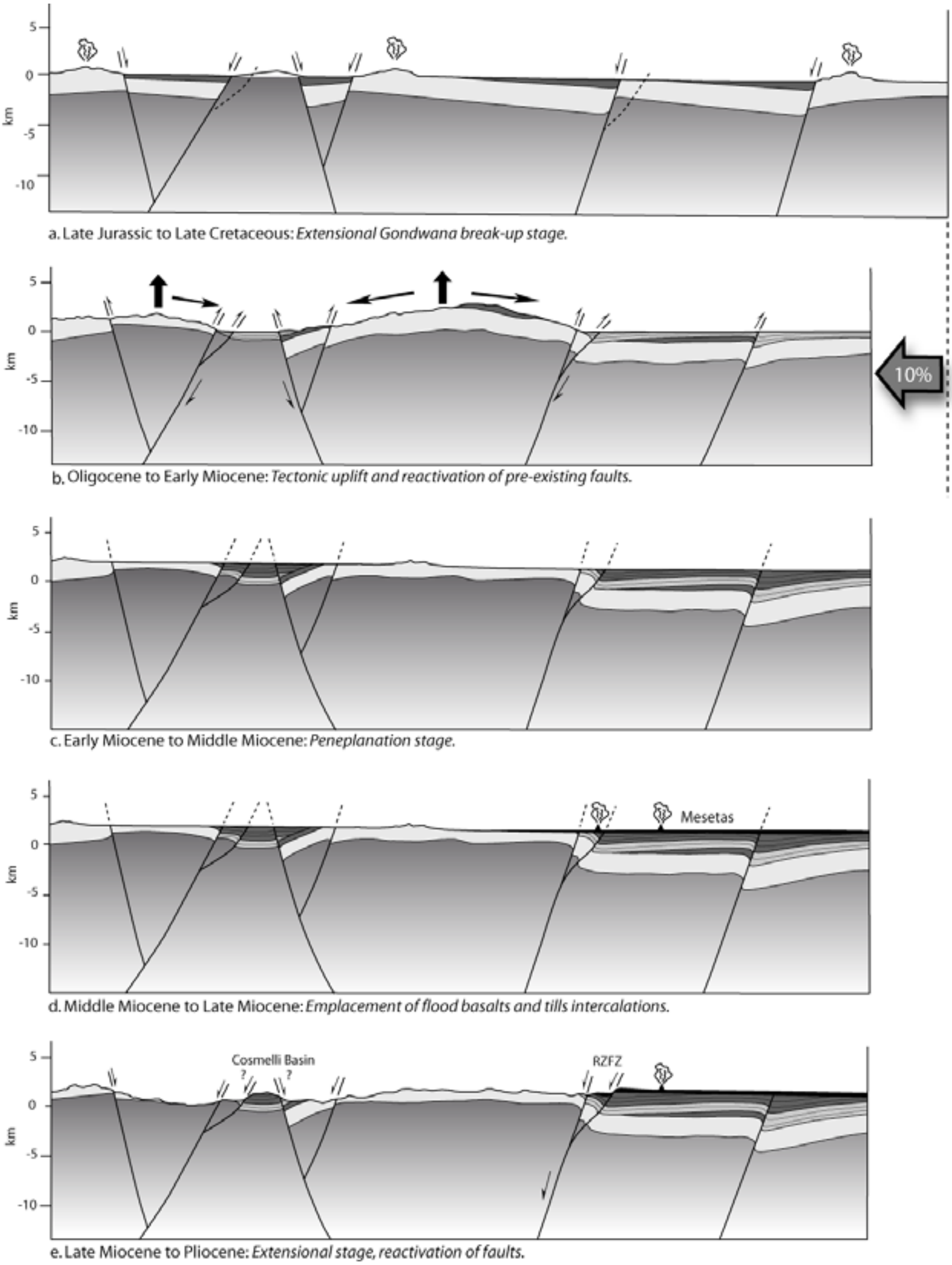
km
5
0
-5
-10
a. Late Jurassic to Late Cretaceous: *Extensional Gondwana break-up stage.*
10%
b. Oligocene to Early Miocene: *Tectonic uplift and reactivation of pre-existing faults.*
c. Early Miocene to Middle Miocene: *Peneplanation stage.*
Mesetas
d. Middle Miocene to Late Miocene: *Emplacement of flood basalts and tills intercalations.*
Cosmelli Basin
?
?
RZFZ
e. Late Miocene to Pliocene: *Extensional stage, reactivation of faults.*

Figure 17

III.2. Apports de la géochronologie et tectonique extensive de la Patagonie Centrale orientale.

Pliocene extensional tectonics in the Eastern Central Patagonian Cordillera : geochronological and new field evidence

Yves Lagabrielle[1], Manuel Suarez[2], Jacques Malavieille[1], Diego Morata[3], Felipe Espinoza[3], René C. Maury[4], **Bruno Scalabrino[1]**, Luis Barbero[5], Rita de la Cruz[2], Eduardo Rossello[6], Hervé Bellon[4].

[1] *Université Montpellier 2, INSU-CNRS, Laboratoire Géosciences Montpellier, place E. Bataillon, 34095 Montpellier Cedex5, France.*

[2] *Servicio Nacional de Geología y Minería, Avenida Santa María 0104, Santiago, Chile.*

[3] *Departamento de Geología, Universidad de Chile, Casilla 13518, Correo 21, Santiago, Chile.*

[4] *CNRS-UMR 6538 Domaines océaniques, UBO-IUEM, place Nicolas-Copernic, 29280 Plouzané, France*

[5] *Departamento de Geologia, Universidad de Cadiz, Espagne.*

[6] *CONICET and Universidad de Buenos Aires, Departamento de Ciencias Geológicas, 1428 Buenos Aires, Argentina.*

Terra Nova, 19, 413-424, 2007.

doi: 10.1111/j.1365-3121.2007.00766.x

Pliocene extensional tectonics in the Eastern Central Patagonian Cordillera: geochronological constraints and new field evidence

Yves Lagabrielle,[1] Manuel Suárez,[2] Jacques Malavieille,[1] Diego Morata,[3] Felipe Espinoza,[3] René C. Maury,[4] Bruno Scalabrino,[1] Luis Barbero,[5] Rita de la Cruz,[2] Eduardo Rossello[6] and Hervé Bellon[4]

[1]*CNRS-UMR 5234, Géosciences Montpellier, Place E. Bataillon, CC 60, 34095, Montpellier Cedex 5, France;* [2]*Servicio Nacional de Geología y Minería, Avenida Santa María 0104, Santiago, Chile;* [3]*Departamento de Geología, Universidad de Chile, Casilla 13518, Correo 21, Santiago, Chile;* [4]*CNRS-UMR 6538 Domaines océaniques, UBO-IUEM, place Nicolas-Copernic, 29280 Plouzané, France;* [5]*Departamento de Geología, Universidad de Cádiz, España;* [6]*CONICET and Universidad de Buenos Aires, Departamento de Ciencias Geológicas, 1428 Buenos Aires, Argentina*

ABSTRACT

Recent field work and review of radiometric data obtained from Neogene lavas and plutonic rocks exposed in the Eastern Central Patagonian Cordillera (46–48°S), which overlie subducted segments of the South Chile Ridge, suggest important Late Miocene to Pleistocene morphological changes in relation to base level variations and/or tectonic events. We present new field observations from a region south of Lago General Carrera-Buenos Aires, between the main Cordillera and the Meseta del Lago Buenos Aires, demonstrating that normal faulting controlled valley incisions and occurred during lava emplacement at 5–4 Ma and after 3 Ma. We also show that the 12 Ma basaltic flows of the Meseta del Lago Buenos Aires (~2000 m a.s.l.) have been subjected to deep incision, with younger lavas dated at 1.2 Ma partially filling the valleys. These incisions are thought to reflect progressive eastward tilting of the entire meseta. Our new observations, together with additional features from Central Patagonia, strongly suggest that tectonic events led to a regional widespread morphological change after 5 Ma. The coincidence in time and space between the subduction of segments of the South Chile Ridge at 6 and 3 Ma causing opening of a slab window, and strong base level variations in the studied area, suggests a cause-and-effect relationship. In Central Patagonia, compressional tectonics ended well before extensional events reported here. Causes of uplift and further extension are probably completely disconnected. The uplift is purely tectonic in origin and occurred prior to the subduction of the South Chile Ridge. Extension should be a consequence of this subduction.

Terra Nova, 19, 413–424, 2007

Introduction

The Eastern Central Patagonian Cordillera, between latitudes 48–46°S, is the section of the southern Andes beneath which the active spreading South Chile Ridge has been subducting during the last 6 Myr (Herron *et al.*, 1981; Cande and Leslie, 1986; Cande *et al.*, 1987; Gorring *et al.*, 1997). This is a key region in which to study the onland tectonic effects of ridge subduction (Flint *et al.*, 1994; Lagabrielle *et al.*, 2004; Ramos, 2005). Three segments of the South Chile Ridge entered the trench at 6, 3, and 0.3 Ma and are presently subducting below this part of South America (Fig. 1a). This situation resulted in the absence of contemporaneous calc-alkaline arc volcanism, in the uplift of the highest mountains of the Patagonian Cordillera (Mt. San Valentín, 4058 m a.s.l.; Mt. San Lorenzo, 3706 m a.s.l.) (Fig. 1a) and in the emplacement of flood basalts inferred to have been generated beneath slab windows (Ramos, 1989; Ramos and Kay, 1992; Demant *et al.*, 1998; Gorring *et al.*, 1997, 2003; Espinoza *et al.*, 2005a,b; Guivel *et al.*, 2005, 2006). It has been shown that an important tectonic activity occurred in the region during the Miocene (Ramos, 1989; Thomson *et al.*, 2001; De La Cruz *et al.*, 2003, 2004; Lagabrielle *et al.*, 2004). In this paper, we present new field observations from a region south of Lago General Carrera-Buenos Aires, which demonstrate that normal faulting controlled valley incisions and occurred during lava emplacement between 5 and 3 Ma, and we discuss the overall implications of this recent tectonic activity in the context of the subduction of the active South Chile Ridge.

Correspondence: Yves Lagabrielle, CNRS-UMR 5234, Géosciences Montpellier, Place E. Bataillon, CC 60, 34095, Montpellier Cedex 5, France. Tel.: +00 33 467 14 35 85; fax: +00 33 467 14 36 42; e-mail: yves.lagabrielle@gm.univ-montp2.fr

Geologic background and timing of deformation events: a review

In Eastern Central Patagonia, Middle Jurassic and Cretaceous volcanics and marine sedimentary rocks unconformably overlie Late Palaeozoic metamorphic rocks (Charrier *et al.*, 1979; Niemeyer *et al.*, 1984; Suárez *et al.*, 1996; De La Cruz *et al.*, 2003, 2004; De La Cruz and Suárez, 2006). The late Early Miocene to Recent stratigraphic sequence, well exposed in the area south of Lago General Carrera-Buenos Aires, shows the following units (Figs 1 and 2): (1) late Early to early Middle Miocene fluvial deposits (Santa Cruz Formation or Zeballos Group, Flint *et al.*, 1994; Ray, 1996; Flynn *et al.*, 2002; De La Cruz and Suárez, 2006); (2) Late Miocene to Recent basalts (Charrier *et al.*, 1979; Suárez and De la Cruz, 2000a,b; Troncoso *et al.*, 2002; Gorring *et al.*, 2003; Lagabrielle *et al.*, 2004; Brown *et al.*, 2004; Espinoza *et al.*, 2005a,b; Guivel *et al.*, 2006); and (3) glacial deposits of Late Miocene–Early Pliocene age and younger, locally interbedded with lava flows of the mesetas (Mercer and Sutter, 1982; Ton-That *et al.*, 1999; Singer *et al.*, 2004).

The orographic front of the Cordillera is formed by the Ibáñez

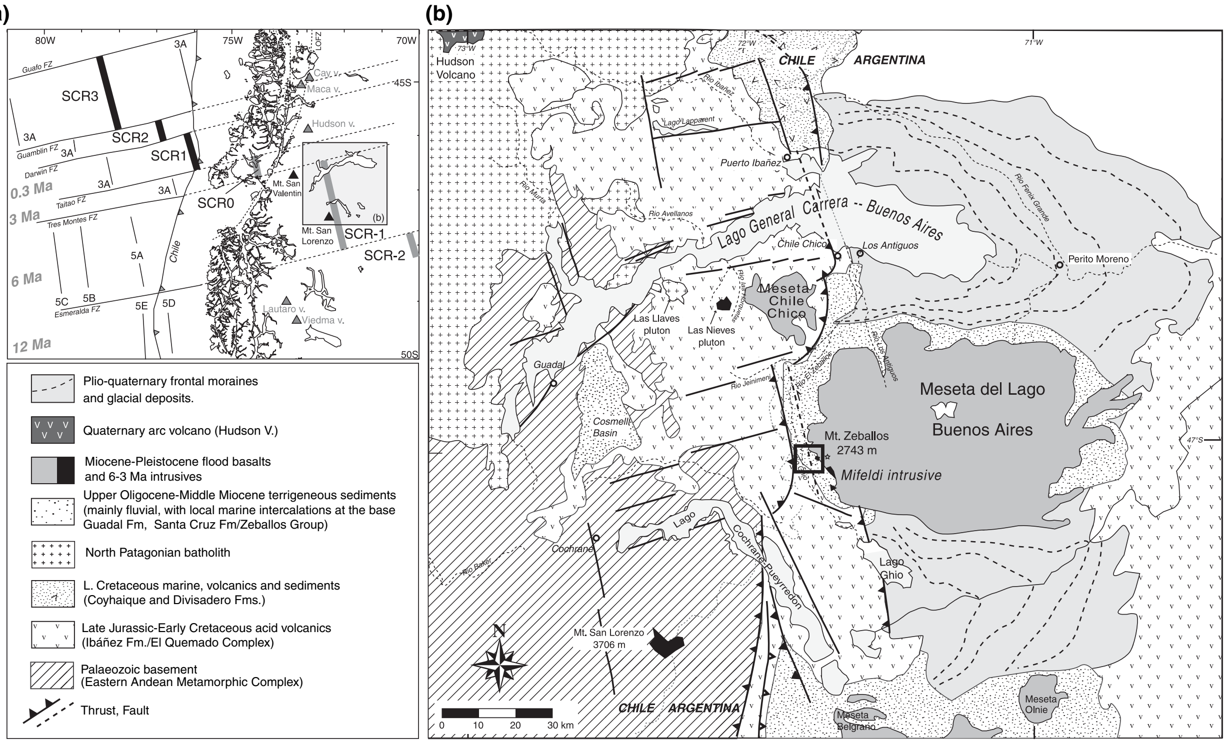

Fig. 1 Geology of the region around the Lago General Carrera-Buenos Aires. Modified from Lagabrielle *et al.* (2004). Frame indicates the location of the Portezuelo area of Alto Río Ghio.

Formation (Middle–Late Jurassic to Early Cretaceous) thrusted to the east over Cretaceous and Cenozoic rocks (Ray, 1996; Suárez and De la Cruz, 2000a; Lagabrielle *et al.*, 2004). The main Cenozoic contractional tectonism occurred during and after the deposition of the Zeballos Group and prior to the emplacement of 12 Ma basalts over an erosional surface that cross-cuts the last thrusts (Lagabrielle *et al.*, 2004, 2006; De La Cruz and Suárez, 2006; Guivel *et al.*, 2006). Basalts from the base of the Meseta Lago Buenos Aires and Meseta Belgrano are 12.1–12.4 Ma, and their equivalents are slightly older (13–14 Ma) farther south at Meseta de la Muerte (Gorring *et al.*, 1997; Guivel *et al.*, 2006).

During the Upper Miocene–Pliocene, the frontal region of the Cordillera experienced an episode of relief inversion revealed by the presence of relict planar surfaces (Avellanos surface, Meseta Chile Chico, Meseta Lago Buenos Aires, Meseta del Guengel, Meseta Belgrano, Fig. 4). Before this event, the overall topography of the Cordillera was smoother than and not so deeply incised as the present-day one (Lagabrielle *et al.*, 2004). The N–S oriented valleys paralleling the front of the Cordillera (Rio Jeinimeni and Rio Ghio valleys), as well as the transverse incision of the Lago General Carrera-Buenos Aires, probably did not exist. These important changes might be linked to vertical tectonic movements of regional importance. However, prior to this work, the lack of robust data prevented discrimination between (a) simple base level variations linked to regional uplift and (b) localized tectonic deformation along discrete fault zones leading to relative uplift and subsidence.

Figure 2 presents the stratigraphy of the volcanic formations of the region and their possible intercorrelations, based on available data in the area of Lago General Carrera-Buenos Aires (Suárez and De La Cruz, 2002). Dated samples were collected in various settings shown in Fig. 4 and Table 1. The most striking results are as follows: (a) basaltic lava flows forming the main plateaus accumulated between 12 and 5 Ma synchronously with fluvioglacial and glacial deposits, well preserved in stratigraphic sections of the Meseta Lago Buenos Aires (Mercer and Sutter, 1982). During this period, the scarps delineating the present-day mesetas obviously did not exist. (b) Basalts dated around 4.5 Ma (Table 1) overlie with a hiatus basalts dated at *c.* 10–8 Ma (area of Pico Solo in Meseta Chile Chico; Figs 2 and 3) and 10–12 Ma (Meseta Chile Chico and Meseta Lago Buenos Aires; Figs 2 and 3), respectively (Espinoza *et al.*, 2005a,b; Guivel *et al.*, 2006). This confirms that change in base level triggering valley incision and relief inversion occurred in the region at least after 5 Ma. (c) In addition, the studied region is characterized by the 6 and 3 Ma emplacement and exhumation of the San Lorenzo and Las Nieves plutons (Welkner, 2000; Suárez and De La Cruz, 2001; Morata *et al.*, 2002) (Fig. 2 and Table 1), which coincide in time and space with the subduction of segments of the South Chile Ridge.

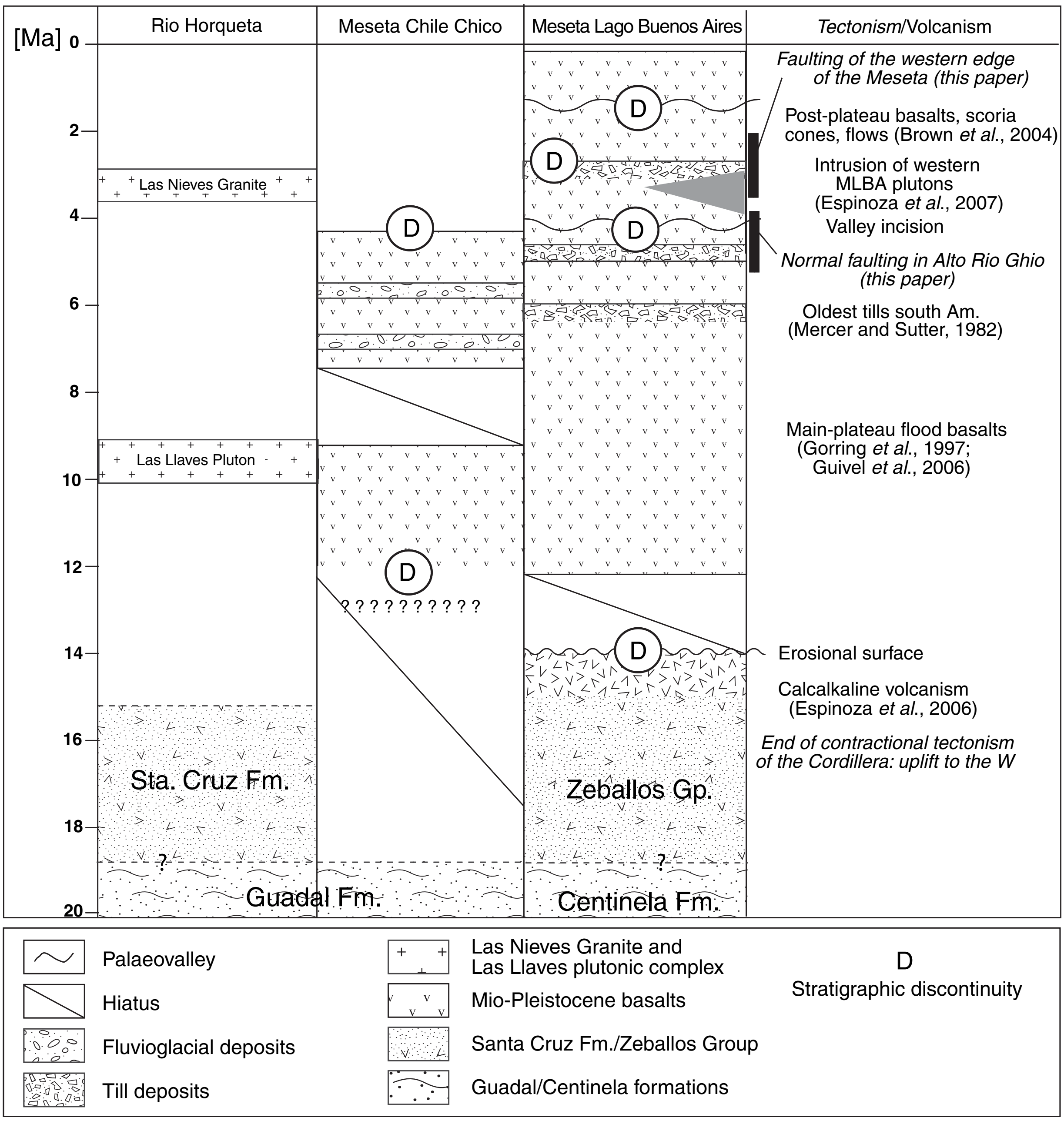

Fig. 2 Schematic Miocene–Pliocene stratigraphy of the study area. MLBA: Meseta Lago Buenos Aries.

Tectonics between 5 and 4 Ma: evidence from the Portezuelo area of Alto Río Ghio

Since Patagonia was covered by thick ice sheets during the Pliocene–Quaternary glacial periods, the most obvious marks of recent tectonic activity have been erased by widespread glacial erosion. This explains why little evidence of recent to active tectonics has been observed so far. In this study, we report evidence of post-5 Ma tectonics from a site located in the Portezuelo area of Alto Río Ghio, on the western side of road R.P. 41, north of Paso Roballos and west of Meseta Lago Buenos Aires (Fig. 4). The site lies along the Rio Zeballos fault zone (Fig. 3), an approximately N–S sinistral transtensional fault system, with possible splays having different trends, which postdates Miocene compressive tectonism in the region and corresponds to a major morphological corridor separating the Meseta Lago Buenos Aires from the Cordillera (Lagabrielle *et al.*, 2004). Here, three basaltic lava flows, locally up to 10 m thick, have been emplaced in a narrow palaeovalley incised in the fluvial sandstones of the Zeballos Group. The lower and upper flows (flows 1 and 3, Fig. 4) gave whole-rock K–Ar ages of 4.98 ± 0.15 and 2.96 ± 0.09 Ma, respectively (samples PG 65

Table 1 Late Miocene–Pliocene K–Ar ages of volcanic rocks from the area of Lago General Carrera-Buenos Aires.

Label in Fig. 3	Article Reference	Location	Sample No.	Location (UTM 19)	Dated Material	Age (Ma)	± error (2σ)
1	a	Avellanos area	Q387	4854211/257617	WR	4.57	0.27
2	b	Río Las Nieves	CC-138	4825965/264583	WR	3.20	0.40
3	c	MCC	PG 36–38	4836043/284123	WR	4.63	0.13
4	c	MCC	PG 138	4836043/284123	WR	4.46	0.22
5	c	MCC	FE01–11	4819707/283249	WR	4.50	0.30
6	c	MCC	FE01–16	4827408/285508	WR	4.60	0.20
7	c	MCC	FE01–36	4831666/280272	WR	4.40	0.80
8	unp. (+)	MCC east edge	CC-270	4831350/287200	WR	5.30	0.40
9	d	Alto Río Ghio	PG 65	4783664/288643	WR	4.98	0.15
10	d	Alto Río Ghio	PG 67	4783664/288643	WR	6.95	0.24
11	d	Alto Río Ghio	PG 69	4778705/292340	WR	4.32	0.23
12	d	Alto Río Ghio	PG 70	4783664/288643	WR	2.96	0.09
13	d	Alto Río Ghio	PG 72	4783664/288643	WR	3.91	0.11
14	d	Alto Río Ghio	PG 75	4785410/286064	WR	4.81	0.32
15	d	NE-MLBA	PG 44	4807449/367743	WR	1.08	0.04
16	d	SE-MLBA	PG 116	4775282/346692	WR	9.97	0.25
17	d	SE-MLBA	PG 119	4781535/348249	WR	10.71	0.29
18	d	SE-MLBA	PG 120	4782842/346203	WR	12.18	0.34
19	d	SE-MLBA	PG 121	4777995/353622	WR	1.19	0.08
20	d	S-MLBA	PG 130	4774013/306399	WR	3.44	0.11
21	d	S-MLBA	PG 132	4774130/306184	WR	3.32	0.10
22	d	S-MLBA	PG 133	4774072/306312	WR	3.64	0.11
23	d	S-MLBA	PG 134	4772347/307422	WR	3.89	0.14
24	e	SW-MLBA	PAT-12	4778705/292340	WR	3.65	0.10
25	e	SW-MLBA	PAT-20	4780366/292728	WR	3.08	0.13
26	e	SW-MLBA	PAT-22	4781845/293488	WR	3.28	0.10
27	unp.	SW-MLBA	PAT-26	4789707/290427	WR	4.52	0.16
28	f	Belgrano	PL9	4700800/312700	WR	3.79	0.13
29	g	San Lorenzo	DW-38	4732496/256521	Bt	6.40	0.40
30	h	San Lorenzo	Q-379	4721955/249109	Bt	6.60	0.50

MLBA: Meseta del Lago Buenos Aires; MCC: Meseta Chile Chico; WR: Whole rock; Bt: Biotite. Data source: (a) Pelleter, 2003; (b) Morata *et al.*, 2002; (c) Espinoza *et al.*, 2005a; (d) Guivel *et al.*, 2006; (e) Espinoza *et al.*, 2006; Espinoza *et al.* 2007; (f) Gorring *et al.*, 1997; (g) Welkner, 1999; (h) Suárez and De La Cruz, 2001; unp.: unpublished data; (+) to be published in Geología del area Chile Chico-Fachinas, escala 1 : 100 000, Carta Geológica de Chile, Serie Geología Básica, Servicio Nacional de Geología y Minería, De La Cruz and Suárez (in preparation).

and PG 70, Table 1). The upper flow extends horizontally farther west and forms the floor of a larger ancient valley, *c.* 3 Ma, which is now incised by the present-day river (Fig. 4). This flow overlies tills that also extend westwards. Therefore, the corridor of the Zeballos fault zone existed at 3 Ma, and relatively old glaciers have flown along it. The intermediate flow (flow 2, Fig. 4) is highly brecciated and includes basaltic blocks of various types, one of them dated at 6.95 ± 0.24 Ma (sample PG 67, Table 1). This block, older than the brecciated flow which surrounds it, might derive from the disaggregation of flows from the base of the Meseta Lago Buenos Aires, which was experiencing active erosion at that time. The basal flow (flow 1) overlies tills and fluvioglacial gravels and conglomerates including numerous cobbles, many of them deriving from the internal part of the Cordillera (plutonic rocks from the batholith, ignimbrites and lavas from the Mesozoic formations). The sediments partly filled the bottom of a narrow palaeovalley and are only locally preserved. Red-coloured conglomeratic layers of till just beneath the flows indicate that the lavas have 'cooked' the glacial sediments (Fig. 5). These features collectively indicate that glaciers have been flowing from the Cordillera into this region at least since 5 Ma, and that basalts were erupted at the time of glacier advance. This is in good agreement with Mercer and Sutter's (1982) observations of tills exposed along the northwestern flank of the Meseta Lago Buenos Aires, which are interbedded between basaltic lava flows dated at *c.* 7 and 4 Ma.

No more than 10 m to the south of the palaeovalley, the Zeballos Group sandstones are intruded by subvertical basaltic dikes forming a basal network merging into a main dike (Fig. 4). The main dike has given a K–Ar whole-rock age of 4.32 ± 0.23 Ma (sample PG 69, Table 1). A lava flow exposed along the road-cut some hundred meters to the north, yielded an age of 4.81 ± 0.32 Ma (sample PG 75, Table 1) and a block from a volcanic cone located at the foot of the main Meseta Lago Buenos Aires scarp was dated at 3.91 ± 0.11 Ma (sample PG 72, Table 1).

New detailed tectonic investigations have been made possible thanks to the development of landslides which occurred in the 2002–2006 period and left fresh exposures along Rio Ghio. This allowed us to recognize that the development of the palaeovalley was controlled by active faulting. Indeed, the Zeballos Group sandstones and the base of the overlying fluvial gravels are affected by a well-marked, eastward dipping brittle cleavage oriented N35–N40, parallel to the palaeovalley axis. The deformed area is more than 10 m wide and locally exposes fault breccias indicating the presence of a major fault zone, oriented N35–N40. The fluvioglacial deposits are locally flattened within the fault zone, with schistosity anastomosing between the cobbles (Fig. 5). Towards the top of the exposure, the schistosity is pervasive, and the Zeballos Group sandstones are cut into microlithons, a few centimeters wide (Fig. 5). The fault plane itself is exposed along the western flank of Rio Ghio and forms a structural surface dipping to the east. Normal offset along this fault controlled the fluvioglacial sedimentation and emplacement of lava flows. Moreover, the dike swarm exposed immediately west of the palaeovalley is cut and offset by a set of westward dipping, conjugate normal faults (Fig. 5). The lowest part of the dike network shows a relatively complex geometry characterized by branching dikelets that escape from the main dike and intrude tectonic breccias because of *in situ* fracturing of the Zeballos Group sandstones. The resulting interfingering

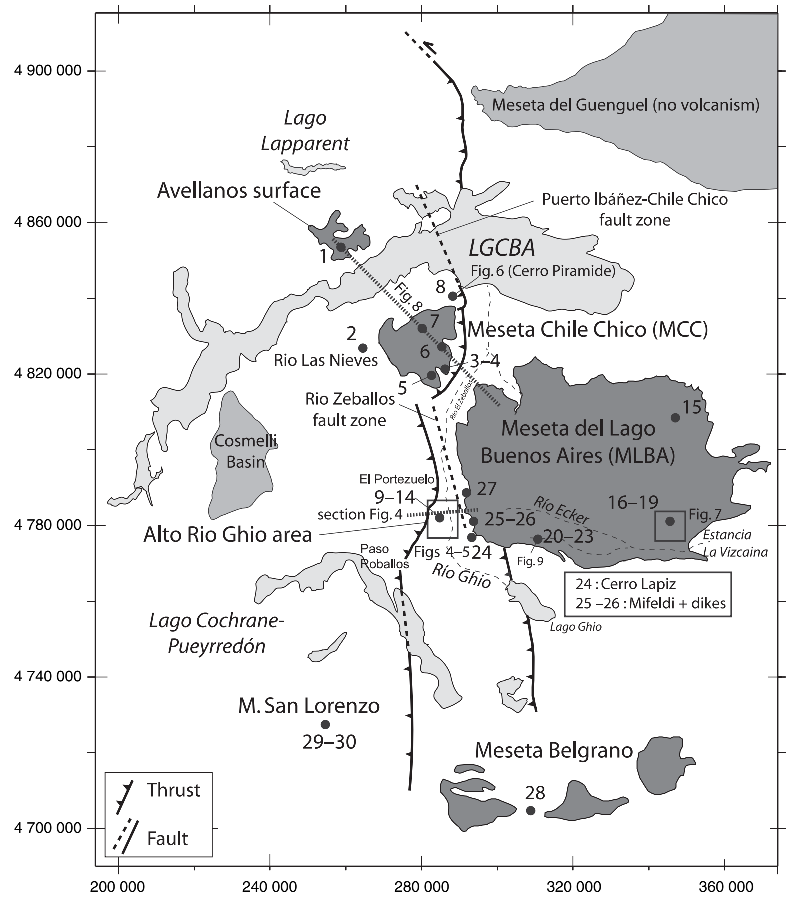

Fig. 3 Simplified map of the region of lakes General Carrera-Buenos Aires and Cochrane-Pueyrredón showing the location of dated samples cited in text. Numbers refer to samples listed in Table 1. The main volcanic mesetas are shown in dark grey, non-volcanic Meseta del Guenguel and Cosmelli Basin are in light grey. LGCBA: Lago General Carrera-Buenos Aries.

of lavas and tectonic breccias demonstrates that faulting and magma emplacement occurred synchronously at 4.3 Ma. Tectonics continued after 4.3 Ma as the same dike is cut by normal faults (Fig. 5). On the eastern side of road R.P. 41, tight steep strike-slip faults trending N110 with a normal component, cut fluvioglacial gravels and the underlying beds of the Rio Zeballos Group. The fluvioglacial deposits can be correlated with those exposed 100 m further west, which underlie flow 1. The different orientation of these faults indicates the presence of a major, complex fault zone in the area, composed of various splays of the Rio Zeballos fault zone.

These new observations have to be correlated with data obtained farther north along the front of the Chile Chico segment of the Cordillera. The front here is a monocline of Jurassic beds steeply dipping to the east, and locally verticalized, at the eastern border of the Meseta Chile Chico (Fig. 6). It connects to a marked tectonic lineament oriented N160–N170, parallel to the Rio Zeballos fault zone, which extends across the Lago General Carrera-Buenos Aires northwest of Puerto Ibáñez (Puerto Ibáñez-Chile Chico fault zone, Fig. 6). The frontal monocline is intruded by a neck, the Cerro Piramide, dated at 5.3 Ma (sample CC-270, Table 1, Fig. 6) in a region where late normal faults have been observed and measured, post-dating the frontal thrust (Lagabrielle *et al.*, 2004). This confirms that the frontal Cordillera was magmatically and tectonically reactivated at around 5 Ma in another region than the Portezuelo area of Alto Río Ghio.

The post-5 Ma tectonic activity: additional lines of evidence

Successive incisions in the Meseta Lago Buenos Aires: mark of progressive tilting?

Evidence for incision of lava flows during the Upper Miocene–Pliocene and early Pleistocene is found in two places on the southern flank of Meseta Lago Buenos Aires. At the headland of a tributary of Río Ecker, on the southwestern flank of the meseta (Fig. 3), basaltic lava flows ranging in age from 3.32 to 3.89 Ma (samples PG 130–134, Table 1) accumulated in a palaeovalley incised within thick flows of the main plateau sequence dated around 12–10 Ma. On the southeastern side of the Meseta Lago Buenos Aires near Estancia La Vizcaina (Fig. 3), a basaltic flow dated at 1.19 Ma (sample PG 121, Table 1) infills a palaeovalley incised within tabular lavas dated from 12.18 Ma (basal flows) to 9.97 Ma (Fig. 7, samples PG 120, 119 and 116 Table 1). Valley incision obviously occurred after the emplacement of the summital tabular flows capping the largest parts of the Meseta Lago Buenos Aires. Available ages range from 12 to 5 Ma for the main-plateau formation, while younger post-plateau basalts form only isolated cones and restricted flows (Mercer and Sutter, 1982; Ton-That *et al.*, 1999; Gorring *et al.*, 2003; Brown *et al.*, 2004; Guivel *et al.*, 2006). Therefore, we infer that the incisions of the Meseta Lago Buenos Aires surface started around 5 Ma. Complementary evidence of relative uplift and tilting of the overall meseta is the flow direction of the most recent post-plateau basalts (< 1 Ma, Brown *et al.*, 2004): all of them spilled eastwards over older flows at the eastern border of the meseta. This is complemented by data on uplift in the Patagonian Cordillera with an important canyon-cutting event which occurred approximately at 1.2 Ma (Rabassa and Clapperton, 1990), and likely represents a continuation of the relief inversion process deduced from the information presented here.

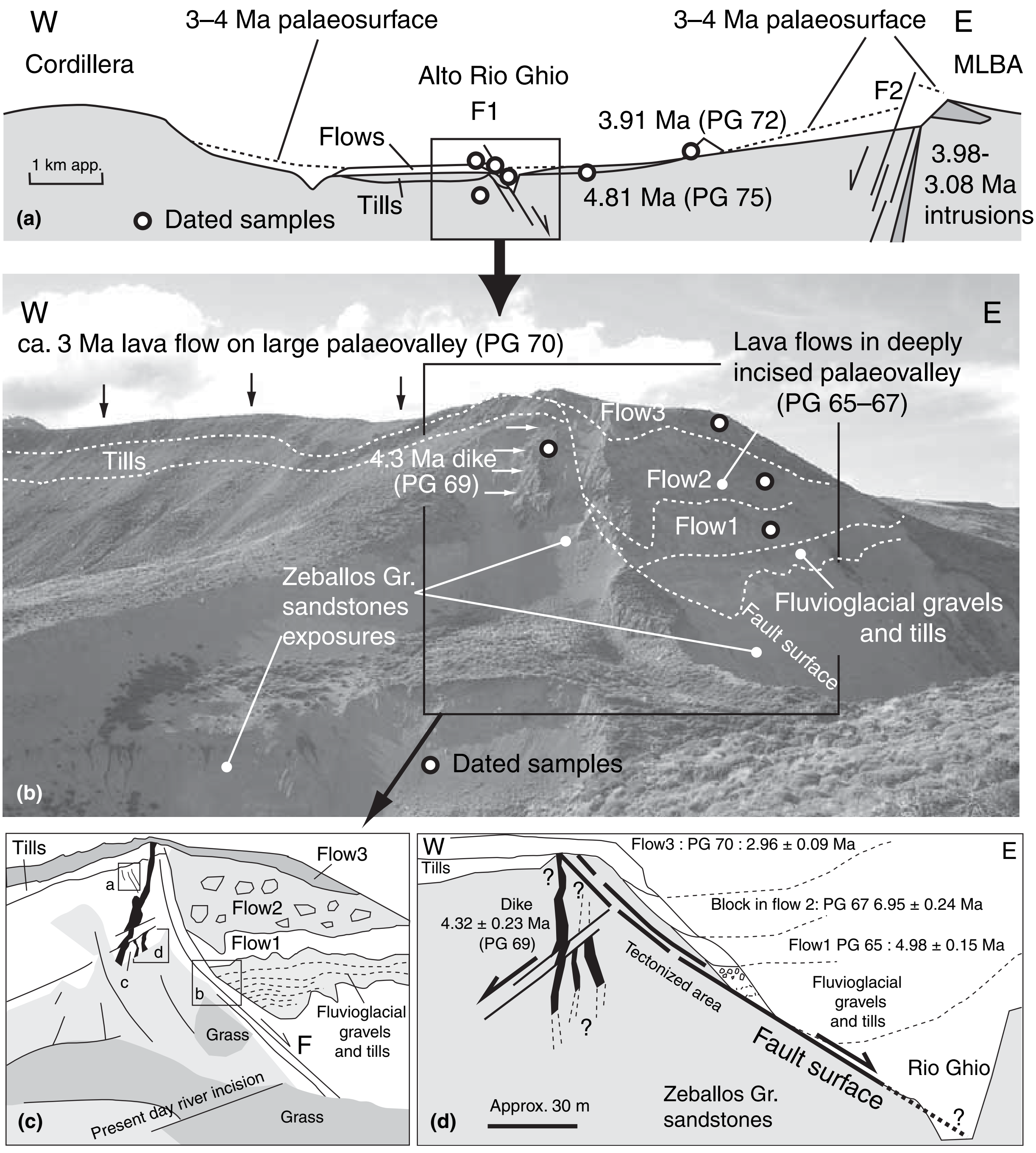

Fig. 4 Superposed basaltic lava flows and river incisions on the western shore of Alto Río Ghio in the Portezuelo area (location in Fig. 3). (a) Simplified E–W section of the Alto Río Ghio area. (b) Photograph of the main exposure (view to the NW) and location of sample sites. (c) Cartoon showing the areas (a, b, c, d) shown in detail in Fig. 5. (d) Interpreted geological section of the studied site. MLBA: Meseta del Lago Buenos Aries.

The 4.5 Ma relict surfaces

Another line of evidence that may indicate abrupt Pliocene morphological changes comes from the occurrence of *c.* 4.5 Ma basalts which accumulated within topographic lows but which now form remnants at different altitudes. Basalts dated at 4.57 ± 0.27 Ma (sample Q387, Table 1) crop out at 2000 m a.s.l. on a remarkably flat palaeosurface in the north side of Lago General Carrera-Buenos Aires (Avellanos palaeosurface) (Fig. 8), and a 4.4 ± 0.8 Ma basalt flow remnant (sample FE01–36, Table 1) is exposed on a conical summit of the Meseta Chile Chico (Cerro Sombrero, 2 km north of Cerro Pico Solo, 2168 m a.s.l.) south of Lago General Carrera-Buenos Aires

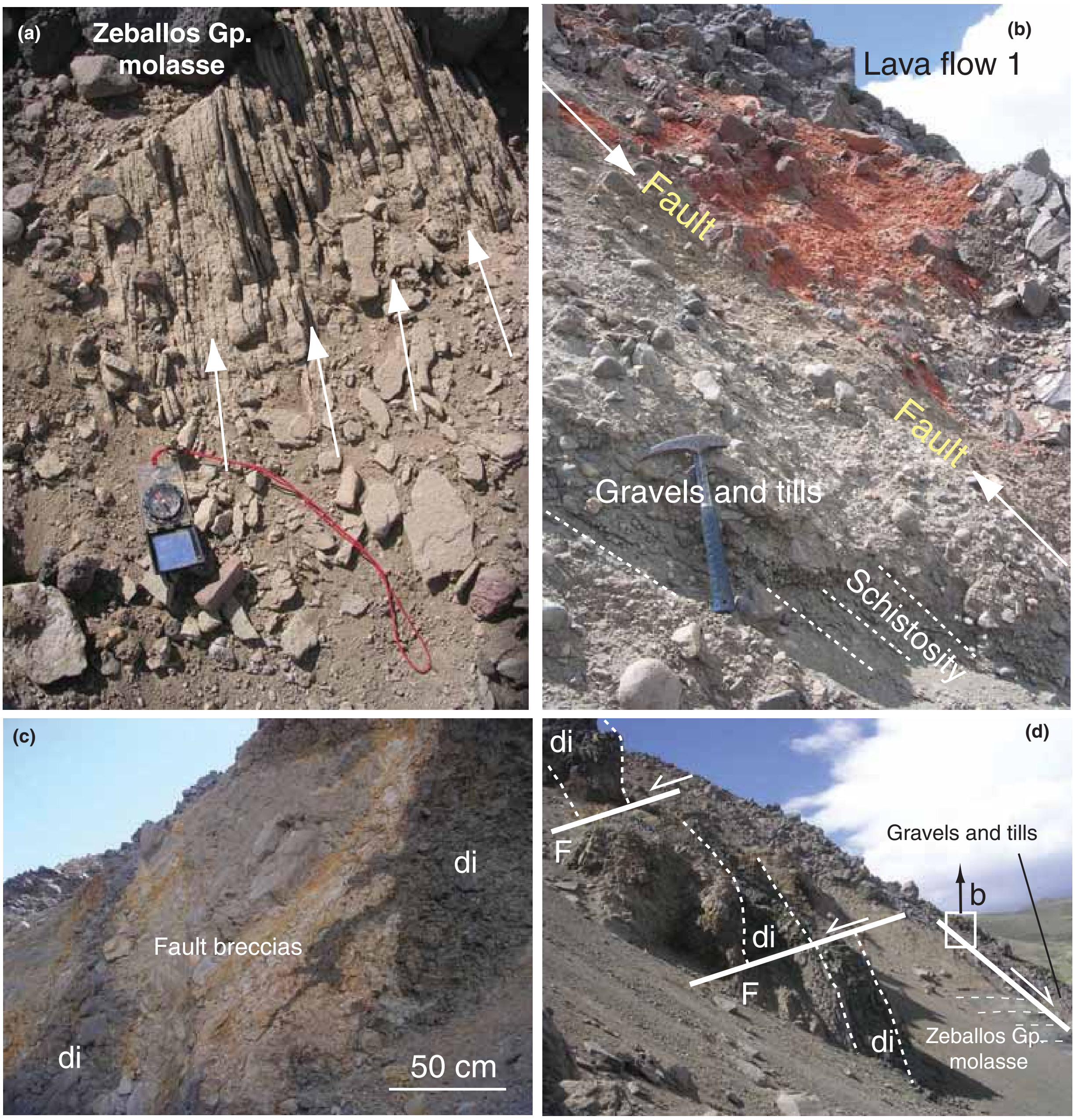

Fig. 5 Some important tectonic features and tectonic–magmatic relationships from the Alto Río Ghio palaeovalley system (Fig. 3). Location of exposures shown in photographs is given in Fig. 4. (a) Brittle cleavage affecting the Zeballos Group sandstones (white arrows). (b) Detailed view of the fault plane and associated schistosity affecting the fluvioglacial formations (area of photo also located in photograph d). Sediments heated by lava flow are red-coloured. (c) Basalt dike (di) penetrating tectonic breccias. (d) Normal faults (F) offsetting the basal dike network (di).

(Fig. 8). Espinoza *et al.* (2005b) documented equivalent chemical signatures for these basalts located on both sides of the lake. Large remnants of a 150 m thick pile of basaltic flows are exposed on the highest part of the southwestern flank of Meseta Chile Chico. A sample from the middle part of this volcanic pile at 1400 m a.s.l. was dated at 4.5 ± 0.30 Ma (sample FE 01–11, Table 1, Fig. 4). Hence, the *c*. 4.5 Ma basalts are exposed at different altitudes on a relatively abrupt terrain of 8–12 Ma flood basalts (Cerro Sombrero area), and also on their basement. As the 4.5 Ma basalts exposed at *c*. 2000 m a.s.l. north and south of Lago General Carrera-Buenos Aires may have formed a continuous lava field accumulated along a former regional depression, the branch of the Lago General Carrera-Buenos Aires which now separates them formed after *c*. 4.5 Ma (Fig. 6). A tectonic process involving local subsidence along transcurrent and normal faults has

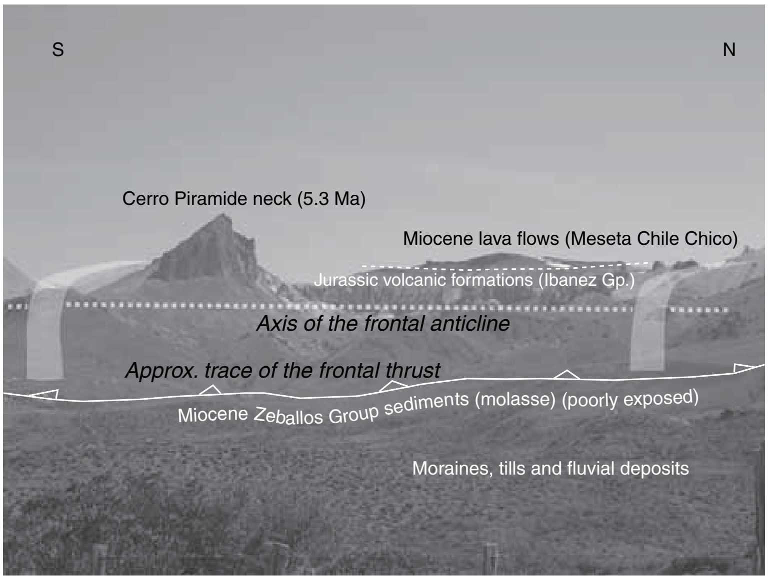

Fig. 6 The Cerro Piramide neck intruding the front of the Cordillera near Chile Chico (location Fig. 3).

been proposed for the origin of the Lago General Carrera-Buenos Aires (Lagabrielle *et al.*, 2004). Finally, observations from the Alto Río Ghio along the N–S trending Zeballos fault zone and the approximately E–W trending Lago General Carrera-Buenos Aires confirm that the disruption and the dissection of the surface which formed the summit of the Cordillera occurred along two main directions (a) parallel to the trend of the Cordillera leading to incisions of Rios Ghio, Jeinimeni and Zeballos and leaving the Meseta Lago Buenos Aires relict surface, and (b) transverse to the Cordillera forming the Lago General Carrera-Buenos Aires depression and leaving the Meseta Chile Chico and Avellanos relict surfaces. N–S disruption started around 5 Ma, while E–W disruption started after 4.5 Ma.

Reactivation and exhumation of the western edge of the Meseta Lago Buenos Aires after 3 Ma

Additional features from the Rio Zeballos–Rio Ghio region indicate that the western border of the Meseta Lago Buenos Aires has experienced post-5 Ma tectonic and magmatic reactivation. Several 3–3.9 Ma subvolcanic acidic rocks (Brown *et al.*, 2004; Espinoza *et al.*, 2006; Espinoza *et al.*, in press) intrude lava flows younger than 5 Ma in the region of Alto Río Ghio, close to Monte Zeballos (Fig. 1b, Table 1). These intrusions (Cerro Lapiz, Mifeldi pluton, Pico Rojo) are aligned along the N170 trending western scarp of the Meseta Lago Buenos Aires. Dikes oriented N160–N170, paralleling the meseta scarp, immediately south of Mifeldi intrusion, have been dated at 3.08 Ma (Espinoza *et al.*, in press).

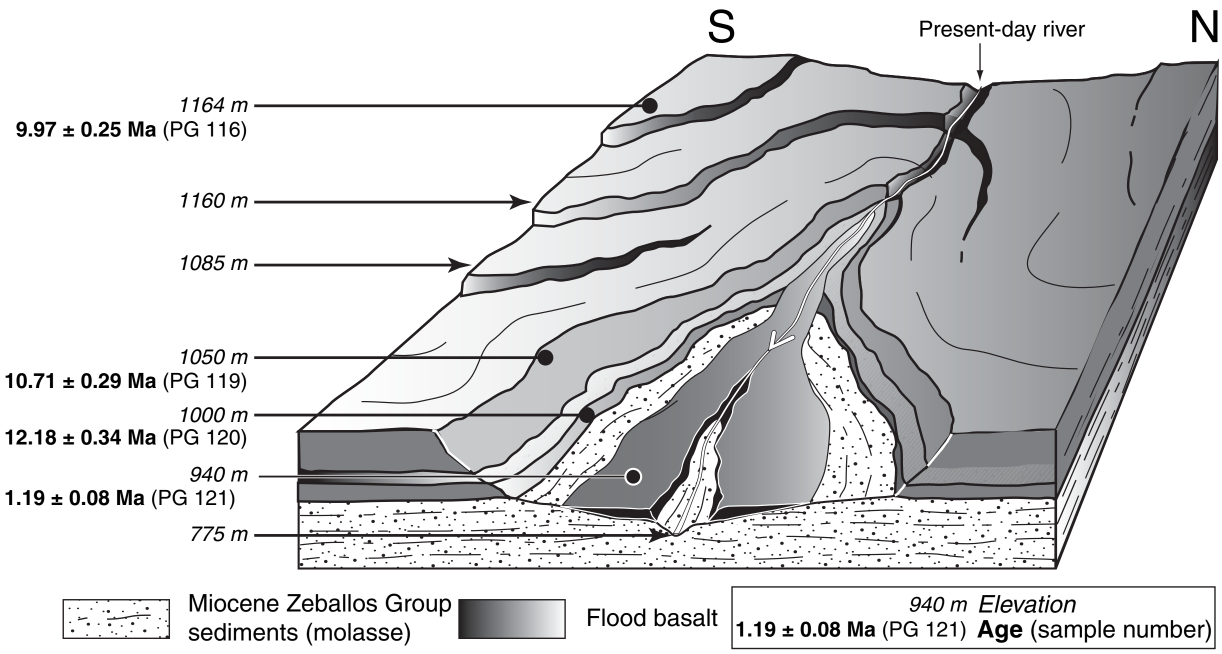

Fig. 7 Block diagram (not to scale) showing the various incisions of lava flows in palaeovalleys sculpted in the southeastern border of Meseta Lago Buenos Aires (see location in Fig. 3). Whole-rock K–Ar ages and elevations of dated samples are shown (Table 1 and Guivel *et al.*, 2006).

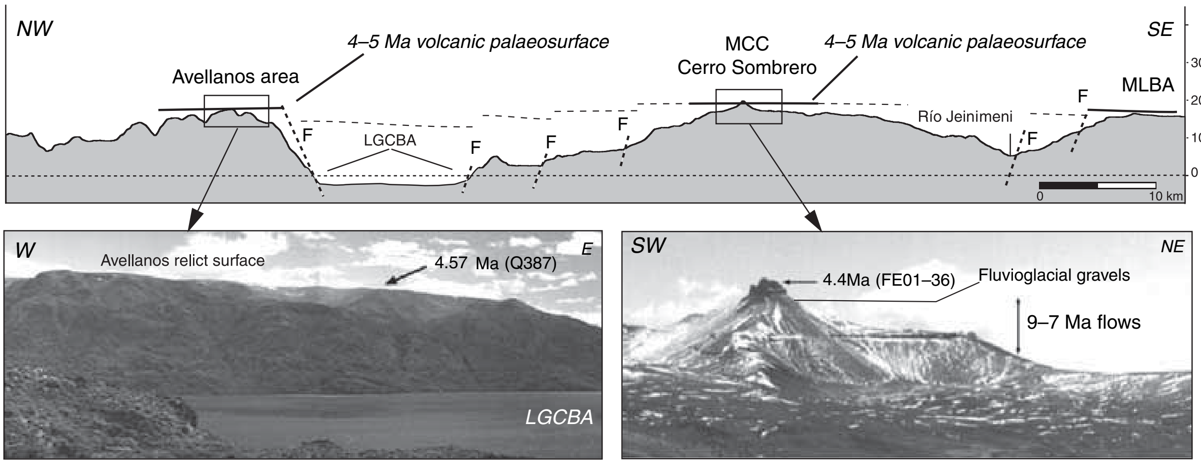

Fig. 8 NW–SE topographic profile across Lago General Carrera-Buenos Aires (LGCBA) with photographs of Avellanos surface and Cerro Sombrero (Meseta Chile Chico, MCC) showing the ages and locations of dated lava flows from both sides of the lake (see location in Fig. 3). F indicates the location of possible post-4 Ma faults that tend to lower the former palaeosurface. MLBA: Meseta Lago Buenos Aires

This indicates a structural control of magma emplacement along faults belonging to the Rio Zeballos fault zone leading to rejuvenation of the western flank of the Meseta Lago Buenos Aires, as suggested in the simplified section in Fig. 4 (fault F2). Relative uplift was probably achieved after 3 Ma.

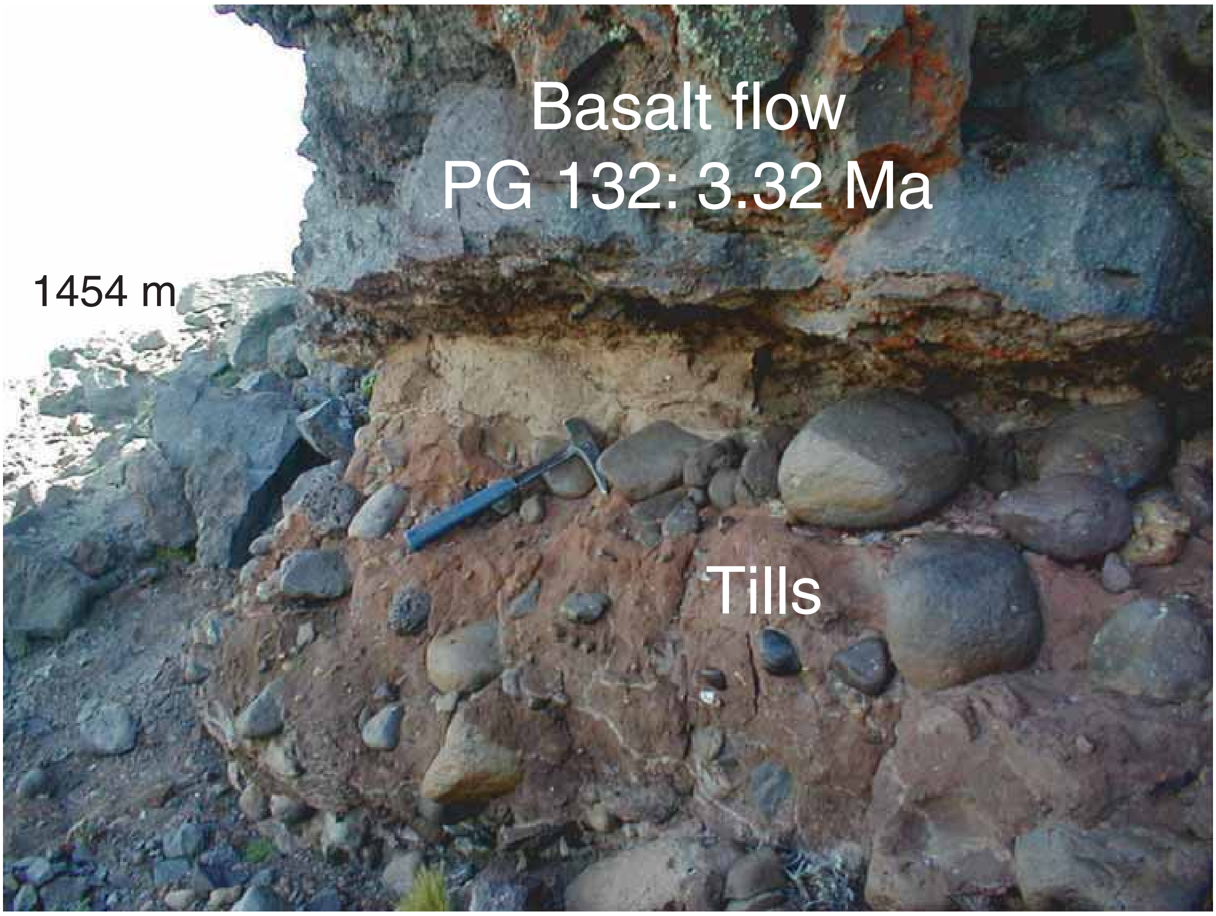

Fig. 9 Photograph of the contact between a 3.32 Ma basalt flow and underlying tills on top of the Meseta Lago Buenos Aires (site location in Fig. 3).

Additional observations from the upper sections of the meseta confirm that vertical displacement occurred along the western and southern scarps of the Meseta Lago Buenos Aires around 3 Ma. Mercer and Sutter (1982) already noticed that the 7–5 Ma tills interbedded between lava flows of the northwestern meseta corner are disconnected from any initial glacial field in the internal Cordillera by the presence of the bounding meseta scarp to the west. We made similar observations but for younger formations on top of the southern scarp of the Meseta Lago Buenos Aires at the site of samples 20–23 (Fig. 4). Here, a till, 40 m thick, is sandwiched between two flows dated at 3.64 and 3.32 Ma (samples PG 133 and 132, respectively, Table 1). The upper part of the till is reddish because of the thermal effect during flow emplacement (Fig. 9). The till is now disconnected from any former glacial relief and from any network of old glacial deposits to the west. This observation confirms that before 3 Ma large glaciers were flowing eastwards from the Cordillera along a former surface locally connected to the Meseta Lago Buenos Aires surface. This connection was disrupted during the 3 Ma event. We infer a normal motion along a fault zone running parallel to the Meseta Lago Buenos Aires western scarp, as suggested in the simplified cross-section in Fig. 4 (fault F2). Further glacial–fluvial erosion and numerous landslides also contributed to scarp retreat.

Discussion and conclusions

The data presented in this paper bring new constraints to the Pliocene tectonic history of Eastern Central Patagonia. We show that the first events leading to the local disruption of the western side of the Meseta Lago Buenos Aires occurred in the Alto Río Ghio region, in relation to extensional displacements along splays of the Rio Zeballos fault zone at around 5–4 Ma. The region was affected again by tectonic disruption, leading to relative uplift of the western scarp of the meseta, after 3 Ma, probably in the period during which its eastern edge was incised by rivers. We infer that uplift and tilting of the Meseta Lago Buenos Aires occurred progressively, with increasing effects from west to east. This can be correlated with the post-plateau volcanic activity of the meseta, which migrated from west to east between 3 and 1 Ma. These results complement previous data indicating fast rates of uplift of the Eastern Patagonian Cordillera between 30 and 8 Ma (Thomson *et al.*, 2001; Haschke *et al.*, 2006), that is prior to the tectonics we identified here and prior to the subduction of the South Chile Ridge segments (Suárez *et al.*, 2000a; Lagabrielle *et al.*, 2004; Ramos, 2005).

The studied region lies above the present-day expected locations of the segments of the South Chile Ridge subducted at 6.0 and 3.0 Ma. A first-order consequence of ridge subduction is the opening of asthenospheric windows in the downgoing slab (Thorkelson, 1996). This allows hot mantle to reach sublithospheric regions, producing first doming and then a weakening of the crust triggering in turn localized collapse. This peculiar geodynamic setting locally modifies the processes governing vertical surface movements of the whole of Patagonia. The tectonic events described here occurred well after the period of compressional tectonics and related continental stacking that led to uplift of the Cordillera at 30–14 Ma (Thomson *et al.*, 2001; Lagabrielle *et al.*, 2004). Therefore they are better explained by a thermal disturbance of the lithospheric mantle beneath Central Patagonia, rather than by subduction-related compressional deformation which is known to have resumed by 12 Ma in this region (Lagabrielle *et al.*, 2004). In addition, the tectonic events evidenced here are approximately synchronous with the 6 and 3 Ma emplacement and exhumation of the San Lorenzo and Las Nieves plutons and in turn coincide in time and space with the subduction of segments of the South Chile Ridge. This suggests causal relationships between deep-seated processes and shallow tectonic evolution, although the thermal–mechanical constraints accounting for such coupling are not yet well understood. The two highest mountains in the Patagonian Cordillera occur in this area (Mts. San Valentín and San Lorenzo), as already noticed by Ramos (1989) and Ramos and Kay (1992). Differential uplift rates, and possible collapse of internal portions of a former compressional belt, would be one of the results of the subduction of an active oceanic ridge under a continent, leading to high erosion and denudation rates. However, whether base level changes leading to valley incision were the result of pure tectonism, or a combination of processes implying isostatic rebound triggered by deglaciation and sea-level variations, is a difficult matter to assess. Glaciers have intermittently occupied parts of Patagonia since the late Miocene–early Pliocene. During melting of the early glaciers, isostatic rebound must have taken place to some extent, adding this component to the spectrum of active forces shaping the area. But this contribution has never been quantified in this region.

Finally, when considering the coincidence in time and place of the development of an asthenospheric window, the occurrence of the highest topographic points in Central Patagonia, the exhumation of young granites and the lack of Pliocene compressional structures, it is tempting to propose that vertical differential displacement related to the occurrence of a slab window under the area may be added to the list of processes responsible for the tectonic evolution of these mountains.

Acknowledgements

This research was funded by grants from the ECOS-CONICYT program (projects C01U01 and C05U01), the Chilean FONDECYT Projects 1000125 and 7000125, and the Servicio Nacional de Geología y Minería (Chile). Field work by YL and JM was possible through grants from the CNRS-INSU DyETI program (France). We are also grateful for the field assistance of Leonardo Zuñiga Díaz. We acknowledge Pr. V. Ramos, an anonymous reviewer and the associate editor for detailed and constructive reviews.

References

Brown, L.L., Singer, B.S. and Gorring, M.L., 2004. Paleomagnetism and 40Ar/39Ar chronology of lavas from Meseta del Lago Buenos Aires, Patagonia. *Geochem. Geophys. Geosyst.*, **5**, Q01H04. doi: 10.1029/2003GC000526.

Cande, S.C. and Leslie, R.B., 1986. Late Cenozoic tectonics of the southern Chile trench. *J. Geophys. Res.*, **91**, 471–496.

Cande, S.C., Leslie, R. B., Parra, J.C. and Hobart, M., 1987. Interaction between the Chile ridge and the Chile trench: geophysical and geothermal evidence. *J. Geophys. Res.*, **92**, 495–520.

Charrier, R., Linares, E., Niemeyer, H. and Skarmeta, J., 1979. K–Ar ages of basalt flows of the Meseta Buenos Aires in southern Chile and their relation to the southeast Pacific triple junction. *Geology*., **7**, 436–439.

De La Cruz, R. and Suárez, M., 2006. Geología del área Puerto Guadal-Puerto Sánchez, Región Aisén del General Carlos Ibáñez del Campo, Escala 1:100.000. *Servicio Nacional de Geología y Minería, Serie Geología Básica, Carta Geológica de Chile, Nº 95*. Santiago, Chile.

De La Cruz, R., Suárez, M., Morata, D., Espinoza, F. and Troncoso, A., 2003. El Cenozoico del Lago General Carrera, Aysén, Chile (46º30'-47º15'S): estratigrafía y tectónica. In: *Congreso Geológico Chileno No. 10*. Concepción.

De La Cruz, R., Welkner, D., Suárez, M. and Quiroz, D., 2004. Geología del área oriental de las hojas Cochrane y Villa O'Higgins, Región Aisén del General Carlos Ibáñez del Campo, escala 1:250.000. *Servicio Nacional de Geología y Minería, Serie Geología Básica, Carta Geológica de Chile, Nº 85*. Santiago, Chile.

Demant, A., Belmar, M., Hervé, F., Pankhurst, R. and Suárez, M., 1998. Pétrologie et géochimie des basaltes de Murta: une éruption sous-glaciaire dans les Andes patagoniennes (46º latitud S), Chili. *Relation avec la subduction de la ride du Chili. C. R. Acad. Sci. Paris*, **327**, 795–801.

Espinoza, F., Morata, D., Polvé Lagabrielle, Y., Maury, R., Guivel, C., Cotten, J., Bellon, H. and Suàrez, M., In press. Pliocene bimodal alkaline magmatism in the back-arc domain of Central Patagonia (47°S) after ridge subduction. *Lithos*, in press.

Espinoza, F., Morata, D., Pelleter, E., Maury, R.C., Suárez, M., Lagabrielle, Y., Polvé, M., Bellon, H., Cotten, J., De la Cruz, R. and Guivel, C., 2005a. Petrogenesis of the Eocene and Mio-Pliocene alkaline basaltic magmatism in Meseta Chile Chico, Southern Patagonia, Chile: evidence for the participation of two slab windows. *Lithos*., **82**, 315–343.

Espinoza, F., Suárez, M., Lagabrielle, Y., Morata, D., Polvé, M., Barbero, L., Maury, R.C., Guivel, C. and De la Cruz, R., 2005b. Tectonics in Central Patagonian Cordillera related to Mio-Pliocene subduction on the Chile Ridge: preliminary morphological, chronological and geochemical evidences. In: *6th International Symposium on Andean Geodynamics-I*, pp. 250–253. Barcelona, España.

Espinoza, F., Morata, D., Polvé, M., Maury, R., Cotten, J., Bellon, H., Guivel, C., Lagabrielle, Y., Suarez, M. and Rosselló, E., 2006. Mio-Pliocene magmatic variability in the Central Patagonia Back-Arc region (47º5'S). In: *The Geological Society of America, Backbone of the Americas: Patagonia to Alaska*, pp. 13–3. 103. Mendoza, Argentina.

Flint, S.S., Prior, D.J., Agar, S.M. and Turner, P., 1994. Stratigraphic and structural evolution of the Tertiary Cosmelli Basin and its relationship to the Chile triple junction. *J. Geol. Soc. London*., **151**, 251–268.

Flynn, J.J., Novacek, M., Dodson, H., Frassinetti, D., McKenna, M., Norell, M., Sears, K., Swisher, C. III. and Wyss, A., 2002. A new fossil mammal assemblage from the southern Chilean Andes: implications for geology, geochronology, and tectonics. *J. South Am. Earth Sci.*, **15**, 285–302.

Gorring, M., Kay, S., Zeitler, P., Ramos, V., Rubiolo, D., Fernández, M. and Panza, J., 1997. Neogene Patagonian plateau lavas: Continental magmas associated with ridge collision at the Chile Triple Junction. *Tectonics*, **16**, 1–17.

Gorring, M., Singer, B., Gowers, J. and Kay, S., 2003. Plio-Pleistocene basalts from the Meseta del Lago Buenos Aires, Argentina: evidence for asthenosphere–lithosphere interactions during slab window magmatism. *Chem. Geol.*, **193**, 215–235.

Guivel, C.H., Morata, D., Pelleter, E., Espinoza, F., Maury, R.C., Lagabrielle, Y., Polvé, M., Bellon, H., Cotten, J., Benoit, M., Suárez, M. and De La Cruz, R., 2005. Geochronology and geochemistry of the Miocene to Recent Patagonian basalts (46-47ºS): evidences for slab tearing due to active spreading ridge subduction. In: *Symposium International on Andean Geodynamics*, pp. 350–353. No. 6 (ISAG 2005, Barcelona), *Extended Abstracts*.

Guivel, C.H., Morata, D., Pelleter, E., Espinoza, F., Maury, R.C., Lagabrielle, Y., Polvé, M., Bellón, H., Cotten, J., Benoit, M., Suárez, M. and De La Cruz, R., 2006. Miocene to Late Quaternary Patagonian basalts (46°S-47°S): Geochronometric and geochemical evidence for slab tearing due to active ridge subduction. *J. Volcan. Geother. Res.*, **149**, 346–370.

Haschke, M., Sobel, E.R., Blisniuk, P., Strecker, M.R. and Warkus, F., 2006. Continental response to active ridge subduction. *Geophys. Res. Lett.*, **33**, L15315, doi: 10.1029/2006GL025972.

Herron, E.M., Cande, S.C. and May, B.R., 1981. An active spreading center collides with a subduction zone; a geophysical survey of the Chile margin triple junction. *Mem. Geol. Soc. Am.*, **154**, 683–701.

Lagabrielle, Y., Suárez, M., Rossello, E., Hérail, G., Martinod, J., Régnier, M. and De La Cruz, R., 2004. Neogene to Quaternary tectonic evolution of the Patagonian Andes at the latitude of the Chile Triple Junction. *Tectonophysics*, **385**, 211–241.

Lagabrielle, Y., Bellon, H., Espinoza, F., Guivel, C.h., Malavielle, J., Maury, R.C., Morata, D., Polvé, M., Rossello, E. and Suárez, M., 2006. Post-Pliocene deformation and uplift of the Patagonian Andes in response to the subduction of the Active Chile Spreading Ridge Center (CSR). *The Geological Society of America, Backbone of the Americas: Patagonia to Alaska*, Paper No. 4-2: 47. Mendoza, Argentina.

Mercer, J.H. and Sutter, J.F., 1982. Late Miocene-Earliest Pliocene glaciation in Southern Argentina: implications for global ice-sheet history. *Palaeog. Palaeoc. Palae*., **38**, 185–206.

Morata, D., Barbero, L., Suárez, M. and De La Cruz, R., 2002. Early Pliocene magmatism and high exhumation rates in the Patagonian Cordillera (46º40'S): K–Ar and fission track data. In: *International Symposium on Andean Geodynamics No. 5 (ISAG 2002)*, pp. 433–436. Toulouse, Francia.

Niemeyer, H., Skarmeta, J., Fuenzalida, R. and Espinosa, W., 1984. Hojas Península de Taitao y Puerto Aisén, Region de Aisén del General Carlos Ibañez del Campo. *Carta Geológica de Chile, 60-61, 1:500.000*. Sevicio Nacional de Geología y Minería, Chile.

Pelleter, E., 2003. *Diversité géochimique et géochronologique des basaltes de la région du Lac General Carrera-Buenos Aires : Nouvelles contraintes sur la subduction de la dorsale active du Chili*. DEA unpublished Thesis, Brest.

Rabassa, J. and Clapperton, C.M., 1990. Quaternary glaciations in the southern Andes. *Quat. Sci. Rev*., **9**, 153–174.

Ramos, V.A., 1989. Andean foothills structures in northern Magallanes Basin, Argentina. *Am. Assoc. Petroleum Geol. Bull.* , **73**, 887–903.

Ramos, V., 2005. Seismic ridge subduction and topography: foreland deformation in the Patagonian Andes. *Tectonophysics*, **399**, 73–86.

Ramos, V.A. and Kay, S.M., 1992. Southern Patagonian plateau basalts and deformation: backarc testimony of ridge collision. *Tectonophysics*, **205**, 261–282.

Ray, F., 1996. Stratigraphical and structural evolution of Tertiary backarc basins in southern Chile (44° to 47°S).

Ph.D. Thesis. (Unpublished). University of Liverpool, 208 pp. U.K.

Singer, B.S., Ackert, R.P. . Jr and Guillou, H., 2004. ^{40}Ar/^{39}Ar and K–Ar chronology of Pleistocene glaciations in Patagonia. *Geol. Soc. Am. Bull.*, **116**, 434–450.

Suárez, M. and De la Cruz, R., 2000a. Tectonics in the eastern-central Patagonian Cordillera (45°30'-47°30' S). *J. Geol. Soc. London*, **157**, 995–1001.

Suárez, M. and De la Cruz, R., 2000b. Geología de la zona del lago General Carrera, Región de Aysén, Chile. In: *Congreso Geológico Chileno No. 9. Actas*, pp. 264–268.

Suárez, M. and De La Cruz, R., 2001. Jurassic to Miocene K–Ar dates from eastern central Patagonian Cordillera plutons, Chile (45º-48ºS) *Geol. Mag.*, **138**, 53–66.

Suárez, M. and De La Cruz, R., 2002. Stratigraphic discontinuities in the Meso-Cenozoic of eastern Aysén, Chile (44º-47ºS). In: *Congreso Geológico Argentino No. 15*), pp. 706–710. **Tomo 1**, El Calafate.

Suárez, M., De La Cruz, R. and Bell, M., 1996. Estratigrafía de la región de Coyhaique (latitud 45º-46ºS); Cordillera Patagónica, Chile. In: *Congreso Geológico Argentino No. 13 y Congreso de Exploración de Hidrocarburos No. 3, 1*, pp. 575–590.

Suárez, M., De La Cruz, R. and Bell, M., 2000a. Timing and origin of deformation along the Patagonian fold and thrust belt. *Geol. Mag.*, **137**, 345–353.

Suárez, M., De la Cruz, R. and Troncoso, A., 2000b. Tropical/Subtropical Upper Paleocene-Lower Eocene fluvial deposits in eastern central Patagonia, Chile (46°45'). *J. South Am. Earth Sci.*, **13**, 527–536.

Thomson, S.N., Hervé, F., Brix, M. and Stockhert, B., 2001. The Mesozoic-Cenozoic denudation history of the southern Chilean Andes and its correlation to different subduction processes. *Tectonics*, **20**, 693–711.

Thorkelson, D.J., 1996. Subduction of diverging plates and the principles of slab window formation. *Tectonophysics*, **255**, 47–63.

Ton-That, R., Singer, B., Mörner, N.A. and Rabassa, J., 1999. Datación de lavas basálticas por ^{40}Ar/^{39}Ar y geología glacial de la región del lago Buenos Aires, Provincia de Santa Cruz, Argentina. *Asoc. Geol. Argentina, Revista.*, **54**, 333–352.

Troncoso, A., Suárez, M., De La Cruz, R. and Palma-Heldt, S., 2002. Paleoflora de la Formación Ligorio Márquez (XI Región, Chile) en su localidad tipo: sistemática, edad e implicancias paleoclimáticas. *Rev. Geol. Chile*, **29**, 113–136.

Welkner, D., 1999. *Geología del área del Cerro de San Lorenzo: Cordillera Patagónica oriental, XI Región de Aysén, Chile (47º25'*-47º50'S). Memoria Título Departamento de Geología. Universidad de Chile. Unpublished.

Received 6 October 2006; revised version accepted 24 July 2007

Chapitre IV :

La Morphologie glaciaire : un marqueur de la tectonique extensive en relation avec l'évolution de la fenêtre asthénosphérique.

Nous avons montré précédemment que la Cordillère de Patagonie Centrale, à la latitude du point triple du Chili, est caractérisée par une phase d'extension importante récente contrôlant en partie l'évolution morphologique actuelle de la chaîne. Ce régime extensif suit une phase de compression responsable de la surrection de la chaîne. Lors de la transition compression/extension, un magmatisme arrière-arc transitionnel à alcalin se met en place. Il est responsable de la formation de plateaux basaltiques tels que la meseta del Lago Buenos Aires actuellement en position de relief inversé. Nous avons montré également que la phase extensive est en relation avec la subduction de la dorsale du Chili et le développement d'une fenêtre asthénosphérique permettant la remontée de manteau chaud au voisinage de la base de la lithosphère.

Dans ce chapitre, nous montrons comment l'évolution Plio-Quaternaire de la Cordillère de Patagonie Centrale peut-être décrite en utilisant comme outil la morphologie glaciaire. Cette partie est présentée sous la forme de trois articles.

Le premier article présente les différentes phases glaciaires successives ayant affecté la Cordillère depuis la fin du Miocène. La Patagonie Centrale est connue pour ses glaciations anciennes, dont les premières sont datées à 7 Ma (Mercer et Sutter, 1982). Dans cet article, nous présentons de nouvelles observations témoignant de phases glaciaires à 7 Ma, 5 Ma et 3 Ma dont les témoins sont soit intercalés entre des laves, soit retrouvés au sommet de la meseta del Lago Buenos Aires pour les plus récentes. Actuellement, ces marqueurs glaciaires sont à la fois, plus élevés que le reste de la Cordillère et déconnectés de tout système glaciaire provenant de l'ouest. Nous suggérons ainsi d'importants mouvements verticaux le long d'un système de failles bordant la partie ouest de la meseta del lago Buenos Aires.

Le second article présenté dans ce chapitre concerne l'utilisation des marqueurs glaciaires perchés de la meseta del Lago Buenos Aires. Grâce aux observations structurales et microtectoniques le long de la bordure ouest de la meseta, nous avons contraint l'amplitude et l'âge de l'extension responsable de la déconnection de la meseta avec le reste de la Cordillère. Cette phase d'extension est datée à 3 Ma et son amplitude varie entre 800 et 3500 mètres. Elle est responsable de l'inversion tectonique négative de la Cordillère ainsi que de la formation des dépressions transverses occupées à partir du Quaternaire par les glaciers de piedmont. Cette phase extensive coincide avec l'ouverture à 3 Ma de la fenêtre asthénosphérique sous la Patagonie Centrale.

Enfin, le troisième article présente les résultats morphostructuraux obtenus dans la région de Coihaique, située à une centaine de kilomètres au nord du point triple du Chili. Cette région présente de très nombreuses analogies morphologiques, topographiques et glaciaires avec la région sud du lac Général Carrera-Buenos Aires. Cependant, les marqueurs glaciaires perchés ne sont pas intercalés avec des laves, ce qui pose un problème de datation. Ceci nous permet néanmoins de proposer que cette région a connu une réorganisation importante des reliefs en relation avec une inversion négative de la chaîne. Bien qu'elle soit située au nord de la position prédite de la fenêtre asthénosphérique, nous proposons que l'extension responsable de la morphologie actuelle est reliée à la présence en profondeur de manteau asthénosphérique chaud migrant vers le nord à travers la fenêtre asthénosphérique en voie d'ouverture.

IV.1. Les glaciations Mio-Pliocène et évolution morphotectonique de la Patagonie Centrale orientale, mesetas del Lago Buenos Aires et Guenguel.

Mio-Pliocene glaciations of Central Patagonia :

New evidence and tectonic implications

Yves Lagabrielle[1], Bruno Scalabrino[1], Manuel Suarez[2] , and Jean-François Ritz[1]

(1) *CNRS-UMR 5234, Géosciences Montpellier, Place E. Bataillon, CC 60, 34095, Montpellier Cedex 5, France*

(2) *Servicio Nacional de Geología y Minería, Avenida Santa María 0104, Santiago, Chile*

Mio-Pliocene glaciations of Central Patagonia :
New evidence and tectonic implications

by :

Yves Lagabrielle[1], **Bruno Scalabrino[1]**, Manuel Suarez[2] , and Jean-François Ritz[1]

(1) *CNRS-UMR 5234, Géosciences Montpellier, Place E. Bataillon, CC 60, 34095, Montpellier Cedex 5, France*

(2) *Servicio Nacional de Geología y Minería, Avenida Santa María 0104, Santiago, Chile*

Submitted to Andean Geology- Revista Geologica de Chile ; accepted with minor revisions 10th June 2009.

Corresponding author :

yves.lagabrielle@gm.univ-montp2.fr

Abstract

Patagonia is well known for spectacular occurrences of a variety of glacial-derived relicts and for a long history of ancient glaciations. In this paper, we first review the diverse evidences that demonstrate the development of glacial-related sedimentation within the Central Patagonia Cordillera since the past 7 Ma. We then describe for the first time well preserved glacial landforms at the top surface of mesetas on both sides of the Lago General Carrera Buenos Aires : the meseta del Guenguel to the north, and the meseta del Lago Buenos Aires to the south. The latter landform, which corresponds to a 3 Ma old paleo-piedmont (after the Ar/Ar dates of the latest lava flows) shows evidence of glacier advances to the NE direction. Over a distance of 20 km, glacial relicts define glacial tongues that were fed by the Cordillera reliefs to the west. These lobes are now beheaded from their westwards sources along a morpho-structural corridor that bounds the meseta del Lago Buenos Aires to the west. These features suggest that recent tectonic causes modified the glacial drainage network of Central Patagonia, and bear important constraints on the history and development of the first glaciations in southern South America.

1. Introduction

The Patagonian Cordillera forms the southern segment of the Andes, north of the Andes of Tierra del Fuego. It was built coevally with the subduction of the southern part of the Chile Spreading Ridge during the Upper Cenozoic. Between latitudes 45° and 47° S the Central Patagonian Cordillera has both the highest mountains (Monte San Valentin, 4058 m a.s.l.) and a deep transverse incision occupied by the Lake General Carrera-Buenos Aires (LGCBA). The northernmost ice-cap in South America occurs in this part of the Cordillera (Campo de Hielo Norte : North Ice Cap, NIC, fig 1). The eastern border of the Cordillera, corresponding to the tectonic front, is marked by a rapid transition to the flat plain region of the pampa and is delineated by a N-S alignment of plateaus or mesetas, preserving perched flat surfaces in response to relief inversion which occurred after 3 Ma (Lagabrielle et al., 2004; 2007; Scalabrino et al., 2009).

Patagonia is well known for spectacular occurrences of a variety of glacial-derived remnants and for a long history of ancient glaciations (Clapperton, 1993; Rabassa et al., 2005). Most of the previous studies which pointed at the abundant relict landforms and deposits of glacial or fluvio-glacial origin refer to glaciations which occurred during the Quaternary (Kaplan et al., 2004; 2005; Rabassa, 2008; Glasser et al., 2008). The maximum areal extent of ice during the Quaternary Period is known as the Greatest Patagonian Glaciation (GPG) and developed between 1.168 and 1.016 Ma (OIS 30–34; Early Pleistocene) (Mercer, 1983; Rabassa et al., 2005). A minimum of eight glaciations occurred in the Middle–Late Pliocene (Oxygen Isotopic Stages 54–82). After the GPG, 14–16 cold (glacial/stadial) geoclimatic events occurred, intercalated with their corresponding warm (interglacial/interstadial) equivalents.

A major characteristic of the glacial history of Patagonia is that numerous testimonies of pre-Pliocene glaciations, some as old as 7 Ma, have been observed in various places (e.g. Mercer, 1983). These are not located within the present-day glacial valleys but are found as remnants preserved on perched relict surfaces, implying complex interaction between mountain building and glacial dynamics. In this paper, we first review the evidence collected so far in Central Patagonia demonstrating the development of glacial-related sedimentation over the reliefs of the Cordillera since ca. 7 Ma. Second, we report the existence of well preserved glacial landforms exposed on the top surface of mesetas on both sides of the Lago General Carrera Buenos Aires : the meseta del Lago Buenos Aires to the south and the meseta del Guenguel to the north. These remnants have been disconnected from the main Cordillera after 3 Ma as shown by Ar/Ar ages from lava flows associated with glacial deposits. This implies important changes in the glacial drainage network of Central Patagonia which occurred around 3 Ma due to tectonic causes. At a broader scale, these findings bear important constraints on the history of the initiation and development of the very first glaciations over entire Southern South America.

2. The geological framework of the Miocene-Pliocene glacial deposits of Central Patagonia

As stressed in the review of section 3 below, inception of the glacial history of Patagonia occurred at or before 7 Ma. Therefore, our understanding of the evolution of the Patagonian glaciations cannot be disconnected from accurate knowledge of the geological evolution of the Cordillera and its piedmont during the Neogene. In particular, we have to evaluate the succession of volcanic and tectonic events which affected Central Patagonia and their possible impacts on the evolution of the glaciations and glacial landscapes. The following section is an overview of the geological evolution of Central Patagonia pointing at the relationships between magmatic and tectonic events on one hand and glacial deposits on the other hand. Such relations are examined in crucial sites such as the mesetas, showing frequent spatial associations of magmatic products and glacial or fluvio-glacial deposits.

In eastern Central Patagonia, Jurassic and Cretaceous volcanics and marine sedimentary rocks unconformably overlie Late Paleozoic metamorphic rocks (Suárez et al. 1996; De La Cruz and Suarez, 2003 ; 2004 ; De La Cruz et al., 2006). The Cenozoic stratigraphic sequence, well exposed in the area south of Lago General Carrera-Buenos Aires, includes: (1) Oligocene marine clastic deposits (Guadal Formation), (2) Miocene fluvial deposits, the so-called « molasse », of the Zeballos group (Flint et al. 1994; Ray, 1996; Flynn et al. 2002; De La Cruz and Suárez, 2006); (3) Late Miocene to Recent basalts forming the prominent flat-topped plateau of Meseta del Lago Buenos Aires (Gorring et al. 2003; Lagabrielle et al. 2004; Brown et al. 2004; Espinoza et al. 2005; Guivel et al. 2006).

The orographic front of the Central Patagonia Cordillera is formed by the Ibáñez Formation (Jurassic to Early Cretaceous), thrusted to the east over Cretaceous and Cenozoic rocks (Suárez and De La Cruz, 2000a; Lagabrielle et al. 2004 ; Scalabrino et al., 2009). The main Cenozoic contractional tectonism occurred during and after the deposition of the Zeballos Group and prior to the emplacement of the alkali basalts of the meseta del Lago Buenos Aires at 14-12 Ma (Lagabrielle et al., 2004, 2006; Guivel et al. 2006; De La Cruz and Suárez, 2006). Therefore, the end of the major contractional event in the region of study can be correlated with the initiation of the subduction of the Chile Ridge at 14-15 Ma in southernmost Patagonia, inducing a different stress regime in the frontal arc region. Between 5 Ma and 3 Ma, renewed orogenic activity, uplift and disruption of former erosional surfaces occurred in relation with activation of strike-slip fault zones and normal inversion of older thrusts (Lagabrielle et al., 2007; Scalabrino et al., submitted).

The Meseta del Lago Buenos Aires (47ºS-71º30'W) is one of the largest (~ 6000 km^2) and most voluminous (ca. 2000 km^3) basaltic plateaus in the back-arc domain of Central Patagonia (figs. 2 and 3). It forms part of the Neogene Patagonian Plateau Lavas province (NPPL, Gorring et al., 1997) outcropping from 46º30' S to 52º S in Argentina. This province has been genetically related to the development of a series of slab windows opened as a consequence of the subduction of the South Chile Spreading Ridge (SCR) under the South American Plate since ~15 Ma (Cande and Leslie., 1986; Ramos and Kay, 1992; Gorring et al., 1997; Gorring and Kay., 2001 ; Gorring et al., 2003 ; Guivel et al., 2006 ; Scalabrino et al., 2009).

The Meseta del Lago Buenos Aires locally exposes spectacular successions of tills and lava flows. In addition, the limit between the Cordillera and the Meseta is also characterized by the existence of numerous recent shallow magmatic intrusions. Both lavas and intrusions have stratigraphical relationships with the glacial deposits, allowing to build accurate chronological schemes for ancient glaciations. For all these reasons this area is of high interest.

The very basal lavas of the Meseta del Lago Buenos Aires have been dated at 16-14 Ma (Espinoza et al., 2008; Boutonnet et al., submitted) and were emplaced during the fluvial sedimentation of the uppermost beds of the Rio Zeballos Group. They show the transition from an arc related source to a more OIB-like source. The main-plateau basaltic pile determining the overall plateau-like morphology of the meseta comprises tabular basaltic lava flows and interbeds of fluvio-glacial deposits emplaced during the Late Miocene-Pliocene

(~12.2-3.3 Ma : Mercer and Sutter, 1982; Ramos and Kay, 1992; Kay et al., 1993; Gorring et al., 1997; Ton-That et al., 1999; Guivel et al., 2006) (figs. 2, 3 and table 1). Later, post-plateau basalts were emplaced in several volcanic pulses during the last 3.3 Ma-100 ka as isolated monogenetic cones and maars (Ton-That et al., 1999; Gorring et al., 2003; Brown et al., 2004, Singer et al., 2004) as well as flows filling valleys incised into the main plateau sequence (Lagabrielle et al., 2007). The post-plateau lavas are volumetrically minor (~600 km^3, Gorring et al., 2003) compared to the main sequence.

In the southwestern border of the Meseta del Lago Buenos Aires, west of Monte Zeballos, several felsic transitional subvolcanic bodies, mostly shallow level plugs, dykes and laccoliths, are exposed at altitudes around 1800-2000 m a.s.l.. The most prominent bodies (Pico Rojo, Mifeldi pluton and Cerro Lápiz peaks) are aligned along a ~N160-170 trending lineament, the Zeballos Fault Zone, paralleling the western edge of the Meseta and marking the morphotectonic front of the Patagonian Cordillera (Giacosa and Franchi, 2001 ; Lagabrielle et al., 2004 ; Scalabrino et al., submitted). They are intrusive into the main-plateau basaltic pile of the Meseta or into the molasse of the Zeballos Group. $^{40}Ar/^{39}Ar$ and whole-rock K-Ar ages dates for the lavas and the felsic intrusions indicate that the emplacement of these rocks occurred between 3.98 and 3.08 Ma synchronously with that of the more mafic, post-plateau basaltic sequence, during a bimodal mafic-felsic magmatic episode devoid of intermediate compositions (Brown et al., 2004 ; Espinoza et al., 2007 ; Boutonnet et al., submitted) The exposure of these bodies along the western scarp of the meseta indicates that a major tectonic disruption occurred here, along the N160 trending Zeballos fault at 3 Ma or immediately after. This event led to the relative uplift of the western border of the meseta with respect to the Cordillera. As shown below, this event had a major impact on the glacial network of this region.

The top surfaces of three other mesetas adjacent to Meseta del Lago Buenos Aires are composed of pre-Quaternary glacial and fluvio-glacial deposits (fig. 1).

(1) On the northern side of the Lake General Carrera-Buenos Aires, the Meseta del Guenguel extends north of Rio Fenix Grande. It has a triangular shape and its maximum elevation reaches 1200 m a.s.l. at its western tip, close to Portezuelo. The Meseta del Guenguel dominates by 1000 m the Lake General Carrera Buenos Aires and the moraines of the Fenix system (fig. 2) deposited by the latest Quaternary glaciers (Singer et al., 2004). By contrast to the Meseta del Lago Buenos Aires, its upper surface is not covered with lava flows. From satellite images, the Meseta del Guenguel paleosurface shows a dendritic relict stream network flowing to the east. Its edges are abruptly cut by post-glacial landslides. Tributaries are

truncated along the southern sharp edge of the meseta in response to recent relief inversion (Lagabrielle et al., 2004).

(2) A northern meseta having the same triangular shape as Meseta del Guenguel is lying north of the Balmaceda Plain (Meseta del Cerro Galera, fig. 1). From satellite images, it also shows a paleo-fluvial network. Its western tip corresponds to Cerro Galera which dominates the depression of Coihaique. No lava flows are reported from the top surface of this meseta.

(3) The Meseta Chile Chico (46.4°S; 2160 m a.s.l.) is the westernmost exposure of Eocene and Mio-Pliocene flood basalt volcanism in Patagonia. The Cenozoic volcanic succession, approximately 1000 m thick, unconformably overlies the Jurassic volcanic rocks of the Ibáñez Group and consists of Late Paleocene-Eocene basalts, Late Oligocene-Early Miocene marine sediments and Late Miocene to Pliocene basalts. These upper basalts, 400 m thick, with alkaline and sub-alkaline affinities gave K/Ar ages ranging between 9.8 Ma ± 0.1 Ma and 4.4 ± 0.8 Ma (Espinoza et al., 2003; De La Cruz and Suárez, in press).

3. Mio-Pliocene Glacial deposits of Central Patagonia : a review

a. The 7 Ma to 5 Ma tills at the northern edge of Meseta Lago Buenos Aires

Some of the oldest Cenozoic glacial deposits recognized in South America have been found in the scarps of the Meseta del Lago Buenos Aires between Rio Jeinimeni and Rio Los Antiguos (Mercer and Sutter, 1982). Till deposited over 30 m in thickness are interbedded with lava flows of the main plateau sequence. Eight lava flows have been dated. The lower basalts yielded whole rock K/Ar ages of 7.34 ± 0.11 to 6.75 ± 0/08 Ma and the upper basalts yielded ages of 5.05 ± 0.07 to 4.43 ± 0.09 Ma (Mercer and Sutter, 1982). In the same locality, Ton-That et al. (1999) have obtained ^{40}Ar-^{39}Ar isochron ages of 5.04 ± 0.04 Ma and 7.38 ± 0.05 Ma for the upper and the underlying basaltic flows, respectively.

b. The 7, 5 and 3 Ma tills at the western edge of Meseta Lago Buenos Aires

Key exposures allowing observations of relationships between glacial deposits, lava flows, dikes and fault surfaces are located west of Meseta Lago Buenos Aires, in the Portezuelo area of Alto Rio Ghio, on the western side of the road R.P. 41, north of Paso Roballos (fig. 4). Here, basaltic lava flows, locally up to 10 m thick, have been emplaced in a paleo-glacial valley trending N35-N40, incised in the fluvial sandstones of the Zeballos Group and filled with glacial sediments (refered to as the paleovalley site hereafter).

(a) Sample from the lower flow in the northern part of the outcrop gave a whole rock K-Ar age of 4.98 ± 0.15 (Lagabrielle et al., 2007). This flow overlies tills and fluvioglacial conglomerates including numerous cobbles deriving from the internal part of the Cordillera (plutonic rocks from the batholith, ignimbrites and lavas from the Mesozoic formations). A new date obtained from a lava flow in direct contact with glacial conglomerates located 200 m south of the previous site gave a Ar-Ar age of 6.85 ± 0.15 Ma (Boutonnet et al., submitted). This is the oldest age for a lava flow in contact with tills obtained at this site. The tills immediately underlying this lava flow display a spectacular red-colour along the contact indicating heating and circulation of hot, oxydizing water during lava emplacement (Plate 1B, 1E). This strongly suggests lava eruption during a glacial period. Close to this site, due to fresh exposures along the current steep valley flank, a spectacular contorted contact between moraine deposits and a lava flow can be observed (Plate 1), indicating that lava flows deformed soft glacial sedimentary deposits and confirming eruption within a glacial landscape. The outcrop belongs to a faulted block, detached along a landslide, avoiding precise correlation with the other dated lavas (Fig. 4).

(b) The intermediate flows are brecciated and include basaltic blocks of various types, one of them dated at 6.95 ± 0.24 Ma. The upper flow gave a K-Ar age of 2.96 ± 0.09 Ma (Lagabrielle et al., 2007) (fig. 4). It extends horizontally farther west over the ancient piedmont surface, developed at the foot of the morphotectonic front of the Cordillera (fig. 5). This paleo-piedmont, at least 3 Ma old, is now incised by the present-day Rio Ghio and is offset to the east by the faults of the Rio Zeballos fault zone which control the western scarp of the meseta.

(c) The upper flow overlies a second layer of tills that also extends westwards towards the front of the Cordillera (fig. 5).

The compilation of ages above indicates glacial advance and related deposition of sediments at least during 3 periods at *ca.* 7 Ma, 5 Ma and 3 Ma (fig. 5). In the same area, a lava flow exposed along the road-cut some hundreds meters to the north, yielded an age of 4.81 ± 0.32 Ma (Lagabrielle et al., 2007). It belongs to a series of flows interbedded with tills, also characterized by the presence of exotic pebbles originating from remote regions of the batholith (Plate 1C). In this region of the Portezuelo area of Alto Rio Ghio, few km norh of the paleovalley, new dating of lava flows confirm that basalts have been erupted between 6 Ma and 3 Ma (Boutonnet et al., submitted).

Evidence of faulting during magmatic activity in Alto Rio Ghio area is deduced from observation made some tens of meters south of the paleovalley. The Zeballos Group sandstones are intruded by subvertical basaltic dikes which are offset by westward dipping, conjugate normal faults. One dike has given a K-Ar whole rock age of 4.32 ± 0.23 Ma (Lagabrielle et al., 2007). Numerous marks of deformation are observed in this site including an eastward dipping brittle cleavage oriented N35-N40, parallel to the paleo-valley axis, affecting both the Zeballos Group sandstones and the base of glacial deposits. This led Lagabrielle et al. (2007) to propose a tectonic control of the paleo-valley. Faulting initiated during the deposition of the first tills and lavas, that is probably as early as 7-6 Ma.

c. Fluvio-glacial conglomerates and tills older than 3 Ma on top surfaces of mesetas

Perched tills and fluvio-glacial deposits have been observed in some localities directly on the top surface of the Meseta del Lago Buenos Aires. First, at the southwestern limit of the plateau, a till, 40 m thick, is sandwiched between two flows dated at 3.64 and 3.32 Ma at 1454 m elevation (Guivel et al., 2006; Lagabrielle et al., 2007, fig. 2, table 1). The upper part of the till is reddish due to thermal effect during flow emplacement. Second, coarse fluvio-glacial gravels and underlying tills have been observed on the western edge of the meseta at 1350 m elevation (D. Morata, pers. comm. Plate 1A). These deposits have been tilted and are covered by a lava flow dated at 5.84+/-0.21 Ma (Guivel et al., 2006, fig. 2, table 1). Third, Mercer and Sutter (1981) relate the presence of a large moraine in their area of study in the northwest corner of the Meseta (fig. 6). Due to its present elevation on the top surface of the meseta and to its location far from the current glacial valley of Lago General Carrera-Buenos Aires, this moraine cannot belong to any of the deposits related to the advance of glaciers during the Quaternary. Therefore, it may be correlated with tills dated between 3.64 and 3.32 at the opposite side of the Meseta.

A sequence of thick tills and fluvio-glacial conglomerates forms the upper part of Cerro Galera, a prominent relief of molasse deposits dominating the Coihaique depression (Scalabrino et al., submitted). This perched sequence, more than 100 m thick, shows a spectacular accumulation of pebbles and boulders within a thin sandy matrix. Most of the blocks are of plutonic origin and derive from the batholith. The till is presently disconnected from any former glacial relief around and from any network of old glacial deposits to the west. No dating of these tills have been performed. Since they cover the upper beds of the Galera Formation, they are younger than 16-14 Ma Their base could be as old as 12 Ma, the age of fluvial conglomerates in the area of Baño Nuevo (Suárez et al., 2007). Further north, in the area of Meseta Boscosa and Baño Nuevo, 60 km NE of Coihaique, tuffs dated at 17 Ma (U-Pb SHRIMP, De La Cruz et al., personal comm.), are overlain by fluvial conglomerates assigned to the late Miocene Galera Formation (dated nearby at 12 Ma; zircon U-Pb SHRIMP from a sample of an intercalated tuff; De La Cruz, Suárez and Fanning, pers. comm.). Varves with dropstones identified as land-slided blocks exposed under cliffs formed by these conglomerates are interpreted as interbedded in them, which allows the inference that the conglomerates are fluvioglacial in origin and that there was a very old glaciation approximately during the late Miocene (Suárez et al., 2007).

In these area, the top of several mountains of the easternmost part of the Cordillera are covered by loose gravels, overlying beds assigned to the Galera Formation and that have been interpreted as representing fluvioglacial deposits of Pliocene or Pleistocene age (Suárez et al., 2007). There are no dates for these deposits that could represent either the eroded remnants of the Galera Formation or younger beds of Pliocene or Pleistocene age. These deposits are disconnected from other glacial forms or deposits and are elevated in several hundreds of meters with respect to the present day river system, implying important uplift since the late Miocene-Pliocene. This was followed by the advance of valley glaciers forming a well developed system of frontal moraines at the northern and eastern margins of the Baño Nuevo plains, that dammed a lake during the Pleistocene (Suárez et al., 2007)

d. Fluvio-glacial and glacial conglomerates on top of the relict Avellanos surface (10-4 Ma)

Relicts of polymictic conglomerates representing fluvioglacial deposits have been found in various places of Central Patagonia, from both sides of the Lake General Carrera Buenos Aires as well as at various localities on the top surfaces of the Mesetas. These deposits are exposed on well defined remnants of a flat paleosurface extending west of the tectonic front, within the Cordillera itself. A well developed paleosurface is the Avellanos peneplain (Lagabrielle et al., 2004; 2007; Scalabrino et al., submitted), that has an average elevation of 2000 m. and is exposed in the internal regions of the Cordillera, north of Lago General Carrera and west of Puerto Ingeniero Ibáñez (fig. 1)., It is a clearly erosional surface, erasing folded Jurassic volcanic rocks and Paleozoic basement. The Avellanos peneplain was present during the Pliocene, as indicated by the age of a 10 m thick basaltic lava flow deposited on it, dated at 4.57 ± 0.27 Ma (Ar/Ar, Guivel et al., 2006). This basaltic flow correlates with the upper basaltic flows on the top of the Meseta Chile Chico, on the opposite side of the Lake, exposed at the same elevation (2,150 m a.s.l) which have been dated at 4.4 ± 0.8 Ma (Espinoza, 2003; the Pico Sur basalts of De La Cruz and Suárez, in press). The latter flow overlies with a hiatus a basaltic lava flow of ca. 8.0 Ma, implying the existence of an erosional surface developed sometime between 8 and 4.5 Ma (De La Cruz and Suárez, in press). Therefore, this erosional surface can be correlated with a depositional surface in the Meseta del Lago Buenos Aires, bracketed between 7 and 5 Ma and where glacial deposits accumulated (Mercer and Sutter, 1982; Ton-That et al., 1999). This indicates that the Avellanos surface was formely connected to a piedmont surface of the mesetas

4. Preserved glacial landforms on the top surfaces of mesetas del Lago Buenos Aires and del Guenguel

Four elongated remnants of glacier outlets, SW-NE oriented, are observed from satellite images and DEM on the NW side of Meseta del Lago Buenos Aires (figs 6 and 7). They parallel a ridge which might correspond to the lateral moraine described by Mercer and Sutter (1982). They are observed in a region devoid of any volcanic cone (fig. 6), contrasting with the remaining surface of the meseta and suggesting that glacial advance avoided the growth of volcanic edifices. To the south, 2 glacial valleys are still in connection with the slopes of the Monte Zeballos, indicating glacial activity during the very recent times. By contrast, the two northernmost outlets appear as truncated valleys (fig. 6) and are disconnected from any current former ice domes in the surroundings.

Glacial geomorphological features are well observed on satellite images, allowing a preliminary analysis, as proposed in figure 8. Landforms include glacial ridges and probable eskers, well developed lateral moraines truncating large volcanic cones, kettles and arcuate frontal moraines (figs 7 and 8). Detailed field work is now needed in order to describe precisely these features and their chronology. The age of the corresponding glaciers is older than 3 Ma, since the isolated volcanic cones and flows of the meseta are often 3 Ma old. This is corroborated by the presence of tills dated around 3 Ma in the western border of the meseta, as reported in section above.

Remnant of a series of arcuate moraines and frontal sandur river indicating the presence of an ancient frontal glacier system can be observed on the south western edge of meseta del Guenguel (fig. 7D). This system is not very well preserved, but the arcuate shape of the corresponding ridges contrasts with the flat surfaces around. This could represent a new evidence that important glaciers developed in Central Patagonia during the Pliocene.

5. Discussion : tectonic and paleoclimatic implications

This study highlights 3 major questions concerning the Miocene-Pliocene tectonic-climatic evolution of the Central Patagonian Cordillera. These questions relate to: (a) the widespread character of the observations reported here, (b) the timing and origin of the processes reponsible for the disconnection of the glacial landforms from the remaining Cordillera, and finally (c) the tectonic-climatic significance of such a major morphological change.

(a) Generalization of the presence of old glacial formations in Central Patagonia and the development of the Avellanos surface.

The compilation of data presented in this study confirms that the oldest known Patagonian glaciation took place between approximately 7 and 5 Ma (Latest Miocene–Earliest Pliocene). The possibility of a ca.12 Ma old glaciation has been also tentatively proposed by Suárez et al. (2007) in the area of Baño Nuevo. This has to be compared to recent results from other regions of Patagonia which also indicate local development of early glaciations. Late Miocene glacial deposits have been recognized in northern Patagonia between lat. 39°S. and 41°S (Schlieder et al., 1988). Suárez and Emparán (1997) report the observation of erratic boulders and glacial striations at about 2.000 m high in the region of Lonquimay (38º30’ S) in Chile, adjacent to the border with Argentina. These erratics occur on hills bordering the present valleys. These feature are probable evidence for an ice cap as far north as latitude 38º30’. The existence of Late Miocene glacial deposits around Lago Cardiel (49°S, 72°15′W in southern South America), as old as 10.5 Ma is reported by Wenzens (2006a). Nine late Miocene glacier advances are identified in this region that until now has been assumed to be unglaciated. Several dating results indicate minimum ages of 6.4 Ma and 6.6 Ma for oldest glaciations of the San Lorenzo and San Martín area. Two further advances have a minimum age of 5.4 Ma.

Our study shows that despite a greater disruption due to recent tectonics, the succession of lavas and tills exposed in Alto Rio Ghio displays similar characteristics to the succession described by Mercer and Sutter (1982) in the northern part of the Meseta del Lago Buenos Aires. In both localities, glacial formations reworking material from remote regions of the Cordillera including the Patagonian Batholith, are comprised between flows dated at 7-6 Ma and 5-3 Ma. In the Alto Rio Ghio area, at least 2 till formations are present and a younger one, dated at 3 Ma is exposed at the same latitude on the top surface of the Meseta (Lagabrielle et al. 2007). This indicates finally that during the 7.3 to 3.0 Ma period, Central Patagonia has experienced at least 3 cycles of glaciation, around 7 Ma, 5 Ma and before 3 Ma, contemporaneous with abundant basalt flooding.

The data from the four mesetas reported here indicate that during the Late Miocene-Pliocene, sometime between 7 and 4.5 Ma and after the deposition of the Rio Zeballos Group (Late Early to early Middle Miocene), glaciers and rivers were flowing to the east or north-east, building a regional morphological smooth surface, known as the Avellanos surface. This surface is erosional in the internal Cordillera. In the piedmont domain to the East, abundant lava flows, now capping the Meseta del Lago Buenos Aires were accumulating locally, probably within large depressed areas of this surface. Interbedding of flows and gravels show that just before or during and after 7 Ma, lavas were synchronously erupted during the fluvial and glacial processes. Finally, between14 Ma and 3 Ma, the region of the Cordillera corresponding to the study area was smoother and not so deeply incised than the current one, The N160 and N-S oriented valleys paralleling the front of the Cordillera (Rio Jeinimeni-Rio Zeballos and Rio Ghio valleys), as well as the transverse incision of the Lago General Carrera-Buenos Aires did not exist (Lagabrielle et al., 2004; Scalabrino et al., submitted). Higher reliefs, the feeders of the paleo-glaciers described in this study were located farther west, suggesting a very different overall morphology of the Cordillera.

(b) Timing and origin of processes responsible for the disconnection of the glacial remnants from the remaining Cordillera.

This study reveals the presence of relict glacial landforms, 3 Ma old and older, preserved on the top surface of the Mesetas del Lago Buenos Aires and del Guenguel. These features are now separated from the rest of the Cordillera by N-S oriented valleys. Mercer and Sutter (1982) already noticed that the 7-5 Ma old tills interbedded between lava flows of the northwestern meseta cormer are disconnected from any initial glacial field in the internal Cordillera due to the presence of the bounding meseta scarp to the west. This already suggested that a tectonic event is responsible for the disconnection of these landforms from the remaining Cordillera (fig. 9). The

observations of truncated valleys developed on the top surface of the meseta as reported in section 4, the age of 3 Ma of the youngest tills exposed on the uppermost sections of the meseta, and the exposure of the 3 Ma Mifeldi pluton along the western scarp of the Meseta, all indicate that this scarp is 3 Ma old or younger. These data and the fact that there is no visible imprint of glacial flow on the Mifeldi cliff and no relict glacial features preserved such as moraines, striations, meltwater channels and other forms related to glacial processes in and around the Mifeldi pluton, show that relatively large glacier outlets left the domain separating the (future) mesetas from the Cordillera at around 3 Ma.

We have shown that first events leading to the local disruption of the western side of the Meseta Lago Buenos Aires occurred in the Alto Rio Ghio region, in relation with displacements along faults oriented N30-N40. This led Lagabrielle et al. (2007) to propose a strong tectonic control of the paleo-valley. Faulting initiated during the deposition of the first tills and lavas, that is probably as early as 7-6 Ma. This N30-N40 faulting direction corresponds to a major orientation of morphotectonic features in Central Patagonia such as the normal fault scarp bounding the Lago Lapparent depression to the north and the tectonic-controlled edges of the central part of Lago General Carrera and the western part of Lago Cochrane-Pueyrredon (Scalabrino et al., submitted). Further north, in the area of Coihaique-Balmaceda, NE faults are a major tectonic element, controlling local lake and river depressions (lagos Pollux and Cástor and ríos Coihaique and Pollux) (De La Cruz et al., 2003). This direction also corresponds to the elongation of the glacier outlets described from the upper surface of the Meseta del Lago Buenos Aires. We may therefore suspect that N30-N40 oriented faults are important elements of the tectonic evolution of the frontal region of the Cordillera between 7 Ma and 3 Ma. They have been active before the initiation of movements along the N160 trending faults which led to relative uplift of the western scarp of the meseta after 3 Ma. These tectonic events have been related to a thermal disturbance of the lithospheric mantle above Central Patagonia which coincides in time and space with the subduction of segments of the South Chile Ridge explaining the vertical differential displacements observed between 7 and 3 Ma (Lagabrielle et al., 2007; Scalabrino et al., submitted).

(c) Tectonic vs. climatic significance of a major morphological change at 3 Ma ?

The landform record provides evidence of glacier advance in the SW-NE direction at 3 Ma, over a surface which is a paleo-piedmont of a former Cordillera. On a relatively short distance of 20 km, we observe more than 4 outlets, not deeply incised, indicating that the pre-3 Ma glaciers were not constrained within narrow valleys. Nevertheless, it is possible that this region of the meseta, despite its present-day elevation, represents a former depressed area, functioning as a collector for the glacier outlets. In any case, before the 3 Ma tectonic crisis, the overall paleotopography of Central Patagonia was smoother than at present, as shown by the envelop of the Avellanos surface formely connected to the meseta surface. Starting at 3 Ma a dramatic change occurred in the entire region of Central Patagonia, corresponding to the

relative uplift of the piedmont domain and to its disconnection from the rest of the Cordillera. This event was accompanied by local collapse of internal basins such as the Lago Lapparent depression and by the rapid subsidence of
the narrow transverse corridors now occupied by Lakes Cochrane-Puyerredon and General Carrera-Buenos Aires (Scalabrino et al., submitted). From this date, glaciers did not expand freely over the piedmont domain but were constrained within narrow valleys. This major change in glacier distribution is mainly due to tectonic causes and triggered in turn major changes in the overall morphology of the Cordillera (figs 9 and 10). However we can not exclude that part of this change has been enhanced due to climatic causes such as increases in the frequency of glacial conditions during the Plio-Quaternary.

Conclusions

We have evidenced, following Mercer and Sutter (1982), the presence of relict glacial landforms, 3 Ma old and older, preserved on the top surface of the Mesetas del Lago Buenos Aires and del Guenguel. New evidence of ancient glaciations will be probably found from explorations of unknown localities in Patagonia. The paleoclimatic impact of these expected findings will be important as late Miocene glacier advances require cold and/or humid conditions which have to be integrated within climatic models of the Neogene. However, at present, the main issue is to decipher the regional significance of these glaciations. There are 2 main possibilities: these are isolated glaciers of mountainous areas such as those already known through the Miocene in Alaska, Greenland and Iceland. These are not necessarily representative of a major continental glaciation (Ehlers and Gibbard, 2007). The second possibility is that these deposits are the testimonies of a former unsuspected large Patagonian Ice Sheet, permanent or partly ephemeral, developed between 7 and 3 Ma and possibly some Ma before, in a period when large ice sheets also developed over Antarctica. Indeed, the ice sheet in Eastern Antarctica reached a maximum size about 15 million years ago (mid-Miocene) and the West Antarctic ice sheet may have developed for the first time also in this period (e.g. Hambrey and McKelvey, 2000).

(a) The first hypothesis implies increased precipitation on relatively high reliefs able to produce abundant ice. In such a case, the mountains had to be much higher at this latitude. However, at the latitude of LGCBA, except in some points such as the Mount San Valentin, there is currently no high relief, rather the Cordillera displays an average low elevation of +

900 m only (Scalabrino et al., submitted). If so, reliefs have either experienced considerable erosion after 3 Ma, or have partly disappeared due to overall collapse of the entire Cordillera. Evidence for local collapse inside the Cordillera as well as normal faulting along the western edges of the mesetas relies on such scenario (Scalabrino et al., submitted).

(b) The second hypothesis implies the temporary development of a large ice cap over the Cordillera before the Quaternary. The 7-3 Ma tills are known from various places and from various mesetas. This suggests a widespread rather than a localized distribution. If these old glaciers are found to be frequently distributed all along Patagonia with the same concentration as deduced from this study, it will be necessary to estimate the total volume of ice stored over the entire Cordillera during the Neogene. This would have an impact on the global water balance and on our understanding of the global climate evolution during the Late Cenozoic. It is clear that a lot of work needs to be done in this direction, based on increased accurate analysis of field data. In that sense, the issues on global climate raised by Mercer and Sutter (1982) following their major discovery on the NW edge of the Meseta del Lago Buenos Aires still remain to be fully addressed, including possible development of early ice sheets in the Northern Hemisphere.

Acknowledgments.

This work was partly funded by grants from the ECOS-sud program and by the Dyeti and Relief programs of the CNRS-INSU, France.

REFERENCES

Bell C. M, and Suárez M. 2000, The Río Lácteo Formation of Southern Chile. Late Paleozoic orogeny in the Andes of southernmost South America, *Journal of South American Earth Sciences Volume 13, Issues 1-2, 1 May 2000, Pages 133-145.*

Boutonnet, E., Arnaud, N., Guivel., C., Lagabrielle, Y., Scalabrino, B., Rossello, E., and ECOS Team. Volcanic and structural effects of a spreading ridge subduction: geochemical and chronological evolution of the Western Meseta del Lago Buenos Aires (MLBA), Patagonia, Chile. Submitted .

Brown, L.L., Singer, B.S. and Gorring, M.L., 2004. Paleomagnetism and $^{40}Ar/^{39}Ar$ chronology of lavas from Meseta del Lago Buenos Aires, Patagonia. *Geochem. Geophys. Geosyst.* 5 (1), Q01H04. doi: 10.1029/2003GC000526.

Caldenius, C. G., 1932, Las glaciaciones Cuaternarias en la Patagonia and Tierra del Fuego: Geografiska Annaler, v. 14, p. 1-164.

Cande, S.C. and Leslie, R.B., 1986. Late Cenozoic tectonics of the southern Chile trench. *J. Geophys. Res.*, 91, 471-496.

Charrier, R., Linares, E., Niemeyer, H. and Skarmeta, J., 1979. K-Ar ages of basalt flows of the Meseta Buenos Aires in southern Chile and their relation to the southeast Pacific triple junction. Geology 7, 436-439.

Clapperton, C.M., 1993, Quaternary Geology and Geomorphology of South America. Elsevier, 779 p.

De La Cruz, R. and Suárez, M., 2006. Geología del área Puerto Guadal-Puerto Sánchez, Región Aisén del General Carlos Ibáñez del Campo, Escala 1:100.000. *Servicio Nacional de Geología y Minería, Serie Geología Básica, Carta Geológica de Chile,* Nº 95. Santiago, Chile.

De La Cruz, R., and Suárez, M. in press. Geología del área Chile Chico-Río de las Nieves, Región Aisén del general Carlos Ibáñez del Campo. Escala 1:100.000. *Servicio Nacional de Geología y Minería, Serie Geología Básica, Carta Geológica de Chile,* Nº 112. Santiago, Chile.

De La Cruz, R., Suárez, M., Morata, D., Espinoza, F. and Troncoso, A., 2003. El Cenozoico del Lago General Carrera, Aysén, Chile (46º30'-47º15'S): estratigrafía y tectónica. *In Congreso Geológico Chileno No. 10,* Concepción.

De La Cruz, R., Welkner, D., Suárez, M. and Quiroz, D., 2004. Geología del área oriental de las hojas Cochrane y Villa O'Higgins, Región Aisén del General Carlos Ibáñez del Campo, escala 1:250.000. *Servicio Nacional de Geología y Minería, Serie Geología Básica, Carta Geológica*

Ehlers, J. & Gibbard, P.L. 2007 The extent and chronology of Cenozoic global glaciation. *Quaternary International* 164-165, 6-20.

Espinoza, F., 2003. Petrologia y geoquimica de los basaltos cenozoicos de la meseta de Chile Chico, 46°35'S- 46°47'S- 71°46'-72°02'W XI region de Aysen, Chile. *Unpublished MSc thesis, Universidad de Chile, Santiago, Chile. 220 pp.*

Espinoza, F., Morata, D., Pelleter, E., Maury, R.C., Suárez, M., Lagabrielle, Y., Polvé, M., Bellon, H., Cotten, J., De la Cruz, R. and Guivel, C., 2005. Petrogenesis of the Eocene and Mio-Pliocene alkaline basaltic magmatism in Meseta Chile Chico, Southern Patagonia, Chile: evidence for the participation of two slab windows. *Lithos,* 82, 315-343.

Espinoza, F., Morata, D., Polvé, M., Lagabrielle, Y., Maury, R. C., Guivel, C., Cotten, J., Bellon, H., Suárez, M. 2008. Bimodal back-arc alkaline magmatism after ridge subduction: Pliocene felsic rocks from Central Patagonia (47ºS). *Lithos*, vol. 101 (1-2), pp. 191-217.

Flint, S.S., Prior, D. J., Agar, S.M. and Turner, P., 1994. Stratigraphic and structural evolution of the Tertiary Cosmelli Basin and its relationship to the Chile triple junction. *J. Geol. Soc. London*, 151, 251-268.

Flynn, J. J, Novacek, M., Dodson, H., Frassinetti, D., McKenna, M., Norell, M., Sears, K., Swisher III, C. and Wyss, A., 2002. A new fossil mammal assemblage from the southern Chilean Andes: implications for geology, geochronology, and tectonics. *J. South Amer. Earth Sc.*, 15, 285-302.

Giacosa R and Franchi M, 2001, Hojas Geológicas 4772-III y 4772-IV Lago Belgrano y Lago Posadas, Provincia de Santa Cruz, *Programa Nacional de Cartas Geológicas de la República Argentina, Boletin N°256, 2001.*

Glasser, N.F., Harrison, S., Winchester, V., and Aniya, M., 2004, Late Pleistocene and Holocene paleoclimate and glacier fluctuations in Patagonia: Global and Planetary Change, v. 43, p. 79-101.

Glasser, N.F., Jansson, K.N., Harrison S., and Kleman, J. 2008. The glacial geomorphology and Pleistocene history of South America between 38°S and 56°S Quaternary Science

Reviews Volume 27, 3-4, 365-390

Gorring M., Kay S., 2001. Mantle processes and sources of Neogene slab window magmas from Southern Patagonia, Argentina, *Journal of petrology, vol. 42, n°6, pp. 1067- 1094.*

Gorring, M., Kay, S., Zeitler, P., Ramos, V., Rubiolo, D., Fernández, M. and Panza, J., 1997. Neogene Patagonian plateau lavas: Continental magmas associated with ridge collision at the Chile Triple Junction. *Tectonics*, 16, 1-17.

Gorring, M., Singer, B., Gowers, J. and Kay, S., 2003. Plio-Pleistocene basalts from the Meseta del Lago Buenos Aires, Argentina: evidence for asthenosphere–lithosphere interactions during slab window magmatism. *Chem. Geol.* 193, 215– 235.

Guivel, Ch., Morata, D., Pelleter, E., Espinoza, F., Maury, R.C., Lagabrielle, Y., Polvé, M., Bellón, H., Cotten, J., Benoit, M., Suárez, M. and De La Cruz, R., 2006. Miocene to Late Quaternary Patagonian basalts (46°S-47°S): Geochronometric and geochemical evidence for slab tearing due to active ridge subduction. *J. Volcan. Geother. Res.,* 149, 346-370.

Kaplan, M.R, Ackert, R.P., Singer, B.S., Douglass, D.C., and Kurz, M.D., 2004, Cosmogenic nuclide chronology of millennial-scale glacial advances during O-isotope stage 2 in Patagonia: Geological Society of America Bulletin, v. 116, p. 308-321.

Kaplan, M.R, Douglass, D.C., Singer, B.S., Ackert, R.P., and Caffee, M.W., 2005, Cosmogenic nuclide chronology of pre-last glaciation maximum moraines at Lago Buenos Aires, 46°S, Argentina: Quaternary Research (in press).

Kay S. M., V.A. Ramos, and M. Marques, 1993, Evidence in Cerro Pampa volcanic rocks for slab-melting prior to ridge-trench collision in southern South America, *Journal of Geology, v. 101, 703-714*.

Lagabrielle Y, Suárez M, Malavieille J, Morata D, Espinoza F, Maury RC, Scalabrino B, Barbero L, De la Cruz R, Rossello E, Bellon H, 2007, Pliocene extensional tectonics in the Eastern Central Patagonian Cordillera: geochronological constraints and new field evidence, *Terra Nova 19 (6), 413–424*.

Lagabrielle Y., Guivel C., Maury R., Bourgois J., Fourcade S., and Martin H., 2000, Magmatic-tectonic effects of high thermal regime at the site of active spreading ridge subduction : the Chile Triple Junction model. *Tectonophysics, n° 326, 3-4, pp. 215-228.*

Lagabrielle, Y., Bellon, H., Espinoza, F., Guivel, Ch., Malavielle, J., Maury, R.C., Morata, D., Polvé, M., Rossello, E. and Suárez, M., 2006. Post-Pliocene deformation and uplift of the Patagonian Andes in response to the subduction of the Active Chile Spreading Ridge Center (CSR). *The Geological Society of America, Backbone of the Americas: Patagonia to Alaska,* Paper No. 4-2: 47. Mendoza, Argentina.

Lagabrielle, Y., Suárez, M., Rossello, E., Hérail, G., Martinod, J., Régnier, M. and De La Cruz, R., 2004. Neogene to Quaternary tectonic evolution of the Patagonian Andes at the latitude of the Chile Triple Junction. *Tectonophysics,* 385, 211-241.

Mercer, J. H. and Sutter, J.F., 1982. Late Miocene-Earliest Pliocene glaciation in Southern Argentina: implications for global ice-sheet history. *Palaeog., Palaeoc., Palae.,* 38, 185-206.

Mercer, J.H., 1983. Cenozoic glaciation in the southern hemisphere. Annual Reviews of Earth and Planetary Science 11, 99–132.,

Hambrey, M.J., and McKelvey, B. Major Neogene fluctuations of the East Antarctic ice sheet: Stratigraphic evidence from the Lambert Glacier region. *Geology*; October 2000; v. 28; no. 10; p. 887-890; DOI: 10.1130/0091-7613(2000)28<887:MNFOTE>2.0.CO;2

Morata, D., Barbero, L., Suárez, M. and De La Cruz, R., 2002. Early Pliocene magmatism and high exhumation rates in the Patagonian Cordillera (46º40'S): K-Ar and fission track data. *In International Symposium on Andean Geodynamics No. 5 (ISAG 2002)*: 433-436. Toulouse, Francia..

Rabassa, J. and Clapperton, C.M., 1990. Quaternary glaciations in the southern Andes. *Quater. Sc. Rev.*, 9, 153-174.

Rabassa, J. and Clapperton, C.M., 1990. Quaternary glaciations in the southern Andes. *Quater. Sc. Rev.*, 9, 153-174.

Rabassa, J., 2008. Late Cenozoic glaciations in Patagonia and Tierra del Fuego. In : The Late Cenozoic of Patagonia and Tierra del Fuego, J. Rabassa, Ed., Developments in Quaternary Science 11, Elsevier, 151-204.

Rabassa, J., Coronato, A/M. and Salemme, M., 2005. Chronology of the Late Cenozoic Patagonian glaciations and their correlation with biostratigraphic units of the Pampean region (Argentina). Journal South Am. Res., 20, 81-103. doi:10.1016/j.jsames.2005.07.004

Ramos, V.A. and Kay., 1992. Southern Patagonian plateau basalts and deformation : backarc testimony of ridge collision. *In : R.A. Olivier, N. Vatin-Pérignon and G. Laubacher (Editors), Andean Geodynamics. Tectonophysics, 205 : 261-282.*

Ramos, V.A., 1989. Andean foothills structures in northern Magallanes Basin, Argentina. American Association of Petroleum Geologist Bulletin 73, 887-903.

Ray, F., 1996. Stratigraphical and structural evolution of Tertiary backarc basins in southern Chile (44° to 47°S). Ph.D. Thesis. (Unpublished), *University of Liverpool:* 208 p. U.K.

Scalabrino B, Lagabrielle Y., De la Rupelle A., Malavieille J., Polvé M., Espinoza F, Morata D., Suarez M., 2009. Subduction of an active spreading ridge beneath Southern South America: A review of the Cenozoic geological records from the Andean foreland, Central Patagonia (46-47°S). *International Journal of Earth Sciences.*

Scalabrino B, Lagabrielle Y., De la Rupelle A., Malavieille J., Polvé M., Espinoza F, Morata D., Suarez M., 2008. Subduction of an active spreading ridge beneath Southern South America: A review of the Cenozoic geological records from the Andean foreland, Central Patagonia (46-47°S). *International Journal of Earth Sciences, in press.*

Scalabrino, B., Lagabrielle, Y., Malavieille, J., Dominguez, S., Melnick., D., Espinoza, F., Suarez, M., Rossello., E. A morphotectonic analysis of Central Patagonian Cordillera. Negative inversion of the Andean belt over a buried spreading center? Submitted to Tectonics.

Scalabrino, B., Lagabrielle, Y., Suarez, M. Mio-Pliocene evolution of the Coihaique basin : New evidence of tectonic rejuvenation of the Central Patagonia Cordillera front. In prep (submitted to Andean Geology)

Schlieder, G., Evenson, E.B., Zeitler, P.K., Stephens, G.C., and Rabassa, J.O., 1988, K/Ar ages and evidence for at least four Plio/Pleistocene glaciations in the northern Patagonian Andes, between Lat. 39 S. and 41 S. (abs.): GSA Annual Meetings with Programs, v. 20, p. A208.

Singer, B.S., Ackert, R.P. Jr., and Guillou, H., 2004, $^{40}Ar/^{39}Ar$ and K-Ar chronology of Pleistocene glaciations in Patagonia: Geological Society of America Bulletin, v. 116, p. 434-450.

Suárez and Emparán, C. 1997. Hoja Curacautín, Regiones de la Araucanía y del Biobio Servicio Nacional de Geología y Minería. Carta Geológica de Chile Nº71, escala 1:250.000, 105 pp.

Suárez, M. and De la Cruz, R. 2000. Tectonics in the eastern-central Patagonian Cordillera (45°30'-47°30' S). *J. Geol.. Soc. London*, 157, 995-1001.

Suárez, M. and De La Cruz, R., 2001. Jurassic to Miocene K-Ar dates from eastern central Patagonian Cordillera plutons, Chile (45º-48ºS) *Geol. Mag.,* 138, 53-66.

Suárez, M., De La Cruz, R. and Bell, M., 1996. Estratigrafía de la región de Coyhaique (latitud 45º-46ºS); Cordillera Patagónica, Chile. *In Congreso Geológico Argentino No. 13 y Congreso de Exploración de Hidrocarburos No. 3*, 1, 575-590.

Suárez, M., De La Cruz, R. and Bell, M.. 2000. Timing and origin of deformation along the Patagonian fold and thrust belt. *Geol. Mag.,* 137, 345-353.

Suarez et al., 2007. To be completed.

Thomson, S.N., Hervé, F., Brix, M. and Stockhert, B., 2001. The Mesozoic-Cenozoic denudation history of the southern Chilean Andes and its correlation to different subduction processes. *Tectonics,* 20, 693-711.

Thorkelson D. J., 1996, Subduction of diverging plates and the principles of slab window formation, *Tectonophysics 255 (1996) 47-63.*

Ton-That, R., Singer, B., Mörner, N.A. and Rabassa, J., 1999. Datación de lavas basálticas por $^{40}Ar/^{39}Ar$ y geología glacial de la región del lago Buenos Aires, Provincia de Santa Cruz, Argentina. *Asoc. Geol.. Argentina, Revista*, 54, 333-352.

Wenzens, G., 2006. Terminal Moraines, Outwash Plains, and Lake Terraces in the Vicinity of Lago Cardiel (49°S; Patagonia, Argentina)—Evidence for Miocene Andean Foreland Glaciations. *Arctic, Antarctic, and Alpine Research*, pp. 276–291 DOI: 10.1657/1523-0430(2006)38[276:TMOPAL]2.0.CO;2

Figure, plate, table captions

Figure. 1. Simplified map of Central Patagonia showing the types localities discussed in text including : the pampa region, the mesetas, and the relict of flat surfaces inside the Cordillera. The contour of the Patagonian slab-window with respect to the location of the active spreading Chile Ridge (SCR) is shown in upper cartoon (CTJ : Chile triple junction).

Figure 2. A 3D view of the Meseta del Lago Buenos Aires (MLBA) and its surroundings based on a SRTM DEM (location in fig. 1). Numbers indicate the main sites where lava flows have been dated since the first work of Mercer and Sutter in 1982, as reported in table 1.

Figure 3. Location of cited tills and fluvio-glacial gravels of Mio-Pliocene age (stars) in Meseta Lago Buenos Aires. Map view and topographic cross-sections. RZFZ : Rio Zeballos Fault Zone.

Figure 4. Photograph of the scarp of the western side of alto Rio Ghio along Ruta 41, exposing a paleo-valley infilled with glacial sediments and lava flows. Numbers correspond to the ages of dated samples of lavas and dikes. Insert shows an idealized E-W section across this outcrop.

Figure 5. Idealized cross-section of the western border of Meseta del Lago Buenos Aires showing the location of faults, tills and lava flows. Vertical exaggeration has been applied partially, in order to enhance the occurrence of till layers.

Figure 6. Topography and satellite image of the Meseta del Lago Buenos Aires showing the main glacial features, 3 Ma old at least, observed at a regional scale.

Figure 7. A : 3D oblique view of the western border of the Meseta del Lago Buenos Aires with some details of glacial features (B and C). D : Remnant of glacial morphology of the southwestern edge of the Meseta del Guenguel.

Figyre 8. Geomorphological map of the western border of the Meseta del Lago Buenos Aires with some details of observed glacial features.

Figure 9. Cartoons depicting the tectonic evolution of the Cordillera piedmont since 14 Ma

Figure. 10. 3D diagrams showing the evolution of the distribution of glaciers in Central Patagonia with emphazis on the consequences of the 3 Ma tectonic event.

Plate 1. Photographs of tills and related glacial features representing evidence of glaciations which developed between 7 and 3 Ma in the western region of Meseta del Lago Buenos Aires. (All photographs by YL, except A by D. Morata).

A : Gradded-bedded fluvio-glacial gravels and tills (upper part of photograph). Northwestern part of meseta Lago Buenos Aires in area of sites 28-30 (fig. 2). These deposits underlie lavas dated around 6.5 – 5 Ma (table 1). Note the presence of white-colored clasts demonstrating alimentation from regions farther west, exposing rocks of the batholith and Ibanez formation.

B : Reddish, « cooked » till due to emplacement of the overlying lava flow in the northern portion of the scarp shown in fig. 4 (paleovalley site of Alto Rio Ghio). This lava flow correlates with a light-grey flow dated at 5 Ma. Thermal interaction between glacial sediments and lavas is currently observed in the area of study (see upper part of photograph D and lower part of photograph E, as well as Lagabrielle et al., 2007). Note the presence of white-colored clasts within the till demonstrating alimentation from regions farther west, exposing the batholith.

C : A contact between a brecciated brown-colored lava flow (between 5 and 3 Ma old) and a till including white-colored clasts deriving from the batholith (Alto Rio Ghio, along Ruta 41, north of the paleovalley site).

D : Gradded-bedded fluvio-glacial gravels and tills in fault contact against molasse deposits (paleovalley site of Alto Rio Ghio, location of photograph in fig. 4).

E : Lava flow in contact with thick till including white-colored clasts deriving from the batholith. Contorted contact indicates interaction during the progression of lava flow on a former glacial landcape.

Table 1. A compilation of ages and location of dated lava flows and dikes from Meseta del Lago Buenos Aires allowing dating of glacial deposits.

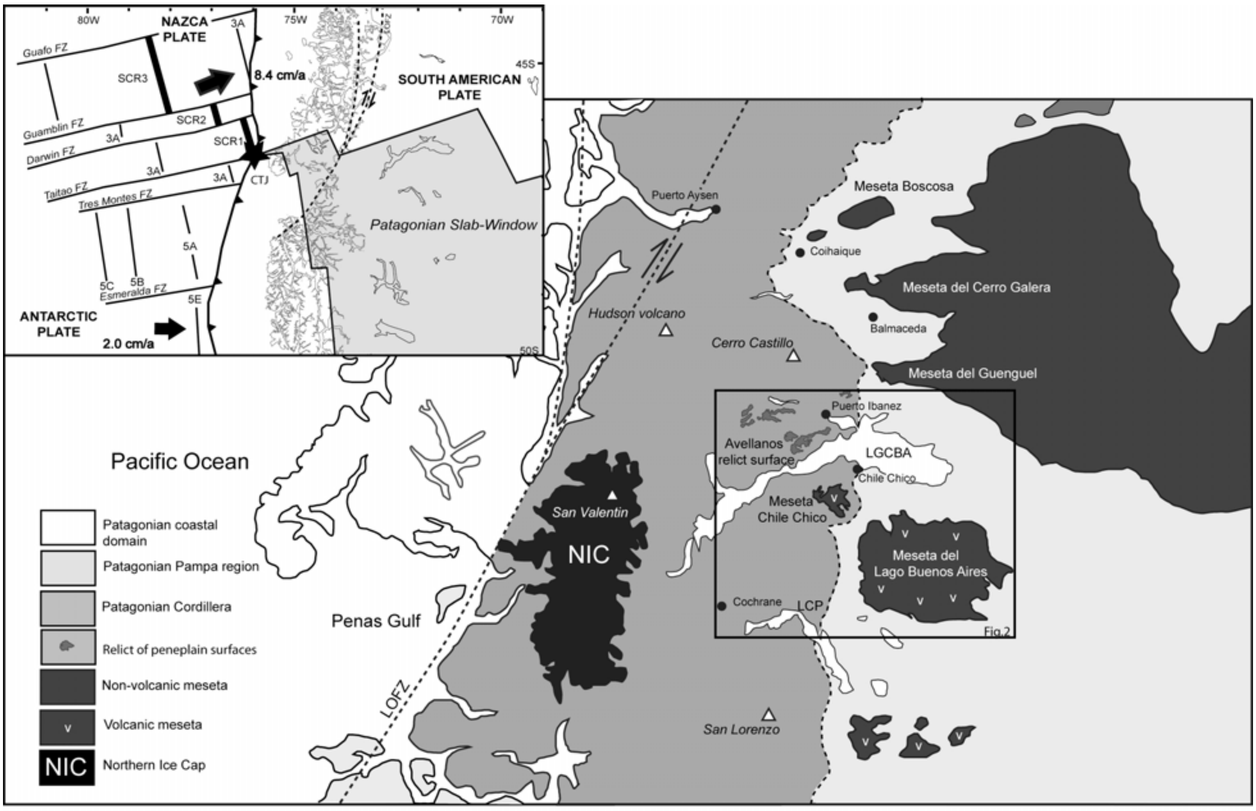

Lagabrielle et al. fig. 1

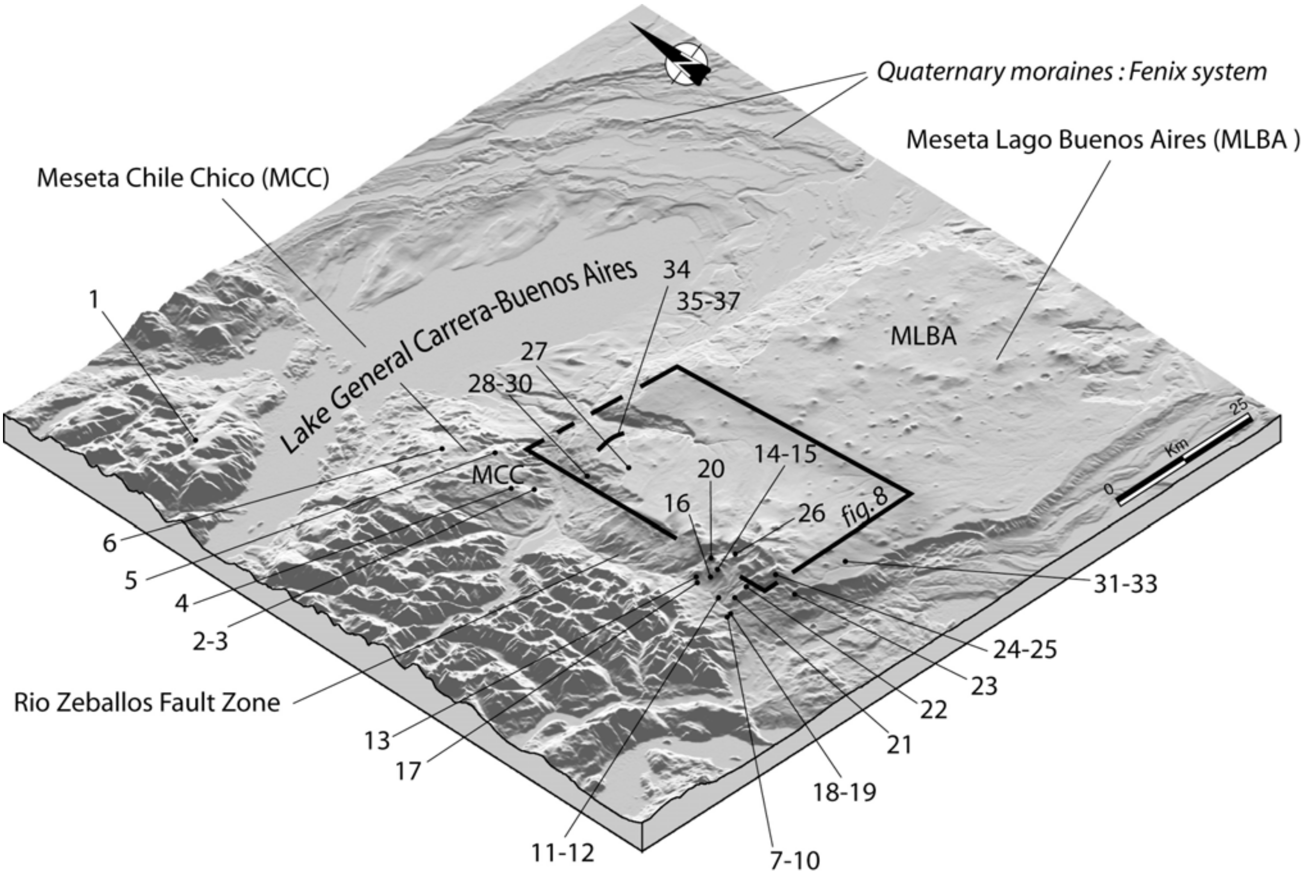

Lagabrielle et al. fig.2

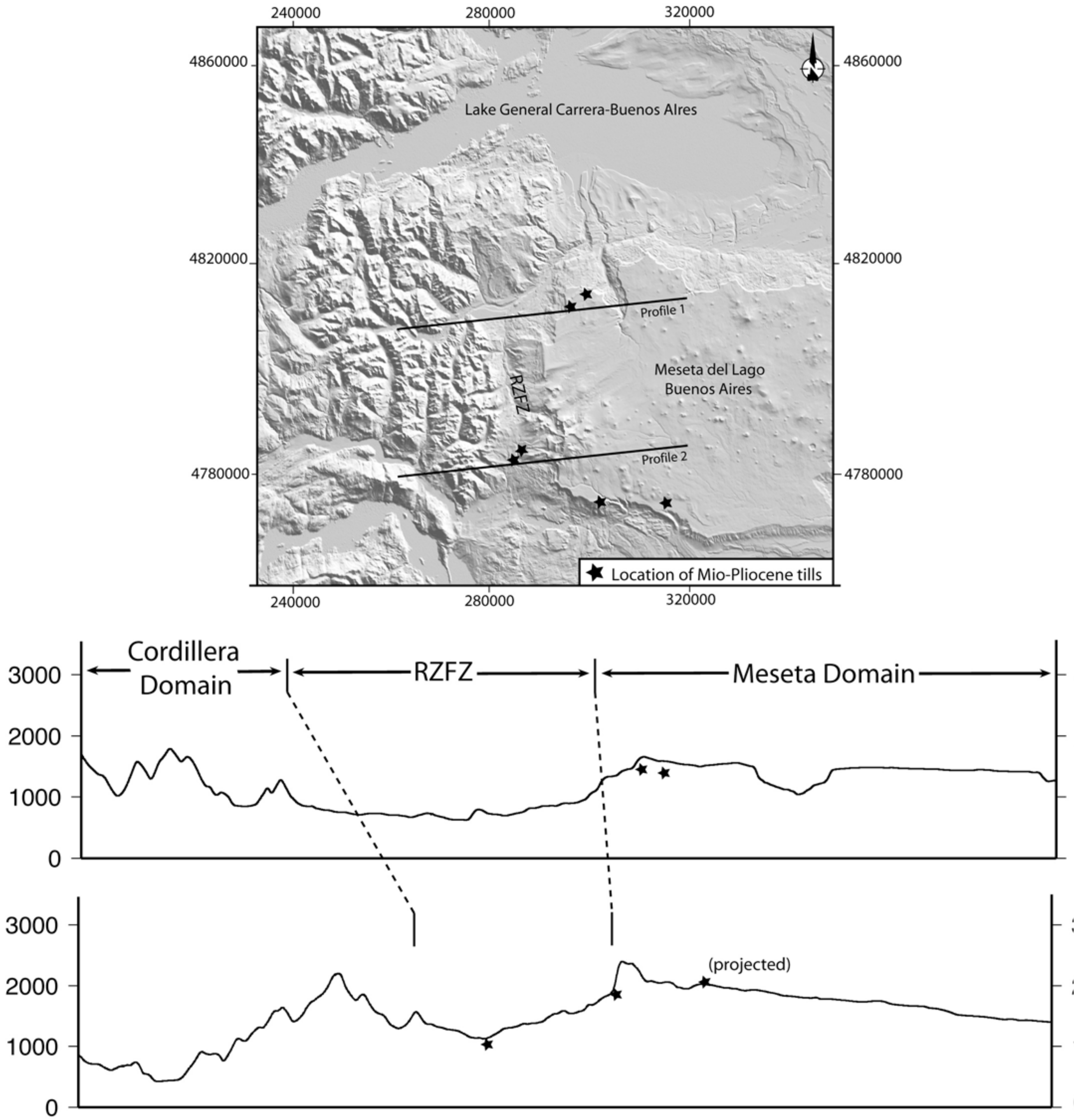

Lagabrielle et al. fig. 3

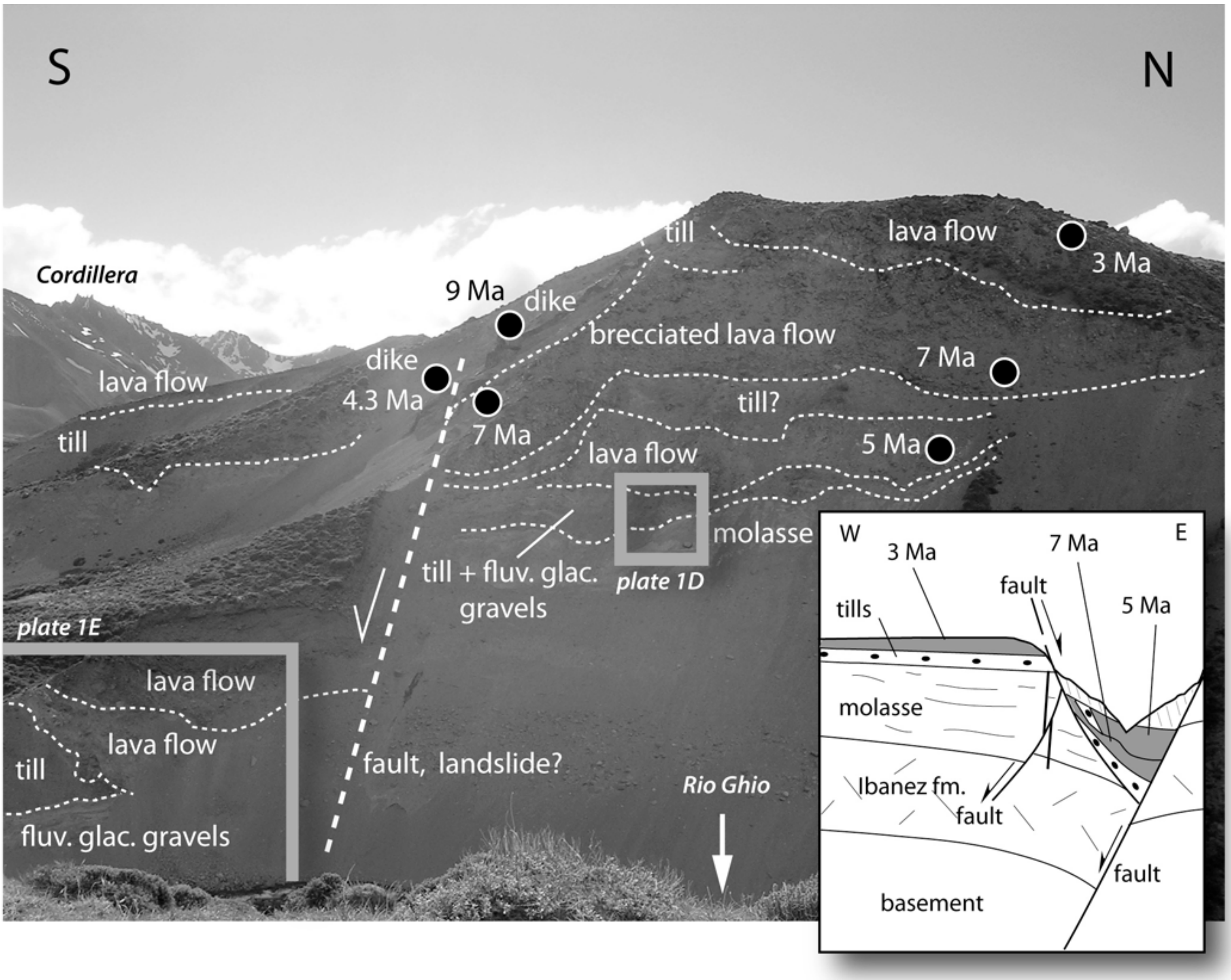

Lagabrielle et al., fig. 4

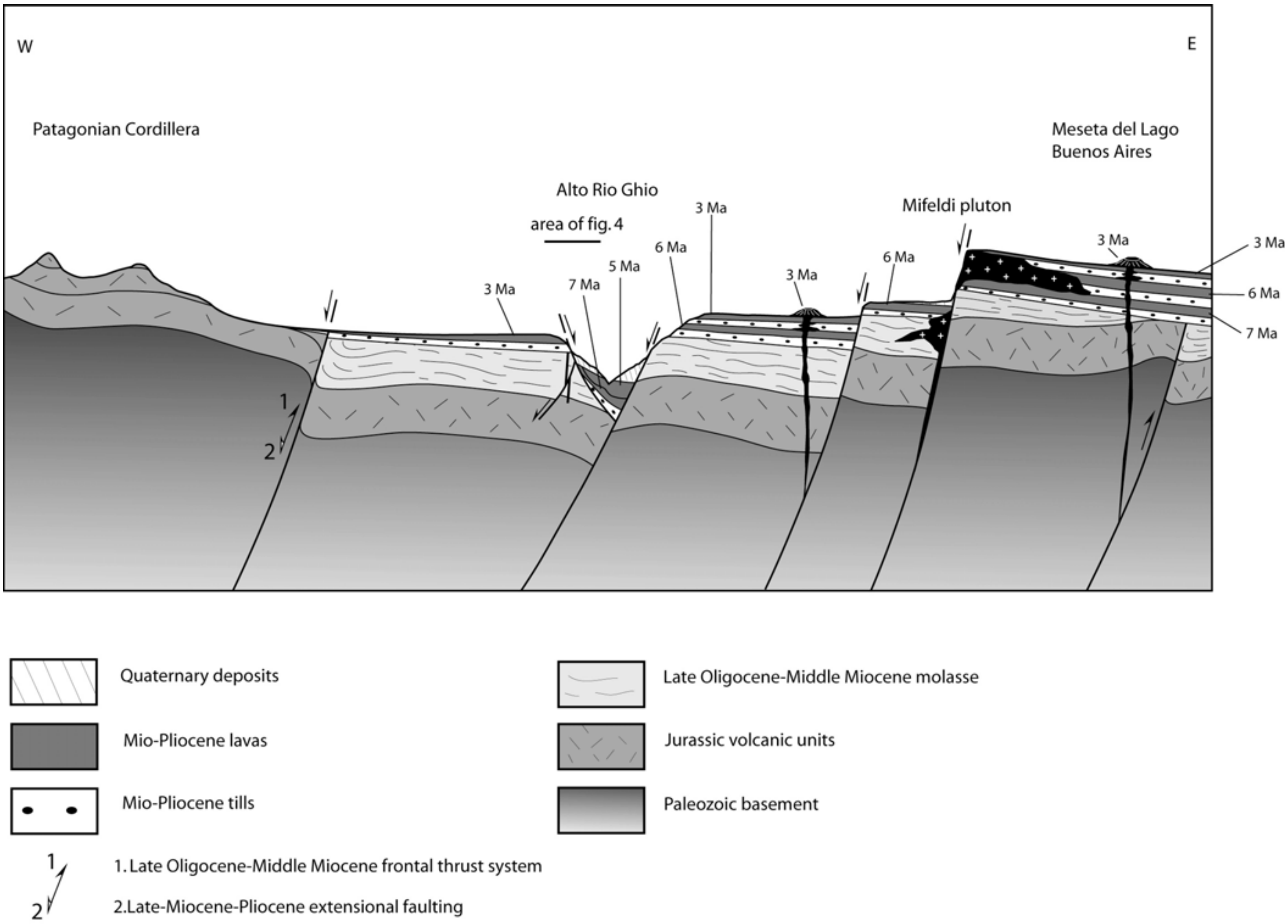

Lagabrielle et al., figure 5

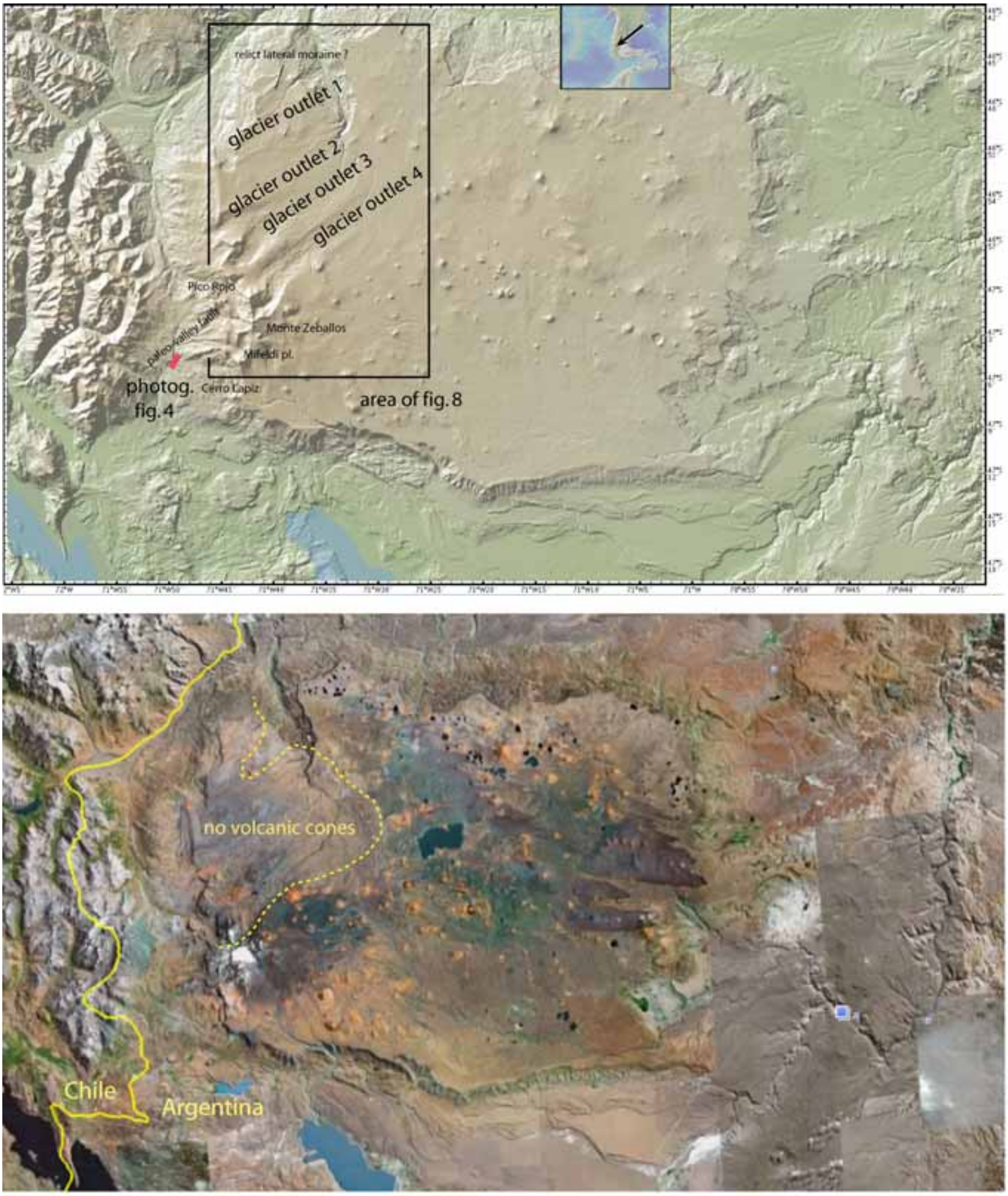

Lagabrielle et al., Figure 6

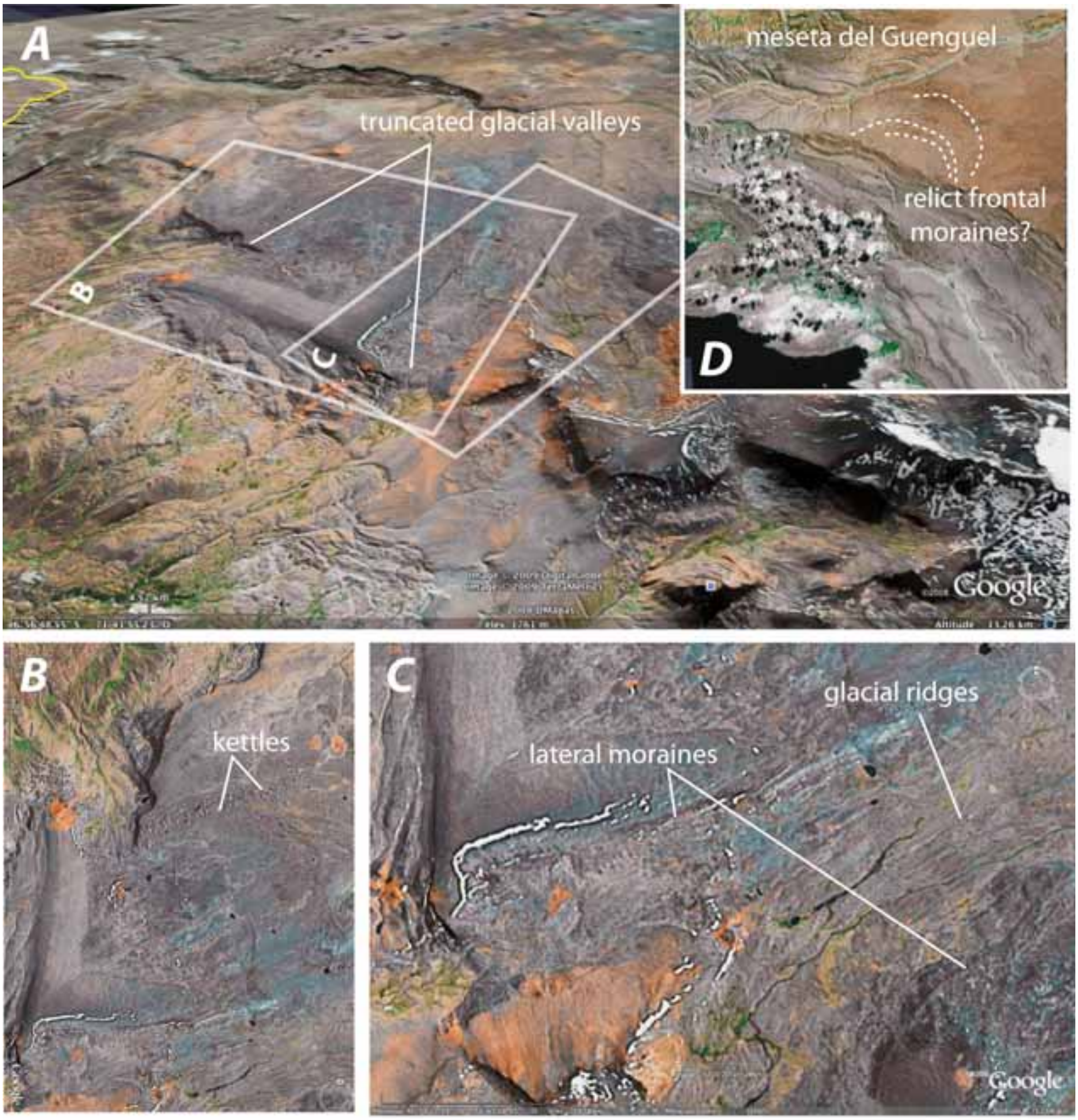

Lagabrielle et al., Fig. 7

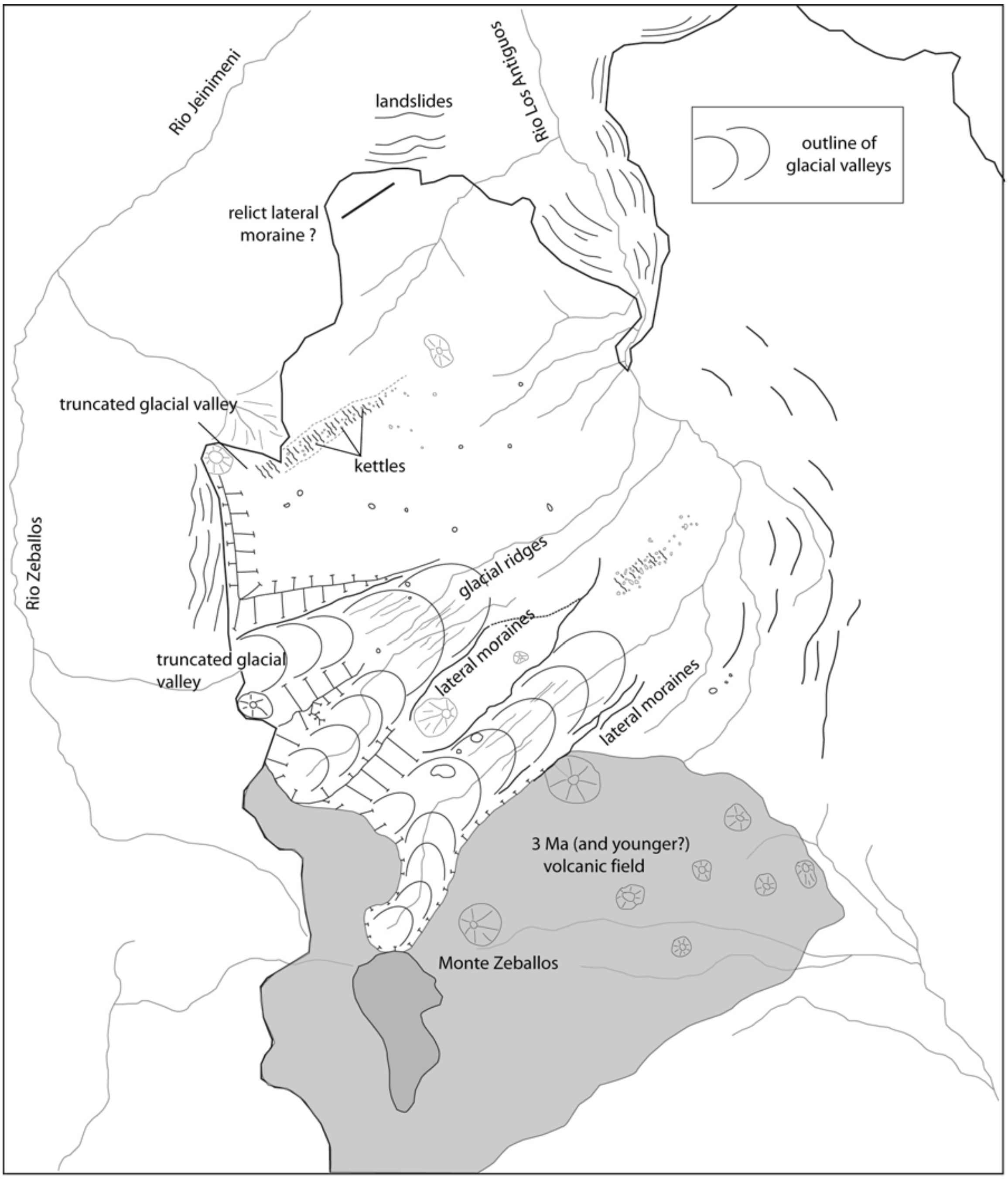

Lagabrielle et al., fig. 8

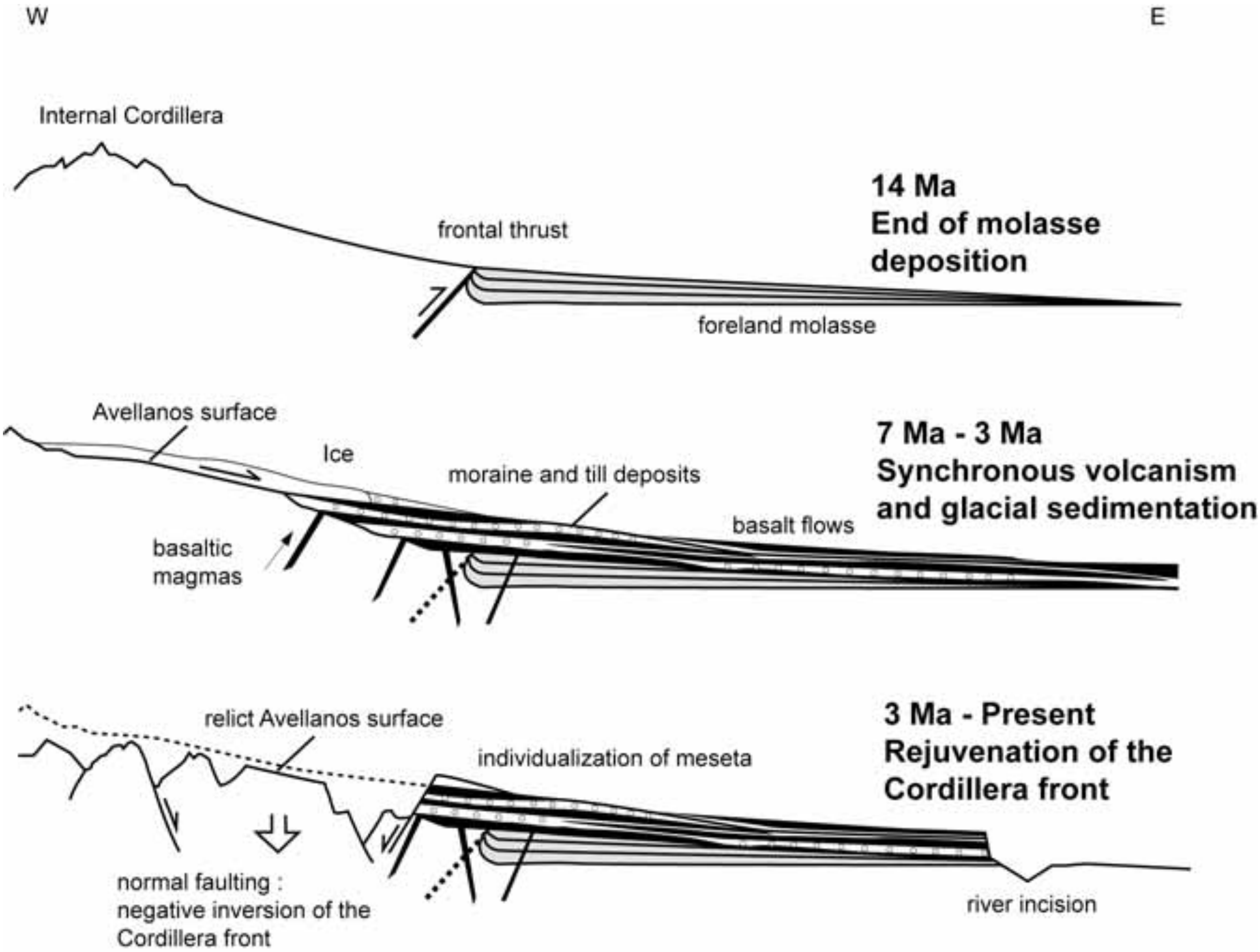

Lagabrielle et al., fig. 9

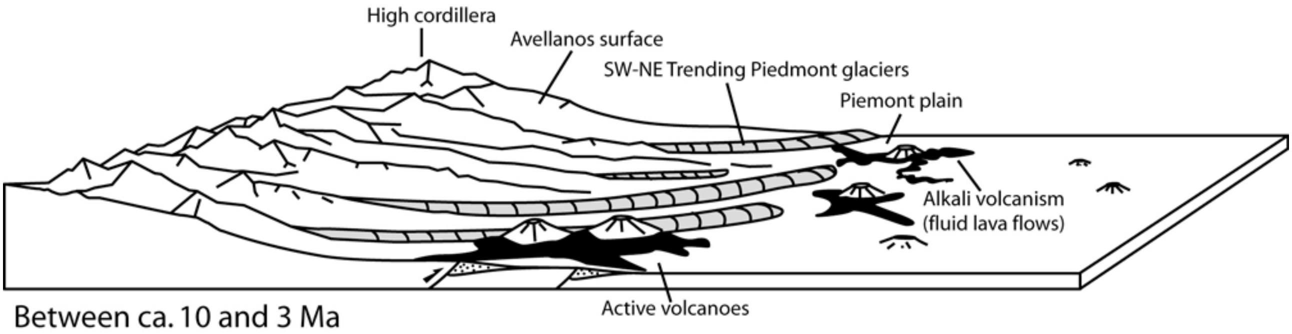

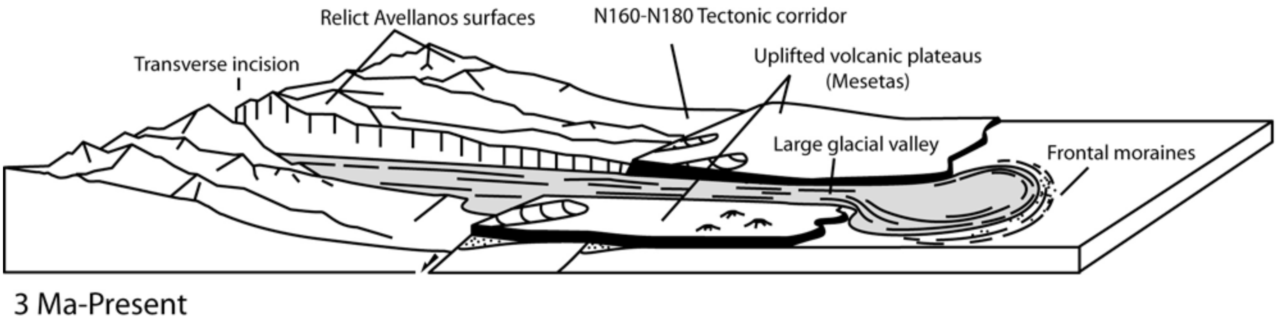

Lagabrielle et al., fig. 10

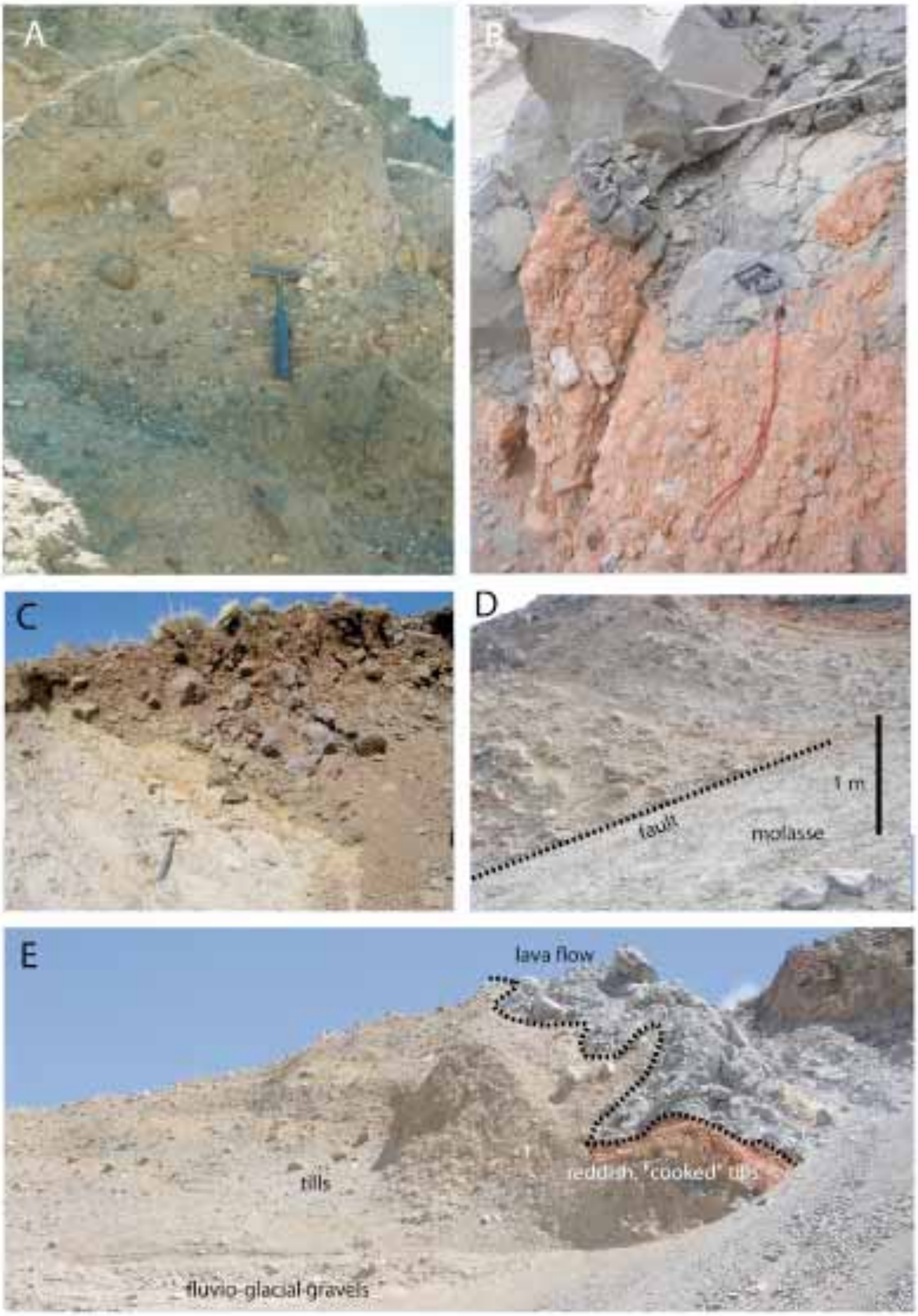

Lagabrielle et al., plate 1

Label in Fig.2	Article Reference	Location	Sample No.	Location (UTM 19)	Dated Materiel	Age (Ma)	± error (2σ)
1	a	Avellanos surface	Q387	4854211/257617	WR	4.57	0.27
2	b	MCC	PG36-38	4836043/284123	WR	4.63	0.13
3	b	MCC	PG138	4836043/284123	WR	4.46	0.22
4	b	MCC	FE01-11	4819707/283249	WR	4.50	0.30
5	b	MCC	FE01-16	4827408/285508	WR	4.60	0.20
6	b	MCC	FE01-36	4831666/280272	WR	4.40	0.80
7	c	Alto Rio Ghio	PG65	4783664/288643	WR	4.98	0.15
8	c	Alto Rio Ghio	PG67	4783664/288643	WR	6.95	0.24
9	c	Alto Rio Ghio	PG69	4783664/288643	WR	4.32	0.23
10	c	Alto Rio Ghio	PG70	4783664/288643	WR	2.96	0.09
11	c	Alto Rio Ghio	PG72	4783664/288643	WR	3.91	0.11
12	c	Alto Rio Ghio	PG75	4785410/286064	WR	4.81	0.32
13	d	South C. Zeballos	PA06-03	4790021/286906	Bt	2.91	0.10
14	d	W-MLBA	PA06-17	4788816/289717	Bt	4.48	0.14
15	d	W-MLBA	PA06-18	4788728/289375	Bt	3.23	0.08
16	d	W-MLBA	PA06-19	4789134/288263	Bt	6.85	0.15
17	d	Alto Rio Ghio	PA06-20a	4789134/288263	Bt	2.12	0.45
18	d	Alto Rio Ghio	PA06-22	4782182/285551	Bt	6.22	0.74
19	d	Alto Rio Ghio	PA06-23	4782182/285551	Bt	9.42	1.42
20	d	W-MLBA	PA06-12	4790274/289079	Bt	2.76	0.07
21	d	SW-MLBA	TM-01	4783140/288460	Bt	4.17	0.16
22	d	SW-MLBA	TM-02	4783332/289383	Bt	6.41	0.22
23	e	SW-MLBA	PAT-12	4778705/292340	WR	3.65	0.10
24	e	SW-MLBA	PAT-20	4780366/292728	WR	3.08	0.13
25	e	SW-MLBA	PAT-22	4781845/293488	WR	3.28	0.10
26	e	SW-MLBA	PAT-26	4789707/290427	WR	4.52	0.16
27	c	NE-MLBA	PG113	4815765/293768	WR	5.84	0.21
28	c	NE-MLBA	PG105		WR	6.53	0.25
29	c	NE-MLBA	PG108		WR	5.80	0.19
30	c	NE-MLBA	PG109		WR	5.64	0.19
31	c	S-MLBA	PG132	4774130/306184	WR	3.32	0.10
32	c	S-MLBA	PG133	4774072/306312	WR	3.64	0.11
33	c	S-MLBA	PG134	4772347/307422	WR	3.89	0.14
34	f	NE-MLBA	8 ages of flows above and below tills			max. 7.00 min. 4.6	
35	g	NE-MLBA			Bt	5.04	0.04
36	g	NE-MLBA			Bt	7.38	0.05
37	h	NE-MLBA				6.53	0.23

a: Pelleter, 2003; b: Espinoza et al., 2005; c: Guivel et al., 2006; d: Boutonnet et al., submitted; e: Espinoza et al., 2006, 2007; f: Mercer and Sutter, 1982; g: Ton-that et al., 1999; h: Morata et al., 2002

Table 1. Lagabrielle et al

IV.2. Morphologie glaciaire et tectonique extensive : Bordure nord-ouest de la meseta del Lago Buenos Aires.

When a subducting spreading ridge triggers relief inversion in Central Patagonia :

Evidence from glacial morphology.

Bruno Scalabrino[1] , Jean-François Ritz[1],Yves Lagabrielle[1]

(1) *CNRS-UMR 5234, Géosciences Montpellier, Place E. Bataillon, CC 60, 34095, Montpellier Cedex 5, France*

When a subducting spreading ridge triggers relief inversion in Central Patagonia: Evidence from glacial morphology

Scalabrino Bruno

Laboratoire Géosciences Montpellier - UMR 5243, Université Montpellier 2, 34095 Montpellier Cedex 05, France.

Ritz Jean-François

Laboratoire Géosciences Montpellier - UMR 5243, Université Montpellier 2, 34095 Montpellier Cedex 05, France.

Lagabrielle Yves

Laboratoire Géosciences Montpellier - UMR 5243, Université Montpellier 2, 34095 Montpellier Cedex 05, France.

Submitted to Geology, 30th August 2009

Corresponding author:

Bruno Scalabrino

Université Montpellier 2, CNRS-UMR5243, Géosciences Montpellier, place E. Bataillon, CC60, 34095 Montpellier Cedex 5, France.

bruno.scalabrino@gm.univ-montp2.fr

ABSTRACT

This study examines the response of the Central Patagonian Cordillera to the subduction of the active South Chile Ridge and the development of the asthenospheric slab window beneath Patagonia since the Pliocene. We investigated the eastern part of the Cordillera where the glacio-volcanic piedmont is topographically-inverted. Glacial morphology and associated deposits capping the top of these piedmonts reveal that during the Pliocene (after 3 Ma), glaciers were flowing to the east over a regional surface connecting the western Cordillera and the paleo-piedmont. N160 trending normal faulting along the western edge of the inverted plateau induces the disruption of this surface after 3 Ma. At a regional scale, extensional tectonics is responsible for a relief inversion which magnitude is comprised between 800 and 3500 meters. Timing of the extensional tectonics is contemporaneous with the subduction of the spreading axis and the development of the slab-window beneath Central Patagonia.

Keywords: Central Patagonia, glacial morphology, relief inversion, active spreading ridge subduction.

1. INTRODUCTION

Since four decades, the question of the impact of a subducting spreading ridge on mantle dynamics and lithosphere/asthenosphere interactions is in debate. A major consequence of such phenomenon would be the formation of an asthenospheric slab window creating a pathway of hot mantellic material beneath the overriding plate inducing abnormal magmatism and a perturbation of the tectonic regime that would become extensional (e.g. Atwater, 1970; Delong et al., 1978; Dickinson and Snyder, 1979, Thorkelson, 1990; Thorkelson, 1996; Breitsprecher and Thorkelson, 2009).

Numerous studies described examples of subducting ridges within circum pacific cordilleras during the Cenozoic (e.g. Palmer, 1968; Dickinson and Snyder, 1979; Garret et al., 1987, Thorkelson, 1990), but the link between the development of an asthenospheric window and the occurrence of an extensional tectonics within the overriding plate is not yet clearly established. In this paper, we analyze this link within a modern example: the Central Patagonian Cordillera, which is a unique region to study interactions between oceanic and continental lithospheres during the subduction of an active spreading ridge beneath a continent. Recent works show that the Central Patagonian Cordillera experienced negative tectonic inversion synchronously with the formation of an underlying slab window (Lagabrielle et al., 2007; Scalabrino et al., in revision). However, the timing and the amplitude of this inversion remain unknown. Here we use the outstanding glacial morphology of Central Patagonia to quantify the age and the vertical deformation associated with the subduction of the South Chile spreading Ridge.

2.TECTONIC SETTING

Located between 45°S and 48°S, the Cordillera was built contemporaneously with the subduction of the South Chile spreading Ridge (SCR). Northwards migration of the SCR since 15 Ma has led to the subduction of several active segments (Figure 1) (Cande and Leslie, 1986). This induces the development of large asthenospheric slab window beneath the upper plate (Fig. 1), especially at 46°S, the latitude of the present-day Chile Triple Junction (CTJ), where the slab window developed since 3 Ma.

The Central Patagonian Cordillera is also known for its evidences of ancient glaciations (e.g. Malagnino, 1995; Rabassa et al., 2005; Lagabrielle et al., in revision). The oldest glacial testimonies - some of these are 7 Ma old (Mercer and Sutter, 1982) - are found east of the cordillera front within abandoned perched relict surfaces. One of the most outstanding features is the meseta del Lago Buenos Aires (MLBA) (Figure 2), between the lake General Carrera-Buenos Aires (LGCBA) and the lake Cochrane-Pueyrredon (LCP). Overlying the Late Oligocene-Middle Miocene foreland basin, the meseta is composed of several voluminous Miocene-Pliocene OIB lava sequences dated between 12 and 3 Ma (Gorring et al., 1997; Guivel et al., 2006). Main lavas are intruded by numerous Late Pliocene-Holocene small volcanic centers (Gorring et al., 2003). Till deposits dated between 7 and 3 Ma are interbedded with the lava sequences (Mercer and Sutter, 1982; Lagabrielle et al., 2007). The meseta MLBA can be described then as an ancient piedmont domain where lavas flows are interbedded with glacial deposits accumulated through time. This domain forms now a perched plateau cut by transverse glacial depressions, such as the LGCBA. In these glacial valleys, moraines are dated between 1 Ma and 13 ka (Ton-That et al., 1999; Singer et al., 2004). The MLBA as the Meseta del Guenguel have been interpreted as base level surfaces that have controlled erosion within the Central Patagonia. Ancient and now perched erosional surfaces as the Avellanos relict surface are interpreted as erosional surface that have been disrupted during the recent tectonic inversion (Scalabrino et al., in revision).

3. MORPHOTECTONICS ANALYSES

In order to characterize the timing and the amplitude of the negative inversion of the Cordillera, we carried out a morphological study of glacial markers within the MLBA. Using satellite images, digital elevation model (DEM SRTM-90m), and extensive field work along the western edge of the meseta del Lago Buenos Aires, we mapped glacial surfaces and associated deposits, and analyzed tectonic markers.

Figure 3 shows the synthesis of our observations along the northwestern edge of the MLBA. 3 main successive glacial stages characterized by glacial surfaces, valleys and moraines, inprint the morphology of the meseta, at an elevation comprised between 1600 m and 2100 m (Figs. 3A and 3B). The upper and oldest glacial surface (Fig. 3B and dark grey on Fig. 3C) corresponds to remnant patches situated above 2000 m high. Gently steeping to the

East, these patches are cut to the West by the N-S trending scarp bounding the northwestern edge of the MLBA. The main patch, ca. 30 km^2, defines a flat "V" shape surface and forms the northern summit flat ridge of the MLBA. Within the ridge, we found few decimetric to plurimetric boulders of Late Jurassic-Early Cretaceous ignimbrites and quartz among the basaltic clastic deposits (Figure 4, photos 1, 2). The lithology of these boulders indicates westerly-derived sources.

The second surface is inset within the highest surface and situated at an elevation between 1845 m and 1900 m. In map, it forms a "I" shape surface which transverse profile defines a U-shaped valley trending NE-SW inset in the older surface (Fig. 3C). The surface interrupts to the West along the N-S trending scarp, as for the highest surface. We also found pebbles of quartz and ignimbrites among the main basaltic debris attesting of westerly-derived sources. The width of this U-shape valley is ~3 km and its longitudinal extend can be estimated at a minimum of 6 km.

The third surface, inset into the two others and therefore younger, reshapes most of the morphology of the meseta, reworking preexisting glacial markers (Figs. 3B, 3C) as well as the main N-S trending scarp along bounding the two previous surfaces. The surface is characterized by several glacial valleys flowing northeastwards which can reach 30 km long, but also by smaller glaciers flowing westwards crossing the main scarp. Within the above-mentioned U-shaped valley, the two opposite flows are separated by a preserved patch corresponding to the second glacial stage (Fig. 3C).

4. STRUCTURAL ANALYSIS

Structurally, the meseta del Lago Buenos Aires is located east of the late Oligocene-middle Miocene morphotectonic front and east of a major tectonic corridor named the Rio Zeballos Fault Zone (Lagabrielle et al., 2004). The northwestern border of the meseta corresponds to a linear vertical cliff trending NNW-SSE with several tilted blocks at its base (Fig. 3D, 4B). Along the base of the cliff, west of the oldest 'V' shape glacial surface, we observed a serie of normal faults trending N140-160°E and dipping steeply to the west (Fig. 4, photo C). Inversion of fault slip data using Etchecopar method (1984) with Célérier (2009) software, allow us to characterize a stress regime close to radial extension with the principal maximum stress axis s1being vertical, s2 sub-horizontal and trending N305°E and s3 the principal minimum stress axis sub-horizontal and trending N215°E. The ellipsoid stress ratio f ($\phi_0 = (\sigma_2-\sigma_3)/(\sigma_1-\sigma_3)$) is comprised between 0.25 and 0. To the south, we observed a drag fold within the main volcanic sequence related to a N-S trending normal fault dipping to the west. We observed few kinematic criteria showing NS to NE-SW normal faulting with a small left-lateral component (Fig. 4, photo 4). Taken their poor number, we could not determine a stress tensor.

Using the stress tensor determined above, we can calculate the kinematics of the Rio Zeballos Fault Zone. Considering N160°E as a mean strike and 70°W as a mean dip, we determine the rake of the slip vector to be comprised between -70 and -90. This suggests that Rio Zeballos Fault Zone had a motion between pure normal faulting and normal faulting with a left-lateral component during the relief inversion.

5. MAGNITUDE OF THE RELIEF INVERSION

In order to constrain the magnitude of the negative tectonic inversion, we focused on two key-areas. The first one is within the northern edge of the LGCBA where normal faulting induced the disruption of the Avellanos erosional surface with the eastern piedmont (Meseta del Guenguel) (Fig. 2). Figure 5A shows piercing lines between the tilted erosional surface and the inverted paleo-piedmont to the east. Within the main oblique normal fault zone, the difference in height between the two surfaces is 3500 m. The second key area is located south of the beheaded glacial valleys of the MLBA (Fig. 2). Here, tills covered by lava flows dated at 3 Ma on the top of the MLBA (Lagabrielle et al., 2007) are also found west of the MLBA in the Rio Ghio valley, several hundreds of meters lower (Figs. 2 and 5). The horizontal projection of tills within the Rio Zeballos Fault Zone defines a 800 m minimum vertical offset.

6. CONCLUSION-DISCUSSION

Our morphological study of glacial markers within the MLBA in Central Patagonia allowed us to characterize the timing and the magnitude of the negative inversion of the Cordillera. Remnants of glacial deposits at the top of the MLBA suggest that glaciers were flowing eastwards over a regional surface connecting the western Cordillera to a paleo-piedmont. These eastwards flowing glaciers postdate the emplacement of the main upper volcanic sequence dated at 3 Ma (Gorring et al., 1997; Guivel et al., 2006), and were interrupted by the occurrence of the normal faulting along the western edge of the MLBA. On the other hand, recent glacial deposits (between 1 Ma and 13 ka in age) found within transverse depressions (LGCBA and LCP) do not show evidences of recent deformations.

Therefore, we can bracket the negative tectonic inversion between 3 and 1 Ma. This timing is consistent with the occurrence of rift-liked alkalin magmatism crisis at the southwestern edge of the MLBA which has been dated at 3 Ma (Espinoza et al., 2008).

Within the MBLA, the inversion was mainly located at its western edge, along the Rio Zeballos fault zone. There, fault slip data analysis allow characterizing a radial extensional regime (Fig. 4A), with a pure normal to normal-sinistral motion along the main fault. Radial extensional deformation is coherent with the formation of transverse and internal depressions driving recent glaciers in Central Patagonia (Lagabrielle et al., 2004; Scalabrino et al., 2009; Scalabrino et al., in revision). The western edge of the MLBA corresponds to the eastern shoulder of a collapsed domain located between the highest relief of Patagonia to the west and the MLBA to the east. After the offset of glacial markers (erosional surface, tills deposits), we estimate the magnitude of the relief inversion of the eastern part of the Cordillera to be comprised between 800 m and 3500 m. This yields a mean vertical slip rate comprised between 0.26 mm/yr and 1.15 mm/yr.

The timing of the extensional deformation deduced from our observations is synchronous with the passage of the subducting spreading South Chile Ridge below the Central Patagonia, resulting in the opening of asthenospheric slab-window at 3 Ma (Lagabrielle et al., 2004; Breitsprecher and Thorkelson, 2009). Upwelling of hot mantle through the slab-window has induced drastic changes in mantle dynamics and in turn regional relief inversion in the Patagonian Cordillera.

ACKNOWLEDGEMENTS

This research was funded by grants from the Chilean-French ECOS-CONICYT program (project C05U01) and CNRS-INSU DyETI and Reliefs programs. Field work by BS and JFR was possible through grants from INSU Dyeti and Relief programs (France). We thank also B. Célérier for helpfull discussion

REFERENCES

Atwater, T., 1970, Implications of plate tectonics for the Cenozoic tectonic evolution of western North America: Geological Society of America Bulletin, v. 81, p. 3513-3536.

Bradley, D., Kusky, T., Haeussler, P., Goldfard, R., Miller, M., Dumoulin, J., Nelson, S.W., and Karl, S., 2003, Geologic signature of early Tertiary ridge subduction in Alaska: In

Sisson, V.B., Roeske, S.M., and Palvis, T.L., eds., Geology of a transpressional orogen developed during ridge-trench interaction along the North pacific margin: Boulder, Colorado, Geological Society of America Special paper, v. 371, p. 19-49.

Breitsprecher, K. and Thorkelson, D.J., 2008, Neogene kinematic evolution of the Nazca–Antarctic–Phoenix slab windows beneath Patagonia and the Antarctic Peninsula: Tectonophysics. doi: 10.1016/j.tecto.2008.02.013

Cande, S.C., Leslie, R.B., 1986, Late Cenozoic tectonics of the Southern Chile Trench: J. Geophys. Res., v. 91, p. 471-496.

Célérier, B., 2009, FSA 32.2. Fault & Stress Analysis software, http://www.pages-perso-bernard-celerier.univ-montp2.fr/software/dcmt/fsa/fsa.html.

Dickinson, W.R., and Snyder, W.S. 1979, Geometry of subducted slab related to the San Andreas transform: Journal of Geology, v.87, p.609-627.

Espinoza, F., Morata, D., Polvé, M., Lagabrielle, Y., Maury, R. C., Guivel, C., Cotten, J., Bellon, H., Suárez, M. 2008, Bimodal back-arc alkaline magmatism after ridge subduction: Pliocene felsic rocks from Central Patagonia (47ºS), Lithos, v. 101 (1-2), p. 191-217.

Etchecopar, A., 1984, Etude des états de contrainte en tectonique cassante et simulations de déformations plastiques (approche mathématique). Unpublished Thèse d'Etat thesis, Université des Sciences et Techniques du Languedoc.

Frohlich, C., 1992, Triangle diagrams: ternary graphs to display similarity and diversity of earthquake focal mechanisms, Physics of the Earth and Planetetary Interiors, v. 75, p. 193-198.

Garret, S.W., Storey, B.C., 1987, Lithospheric extension on the Antarctica Peninsula during Cenozoic subduction: In Extension in the basin and Range Province and East Pacific Margin, Geological Society, London, Special Publications, v. 28, pp. 419-431.

Gorring, M., Kay, S., Zeitler, P., Ramos, V., Rubiolo, D., Fernandez, M., Panza, J., 1997, Neogene Patagonian plateau lavas: continental magmas associated with ridge collision at the Chile Triple Junction: Tectonics, v. 16, p. 1-17.

Gorring, M., Singer, B., Gowers, J., Kay, S., 2003, Plio-Pleistocene basalts from the Meseta del Lago Buenos Aires, Argentina : evidence for asthenosphere-lithosphere interactions during slab-window magmatism: Chem. Geol., v. 193, p. 213-235.

Gripp, A.E., Gordon, R.G., 1990. Current plate velocities relative to the hotspots incorporating the NUVEL-1 global plate motion model. Geophysical Research Letters 17, 1109-1112.

Guivel, C., Morata, D., Pelleter, E., Espinoza, F., Maury, R.C., Lagabrielle, Y., Polvé, M., Bellon, H., Cotten, J., Benoit, M., Suarez, M., de la Cruz, R., 2006, Miocene to Late Quaternary Patagonian basalts (46°-47°S) : Geochronometric and geochemical evidence for slab tearing due to active spreading ride subduction: Journal of Volcanology and Geothermal research, v. 149, p. 346-370.

Lagabrielle, Y., Suarez, M., Rossello, E.A., Hérail, G., Martinod, J., Régnier, M., de la Cruz, R., 2004, Neogene to Quaternary tectonic evolution of the Patagonian Andes at the latitude of the Chile Triple Junction: Tectonophysics, v. 385, p. 211-241.

Lagabrielle, Y., Suarez, M., Malavieille, J., Morata, D., Espinoza, F., Maury, R., Scalabrino, B., de la Cruz, R., Rossello, E., Barbero, L., Bellon, H., 2007, Pliocene extensional tectonics in Eastern Central Patagonian Cordillera : geochronological constraints and new field evidence: Terra Nova, v. 19, p. 413-424.

Lagabrielle, Y., Scalabrino, B., Suarez, M., Ritz, J.F. Mio-Pliocene glaciations of Central Patagonia: New evidence and tectonic implications. Accepted to Andean Geology, special volume.

Malagnino E., 1995, The discovery of the oldest extra-Andean glaciation in the Lago Buenos Aires Basin, Argentina. Quaternary of South America and Antarctic Peninsula 9 (1991), Rabassa & Saleme Eds., Balkema, v. 4, p. 69-83.

Mercer, J.H., Sutter, J.F., 1982, Late Miocene-Earliest Pliocene Glaciation in Southern Argentina : implications for global ice-sheet history: Paleogeography, Paleoclimatology, Paleoecology v. 38, p. 185-206.

Palmer, H., 1968, East Pacific rise and westward drift of the North America: Nature, v. 220, p. 341-345.

Petit, J.P., 1987. Criteria for the sense of movement on fault surfaces in brittle rocks, Journal of Structural Geology, v. 9 (5-6), p. 597-608.

Rabassa, J., Coronato, A/M. and Salemme, M., 2005. Chronology of the Late Cenozoic Patagonian glaciations and their correlation with biostratigraphic units of the Pampean region (Argentina) : Journal South Am. Res., v. 20, p. 81-103.

Ritz, J.F., 1994, Determining the slip vector by graphical constructiuon : use of a simplified représentation of the stress tensor, Journal of Structural Geology, vol. 16 (5), p. 737-741.

Scalabrino, B., Lagabrielle, Y., de la Rupelle, A., Malavieille, J., Polvé, M., Espinoza, F., Morata, D., Suarez, M., 2009, Subduction of an Active Spreading Ridge beneath Southern South America: A review of the Cenozoic geological records from the Andean foreland, Central Patagonia (46-47°S): In S. Lallemand and F. Funiciello (eds.), Subduction Zone Geodynamics, DOI 10.1007/978-3-540-87974-9, Springer-verlag Berlin Heidelberg, p. 227-246.

Scalabrino, B., Lagabrielle, Y., Malavieille, J., Dominguez, S., Melnick., D., Espinoza, F., Suarez, M., Rossello., E. A morphotectonic analysis of Central Patagonian Cordillera. Negative inversion of the Andean belt over a buried spreading center? Accepted pending minor revisions to Tectonics.

Thorkelson, D.J., 1990, Tectonic and magmatic aspects of slab window, Geol. Assoc. Can. Progr. Abstr., 15, A105.

Thorkelson D.J.; 1996, Subduction of diverging plates and the principles of slab window formation, Tectonophysics v. 255, p. 47–63.

Ton-That, R., singer, B., Morner, N-A, Rabassa, J., 1999, Datacion de lavas basalticas por $^{40}Ar/^{39}Ar$ y geologia glacial de la region del Lago Buenos Aires, provincia de Santa Cruz, Argentina: Asociacion Geologica Argentina, Revista (Buenos Aires) v. 54 (3), p. 333-352.

Singer, B.S., Ackert, R.P., Guillou, H., 2004, $^{40}Ar/^{39}Ar$ and K/Ar chronology of Pleistocene glaciations in Patagonia: Geological Society of America v. 116 (3/4), p. 434-450.

Wilson, J.T., 1988, Convection tectonics: Some possible effects upon the Earth's surface of flow from the deep mantle: Canadian Journal of Earth Sciences, v. 25, p. 1199-1208.

Figure Captions:

Figure 1. Tectonic setting and simplified tectonic data of southern South America (see Scalabrino et al., 2009 for references). Relative motions between plates are from model NUVEL-1 of Gripp and Gordon (1990). Location of the study area is represented by black frame.

Figure 2. Digital Elevation Model (DEM SRTM-90 m) of the eastern Central Patagonian Cordillera showing main topographic anomalies. Black frame shows the location of morphological and structural analysis discussed in the text.

Figure 3. A: Landsat image of the northwestern side of the meseta del Lago Buenos Aires, including the Cordillera (left), the Rio Zeballos Fault Zone (middle) and the topographically-inverted meseta del Lago Buenos Aires (right). White eyes and numbers indicate location and orientation of photographs of Figure 4. White circles indicate the location of structural analysis. B: Photograph of the successive glacial valleys on the northwestern edge of the MLBA. C: Simplified map of the glacial morphological observations showing the three main glacial surfaces. The highest surface with post 3 Ma-old westerly-derived glacial deposits is represented in dark grey. D: Simplified tectonic and geologic map of the northwestern edge of the MLBA.

Figure 4: Potographs 1-2: Westerly-derived boulder and pebbles of Jurassic-Cretaceous ignimbrites covering the upper surface (2200 m a.s.l) of the MLBA (person for scale). Photographs 3-4: Pictures of the main scarp and of the drag fold, north and south of the beheaded valley respectively, related to N160 trending normal faults. A-B: Associated stereographic, equal area, lower hemisphere projections of faults slip data (FSA 30.5, Célérier

et al., 2008), and representation of the ellipsoid stress ration defining radial extensional regime (representation after Ritz et al., 1994)..

Figure 5: A. Topographic section across the tilted erosional surface and the topographically-inverted paleo-piedmont north of the LGCBA showing offset ranges along main normal fault. B. Topographic cross-section south of the study area where 3 Ma-old tills sequence are shifted more than 800 meters.

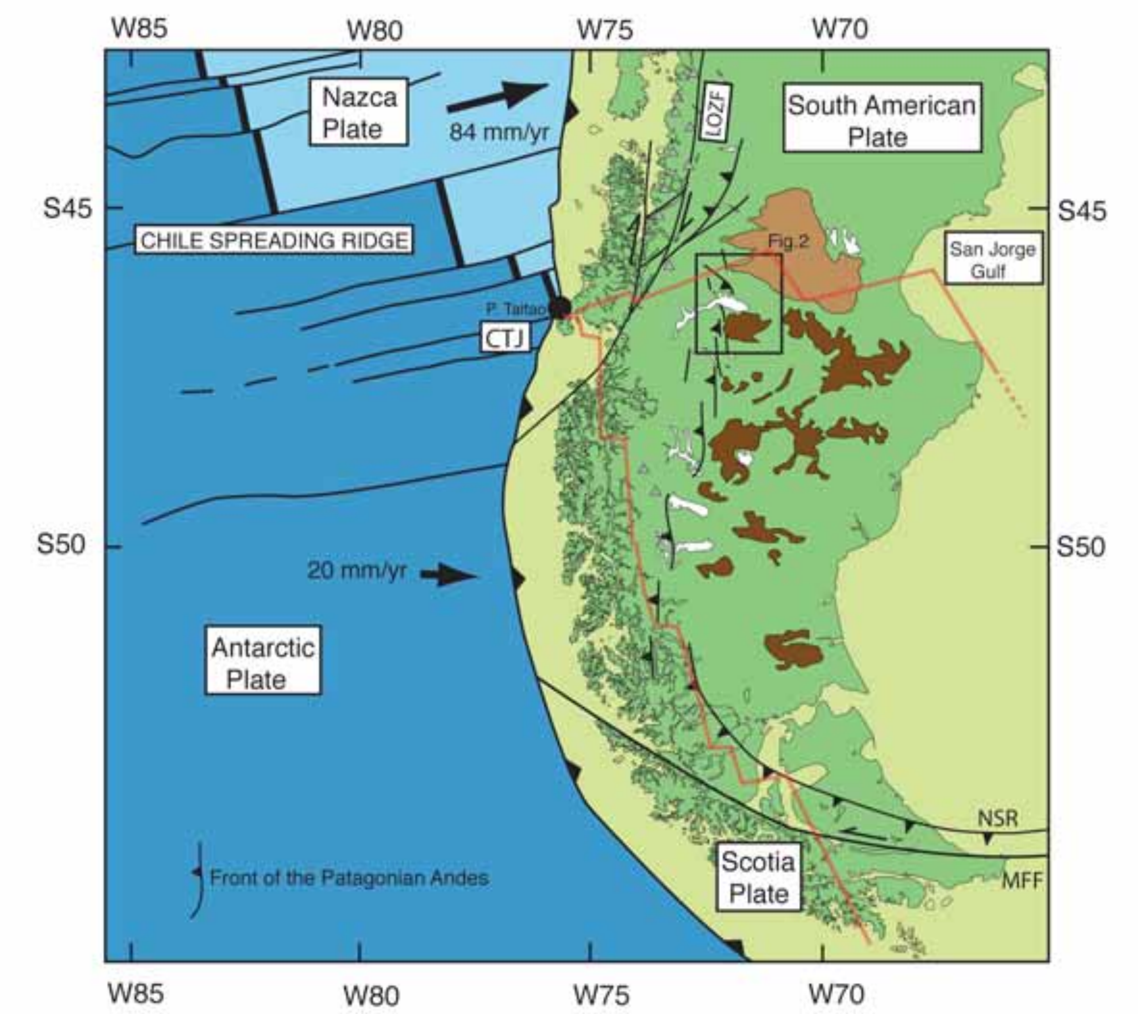

Fig. 1 Scalabrino et al.

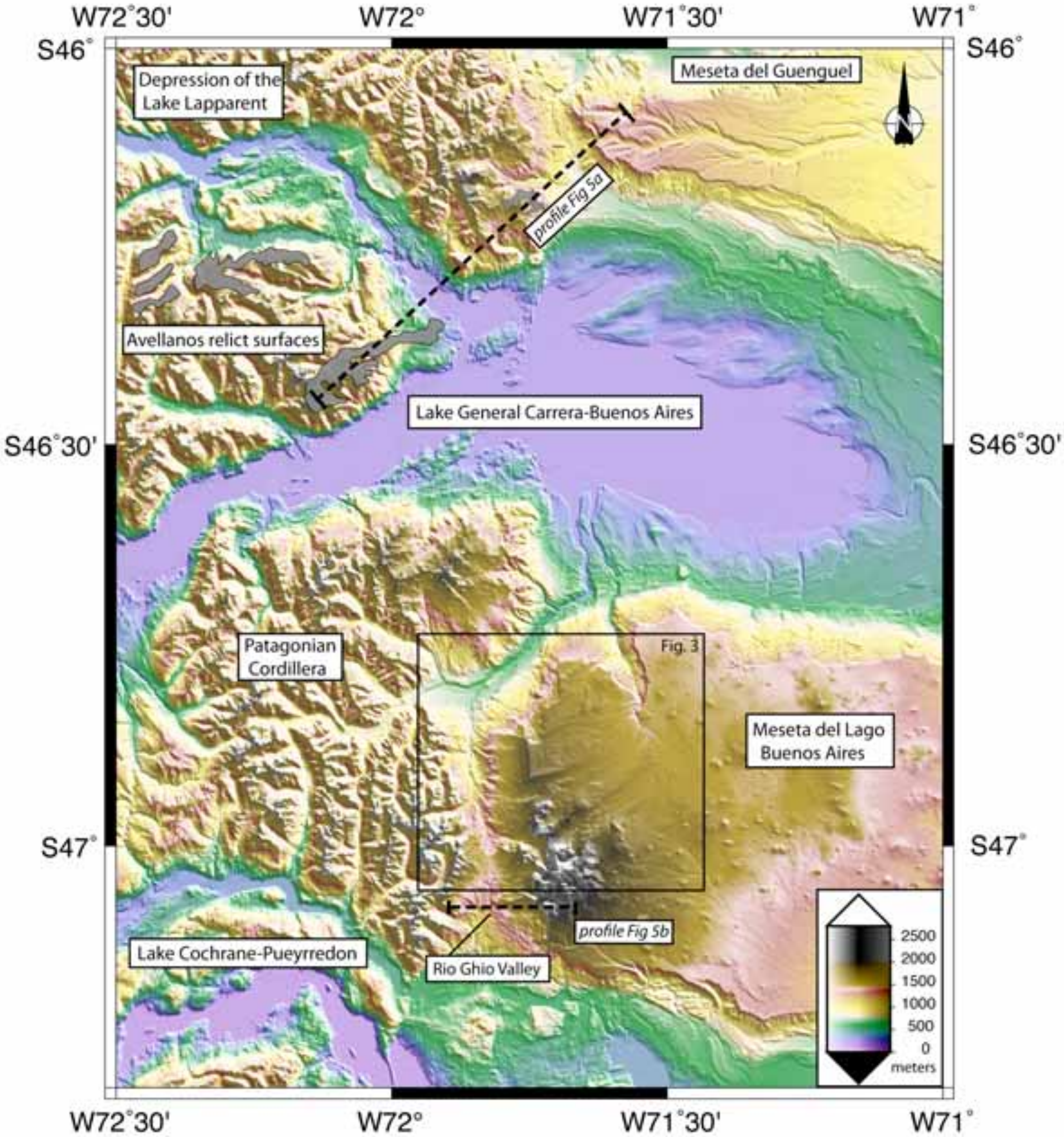

Fig. 2 Scalabrino et al.

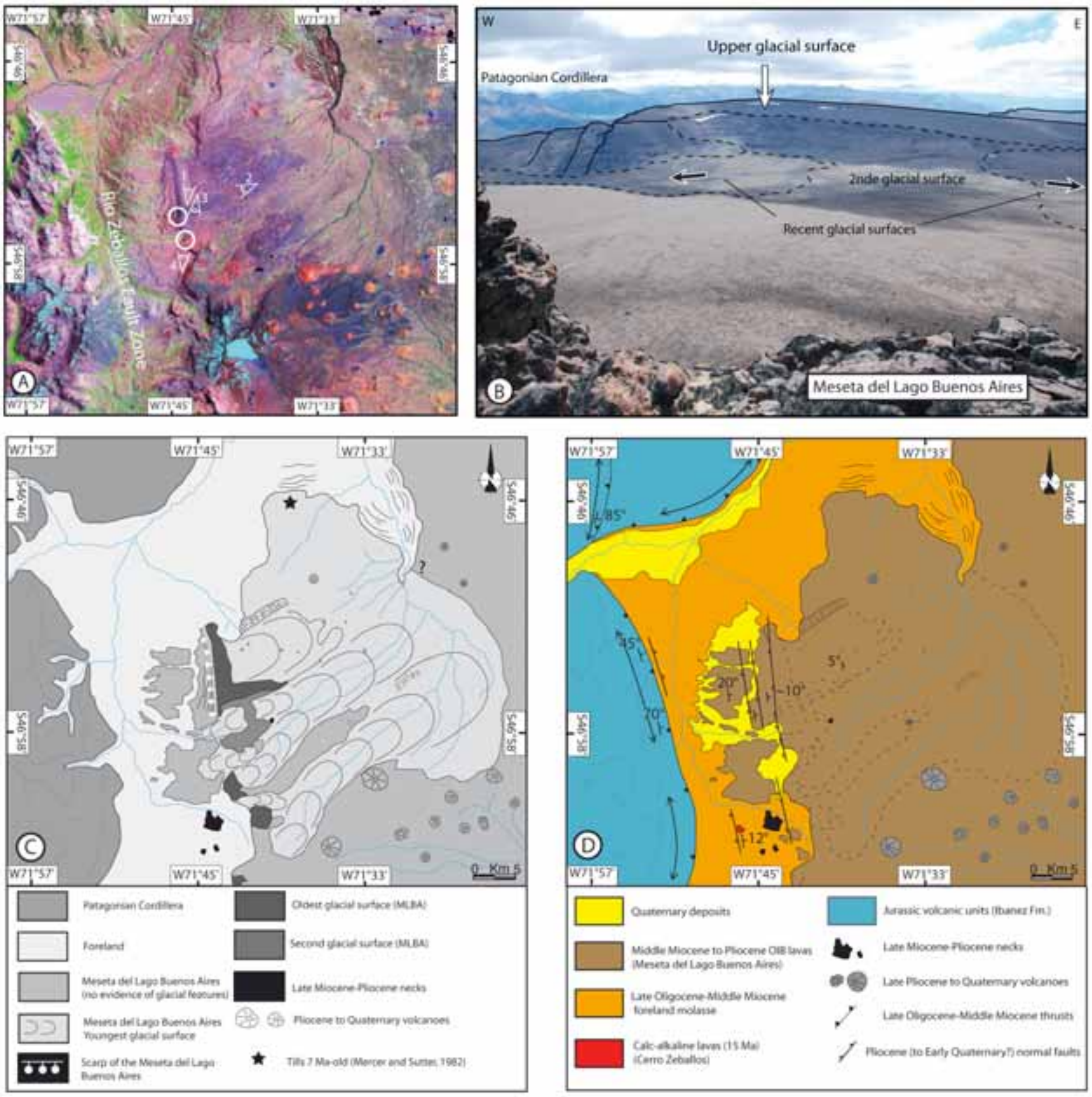

Fig. 3 Scalabrino et al.

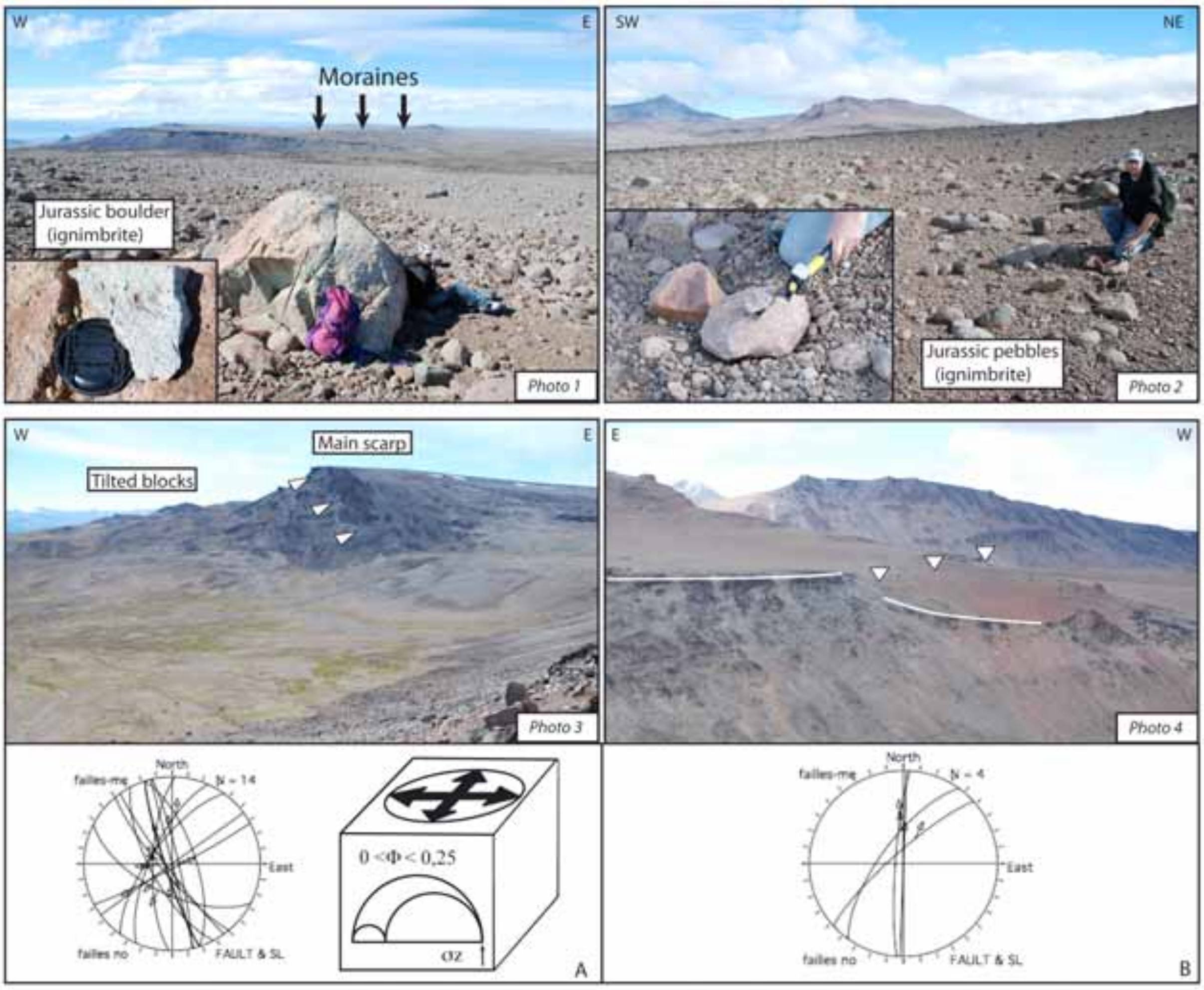

Fig. 4 Scalabrino et al.

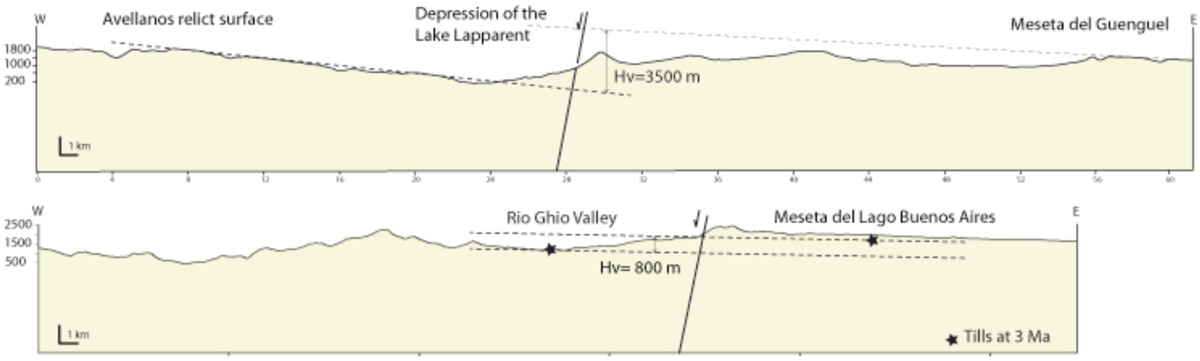

Fig. 5 Scalabrino et al.

IV.3. Evolution morphotectonique de la région de Coihaique (Aysen). Influence de la subduction de la dorsale du Chili au nord du point triple.

Oligocene to recent morphostructural evolution of the Coihaique area (Aysen region), Central Patagonia.

Tectonic events at the tip of a propagating slab window.

Bruno Scalabrino[1] ; Yves Lagabrielle[1] ; Manuel Suarez[2]

[1] *Université Montpellier 2, INSU-CNRS, Laboratoire Géosciences Montpellier, place E. Bataillon, 34095 Montpellier Cedex 5, France.*

[2] *Servicio Nacional de Geologìa y Minerìa, Avenida Santa Marìa 0104, Santiago, Chile.*

Oligocene to Recent morphostructural evolution of the Coihaique area (Aysen region), Central Patagonia.

Tectonic events at the tip of a propagating slab window.

Scalabrino, B[1]., Lagabrielle, Y[1]., Suarez, M[2].

[1] *Université Montpellier 2, INSU-CNRS, Laboratoire Géosciences Montpellier, place E. Bataillon, 34095 Montpellier Cedex 5, France.*

[2] *Servicio Nacional de Geologìa y Minerìa, Avenida Santa Marìa 0104, Santiago, Chile.*

Submitted to Andean Geology special volume

Corresponding author:

Bruno Scalabrino

Université Montpellier 2, CNRS-UMR5243, Géosciences Montpellier, place E. Bataillon, CC60, 34095 Montpellier Cedex 5, France.

bruno.scalabrino@gm.univ-montp2.fr

Abstract :

We conducted a preliminary morphological and structural analysis of the region of Coihaique (Aysen region, Central Patagonia), based on DEM's data and field observations coupled with a review of literature in order to study the possible on-land effects of the subduction of the active South Chile spreading Ridge (SCR). This region is characterized by an average very low elevation reaching 780 m, and shows a number of peculiar features not expected in a "normal" subduction belt. The Patagonian Cordillera exhibits a central low elevated domain, where high relief should be expected. This depressed area is flanked by western and eastern regions of higher elevation. To the east, the meseta del Cerro Galera dominates the low elevated domains. It corresponds to a former piemont and it is composed of Oligocene-Miocene foreland molasse capped by Late Miocene-Pliocene till deposits attesting that during this period, the morphology of the Cordillera was characterized by large glaciers flowing to the east. At present time, the Patagonian Cordillera is separated from the meseta by an oblique tectonic corridor and internal depression localizing recent vertical movements. It is shown that a negative inversion related to extensional and strike-slip faulting occurred in the frontal region of the Cordillera after the deposition of the till sequence. We propose that the extensional tectonics is related to the asthenospheric slab window beneath the South American plate. Located north of the predicted position of the slab window, the Coihaique region represents the northern tip of an extensional propagating domain ahead the slab-window termination. Upwelling of hot mantle through the slab-window can influenced the mantle dynamics by northwards asthenospheric spreading, leading to the weakening of the crust and in turn, to local to regional collapse of the Central Patagonian Cordillera.

Key words : morphostructural, relief inversion, extension, Central Patagonia, active spreading ridge subduction.

1. Introduction

The Andean chain borders the entire western margin of South America where different oceanic plates have been subducted. It represents a belt of thickened and/or thinned crust resulting from oblique to horizontal shortening, extension and magmatic cycles occuring during the Late Mesozoic and Cenozoic.

The Patagonian Cordillera forms the southernmost Andes and was built coevally with the Upper Cenozoic subduction of the southern portion of the Chile spreading ridge. The Chile Triple junction, now located at 46°12'S, is the point where the Nazca, Antarctic and South American plates meet (Figs. 1-2). Since 14 Ma, the CTJ is migrating northward as a result of oblique collision between the South Chile Ridge and the southernmost tip of the South America (Herron et al., 1981; Cande and Leslie., 1986; Cande et al., 1987; Nelson et al., 1994; Bangs and Cande, 1997; Tebbens and Cande, 1997; Tebbens., 1997). Subduction of several spreading segments leads to the development of a large asthenospheric slab window beneath Patagonia (Fig. 2) (Ramos and Kay, 1992; Gorring et al., 1997; Lagabrielle et al., 2004; Breitsprecher and Thorkelson, 2008; Scalabrino et al., 2009). Similar opening of asthenospheric window is reported from other tectonic settings as northwestern America (Dickinson and Snyder, 1979; Thorkelson, 1996; Bradley et al., 2003) and west Antarctic Peninsula (Garret et al., 1987). Therefore, the Chile-Argentina Patagonian region constitutes an appropriate natural laboratory in order to study on-lands effects of the subduction and the migration of an active spreading ridge.

The Patagonian Cordillera is topographically different from the Northern Andes. Between 45°S and 50°S, Central Patagonian is characterized by the occurrence of few hight summits which border the Pacific coastline (Northern and Southern Ice Caps with the Mt San Valentin, 4058m a.s.l…) juxtaposing deep transverse depressions occupied by post glacial lakes (Lake General Carrera Buenos Aires, Lake Cochrane-Pueyrredon) (Fig. 1-2). The northern part of the Patagonian Cordillera (44°S-48°S) lacks very large thrusts and total shortening remains low along this region characterized by a non-thickened crust (Introcaso et al., 1996; Tassara et al., 2003).

The region of Coihaique-Balmaceda, between 44°S-46°S, is located north of the present-day Chile Triple Junction. This region is a limit between two different subduction situations (Figs. 1-2): (1) south of 46°S, the Antarctic oceanic lithosphere which approaches the trench is older towards the west and arc-volcanism exhibits adakitic affinity (Stern, 1990),

(2) north of 46°S, the Nazca oceanic lithosphere is younger towards the east and volcanoes of the arc have a calk-alkaline affinities as examplified by the compostion of erupted products of Hudson volcano (Naranjo et al., 1993; Gutierrez et al., 2005). The Coihaique region corresponds also to a limit between two different tectonic settings (Fig. 1): (1) south of 46°S, the South American plate is characterized by a series of easterly vergent thrusts juxtaposing Mesozoic-Cenozoic internal units over Cenozoic molasse deposits with a relatively low amount of shortening, (2) north of 46°S, the Patagonian Cordillera is controlled by several splays of the long-lived active dextral system of the Liquine-Ofqui fault Zone (Hervé et al., 1994; Cembrano et al., 1996, 2000, 2002 and Rosenau et al., 2006).

Tectonic effects of ridge subduction have been already considered in the forearc and in the intra-arc region of Patagonia (Forsythe and Nelson, 1985; Nelson et al., 1994; Thomson et al., 2001; Cembrano et al., 1996, 2002) and in the back-region firstly south of the present Chile Triple Junction (Ramos, 1989; Flint et al., 1994; Suarez et al., 2000; Morata et al., 2002) and second at the Chile Triple Junction (Lagabrielle et al., 2004, 2008; Scalabrino et al., 2007; 2009a; 2009b). However, no detailed morphostructural data are available so far from the region of Coihaique, north of the Chile Triple Junction.

In this study, we present preliminary morphostructural and tectonic data collected from the area of Coihaique based on DEM and Landsat mosaic interpretations and on field observations. We propose a Miocene-Pliocene morphostructural evolution of the Patagonian Cordillera in relation with the suduction of the South Chile Ridge in an area of 100 x 100 km, between 45°S and 46°S.

2. Plate configuration

During Oligocene times, the south South American margin was characterized by the subduction of the Farallon-Nazca plate following three successive kinematic stages: between 40 Ma to 26 Ma, convergence rate increases from 35±25 mm/a to 112±8 mm/a (Pardo-Casas and Molnar, 1987) and the direction of the Nazca (ex-Farallon plate) plate with respect to South America becomes more orthogonal. Since 20 Ma, the direction is slightly oblique (Pardo-Casas and Molnar, 1987; Somoza, 1998). Subduction of the South Chile Spreading Ridge started at 15 Ma at the southern tip of the southern South America. Obliquity of the South Chile Ridge has induced a northward migration of the Chile Triple Junction and is presently entering the Chile trench at 46°12'S. Since 15 Ma, four spreading segments have been subducted beneath the South American plate inducing the development of a large slab window.

North of the Chile Triple Junction, the present-day relative motion vector of the Nazca and South American plates is trending N80 (Gripp and Gordon, 1990; De Mets et al., 1990) with a magnitude of 84 mm/a (Fig. 2). Oblique subduction has led to tectonic partitioning in the Cordillera, and part of the convergence has been accommodated along the Liquine-Ofqui dextral strike-slip fault zone north of the Chile Triple Junction (Hervé, 1994; Cembrano et al., 1993,1996, 2002). South of the Chile Triple Junction, current convergence between the Antarctic and South American plates occurs at a rate of 20 mm/yr, in an E-W direction (Fig. 2) (Gripp and Gordon, 1990; De Mets et al., 1990).

3. Geological setting

Upper-Middle Jurassic volcanic rocks of the Ibáñez Formation are the oldest rocks in the Coihaique-Balmaceda area (Fig. 3). They represent the youngest event of a widespread, mainly silicic volcanism that covered most of Patagonia from the Early to Late Jurassic. These rocks unconformably overlie Paleozoic basement rocks well-observed more to the south close to Lake General Carrera-Buenos Aires area (LGCBA) (Niemeyer et al., 1984; Charrier et al., 1979; Suárez et al. 1996; De La Cruz et al. 2003a, 2005, 2006). During the Earliest Cretaceous, a back-arc epicontinental sea representing the northwestern continuation of the Austral Basin covered the region (Bell and Suárez, 1997). The marine transgression is represented by the Coihaique Group (Fig. 3). From base to top this group is composed of three different formations. First, the shallow marine calcareous, sandstones, tuffs and oyster beds of the Toqui Formation, 70 m thick (De la Cruz et al., 2003b; Suárez and de la Cruz, 1994a) unconformably overlie the Jurassic volcanics with angular to erosive contacts. Second, the fossiliferous black shales of the Katterfeld Formation, 200 m thick (De la Cruz et al., 2003b) overlie the Toqui Formation. These rocks are overlain by the marine sandstones and shales of the Apeleg Formation, 400m thick.

The geological Cenozoic record in the area is essentially represented by volcanic and intrusive rocks, with subordinate sedimentary rocks. The bedded rocks firstly comprise late Early Cretaceous rocks of the Divisadero Formation (Fig. 3) (Heim, 1940), which consist of

800 to 1500 m of volcanoclastic deposits. Locally, this formation has an erosive contact with the Ibáñez and Apeleg formations (De la Cruz et al., 2003b). Secondly, Late Cretaceous (82-75 Ma, de la Cruz et al., 2003b) volcanic rocks of the El Toro Formation consists of approximatively 450 m thick of andesits and basaltics lavas which outcrop on the northeastern part of the area. Thirdly, the eastern and southeastern part of the Coihaique-Balmaceda area is characterized by the exposure of the Late Paleocene-Eocene Balmaceda Basalts (59-56 Ma, Suárez et al., 1996; De la Cruz et al., 2003b). They consist of a 450 m thick pile of tholeiites and alkali basalts with OIB signature (Demant et al., 1996; Morata et al., 2002; Parada et al., 2001). This formation is unconformably overlain by fluvial deposits with tuffs intercalations of the Oscuro Formation assigned to the Early Miocene (Fig. 3) (Ray, 1996). Finally, well bedded sequences formed by Miocene westerly-derived fluvial deposits, are exposed in the eastern side of the area (Fig. 3) (meseta del Cerro Galera). This sequence consists of conglomerates with sandstone intercalations reaching approximatively 500 m in thickness. This sequence is younger than the Santa Cruz Formation well-observed south of the LGCBA, on the Cosmelli Basin and west of the morphotectonic front of the Cordillera (Ray, 1996) and related to the Oligocene-Miocene compressional stage. The older marine sequence of the Guadal Formation well known farther south is not exposed in this area. The top of the Cerro Galera Formation and above the Galera Formation is also characterized by the exposure of till deposits outcropping at the Cerro Galera (1460 m.a.s.l) (see section 4.2) (Figs. 3-4). They can be correlated with the Late Miocene- Early Pliocene till deposits of the meseta del Lago Buenos Aires south of the LGCBA described by Mercer and Sutter, 1982 and Lagabrielle et al., (2007) and dated at 7-3 Ma, and with the deposits assigned to the Galera Formation in the area of Baño Nuevo, 75 km northeast of Coihaique (Suárez et al., 2007).

The intrusive rocks are mainly represented by the Patagonian Batholith which displays Early Cretaceous to Miocene ages (Halpern and Fuenzalida, 1978; Pankhurst et al., 1999; Suárez and de la Cruz, 2001; Morata et al., 2002). It crops out in the northwestern and southwestern sides of the region. In the region of Coihaique, several small plutonic bodies are associated with the Patagonian Batholith, such as the Elizalde Plutonic Complex located in the southwestern side of the area. This complex has a wide range of compositions between granite to gabbro with Early-early Late Cretaceous ages (Pankhurst et al., 1999; Suárez and De la Cruz, 2001; Morata et al., 2002). South of Coihaique, small acidic porphyric bodies intrude the Katterfeld, Apeleg and Divisadero Formations as the Cerro Mac Kay which has a K-Ar age of 63 ± 2 Ma (Fig. 3) (De la Cruz et al., 2003b). Oligocene intrusive rocks are represented by the Bandurrias gabbros and by basic to intermediate hypabissal bodies outcropping close to the Coihaique and Foitzick Fault Zones respectively and which can be linked to magmatism arc related to the Nazca subduction (De la Cruz et al., 2003b).

Quaternary deposits represent a large part of the Coihaique area and comprise Pleistocene to Holocene glacial and fluvial materials. Glacial materials correspond to recent glaciations, which occurred during the Quaternary and can be correlated to the numerous glacial deposits well-documented in LGCBA area (Ton-That et al., 1999; Singer et al., 2004).

As shown on the cross-section (Fig. 4) constructed using data gathered from former studies of De La Cruz et al (2003b) merged with results of recent structural field works, the bedded rocks are in general, subhorizontal or weakly folded, indicating little amount of shortening. This area exhibits a thick-skinned tectonic style mainly controlled by high dipping faults, probably corresponding to reactivated older faults. Here, NNW-SSE and NE-SW trending faults have senestral, dextral and normal components and mainly affect Cretaceous Formation (Fig. 4). Origin and evolution of fault zone, and tectonic corridors will be discussed in this paper.

4. Geomorphology of the Coihaique-Balmaceda region

In the following section, we describe the most peculiar morphological features of the Patagonian Cordillera at the latitude of Coihaique based on the analysis of a digital elevation model (DEM SRTM-90 m) in an area of 100x200 km between S45° and S46°.

4.1. General characteristics.

The present-day topography of the Patagonian Cordillera is clearly different from that of rest of the Andes. Between 45°S and 55°S, the mean elevation of the Cordillera is around 1000 m.a.s.l (Montgomery et al., 2001). At the latitude of the Chile Triple Junction, the mean relief elevation is 900 meters (Scalabrino et al., 2007) with highest peaks of the Patagonian Cordillera culminating around 4000 m.a.s.l (western part of the Cordillera, Mt San Valentin, 4058 m.a.s.l). As shown on the calculated profile of the mean topography exhibited in figure 5b, the average elevation of the Coihaique-Balmaceda region is about 780 m. Mean elevation of peaks is around 1500 m with highest peaks reaching 2000 m and dominating an internal area showing low elevation. Here, the Patagonian Cordillera is flanked to the west by a low-elevated domain limited by the active Liquine-Ofqui Fault Zone separating the Taitao Peninsula from the continent (Fig. 5a). To the east, the Patagonian Cordillera is flanked by the Pampean domain characterized by wide areas of homogeneous topography including flat plains and several mesetas (Fig 5a). Figure 5b corresponds to a topographic profile at latitude S45°45'. It shows the typical pattern of this region, characterized by two opposite, western and eastern regions of relatively high elevation, braketing an axial low-elevated region. The axial low-elevated region is located between the Cordillera to the west and the meseta del Cerro Galera to the east, and occurs surprisingly in a position where higher reliefs should be expected in the case of a normal subduction belt. Both flanking regions of higher elevation are characterized by top surface having opposite slopes. Here, the western region includes high relief of the Patagonian Cordillera, reaching between 1000 and 2000 meters and characterized by deeply incised valleys. The eastern region comprises remarkable flat surfaces (mesetas) gently dipping eastwards. Between these two domains, the Patagonian Cordillera shows a low-elevated domain exhibiting westwards general slope locally affected by steps having eastwards slope.

4.2. The meseta del Cerro Galera: a topographically inverted basin

The morphology of the eastern part of the Patagonian Cordillera is characterized by a succession of plateaus of sedimentary composition (Figs 2-5a). Three meseta have been observed from the north to the south: the meseta Boscosa, the meseta del Cerro Galera and the meseta del Guenguel. Here, we focus on the meseta del Cerro Galera, the largest sedimentary plateau in this area. The flat-topped meseta del Cerro Galera is made up of continental Miocene syn-orogenic sediments (de la Cruz et al., 2003b). A shown on figure 6, the top surface of the meseta is characterized by the exposure of till deposits capping the molasse sequence with an erosive contact. This sequence, younger than 12 Ma (the age of the upper syn-orogenic sediments) (comm. Pers. M. Suárez), contains heterometric pebbles of granite and basalts with a thin sandy matrix (Fig. 6). The elevation of the meseta varies from 1465 m (Cerro Galera) to 500 meters from west to east. The meseta shows a gentle slope dipping to the east and exhibits a well-preserved eastward dendritic relict stream network cut by present-day landslide along its southern edge (Fig. 5a). This depositional surface is presently disconnected from the rest of the Cordillera by NE-SW oriented corridors and internal depression as discussed below. Similar topographic and morphologic anomalies and stratigraphic characteristics have been reported from studies of the meseta Boscosa and the meseta del Guenguel (Lagabrielle et al., 2004).

4.3. Depression and corridors inside the Central Patagonian Cordillera.

At the latitude of the meseta del Cerro Galera, the Patagonian Cordillera lacks high reliefs and exhibits two peculiar topographic anomalies, the depression of Coihaique and the Castor-Pollux oblique corridor, as observed on figures. 5a-b. Contrary to internal depressions of the Lake General Carrera-Buenos Aires and the Lake Cochrane-Pueyrredon farther south, these two topographic lows are not occupied by a post-glacial lake. However, glacial deposits, located 50 km east of Balmaceda testifie Plio-Quaternary glacial stages (Fig. 3).

The depression of Coihaique consists of a low-elevated area bordered by the Cordillera to the west and by the Castor-Pollux oblique corridor to the east. This basin is a sharply defined rhomboidal area, with an area of ca. 400 km^2. Its elevation is comprised between 230 m a.s.l and 600 m a.s.l., with the lowest part located on the northwestern edge of the depression (around 220 m a.s.l, few kilometers south of Coihaique) (Figs. 5a-b) The Coihaique depression is delineated to the south by a topographic jump of more than 1000 meters corresponding to the N120 trending, El Ministro senestral fault (De la Cruz et al., 2003b). This morphological boundary corresponds to the northern ending of the en-échelon thrust system, inherited from the late Oligocene-Middle Miocene compressional episode, as proposed by Lagabrielle et al., (2004). To the west, the depression of Coihaique is separated from the Cordillera by several topographic steps delimited by N120 to N140 trendings faults, a possible continuity of the El Ministro fault system. To the north, the Coihaique depression is bounded by a major NE trending fault system, the Coihaique fault zone, separating the basin from the rest of the Cordillera (De la Cruz et al., 2003b).

Few kilometers to the east, the central low-elevated domain is also characterized by a topographic anomaly corresponding to the Castor-Pollux corridor (Figs 3-7). This corridor is located east of the Coihaique depression and bounds the western border of the meseta del Cerro Galera (Fig 7). It is composed of 2 parts, from the west to the east: (1) a N160 trending corridor where elevations are comprised between 450 m a.s.l and 650 m a.s.l, with a general westwards slope, and by (2) a N40 trending corridor where post-glacial lakes have been emplaced (Lake Castor, Lake Pollux, Lake Frio). Here, elevations are comprised between 500 m a.s.l and 900 m a.s.l, locally affected by southeastwards steps. These two morphological corridors are separated by a major N160 trending fault well observed on the DEM (Fig. 5a-8), which isolates tilted domains.

This area is also characterized by drainage network anomalies. Drainage inversion, with ancient rivers originally flowing towards the east and later, to the west, is a common observation in Central Patagonia. It has been recognized in the Rio Chacabuco, south of the Lake General Carrera-Buenos Aires, formerly flowing to the Atlantic and currently to the Pacific (Péri et al., 2008). Here, drainage inversion is observed in the case of the Rio Simpson (Fig. 8). This river was originally flowing to the Atlantic Ocean, from the high reliefs of the Cordillera to the flat lying “pampas”. It changes its course flowing across the Patagonia Cordillera within Quaternary glacial valley, and crosses the depression of Coihaique (Fig. 8). The Rio Simpson ends its course in the Pacific Ocean at Puerto Aysen.

5. Structure of the Coihaique area

The morphology of the area of Coihaique exhibits a peculiar pattern including peaks, narrow depressions and flat topographically inverted plateaus at an average elevation of 780 meters (Fig. 5). Since Patagonia was covered by thick ice sheets during the Pliocene-Quaternary glacial periods, the most obvious marks of recent tectonic activity have been erased by widespread glacial erosion. This explains why little evidence of recent to active tectonics has been observed. In this section, we discuss the tectonic significance of the sharp boundaries of the internal depression and oblique corridor on the basis of: (1) the interpretation of DEM and satellite images and (2) field tectonic data combined with analysis of geomorphology.

5.1. The depression of Coihaique

Located at around 100 km east of the Liquine-Ofqui Fault Zone, the depression of Coihaique is a low-elevated area bounded to the west by the Patagonian Cordillera. The rhomboidal aspect of this depression strongly suggests a tectonic control even if Quaternary glaciers strongly impacts the present-day morphology. It exposes Cretaceous sedimentary formations and Quaternary deposits (Figs. 3-4), and is bounded to the north by the NE trending Coihaique fault zone. This fault zone, 20 km long, has a dextral transtensional motions (De la Cruz et al., 2003b). It controls the location of Oligocene gabbros aligned along it, suggesting that this fault zone was active during this period (De la Cruz et al., 2003) (Fig. 3). Post-Oligocene testimonies of tectonic activity along this fault zone remain poor because of the lack of pre-Quaternary formations in this area. Nevertheless, this fault zone corresponds to a major topographic boundary between the northern Cordillera and the depression of Coihaique strongly suggesting activity during Pliocene times. To the west, the depression of Coihaique is bounded by several N160 trending accidents, well observed on DEM's image. Here, previous work of de la Cruz et al (2003b) has shown that this fault system affect Cretaceous formations without clear criteria of displacement. But linear aspect of the faults suggests dominant strike-slip and/or normal motion. As shown on the DEM, this fault system controls the morphology of this area characterized by well delimeated blocks close to the Lake Elizalde. To the south, this fault zone connects the northwestern extension of the N120 trending El Ministro fault zone. To the east and approximately 20 km to the western border of the depression, the low-elevated domain of Coihaique is controlled by a major 40 km long, N170 trending fault, named the Foitzik fault (de la Cruz et al., 2003b). Here, microtectonic analysis along fault-related scarps, affecting Jurassic units, indicate a dextral strike-slip motion with normal component (Fig. 9). The lack of recent formations along this fault does not allow us to date the activity of the fault. Nevertheless, as shown on Figs. 8 and 9, this fault controls the present-day morphology of the eastern part of the depression of Coihaique suggesting a recent activity (even if Holocene deposits, along the Rio Simpson, are not affected). To the south, the depression of Coihaique is bounded by the sinistral, N120 trending, El Ministro fault. Here, no evidence of vertical movements has been observed but several minor faults, associated to it, along the Austral Road, exhibit transtensive component along NNW dipping accidents. Finally, the overall outline of the depression of Coihaique with its tectonic-controlled edges suggest a pull-apart structure related to sinistral strike-slip faults.

5.2. The Castor-Pollux oblique corridor

Located on the eastern side of the depression of Coihaique, the Castor-Pollux corridor corresponds to a major morphological boundary between the Patagonian Cordillera and the depositional surface of the meseta del Cerro Galera (Figs. 3-7). This corridor is composed of 2 parts. To the west, the Castor-Pollux corridor is delimited by the Foitzick fault and to the east by the N160 trending, sinistral fault of El Cordon La Galera. This fault, affecting Cretaceous formations, has been described by de la Cruz et al (2003b) as a 30 km long, senestral fault connecting to the south the El Ministro fault. The Cordon la Galera fault is well-observed on the DEM's and marks the topography by a west facing scarp more than 200 meters high. To the east, the Castor-Pollux corridor is characterized by a NE trending branch where N45 trending faults have been defined (Fig. 8). Along this branch, few 5 to 20 km long, normal faults have been mapped, some of them connecting the Cordon la Galera fault. Here, normal faults locally control the emplacement of post-glacial lakes as the lake Pollux and the lake Castor. These faults delimit tilted blocks with NW and SE tilting, as observed on the northern edge of the lake Pollux, where a NE trending block is southeasterly tilted. Several normal faults have been observed right at the front of the western scarp of the molasse of the meseta del Cerro Galera, which control easterly and southeasterly dipping blocks (Fig. 8). But in this area, the lack of recent deposits affected by faulting combined with the absence of kinematic criteria avoid well-constrained timing of the deformation.

6. Discussion-Conclusion

6.1. The Central Patagonia: a peculiar morphological pattern

This compilation of morphological and tectonic data concerns a portion of the Patagonian Cordillera located north of the present-day Chile Triple Junction. This portion of the Cordillera is characterized by a number of striking features, some of them being rarely observed along "normal" subduction belts.

(i) The Central Patagonia, at the latitude of Coihaique, is characterized by a short wavelength topography and highly contrasted reliefs with an average anomalous low elevation of ca. 780 m.

(ii) The morphology of the Coihaique region strongly contrasts with the rest of the northernmost Andes. Here, the Central Patagonia exhibits a central depressed area, the depression of Coihaique, with a mean low elevation of ca. 200 m only, flanked by western and eastern regions of higher elevation. The central depressed area, composed of 2 domains, is also characterized by westward and eastward steps delineated by major faults. This central depression which, displays typical features of tectonically controlled area as pull-apart basin occurs in a position where higher reliefs should be expected in the case of a normal subduction belt. Similar morphostructural pattern was described southward, in the region of the Lake General Carrera-Buenos Aires (Scalabrino et al., 2007; 2009b).

(iii) The eastern part of the Central Patagonia belt, which corresponds to the ancient paleo-piemont of the Cordillera (meseta del Cerro Galera), is now disconnected from the rest of the belt. Disconnection is due to N160 and N45 trending morphotectonic corridors, which localized post Miocene-Pliocene vertical movements.

6.2. Origin and significance of tectonically-controlled area

Located west of the continental Miocene foreland of the meseta del Cerro Galera, the Castor-Pollux tectonically controlled corridor corresponds to a major morphological and tectonic boundary between the Cordillera and the paleo-piemont. As shown previously, this system is composed of N160 trending major strike-slip faults (Foitzick and Cordon la Galera faults), associated with N45 normal branches connecting to the N160 sturctures. This pattern has been also described farther south, close to the Lake General Carrera-Buenos Aires, where similar structures have been observed. Here, 100 km to the south, it has been suggested that this structure corresponds to the frontal thrust system of the Patagonian Cordillera, an en-échelon oblique system, ending with the El Ministro fault located 50 km south of Coihaique (Lagabrielle et al., 2004). This en-échelon thrust system has been the site of compressional tectonics during the Late Oligocene-Middle Miocene ages (Lagabrielle et al., 2004) with the last compressional pulse at around 15 Ma (Lagabrielle et al., 2004; Scalabrino et al., 2009a). The Cordon la Galera fault connects to the south with the El Ministro fault, and to the northeast with the Pollux-Castor fault. This fault system is located 5 to 10 km to the west of the scarp of the Miocene depositional center of the meseta del Cerro Galera now topographically inverted. We suggest, as close to the Lake General Carrera-Buenos Aires, that this fault system has been the Oligocene? - Miocene frontal thrust system, linked to the compressional episode, which occurred in Central Patagonia in relation with the approach of the Chile Ridge to the Chilean trench. Here, oblique compressional tectonics leads to the tectonic uplift of the Cordillera and in turn to the deposition of molasse sediments. Moreover, no testimonies of compressional structures have been observed here except molasse sequences. With an overall view of the Cordillera, the lack of important fold and thrust indicates that this part of the Central Patagonia did not experienced important shortening (Fig. 4). Compressional tectonics was localized along high dipping faults, probably corresponding to Cretaceous normal faults inverted during successive tectonic stages also suggested by De la Cruz et al (2003b).

As observed on the meseta del Cerro Galera, the Miocene molasse sequence is capped, with an erosive contact, by late Miocene-Pliocene till deposits. Here, the age of the fluvio-glacial deposits is younger that the Middle Miocene but contrary to the meseta del Lago Buenos Aires, till deposits are not interbedded with lavas which avoid more precise dating. But, corroborating earlier work by Mercer and Sutter, 1982, Lagabrielle et al (this volume) have shown that the till deposits of the meseta del Lago Buenos Aires, are dated at 7, 5 and 3 Ma. We therefore suggest that this sequence of the meseta del Cerro Galera is likely to be comprised between 7 and 3 Ma. This implies that during the Late Miocene-Pliocene, the morphology of the Central Patagonian Cordillera was totally different from the present-day morphology. The cordillera was connected to the meseta del Cerro Galera, and glaciers and rivers were flowing to the east over a large surface.

Our observations of the present-day morphology show that the meseta del Cerro Galera currently lies 700 m higher than the Castor-Pollux corridor and 100 to 400 m higher than the rest of the Cordillera. This implies that the Castor-Pollux corridor has been the site of post Miocene-Pliocene vertical movements along N45 and N160 normal faults, even if Holocene glacier deeply modified the morphology at some places; notably by erasing recent fault scarps. This event can be viewed as the negative inversion of pre-existing faults in relation with post Miocene-Pliocene extensional/transtensional tectonics, as also suggested farther south, where extensional tectonics can be dated between 3 Ma and 1 Ma (Scalabrino et al., 2009b).

Scalabrino et al (2009b) have shown that tectonic inversion of the frontal region of the Central Patagonia cordillera is also characterized by the collapse of basin located close to the former tectonic front. Here, the Coihaique depression is one of the best examples, with the Lapparent depression farther south, of such a depression. These depressions have polygonal shapes defined by sharp and linear outlines, strongly suggest a pull-apart like structure. Our morphological analysis suggests that the extensional/transtensional event responsible for the collapse of the crust is coeval with the disconnection of the Cordillera from the meseta del Cerro Galera in response to the negative inversion of the frontal region. Here, the development of these depressions led to the deviation of main glaciers which invaded the topographic low areas.

6.3. Evolution of the Central Patagonian Cordillera and the subduction of the Chile Spreading Ridge

The northwards migration of the South Chile Ridge subduction induces the subduction of several segments especially at 6, 3 and 0.3 Ma leading to the development of a large asthenospheric slab window beneath the upper plate. As suggested by Breitsprecher and Thorkelson (2008), the slab window has developed since 3 Ma at the latitude of the present-day triple junction, in the area of the Lake General Carrera-Buenos Aires, 100 km south of Coihaique. Here, it has been recently proposed that negative tectonic inversion of the Cordillera, which occurred between 3 Ma and 1 Ma, was linked to the slab-window at depth (Fig. 11) (Scalabrino et al., 2009b).

The morphostructural evolution of the Central Patagonia at the latitude of Coihaique is linked to the subduction of the South Chile Ridge since the Oligocene. Three stages have been outlined:

1. During the Oligocene-Middle Miocene, the South Chile Ridge approaches the Chile trench and starts his subduction at around 15 Ma at the southern tip of Patagonia. Tectonic coupling at the trench increases coevally and drives oblique compressional tectonics in the upper plate. During this period, the Patagonian Cordillera is characterized by tectonic uplift with low rate of shortening and by the deposition of continental molasse to the east including the molasse of the meseta del Cerro Galera (Fig. 10a). Here, tectonic uplift is controlled by high dipping faults, corresponding to Cretaceous normal faults, inverted during the compressional stage. The late compressional pulse occurs at around 15-12 Ma as shown by the age of the upper bed of the molasse sequence capped by fluvio-glacial deposits. This timing is also recorded farther south along the N-S morphotectonic front south of the lake General Carrera-Buenos Aires (Lagabrielle et al., 2004; Scalabrino et al., 2009a).
2. Following the compressional episode, major glaciations affect the Central Patagonia, from this area to the southern part of Patagonia as shown by Miocene-Pliocene till deposits observed on topographically-inverted mesetas (Meseta del Lago Buenos Aires). At that time, the Cordillera is characterized by large glaciers flowing to the east over a regional surface

(Fig. 10b). In the present study area, testimonies of late Miocene-Pliocene glacier are observed on the meseta del Cerro Galera, where a till sequence of 300 m thick containing granite and basalt pebbles overlie the foreland molasse (Fig. 6).

3. During the Pliocene, the Central Patagonia cordillera has experienced drastic morphological changes, related to the negative tectonic inversion of the front of the belt and to the development of internal pull-apart basins (Fig. 10c). Vertical movements along oblique corridor lead to the disconnection of eastern depositional center from the rest of the Cordillera. Development of topographic low-elevated domains inside the Cordillera also induces drastic changes on the glacier network. Tectonic depressions have driven the course of the Pleistocene-Holocene glaciers (Fig. 10c). At this time, the slab-window is under the lake General Carrera-Buenos Aires region, at the latitude of the present-day triple junction, where negative tectonic inversion has been observed (Scalabrino et al., 2007; 2009b; Lagabrielle et al., this volume).

In the present-day predicted position of slab-window according to the 2D Neogene kinematic reconstruction of Breitsprecher and Thorkelson (2008), the area of Coihaique is not located above the slab-window (Fig. 11). Contrary to the southernmost region, this area do not exhibits Pliocene OIB lava sequence as the meseta del Lago Buenos Aires where post 3 Ma lavas have been related to the slab-window (Guivel et al., 2006). But, geophysical evidence as, high heat flow reaching 160 mW/m2 (Hamza and Munoz, 1996), large negative Bouguer anomaly (Murdie et al., 2000) and low Vs velocities at 100 km depth revealed by tomography (Heintz et al., 2005) suggest the presence of hot mantle beneath a thin lithosphere at a regional-scale. Nevertheless, the similar structural and morphological pattern of the Coihaique region suggests also that the upwelling of hot mantle through the slab-window can influenced the mantle dynamics by northwards asthenospheric spreading beneath Central Patagonia. In this context, the Coihaique region represents the north tip of an extensional domain propagating northwards ahead the northern boundary of the slab window, in continuity with the area of the Lake General Carrera-Buenos Aires (Fig. 11). Similar pattern was also described 50 km farther north, close to the Lago Fontana fold and thrust belt, where Folguera and Iannizzotto (2004) have suggested extensional tectonics since 5 Ma. Upwelling of hot mantle beneath Patagonia is likely to have induced drastic changes in the mantle dynamics and in turn led to the weakening of the crust and, to local and regional collapse of the Central Patagonian Cordillera.

Acknowledgements

This research was funded by grants from the Chilean-French ECOS-CONICYT program (project C05U01) and CNRS-INSU DyETI and Reliefs programs. We also thank the field assistance of Leonardo Zuñiga Díaz.

References

Bangs, N.L., Cande, S.C., Lewis, S.D., Miller, J.J., 1992. Structural framework of the Chile margin at the Chile Ridge collision zone. Proc. Ocean Drilling Program. Initial report 141, 11-21.

Bell, C.M., Suarez, M., 1997. The lower Cretaceous Apeleg Formation of the Aisen Basin, Southern Chile. Tidal sandbar deposits of an epicontinental sea. Revista Geologica de Chile, Vol. 24, No. 2, p. 203-225.

Bradley, D., Kusky, T., Haeussler, P., Goldfard, R., Miller, M., Dumoulin, J., Nelson, S.W., and Karl, S., 2003. Geologic signature of early Tertiary ridge subduction in Alaska. In Sisson, V.B., Roeske, S.M., and Palvis, T.L., eds., Geology of a transpressional orogen developed during ridge-trench interaction along the North pacific margin: Boulder, Colorado, Geological Society of America Special paper 371, p. 19-49.

Breitsprecher, K. and Thorkelson, D.J., 2008. Neogene kinematic evolution of the Nazca–Antarctic–Phoenix slab windows beneath Patagonia and the Antarctic Peninsula. Tectonophysics. doi: 10.1016/j.tecto.2008.02.013

Cande, S.C., Leslie, R.B., 1986. Late Cenozoic tectonics of the Southern Chile Trench. J. Geophys. Res. 91, 471-496.

Cande, S.C., Leslie, R.B., Parra, J.C., Hobart, M., 1987. Interaction between the Chile ridge and the Chile trench : geophysical and geothermal evidence. J. Geophys. Res. 92, 495-520.

Cembrano, J., Hervé, F., 1993. The Liquine-Ofqui fault zone : A major Cenozoic strike-slip duplex in Southern Andes. Second International Symposium on Andean Geodynamics, Oxford (UK), extended abstract, ORSTOM editions.

Cembrano, J., Hervé, F., Lavenu, A., 1996. The Liquine-Ofqui fault zone : A long-lived intra-arc fault system in Southern Chile. Tectonophysics 259, 207-224.

Cembrano, J., Lavenu, A., Reynolds, P., Arancibia, G., Lopez, G., Sanueza, A., 2002. Late Cenozoic transpressional ductile deformation north of the Nazca-Sout America-Antarctica triple junction. Tectonophysics 354, 289-314.

Charrier, R., Linares, E., Niemeyer, H., Skarmeta, J., 1979. K-Ar ages of basalt flows of the Meseta Buenos Aires in southern Chile and their relation to the southeast Pacific triple junction. Geology 7, 436-439.

De La Cruz, R., Suárez, M., Morata, D., Espinoza, F. and Troncoso, A., 2003a. El Cenozoico del Lago General Carrera, Aysén, Chile (46º30'-47º15'S): estratigrafía y tectónica. *In Congreso Geológico Chileno No. 10,* Concepción.

De La cruz, R., Suarez, M., Belmar, M., Quiroz, P.T., Bell, M., 2003b. Geologia del area Coihaique-Balmaceda, Región Aisén del General Carlos Ibáñez del Campo, Escala 1:100.000. *Servicio Nacional de Geología y Minería, Serie Geología Básica, Carta Geológica de Chile.* Santiago, Chile.

De La Cruz, R. and Suárez, M., 2006. Geología del área Puerto Guadal-Puerto Sánchez, Región Aisén del General Carlos Ibáñez del Campo, Escala 1:100.000. *Servicio Nacional de Geología y Minería, Serie Geología Básica, Carta Geológica de Chile.* Santiago, Chile.

De La Cruz, R., Welkner, D., Suárez, M. and Quiroz, D., 2004. Geología del área oriental de las hojas Cochrane y Villa O'Higgins, Región Aisén del General Carlos Ibáñez del Campo, escala 1:250.000. *Servicio Nacional de Geología y Minería, Serie Geología Básica, Carta Geológica de Chile,* 85. Santiago, Chile.

DeMets, C., Gordon, R.G., Argus, D.F., Stein, S., 1990. Current plate motions. Geophys. J. Int. 101, 425-478.

Demant, A., Hervé, F., Pankhurst, R.J., Suarez, M., 1996. Geochemistry of early tertiary back-arc basalts from Aysen, southern Chile (44°-46°S) : geodynamic implications. In International Sympsium of Andean Geodynamics, NO.3, Proceedings, p. 555-558. Saint Malo.

Dickinson, W.R., and Snyder, W.S. 1979. Geometry of subducted slab related to the San Andreas transform. Journal of Geology, v.87, p.609-627.

Flint, F.F., Prior, D.J., Agar, S.M., Turner, P., 1994. Stratigraphic and structural evolution of the tertiary Cosmelli basin and its relationships to the Chile Triple Junction. Journal of Geological society of London 151, p. 251-268.

Folguera, A., Iannizzotto, N.F., 2004. The Lagos La Plata and Fontana fold-and-thrust belt: long-lived orogenesis at the edge of western Patagonia. Journal of South American Earth Sciences 16, p. 541-566.

Forsythe, R.D., Nelson, E.P., 1985. Geological manifestations of ridge collision : évidence from the Golfo de Penas- Taitao basin, southern Chile. Tectonics 4, 477-495.

Garret, S.W., Storey, B.C., 1987. Lithospheric extension on the Antarctica Peninsula during Cenozoic subduction. In Extension in the basin and Range Province and East Pacific Margin, Geological Society, London, Special Publications, v. 28, pp. 419-431.

Gorring, M., Kay, S., Zeitler, P., Ramos, V., Rubiolo, D., Fernandez, M., Panza, J., 1997. Neogene Patagonian plateau lavas : continental magmas associated with ridge collision at the Chile Triple Junction. Tectonics 16, 1-17.

Gripp, A.E., Gordon, R.G., 1990. Current plate velocities relative to the hotspots incorporating the NUVEL-1 global plate motion model. Geophysical Research Letters 17, 1109-1112.

Guivel, C., Morata, D., Pelleter, E., Espinoza, F., Maury, R.C., Lagabrielle, Y., Polvé, M., Bellon, H., Cotten, J., Benoit, M., Suarez, M., de la Cruz, R., 2006. Miocene to Late Quaternary Patagonian basalts (46°-47°S) : Geochronometric and geochemical evidence for slab tearing due to active spreading ride subduction. Journal of Volcanology and Geothermal research 149, 346-370.

Gutierrez, F., Gioncada, A., Gonzalez Ferran, O., Lashen, A., mazzuoli, R., 2005. The Hudson volcano and surrounding monogenetic centers (Chilean Patagonia): An example of volcanism associated with ridge-trench collision environment. Journal of Volcanology and Geothermal Research 149, 346-370.

Halpern, M., Fuenzalida, R., 1978. Rb-Sr geochronology of a transect of the Chilean Andes between latitudes 45°S and 46°S. Earth and Planetary Science Letters, vol.41, p. 60-66.

Hamza, V.M., Munoz, M., 1996. Heat flow map of South America. Geothermics 25(6), 599-646.

Heim, A., 1940. Geological observations in the Patagonian Cordillera (Preliminary Report). Eclogae Geologicae Helvetiae, vol.33, p. 25-51. Traducion in Boletin Minero, vol.54, No.507, p.646-649.

Heintz M., Debayle, E., Vauchez. A., 2005. Upper mantle structure of the South America continent and neighboring oceans from surface wave tomography. Tectonophysics, 406, 115-139.

Herron, E.M., Cande, S.C., Hall. B.R., 1981. An active spreading center collides with a subduction zone ; geophysical survey of the Chile margin triple junction. Memoir-Geological Society of America 154, 683-701.

Hervé, F., 1994. The Southern Andes between 39°S and 44°S latitude : the geological signature of a transpressive tectonic regime related to a magmatic arc. In : Reutter, K-J., Scheuber, E., Wigger, P.J., (Eds), Tectonics of the Southern central Andes. Springer, Berlin, pp.243-248.

Introcaso, A., Pacino, M.C., Guspi, F., 1996. The Argentina- Chile Andes. Crustal thickness, isostasy, shortening and anomaly prediction from gravity studies. Third ISAG, St Malo (France).

Lagabrielle, Y., Suarez, M., Rossello, E.A., Hérail, G., Martinod, J., Régnier, M., de la Cruz, R., 2004. Neogene to Quaternary tectonic evolution of the Patagonian Andes at the latitude of the Chile Triple Junction. Tectonophysics 385, 211-241.

Lagabrielle, Y., Suarez, M., Malavieille, J., Morata, D., Espinoza, F., Maury, R., Scalabrino, B., de la Cruz, R., Rossello, E., Barbero, L., Bellon, H., 2007. Pliocene extensional tectonics in Eastern Central Patagonian Cordillera : geochronological constraints and new field evidence. Terra Nova.

Lagabrielle, Y., Scalabrino, B., Suarez, M., Ritz, J.F. Mio-Pliocene glaciations of Central Patagonia: New evidence and tectonic implications. Submitted to Andean Geology, special volume (this volume).

Montgomery, D.R., Balco, G., Willett, S.D., 2001. Climate, tectonics, and morphology of the Andes. Geology, vol.29, No.7, pp. 579-582, DOI: 10.1130/0091-7613(2001).

Morata, D., Barbero, L., Suarez, M., de la Cruz, R., 2002. Early Pliocene magmatism and high exhumation rates in the Patagonian Cordillera (46°40'S) : K-Ar, and fission track data. International Symposium on Andean Geology (ISAG), Toulouse, France, pp. 433-436.

Murdie, R., Styles, P., Prior, D.J., Daniel, A.J., 2000. A new gravity map of Southern Chile and its preliminary interpretation. Revista Geologica de Chile 27 (1), 49-63.

Naranjo, J.A., Moreno, H., Banks, N., 1993. La erupcion del volcan Hudson en 1991 (46°S), Region XI, Aysen. Servicio nacional de Geologia y Mineria, Boletin, No. 44, 50 p.

Nelson, E., Forsythe, R., Diemer, J., Allen, M., Urbina, O., 1993. Taitao ophiolite : a ridge collision ophiolite in the forearc of the southern Chile (46°S). Revista Geologica de Chile 20(2), 137-165.

Niemeyer, H., Skarmeta, J., Fuenzalida, R and Espinosa, W. 1984. Hojas Peninsula de Taitao y Puerto Aisen, Region de Aisen del General Carlos Ibanez del Campo. Carta Geologica de Chile, 60-61, 1:500.000. Sevicio Nacional de geololgia y Mineria, Chile.

Pankhurst, R.J., Weaver, S.D., Hervé, F., Larrondo, P., 1999. Mesozoic-Cenozoic evolution of the North Patagonian Batholith in Aysen, southern Chile. Journal of the Geological Society (London), 156.

Parada, M.A., Lashen, A., Palacios, C., 2001. Ages and geochemistry of Mesozoic-Eocene back-arc volcanic rocks in the Aysen region of the Patagonian Andes, Chile. Revista Geologica de Chile, vol.28, No.1, p. 25-46.

Pardo-Casas, F., Molnar, P., 1987. Relative motion of the Nazca (Farallon) and South America plates since Late Cretaceous time. Tectonics 6 no 3, 233-248.

Péri, V.G., Rossello, E.A., Lagabrielle, Y., Scalabrino, B., 2008. Geomorfologia cuantitativa aplicada sobre modelos digitales de elevacion al este del Punto Triple Chile (Patagonia). XVII Congreso Geologico Argentino, poster, Jujuy, Argentina.

Ramos, V.A., 1976. Estratigrafia de los Lagos La Plata y Fontana, Provincia de Chubut, Republica Argentina. In Congreso Geologico Chileno, No.1, Actas, vol.1, p A43-A63. Santiago.

Ramos, V.A., 1989. Andean foothills structures in the northern Magallanes Basin, Argentina. American Association of Petroleum Geologist Bulletin 73, 887-903.

Ramos, V., Kay, S.M., 1992. Southern Patagonian plateau basalts and déformation : backarc testimony of ridge collision. Tectonophysics 205, 261-282.

Ray, F.M., 1996. Stratigraphical and structural evolution of Tertiary backarc basins in Southern Chile (44°S-47°S). University of Liverpool, England, 208 pp. Unpublished PhD Thesis.

Roseneau, M., Melnick, D., Echtler, H., 2006. Kinematic constraints on the intra-arc shear and strain partitionning in the southern Andes between 38°S and 42°S latitude. Tectonics vol. 25, TC4013, doi: 10.1029/2005TC001943.

Scalabrino, B., Lagabrielle, Y., de la Rupelle, A., Malavieille, J., Polvé, M., Espinoza, F., Morata, D., Suarez, M., 2009a. Subduction of an Active Spreading Ridge beneath Southern South America: A review of the Cenozoic geological records from the Andean foreland, Central Patagonia (46-47°S). In S. Lallemand and F. Funiciello (eds.), Subduction Zone Geodynamics, DOI 10.1007/978-3-540-87974-9, Springer-verlag Berlin Heidelberg, pp. 227-246.

Scalabrino, B., Ritz, J.F., Lagabrielle, Y., 2009b. Using glacial morphology to constrain the impact of the Chile active Spreading Ridge subduction in Central Patagonia. Geophysical Research Abstracts, oral, vol. 11, EGU 2009-8518, 2009. EGU General Assembly 2009.

Scalabrino, B., Lagabrielle, Y., Malavielle, J., Dominguez, S., Espinoza, F., Suarez, M., Morata, D., Rossello, E. (2007). Impact of the spreading ridge subduction on the morphotectonic evolution of the Patagonian Cordillera since 15 Ma (latitude of the Chile Triple Junction, CTJ) ; GEOSUR 2007, *International Geological Congress on the Southern Hemisphere*, Santiago, Chile.

Singer, B.S., Ackert, R.P., Guillou, H., 2004. $^{40}Ar/^{39}Ar$ and K/Ar chronology of Pleistocene glaciations in Patagonia. Geological Society of America 116, no. 3/4, 434-450.

Somoza, R., 1998. Updated nazca (Farallon)-South American relation motion during the last 40 Ma. Implications for mountain building in the Central Andean region. Journal of South American Earth Sciences 11, 211-215.

Stern, C.R., Zartman, F.A., Futa, K., Zartman, R.E., Peng, Z., Kyser, T.K. 1990. Trace-element and Sr, Nd, Pb, and O isotopic composition of Pliocene and Quaternary alkali basalts of the Patagonian Plateau lavas of the Southermost South America. Contributions to Mineralogy and Petrology 104, 294-308.

Suarez, M., de la Cruz, R., 1994a. Estratigrafia y paleogeografia mesozoica de Aisen nororiental (45°S-46°S), Chile. In Congreso Geologico Chileno, No.7, Actas, vol.1, p. 538-542. Concepcion.

Suarez, M., de la Cruz, R., 1996. Estratigrafia y tectonica de la zona sureste del Lago General Carrera (46°30'-47°S), Cordillera Patagonica, Chile. In Congreso Geologico Argentino, No.13 y Congreso de Exploracion de Hidrocarburos, No.3, Actas, vol. 1, p. 425-432. Buenos Aires.

Suarez, M., de la Cruz, R., 2000. Tectonics in the eastern central Patagonian Cordillera (45°30'-47°30'S). Journal of the Geological Society (London) 157, 995-1001.

Suarez, M., de la Cruz, R., 2001. Jurassic to Miocene K-Ar dates from eastern central Patagonian Cordillera plutons, Chile (45°-48°S). Geological Magazine 138 (1), 53-66.

Tassara A., Yanez, G., 2003. Relacion entre el espesor elastico de la litosfera y la segmentacion tectonica del margen andino (15°-47°S). Revista Geologica de Chile, vol 30, no.2, p. 159-186.

Ton-That, R., Singer, B., Mörner, N-A., Rabassa, J., 1999. Datacion de lavas basálticas por 40Ar/39Ar y geologia glacial de la region del Lago Buenos Aires, província de Santa Cruz, Argentina; Asociacion Geológica Argentina, Revista (Buenos Aires) 54 (4), 333-352.

Tebbens, S.F., Cande, S.C., 1997. Southeast Pacific tectonic evolution from the early Oligocene to Present. Journal of Geophysical Research 102, 12061-12084.

Tebbens, S.F., Cande, S.C., Kpovacs, L., Parra, J.C., Labrecque, J.L., Vergara, H., 1997. The Chile Ridge : A tectonic framework. Journal of Geophysical Research 102, 12035-12059.

Thomson, S.N., Hervé, F., Stockhert, B., 2001. Mesozoic-Cenozoic denudation history of the patagonian Andes (Southern Chile) and its correlation to different subduction processes. Tectonics 20, 693-711.

Thorkelson D.J.; 1996. Subduction of diverging plates and the principles of slab window formation, *Tectonophysics* 255, pp. 47–63.

Figure Captions

Figure 1. Location of the study area in Central Patagonian Cordillera (blue frame) and simplified tectonic features of the southern South America (see Scalabrino et al., 2009 for references). The predicted location of the Patagonian slab window beneath the South American plate is also shown (red lines) (after Breitsprecher and Thorkelson, 2008). Land topography corresponds to a Global Digital Elevation Model derived from *GTOPO30 EROS Data Center-USGS*, combined to the bathymetry data of the East Pacific Ocean of Smith and Sandwell (1997).

Figure 2. a) Simplified map of central Patagonia showing the main morphostructural domains discussed in the text including: the Cordillera, the meseta and the pampa domain. The black frame corresponds to the study area. LOFZ: Liquine-Ofqui Fault Zone; NIC: Northern Ice Cap; LGCBA: Lake General Carrera-Buenos Aires; LCP: Lake Cochrane-Pueyrredon; LL:

Lake Lapparent. b) Plate tectonic setting of the South America and main features of the subducting South Chile Ridge, including transform fault zones (FZ) and active spreading segments (thick black lines) (adapted from Tebbens et al., 1997; Ramos, 1989; DeMets et al., 1990; Cembrano et al., 1996; Guivel et al., 1999). Location of the 2D predicted Patagonian slab-window is shown by grey area (after Breitsprecher and Thorkelson, 2008). CTJ: Chile Triple Junction.

Figure 3. Geological map of the Central Patagonian Cordillera in the Coihaique-Balmaceda area (adapted from De La Cruz et al., 2003). Line AA' indicates the position of regional section of Fig. XX. CF: Castor Fault; PF: Pollux fault; FFZ: Foitzick Fault Zone; EMFZ: El Ministro Fault Zone; CFZ: Coihaique Fault Zone. LA: Lake Atravesado; LE: Lake Elizalde; LLP: Lake La Paloma; LP; Lake Pollux; LC: Lake Castor; LF: Lake Frio.

Figure 4. Regional W-E trending cross-section of the Central Patagonian Cordillera at the latitude of the meseta del Cerro Galera (latitude S45°45'). Line AA' in Fig. 3 (modified from De La Cruz et al., 2003).

Figure 5. a) Digital Elevation Model (DEM SRTM-90 m) of the Central Patagonian Cordillera between 45°S and 46°5'S, showing the location of Coihaique (Chile), Balmaceda (Argentina) and the mesetas. LGCBA: Lake General Carrera-Buenos Aires; DLL: Depression of the Lake Lapparent; LOFZ: Liquine-Ofqui Fault Zone. b) Numerical W-E trending topographic section of the Central Patagonian Cordillera along the Coihaique-meseta del Cerro Galera area. Here, the different domains discussed in the text are also shown.

Figure 6. Some stratigraphic features of the meseta del Cerro Galera (location in Fig. 2). a) Panoramic view of the western edge of the meseta del Cerro Galera, exposing Miocene foreland molasse of the Cerro Formation. b-c) Top of the meseta del Cerro Galera at around 1460 meters where Late Miocene-Pliocene westerly-derived fluvio-glacial deposits overlie foreland molasses. d-e) Photographies of the Late-Miocene-Pliocene fluvio-glacial deposits characterized by heterometric and polygenic pebbles with sandy matrix.

Figure 7. Photograph of the Castor-Pollux oblique corridor localized east of the Patagonian Cordillera. This photograph, which was taken from the top of the meseta del Cerro Galera, shows the disconnection of the Miocene depositional center from the rest of the western Cordillera.

Figure 8. Digital Elevation Model (DEM SRTM-90m) of the depression of Coihaique and of the Castor-Pollux tectonic-controlled corridor. It shows the main structural boundary and the disconnection of the meseta del Cerro Galera from the rest of the Cordillera. It exhibits also the drainage inversion of the Rio Simpson related to the negative inversion of the Patagonian Cordillera.

Figure 9. Photograph of the northern edge of the depression of Coihaique along the Foitzick fault zone. It shows the control of the depression by this dextral, with normal component, fault.

Figure 10. 3D schematic diagrams illustrating the evolution of the Patagonian Cordillera since the Oligocene at the latitude of Coihaique.

Figure 11. Illustration of the consequence of the subduction of the South Chile Ridge north of the Chile Triple Junction. Our observations suggest a northward propagation of the extensional tectonics as represented by a red arrow. The position of the Patagonian slab window is shown by a grey area (after Breitsprecher and Thorlkelson, 2008). Red arrow indicates the location of the tectonically-inverted Cordillera.

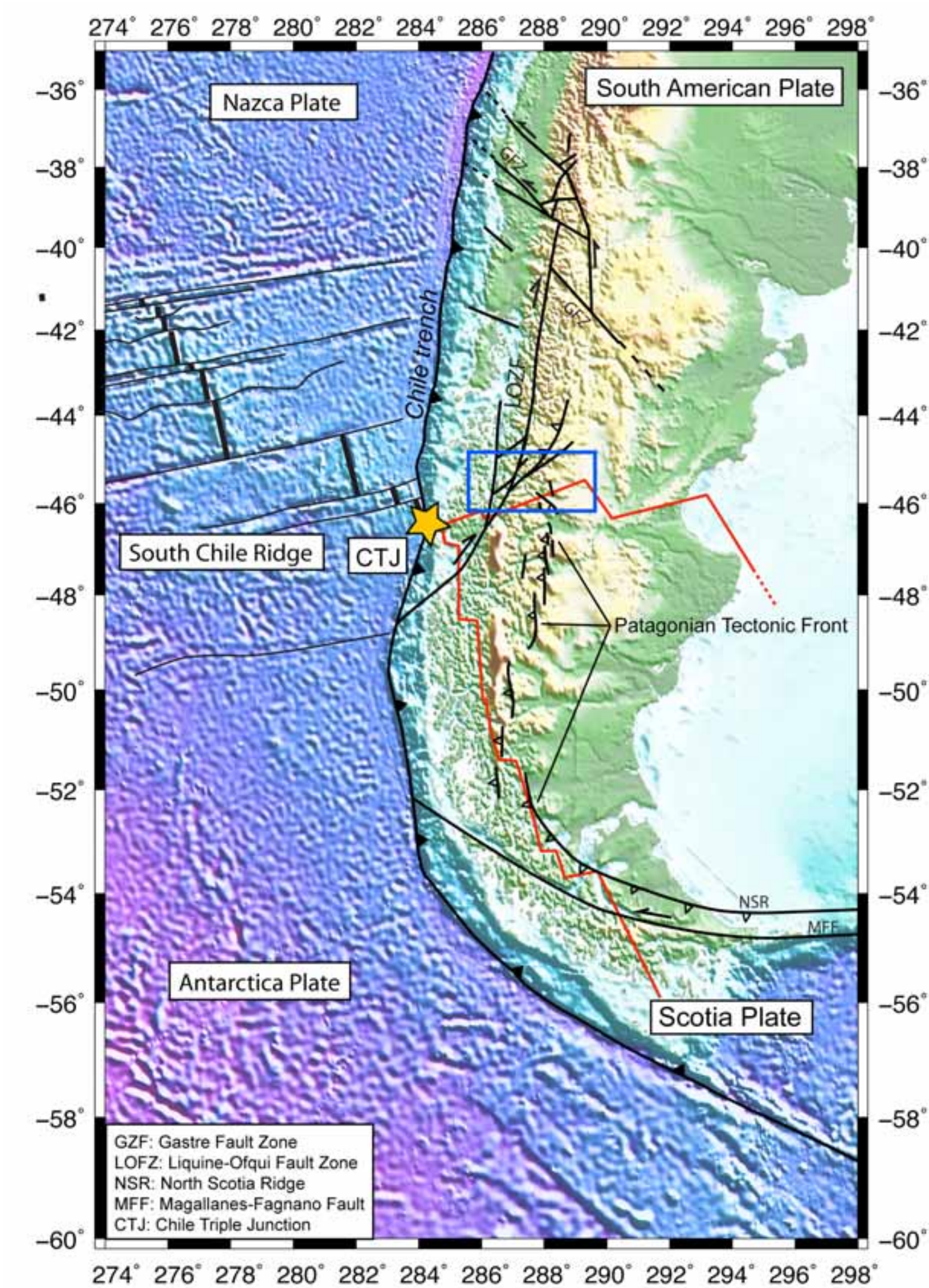

Fig. 1 Scalabrino et al.

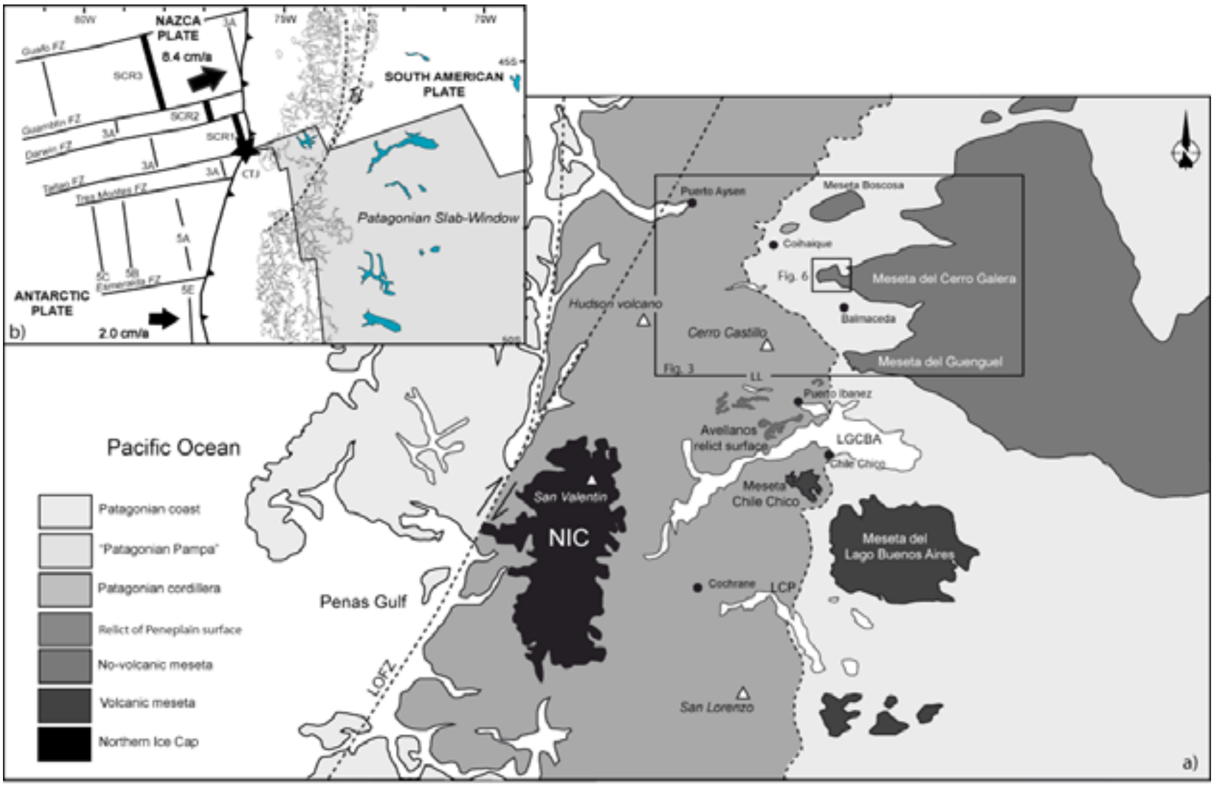

Fig.2 Scalabrino et al.

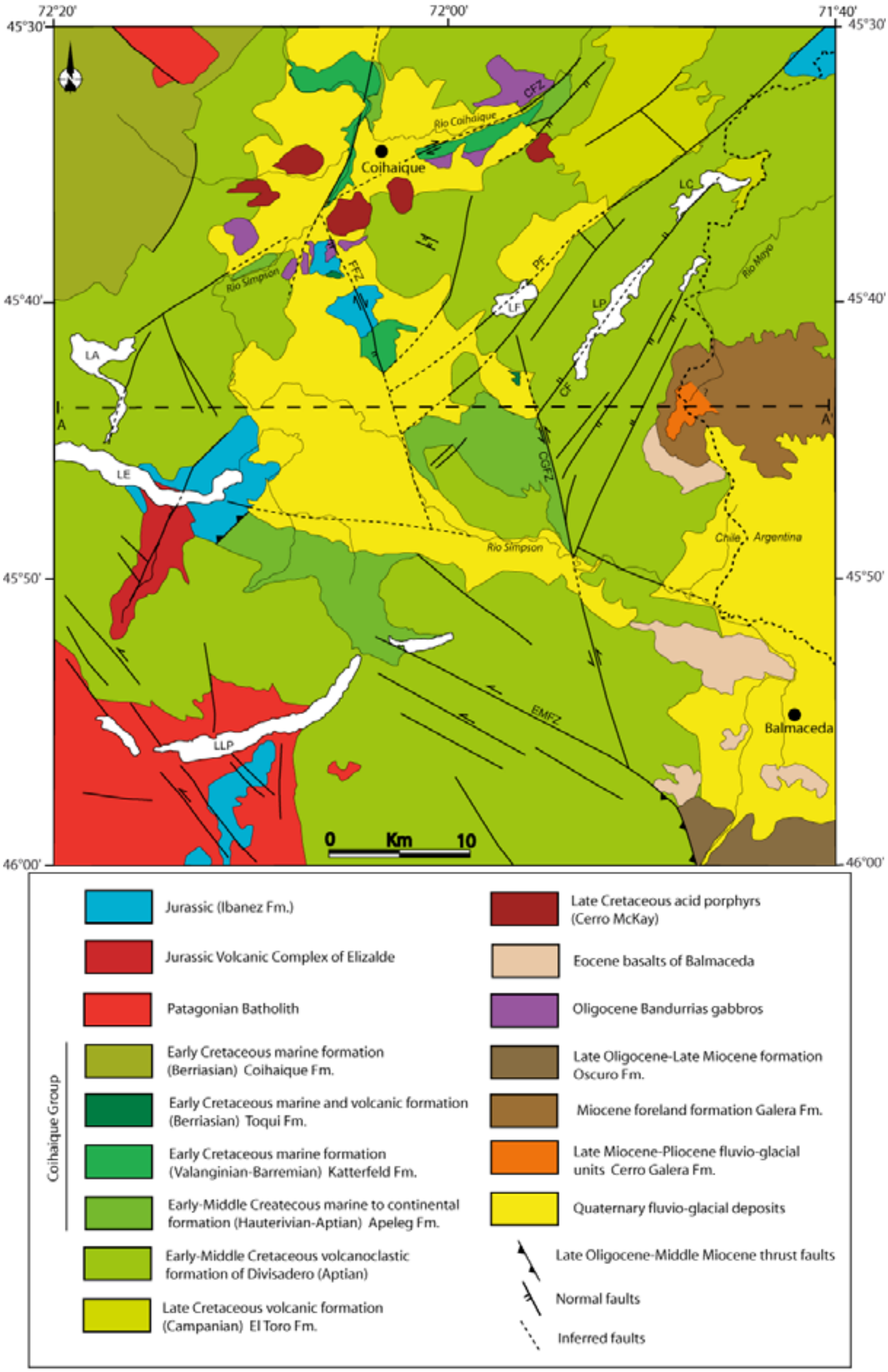

Figure 3 Scalabrino et al.

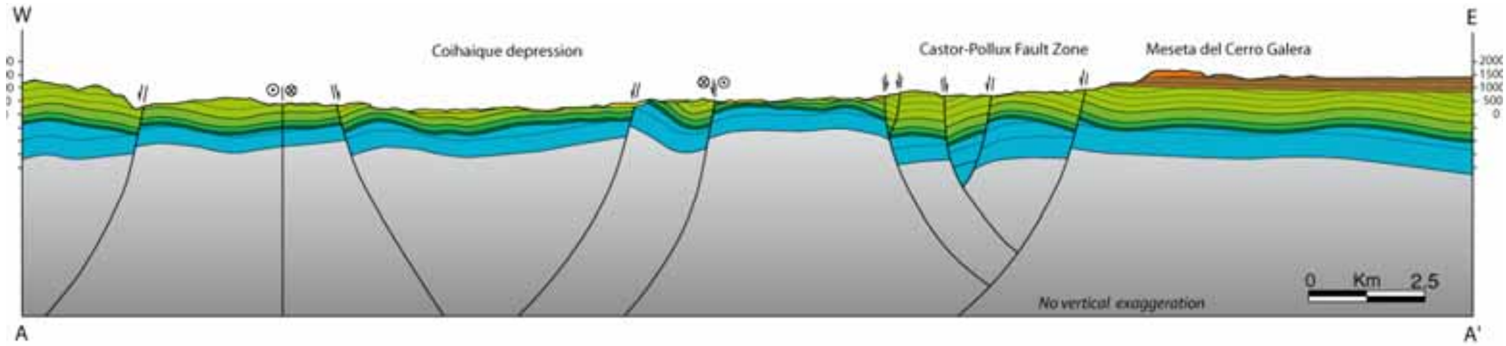

Fig. 4 Scalabrino et al.

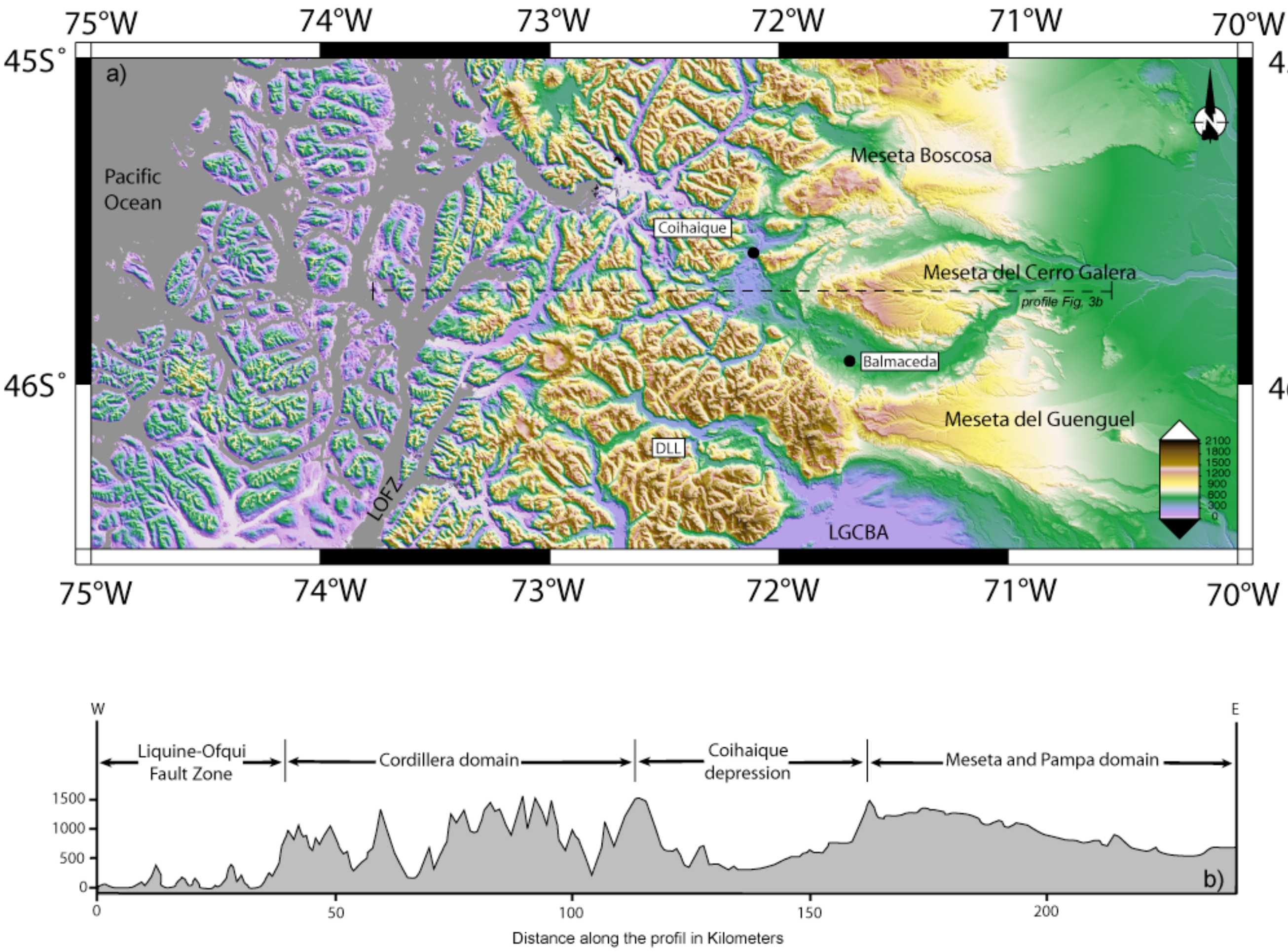

Fig. 5 Scalabrino et al.

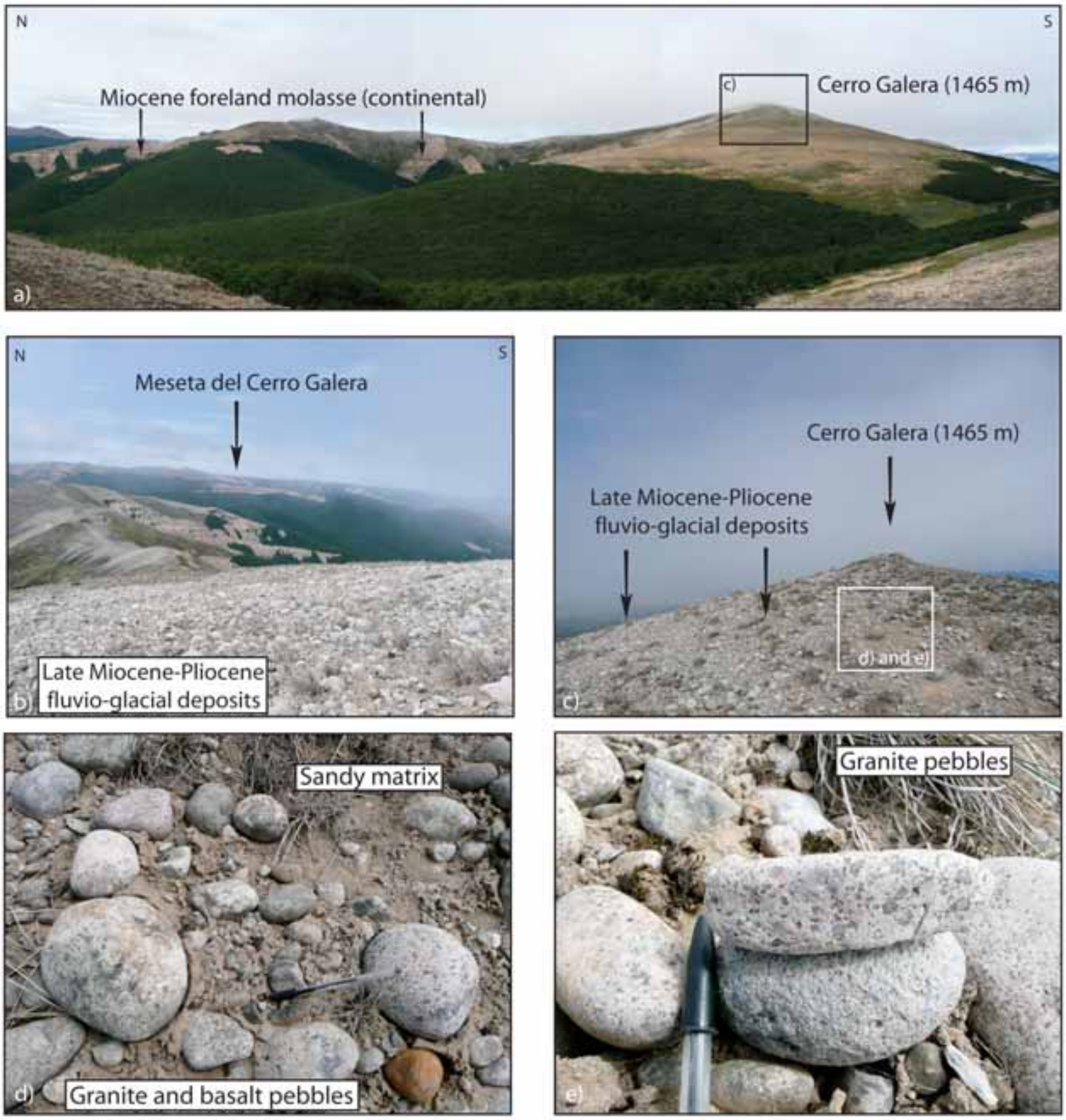

Fig. 6 Scalabrino et al.

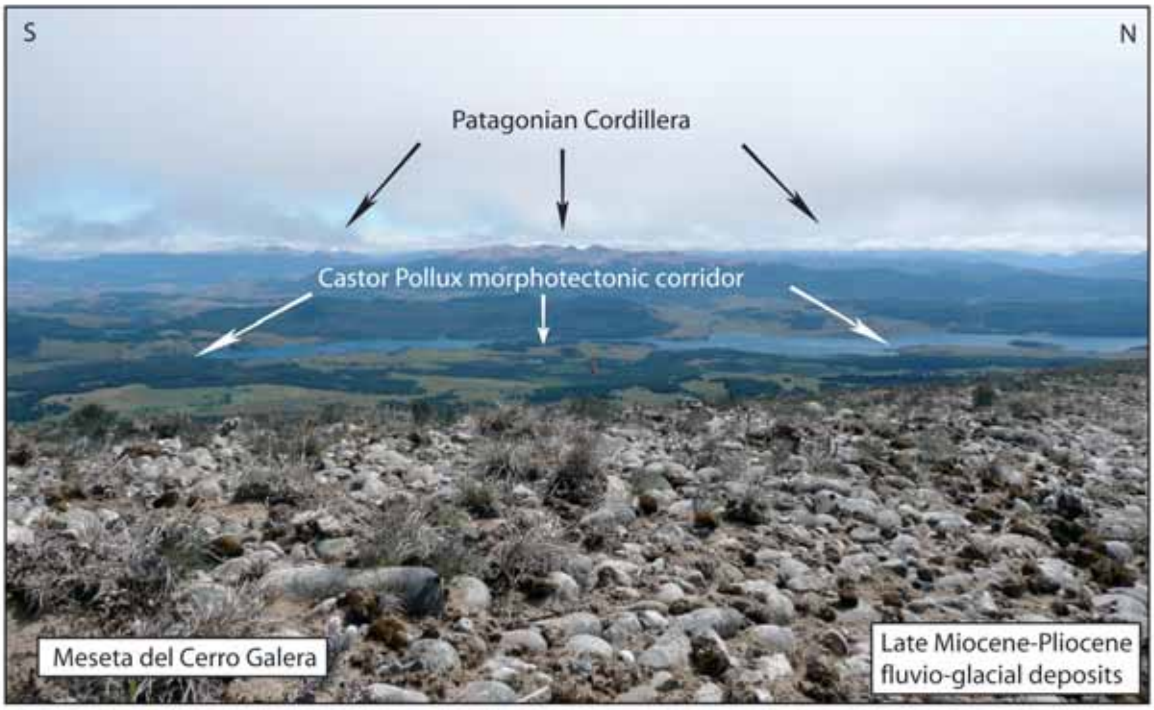

Fig. 7 Scalabrino et al.

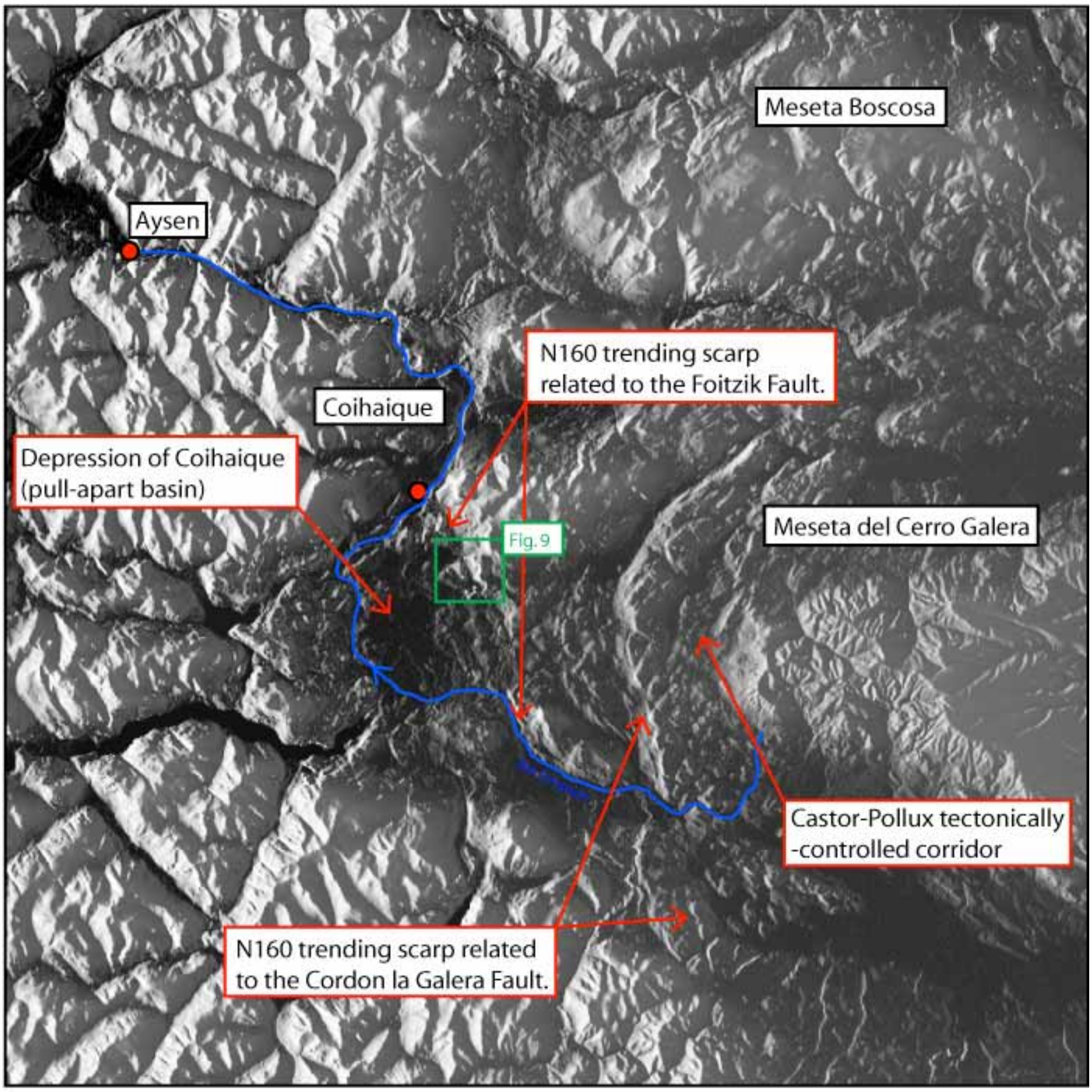

Fig. 8 Scalabrino et al.

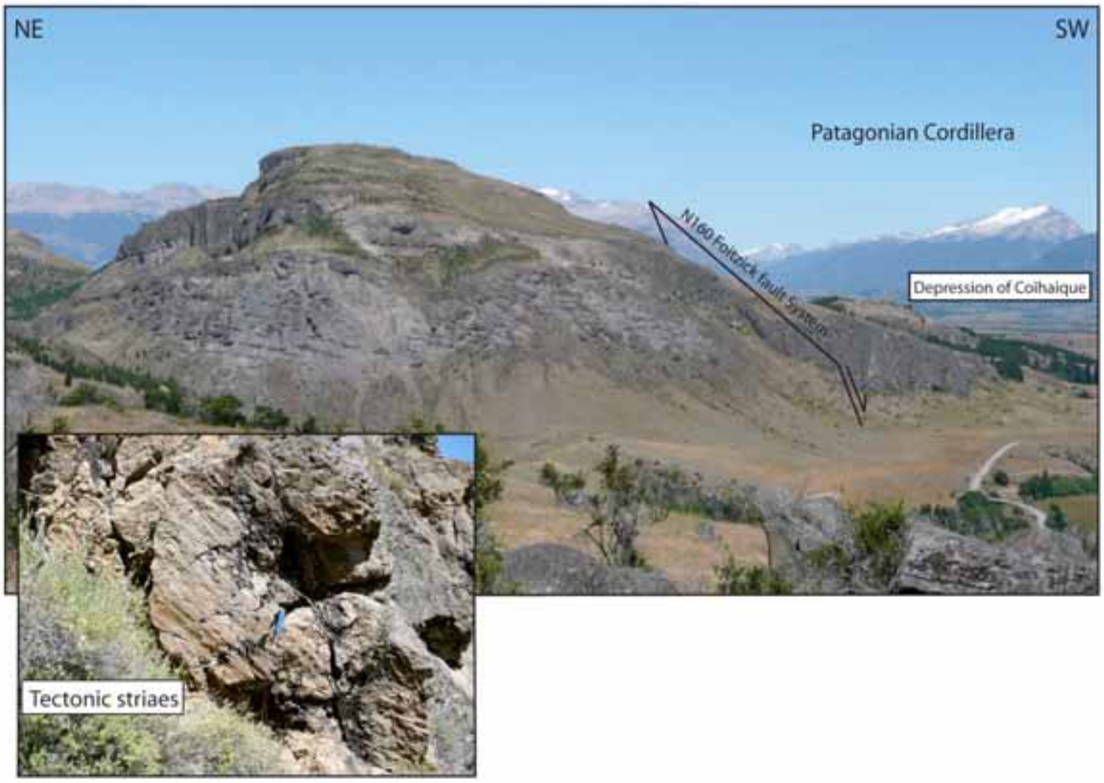

Fig. 9 Scalabrino et al.

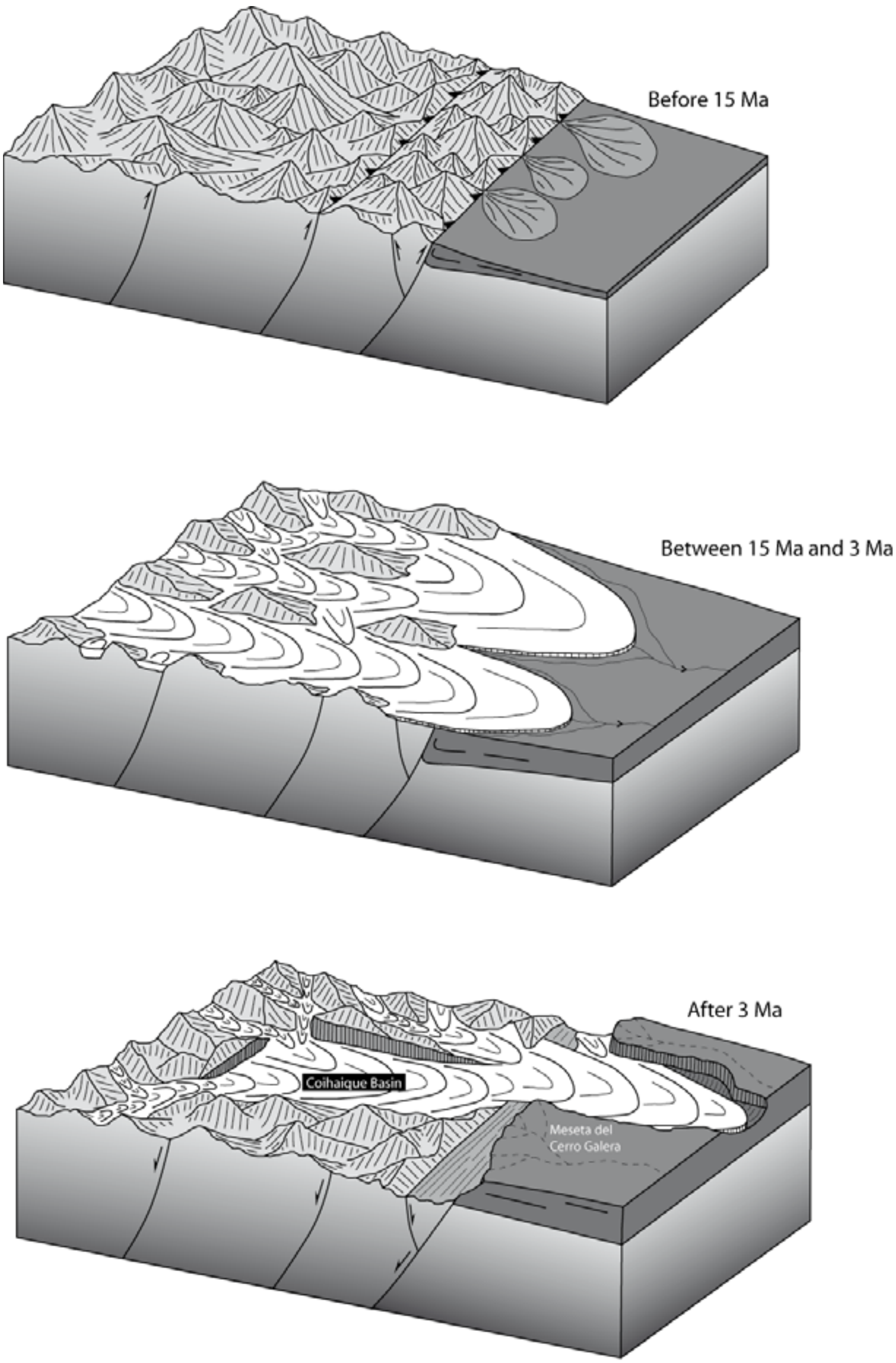

Fig. 10 Scalabrino et al.

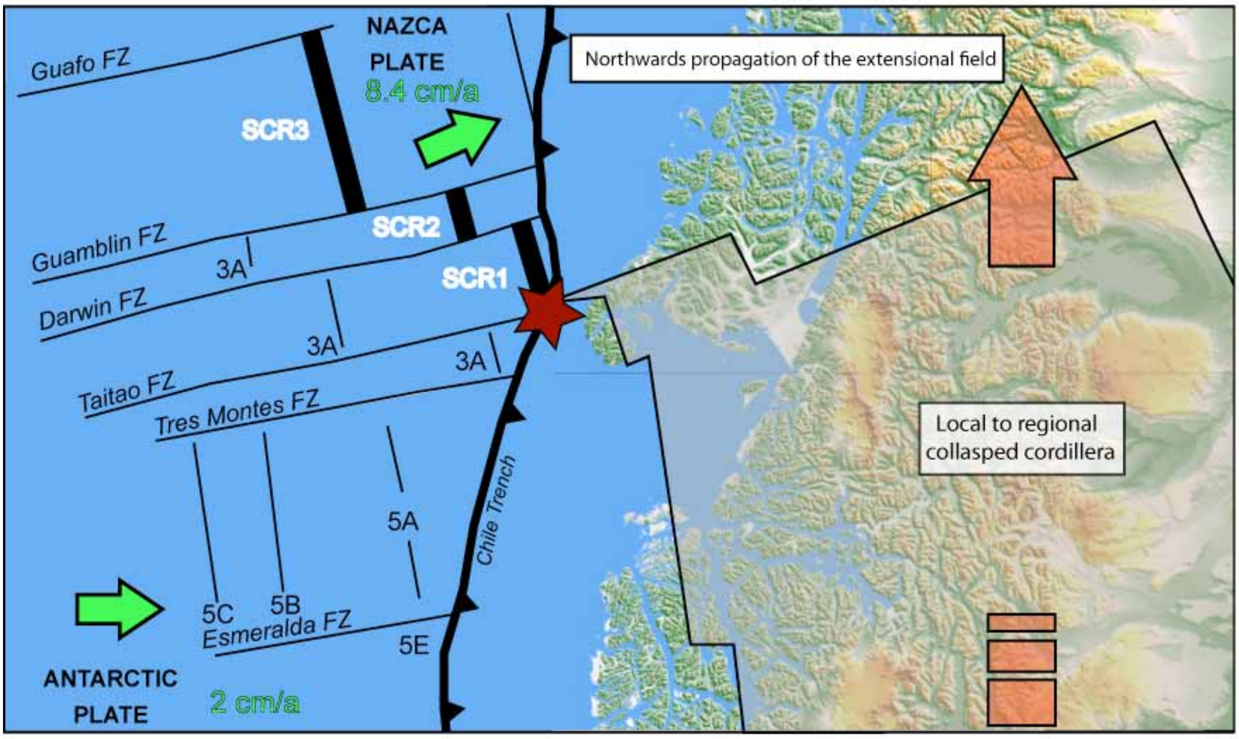

Fig. 11 Scalabrino et al.

Chapitre V :

Conclusion générale et perspectives.

Un modèle d'évolution des chaînes circum-Pacifique lors de la subduction de dorsale active.

V.1. Conclusion : Réponse de la Cordillère de Patagonie Centrale à la subduction de la dorsale du Chili.

Cette étude, réalisée suivant une approche pluridisciplinaire, apporte de nouvelles données structurales, morphologiques et chronologiques pour contraindre notre compréhension de l'évolution morphotectonique de la Cordillère de Patagonie entre le Miocène et le Quaternaire lors de la subduction de la dorsale active du Chili. Plus généralement, le problème abordé dans ce travail concerne les effets géologiques de la subduction d'une dorsale active et du développement d'une fenêtre asthénosphérique sur l'évolution géologique de la plaque continentale supérieure.

La Cordillère des Andes est marquée par la subduction de plusieurs anomalies topographiques et structurales, dont la dorsale du Chili dans la partie australe de la chaîne. Depuis 18 Ma, la Cordillère de Patagonie Centrale correspond ainsi à une région de transition entre deux systèmes de subduction différents. Au nord, la subduction de la plaque Nazca, initiée au Mésozoïque, est rapide et oblique. Au sud, la subduction de la plaque Antarctique est orthogonale. A cette plaque océanique jeune et chaude sont donc associées une diminution du pendage du panneau plongeant et une diminution des taux de subduction.

L'une des caractéristiques majeure de la Patagonie Centrale est sa topographie particulière bien différente de celle attendue pour une chaîne de subduction classique le long d'une marge active. En effet les reliefs à faible altitude de cette région, s'étendant jusqu'en Terre de feu, contrastent avec les hauts reliefs du reste de la Cordillère des Andes. Afin d'expliquer cette topographie et la morphologie actuelle si particulière de la Cordillère de Patagonie Centrale, il est essentiel de pouvoir caractériser le régime tectonique de la plaque supérieure et de le mettre en relation avec la subduction de la dorsale active du Chili et le développement d'une fenêtre asthénosphérique sous la plaque continentale. Dans notre travail, nous avons décrit cette déformation récente, ce qui n'avait pas été fait jusqu'à présent et nous l'avons replacé dans un calendrier le plus précis possible. Il reste à mieux comprendre les aspects rhéologiques concernant l'ensemble de la lithosphère. Ceci pourrait faire l'objet d'un travail complémentaire, faisant appel à un important volet de modélisation assimilant les contraintes structurales et temporelles établies dans le cadre de cette thèse.

Les principaux résultats de cette thèse peuvent être résumés ainsi.

1) L'étude structurale et morphologique de la Cordillère de Patagonie Centrale à la latitude du point triple du Chili (46°12'S de latitude) nous a permis de proposer que ce segment des Andes australes a subi une inversion tectonique négative majeure au cours du Néogène. Bordée à l'ouest par les hauts reliefs du Northern Ice Cap (NIC) culminant localement à plus de 4000 mètres d'altitude et à l'est par les hauts plateaux volcaniques et/ou sédimentaires (mesetas), la Patagonie Centrale est caractérisée par une zone centrale déprimée, marquée par la présence de dépressions transverses et internes à la chaîne contrôlées par des failles normales. De ce fait, les particularités topographiques, structurales et morphologiques de la Cordillère de Patagonie Centrale suggèrent une topographie de type rift.

2) Après une phase de raccourcissement responsable de la surrection de la chaîne entre l'Oligocène et le Miocène moyen (30-14 Ma) (Thomson et al., 2001 ; Lagabrielle et al., 2004), l'évolution morphostructurale de la Patagonie Centrale est caractérisée par une phase d'érosion majeure responsable de la formation de surfaces d'aplanissement en altitude. Les dépôts d'origine fluvio-glaciaire observés au niveau du piedmont de la chaîne et intercalés entre des coulées basaltiques formant les mesetas nous ont permis de proposer qu'entre 7 et 3 Ma, la Patagonie Centrale est marquée par de grandes phases glaciaires recouvrant l'ensemble de la Cordillère, synchrone d'un volcanisme important. Nos données structurales et morphologiques nous permettent de suggérer qu'à partir de la fin du Miocène-Pliocène, la Cordillère se présente comme un vaste dôme d'origine thermique en relation avec les premiers stades de remontée de matériel asthénosphérique chaud à travers la fenêtre asthénosphérique. Puis au Pliocène, le régime tectonique de la chaîne devient principalement de type extensif. La déformation est localisée généralement au niveau de failles polyphasées. Nous proposons que le régime extensif, de type radial, est responsable des caractéristiques majeures suivantes :

→ la formation de dépressions transverses et internes dont les bordures sont principalement contrôlées par des systèmes de failles polyphasées N45-50 et N160-170 à composantes normales et décrochantes. Ces dépressions canalisent au cours du Quaternaire les glaciers de piedmont de Patagonie Centrale. Ces caractéristiques sont observées depuis la latitude du Point Triple jusqu'en Terre de Feu.

→ l'inversion négative du front morphotectonique situé à l'est de la Cordillère le long duquel, des zones de failles orientées N160 localisent les mouvements verticaux Pliocène . Cette extension est associée à un magmatisme alcalin important de type 'rifting'.

→ la déconnexion du piedmont avec le reste de la Cordillère est accompagnée par le basculemnt des surfaces d'érosion observées dans les parties internes de la chaîne. La position en relief inversé des zones de dépôts formant actuellement les hauts plateaux à l'est de la Cordillère (mesetas) et leur déconnexion avec le reste de la cordillère sont l'une des particularités majeure de l'évolution du relief en relation avec le régime extensif à transtensif.

→ à l'échelle de la Cordillère, l'inversion tectonique négative est responsable de l'effondrement régional de l'ensemble de la chaîne entre les hauts reliefs occidentaux (NIC) et les mesetas.

3) L'analyse structurale et morphologique détaillée de la bordure ouest des plateaux volcano-sédimentaires tels que la meseta del Lago Buenos Aires a également contribué à la compréhension de l'évolution récente de la Cordillère de Patagonie Centrale. Nous avons montré à partir de marqueurs glaciaires et des dépôts associés observés au sommet de la meseta del Lago Buenos Aires, qu'à 3 Ma, les glaciers provenant des parties internes de la chaîne s'étendaient jusqu'au niveau du piedmont patagonien. La déconnexion entre les zones d'accumulation à l'ouest (plusieurs centaines de kilomètres) et les zones de dépôts à l'est s'effectue après 3 Ma le long de zones de failles situées entre le front morphotectonique et les plateaux. L'amplitude de la déformation extensive, au niveau de la partie orientale de la chaîne, est comprise entre 800 mètres et 3500 mètres. Cette phase extensive post-3Ma, responsable de l'inversion négative du relief décrite précédemment, induit un changement majeur dans la dynamique glaciaire. Les glaciers d'âge Mio-Pliocène s'écoulaient sur l'ensemble de la Cordillère tandis que les glaciers quaternaires sont canalisés au niveau des dépressions tectoniques formées à partir de 3 Ma.

4) D'un point de vue géodynamique, la subduction de la dorsale du Chili induit la formation d'une fenêtre asthénosphérique sous le continent sud-américain (e.g. Gorring et al., 1997 ; Lagabrielle et al., 2004 ; Breitsprecher et Thorkelson, 2009). A la latitude du point triple du Chili, Breitsprecher et Thorkelson, (2009) proposent que la fenêtre asthénosphérique se développe sous la Patagonie Centrale à partir de 3 Ma. La remontée de matériel asthénosphérique chaud à travers cette ouverture, montrée par diverses données de géophysique (e.g. Murdie et Russo, 1999 ; Murdie et al., 1999 ; Heintz et al., 2005 ;

Artemieva, 2006) provoque des perturbations thermiques à la base de la lithosphère continentale amincie. Il a été proposé que le magmatisme alcalin observé dans les parties internes et orientales de la Cordillère correspond à une crise magmatique majeure en relation avec les perturbations thermiques en profondeur (e.g. Morata et al., 2002 ; Gorring et al., 2003 ; Guivel et al., 2006 ; Espinoza et al., 2005). La présence de matériel chaud à la base de la lithosphère induirait la formation d'un dôme thermique régional, également suggéré par Guillaume (2009), suivie par l'instauration d'un régime extensif à 3 Ma. Ces résultats nous permettent de montrer que l'évolution morphostructurale et magmatique de la Cordillère est en relation directe avec le développement de la fenêtre asthénosphérique sous la Patagonie Centrale à cette même époque.

5) Lors de cette étude nous nous sommes également intéressés à l'évolution morphotectonique située au nord du point triple du Chili, aux environs de Coihaique (45°30'S et 46°S). Les caractéristiques topographiques, morphologiques et structurales indiquent une inversion négative du relief en relation avec une phase d'extension Plio-Quaternaire. Bien que les marqueurs magmatiques récents liés à la fenêtre asthénosphérique soient faiblement représentés, les séquences glaciaires d'âge Mio-Pliocène observées au niveau de plateaux topographiquement inversés et plus élevés que le reste de la Cordillère suggèrent une évolution comparable à celle décrite plus au sud. Nous proposons donc que l'ouverture de la fenêtre asthénosphérique induite par la subduction de la dorsale active du Chili affecte aussi les régions situées immédiatement au nord du point triple. Trois hypothèses peuvent être proposées :

→ Soit la taille de la fenêtre asthénosphérique est plus importante que celle prédite par Breitsprecher et Thorkelson, (2009). En effet, leurs travaux de reconstitution sont basés essentiellement sur la géométrie de la subduction de la dorsale du Chili. Ils ne tiennent pas compte des processus d'érosion thermique et de slab-pull de la plaque Nazca en subduction tendant à élargir la fenêtre asthénosphérique.

→ Soit des courants asthénosphériques latéraux, passant à travers la fenêtre, induisent une perturbation thermique de la région. Cette hypothèse a également été proposée par Folguera et al. (2006) afin d'expliquer certaines particularités structurales et magmatiques de la Cordillère de Patagonie entre 44°30'S et 45°S et par Guillaume (2009) afin d'expliquer les épanchements basaltiques de la vallée du Rio Senguerr étudiés par Bruni, (2007), à 200-300 km au nord du point triple.

→ Soit la déchirure du slab se propage comme proposé dans le modèle de Guivel et al. (2006), ce qui tendrait à conforter celui-ci.

En raison de l'absence de données structurales et tectoniques plus précises au nord de Coihaique, il nous est difficile de discuter ces hypothèses avec plus de détails.

V.2. Perspectives concernant le chantier Patagonie

Les résultats de ce travail ont apporté de nouvelles informations fondamentales dans l'étude de l'évolution des chaînes de subduction en interactions avec une dorsale active en subduction. L'étude pluridisciplinaire mise en œuvre ici nous a permis de mieux contraindre l'évolution de l'unique exemple de Cordillère affectée par la subduction d'une dorsale active sous un continent. Un certain nombre de perspectives sur les travaux futurs à envisager s'offrent ainsi.

→ Dans le cadre de la caractérisation de la déformation extensive responsable de l'effondrement local à régional de la Patagonie Centrale, des analyses morphologiques et tectoniques détaillées sont nécessaires dans la partie ouest de la chaîne. Initiés lors d'une mission d'exploration en 2008, ces travaux permettraient tout d'abord de mieux caractériser l'extension sur la bordure ouest du domaine effondré à partir d'analyses morphotectoniques au niveau de surfaces d'érosion perchées et de vallées glaciaires d'âge Holocène. Dans un second temps, à partir de la thermochronologie basse température (U-TH/He), il serait possible de quantifier les taux de dénudation et l'âge de la déformation le long des principaux segments de failles contrôlant la bordure ouest de la chaîne.

→ En ce qui concerne la Cordillère patagonienne située au sud de notre zone d'étude, la présence de dépressions transverses à la chaîne et de plateaux volcano-sédimentaires perchés suggère une évolution similaire à celle proposée à la latitude du point triple du Chili. Il serait primordial d'effectuer une analyse structurale détaillée de chaque dépression décrite par Diraison et al, (1997), du front morphotectonique et des bordures ouest des mesetas dans le but de caractériser et de dater l'extension. Si nos hypothèses concernant les relations entre un régime extensif en surface et l'ouverture d'une fenêtre asthénosphérique sous le continent sont correctes, nous devrions obtenir une progression d'âges de plus en plus jeunes en allant vers la latitude du point triple, témoins du développement de la fenêtre asthénosphérique et de sa migration vers le nord.

Pour les régions situées au nord du point triple du Chili (environ 40°S-44°S), il s'agirait de compléter les travaux de Folguera et al, (2006) et de Bruni (2007). Ici, l'extension doit débuter dans des temps plus récents encore que dans notre zone d'étude. Dans le cas d'un régime extensif très récent, ou non initié, la préservation d'une surface d'érosion régionale (non affectée par la déformation extensive) apporterait de plus amples informations sur les processus d'érosion affectant la Cordillère pendant une période de transition entre un régime compressif et un régime extensif. Il s'agirait donc d'effectuer une reconnaissance pour rechercher des témoins d'une telle surface.

→ D'un point de vue paléoclimatique, l'étude des séquences volcano-sédimentaires perchées situées à l'est de la Cordillère permettra d'établir la chronologie des phases glaciaires au cours du Miocène. En effet, nous avons confirmé que la Cordillère a connu des glaciations majeures entre 7 Ma et 3 Ma. Il serait intéressant d'étendre notre analyse plus au sud où des indices de glaciation datée à 10.5 Ma ont été observés à environ 49°S (Wenzens et al., 2006). Ceci permettrait alors de mieux contraindre l'importance des phases glaciaires dans les Andes australes et plus particulièrement leur initiation et leurs conséquences sur le climat mondial au cours du Miocène.

V.3. Subduction de dorsale et chaînes de type 'andin' : vers un modèle à l'échelle du Pacifique.

Pour clore ce travail, nous considérons le problème étudié en Patagonie à l'échelle de l'ensemble des chaînes circum-Pacifique dont les interactions avec les dorsales actives en subduction ont été nombreuses au cours du Méso-Cénozoïque. Notre première approche se fait à partir de la compilation des données structurales et magmatiques relatives aux différents cas de subduction de dorsale cités par la littérature (Figure V.1). Pour chaque contexte, la vitesse relative de convergence à la fosse, le régime tectonique et le magmatisme sont représentés entre le Crétacé et le Quaternaire. Cette figure illustre, en fonction de la vitesse de convergence à la fosse, le régime tectonique de la plaque supérieure et le magmatisme associé. Nous remarquons que pour chaque cas, l'entrée en subduction d'une dorsale active induisant la formation d'une fenêtre asthénosphérique, est en relation avec une diminution des taux de convergence. Simultanément, le régime de la plaque supérieure est marqué par une transition d'un régime compressif à un régime extensif.

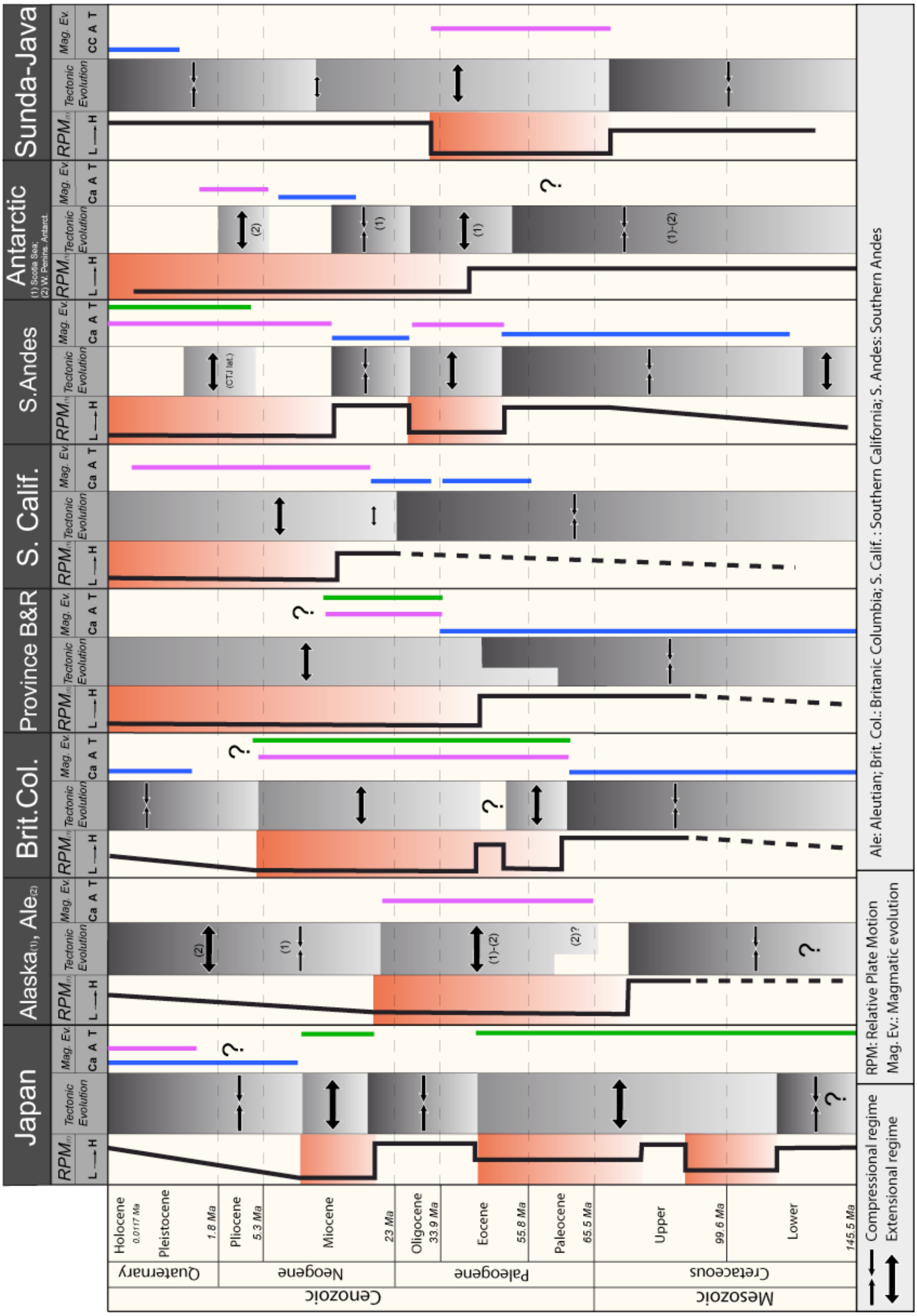

Figure V.1 : Tableau illustrant les relations temporelles entre l'arrivée en subduction d'une dorsale à la fosse (diminution des vitesses de convergence) et la formation d'une fenêtre asthénosphérique (dégradé rouge) avec la transition d'un régime compressif à un régime extensif majeur accompagné d'un magmatisme alcalin à tholéitique en position arrière-arc (Ca : Calco-alcalin, A : Alcalin, T : Tholéiitique).

Cette corrélation est très bien contrainte au niveau du Japon, de la Colombie Britannique, de la province du Basin and Range, de la Basse Californie et des Andes du sud (Figure. V.1). En ce qui concerne les autres contextes présentés, la phase d'extension liée à la présence de manteau chaud sous la plaque continentale est seulement suggérée. Nous remarquons également que le régime extensif peut-être suivi par une phase de compression, pouvant réactiver les structures préexistantes, en relation avec une augmentation des vitesses de convergence. Cette augmentation peut être reliée dans certains cas à une réorganisation des plaques en présence, tel que l'individualisation d'une nouvelle plaque, cas observé en Colombie Britannique lors de la formation de la plaque Explorer à la fin du Cénozoïque.

En ce qui concerne le magmatisme observé au niveau des Cordillères circum-Pacifique, nous remarquons un changement majeur dans la signature et la localisation des séquences magmatiques. Lors d'une subduction 'normale' de lithosphère océanique, le magmatisme est caractérisé principalement par des produits calco-alcalin d'arc. Dans le cas de la subduction d'une dorsale active et du développement d'une fenêtre asthénosphérique, le magmatisme d'arc cesse. La remontée de matériel asthénosphérique à travers la fenêtre induit un magmatisme d'arrière-arc de type alcalin à tholéiitique, particularité observé dans plusieurs régions telles que le Japon, la province du Basin and Range, en Basse Californie, en Antarctique et en Patagonie.

La compilation des caractéristiques tectono-magmatiques à travers diverses chaînes, nous permet de proposer un modèle d'évolution générale des chaînes de subduction circum-Pacifique depuis un stade de subduction 'froide' jusqu'à un stade de subduction 'chaude' lors du développement d'une fenêtre asthénosphérique (Figure. V.2). Ce travail fait l'objet d'un article à soumettre à *Nature to Geosciences*, dont les grandes articulations seront présentées ci-après. Les différentes caractéristiques du modèle sont les suivantes.

• Le premier stade est caractérisé par la subduction d'une plaque océanique mature et dont la vitesse de convergence est constante. La subduction continue depuis plusieurs dizaines de millions d'années entraîne une force de slab-pull importante. Le régime tectonique de la plaque supérieure est généralement marqué par une phase de compression majeure induisant la surrection de la chaîne (Figure. V.2A). Simultanément, le magmatisme de type calco-alcalin est dominant au niveau de l'arc magmatique.

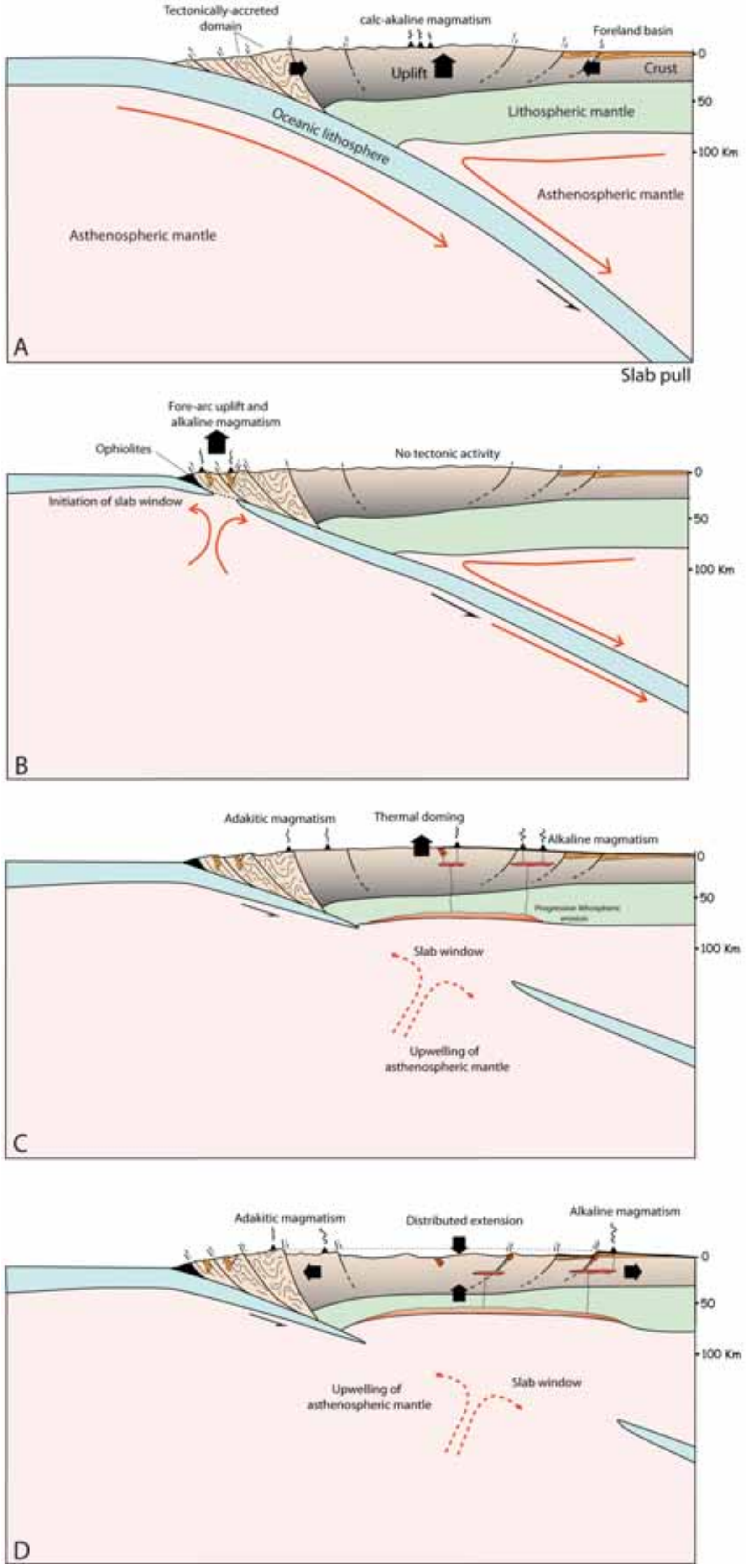

Figure. V.2 : Modèle d'évolution générale des chaînes de subduction circum-Pacifique interagissant avec une dorsale active en subduction, depuis un stade de subduction'froide' à un stade de subduction 'chaude'.

• Lors de l'entrée en subduction d'une dorsale active, la vitesse de convergence à la fosse diminue. Le domaine avant-arc est fortement perturbé par la collision de la dorsale avec la fosse et par l'initiation de l'ouverture de la fenêtre asthénosphérique (Figure. V.2B). Les sédiments accrétés le long de la fosse subissent une déformation majeure et une surrection générale. Ce domaine est également marqué par l'accrétion d'ophiolites et la mise en place d'un magmatisme alcalin à tholéiitique en relation avec des anomalies de températures en profondeur. En ce qui concerne le domaine de l'arc magmatique, l'activité volcanique cesse. Le domaine arrière-arc est, quant à lui, marqué par une quiescence tectonique, du fait de la diminution importante du couplage mécanique à la fosse (Figure. V.2B).

• La subduction de la dorsale se poursuit et l'ouverture de la fenêtre asthénosphérique s'accroît (Figure. V.2C). La plaque océanique nouvellement subduite s'enfonce à faible vitesse sous la plaque continentale tandis que la lithosphère océanique précédemment subduite continue à plonger rapidement dans le manteau asthénosphérique. Ce différentiel de vitesse élargit ainsi la fenêtre. La subduction froide est remplacée par une subduction chaude où le matériel asthénosphérique chaud remonte à travers la fenêtre. La plaque supérieure est caractérisée par une surrection thermique générale induisant un dôme de grande amplitude (Figure. V.2C). Simultanément, le domaine arrière-arc est marqué par une phase de magmatisme alcalin à tholéiitique (suivant les contextes) construisant de grandes provinces magmatiques.

• Lors du dernier stade, la fenêtre asthénosphérique de taille conséquente favorise la remontée massive de manteau asthénosphérique affectant thermiquement l'ensemble de la base de la lithosphère continentale. Le régime de déformation est principalement extensif, provoquant l'effondrement local à régional de la Cordillère, bordée de part et d'autres par des hauts reliefs (Figure. V.2D). Cette extension est de plus ou moins grande amplitude (certains contextes sont caractérisés par la dénudation de roches profondes) en fonction de l'héritage géologique et structural de la chaîne et de la configuration de la dorsale en subduction. Pendant cette période, le magmatisme de type alcalin (à tholéiitique) est toujours actif (Figure. V.2D). Nous remarquons également l'activité magmatique de type adakitique en domaine d'arc permettant de contraindre la limite de la fenêtre asthénosphérique proche de la fosse.

Toutefois, des études morphologiques et structurales complémentaires doivent être réalisées afin de mieux comprendre les transitions entre les régimes de déformation, l'initiation d'un dôme thermique et la mise en place d'un régime extensif associé à un magmatisme alcalin arrière-arc de grande ampleur, en relation avec le développement d'une fenêtre asthénosphérique.

Ce modèle permet finalement d'expliquer comment s'effectuent sur des cycles longs de plusieurs dizaines de millions d'années la croissance, la stabilisation, puis 'l'atténuation' progressive par tectonique extensive des chaînes de montagne liées aux zones de subduction. Pour parfaire ce modèle, il faut poursuivre l'établissement de calendrier précis, zone par zone, des différentes phases de croissance des chaînes péri-Pacifique sur la base du tableau de la figure V.1. Il faut également identifier sur le terrain, pour chaque chaîne, les preuves tangibles d'une phase d'extension syn à post-subduction de dorsale. S'agissant de déformation de faible amplitude, la tâche peut être rendue très difficile notamment dans les régions tropicales très couvertes ou aux hautes latitudes, en raison de l'érosion glaciaire souvent plus efficace que la seule tectonique récente pour façonner les paysages.

Annexes

XII Congreso Geológico Chileno
Santiago, 22-26 Noviembre, 2009

Neotectonics along the eastern flank of the North Patagonian Icefield, southern Chile: Cachet and Exploradores fault zones

Melnick, D.[1], Georgieva, V.[1], Lagabrielle, Y.[2], Jara, J.[3], Scalabrino, B.[2], Leidich, J.[4]

(1) Institute of Geosciences, University of Potsdam, 14476 Potsdam, Germany

(2) UMR 5243 Géosciences Montpellier, Université de Montpellier 2, Place Eugène Bataillon, CC 60, 34095 Montpellier Cedex 5, France

(3) Departamento de Ciencias de la Tierra, Universidad de Concepción, Chile

(4) Patagonia Adventure Expeditions, Casilla 8, Cochrane, Chile

melnick@geo.uni-potsdam.de

Introduction

In the southern Andes, the North Patagonian Icefield (NPI) is a poorly-known region in terms of geology and neotectonics that marks a major topographic anomaly at the transition between the Austral and Patagonian Andes. The NPI is located immediately east of the Nazca-Antarctic-South America Triple Plate Junction, where the Chile Rise collides against the margin (Fig. 1A). Since 14 Ma, this Triple Junction has migrated northward as a result of oblique plate convergence, resulting in collision, and subduction, of two relatively short ridge segments in the Golfo de Penas region at 6 and 3 Ma, and at present of one segment immediately north of the Taitao Peninsula [1]. Oblique plate convergence in addition to collision of these ridge segments resulted in formation of a forearc sliver, the Chiloe block, which is decoupled from the South American foreland by the Liquiñe-Ofqui fault zone

Here we present geomorphic and structural field evidences that report neotectonic activity in the internal part of the orogen, at the flanks of the NPI (Fig. 1A and 1B). We define two hitherto unrecognized fault systems, the Cachet and Exploradores faults, which run along the eastern and northeastern foothills of the NPI, respectively. Based on the offset of deep glacial valleys, we suggest that both faults have been active at least during the past ~3 m.y. We integrate the kinematics of these two fault systems with data from the Liquiñe-Ofqui fault zone, to propose a simple neotectonic model, which may help to explain the topographic anomalies in the NPI region. Furthermore, we describe the occurrence of several glacial-dammed lakes that occur along the main trace of the Cachet fault zone caused by drainage capture and fragmentation associated to strike-slip deformation. Due to the unstable position of these lakes, we emphasize the hazard of outburst megaflood events.

Geologic and morphotectonic setting of the NPI

The NPI is a flat-topped massif capped by an ice shield bounded by steep flanks. The flat ice shield has at a mean elevation of 1.500 m, and several nunataks emerging out of the ice cap reaching the highest elevation of 4.057 m at Cerro San Valentín. Immediately north of San Valentín, the mean elevation of the Andean cordillera decrease to ~1.000 m, with a few outliers formed by recent volcanoes that occasionally reach ~2.000 m. The core and highest parts of the NPI are formed by Paleozoic metamorphic rocks intruded by Jurassic to Miocene plutons of the Patagonian batholith. To the east of the NPI, deformed Jurassic to Miocene units integrate the Patagonian fold-and-thrust belt, which records phases of shortening and uplift during the late Cretaceous to Eocene and Oligocene to middle Miocene (Ref. [1] and references therein). Subsequently to this main phase of mountain building, only minor extensional deformation has been documented in the foreland adjacent to the Lago General Carreras. Normal faulting in this region is associated to the effusion of alkaline basalts and formation of vast plateau surfaces referred to as 'Mesetas'. Both extension and alkaline volcanism has been related to subduction of the Chile Rise resulting in opening of an astenospheric window and weakening of the lower crust [2] (and references therein).

The Cachet and Exploradores faults

The NPI is bounded along its eastern foothills by the Cachet fault system, which consists of a few dextral strike-slip fault strands that strike north-south. Continuous fault segments extend between the headwaters of the Ventisquero River at the southeastern tip of the NPI northward crossing the Pared Norte, Colonia, and Nef glaciers until the Soler River. North of Soler, the fault system looses continuity and grades to NNW-SSE oriented, en échelon faults, which extend northward probably until Lago Norte and the southeastern sector of the Exploradores glacier. Along the northern foothills of the NPI, the Cachet system is intersected by the Exploradores fault system, which consists of northwest-southeast oriented, southwest-dipping reverse faults with a minor strike-slip component. The Exploradores fault system controls the occurrence of the Exploradores-Bayo valley, the first to cut through the entire Andean Main Cordillera north of the NPI.

The Cachet fault marks a major axial drainage at the foothills of the NPI. Dextral slip along the Cachet fault resulted in the progressive deflection of the Nef, Colonia, and Pared Norte glaciers and consequently in the formation of several beheaded glacial valleys. These valleys are located in a hanging position along the eastern fault block (Fig. 1B and 1C). Glacial erosion along large-drainage glaciers as Soler and Colonia has outpaced strike-slip motion of the Cachet fault resulting in deflection of the glacier but continuous drainage across the fault. On the other hand, strike-slip motion across glacier with smaller drainages resulted in the formation of hanging valleys and drainage captures by the stream parallel to the fault (Fig. 1B and 1C). Based on correlation of the beheaded valleys floors and ridge crests, we estimate the total dextral offset along the Cachet fault, which decreases from ~6 to 4 km between the Pared Norte and Soler Valleys. In outcrops it is possible to recognize that some faults of the Cachet system have a minor extensional component (Fig. 1B and 1C).

I.1. *Glacial-dammed lakes as a result of strike-slip deformation along the Cachet fault*

As a result of dextral strike-slip deformation, several glacier-dammed lakes occur along the axial valley controlled by the Cachet Fault. The largest of these lakes are the Cachet 2 and Arco lakes, which are dammed by the deflected Colonia glacier. The Colonia glacier has the largest drainage area along the eastern NPI. Enhanced deflation lead to the occurrence of two sudden jökulhlaups, or glacial lake outburst floods, during April, October, and December 2008. The unstable position of Soler, Cachet 2, Arco, and Guillermo lakes, all located along the trace of the Cachet fault, which are dammed either directly by ice or by lateral moraines of the major glaciers, makes this region particularly prone to the occurrence of outburst flooding events.

I.2. *Discussion*

We interpret margin-parallel strike-slip deformation along the eastern flank of the NPI to arise from localized, oblique collision of three segments of the Chile Rise at 6, 3, and 0 Ma in the Golfo de Penas region. This resulted in decoupling of the NPI from the Patagonian foreland. We suggest that northward motion of the NPI is accommodated by the Exploradores and other reverse fault systems along its northern flank, which act as crustal ramp. This would explain the highest topography at the northern edge of the NIP. The margin-normal extensional deformation observed locally along the Cachet fault may be interpreted as a result of lower crustal weakening by subduction of slab windows after collision of Chile Rise segments, which would induce a minor extensional collapse of the NPI. Our integrated geomorphic and structural observations revealed the existence of neotectonic features at the foothills of the NPI; some of these faults are potentially active and we expect that work currently in progress (thermochronology, structural, paleomagnetism) will help to quantify their rates and tectonic significance.

Figure 1. A: Regional location map and major fault zones. LOFZ: Liquiñe-Ofqui fault zone; EFZ: Exploradores fault zone. NPI: North Patagonian Icefield. B: Geological map of the eastern NPI flank. Pz: Paleozoic metamorphic rocks (metasediments and ultramafics); Jrg: Jurassic granites (after geologic map of Chile); KMg: Cretaceous-Miocene intrusives; Qs: Quaternary sediments. C: Panoramic view of the deflected Nef glacier. Mount San Lorenzo can be seen in the background. A hanging beheaded valley is appreciated

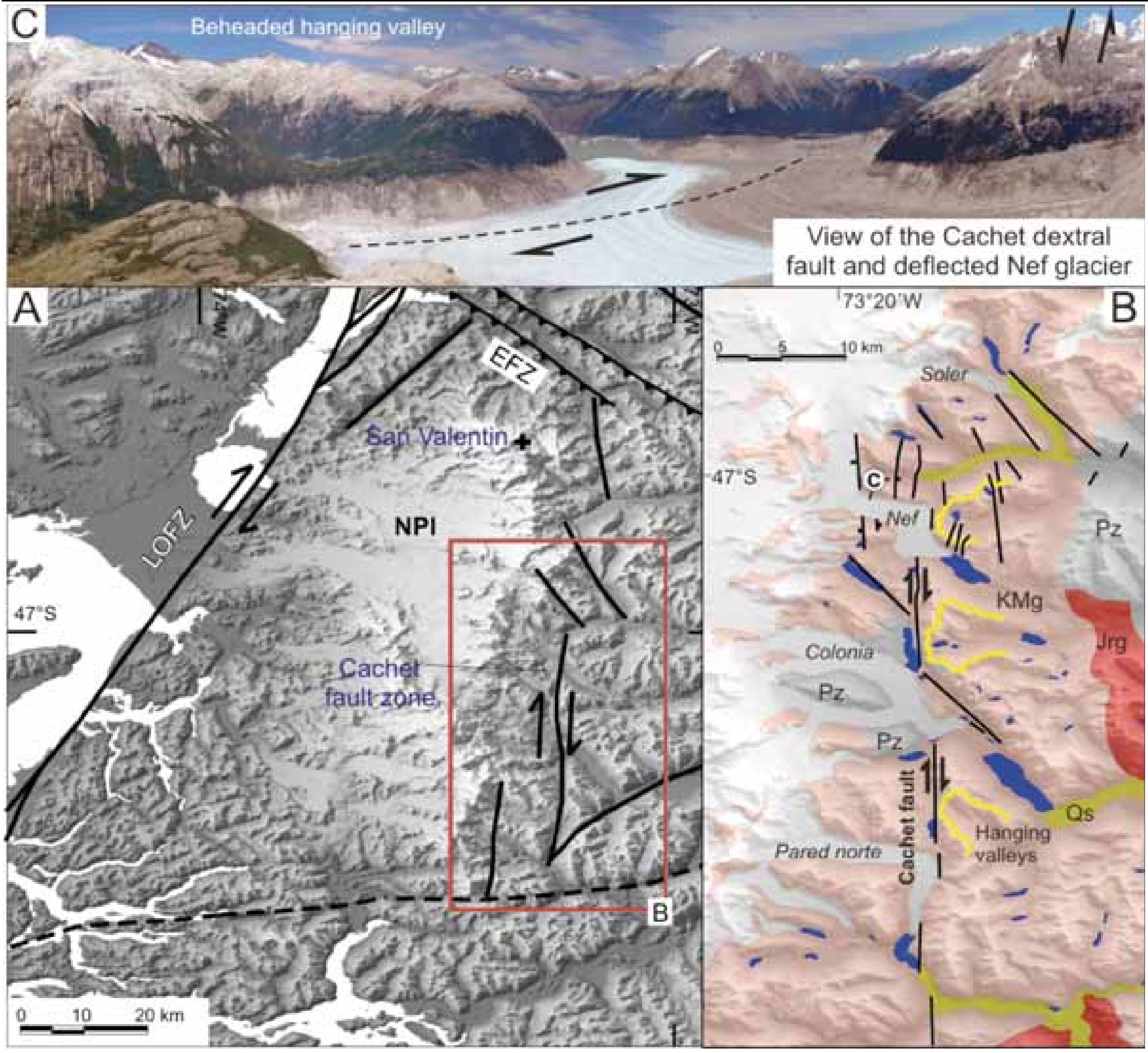

Referencias

[1] Lagabrielle, Y. *et al.* (2004) Neogene to Quaternary tectonic evolution of the Patagonian Andes at the latitude of the Chile Triple Junction. *Tectonophysics*, vol. 385, 211-241.

[2] Lagabrielle, Y. *et al.* (2007) Pliocene extensional tectonics in the Eastern Central Patagonian Cordillera: Geochronological constraints and new field evidence. *Terra Nova*, vol. 19, 413-424.

Subduction of the South-Chile active spreading ridge: A 17 Ma to 3 Ma magmatic record in Central Patagonia (Western edge of Meseta del Lago Buenos Aires, Argentina).

Boutonnet E. [a,b,1], Arnaud N. [a], Guivel C. [c], Lagabrielle Y. [a], **Scalabrino B.** [**a**], Espinoza F. [d]

[a] *CNRS-UMR 5243 Géosciences Montpellier, Université Montpellier 2, CC 60, Place Eugène Bataillon, Montpellier Cedex5, 34095, France.*
[b] *CNRS-MR 5570 Laboratoire des Sciences de la Terre, ENS-UCBL Lyon, Université de Lyon1, 2 rue Raphaël Dubois, Villeurbanne cedex, 69622, France*
[c] *UMR 6112 Planétologie et Géodynamique, Université de Nantes, Nantes, France.*
[d] *Departemento de Geologia, Universidad de Chile, Castilla 13518, Correo 21, Santiago, Chile.*

Corresponding author: Emmanuelle Boutonnet.

e-mail : emmanuelle.boutonnet@ens-lyon.fr

Tel : (+33)4 72 44 84 90

Fax : (+33)4 72 44 85 93

[1] Present address:

Laboratoire des Sciences de la Terre, ENS-UCBL Lyon, Université de Lyon1, 2 rue Raphaël Dubois, Villeurbanne cedex, 69622, France.

Abstract

The Chile Triple Junction is a natural laboratory to study the interactions between magmatism and tectonics during the subduction of an active spreading ridge beneath a continent. The MLBA plateau (Meseta del Lago Buenos Aires) is one of the Neogene alkali basaltic plateaus located in the back-arc region at the latitude of the current Chile triple Junction. The genesis of MLBA can be related with successive opening of slabs windows beneath Patagonia: within the subducting Nazca plate itself and between the Nazca and Antartica plates. Detailed $^{40}Ar/^{39}Ar$ dating and geochemical analysis of bimodal magmatism from the western flank of the MLBA show major changes in the back-arc magmatism which occurred between 14.5 Ma and 12.5 Ma with the transition from calc-alkali lavas (Cerro Zeballos) to alkali lavas (MLBA) in relation with slab window opening. In a second step, at 4- 3 Ma, alkaline felsic intrusions were emplaced in the western flank of the MLBA coevally with the MLBA basalts with which they are genetically related. These late OIB-like alkaline to transitional basalts were generated by partial melting of the subslab asthenosphere of the subducting Nazca plate during the opening of the South Chile spreading ridge-related slab window. These basalts differentiated with small rates of assimilation in shallow magmatic chambers emplaced along transtensional to extensional zones where magmas could be stored. The close association of bimodal magmatism with extensional tectonic features in the western MLBA is a strong support to the model of Patagonian collapse event proposed to have taken place between 5 and 3 Ma as a consequence of the presence of the asthenospheric window (SCR-1 segment of South Chile Ridge) below the MLBA location.

Key words: Subduction, spreading ridge, bimodal back-arc, magmatism, Patagonia

1. Introduction

Recent studies of the effects of active spreading ridge subduction beneath a continent have revealed the importance of back-arc magmatism as well as crustal extension following shortening and in some cases, large scale doming. This peculiar evolution which implies opening of an asthenospheric slab window and a weakening of the lower crust due to abnormal heatflow in response to the subduction of a hot mantle, is known from various subduction belts worldwide including the North and South American Cordillera (*Scalabrino et al., 2009; Scalabrino et al., in review; Guillaume et al., 2009*), Antarctica Peninsula (*Hole and Larter, 1993 ; Weaver et al., 1994*), Japan (*Marshak and Karig, 1977; Kiminami et al., 1994; Osozawa and Yoshida, 1997*) and Solomon sea (*Johnson et al., 1987*). Central Patagonia is one of the key region where basic observations on the magmatic effects of slab window and on the behaviour of a continental crust overriding a subducted ridge have been made in the last 15 years (*Ramos Kay, 1992; Gorring, et al., 1997; Lagabrielle et al., 2004*).

The Patagonia Cordillera has been concerned since 15 Ma by the oblique subduction of the South Chile spreading Ridge (SCR). During the subduction of a spreading ridge, the axial accretion ceases leading to the opening of a slab window below the continent (*Thorkelson et al., 1996*). This phenomenon drives major and various magmatic and tectonic consequences. The Central Patagonia located at the latitude of the current Chile Triple Junction (CTJ) where the Antarctic, Nazca and South America plates meet, is a unique place where records of volcanic activity in the time span of 17 Ma to present are located in a same area, at the western border of Meseta del Lago Buenos Aires (MLBA) (*fig.1*). This situation allows to study in a single geological section the transition from a “normal subduction” to the progressive opening of a slab window. Preliminary studies of the western border of the MLBA concentrated on recent bimodal volcanic products (*Espinoza et al., 2008*) and on tectonic and glacial aspects emphasizing post-3 Ma tectonic activity in relation with a negative inversion of the Cordillera front in this area (*Lagabrielle et al., 2007; Lagabrielle et al., submitted; Scalabrino et al., in review*). In this paper we describe in detail the geology of a restricted place where a continuous transition between sedimentary and volcanic rocks belonging to the 17 to 2 Ma period can be observed at the tectonic front of the Cordillera. This study aims at understanding the magmatic and tectonic implications of the presence of a slab window at the current CTJ latitude almost 300 km east from the trench (notably their relationships with extensional tectonics) in the MLBA region. Petrological, geochemical and geochronological characteristics of bimodal magmatism of the western MLBA and its relationships in space and time with the calc-alkaline/ alkaline transition and extensional tectonics allow developing a global model for the spreading ridge subduction context for the past 15 Ma.

2. Regional geology

2.1. Geological setting

The Andean cordillera results from the subduction of the Pacific Ocean plate beneath the South American plate since the Late Mesozoic and Cenozoic (*Cande and Leslie, 1986*). Tectonic and magmatic activities in the Patagonian Andes display numerous features specifically related to the subduction of the South Chile Ridge (SCR), which separates the Antarctic plate (south) and the Nazca plate (north), since 15 Ma. The Chile Triple Junction (CTJ) migrates northwards with a rate of 160mm/yr as a result of the oblique collision between the ridge and the trench (*Herron et al., 1981; Cande and Leslie, 1986; Cande et al., 1987; Nelson et al., 1994; Bangs and Cande, 1997; Tebbens and Cande, 1997, Tebbens et al., 1997*). Its present location at 46°12'S is marked by a gap in the calc-alkaline volcanic belt between the South Volcanic Zone (SVZ) and the Austral Volcanic Zone (AVZ) (*fig.1*) (*Stern et al., 1990; Ramos and Kay, 1992*). The SCR is segmented, each segment already subducted being named relatively to its distance away from the trench. The subduction of the presently farthest SCR-4 segment started at 15- 14 Ma, that of SCR-3 at 14- 13 Ma, SCR-2 at 12 Ma, SCR-1 at 6 Ma, SCR0 at 3 Ma and finally SCR+1 is being subducted since 0.3 Ma. The location of these subducted segments beneath Patagonia is evaluated thanks to the magnetic anomaly patterns (*Cande and Leslie, 1986; Guivel, 1999; Lagabrielle et al., 2004; Breitsprecher and Thorkelson, 2009*).

East of the Andean cordillera, the Patagonian back-arc is characterized by a regional-scale basaltic province named Neogene Patagonian Plateau (called Mesetas) Lavas (NPPL, *Gorring et al., 1997*) with OIB-like affinities but which emplacement seems to be related neither with a hotspot track nor back-arc extension (*Ramos and Kay, 1992*). Numerous authors have proposed that these basalts were produced by decompression melting of subslab asthenospheric mantle upwelling through a slab window (*Ramos and Kay, 1992; Kay et al., 1993; Gorring et al., 1997, 2003; D'Orazio et al., 2000, 2001, 2003; Gorring and Kay,* *2001*). The Mesetas location is apparently consistent with the successively opening slab windows (*Gorring et al., 1997; Gorring and Kay, 2001*). The main tectonic effect related to the subduction of very young oceanic lithosphere is an increase in tectonic coupling at the trench before ridge subduction followed by local collapse of the Cordilleran belt due to migration of the slab window beneath the continent. A compressive phase is related to the important coupling at ca. 15Ma and it reactivated oldest faults at the front of the Cordillera (*Scalabrino et al., in review*) which is now marked by a forearc Miocene basin. In the case of the Patagonian belt, the local collapse is marked by the presence of internal, recent grabens and deep transverse depressions (Lake General Carrera Buenos Aires, LGCBA, -385m), together with a negative inversion of the Cordillera front well observed at the western border of the MLBA (*Lagabrielle et al., 2005, 2007, Scalabrino et al.,2009; Scalabrino et al., in review*).

2.2. The Meseta del Lago Buenos Aires area.

The Meseta del Lago Buenos Aires (MLBA) is one of the largest (~6 000 km^3) most voluminous basaltic plateau (or Meseta) of the NPPL. It is located south of the Lake General Carrera Buenos Aires (LGCBA), at the latitude of the CTJ, and ca. 300 km east from the trench. To the west of the study area (*fig.2a*), the Cordillera is constructed by slightly deformed sequences of the Jurassic Ibañez Group (part of the Mesozoic Chon-Aike acid large Igneous Province; *Pankhurst et al., 1998*). This sequence contains felsic volcanism, tuffs and continental sedimentary deposits and overlies unconformably the Eastern Andean Metamorphic Complex. Late Jurassic to Lower Cretaceous marine sedimentary rocks overlies diachronically the Ibañez Group (*Suarez et al., 1997*). The last major compressive phase which affected the Patagonian fold and thrust belt occurred at ca. 20 -15 Ma (*Lagabrielle et al., 2004*). This event is sealed in the studied area by the synorogenic sediments of the Rio Zeballos Molasse Group (late Oligocene to early Middle Miocene, *Marshall and Salinas, 1990; Flint et al., 1994; Escosteguy et al., 2002*). The 300 m-thick basal lava sequence of the MLBA overlies unconformably the Molasse and locally the Jurassic volcanics. The main-plateau basaltic pile (ca. 1 500 km^3) which determines the overall plateau-like morphology is composed by tabular basaltic lava flows and necks (*Busteros and Lapido, 1983; Giacosa and Franchi, 2001*). It was essentially emplaced during Late Miocene- Lower Pliocene (~12.2 – 3.3 Ma, *Guivel et al., 2006*). A second and volumetrically minor event (ca. 300 km^3) occurred during the last 3.3 Ma – 100 ka. These later MLBA post-plateau basalts (*Ton That et al.,* *1999; Gorring et al., 2003; Brown et al., 2004; Singer et al., 2004*) were emplaced as monogenic cones, maars and fluid lava flows filling incisions and valleys.

Numerous authors associate the main-plateau magmatic event with the opening of a slab window beneath the plateau location as a consequence of the subduction of SCR-1 segment under Patagonia since 6 Ma (*Cande and Leslie, 1986; Ramos and Kay, 1992; Gorring et al., 1997; Gorring and Kay, 2001*). However, a recent chronological and petrogenetic study of the Miocene MLBA main-plateau basalts (*Guivel et al., 2006*) has shown that the spatial distribution and early genesis of these OIB-like basalts are better explained by a model involving the opening of a slab tear in the subducting Nazca plate. This tearing is a consequence of the important coupling in the trench zone at 15 Ma. It evolved into a unique slab window parallel to the trench and explains the location of alkaline magmatism in back-arc region at 12 Ma. Concerning the post-plateau event, the hypothesis of a slab window related to the SCR-1 segment is consistent in time and space (*Gorring et al., 2003; Guivel et al., 2006*).

Along the western border of the MLBA, the Rio Zeballos Fault Zone is an approximately N-S sinistral transtensional fault system witch postdates Miocene compressive tectonics in the region and corresponds to a major morphological corridor separating the MLBA from the Cordillera (*Lagabrielle et al., 2004, 2007*). Close to the Monte Zeballos, several felsic and mafic sub-volcanic bodies are intrusive into the meseta or into the Zeballos Molasse Group (*fig.2b*). K/Ar dates reported by *Espinoza et al. (2008)* for the southernmost felsic intrusions and lava flows indicate ages between 3.65±0.1 Ma (alkali granite of Cerro Lapíz neck) and 3.08±0.13 Ma (microsyenite of Mifeldi neck). The chronological data indicate that the emplacement of the felsic rocks occurred more or less synchronously with that of the post-plateau basaltic sequence. Chemically, these rocks have A_1-type granitoid affinities. They are interpreted as products of fractional crystallization from a primitive source, similar to post-plateau coeval basalts, with small rates of assimilation of host Jurassic tuffs (*Espinoza et al., 2008*) in a shallow magmatic reservoir. Alkaline bimodal magmatism is typically found in extensional tectonic settings such as continental rift zones. In the present case, the intrusions are aligned along the Zeballos Fault Zone, which is interpreted as a recent extensional zone (*Lagabrielle et al., 2006, 2007, Scalabrino et al., 2009, in review*). The transtensional or extensional event in the valley, in possible relation with the presence of the SCR-1 segment just beneath, is dated between 5 and 3 Ma.

3. Field observations

Three sites were sampled during fieldwork investigations in 2006 and 2007 (*fig.2b*). All samples were taken in the Rio Ghio/ Rio Zeballos valley which borders MLBA to the west. This N160-170 tectonic corridor (*Lagabrielle et al., 2004, 2007*) is defined by the morphotectonic front of the Patagonian cordillera to the west and by the vertical scarp of MLBA to the east. Samples are representative of the main morphological and geological units. Most of the studied rocks are fresh enough for geochemical analysis (Loss on Ignition – LOI values lower than 2 wt %); some samples have a high LOI (higher than 3 wt %) (see *table1*) and consequently their geochemical characteristics will be considered with care.

3.1. Pico Rojo dikes, necks and lava flows series.

Pico Rojo (47°00’S, 71°45’W) microsyenitic peak (PA-06-13, *fig.2b*)) is an important sub-circular neck, rimmed to the east by a glacial valley which has erased any visible contact with the MLBA basalts. Other magmatic rocks outcrop south of Pico Rojo as lavas, dikes and smaller necks crosscutting the Miocene sediments. No field relationships were observed between these intrusives and MLBA contrary to the Mifeldi microsyenite (9 km south from Pico Rojo, *Espinoza et al., 2008*) which clearly intrudes the MLBA basalts. Three necks (PA-06-12/17/18), one dike (PA-06-15) and two lava flows (PA-06-16/19) were sampled in order to be dated and chemically analyzed and offer new and complementary data to the study by *Espinoza et al. (2008).*

3.2. Cerro Zeballos hill

A second sampled zone is a remnant relief, the Cerro Zeballos hill, located in the middle of the Rio Zeballos valley, a few kilometers west from Pico Rojo (*fig.2b*, 47°00’S, 71°47’W). The hill is principally composed of sandstones and conglomerates of the Zeballos molassic Group. Cm to dm-sized clasts of lava (PA-06-05/06/07) are found within the molasse beds. They are possible remnants of calc-alkaline/alkaline eruptive episode which occurred during the molasse deposition and may thus bracket this major geochemical transition. Two basaltic to andesitic flows (PA-06-10/11) constitute the top of the hill. This ca. 25 m thick volcanic sequence (Zeballos Volcanic Sequence, *Espinoza et al., submitted*) rests unconformably over the sediments. Close to the hill, two east-west oriented basaltic dikes (PA-06-03/20) which likely represent the feeders of the overlying MLBA lava flows crosscut the Zeballos Molasse Group.

3.3. Alto Rio Ghio dikes and lava flows.

A third sampled zone is a 6- 7 Ma-old paleovalley, the Alto Rio Ghio (*Lagabrielle et al., 2007, submitted*) located in the present-day Rio Ghio valley (*fig.2b*, 47°04'S, 71°49'W), few kilometers south from Cerro Zeballos, where the Zeballos molassic Group is covered by flows of MLBA-type basalts (PA-06-22/24), intruded by dikes (PA-06-23/25) and locally incised by rivers and glaciers. Their chronological studies might give information on paleosurfaces, glacier, river incisions and tectonics since 5 Ma. In order to enlarge the studied field, three basaltic flows were sampled eastwards at the foot of the Meseta (TM01/02/03) to gain information on MLBA basalts origin and their possible relationships with felsic rocks.

4. Analytical methods

22 samples were selected for major and trace element analyses (7 from Pico Rojo intrusions and lava flows series, 2 from the east-west dikes, 5 from Cerro Zeballos, 5 from the Alto Rio Ghio and 3 lava flows at the foot of the Meseta) and 18 of them were dated by the $^{40}Ar/^{39}Ar$ method. Whole-rock mesostasis, glass and feldspar Ar-Ar ages were obtained at the geochronology laboratory of Geosciences Montpellier (Université de Montpellier 2, France) following a protocol similar to that described in *Garcia et al. (2003)*. Analyses were performed on the 150- 250 µm-size fraction after separation with Frantz magnetic separator, heavy liquids and finally by hand picking under a binocular microscope. For each sample, one or more aliquots on different separates (typically feldspar and volcanic glass), were irradiated at the McMaster reactor, Ontario, in the 5C position for 26 h under a 10^{18} neutrons $cm^{-2}s^{-1}$ flux during December 2007. Irradiation interference on K, Ca and Cl were corrected by irradiation of KCl and CaF_2 pure salts. J factor was estimated by the use of duplicates of the Fish Canyon sanidine standard with an age of 28.02 ± 0.16 Ma (*Renne et al., 1998*) with reproductive values within 0.6%.

The samples were analyzed in Geosciences Montpellier. Samples were loaded in aluminum packets into a double vacuum Staudacher type furnace, which temperature is calibrated by means of a thermocouple, and step heated. The gas was purified by the means of cold traps with liquid air and Al-Zr getters during 5 mn. Once cleaned, the gas was introduced into a VG3600 mass spectrometer, and 1 min were allowed for equilibration before analysis was done statically. Signals were measured by the mean of a Faraday cup with a resistor of 10^{11} ohm for ^{40}Ar and ^{39}Ar while ^{39}Ar, ^{38}Ar, ^{37}Ar and ^{36}Ar were analyzed with a photomultiplier after interaction on a Daly plate. Gain between both collectors was estimated by duplicate analysis of ^{39}Ar on both during each analysis, and also by statistical analysis on a period of several years. This gain was in average of 54 and is know at better than 1.5%. This error is included in the age calculation, along with analytical errors on each signal and errors on the blank values. Detail analytical results are available from the authors upon request. Age plateau given are weighted mean plateaus (*Fleck et al., 1977*) which error takes the error on the J factor into account, but plateau criterion were rarely achieved, and sometimes simple mean age is given. The isochron ages are obtained in an inverse isochron diagram of $^{36}Ar/^{40}Ar$ versus $^{39}Ar/^{40}Ar$ (*Roddick et al., 1980*), which allows homogeneous excess components to be individualized in many occasions. Errors on age and intercept age include individual errors on each point and linear regression by York's method (*York, 1969*). The goodness of it relative to individual errors is measured by Mean Square Weighted Deviation (MSWD).

Classical furnace step heating was conducted and yielded age spectra from which plateau and isochron ages were calculated and are shown side by side to assess potential excess argon problems. If the inverse isochron age is close to the plateau age and $^{40}Ar/^{36}Ar$ is not significantly different from present day $^{40}Ar/^{36}Ar$ atmospheric ratio (295.5), we consider that the plateau age is reliable. When this is not the case, we prefer to rely on the inverse isochron age if this one is well determined.

Mineral chemistry was carried out using the five spectrometer probe CAMECA SX100 of Geosciences Montpellier (France). Major and selected trace elements analyses were performed on agate-ground powders by ICP-AES at the chemical laboratory of the Université de Bretagne Occidentale (Brest, France). All data were calculated using IWG-GIT, BE-N, AC-E, PM-S and WS-E as standards. Specific details for the analytical methods and sample preparation can be found in *Cotten et al. (1995)*. Relative standard deviation is generally ca. 5%. Other trace element analyses for 12 samples were performed by ICP-MS at the chemical laboratory of the Université de Bretagne Occidentale (Brest, France). Data quality was controlled by running BCR-2 and BIR1 standards. Relative standards deviations are generally ≤5%.

5. Petrologic and geochemical data

5.1. Petrography and mineral chemistry

5.1.1. Cerro Zeballos lavas and clasts in molasse.

The Cerro Zeballos volcanics present typical porphyritic textures with phenocrysts of olivine (in the case of basalts), pyroxenes, amphibole (in the case of andesites), plagioclases and Fe-Ti oxides ($Ti_{7-18}Fe_{82-93}$) set in a fine grained crystalline groundmass principally made up of plagioclase laths and opaque oxides. The capping basalt (PA-06-11) is highly porphyritic and is composed of almost completely altered (iddingsite) subhedral olivine (Fo_{38-45}), subhedral to euhedral oscillatory-zoned diopside ($Wo_{47-48}En_{38}Fs_{14-15}$) and zoned calcic plagioclase phenocrysts with anorthite core ($An_{89-91}Ab_{8-11}Or_{0-1}$) and Na-richer rim ($An_{57-79}Ab_{20-40}Or_{1-3}$) (*fig.3*). The andesite flow (PA-06-10) and inclusion (PA-06-07) are porphyritic and homogenous. They contain variables amounts of zoned Ca-amphiboles phenocrysts. Plagioclase with complex oscillatory pattern is an abundant primary phase with calcic core ($An_{80-95}Ab_{5-20}Or_{0-1}$) and more sodic rims ($An_{38-67}Ab_{32-59}Or_{1-3}$). The phenocryst assemblage is completed Fe-Ti oxides plus augite and diopside ($Wo_{45-48}En_{35-41}Fs_{14-17}$) partly replaced by amphibole. Groundmasses of all these samples are made up by microcrysts with composition similar to those of the phenocrysts.

5.1.2. Basaltic intrusives and lava flows in the Pico Rojo area and in the Alto Rio Ghio area.

Basaltic lavas include samples PA-06-03 and PA-06-20 E-W dikes near Cerro Zeballos, PA-06-17/18/19 in Pico Rojo area and all the samples from the Alto Rio Ghio site. The two E-W dikes around Cerro Zeballos (PA-06-03 and PA-06-20) present a clear fluidal texture. South from Pico Rojo, a neck (PA-06-17) is the microgranular equivalent of the lava flow PA-06-19 with few phenocrysts of plagioclase and clinopyroxene. The southernmost neck (PA-06-18) has no Fe-Mg minerals. Further to the south, two dikes in the Alto Rio Ghio area (PA-06-23 and PA-06-25) display an altered glass with crystallized calcite into vesicles and very few Mg-Fe minerals. This alteration is correlated with high LOI (5.79 and 5 wt% respectively). Contrary to the dikes, the two lava flows of the Alto Rio Ghio area (PA-06-22 and PA-06-24) present large olivine and plagioclase phenocrysts, with interstitial clinopyroxene in the case of PA-06-22. Only the samples PA-06-03/20/17 were analyzed by microprobe. These basaltic neck and dikes are aphyric to moderately porphyritic with occasional plagioclases, clinopyroxenes ($Wo_{38-46}En_{35-49}Fs_{14-20}$) (*fig.3b*) and olivine (Fo_{46-57}) phenocrysts. Two families of basaltic rocks can be separated based on porphyritic plagioclase compositions. The basaltic neck contains Ca-plagioclases ($An_{72-78}Ab_{21-27}Or_{1-2}$) whereas the two E-W basaltic dikes contain Na-richer plagioclases ($An_{52-63}Ab_{36-45}Or_{2-4}$) and K-feldspar. Their glassy to microlitic groundmass contains plagioclase laths, olivine, clinopyroxene, Ti-magnetite ($Ti_{12-28}Fe_{72-88}$) and glass.

5.1.3. Differentiated intrusives and lava flows restricted to the Pico Rojo area.

These differentiated rocks are inequigranular holocrystalline rocks with roughly round minerals and no or little fluidal texture except the neck near Pico Rojo (PA-06-12) which presents elongated plagioclases. In this rock, rare phenocrysts of olivine (Fo_{25-35}), Ti-magnetite ($Ti_{24}Fe_{76}$) and weakly zoned feldspar, from andesine to anorthosite ($An_{21-41}Ab_{54-63}Or_{5-16}$) (*fig.3a*), set in a fine-grained groundmass composed principally of plagioclase laths and to a lesser extent by pyroxene and oxides microcrysts with compositions similar to those of the phenocrysts. Pico Rojo neck (PA-06-13) is made of little globular minerals of plagioclase, oxides and clinopyroxene. A massive porphyritic trachytic lava flow (PA-06-16) and its intrusive dike (PA-06-15) sampled close to Pico Rojo neck are characterized by numerous plagioclases and Fe-olivine phenocrysts. In the dike (PA-06-15), the andesine plagioclase ($An_{26-46}Ab_{51-62}Or_{3-13}$) and anorthoclase ($An_{12-13}Ab_{65-66}Or_{20-23}$) phenocrysts are rarely zoned. This rock displays two families of olivine ($Mg_{14-19}Fe_{81-86}$ and $Mg_{34-37}Fe_{63-66}$) which present disequilibrium with the groundmass composed of Fe-Ti oxides with variable compositions, sanidines ($An_{0-8}Ab_{56-67}Or_{25-43}$), and augites ($Wo_{36-45}En_{22-37}Fs_{22-33}$). The upper lava flow (PA-06-16) is made up of phenocrysts of Fe-olivine ($Mg_{11-15}Fe_{85-89}$), normally-zoned feldspar with andesine core ($An_{25-30}Ab_{60-70}Or_{5-10}$) and anorthosite to sanidine rims ($An_{0-8}Ab_{56-67}Or_{25-43}$), set in a groundmass mainly composed of anorthoclase laths ($An_{6-15}Ab_{65-76}Or_{10-30}$), Fe-Ti oxides and green augite ($Wo_{44-45}En_{25-27}Fs_{28-30}$).

5.2. Geochemistry and samples classification.

5.2.1. Major elements and petrographic types.

The geochemical compositions are given in *Table 1*. SiO_2 concentrations and Mg# of analyzed rocks range respectively from 46.3 to 61.7 wt% and from 67 to 16 (see *Table1*). Our sampling set contains only one primitive basalt (Mg#>65). In the TAS (total alkalis vs. silica) diagram (*fig.4*), the samples plot both up and down the limit between alkalic and subalkalic compositions. The distribution of our samples can be separated in four groups. Group 1 samples plot in the alkalic basalts – hawaite field (Mg# = 35- 48), group 2 samples plot in the subalkalic basalt – basaltic andesite fields (Mg# = 45- 67), group 3 samples plot in the calc-alkaline andesite – trachyandesite field (Mg# = 41- 53) and group 4 plot in the differentiated trachyandesite – trachyte field (Mg# = 16- 30). The first group contains the two E-W dikes at the foot of Cerro Zeballos (PA-06-03/20), the southernmost neck close to Pico Rojo (PA-06-18) and two samples taken east of the Rio Ghio valley (TM01/02). The second group contains a lava flow (PA-06-19) and a neck (PA-06-17) close to Pico Rojo, most of the basaltic dikes, and lava flows sampled near the Alto Rio Ghio area (PA-06-22/23/24/25, TM03). All the samples of the third group were sampled at the Cerro Zeballos hill (PA-06-05/06/07/10/11) and define a high-K calc-alkaline trend in the K_2O vs. SiO_2 diagram. Sample PA-06-11 is rather primitive and plots in the group 2 field in the TAS diagram. However, its porphyritic texture and its zoned plagioclases and clinopyroxenes indicate that this basalt is probably calc- alkaline and belong to the Cerro Zeballos group 3. Finally, all the samples of the fourth group belong to the felsic dike, neck and lava flow series close to Pico Rojo (PA-06-12/13/15/16).

Contrary to the MLBA post-plateau basalts (*Guivel et al., 2006*), most of the alkalic lavas of group 1 do not contain normative nepheline, but only olivine, hypersthene, diopside, orthoclase and plagioclase plus accessory phases. This feature can be related to the differentiation rate which is probably higher for our samples than that of the MLBA samples. All the felsic rocks of group 4 except the dike south from Pico Rojo sample (PA-06-12) are quartz-normative (less than 6%). In groups 2 and 3, only the most primitive basaltic flow of the top of Cerro Zeballos (PA-06-11) displays nepheline in its CIPW norm, while most of the other samples are quartz-normative, particularly those of Cerro Zeballos.

5.2.2. Classification based on Ti vs. La/Nb diagram.

Stern et al. (1990), Gorring et al. (1997, 2003) Gorring and Kay (2001), Espinoza et al.

(2005) and *Guivel et al. (2006)* have shown that some Patagonian main-plateau and post-plateau basalts display weak to moderate subduction-related geochemical imprints expressed by relative depletions in High Field Strength Elements (HFSE) vs. Large Ion Lithophile Elements (LILE) and Light Rare-Earth Element (LREE), and sometimes as well by specific isotopic signatures. These features are clearly observed in the MLBA data set (*Guivel et al., 2006*) in which about 30% of the basalts have La/Nb ratios greater than unity (up to 1.2) and TiO_2 contents usually lower than 2 wt%. Their relative depletion in Nb is unlikely to result from fractionation of Ti-magnetite during differentiation because their Nb contents increase with decreasing Mg numbers (*Guivel et al., 2006*). Consequently, we have also identified geochemical groups for our group 1 and 2 basaltic samples thanks to the Ti vs. La/Nb diagram (*fig.5*) which discriminates clearly those source patterns.

All basalts and hawaites of group 1 plot in the MLBA alkali basalts field defined by *Guivel et al. (2006)* characterized by La/Nb<1.2 and TiO_2>1.75 wt%. All group 3 calc- alkali lavas but PA-06-11 plot in the South Volcanic Zone (SVZ) field defined by La/Nb >2.5 and TiO2<1.5 wt%. Group 2 samples and PA-06-11 basalt plot between the MLBA alkali basalts field and the SVZ calc-alkaline rocks field. *Stern et al. (1990)* termed these basalts "transitional basalts" and we will use this name to designate samples of group 2 lavas that present characteristics transitional between alkaline and calc- alkaline imprint. Two patterns can be distinguished in this transitional composition field. The first one corresponds to MLBA transitional basalts defined by *Guivel et al. (2006)*, characterized approximately by 1<La/Nb<2 and 1<TiO_2<1.75 wt%. Three samples from around Alto Rio Ghio area and the Cerro Zeballos upper lava flow sample plot in this field, displaying moderate subduction related imprint. But other samples belonging to group 2 and 3 display more calc-alkaline signature with a higher La/Nb ratio. Those geochemical features can be compared with those of the southernmost volcano of SVZ, the Hudson volcano. This volcano has a calc-alkaline signature influenced by alkaline affinities from the nearly asthenospheric window (*Gutierrez et al., 2005*), with compositions corresponding to our transitional to calc-alkaline samples in the TiO_2 vs. La/Nb diagram. Finally, Group 4 samples represented by differentiated rocks are not plotted in this diagram.

5.2.3. Trace-element compositions.

A further discrimination has been operated within our data set, since basaltic lavas from both MLBA and our group 1 alkali basalts (*fig.6a*) display chemical features very similar to those considered typical of Ocean Island Basalts (OIB), as already shown by previous authors (*Hawkesworth et al., 1979; Baker et al., 1981; Ramos and Kay, 1992*). The main plateau alkali basalts display levels of LILE and LREE enrichment similar to those of transitional basalts (average primitive mantle normalized, $(La/Nb)_N$=2.71 for alkali basalts, $(La/Nb)_N$=2.84 for transitional basalts) but slightly lower than that of the post plateau lavas (average $(La/Sm)_N$=3.80, *Guivel et al., 2006*). Our sample data is better fitted by the main-plateau field in the incompatible trace-element pattern diagram and particularly with an average $(La/Nb)_N$=2.97. Both transitional rocks of MLBA and group 2- 3 samples (*fig.6b*) share close trace-elements features. They display LILE and LREE-enriched pattern and are noticeably but variably depleted in Nb and this anomaly is attenuated with increasing differentiation. So, the Nb depletion is pristine and linked to the nature of the magma source. Most of our group 2 transitional samples and all group 3 calc- alkali samples present a higher Nb anomaly than MLBA transitional lavas and this observation confirms that our sampling contains more calc-alkaline-influenced rocks than MLBA transitional basalts. All the studied group 4 felsic rocks (*fig.6*) are also enriched in LILE and HREE ($(La/Sm)_N$=3.4 –4.18) with LREE fractionation increasing with differentiation, as *Espinoza et al. (2008)* observed on other felsic rocks. All exhibit a sub-horizontal Heavy REE (HREE) patterns ($(Dy/Yb)_N$=1.26 –1.33), but, contrary to *Espinoza et al. (2008)* samples, none of our studied rocks show a negative Eu anomaly.

6. Ar- Ar geochronology

6.1. Cerro Zeballos lavas and volcanic clasts.

The ^{40}Ar-^{39}Ar ages are given in *Table 2*. All the calc-alkali lavas display ages between 16.98 and 12.4 Ma (*fig.7*). Thus, they were erupted well before the onset of the main-plateau magmatic event of the MLBA (12.36 ±0.33 Ma, *Guivel et al., 2006*). The upper basaltic lava flow (PA-06-11) provides a Ar/Ar isochrone age (*fig.8*) of 12.4 ±1.56 Ma and the andesite from the pyroclastic flow just below (PA-06-10) provides a Ar/Ar plateau age of 14.48 ±0.2 Ma. *Espinoza et al. (submitted)* dated also these lava flows and the resulting K/Ar ages are respectively 14.48 ±0.36 Ma and 15.03 ±0.36 Ma. We prefer our ^{40}Ar-^{39}Ar ages because the present results method reveals Ar excess in the samples, particularly for the uppermost lava flow, that K/Ar results can not account for. We dated three andesitic clasts found coarse breccias levels of the molasse (PA-06-06/05/07). They display Ar/Ar plateau ages of 16.05 ±0.4 Ma, 16.73 ±0.21 Ma and 16.98 ±0.36 Ma respectively. Several basaltic andesite to trachy-andesite clasts have also been dated by *Espinoza et al. (submitted)* and the resulting K/Ar ages are 14.82 ±0.35 Ma and 16.52 ±0.39 Ma. Those ages are consistent with the ^{40}Ar-^{39}Ar ages obtained by *Blisniuk et al. (2005)* on tuffs interbedded with sediments of the Santa Cruz Formation near Lago Posadas (22 – 14 Ma) and with the age of several subvolcanic calc- alkaline bodies exposed close to the studied area and far to the south (Cerro Indio and Cerro Negro del Ghio : 18 – 13Ma, *Ramos, 2002* ; Cerro Moyano : 16 ±1 Ma, *Linares and Gonzalez, 1990*). These results indicate that a calc-alkaline volcanic activity was synchronous with the deposition of synorogenic sediments during the compressive phase at ca. 20 – 15 Ma, before the MLBA episode, that is before ridge subduction.

6.2. Basaltic intrusives and lava flows.

The basaltic intrusives and lava flows of the northern part of the studied area (near Pico Rojo intrusive) yielded ages between 6.85 and 2.12 Ma (*fig.7*), and those of the southern part of the studied area (east from Mifeldi intrusion) present ages between 9.42 and 4.17 Ma. Only three alkali basalts can be clearly associated with the post-plateau event with ages younger than 3.3 Ma (*Ton-That et al., 1999; Brown et al., 2004; Guivel et al., 2006*). The two E-W alkali basaltic dikes located south of Cerro Zeballos hill (PA-06-03/20) display close and recent isochrone ages (*fig.8*) of 2.94 ±0.1 Ma and 2.12 ±0.45 Ma. The southernmost alkali basaltic neck south of Pico Rojo (PA-06-18) presents a well constrained plateau age of 3.23 ±0.08 Ma whereas the basaltic lava flows in the valleys east of Mifeldi (TM01/02, PA-06-22) are older, with ages of 4.17±0.16 Ma, 6.41 ±0.22 Ma and 6.44 ±0.56 Ma respectively. The oldest analyzed rock (except in Cerro Zeballos) is a transitional black dike (PA-06-23) dated at 9.42 ±1.42 Ma in the Alto Rio Ghio area. The transitional-affinity lava flow PA-06-19 close to Pico Rojo neck is dated at 6.85 ±0.15 Ma (^{40}Ar-^{39}Ar plateau age) and the neck PA-06-17 displays a maximum plateau age of 4.48 ±0.17 Ma.

6.3. Differentiated intrusives and lava flows.

The trachyandesitic dike (PA-06-12) close to Pico Rojo neck (*fig.7*) displays a ^{40}Ar-^{39}Ar age of 2.76 ±0.07 Ma (average age calculated on consecutive steps) (*fig.8*). The trachyandesitic dike (PA-06-15) and the trachytic lava flow (PA-06-16) south from the neck are respectively dated at 4.41 ±0.54 Ma (plateau age) and 3.1 ±0.08 Ma (plateau age). These ages closely match those obtained by *Espinoza et al. (2008)* on Pico Rojo (3.98 ±0.1 Ma), as well as on felsic products erupted about 9 km south of Pico Rojo, which display K/Ar ages between 3.65 ±0.10 Ma (Cerro Lapíz granitic neck) and 3.08 ±0.13 Ma (microsyenitic dike close to Mifeldi neck, *Espinoza et al., 2008*). The felsic magmatism is coeval with the 3.2 ±0.4 Ma old Las Nieves pluton (*Morata et al., 2002*), exposed 55 km northwest and is roughly synchronous with the beginning of the post-plateau basaltic event (3.4- 3.3 Ma, *Ton-That et al., 1999; Brown et al., 2004; Guivel et al., 2006*).

7. Petrogenetic processes

7.1. Origin of the Cerro Zeballos transitional lavas

7.1.1.Geochemical features and magma sources.

The lavas flows and the clasts in the Zeballos group sediments present both alkaline (HREE and LILE enrichment) and calc-alkaline (Nb and Ti depletions) signatures. These features are also observed in the MLBA transitional lavas, and could suggest that their genesis was controlled by a mixing process between a component related to the alkali basalts (subslab OIB-source) and a contaminant characterized by a selective depletion in Ti and Nb. The possible contaminants could be the same as those invoked to explain the MLBA transitional signature : 1) rutile-bearing restites of partially melted oceanic crust from the edges of the asthenospheric window incorporated in the mantle (*Guivel et al., 2006*), 2) oceanic sediments, 3) calc-alkaline event residue stored in the Patagonian basal crust (*D'Orazio et al., 2001*). These hypotheses however are not sufficient to explain the Cerro Zeballos peculiar chemical and petrological characteristics, particularly high SiO_2, high Th/Yb and La/Nb ratios (*Espinoza et al., submitted)*, high K_2O and presence of amphiboles.

Major and trace element plots suggest derivation by fractional crystallization of the Zeballos Volcanic Sequence from a parental basaltic liquid, similar to basalt PA-06-11, with crystallization temperatures between 980 and 880°C for pressures of 1 and 0.5 GPa respectively (*Espinoza et al., submitted*). The absence of Eu depletion in REE- patterns indicates that crystallization occurred in high fO_2 conditions. Small plutonic bodies (Cerro Indio and Cerro Negro) of ca. 16- 13 Ma just south of the Alto Rio Ghio and intrusive inside cretaceous basement could be deeper equivalents to the erupted rocks from the Zeballos magmatic group. Apart from the group 3 lavas particular signature, a main issue concerning the Zeballos Volcanic Sequence is the presence of strong calc-alkaline affinities in parental magmas of these lavas, at ca. 300 km east from the trench between 16 and 12 Ma. *Espinoza et al (submitted)* noticed that group 3 lavas geochemical features, as high K_2O contents or La/Nb and La/Yb ratios, are very similar to those of the flat-slab region lavas (Poncho volcanic complex 31.5°S, *Kay and Gordillo (1994)*, Chachaués volcanic complex 37°S, *Kay et al. (2006)*). This leads to propose a shallow subduction model (*Espinoza et al., submitted)* to explain the presence of a back-arc calc-alkaline event at 16- 12 Ma in the western MLBA area.

7.1.2. The shallow plate subduction model.

In the case of central Chile/ Argentina, the Andean flat-slab region has recorded the magmatic and tectonic effects of the shallowing of the subducting Nazca plate since ca. 8Ma. Models involving the generation of a secondary hydration front by slab dehydration and mantle-wedge processes at ca. 500 km east of the present trench (e.g. *Tatsumi and Eggins, 1995 ; Grove et al., 2003*) leading to magmatism with strong arc-like component and high K_2O contents have been proposed to explain the genesis of the Pocho volcanic complex (*Kay and Gordillo, 1994; Kay and Mpodozis, 2002*) in the Chilean flat-slab region and the Chachahuén volcanic complex (*Kay et al., 2006 ; Kay and Ramos, 2006*) in the Neuquén basin. In each case, the shallow subduction is linked with an important coupling near the trench triggered by the subduction of a volcanic ridge. In Patagonia, shallowing syncollisional subduction was suggested by *Gorring et al. (1997)* in relation with the subduction at ca. 15 Ma of the active Chile ridge.

We infer that the subduction of young and buoyant oceanic lithosphere would cause a progressive decrease of the slab dip between ca. 20 and 15 Ma (*fig.9*). North of the CTJ, the oceanic lithosphere is younger oceanward and therefore, the slab is shallowing progressively since millions of years beneath south Patagonia. This event can be related in time and space with the compressive event in Patagonia (*Lagabrielle et al, 2004*) that begins at ca. 20 Ma and ends at ca. 15 Ma with a major contractional phase as the SCR starts to be subducted. Slab shallowing would drive to the migration of the arc towards the East and inducing the genesis of a second hydration front at ca. 300 km east from the trench. Long-term flat-slab magmatism should lead to a more arc-like signature (*Kay and Gordillo (1994)*, *Kay et al. (2006)*). Patagonian lavas keep calc-alkaline to transitional affinities between 17 and 14.5 Ma. This feature has been explained by a transitory flat-slab subduction followed by slab window opening at 12.5 Ma (*fig.9*, *Espinoza et al., submitted*). Slab window could open due to slab tear (*Guivel et al., 2006*) as a consequence of the important coupling near the trench. This leads to an attenuation of the arc-like signature and to the eruption of the MLBA lavas having a typical alkali signature.

7.2. Bearing on the timing of the calc-alkaline to alkaline transition and the development of the slab window.

The Cerro Zeballos hill is an ideal site to study the transition and mixing between subduction calc-alkali magmatism and alkali magmatism and the possible links with the development of a slab window beneath Patagonia. The upper lava flow on the top of Cerro Zeballos hill is synchronous with the onset of the MLBA magmatic event. If the flat-slab model is admitted, the Cerro Zeballos lavas are considered as "normal-subduction" products and the transition has to be found between the Zeballos sequence and the basal MLBA basalts. The crucial question is to decipher if PA-06-11 belongs to the calc-alkaline event (group 3) or to the MLBA transitional event (group 2). Petrology and geochemistry (*Espinoza et al., submitted*) indicate that this sample has a strong calc-alkaline imprint which is not correlated to its low-differentiation rate and consequently, it could be related to the end of the calc-alkaline event in this area at 12.4 Ma. In this case, all the Cerro Zeballos lavas are subduction-related and were generated earlier than the slab window opening. Following these hypothesis, the transition is dated between ca. 12.4 ±1.56 Ma (PA-06-11 sample, top of the hill) and 12.36 ±0.33 Ma (infra-volcanic alkali intrusion and oldest MLBA event-related sample, *Guivel et al. (2006)*). The Pa-06-11 magma could also be a mixing between the last calc-alkaline magmas and the first MLBA-type transitional magmas. The bad resolution on the age of the capping lava flow has a great influence on this transition age.

7.3. Genesis of Western MLBA bimodal magmatism.

7.3.1. Fractional crystallization of alkali basaltic magmas.

Two main hypotheses have been proposed to explain the genesis of bimodal alkaline magmatism. One states a genetic relationship between mafic and felsic group 4 rocks through fractional crystallization processes with variable crustal contamination (*Espinoza et al., 2008*). The other hypothesis invokes the genesis of mafic and felsic lavas from different sources, the basic rocks derived directly from mantle partial melting and the felsic rocks from anatexis of crustal country rocks (*Whalen et al., 1987*). Our geochemical studies are in favour of the former hypothesis. Ratios of incompatible elements such as LILE/HFSE ratios should remain constant or increase in liquid formed by partial melting of crustal rocks during crustal anatexis because LILE are more incompatible than HFSE (*Ayers and Harris, 1997*). The crustal country rocks have LILE/HFSE ratios (Jurassic volcanic Ibañez formation: Rb/Nb= 6.1 -24, Ba/Nb= 96- 218; metamorphic basement: Rb/Nb= 7, Ba/Nb= 34, *Kilian and Behrmann, 2003*) higher than the studied felsic rocks (Rb/Nb= 1.1- 1.9, Ba/Nb= 17.9- 23.4). *Espinoza et al., 2008* show that Sr and Nd isotopic signatures of the felsic W-MLBA rocks are similar to those of the post-plateau MLBA basalts and not consistent with those of the possible crustal sources. Hence, there are neither isotopic nor incompatible trace element arguments supporting the derivation of the felsic rocks (group 4) of western MLBA from anatectic processes involving the crustal rocks.

The huge volumetric dominance of basalts over the felsic rocks also favours the fractional crystallization process as well as petrographical and geochemical evidence suggesting progressive evolution in the alkali trend : the Fe-rich olivines, the Ti-rich (0.5 to 0.8%) clinopyroxenes and the lack of orthopyroxenes mark affinities of felsic rocks with alkali series. In the Nb/Yb vs. La diagram (*fig.10*), the fractional crystallization is marked by an horizontal trend because Nb and Yb do not fractionate during this process. La represents the differentiation degree and Nb/Yb ratio permits the vertical separation of the different sources relatively to Nb anomaly. The felsic rocks plot immediately to the right of the alkali basalts field, which confirms that they are cogenetic with MLBA alkali basalts. Major and trace elements trends are in agreement with crystal fractionation: the negative correlation of MgO, FeO, CaO, Sr and TiO_2 contents versus SiO_2 (*fig.11*) might be explained as a consequence of fractionation of olivine, clinopyroxene, plagioclase and Fe-Ti oxides respectively. The positive correlation of K_2O, Ba and Rb contents versus SiO_2 shows that there is no sanidine in the early phases. Most of the Mifeldi region felsic rocks show similar pattern except Cerro Lapíz granite neck (*Espinoza et al., 2008*). Finally, the ages of the felsic rocks (4.5- 2.5 Ma) indicate that the felsic event occurred at the chronological transition between the main-plateau and the post-plateau magmatic events.

7.3.2. Physical and chemical conditions of fractional crystallization.

Most of the differentiated (SiO_2< ca. 63%) felsic rocks of western MLBA present no or little Eu anomaly (*fig.6*). This feature can be explained by O_2-fugacity (f_{O2}) dependent compatibility of Eu in plagioclases in the first stages of fractional crystallization. The Fe-Ti oxides compositions give indications on T and f_{O2} conditions in the magmatic chamber where those oxides crystallised. *Ghiorso and Sack (1991)* calibrated the T- f_{O2} from two Fe-Ti oxides solid solutions, Magnetite (Fe_3O_4) – Ulvöspinel ($FeTiO_4$) and Ilmenite ($FeTiO_3$) – Hematite (Fe_2O_3). The Fe-Ti oxides compositions of PA-06-15 sample, plotted in the XIlm vs. XUlv diagram (*Lattard et al., 2005*) (*fig.12*), give a temperature of ca. 1 000°C and a very high log(fO_2) of -4.2 (for comparison, SVZ log(fO_2)= -12 to -14.7 for T= 720 – 850°C, *Gutierrez et al. (2005)*). These high fO_2 conditions are consistent with the lack of Eu anomaly. These observations confirm *Espinoza et al. (2008)* conclusions and are consistent with the genesis of felsic rocks through low-pressure and high fO_2 fractional crystallization of mafic magmas in shallow crustal chambers. As a test, a model of closed system fractional crystallization of alkali mafic magmas was conducted with PA-06-03 sample composition, by simple mass balance calculation using major elements, with olivine, clinopyroxene, plagioclase and Fe-Ti oxides fractionation (with composition measured in the PA-06-03 basalt). The results are given in *table 3*. The Pico Rojo dike (PA-06-12) can be obtained with 50% fractional crystallization whereas the felsic dike and lava flow (PA-06-15/16) need larger degrees of crystallization (60% and 65% respectively). These large degrees of fractionation are in agreement with the small volume of erupted differentiated samples compared to the basaltic pile.

However, closed-system fractional crystallization fails to explain some characters such as high concentrations of some incompatible elements (e.g. Th and La, *Espinoza et al., 2008*) for which open-system models must be involved. AFC model (*DePaolo (1981)*) following *Espinoza et al. (2008)* were tested using a primitive alkali basaltic source (with PA-06-03 chemistry) and choosing as a contaminant a Middle Jurassic rhyolitic tuff from the Ibañez formation. The model was tested with incompatible element ratios (Sr/La vs. La/Nb) and the best model indicates 30% of assimilation (assimilation vs. crystallization ratio r=0.3) and a low bulk distribution coefficient for Sr (D_{Sr}) of 1.1. These results must be considered with care because AFC is an under-constrained model and just gives plausible fractional crystallization conditions.

7.4. Origin of the alkali main to post-plateau basalts

The studied felsic W-MLBA rocks derive from MLBA-type alkali basalts and provide ages corresponding to the end of the main plateau event (9.4 to 3.3 Ma) and to the onset of the post-plateau event (3.3 to 2.1 Ma). Basaltic alkaline post-plateau basalts have a relatively strong OIB-like geochemical signature which has been interpreted by *Gorring et al. (2003)* as a consequence of their derivation from an OIB-source involving the deep asthenospheric mantle. The melting of this OIB-source is generally related to a hotspot (*Johnston et al., 1997*) but in the Patagonian ridge-subduction context, this phenomenon is not necessary. Indeed, the opening of a slab window induces deep subslab asthenosphere decompression and melting (*Thorkelson et al., 1996*). The studied alkali post-plateau basalts are linked to the SCR-1 asthenospheric window beneath the region since about 3.3 Ma. In order to explain the main-plateau OIB-like geochemical signature before 3.3 Ma, other models of slab window were invoked as a tearing in the subducting slab (*Guivel et al, 2006*).

The alkali main-plateau and post-plateau basalts may derive from similar types of enriched mantle source (Sr and Nd isotopic ratios, *Gorring et al., 2003; Guivel et al., 2006*). However, the variable slopes of their incompatible trace element pattern are consistent with variable degrees of partial melting of such a source. The geochemistry of post-plateau MLBA basalts is consistent with 1.5 – 5% melting of a mantle source in which garnet is slightly more abundant than spinel. Main plateau alkali lavas would derive from somewhat larger (5- 10%) melting degrees of less garnet-rich source (*Luhr et al., 1995*; *Guivel et al., 2006*). As we have no primitive basalts (Mg#<63), it is difficult to estimate the fusion rate in our study.

8. Magmatic evolution of the Cordillera-MLBA junction from 14 Ma to present, links with the morphotectonic evolution.

8.1 Paleotopography between 14 and 12 Ma : dating the end of the contractional tectonics

The Cerro Zeballos pyroclastic flow that directly overlies the Zeballos group sediments (PA-06-10) gives a local minimum age for the upper beds of the Molasse at 14.48 ±0.2 Ma.

This pyroclastic flow therefore seals a paleosurface topping the molasse, about 14.5 Ma old. Its base represents the very last record of the detrital sedimentation in the former Cordillera piemont of Central Patagonia. The molasse correlates with the Santa Cruz Formation known in all of Patagonia, which is a sequence of clastic fluvial deposits dominated by sand-, silt- and claystone beds locally with conglomerates, resting over the Centinela Formation and recording the end of marine conditions. Since the 14.48 ±0.2 Ma-old lava flow of Cerro Zeballos remains almost horizontal, this paleosurface apparently did not experienced further deformation, at least no later important tilting, suggesting that it also corresponds to the age of the last contractional event in this region. The following alkali flows were emplaced at ca. 12.4 Ma in the MLBA area. These flows belong to an episode of regional extension marking the onset of the construction of the entire MLBA pile. This main episode of alkali basalt flooding, which occurred between 12 and 9 Ma is known indeed from all parts of the MLBA (*Guivel et al., 2006*). Numerous dikes and intrusions in the region also yielded ages comprised between 12 and 9 Ma (*Guivel et al., 2006*).

A fundamental feature regarding the timing of the contractional events at the Cordillera front is that the basal lavas of the meseta are never engaged within thrust faults which affect the Jurassic Ibañez group and the Oligocene-Miocene molasse. Moreover, immediately north of Lago Ghio, the basal lava flows have been erupted unconformably over a flat surface erasing a main thrust front separating the basement to the west, from the molasse to the east (*Giacosa and Franchi, 2001*). This clearly indicates that an erosional surface developed before 12 Ma, erasing some local reliefs inherited from the frontal tectonics and contributing to the sedimentation of the very last molasse deposits. Tectonics might have ceased well before this erosive event and there is no indications allowing to determine precisely the age of the last contractional displacements along faults forming the Cordillera front of Central Patagonia. The age of the Santa Cruz Formation near Lake Cochrane-Puyerredon was constrained by *Blizniuk et al. (2005)* between 22 and 14 Ma, with an important change in $d^{13}C$ and $d^{18}0$ at 16.5 Ma, indicative of one kilometre rapid uplift. At 14 Ma, the deposition ends due to absence of erosion in response to the rain shadow effect of the uplifted Cordillera. Therefore, we may conclude that after a peak at 16 Ma, the tectonic activity of the Cordillera front progressively decreased until 14 Ma. Both slow down in tectonic and rain shadow induced cessation of fluvial sedimentation. Erosion and ablation of frontal reliefs occurred before 12.5 Ma. This progressive change in the regional stress conditions of the frontal Cordillera can be correlated with the initiation of the subduction of Chile ridge at 15- 14 Ma

(*Lagabrielle et al., 2004*). A dramatic change in climatic conditions occurred later, between 12 and 7 Ma, with the development of the very first glaciations which affected also the piemont region (*Mercer and Sutter, 1982* ; *Lagabrielle et al., submitted*).

8.2 Paleotopography, volcanism and glacial sedimentation : the 7-3 Ma period

The geometry of the western side of the MLBA between 7 and 3 Ma can be constrained by the ages of several lava flows lying directly over the molasse or over glacial sediments and sealing paleosurfaces. In the Alto Rio Ghio area, basaltic lava flows, locally up to 10 m thick, have been emplaced in a paleovalley trending N35 -N40, incised in the fluvial sandstones of the Zeballos Group and filled with glacial sediments. Our new date at this site is obtained from a lava flow in direct contact with glacial conglomerates which gives an Ar-Ar age of 6.44 ± 0.56 Ma (PA-06-22). Sample from a flow in the northern part of the outcrop, located 200 m from our sample site gave a whole rock K-Ar age of 4.98 ± 0.15 Ma (*Lagabrielle et al., 2007*). Both flows overlie tills and fluvioglacial conglomerates including numerous clasts deriving from the internal part of the Cordillera (plutonic rocks from the batholith, ignimbrites and lavas from the Mesozoic formations). Our age is the oldest age for a lava flow in contact with tills obtained at this site. The tills immediately underlying this lava flow display a spectacular red-colour indicating contact heating. This strongly suggests lava eruption during a glacial period. Previous studies at this site from a brecciated flow yielded ages of 6.95 ± 0.24 Ma and 2.96 ± 0.09 Ma (*Lagabrielle et al., 2007*). The youngest flow extends horizontally farther west and forms the ancient piemont surface, developed at the foot of the morphotectonic front of the Cordillera. This upper flow overlies a second layer of tills that also extends westwards towards the front of the Cordillera. This set of ages indicates glacial advance and related deposition of sediments at least during 3 periods at ca. 7 Ma, 5 Ma and 3 Ma.

Numerous marks of deformation as well as a major normal fault are observed in this site. This led *Lagabrielle et al. (2007)* to propose a strong tectonic control of the Alto Rio Ghio area. Faulting initiated during the deposition of the first tills and lavas, that is probably as early as 7-6 Ma. The oldest known basaltic lava flow outside the Alto Rio Ghio area is located about 5 km west from the MLBA edge and is dated at 6.85 ±0.15 Ma (PA06-19). During lava eruption, the molasse was thus still exposed in this area, whereas some ten of kilometres eastward, 12 Ma to 7 Ma old alkali flows already covered the Cordillera piemont.

This can be due to the persistence of a paleo-relief of molasse or this may suggest tectonic rejuvenation at 7-6 Ma, in relation with normal faulting, as revealed by the Alto Rio Ghio area faulting, leading to exhumation of the molasse.

Finally, the large set of geochronological data obtained from the Alto Rio Ghio area reveals a typical succession of lava flows and glacial sediments between 7 and 3 Ma. It indicates a similar geology to that of the rest of the Meseta del Lago Buenos Aires extending largely immediately to the east. Hence we infer that the Alto Rio Ghio area is a remnant of the westernmost edge of the Meseta which has been down-faulted due to (trans-) tensive faulting along the Rio Zeballos fault zone (*Lagabrielle et al., 2007, submitted* ; *Scalabrino et al., in review*). As shown in the following section, disruption started around 3 Ma, in response to the tectonic rejuvenation of the Cordillera front and coevally with the 3 Ma syn-tectonic magmatism of the Rio Zeballos fault zone.

8.3 Important changes at 4 -3 Ma : the magmatic-tectonic rejuvenation.

Two molasse paleosurfaces were sealed at 3.23 ±0.08 Ma (PA06-18) and 3.1 ±0.08 Ma (PA06-16) close to the current MLBA border. Abundance of coeval magmatic ages indicate that a major event occurred around 4 -3 Ma. Our ages together with former ages show a relative homogeneity between 4.41 ±0.54 Ma and 2.76 ±0.07 Ma, near Pico Rojo neck and between 3.65 ±0.1 Ma and 3.08 ±0.13 Ma near Mifeldi intrusion (*fig.7*) (*Espinoza et al., 2008*). The Mifeldi pluton is a lenticular-shaped intrusion now exposed along a ~200m high N-S trending vertical scarp which coincides here with the MLBA border. This pluton intrudes the Mio-Pliocene basalts of the upper sequence of the MLBA as demonstrated by exposures well observed on both edges of the pluton (*Espinoza et al., 2005*). The Cerro Lapíz neck is the core of a major eroded volcano, located 4 km to the south. It is intrusive into the Mio-Pliocene basalts and is a more differentiated equivalent of Pico Rojo. *Figure 13* summarizes these geometrical constraints. The close association between the neck and dike structures, and acid volcanism calls for the existence of now eroded voluminous aerial volcanic constructions. Therefore, the 4 -3 Ma old landscape of this region was probably very different from the current one.

The 4 -3 Ma old bimodal intrusions and dikes outcropping close to the western edge of MLBA are aligned along the N160- 170 trending lineament of the Zeballos Fault Zone. This fault zone coincides with the western border of MLBA and is topographically associated with significant morphological scarps and aligned landslides suggesting a strong tectonic control (*Lagabrielle et al., 2007*). This magmatic lineament is associated with normal and strike-slip faults, that were active from 6 Ma to 3 Ma, probably inversing inherited faults associated with the Cordilleran construction (*Suarez et al., 2000; Lagabrielle et al., 2004, Scalabrino et al., in review*). Moreover, the entire western part of MLBA close to this lineament presents an overall doming visible in high-resolution MNT (*Lagabrielle et al., 2004, 2007, Scalabrino et al., 2009 ; Scalabrino et al., in review*) suggesting morphological inflation due to intrusion of a larger laccolith underlying Monte Zeballos (*fig.13*). These features collectively suggest a strong structural control on the location of magma emplacement. Offset along the main normal fault was probably not greater that 500 m; indeed, the intrusions have been emplaced at depth sufficient to crystallize grained or micrograined intrusions but rather superficially in the core of the former western-MLBA volcanoes. Relatively moderate tectonic offset, together with strong erosion were needed to exhume these shallow bodies.

All the differentiated products were emitted between 4.50 and 2.75 Ma as a series of intrusions and lava flows aligned along the N160- 170 trending lineament of Zeballos Fault Zone whereas MLBA basaltic products have a larger time and space repartition (post plateau basalts covered all the MLBA surface between 3.3 Ma and 110 ka, *Guivel et al. (2006)*). The felsic event is thus clearly restricted in time and space, suggesting tight relationships between a regional extension event and the genesis of these rocks. In active rifts, aligned alkali intrusions and bimodal magmatism are common because normal faulting allows upwelling of magmas to upper crustal levels. These magmas are stored and experience differentiation in newly created spaces thanks to active extension. They finally erupt through the same fault network which allowed earlier magmatic processes. The presently studied area is of course not a large continental rift zone. Nevertheless, it is an area where collapse and extension took place between 6 and 3 Ma (*Lagabrielle et al., 2004, 2007; Scalabrino et al., in review*), particularly in the Rio Ghio / Rio Zeballos valley region. This event could allow for the creation of small magmatic chambers in the crust where the alkali magma differentiation would be able to occur with small rates of assimilation.

The region south of LGCBA is located just above the estimated present-day location of the subducted (ca. 6 Ma ago) SCR-1 segment of the SCR (*Cande and Leslie, 1986*) and geophysical studies clearly indicate the occurrence of a thermal and compositional mantle anomaly below the region since, at least, Eocene times (*Ramos and Kay, 1992; Gorring et al.,* *1997; Murdie et al., 2000; Gorring and Kay, 2001; Gorring et al., 2003*). The consistency of ages and localization of the felsic magmatism with the collapsed zone is probably not casual and calls for regional control of the volcanic field.

8.4. Tectono-magmatic model of western-MLBA border evolution.

A tentative sketch for the proposed tectono-magmatic model of the W-MLBA evolution is shown in *Figure 14*. Between 12 and 8 Ma (*fig.14a*), important volumes of alkaline to transitional basalts are emplaced on a paleotopography deriving from the erosion of Patagonian cordillera tectonic front at ca. 16 Ma. OIB-type magmas would be generated by the partial melting of the subslab asthenospheric mantle uprising through a slab window, as a tear in the slab (*Guivel et al., 2006*). At 6 Ma, the SCR-1 ridge segment subducted and a main to post-plateau alkali and transitional magmatic event occurred at ca. 5- 3 Ma (*fig.14b*) being related to the location of the corresponding slab window beneath the region (*Gorring et al., 2001; Guivel et al., 2006*). Associated to the magmatic event, negative inversion occurred between 5 and 3 Ma, as observed in the Rio Ghio/ Rio Zeballos valley (*Lagabrielle et al., 2005, 2007; Scalabrino et al., 2009 ; Scalabrino et al., in review*). This extensional event may have started earlier (7- 6 Ma) as suggested by the normal faulting in the Rio Ghio area. At around 5- 4 Ma, it allowed the emplacement of shallow magma chambers along the tectonic corridor, probably in the Jurassic Ibañez group or within the underlying metamorphic basement. The basalts could then either erupt directly at the surface or locally differentiate with small rates of assimilation (ca. 30%). At ca. 4 Ma, the felsic lavas are emplaced within the Zeballos group sediments or the MLBA basalts as necks, dikes and lava flows following the N160- 170 fault zone along the western MLBA flank. This leads to the bimodal magmatism. At or after ca. 3 Ma, normal faults activity lead to the disruption of the region, to the uplift of the meseta border, to the exposure of the felsic intrusions, and to the onset of erosion of the 3 Ma volcanoes. From 3.3 Ma to 110 ka, the MLBA basaltic post-plateau magmatism was still active but without any differentiation. Since 3 Ma, the core of the former volcanoes have been exhumed (*fig.14c*) and the western border of MLBA has been modified by landslides. Glaciers which were flowing over the paleosurface of the Meseta are now restricted to Quaternary glacial valleys deeply incised to the north and to the south of the current meseta edges (*Lagabrielle et al., submitted*).

9. Conclusions.

The western flank of the MLBA is a key area to study the volcanic and structural effects of the subduction of the SCR. The ^{40}Ar-^{39}Ar ages and the geochemical analysis allow us to reconstitute the magmatic events and their interactions with tectonics. Major changes in the back-arc magmatism occurred at ca. 12.5 Ma with the transition from calc-alkali lavas (Cerro Zeballos) to transitional/ alkali lavas (MLBA). This transition is related to the opening of a slab window beneath the region. The calc-alkaline lavas likely derive from a temporary flat subduction configuration and the migration of the hydration front eastwards. A series of alkaline felsic intrusions, ranging from trachy-andesite to trachyte (and alkali microgranites), associated trachytic lava flows, dated between 4 and 3 Ma, occur in the western flank of the MLBA. These lavas are synchronous with the transition from main to post-plateau MLBA magmatism and they are genetically related. These OIB-like alkali to transitional basalts are generated by partial melting of the subslab asthenosphere of the subducting Nazca plate during the opening of the South Chile Ridge spreading ridge-related slab window. These basalts differentiated with small rates of assimilation in shallow magmatic chambers emplaced along transtensional to extensional (rift-like) zones where magmas could be stored (as western MLBA area) during the Patagonian collapse event between 6 and 3 Ma. The collapse event is a consequence of the presence of the asthenospheric window (SCR-1 segment of South Chile Ridge) below the MLBA. The structure inherited from this event lead to the emplacement of the bimodal magmas along the N160 – 170 tectonic corridor (the Zeballos Fault Zone). The proposed model explains both magmatic and tectonic characteristics of Western-MLBA zone and it can probably be applied to other zones where felsic Magmatism is associated with a collapse event in spreading ridge subduction contexts.

Acknowledgements:

The authors would like to thank Céline Liorzou and Claire Bassoulet for the ICP-AES and ICP-MS analyses (UMR 6 538, Brest, France). This work was made possible through grants from the ECOS-Sud program and from the Relief program (INSU-CNRS, France).

References:

Ayers, M., Harris, N., 1997. REE fractionation and Nd-isotope disequilibrium during crustal anatexis: constraints from Himalayan leucogranites. Chemical Geology, 139: 249–269.

Baker, P. E., Rea, W. J., Skarmeta, J., Caminos, R., Rex, D. C., 1981. Igneous History of the Andean Cordillera and Patagonian Plateau around Latitude 46 degrees S. Philosophical Transactions of the Royal Society of London. Series A, Mathematical and Physical Sciences, 303 (1474): 105-149.

Bangs, N.L., Cande, S.C., Lewis, S.D., Miller, J.J., 1992. Structural framework of the Chile margin at the Chile Ridge collision zone. Proceedings of Ocean Drilling Program Initial Report, 141: 11–21.

Bell, C. M. and Suárez, M., 2000. The Río Lácteo Formation of Southern Chile. Late Paleozoic orogeny in the Andes of southernmost South America. Journal of South American Earth Sciences, 13 (1-2): 133-145.

Bjerg, E.A., Ntaflos, T., Kurat, G., Dobosi, G., Labudia, C.H., 2004. The upper mantle beneath Patagonia, Argentina, documented by xenoliths from alkali basalts. Journal of South American Earth Sciences, 18: 125–145.

Blisniuk, P.M., Stern, L.A., Chamberlain, C.P., Idleman, B., Zeitler, P.K., 2005. Climatic and ecologic changes during Miocene surface upliflt in the southern Patagonian Andes. Earth and Planetary Science Letters, 230: 125-142.

Breitsprecher, K. and Thorkelson, D.J., 2009. Neogene kinematic history of Nazca-Antarctic-Phoenix slab window beneath Patagonia and the Antarctic Peninsula. Tectonophysics: 464: 10-20.

Brown, L.L., Singer, B.S., and Gorring, M.L., 2004. Paleomagnetism and 40Ar/39Ar Chronology of Lavas from Meseta del Lago Buenos Aires, Patagonia. Geochemistry, Geophysics, Geosystems, 5 (1): Q01H04.

Busteros, A. and Lapido, O., 1983. Rocas basicas en la vertiente noroccidental de la meseta del lago Buenos Aires, provincia de Santa Cruz. Asociación Geológica Argentina, Revista XXXVIII (3-4): 427-436.

Cande, S.C., Leslie, R.B., 1986. Late cenozoic tectonics of the southern Chile trench. Journal of Geophysical Research, 91 (B1): 471-496.

Cande, S.C., Leslie, R.B., Parra, J.C., Hobart, M., 1987. Interaction between the Chile ridge and Chile trench : geophysical and geothermal evidence. Journal of Geophysical Research, 92 (B1): 495-520.

Cembrano, J., Hervé, F., Lavenu, A., 1996. The Liquine Ofqui fault zone: a long-lived intra-arc fault system in southern Chile. Tectonophysics, 259: 55–66.

Cole, R.B., Stewart, B.W., 2007. Continental margin volcanism at sites of spreading ridge subduction: Examples from southern Alaska and western California. Tectonophysics, 464(1-4): 118-136.

Corgne, A., Maury, R.C., Lagabrielle, Y., Bourgois, J., Suarez, M., Cotton, J. and Bellon, H., 2001. The diversity of basalts from Patagonia at the latitude of the Chile triple junction (46°–47°S). Additional data and implications on the subduction processes. Comptes Rendus de l'Académie des Sciences - Series IIA - Earth and Planetary Science, 333 (7): 363-371.

Cotton, J., Le Dez, A., Bau, M., Caroff, M., Maury, R.C., Dulski, P., Fourcade, S., Bohn, M. and Brousse, R., 1995. Origin of anomalous rare-earth element and yttrium enrichments in subaerially exposed basalts: Evidence from French Polynesia. Chemical Geology, 119 (1-4): 115-138.

Demant, A., Suarez, M. et De La Cruz, R., 2007. Geocronología y petroquímica de sucesiones volcánicas del Cretácico Superior-¿Paleógeno? del este de la Cordillera Patagónica oriental (45°15'-45°40'S). Rev. geol. Chile, 34: 3-21.

DeMets, C., Gordon, R.G., Argus, D.F. and Stein, S., 1990. Current plate motions. Geophys. J. Int., 101 (2), 425-478.

DePaolo, D.J., 1981. Trace element and isotopic effects of combined wallrock assimilation and fractional crystallization. Earth and Planetary Science Letters, 53: 189–202.

D'Orazio, M., Agostini, S., Mazzarini, F., Innocenti, F., Manetti, P., Haller, M.J., Lahsen A., 2000. The Pali Aike volcanic field, Patagonia: slab-window magmatism near the tip of South America. Tectonophysics, 321: 407-427.

D'Orazio, M., Agostini, S., Innocenti, F., Haller, M.J., Manetti, P., Mazzarini. F., 2001. Slab window-related magmatism from southernmost South America: the Late Miocene mafic volcanics from the Estancia Glencross Area (~52oS, Argentina-Chile). Lithos, 57 (2): 67-89.

D'Orazio, M., Innocenti, F., Manetti, P., Tamponi, M., Tonarini, S., Gonzalez-Ferran, O., Lahsen, A., Omarini, R., 2003. The Quaternary calc-alkaline volcanism of the Patagonian Andes close to the Chile triple junction: geochemistry and petrogenesis of volcanic rocks from the Cay and Maca volcanoes (~ 45°S, Chile). Journal of South American Earth Sciences, 16: 219–242.

D'Orazio, M., Innocenti, F., Manetti, P., Haller,http://www.sciencedirect.com/science?_ob=ArticleURL&_udi=B6VDS-4FBW5SC-2&_user=2402213&_rdoc=1&_fmt=&_orig=search&_sort=d&view=c&_acct=C000041118&_version=1&_urlVersion=0&_userid=2402213&md5=db76a92bc1ba1124a6a503ea475f2177 - aff3#aff3 M.J., Di Vincenzo,http://www.sciencedirect.com/science?_ob=ArticleURL&_udi=B6VDS-4FBW5SC-2&_user=2402213&_rdoc=1&_fmt=&_orig=search&_sort=d&view=c&_acct=C000041118&_version=1&_urlVersion=0&_userid=2402213&md5=db76a92bc1ba1124a6a503ea475f2177 - aff2#aff2 G., and Tonarini, S. 2004. The Late Pliocene mafic lavas from the Camusú Aike volcanic field (~50°S, Argentina): Evidence for geochemical variability in slab window magmatism. Journal of South American Earth Sciences, 18 (2): 107-124.

Eby, G.N., 1992. Chemical subdivision of the A-type granitoids: Petrogenetic and tectonic implications. Geology, 20 (7): 641–644.

Espinoza, F., 2003. Petrologia y geoquimica de los basaltos cenozoicos de la meseta de Chile Chico, 46°35'S- 46°47'S- 71°46'-72°02'W XI region de Aysen, Chile. Ph.D. Thesis, Universidad de Chile, Santiago, Chile. 220 pp.

Espinoza, F., Morata, D., Pelleter, E., Maury, R.C., Suárez, M., Lagabrielle, Y., Polvé, M., Bellon, H., Cotten, J., De la Cruz, R., and Guivel, C., 2005. Petrogenesis of the Eocene and Mio- pliocene alkaline basaltic magmatism in Meseta Chile Chico, southern Patagonia, Chile : evidence of the participation of two slab windows, Lithos., 82: 315-343.

Escosteguy, L., Dal Molin, C., Franchi, M., Geuna, S., Lapido, O., 2002. Estratigrafia de la cuenca de los rios El Zeballos y Jeinemeni, Noroeste de la provincia de Santa Cruz. In XV Congreso Geologico Argnetino, El Calafate, 2002.

Espinoza, F., Morata, D., Pelleter, E., Maury, R.C., Suárez, M., Lagabrielle, Y., Polvé, M., Bellon, H., Cotten, J., De la Cruz, R., Guivel, C., 2005. Petrogenesis of the Eocene and Mio-Pliocene alkaline basaltic magmatism in Meseta Chile Chico, Southern Patagonia, Chile: evidence for the participation of two slab windows. Lithos 82: 315–343.

Espinoza, F., Morata, D., Polvé, M., Lagabrielle, Y., Maury, R.C., De la Rupelle, A., Guivel, C., Cotton, J., Bellon, H., Suárez, M. Middle Miocene calc-alkaline volcanism in central Patagonia back-arc (47°S) : petrogenesis and implications for slab dynamics. Submitted to Andean geology.

Espinoza, F., Morata, D., Polvé, M., Lagabrielle, Y., Maury, R.C., Guivel, C., Cotton, J., Bellon, H., Suárez, M., 2008. Bimodal back-arc alkaline magmatism after ridge subduction: Pliocene felsic rocks from Central Patagonia (47°S). Lithos 101: 191-217.

Fleck, R.J, Sutter, J.F. and Elliot, D.H., 1977. Interpretation of discordant 40Ar/39Ar age-spectra of Mesozoic tholeiites from Antarctica. Geochim. Cosmochim. Acta, 41: 15–32.

Flint, S. S, Prior, D. J., Agar, S. M. and Turner, P., 1994. Stratigraphic and structural evolution of the Tertiary Cosmelli Basin and its relationship to the Chile triple junction. Journal of the Geological Society, 151 (2): 251-268.

Garcia, S., Arnaud, N. O., Angelier, J., Bergerat, F., and Homberg, C., 2003. Rift jump process and new paleorift location in northern Iceland for the last 10Ma based on 40Ar/39Ar geopchronology. Earth and Planetary Science Letters, 214 (3-4): 529-544.

Garret, S.W., Storey, B.C., 1987. Lithospheric extension on the Antarctica Peninsula during Cenozoic subduction. In Extension in the basin and Range Province and East Pacific Margin. Geological Society, London, Special Publications, 28: 419–431.

Ghiorso, M.S., Sack, R.O., 1991. Fe–Ti oxide geothermometry. Thermodynamic formulation and the estimation of intensive variables in silicic magmas. Contributions to Mineralogy and Petrology, 108: 485–510.

Giacosa, R. and Franchi, M., 2001. Hojas Geológicas 4772-III y 4772-IV Lago Belgrano y Lago Posadas, Provincia de Santa Cruz. Programa Nacional de Cartas Geológicas de la República Argentina, Boletin n°256, 2001.

Gorring, M., Kay S., Zeitler, P., Ramos, V., Rubiolo, D., Fernandez, M., Panza, J., 1997. Neogene Patagonian plateau lavas : Continental magmas associated with ridge collision at the Chile Triple Junction. Tectonics, 16 (1): 1-17.

Gorring, M., Kay, S., 2001. Mantle processes and sources of Neogene slab window magmas from Southern Patagonia, Argentina, Journal of petrology, 42 (6): 1067- 1094.

Gorring, M., Singer, B., Gowers, J., Kay, S.M., 2003. Plio-pleistocene basalts from the Meseta del Lago Buenos Aires, Argentina: evidence for asthenosphere-lithosphere interactions during slab window magmatism, Chemical geology, 193 (3-4): 215-235.

Grove, T.L., Elkind-Tanton, L.T., Parman, S.W., Chatterjee, N., Müntener, O., Gaetani, G.A., 2003. Fractional crystallization and mantle-melting controls on calc-alkaline differentiation trends. Contributions to Mineralogy and Petrology, 145: 515-533.

Guillaume, B., Martinod, J., Husson, L., Roddaz, M., and Riquelme, R., 2009. Neogene uplift of central eastern Patagonia: Dynamic response to active spreading ridge subduction? Tectonics, 28, TC2009.

Guivel, C., Lagabrielle, Y., Bourgois, J., Maury, R.C., Fourcaded, S., Martin, H., Arnaud, N., 1999. New geochemical constraints for the origin of ridge-subduction-related plutonic and volcanic suites from the Chile Triple Junction (Taitao Peninsula and Site 862, LEG ODP141 on the Taitao Ridge). Tectonophysics 311: 83–111.

Guivel, C., Morata, D., Pelleter, E., Espinoza, F., Maury, R.C., Lagabrielle, Y., Polve, M., Bellon, H., Cotton, J., Benoit, M., Suarez, M., De la Cruz, R., 2006. Miocene to Late Quaternary Patagonian basalts (46–478S): Geochronometric and geochemical evidence for slab tearing due to active spreading ridge subduction. Journal of Volcanology and Geothermal Research, 149: 346–370.

Gutierrez, F., Gioncada, A., Gonzalez Ferran, O., Lahsen, A., Mazzuoli, R., 2005. The Hudson Volcano and surrounding monogenetic centres (Chilean Patagonia): An example of volcanism associated with ridge–trench collision environment. Journal of Volcanology and Geothermal Research, 145: 207– 233.

Hawkesworth, C.J., Norry, M.J., Roddick, J.C., Baker, P.E., Francis, P.W., Thorpe, R.S., 1979. 143Nd/144Nd, 87Sr/86Sr and incompatible trace element variation in calc-alkaline andesitic and plateau lavas from South America. Earth and Planetary Science Letters, 42: 45-57.

Heintz, M., Debayle, E., Vauchez, A., 2005. Upper mantle structure of the South American continent and neighboring oceans from surface wave tomography. Tectonophysics 406: 115–139.

Herron, E.M., Cande, S.C. and Hall, B.R., 1981. An active spreading center collides with a subduction zone: a geophysical survey of the Chile margin triple junction. In: L.D. Kulm, J. Dymond, E.J. Dasch, D.M. Hussong and R. Roderick (Editors), Nazca Plate: Crustal Formation and Andean Convergence. Geol. Soc. Am. Mem., 154: 683-701.

Hervé, F., Demant, A., Ramos, V.A., Penkhurst, R.J., Suárez, M., 2000. The southern Andes. In Tectonic evolution of south America, Rio de Janeiro, 2000: 605-634.

Hole, M.J., Rogers, G., Saunders, A. and Storey, M., 1991. Relation between alkalic volcanism and slab-window formation. Geology, 19: 657-660.

Johnson, R.W., Jacques, A.L., Langmuir, C.H., Perfit, M.R., Staudigel, H., Dunkley, P.N., Chappell, B.W., and Taylor, S.R., 1987. Ridge subduction and forearc volcanism: petrology and geochemistry of rocks dredged from the western Solomon arc and Woodlark basin. In: Marine Geology, Geophysics, and Geochemistry of the Woodlarck-Basin-Solomon Islands, B. Taylor and N.F. Exon, eds., Circum Pacific Counc. Energy Miner. Resour., Houston, TX., 155-226.

Johnston, S.T., Thorkelson, D.J., 1997. Cocos-Nazca slab window beneath Central America. Earth and Planetary Science Letters, 146: 465-474.

Jolly, W.T., Lidiak, E.G., Dickin, A.P., 2007. Bimodal volcanism in northeast Puerto Rico and the Virgin Islands (Greater Antilles Island Arc): Genetic links with Cretaceous subduction of the mid-Atlantic ridge Caribbean spur. Lithos, 103: 393-414.

Kay, S. M., Ramos, V.A. and Marques, M., 1993. Evidence in Cerro Pampa volcanic rocks for slab-melting prior to ridge-trench collision in southern South America. Journal of Geology, 101: 703-714.

Kay, S.M., and Gordillo, C.E., 1994. Pocho volcanic rocks and the melting of depleted continental lithosphere above a shallowly dipping subduction zone in the Central Andes. Contributions to Mineralogy and Petrology, 117: 25-44.

Kay, S.M., and Mpodozis, C., 2002. Magmatism as a probe to the Neogene shallowing of the Nazca plate beneath the modern Chilean flat-slab. Journal of South American Earth Sciences, 15 (1): 39-57.

Kay, S.M., Mancilla, O., Copeland, P., 2006. Evolution of the late Miocene Chachahuén volcanic complex at 37°S over a transient shallow subduction zone under the Neuquén Andes. In: Kay S.M., Ramos V., 2006. Evolution of an Andean margin : A tectonic and magmatic view from the Andes to the Neuquén Basin (35°-39°S lat). Geological Society of American Special Paper, n°407, 215-246.

Kilian, R., Behrmann, J., 2003. Geochimical constraints on the sources of southern Chile trench sediments and their recycling in arc magmas of the Southern Andes. Journal of the Geological Society (London), 160: 57- 70.

Kinimani, K., Miyashita, S. and Kawabata, K., 1994. Ridge collision and in situ greenstones: An example from the Late Cretaceous Ryukyu Islands and southwest Japan margin. The Island Arc, 3: 103-111.

Lagabrielle, Y., Guivel, C., Maury, R., Bourgois, J., Fourcade, S., and Martin, H., 2000. Magmatic-tectonic effects of high thermal regime at the site of active spreading ridge subduction : the Chile Triple Junction model. Tectonophysics, 326 (3-4): 215-228.

Lagabrielle, Y., Suarez, M., Rossello, E., Hérail, G., Martinod, J., Régnier, M., de La Cruz, R., 2004. Neogene to quaternary tectonic evolution of the Patagonian Andes at the latitude of the Chile Triple Junction. Tectonophysics, 385: 211-241.

Lagabrielle, Y., Suárez, M., Malavieille, J., Morata, D., Espinoza, F., Maury, R.C., Scalabrino, B., Barbero, L., De la Cruz, R., Rossello, E., Bellon, H., 2007. Pliocene extensional tectonics in the Eastern Central Patagonian Cordillera: geochronological constraints and new field evidence. Terra Nova 19 (6): 413–424.

Lagabrielle, Y., Scalabrino, B., Suarez, M., Ritz, J.F. Mio-Pliocene glaciations of Central Patagonia : New evidence and tectonic implications, Submitted to Andean Geology-Revista Geologica de Chile.

Lattard, D., Sauerzapf, U., Kasemann, M., 2005. New calibration data for the Fe–Ti oxide thermo-oxybarometers from experiments in the Fe–Ti–O system at 1 bar, 1 000–1 300°C and a large range of oxygen fugacities. Contrib. Mineral Petrol, 149: 735–754.

Linares, E., and Gonzales, R.R., 1990. Catalógo de edades radiométricas de la Républica Argentina 1957-1987. Asociacion Geológica Argentina, Publicaciones Especiales Serie B, Didactica y Complementaria, 19: 1-628.

Luhr, J.F., Aranda-Gomez, J.J., Housh, T.B., 1995. San Quintin volcanic field, Baja California Norte, Mexico: geology, petrology and geochemistry. Journal of Geophysical Research 100, 10353– 10380.

Marshak, R.S., et D.E. Karig, 1977. Triple junctions as a cause for anomalously near-trench igneous activity between the trench and volcanic arc, Geology, 5: 233-236.

Marshall L.G., Salinas, P., 1990. Stratigraphy of the Río Frías formation (Miocene), along the Alto Río Cisnes, Aysén, Chile. Revista Geológica de Chile, 17: 57–88.

Mehier B., 1995. Magmatisme et tectonique des plaques, Paris, Ellipses, 256 pp.

Mercer, J.H., Sutter, J.F., 1982. Late Miocene-Earliest Pliocene Glaciation in Southern Angentina: implications for global ice sheet history. Palaeogeography, Paleoclimatology, Palaeoecology, 38: 185-206.

Morata, D., Barbero, L., Suarez, M., De la Cruz, R., 2002. Early Pliocene magmatism and high exhumation rates in the Patagonian Cordillera (46840VS): K–Ar and fission track data. Fifth International Symposium on Andean Geology. ISAG, Toulouse, France, pp. 433–436.

Murdie, R.E., Style, P., Prior, D., 2000. A new gravity map of southern Chile and its preliminary interpretation. Rev. geol. Chile, 27 (1): 49-63.

Nelson, E., Forsythe, R., Arit, I., 1994. Ridge collision tectonics in terrane development. Journal South American Earth Sciences, 7: 271-278.

O'Neill, H.S.C., Pownceby, M.I., 1993. Thermodynamic data from redox reactions at high temperatures. I. An experimental and theoretical assessment of the electrochemical method using stabilized zirconia electrolytes, with revised values for the Fe– ’’FeO’’, Co–CoO, Ni–NiO and Cu–Cu2O oxygen buffers, and new data for the W–WO2 buffer. Contrib Miner Petrol, 114: 296– 314.

Osozawa, S., and Yoshida, T. 1997. Arc-type and intraplate-type ridge basalts formed at the trench-trench-ridge triple junction: implication for the extensive sub-ridge mantle heterogeneity. The island arc, 6: 197-212.

Pallares, C., Maury, R.C., Bellon, H., Royer, J-Y., Calmus, T., Aguillón-Robles, A., Cotton, J., Benoit, M., Michaud, F., Bourgois, J., 2007. Slab-tearing following ridge-trench collision: Evidence from Miocene volcanism in Baja California, México. Journal of Volcanology and Geothermal Research, 161: 95–117.

Pankhurst. R.J., Weaver. S.D., Hervé. F., Larrondo. P., 1999. Mesozoic-Cenozoic evolution of the North Patagonian Batholith in Aysén, southern Chile. Journal of the geological society of London, 156: 673-694.

Parada, M.A., Lahsen, A., Palacios, C., 2001. Ages and geochemistry of Mesozoic- Eocene back-arc volcanic rocks in the Aysén region of the Patagonian Andes, Chile. Revista Geológica de Chile, 28 (1): 25-46.

Pardo-Casas, F., Molnar, P., 1987. Relative motion of the Nazca (Farallón) and South American plates since Late Cretaceous time. Tectonics, 6: 233-248.

Ramos, V.A. and Kay, S.M., 1992. Southern Patagonian plateau basalts and deformation : backarc testimony of ridge collision. In : R.A. Olivier, N. Vatin-Pérignon and G. Laubacher (Editors), Andean Geodynamics. Tectonophysics, 205 : 261-282.

Ramos, V.A and Aleman, A., 2000. Tectonic evolution of the Andes. In: Tectonic evolution of south America, Rio de Janeiro, 2000: 635-685.

Ramos, V.A., Cristallani, E.O., López, D., 2002. The Pampean flat slab of the Central Andes. Journal of South American Earth Sciences, 11: 211-215.

Renne, P.R., Swisher, C.C., Deino, A.L., Karner, D.B., Owens, T.L., and DePaolo, D.J., 1998. Intercalibration of standards, absolute ages and uncertainties in 40Ar/ 39Ar dating. Chemical Geology, 145(1-2): 117-152.

Roddick, J.C., Cliff, R.A., Rex, D.C., 1980. The evolution of excess argon in alpine biotites. Earth Planet. Sci. Lett, 48: 185-208.

Scalabrino, B., Lagabrielle, Y., Malavieille, J., Dominguez, S., Morata, D., Espinoza, F., Suarez, M., Rossello, E., 2007. Impact of spreading ridge subduction on the morphotectonic evolution of the Patagonian Cordillera since 15 Ma (latitude of the Chile Triple Junction, CTJ). Poster, GEOSUR 2007 International Geological Congress on the Southern hemisphere, Santiago, Chile.

Scalabrino, B., Lagabrielle, Y., De la Rupelle, A., Malavieille, J., Polvé, M., Espinoza, F., Morata, D., Suarez, M., 2009. Subduction of an Active Spreading Ridge Beneath Southern South America: A Review of the Cenozoic Geological Records from the Andean Foreland, Central Patagonia (46-47°S). In: S. Lallemand and F. Funiciello (eds.), Subduction Zone Geodynamics, Springer-Verlag Berlin Heidelberg 2009 IJES volume special subduction conference.

Scalabrino, B., Lagabrielle, Y., Malavieille, J., Dominguez, S., Morata, D., Espinoza, F., Suarez, M., Rossello, E., in review. A morphotectonic analysis of Central Patagonian Cordillera. Negative inversion of the Andean belt over a buried spreading center? Accetped to Tectonics, minor revisions

Singer, B.S., Ackert Jr., R.P., Guillou, H., 2004. 40Ar/39Ar and K–Ar chronology of Pleistocene glaciations in Patagonia. Geological Society of America Bulletin, 116: 434–450.

Spencer, K., Lindsley, D., 1981. A solution model for coexisting iron-titanium oxides, American Mineralogist, 66: 1189-1201.

Stern, C.R., Zartman, F.A., Futa, K., Zartman, R.E., Peng, Z., Kyser, T.K., 1990. Trace-element and Sr, Nd, Pb, and O isotopic composition of Pliocene and Quaternary alkali basalts of the Patagonian Plateau lavas of southernmost South America. Contrib. Mineral. Petrol. 104: 294–308.

Suárez, M., De La Cruz, R., 2000. Edades del Grupo Ibáñez en la parte oriental del Lago General Carrera (46°-47° LS), Aysén, Chile. In: Congreso Geológico Chileno, No. 8, Actas 2: 1548-1551.

Suárez, M., De La Cruz, R., and Bell, C. M., 2000. Timing and origin of deformation along the Patagonian fold and thrust belt. Geological Magazine, Cambridge University Press, 137: 345-353.

Suárez, M., and De La Cruz, R. 2001. Jurassic to Miocene K–Ar dates from eastern central Patagonian Cordillera plutons, Chile (45°–48° S). Geological Magazine, Cambridge University Press, 138: 53-66.

Suárez, M., Lagabrielle, Y., Malavieille, J., Morata, D., Espinoza, F., Maury, R., Scalabrino, B., Barbero, L., De la Cruz, R., Rossello, E., Bellon, H. Vertical tectonics in Eastern Central Patagonian Cordillera during the Miocene-Pleistocene: geomorphological and radiochronological evidence. Submitted to Terra Nova, oct. 2006.

Sun, S., McDonough, W.F., 1989. Chemical and isotopic systematics of oceanic basalts; implications for mantle composition and processes. Saunders, A.D., Norry, J.M. (Eds.), Magmatism in the Ocean Basins. Geological Society of London Special Publication, 42: 313–345.

Tatsumi, Y., and Eggins, S., 1995. Subduction Zone magmatism. Blackwell Publishing, pp.224.

Tebbens, S. F., Cande, S.C. 1997. Southeast Pacific tectonic evolution from early Oligocene to Present, Journal of Geophysical Research, 102: 12 061-12 084.

Tebbens, S. F., Cande, S. C., Kovacs, L., Parra, J. C., LaBrecque, J. L., Vergara, H., 1997. The Chile ridge : a tectonic framework. Journal of Geophysical Research, 102 (B6): 12 035-12 060.

Thorkelson, D.J., 1996. Subduction of diverging plates and the principles of slab window formation. Tectonophysics, 255: 47-63.

Ton-That, T., Singer, B.S., Mörner, N.A., and Rabassa, J., 1999. Datación por el método 40Ar/39Ar de lavas basalticas y geología del Cenozoico superior en la región del Lago Buenos Aires, provincia de Santa Cruz, Argentina. Revista de la Asociación Geológica Argentina, 54: 333-352.

Weaver, S.D., Storey, B.C., Pankhurst, R.J., Mukasa, S.B., DiVenere, V.J. and Bradshaw, J.D., 1994. Antarctica-New Zealand rifting and Marie Byrd Land lithospheric magmatism linked to ridge subduction and mantle plume activity. Geology, 22: 811-814.

Whalen, J.B., Currie, K.L., Chappell, B.W., 1987. A-type granites: geochemical characteristics, discrimination and petrogenesis. Contributions to Mineralogy and Petrology, 95: 407–419.

York, D., 1969. Least squarefitting of a straight line with correlated errors. Earth Planet. Sc. Lett., 5: 320-324.

Figures Captions:

Figure 1. Present day tectonic setting of Southern South America (modified from *Espinoza et al., 2008*). South Chile Ridge (SCR) segments, Chile Triple Junction (CTJ) (after *Cande and Leslie, 1986*) and the Neogene Patagonian Plateau Lavas (*Gorring et al., 1997*) location are shown. White arrows indicate the relative plate motion of the Nazca plate with respect to Antarctic plate and grey arrows indicate the relative motion of the oceanic plates with respect to South American Plate. The relative velocities are from *DeMets et al., 1990*. Expected positions of subducted segments of the SCR (SRC0 to SCR-2) segments below Patagonia are estimated by *Cande and Leslie, 1986* and *Guivel et al., 2006*. Gray numbers on dashed lines indicate the age of collision of the different segments of SCR with the Chile trench. MLBA : Meseta del Lago Buenos Aires.

Figure 2. a) Simplified geological section from the Patagonian batholith to the foreland basin (modified from *Lagabrielle et al., 2004*) showing the Zeballos Fault Zone west from the MLBA and the main geological units. Section has a vertical exaggeration. b) Topographic map of the area of the western MLBA (Landsat images compilation) with geological indications (from *Giacosa et Franchi, 2001*). The location of most of our samples is indicated with spots which color indicate the geochemical group : black for alkali basalts, white for felsic rocks and grey for transitional and calc-alkaline basaltic to andesitic rocks; the non-colored zones are covered by quaternary deposits. The Andean subduction front is represented by the line with black triangles.

Figure 3. a) Ab-An-Or compositional triangles for feldspars phenocrysts and groundmass of W-MLBA felsic and mafic (Cerro Zeballos basalts and MLBA basalts) rocks. b) Classification diagram for pyroxene phenocrysts and groundmass of W-MLBA rocks.

Figure 4. Total alkali vs. silica (TAS) classification diagram (*Cox et al., 1979*) for the magmatic rocks of western MLBA recalculated to 100 wt% anhydrous basis. The dashed line represents the boundary between alkaline and sub-alkaline series. We separate four groups of magmatic rocks (see section 5.2.1): (1) alkali basalts - hawaites, (2) sub-alkali basalts to basaltic andesites, (3) calc-alkali andesites – trachy- andesites and (4) alkali felsic rocks.

Figure 5. TiO_2 vs. La/Nb discrimination diagram for the western MLBA group1, 2 and 3 rocks. The alkali basalts and transitional basalts groups are clearly separated. The fields of MLBA alkali and transitional basalts (*Guivel et al., 2006*) and South Volcanic Zone calc-alkali basalts (*Gutierrez et al., 2005*) are also represented. Some of our transitional and calc-alkaline basalts plot in the Hudson (southernmost volcano of SVZ, *Gutierrez et al., 2005*) field. See section 5.2.2 for explanations.

Figure 6. MORB-normalized REE diagram (*Sun and MacDonough, 1989*) for Pliocene W-MLBA felsic rocks compared with (a) alkali basalts and (b) transitional basalts (our study and *Guivel et al., 2006*). The dashed lines represent the felsic rocks studied by *Espinoza et al. (2008)* near Mifeldi intrusion and the continuous lines represent our studied rocks. The most differentiated rocks (Cerro Lapíz) shows an Eu anomaly.

Figure 7. Location and selected ^{40}Ar-^{39}Ar ages (Ma $\pm 1\sigma$) of studied intrusions and lava flows (a) in Cerro Zeballos hill and (b) in the Rio Ghio/ Rio Zeballos valley. The ages of *Espinoza et al. (2008)* around Mifeldi microsyenite are represented too. The Cerro Zeballos rocks are emplaced before the MLBA basaltic event (before 12.5 Ma) whereas most of the other mafic and felsic rocks belong to the transition between main and post plateau magmatism period (around 5 Ma).

Figure 8. Details of the ^{40}Ar-^{39}Ar ages measures. The plateau-age calculations correspond to the samples with no excess argon whereas the isochrone ages are preferred when the sample has a clear excess.

Figure 9. The shallow-slab subduction model (*Espinoza, Thesis 2007*) presented thanks reconstitutions of plate motions (*Breitsprecher et al., 2009 : Scalabrino et al., in review)* and schematic sections. The subduction of young and buoyant oceanic lithosphere would cause a progressive decrease of the slab dip between ca. 30 and 17 Ma (A- B). This drives to migration of the arc towards the East and is related to the genesis of a second hydration front at ca. 300 km east from the trench and calc-alkaline magmatism between 16 and 14 –12 Ma (C) At 12.5 Ma, an asthenospheric window opens in the subducting plate, driving to the alkali- transitional MLBA magmatism (D).

Figure 10. Nb/Yb vs. La discrimination diagram for the W-MLBA mafic and felsic studied rocks. The La value traces differentiation while Nb/Yb ratio discriminates the alkali basalts from the calc-alkali basalts. This ratio does not change during fractional crystallization and thus the felsic rocks plot to the right from their cogenetic alkali basalts. The bibliographic references are (1) our study, (2) *Gutierrez et al., 2005*, (3) *Guivel et al., 2006*, (4) *Espinoza et al., 2008*.

Figure 11. a) Selected major (wt.%) and trace elements (ppm) vs. SiO_2 for W-MLBA felsic and mafic rocks. The field of MLBA alkali basalts (*Guivel et al., 2006*) and felsic rocks studied by *Espinoza et al., 2008* are also represented. Two trends from basalts to differentiated rocks are observed, one from alkali basalts and one from transitional basalts. b) MORB-normalized trace-element diagram (*Sun and MacDonough, 1989*) showing the differences between alkali basalts and differentiated felsic rocks for each element. These differences can be interpreted as element fractionation during crystallization (see section 7.3.1 for details).

Figure 12. Calibration diagram of temperature and oxygen fugacity with the composition of two solid solutions of Fe-Ti oxides (Ilmenite- hematite and Ulvöspinel- Magnetite, *Ghiorso and Sack, 1991; Lattard et al., 2005*). The field of a trachy-andesitic sample (PA-06-15) oxides composition shows temperature conditions of about 1 000°C and a DNNO~ 2.5, which correspond to a f_{O2}~-4.2.

Figure 13. E-W synthetic interpreted section of the western-MLBA border. Several sections were compiled along a ca. 9 km transect. Three samples give spatial geometric constrains. Intrusions are emplaced inside MLBA and the molasse sediments. The normal faults might control the location of these intrusions and erupted lava flows. The magmatic chamber is probably located in the Jurassic Ibañez group where the differentiation through a factional crystallization with small rates of assimilation process occurred.

Figure 14. Synthetic geodynamical model of W-MLBA evolution between 12 and sub-actual times. The first cartoon shows the main plateau basalts emplacement in a tectonically controlled basin between 12 Ma and 4 Ma. Then, a collapse event lead to the genesis of felsic magmas in a shallow magmatic chamber beneath the W-MLBA border at the transition between the main and the post-plateau magmatic events. Alkali magmas emplaced after 3.3

Ma correspond to the MLBA post-plateau event. Finally, after the end of the extension, the western flank of the plateau is dissected by landslides and glacial erosion which allow for the extrusion of the deep structures.

Tables captions:

Table 1. Representative ICP-MS and ICP-AES geochemical analysis of Western-MLBA felsic and mafic rocks.

Table 2. Selected $^{40}Ar/^{39}Ar$ ages. For each sample, the plateau age and the isochron age are given. The age in bold characters is the chosen age for the sample.

Table 3. Used conditions for the model of closed system fractional crystallization of alkali mafic magmas with PA-06-03 sample composition, by simple balance mass calculation using major elements with olivine, clinopyroxene, plagioclase and Fe-Ti oxides fractionation.

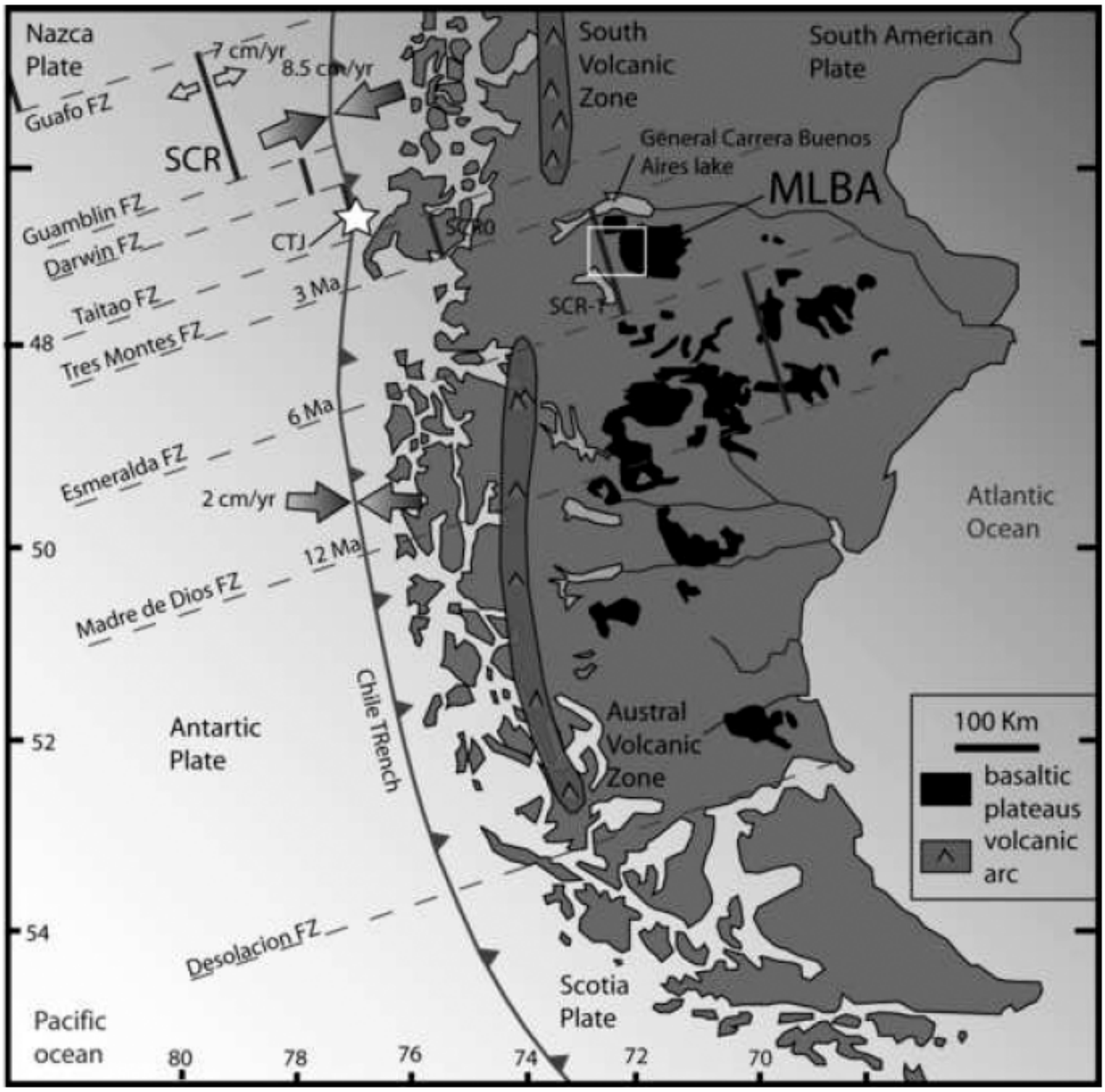

Nazca Plate
7 cm/yr
8.5 cm/yr
Guafo FZ
SCR
South Volcanic Zone
South American Plate
General Carrera Buenos Aires lake
MLBA
Guamblin FZ
Darwin FZ
CTJ
SCR0
Taitao FZ
3 Ma
SCR-1
Tres Montes FZ
48
6 Ma
Esmeralda FZ
2 cm/yr
Atlantic Ocean
50
12 Ma
Madre de Dios FZ
Chile TRench
Antartic Plate
52
Austral Volcanic Zone
100 Km
basaltic plateaus
volcanic arc
54
Desolacion FZ
Scotia Plate
Pacific ocean
80
78
76
74
72
70

Figure 1

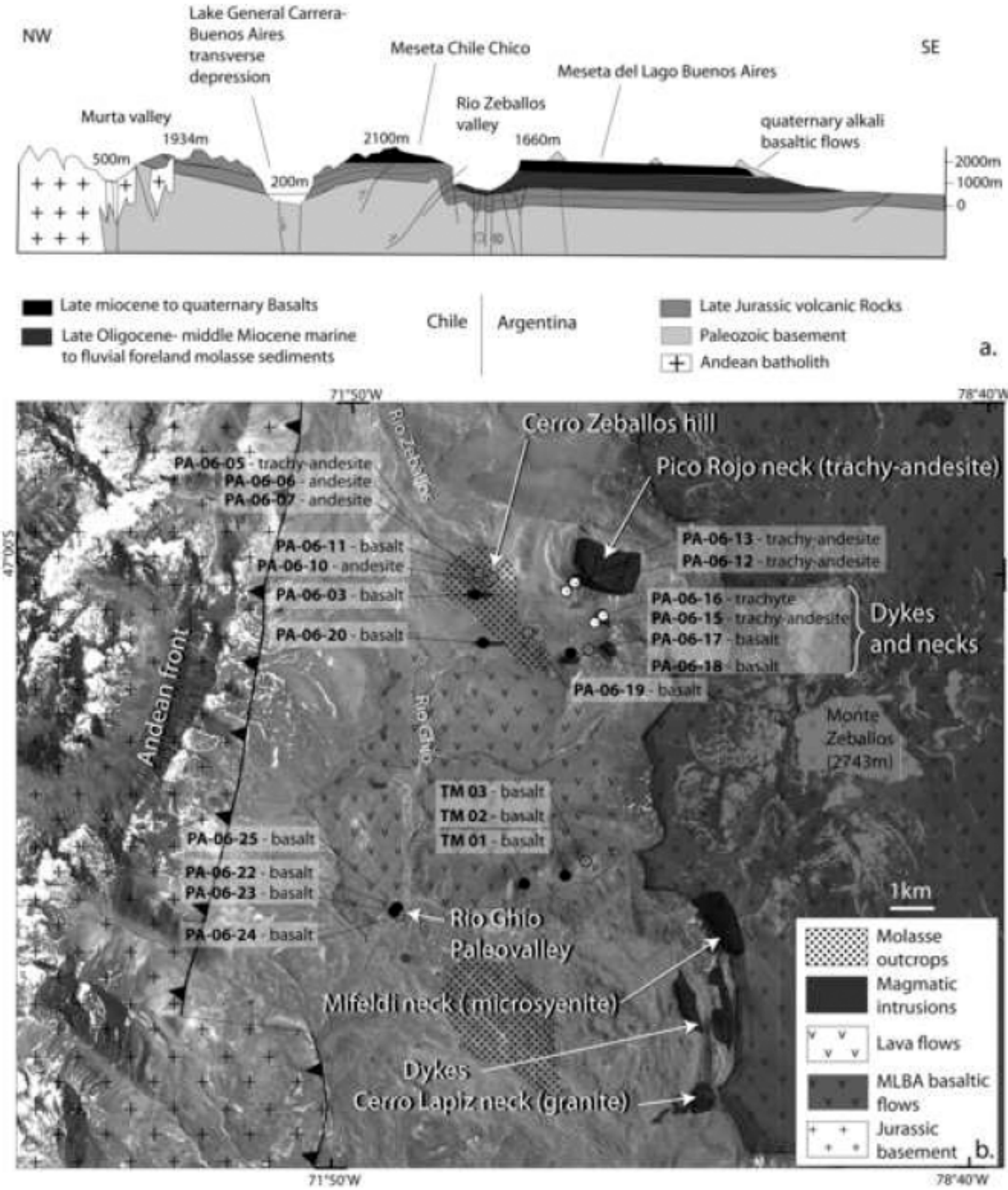
NW
Lake General Carrera-Buenos Aires transverse depression
Meseta Chile Chico
SE
Meseta del Lago Buenos Aires
Rio Zeballos valley
Murta valley
1934m
2100m
1660m
quaternary alkali basaltic flows
500m
200m
2000m
1000m
0
Late miocene to quaternary Basalts
Late Oligocene- middle Miocene marine to fluvial foreland molasse sediments
Chile
Argentina
Late Jurassic volcanic Rocks
Paleozoic basement
Andean batholith
a.
71°50'W
78°40'W
47°00'S
Cerro Zeballos hill
Pico Rojo neck (trachy-andesite)
PA-06-05 - trachy-andesite
PA-06-06 - andesite
PA-06-07 - andesite
PA-06-11 - basalt
PA-06-10 - andesite
PA-06-03 - basalt
PA-06-20 - basalt
PA-06-13 - trachy-andesite
PA-06-12 - trachy-andesite
PA-06-16 - trachyte
PA-06-15 - trachy-andesite
PA-06-17 - basalt
PA-06-18 - basalt
Dykes and necks
PA-06-19 - basalt
Rio Zeballos
Rio Ghio
Andean front
Monte Zeballos (2743m)
TM 03 - basalt
TM 02 - basalt
TM 01 - basalt
PA-06-25 - basalt
PA-06-22 - basalt
PA-06-23 - basalt
PA-06-24 - basalt
Rio Ghio Paleovalley
1km
Mifeldi neck (microsyenite)
Dykes
Cerro Lapiz neck (granite)
Molasse outcrops
Magmatic intrusions
Lava flows
MLBA basaltic flows
Jurassic basement
b.

Figure 2

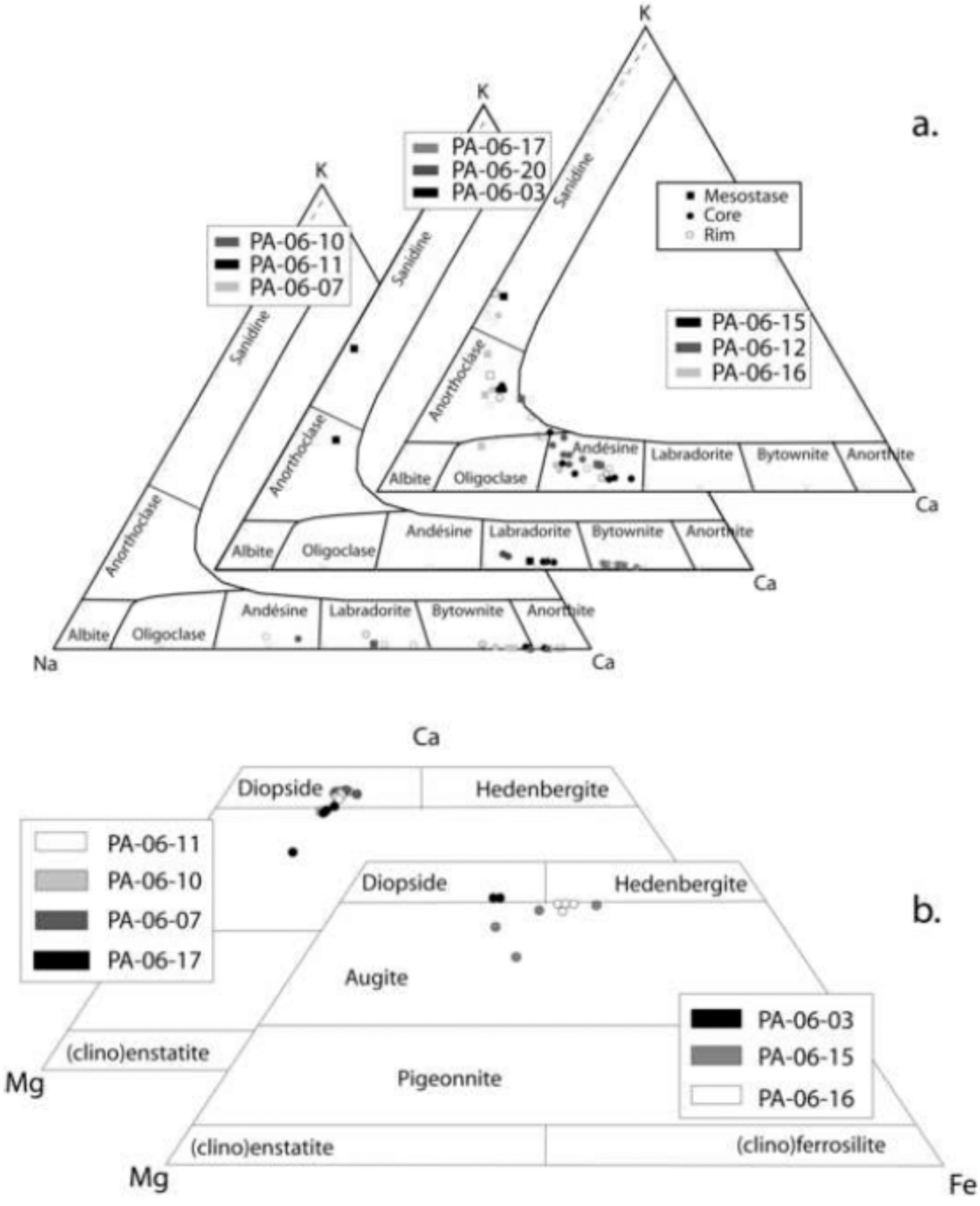
a.
K
PA-06-10
PA-06-11
PA-06-07
Sanidine
Anorthoclase
Albite
Oligoclase
Andésine
Labradorite
Bytownite
Anorthite
Na
Ca
K
PA-06-17
PA-06-20
PA-06-03
K
Mesostase
Core
Rim
PA-06-15
PA-06-12
PA-06-16
b.
Ca
Diopside
Hedenbergite
PA-06-11
PA-06-10
PA-06-07
PA-06-17
Augite
Pigeonnite
(clino)enstatite
(clino)ferrosilite
PA-06-03
PA-06-15
PA-06-16
Mg
Fe

Figure 3

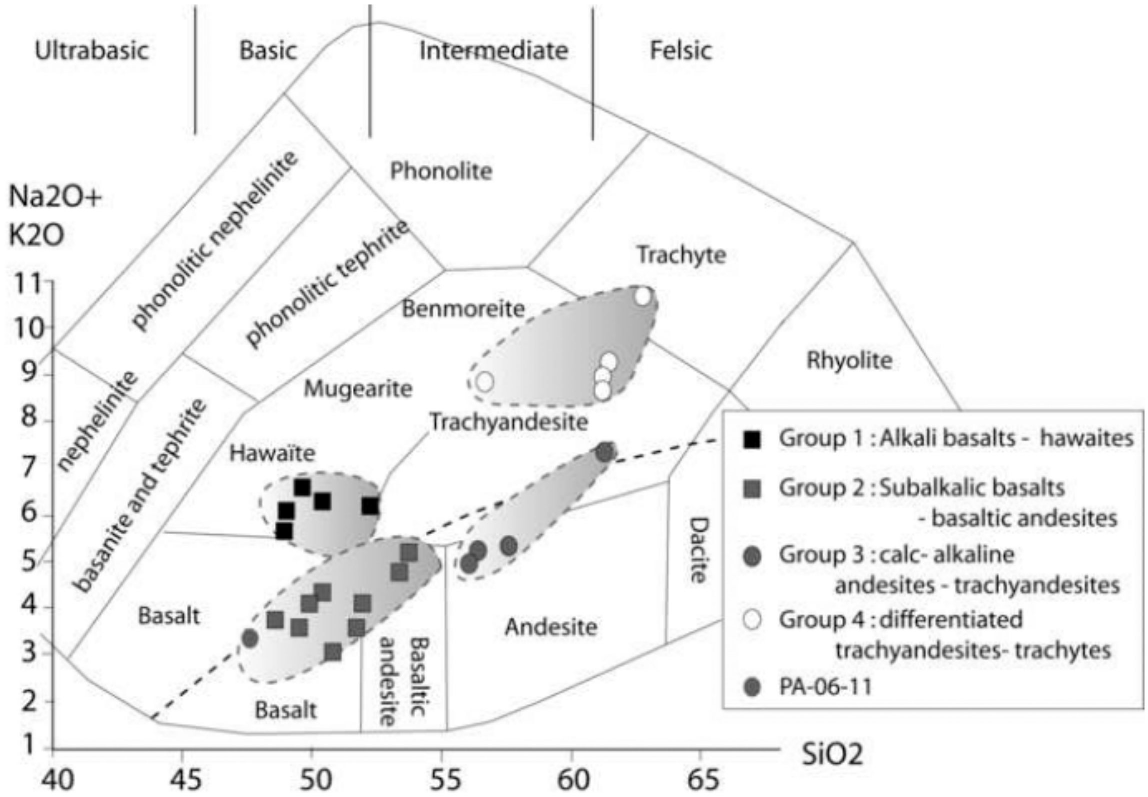

Ultrabasic
Basic
Intermediate
Felsic
Na2O+
K2O
Phonolite
phonolitic nephelinite
phonolitic tephrite
Trachyte
Benmoreite
Rhyolite
nephelinite
Mugearite
basanite and tephrite
Trachyandesite
Hawaïte
Dacite
Basalt
Andesite
Basaltic andesite
Basalt
SiO2
Group 1 : Alkali basalts - hawaites
Group 2 : Subalkalic basalts - basaltic andesites
Group 3 : calc- alkaline andesites - trachyandesites
Group 4 : differentiated trachyandesites- trachytes
PA-06-11

Figure 4

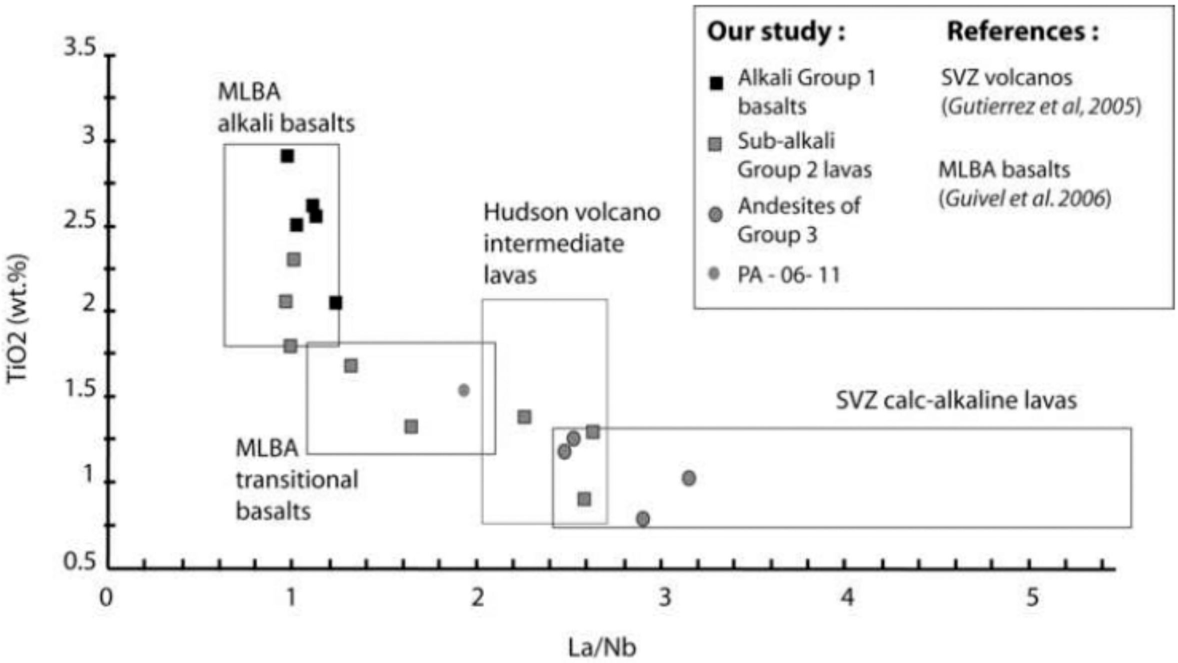

Our study :
Alkali Group 1 basalts
Sub-alkali Group 2 lavas
Andesites of Group 3
PA - 06- 11
References :
SVZ volcanos (Gutierrez et al, 2005)
MLBA basalts (Guivel et al. 2006)
MLBA alkali basalts
Hudson volcano intermediate lavas
MLBA transitional basalts
SVZ calc-alkaline lavas
TiO2 (wt.%)
La/Nb
3.5
3
2.5
2
1.5
1
0.5
0
1
2
3
4
5

Figure 5

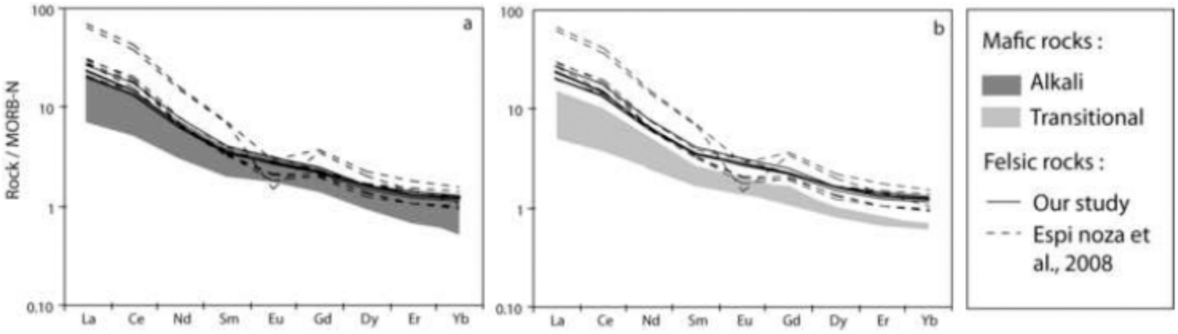

a
b
Rock / MORB-N
100
10
1
0.10
La
Ce
Nd
Sm
Eu
Gd
Dy
Er
Yb
Mafic rocks :
Alkali
Transitional
Felsic rocks :
Our study
Espi noza et al., 2008

Figure 6

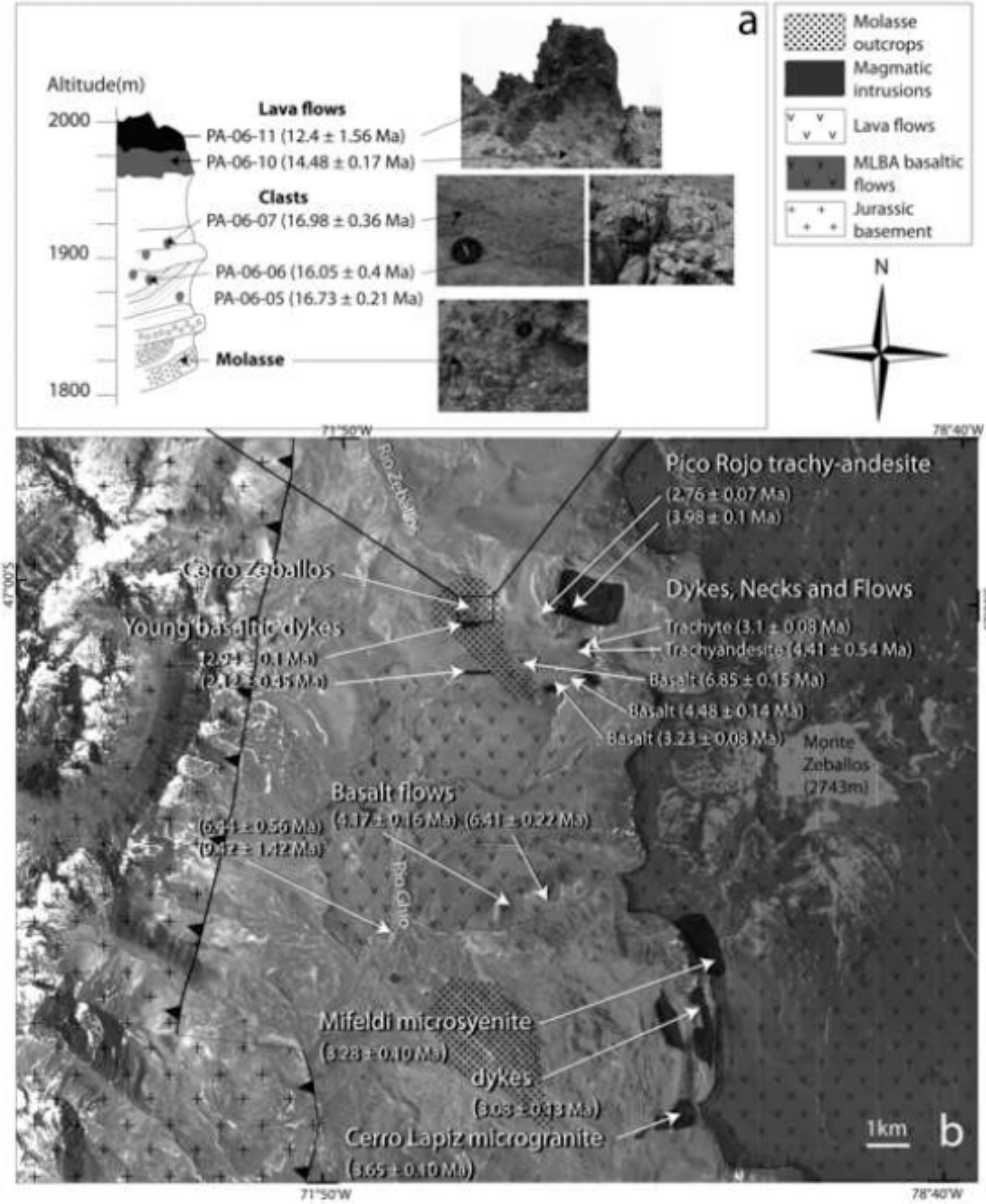

a
Altitude(m)
2000
1900
1800
Lava flows
PA-06-11 (12.4 ± 1.56 Ma)
PA-06-10 (14.48 ± 0.17 Ma)
Clasts
PA-06-07 (16.98 ± 0.36 Ma)
PA-06-06 (16.05 ± 0.4 Ma)
PA-06-05 (16.73 ± 0.21 Ma)
Molasse
Molasse outcrops
Magmatic intrusions
Lava flows
MLBA basaltic flows
Jurassic basement
N
Pico Rojo trachy-andesite
(2.76 ± 0.07 Ma)
(3.98 ± 0.1 Ma)
Cerro Zeballos
Dykes, Necks and Flows
Young basaltic dykes
Trachyte (3.1 ± 0.08 Ma)
Trachyandesite (4.41 ± 0.54 Ma)
Basalt (6.85 ± 0.15 Ma)
Basalt (4.48 ± 0.14 Ma)
Basalt (3.23 ± 0.08 Ma)
Monte Zeballos (2743m)
Basalt flows
Mifeldi microsyenite
dykes
Cerro Lapiz microgranite
1km
b

Figure 7

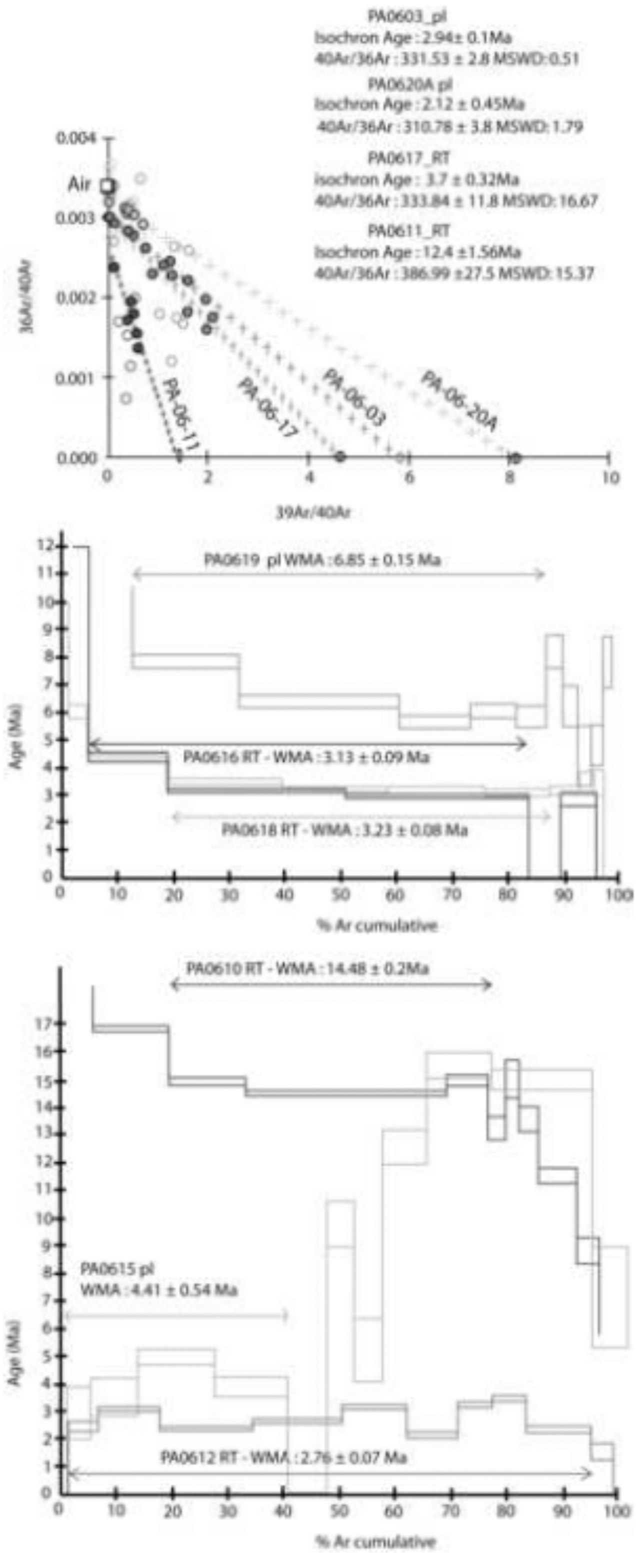
PA0603_pl
Isochron Age : 2.94± 0.1Ma
40Ar/36Ar : 331.53 ± 2.8 MSWD:0.51
PA0620A pl
Isochron Age : 2.12 ± 0.45Ma
40Ar/36Ar : 310.78 ± 3.8 MSWD:1.79
PA0617_RT
Isochron Age : 3.7 ± 0.32Ma
40Ar/36Ar : 333.84 ± 11.8 MSWD:16.67
PA0611_RT
Isochron Age : 12.4 ±1.56Ma
40Ar/36Ar : 386.99 ±27.5 MSWD:15.37
Air
36Ar/40Ar
39Ar/40Ar
PA-06-11
PA-06-17
PA-06-03
PA-06-20A
PA0619 pl WMA : 6.85 ± 0.15 Ma
PA0616 RT - WMA : 3.13 ± 0.09 Ma
PA0618 RT - WMA : 3.23 ± 0.08 Ma
Age (Ma)
% Ar cumulative
PA0610 RT - WMA : 14.48 ± 0.2Ma
PA0615 pl
WMA : 4.41 ± 0.54 Ma
PA0612 RT - WMA : 2.76 ± 0.07 Ma
Age (Ma)
% Ar cumulative

Figure 8

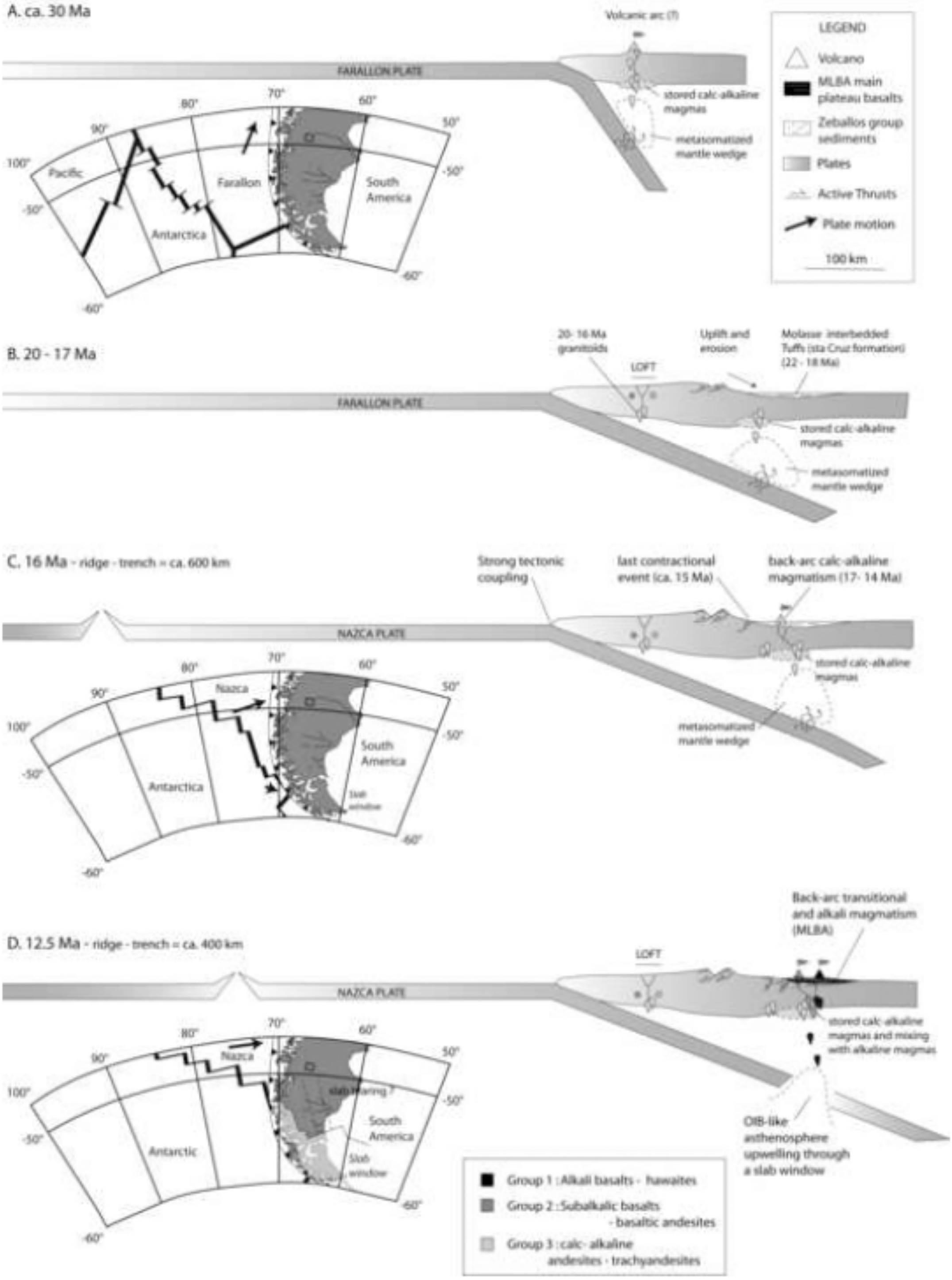
A. ca. 30 Ma
Volcanic arc (?)
FARALLON PLATE
stored calc-alkaline magmas
metasomatized mantle wedge
LEGEND
Volcano
MLBA main plateau basalts
Zeballos group sediments
Plates
Active Thrusts
Plate motion
100 km
Pacific
Antarctica
Farallon
South America
B. 20 - 17 Ma
20- 16 Ma granitoids
LOFT
Uplift and erosion
Molasse interbedded Tuffs (sta Cruz formation) (22 - 18 Ma)
stored calc-alkaline magmas
metasomatized mantle wedge
C. 16 Ma - ridge - trench = ca. 600 km
Strong tectonic coupling
last contractional event (ca. 15 Ma)
back-arc calc-alkaline magmatism (17- 14 Ma)
NAZCA PLATE
stored calc-alkaline magmas
metasomatized mantle wedge
Nazca
Antarctica
South America
Slab window
D. 12.5 Ma - ridge - trench = ca. 400 km
Back-arc transitional and alkali magmatism (MLBA)
LOFT
NAZCA PLATE
stored calc-alkaline magmas and mixing with alkaline magmas
OIB-like asthenosphere upwelling through a slab window
Nazca
slab tearing ?
Antarctic
South America
Slab window
Group 1 : Alkali basalts - hawaites
Group 2 : Subalkalic basalts - basaltic andesites
Group 3 : calc- alkaline andesites - trachyandesites

Figure 9

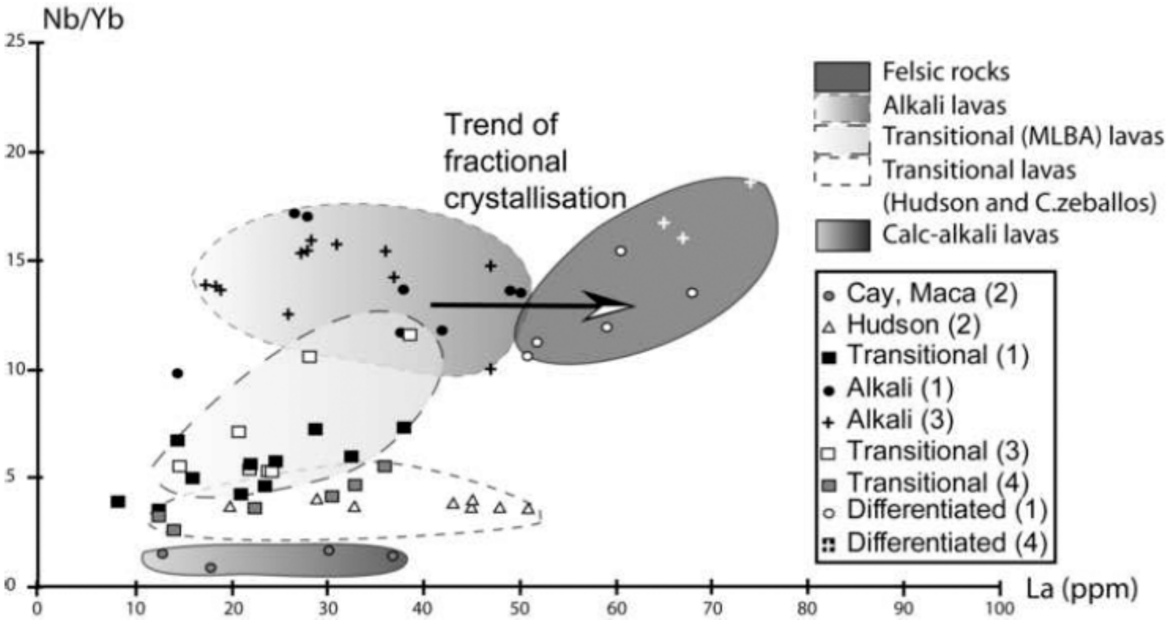

Nb/Yb
25
20
15
10
5
0
0
10
20
30
40
50
60
70
80
90
100
La (ppm)
Trend of fractional crystallisation
Felsic rocks
Alkali lavas
Transitional (MLBA) lavas
Transitional lavas
(Hudson and C.zeballos)
Calc-alkali lavas
Cay, Maca (2)
Hudson (2)
Transitional (1)
Alkali (1)
Alkali (3)
Transitional (3)
Transitional (4)
Differentiated (1)
Differentiated (4)

Figure 10

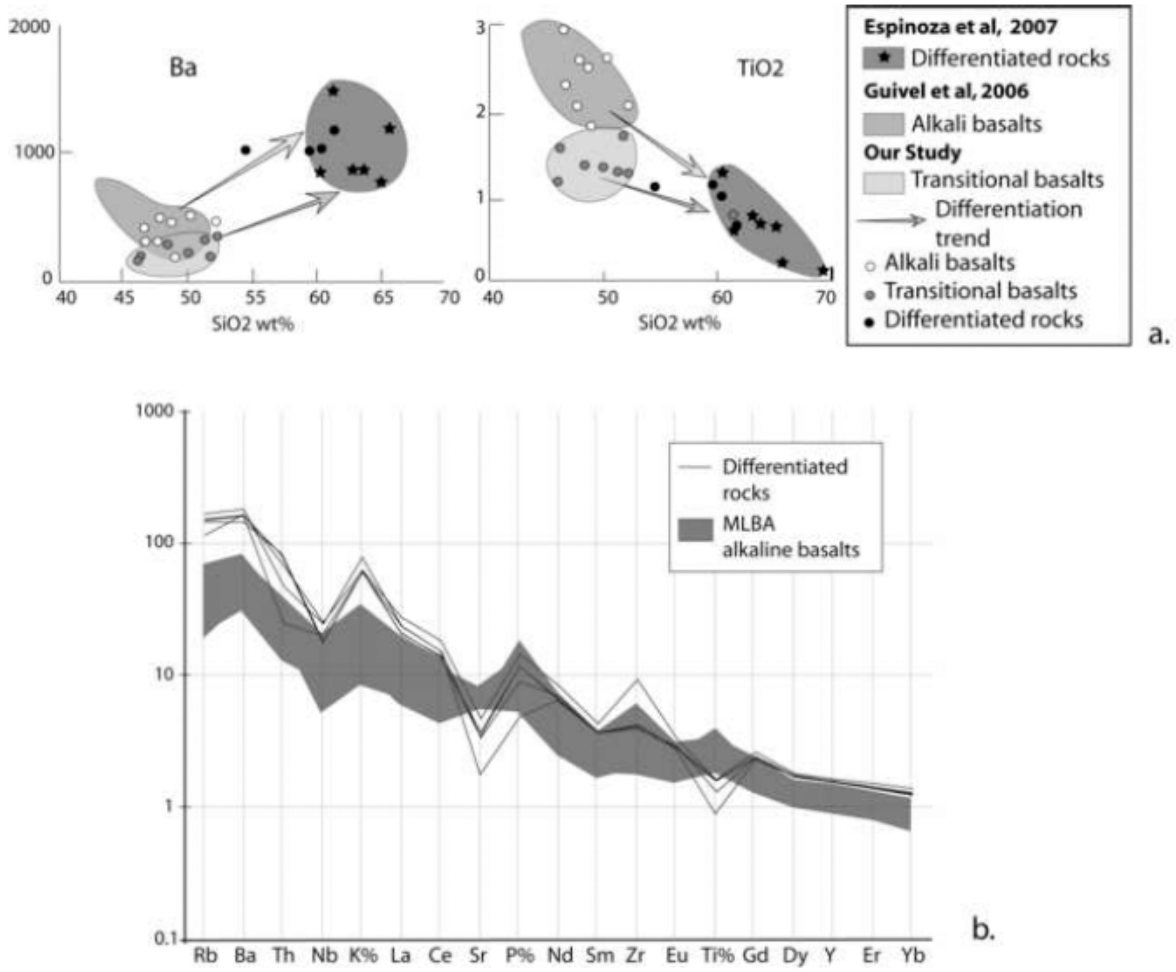

2000
1000
0
Ba
40
45
50
55
60
65
70
SiO2 wt%
3
2
1
0
TiO2
40
50
60
70
SiO2 wt%
Espinoza et al, 2007
Differentiated rocks
Guivel et al, 2006
Alkali basalts
Our Study
Transitional basalts
Differentiation trend
Alkali basalts
Transitional basalts
Differentiated rocks
a.
1000
100
10
1
0.1
Differentiated rocks
MLBA alkaline basalts
Rb
Ba
Th
Nb
K%
La
Ce
Sr
P%
Nd
Sm
Zr
Eu
Ti%
Gd
Dy
Y
Er
Yb
b.

Figure 11

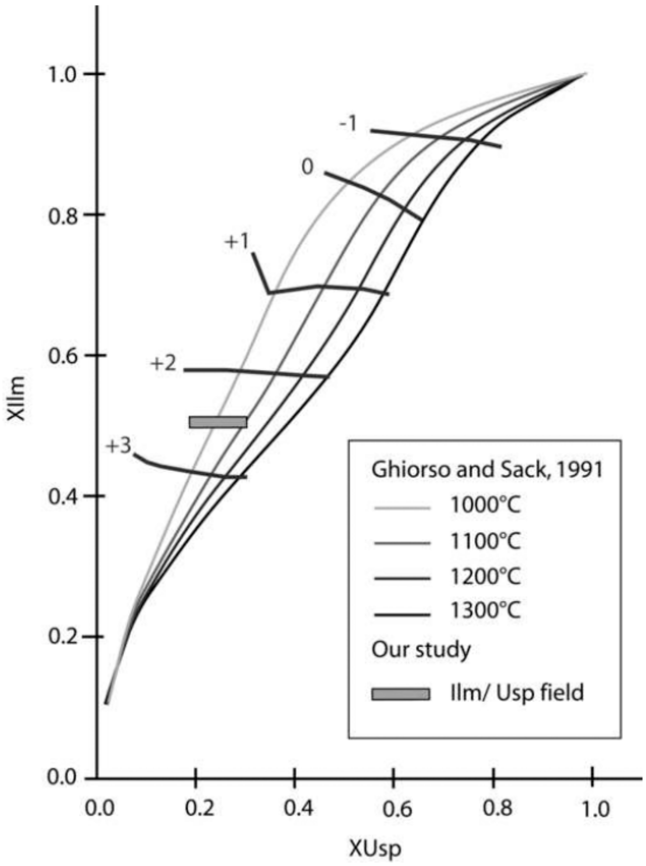

1.0
0.8
0.6
0.4
0.2
0.0
XIlm
0.0
0.2
0.4
0.6
0.8
1.0
XUsp
-1
0
+1
+2
+3
Ghiorso and Sack, 1991
1000°C
1100°C
1200°C
1300°C
Our study
Ilm/ Usp field

Figure 12

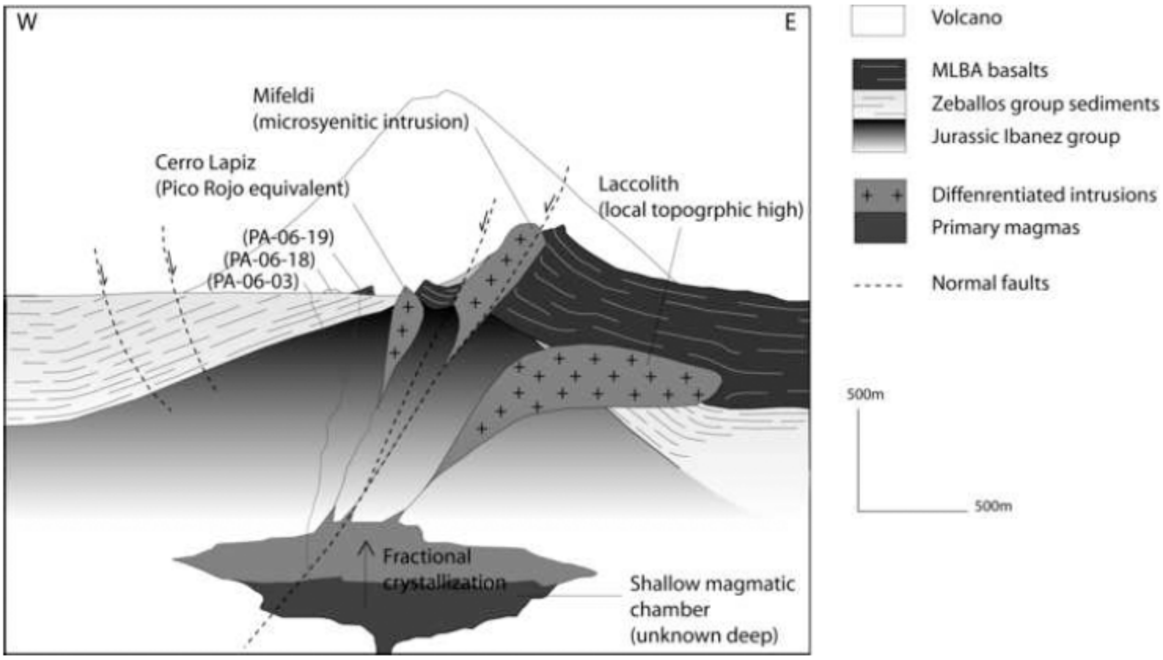

W
E
Mifeldi
(microsyenitic intrusion)
Cerro Lapiz
(Pico Rojo equivalent)
Laccolith
(local topogrphic high)
(PA-06-19)
(PA-06-18)
(PA-06-03)
Fractional
crystallization
Shallow magmatic
chamber
(unknown deep)
Volcano
MLBA basalts
Zeballos group sediments
Jurassic Ibanez group
Diffenrentiated intrusions
Primary magmas
Normal faults
500m
500m

Figure 13

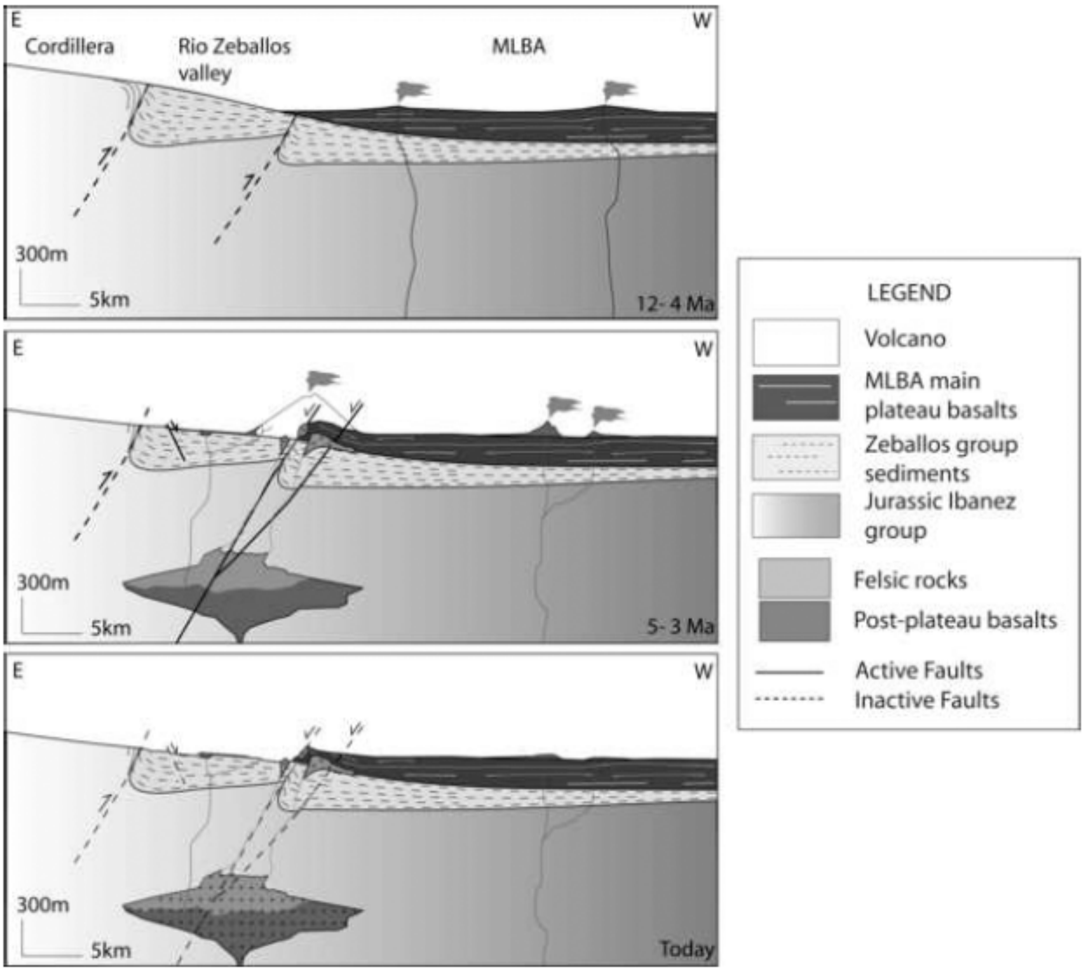

E
W
Cordillera
Rio Zeballos valley
MLBA
300m
5km
12- 4 Ma
5- 3 Ma
Today
LEGEND
Volcano
MLBA main plateau basalts
Zeballos group sediments
Jurassic Ibanez group
Felsic rocks
Post-plateau basalts
Active Faults
Inactive Faults

Figure 14

Références

Allan, J.F., Chase, R.L., Cousens, B., Michael, P.J.? Gorton, M.P. Scott, S.D., 1993. The Tuzo Wilson volcanic field, NE Pacific: alkaline volcanism at a complex, diffuse, transform-trench-ridge triple junction. *Journal of Geophysical Research, 98*, 22367-22387.

Allmendinger, R.W., Jordan, T.E., Kay, S.M., et Isacks, B., 1997, The evolution of the Altiplano-Puna Plateau of the central Andes. *Annual Review of Earth and Planetary Sciences, 25*, 139-174.

Altenberger, U., Oberhansli, R., Putlitz, B., Wemmer, K., 2003. Tectonic controls and Cenozoic magmatism at the Torres del Paine, southern Andes (Chile, 51°10'S). *Revista geologica de Chile, 30 (1),* 65-81.

Artemieva I.M., 2006. Global 1°x1° therma model TC1 for the continental lithosphere: Implications for the lithosphere secular evolution. *Tectonophysics, 416*, 245-277.

Atwater, T., et Severinghaus, J., 1989. Relative plate motions in Northeast Pacific, 85 Ma to présent, as recorded by magnetic lineation pattern. *International Geological Congress, Abstract, 28 (1)*, 60.

Atwater, T., et Stock, J., 1998. Pacific-North America plate tectonics of the Neogene southwestern United States: an update. *International Geology Review, 40 (5),* 375-402.

Audoine, E., Savage, M.K., Gledhill, K., 2000. Seismic anisotropy from local earthquakes in the transition region from a subduction to a strike-slip plate boundary, New Zealand. *Journal of Geophysical Research, 105 (B4)*, 8013-8033.

Babcock, S., Burmester, R.F., Engebretson, D.C., Warnock, A., Clark K.P., 1992. A rifited margin origin for the Crescent Basalts and related rocks in the northern Coast Range volcanic province, Washington and British Columbia. *Journal of Geophysical. Research, 97*, 6799–6821.

Barker, P.E., Buckley, F., Rex, D.C., 1977. Cenozoic volcanism in the Antarctic. *Philosophical Transactions of the Royal Society of London, 279 (963)*, 131-142.

Barker, P.F., Barber, P.L., King, E.C., 1984. An early Miocene ridge crest-trench collision on the South Scotia Ridge near 36°W. *Tectonophysics, 102 (1-4)*, 315-332.

Baumgartner, L.K., Jurgen , M., Darbellay, B., Putlitz, B., Robyr, M., 2006. The geology of the Torres del Paine laccolith, S-Chile. *Conference on BackBone of the Americas-Patagonia to Alaska, Mendoza (Argentina).*

Beck, S.L., Zandt, G., Myers, S.C., Wallace, T.C., Silver, P.G., Drake, L., 1996. Crustal thickness variations in the Central Andes. *Geology, 24*, 407-410.

Bell, M., Suarez, M., 2000. The Rio Lacteo Formation of southern Chile. Late Paleozoic orogeny in the Andes of the southernmost South America. *Journal of South American Earth Sciences 13*, 133-145.

Biddle, K.T., Uliana, M.A., Mitchum, R.M., Fitzgerald, M.G., Wright, R.C., 1986. The stratigraphic and structural evolution of the central eastern Magallanes basin, southern South America; *In Allen, P., Homewood, P., (eds.). Foreland Basins. International Association of Sedimentologists Special Publication, 8*, 41-61.

Bol, A.J., Coe, R.S., Gromme, C.S., Hillhouse, J.W., 1992. Paleomagnetism of the Ressurection Peninsula, Alaska: Implications for the tectonics of southern Alaska and the Kula-Farallon Ridge. *Journal of Geophysical Research, 97*, 17213-17232.

Bourgois, J., Toussaint, J.F., Gonzalez, H., Orrego, A., Azema, J., Calle, B., Desmet, A., Murcia, A., 1985. Ophiolites from the Colombian Andes: Structural evolution and geodynamic significance. *Memorias- Congreso Latinoamericano de Geologia, 6 (1)*, 78.

Bourgois, J., Lagabrielle, Y., Maury, R.C., Le Moigne, J., Vidal, P., Cantagrel, J.M., Martin, H., Urbina, O., 1992. Geologie de la Péninsule de Taitao (Point Triple du Chili, 46°-47°S): obduction de l'ophiolite de Bahia Barrientos entre le Miocène et le Pléistocène. *Transactions of the American Geophysical Union, 73 (43)*, 592.

Bourgois, J., Lagabrielle, Y., Le Moigne, J., Urbina, O., Janin, M.C., Beuzart, P., 1993. Preliminary results of a field study of the Taitao ophiolite (Southern Chile): implications for the evolution of the Chile triple junction, *Ofioliti, 18 (2)*, 113-129.

Bourgois, J., Martin, H., Lagabrielle, Y., Le Moigne, J., Furtos-Jara, J., 1996. Subduction erosion related to spreading-ridge subduction: Taitao Peninsula (Chile margin triple junction area). *Geology, 24 (8)*, 723-726.

Bourgois, J., et Michaud, F., 2002. Comparison between the Chile and Mexico triple junction areas substantiates slab window development beneath northwesterb Mexico during the past 12-10 Myr. *Earth and Planetary Earth Sciences, 201*, 35-44.

Bowman, J.R., Sisson, V.B., Valley, J.W., Palvis, T.L., 2003. Oxygen isotope constraints on fluid infiltration associated with high-temperature-low-pressure metamorphism (Chugach metamorphic complex) within the Eocene southern Alaska forearc. In Sisson, V.B., Roeske, S.M., and Palvis, T.L., eds., Geology of a transpressional orogen developed during ridge-trench interaction along the North pacific margin. Boulder, Colorado, *Geological Society of America Special paper 371*, 237-252.

Bradley, P.M., Haeussler,P., Nelson, S., Krusky, T., Donley, D.T., Goldfard, R., 1995. Geological effects of Paleogene ridge subduction, Kenai Peninsula, Southern Alaska. *Abstract, Geological Society of America 27 (5),* 7.

Bradley, D., Kusky, T., Haeussler, P., Goldfard, R., Miller, M., Dumoulin, J., Nelson, S.W., and Karl, S., 2003. Geologic signature of early Tertiary ridge subduction in Alaska. In Sisson, V.B., Roeske, S.M., and Palvis, T.L., eds., Geology of a transpressional orogen developed during ridge-trench interaction along the North pacific margin. Boulder, Colorado, *Geological Society of America Special paper 371*, 19-49.

Breitsprecher, K., Thorkelson, D.J., Groome, W.G., Doastal, J., 2003. Geochemical confirmation of the Kula-Farallon slab window beneath the Pacificv Northwest in Eocene time. *Geology, 31 (4)*, 351-354.

Breitsprecher, K. et Thorkelson, D.J., 2009. Neogene kinematic evolution of the Nazca–Antarctic–Phoenix slab windows beneath Patagonia and the Antarctic Peninsula. *Tectonophysics, 464*, 10-20. doi: 10.1016/j.tecto.2008.02.013

Bruce, Z.R.V., 2001. Mesozoic Geology of the Puerto Ingeniero Ibanez area, 46° South, Chilean Patagonia. *PhD Thesis, unpublished*, University of Canterbury.

Bruni, S., 2007. The Cenozoic back-arc magmatism of Central Patagonia (44°-46°S): activation of different mantle domains in space and time. *PhD thesis*, Universitá di Pisa, 159 p.

Burns, W., Jordan, T.E., Copeland, P., Kelley, S.A., 2006. The case for extensional tectonics in the Oligocene-Miocene Southern Andes as recorded in the Cura Mallin basin (36°S-38°S). *In Kay,* *S.M., et al (eds.). Evolution of an Andean margin: atectonic and Magmatic view from the Andes to the Neuquen Basin (35°39°S). Geological Society of America Special Paper, 407*, 163-184.

Burov, E., et Diament, M., 1996. Isostasy, equivalent elastic thickness, and inelastic rheology of continents and oceans. *Geology, 24 (5),* 419-422.

Cande, S.C., Leslie, R.B., 1986. Late Cenozoic tectonics of the Southern Chile Trench. *Journal of Geophysical Research, 91*, 471-496.

Cande, S.C., Leslie, R.B., Parra, J.C., Hobart, M., 1987. Interaction between the Chile ridge and the Chile trench : geophysical and geothermal evidence. *Journal of Geophysical Research, 92*, 495-520.

Castro, A., Fernandez, C., de la Rosa, J.D., Moreno-Ventas, I., El Hmidi, H., El-Biad, M., Bergamin, J.F., Sanchez, N., 1996. Triple junction migration during Paleozoic plate convergence : The Aracena metamorphic belt, Hercynian Massif, Spain. *Geologische Rundschau, 85*, 180-185.

Castro, A., Fernandez, C., El-Hmidi, H., El-Biad, M., Diaz, M., de la Rosa, J.D., Stuart, F., 1999. Age constraints to the Relationship between magmatism, metamorphism and tectonism in the Aracena metamorphic belt, southern Spain. *International Journal of Earth Sciences, 88*, 26-37.

Celaya, M., McCabe, R., 1987. Kinematic model for the opening of the Sea of Japan and the Charrier, R., Baeza, O., Elgueta, S., bending of the Japanese islands. *Geology, 15 (1)*, 53-57.

Cembrano, J., Hervé, F., Lavenu, A., 1996. The Liquine-Ofqui fault zone : A long-lived intra-arc fault system in Southern Chile. *Tectonophysics 259*, 207-224.

Cembrano, J., Lavenu, A., Reynolds, P., Arancibia, G., Lopez, G., Sanueza, A., 2002. Late Cenozoic transpressional ductile deformation north of the Nazca-Sout America-Antarctica triple junction. *Tectonophysics 354*, 289-314.

Charrier, R., 1984. Areas subsidentes en el borde occidental de la Cuenca de tras-arco jurasico-cretacica, Cordillera principal Chilena, entre 34°S y 34°30'S. *IX^e Congreso Geologico Argentino (Bariloche), Actas 2*, 107-124.

Charrier, R., Baeza, O., Elgueta, S., Flynn, J.J., Gans, P., Kay, S.M., Munoz, N., Wyss, A.R., Zurita, E., 2002. Evidence for Cenozoic extensional basin development and tectonic inversion south of the flat-slab segment, southern Central Andes, Chile (33°S-36°S.L.). *Journal of South American Earth Sciences, 15*, 117-139.

Cloos, M., 1993. Lithospheric buoyancy and collisional orogenesis ; subduction of oceanic plateaus, continental margins, Island arcs, spreading ridges and seamounts. *Bull. Geol. Soc. Am., 105 (6)*, 715-737.

Cobbold, P.R., et Rossello, E.A., 2003. Aptian to récent compressional déformation, foothills of the Neuquen Basin, Argentina. *Marine and Petroleum Geology, 20 (5)*, 429-443.

Cole, R.B., et Basu, A.R., 1992. Middle tertiary volcanism during ridge-trench interactions in western California. *Sciences, 258*, 793-796.

Cole, R.B., et Basu, A.R., 1995. Nd-Sr isotopic geochemistry and tectonics of ridge subduction and middle Cenozoic volcanism in the western California. *Geological Society of America Bulletin, 107 (2)*, 167-179.

Cole, R.B., Nelson, S.W., Layer, P.W., Oswals, P.J., 2006. Eocene volcanisml above a depleted mantle slab window in Southern Alaska. *Geological Society of America Bulletin, 118 (1-2)*, 140-158.

Cole, R.B., et Stewart, B.W., 2009. Continental margin volcanism at sites of spreading ridge subduction : Examples from southern Alaska and western California. *Tectonophysics, 464 (1-4)*, 118-136.

Colleta, B., Roure, F., de Toni, B., Loureiro, D., Passalacqua, H., Gou, Y., 1997. Tectonic inheritance, crustal architecture and contrasting structural styles in the Venezuela Andes. *Tectonics, 16 (5),* 777-794.

Coney, P.J., 1987. The regional tectonic setting and possible causes of Cenozoic extension in the North American Cordillera. *Geological Society Special Publications, 28*, 177-186.

Coutand, I., Diraison, M., Cobbold, P.R., Gapais, D., Rossello,E.A., Miller, M., 1999. Structure and kinematics of a foothills transect, Lago Viedma, Southern Andes (49°30'S). *Journal of South America Earth Sciences (Oxford) 12,* 1-15.

Coutand, I., Carrapa, B., Deeken, A., Schmitt, A.K., Sobel, E.R., Srecker, M.R., 2006. Propagation of orographic barriers along an active range front : insights from Sandstone petrography and detritial apatite fission-track thermochronology in the intramontane Angastaco Basin, NW Argentina. *Basin Research, 18 (1),* 1-26.

Cooper, A.K., Marlow, M.S., Scholl, D.W., Stevenson, A.J., 1992. Evidence for Cenozoic crustal extension in the Bering Sea region. *Tectonics, 11 (4)*, 719-731.

Cross, T.A., et Pilger, R.H., 1982. Controls of subduction geometry, location of magmatic arcs, and tectonics of arc and back-arc regions. *Bull. Geol. Soc. Am., 93 (6),* 545-562.

Cunningham, W.D., 1993. Strike-slip faults in the southernmost Andes and the development of the Patagonian orocline. *Tectonics, 12 (1)*, 169-185.

Daly, M., 1989. Correlations between Nazca/Farallon plate kinematics and forearc evolution in Ecuador. *Tectonics, 8(4),* 769-790.

Dalziel, I.W.D., de Wit, M.F., Palmer, K.F., 1974. Fossil margin basin in the Southern Andes. *Nature, 250 (5464),* 291-294.

Dalziel, I.W.D., 1981. Back-arc extension in the Southern Andes: a review and critical reappraisal. *Philosophycal Transactions Royal Society of London, A300*, 319-335.

Dalziel, I.W.D., et Forsythe, R.D., 1985. Andean evolution and the terrane concept. Tectonostratigraphy Terranes of the Circum-Pacific Region. *Earth Sciences Series, 1,* 565-581.

Debayle, E., 2005. Global tomography of the upper mantle and transition zone. *Fall Meeting on American geophysical Union (AGU 2005),* San Francisco, Californie (USA).

De La Cruz, R., Suárez, M., Morata, D., Espinoza, F. and Troncoso, A., 2003. El Cenozoico del Lago General Carrera, Aysén, Chile (46º30'-47º15'S): estratigrafía y tectónica. *In Congreso Geológico Chileno No. 10,* Concepción.

De La Cruz, R., Welkner, D., Suárez, M. and Quiroz, D., 2004. Geología del área oriental de las hojas Cochrane y Villa O'Higgins, Región Aisén del General Carlos Ibáñez del Campo, escala 1:250.000. *Servicio Nacional de Geología y Minería, Serie Geología Básica, Carta Geológica de Chile,* 85. Santiago, Chile.

De La Cruz, R. and Suárez, M., 2005. Geología del área Puerto Guadal-Puerto Sánchez, Región Aisén del General Carlos Ibáñez del Campo, Escala 1:100.000. *Servicio Nacional de Geología y Minería, Serie Geología Básica, Carta Geológica de Chile.* Santiago, Chile.

De La Cruz, R. and Suárez, M., 2006. Geología del área Puerto Guadal-Puerto Sánchez, Región Aisén del General Carlos Ibáñez del Campo, Escala 1:100.000. *Servicio Nacional de Geología y Minería, Serie Geología Básica, Carta Geológica de Chile.* Santiago, Chile.

DeLong, S.E., Scharz, W.M., Anderson, R.N., 1979. Thermal effects of ridge subduction. *Earth and Planetary Sciences Letters, 44*, 239-246.

DeMets, C., Gordon, R.G., Argus, D.F., Stein, S., 1990. Current plate motions. *Geophysical Journal International, 101*, 425-478.

Deverchère, J., 1988. Extension crustale dans un contexte de convergence de plaques : l'exemple des Andes du Pérou Central contraint par des données sismotectoniques. *Thèse de 3ème cycle*, université de Paris-Sud, centre d'Orsay.

Dickinson, W.R., and Snyder, W.S. 1979. Geometry of subducted slab related to the San Andreas transform. *Journal of Geology, 87*, p.609-627.

Diraison, M., Cobbold, P.R., Gapais, D., Rossello, E.A., 1997. Magellan strait : Part of a Neogene rift system. *Geology, 25*, 703-706.

Diraison, M., Cobbold, P.R., Gapais, D., Rossello, E.A., Le Corre, C., 2000. Cenozoic crustal thickening, wrenching and rifting in the foothills of the southernmost Andes. *Tectonophysics 316,* 91-119.

Dixon, J.M., et Farrar, E., 1980. Ridge subduction, eduction, and the Neogene tectonics of southwestern North America. *Tectonophysics, 67 (1-2)*, 81-99.

D'Orazio, M., Agostini, S., Innocenti, F., Haller, M., Manetti, P., Mazzarini, F., 2001. Slab-window-related magmatism from southernmost South America : The Late Miocene mafic volcanics from the Estancia Glencross area (~ 52°S Argentina-Chile). *Lithos 57*, 67-89.

Edwards, B.R., et Russel, J.K., 1999. Northern Cordilleran volcanic province : A northern Basin and Range ? *Geology, 27 (3)*, 243-246.

Espinoza, F., Morata, D., Pelleter, E., Maury, R.C., Suarez, M., Lagabrielle, Y., Polvé, M., Bellon, H., Cotten, J., de la Cruz, R., Guivel, C., 2005. Petrogenesis of the Eocene and Mio-Pliocene alkaline basaltic magmatism in Meseta Chile Chico, Southern Patagonia, Chile : evidence for the participation of two slab windows. *Lithos, 82 (3-4)*, 315-343.

Espurt, N., Funiciello, F., Martinod, J., Guillaume, B., Regard, V., Faccenna, C., Brusset, S., 2008. Flat subduction dynamics and deformations of the South American plate: insights from analogue modeling. *Tectonics, 27*, doi:10,1029/2007TC002175.

Eagles, G., Livermore, R.A., Fairhead, J.D., Morris, P., 2005. Tectonic evolution of the west Scotia Sea. Journal of Geophysical Research, 110 (B02), doi:10.1029/2004JB003154.

Espinoza, F., 2003. Petrologia y Geoquimica de los basaltos cenozoicos de la meseta Chile Chico, XI region de Aysen, Chile. *Unpublished thesis*, Universidad de Chile.

Espinoza, F., Suarez, M., Lagabrielle, Y., Morata, D., Polve, M., Barbero, L., Maury, R.C., Guivel, C., De la Cruz., 2005. Tectonics in Central Patagonian Cordillera related to Mio-Pliocene subduction on the Chile Ridge: preliminary morphological, chronological and geochemical evidences. *6th International Symposium on Andean Geodynamics-ISAG, Barcelone (Espagne)*, 250-253.

Espinoza, F., Morata, D., Polve, M., Lagabrielle, Y., Maury, R.C., Guivel, C., Cotton, J., Bellon, H., Suarez, M., 2008. Bimodal back-arc alkaline magmatism after ridge subduction: Pliocene felsic rocks from central Patagonia (47°S). *Lithos, 101 (3-4)*, 191-217.

Farias, M., Charrier, R., carretier, S., Martinod, J., Fock, A., Campbell, D., Caceres, J., Comte, D., 2008. Late Miocene high and rapid surface uplift and its erosional response in the Andes of central Chile (33°S-35°S). Tectonics, 27, TC1005, doi:10.1029/2006TC002046.

Farrar, E., et Dixon, J.M., 1993. Ridge subduction: kinematics and implications for the nature of mantle upwelling. *Canadian Journal of Earth Sciences, 30 (5)*, 893-907.

Ferrari, L., Valencia-Moreno, M., Bryan, S., 2006. Magmatism and tectonics of the Sierra Madre Occidental and its relation with the evolution of the western margin of North America. *Geological Society of America.*

Folguera, A., Zapata, T., Ramos, V.A., 2006. Late Cenozoic extension and evolution of the Neuqeuen Andes. *In Kay, S.M., et al (eds.). Evolution of an Andean margin: atectonic and Magmatic view from the Andes to the Neuquen Basin (35°39°S). Geological Society of America Special Paper, 407*, 267-285.

Forsythe, R., et Nelson, E., 1985. Geological manifestations of ridge collision: evidence from the Golfo de Penas-Taitao Basin, southern Chile. *Tectonics, 4 (5)*, 477-495.

Forsythe, R., Nelson, E., Carr, M., Kaeding, M., Herve, M., Mpodozis, C., Sffia, J., Harambour, S., 1986. Pliocene near-trench magmatism in Southern Chile: a possible manifestation oif ridge collision. *Geology, 14*, 23-27.

Forsythe, R., et Prior, D., 1992. Cenozoic continental geology of South American and its relation to the evolution of the Chile Triple Junction. *Proceedings of the Ocean Drilling Program, Part A: Initials Reports, 141*, 11-21.

Fouch, M.J., Fischer, K.M., 1996. Mantle anisotropy beneath Nortwest pacific subduction zones. *Journal of Geophysical Research, 101 (B7),* 15987-16002.

Fouch, M.J., Fischer, K.M., 1998. Shear wave anisotropy in the Mariana subduction zone. *Geophysical Research Letters, 25 (8),* 1221-1224.

Fox, K.F., Fleck, R.J., Curtis, G.H., Meyer, C.E., 1985. Implications of the northwestardly younger age of the volcanic rocks of west-central California. *Geological Society of America Bulletin, 96 (5),* 647-654.

Frederiksen, A.W., Bostock, M.G., VanDecar, J.C., Cassidy, J.F., 1998. Seismic structure of the upper mantle beneath the northern Canadian Cordillera from teleseismic travel-time inversion. *Tectonophysics, 294*, 43-55.

Galland, O., Hallot, E., Cobbold, P.R., Ruffet, G., 2007. Volcanism in a compressional Andean setting: A structural and geochronological study of Tromen volcano (Neuquen province, Argentina). *Tectonics, 26*, TC4010, doi:10.1029/2006TC002011.

Garret, S.W., et Storey, B.C., 1987. Lithospheric extension on the Antarctic Peninsula during Cenozoic subduction. *In Coward, M.P., Dewey, J.F., Hancock, P.L., (eds), 1987, Continenetal Extensional Tectonics, Geological Society Special Publication, 28*, 419-431.

Garver, J.I., Schiffman,C.R., Perry, S.E., 2003. Rapid tectonic exhumation of the Cordillera Blanca. *Geological Society of America Abstracts with Programs, 35*, p.429.

Garzione, C.N., Hoke, G.G., 2006. Paleoelevation and geomorphic constraints on the late Miocene rise of the Andes: geodynamic implications for the growth of orogenic plateaus. *Geochimica and Cosmochimica Acta, 70 (18s), A195*.

Gerbault, M., Martinod, J., Hérail, G., 2002. Possible Orogeny-parallel Lower Crustal Flow and Thickening in the Central Andes. *Tectonophysics, 5th ISAG 2002 Special Issue (ISAG 5th, Toulouse, 2002) edited by M.Gerbault, G. Hérail and J. Martinod, 399, 1-4*, 1-13.

Giambiagi, L.B., Ramos, V.A., Godoy, E., Alvarez, P.P., Orts, S., 2003. Cenozoic deformation and tectonic style of the Andes, between 33° and 34° south latitude. Tectonics, 22 (4), 1041, doi:10.1029/2001TC001354.

Gill, J.B., 1981. Orogenic andesites and plate tectonics. *Springer-Verlag*, New-York, 390.

Godoy, E., Yanez, G., Vera, E., 1999. Inversion of an Oligocene volcanotectonic basin and uplifting of its surimposed Miocene magmatic arc in the Chilean Central Andes: first seismic and gravity evidences. *Tectonophysics, 306 (2),* 217-236.

Gorring, M., Kay, S., Zeitler, P., Ramos, V., Rubiolo, D., Fernandez, M., Panza, J., 1997. Neogene Patagonian plateau lavas : continental magmas associated with ridge collision at the Chile Triple Junction. *Tectonics, 16*, 1-17.

Gorring, M., Kay, S., 2001. Mantle processes and sources of Neogene slab window magmas from Southern Patagonia. *Argentina. J. Petrol. 42*, 1067-1094.

Gorring, M., Singer, B., Gowers, J., Kay, S., 2003. Plio-Pleistocene basalts from the Meseta del Lago Buenos Aires, Argentina : evidence for asthenosphere-lithosphere interactions during slab-window magmatism. *Chem. Geol. 193*, 213-235.

Grégory-Wodzicki, K.M., 2000. Uplift history of the central and northern Andes: a review. *Geological Society of America Bulletin, 112*, 1092-1205.

Groome, G.W., Thorkelson, D.J., Friedman, R.M., Mortensen, J.K., Massey, N.W.D., Marshall, D.D., Layer, P.W., 2003. Magmatic and tectonic history of the Leech River Complex, Vancouver Island, British Columbia: Evidence for ridge-trench intersection and accretion of the Crescent Terrane. In Sisson, V.B., Roeske, S.M., and Palvis, T.L., eds., Geology of a transpressional orogen developed during ridge-trench interaction along the North pacific margin. Boulder, Colorado, *Geological Society of America Special paper 371*, 327-353.

Groome, G., Thorkelson, J.D., 2009. The three-dimensional thermo-mechanical sugnature of ridge subduction and slab window migration. *Tectonophysics, 464*, 70-83.

Guillaume, B., 2009. Evolution Cénozoique des Andes méridionales: approche morphotectonique, géochronologique et apports *de la modélisation analogique. Thèse de doctorat, Université de Toulouse III, Paul Sabatier*, 330 pp.

Guivel, C., 1999. Subduction d'une dorsale océanique active: Interactions magmatiques et tectoniques. Le cas du point triple du Chili. *Thèse de doctorat*, Université de Bretagne Occidentale, France, 268 pp.

Guivel, C., Lagabrielle, Y., Bourgois, J., Maury, J.C., Fourcade, S., Martin, H., Arnaud, N., 1999. New geochemical constraints for the origin of ridge-subduction-related plutonic and volcanic suites from the Chile Triple Junction (Taitao Peninsula and site 862, LEG ODP141 on the Taitao Ridge). *Tectonophysics, 311 (4)*, 83-111.

Guivel, C., Lagabrielle, Y., Bougois, J., Martin, H., Arnaud, N., Fourcade, S., Cotton, J., Maury, R.C., 2003. Very shallow melting of oceanic crust during spreading ridge subduction: origin of near trench Quaternary volcanism at the Chile Triple Junction. *Journal of Geophysical Research, 108 (B7)*, 1-19.

Guivel, C., Morata, D., Pelleter, E., Espinoza, F., Maury, R.C., Lagabrielle, Y., Polvé, M., Bellon, H., Cotten, J., Benoit, M., Suarez, M., de la Cruz, R., 2006. Miocene to Late Quaternary

Patagonian basalts (46°-47°S) : Geochronometric and geochemical evidence for slab tearing due to active spreading ride subduction. *Journal of Volcanology and Geothermal Research, 149*, 346-370.

Gutscher, M.A., Malavieille, J., Lallemand, S., Collot, J.Y., 1999b. Tectonic segmentation of the North Andean margin: impact of the Carnegie Ridge collision. *Earth and Planetary Science Letters, 168 (3-4)*, 255-270.

Gutscher, M.A., Spakman, W., Bijwaard, H., Engdalh, E.R., 2000. Geodynamics of flat subduction. Seismicity and tomographic constraints from the Andean margin. *Tectonics, 19*, 814-833.

Halpern , M., 1973. Regional Geochronology of Chile South of 50°S Latitude. *Geological Society of America Bulletin, 84 (3),* 1113.

Hamza, V.M., et Munoz, M., 1996. Heat flow map of South America. *Geothermics; 25 (6),* 599-646.

Hauessler, P.J., Bradley, D.C., Goldfarb, R.J., 2003. Brittle deformation along the Gulf of Alaska margin in response to Paleocene-Eocene triple junction migration. In Sisson, V.B., Roeske, S.M., and Palvis, T.L., eds., Geology of a transpressional orogen developed during ridge-trench interaction along the North pacific margin. Boulder, Colorado, *Geological Society of America Special paper 371*, 119-140.

Heintz M., Debayle, E., Vauchez. A., 2005. Upper mantle structure of the South America continent and neighboring oceans from surface wave tomography. *Tectonophysics, 406*, 115-139.

Helffrich, G., Douglas, A.W., Vera, E., Barrientos, S., Shore, P., Robertson, S., Adaros, R., 2002. A teleseismic shear-wave splitting study to investigate mantle flow around South America and implications for plate-driving forces. *Geophysical Journal International, 149*, 1-7.

Hervé, F., Suarez, M., Puig, A., 1984. The Patagonian Batholith S of Tierra del Fuego, Chile: Timing and tectonic implications. *Journal of Geological Society of London, 144*, 909-917.

Hervé, F., 1993. Paleozoic metamorphic complexes in the Andes of Aysen, Southern Chile. *Proceedings of the first Circum-Pacific and Circum-Atlantic Terrane Conference, Guanajuato, Mexico*, 64-65.

Hervé, F., 1994. The Southern Andes between 39° and 44°S Latitude: the geological signature of a transpressive tectonic regime related to a magmatic arc. *K.J. Reutter, E. Scheuber and P.J. Wigger. Tectonics of the Southern Central Andes, Structure and Evolution of an Active Continental Margin,* 249-261, Springer Verlag, Berlin.

Hervé, F., Aguirre, L., Godoy, E., Massone, H., Morata, D., Pankhurst, R., Ramirez, E., Sepulveda, V., Wilner, A., 1998. Meuvos antecedentes acerca de la edad y las conditiones P-T de los complejos metamorficos en Aysen. *X Congreso Latinoamericano de Geologia y VI Congreso Nacional de Geologia Economica. Actas, II*, 134-137.

Hervé, F., Demant, A., Ramos, V.A., Pankhurst, R.J., Suarez, M., 2000. The Southern Andes. *In Cordani, U.J., Milani, E.J., Thomaz Filho, A., Campos, D.A., (eds.). Tectonic evolution of South America, 31st International Geologic Congress*, 605-634.

Hervé, F., Pankhurst, R.J., Fanning, M.C., Calderon, M., Yaxley, G.M., 2007. The South Patagonian Batholith: 150 Myr of granite magmatism on a plate margin. Lithos, 97, 373-394.

Heuret, A., et Lallemand, S., 2005. Plate motions, slab dynamics and back-arc deformation. *Physics of the Earth and Planetary Science Letters, 256*, 473-483.

Hibbard, J.P., Karig, D.E., 1990a. Structural and magmatic responses to spreading ridge subduction: An example from Southwest Japan. *Tectonics, 9 (2),* 207-230.

Hibbard, J.P., et Karig, D.E., 1990b. Alternative plate model for the early Miocene evolution of the Southwest Japan margin. *Geology, 18 (2)*, 170-174.

Hiramatsu, Y., Ando, M., Tsukuda, T., Ooida, T., 1998. Three dimensional image of the anisotropic bodies beneath central Honshu, Japan. *Geophysical Journal International, 135 (3)*, 801-816.

Hole, M.J., Graeme, R., Saunders, A.D., Storey, M., 1991. Relation between alkalic volcanism and slab-window formation. *Geology, 19 (6),* 657-660.

Hole, M.J., et Larter, R.D., 1993. Trench-proximal volcanism following ridge crest-trench collision along the Antarctic Peninsula. *Tectonics, 12 (4)*, 897-910.

Horai, K., et Uyeda, S., 1963. Terrestrial heat flow in Japan. *Nature, 199*, 364-365.

Hyndman, R.D., et Lewis, T.J., 1999. Geophysical conséquences of the Cordillera-Craton thermal transition in southwestern Canada. *Tectonophysics, 306 (3-4)*, 397-422.

Introcaso, A., Pacino, M.C., Fraga, H., 1992. Gravity, isostasy and Andean crustal shortening between latitudes 30° and 35°S. *Tectonophysics, 205 (1-3),* 31-48.

Isacks, B.L., 1988. Uplift of the Central Andean Plateau and bending of the Bolivian Orocline. *Journal of Geophysical Research, 93 (B4)*, 3211-3231.

Iwamori, H., 2000. Thermal effects of ridge subduction and its implications for the origin of granitic batholith and paired metamorphic belts. *Earth and Planetary Science Letters, 181 (1-2)*, 41-46.

Jaillard, E., Ordonnez, M., benitez, S., Berrones, G., Jimenez, N., Montenegro, G., Zambrano, I., 1995. Basin development in an accretionary, oceanic-floored fore-arc setting : southern coastal Ecuadore during Late Cretaceous-late Eocene time. *AAPG Memoir, 62*, 615-631.

Jaillard, E., Laubacher, G., Bengtson, P., Dhondt, A.V., Bulot, L.G., 1999. Stratigraphy and évolution of the Creatceous forearc Celica-Lancones Basin of southwestern Ecuador. *Journal of South American Earth Sciences, 12 (1)*, 51-68.

Johnson, C.M., O'Neil, J.R., 1984. Triple junction magmatism : a geochemical study of Neogene volcanic rocks in western California. *Tectonophysics, 71 (2),* 241-263.

Johnson, R.W., Jaques, A.L., Langmuir, C.H., Perfit, M.R., Dunkley, S.H.P.N., Chappel, B.W., Taylor, S.R., 1987. Ridge subduction and forearc volcanism :petrology and geochemistry of rocks dredged from the western Salomon arc and Woodlark basin. 155-226.

Johnston, S.T., et Thorkelson, D.J., 1997. Cocos-Nazca slab window beneath Central America. *Earth and Planetary Earth Sciences, 146 (3-4)*, 465-474.

Jordan, T.E., Isacks, B., Allmendinger, R., Brewer, J., Ramos, V.A., Ando, C., 1983. Andean tectonics related to geometry of the subducté Nazca plate. *Geological Society of America Bulletin, 94*, 341-361.

Jordan, T.E., Burns, W.M., Veiga, R., Pangaro, F., Copeland, P., Kelley, S., Mpodozis, C., 2001. Extension and basin formation in the southern Andes caused by increased convergence rate : A mid-Cenozoic trigger for the Andes. *Tectonics, 20 (3)*, 308-324.

Kaeding, M., Forsythe, R.D., Nelson, E.P., 1990. Geochemistry of teh Taitao ophiolite and near-trench intrusions from the Chile Margin Triple Junction. *Journal of South American Earth Sciences, 3 (4)*, 161-177.

Kay, M., Mpodozis, C., Ramos, V.A., Munizaga, F., 1991. Magma source variations for mid to late Tertiary volcanic rocks erupted over a shallowing subduction zone and through a thickening crust in the Main Andean Cordillera (28-33°S). *In Harmon, R.S., Rapela, C., (eds.). Andean Magmatism and its tectonic Setting. Geological Society of America Special Paper, 265*, 113-137.

Kay, M., Ramos, V.A., Marquez, M., 1993. Evidence in Cerro Pampa volcanic rocks for slab-melting prior to ridge-trench collision in southern South America. *Journal of Geology, 101 (6)*, 703-714.

Kay, S.M., Mpodozis, C., Coira, B., 1999. Neogene magmatism, tectonism, and mineral deposits of the Central Andes (22°S to 33°S). *In Skinner, B., (ed.). Geology and Mineral Deposits of Central Andes. Society of Economic geology, Special Publication, 7*, 27-59.

Kay , S.M., et Mpodozis, C., 2002. Magmatism as a probe to the Neogene shallowing of the Nazca plate beneath the modern Chilean flat-slab. *Journal of South American Earth Sciences, 15*, 39-57.

Kinimani, K., Miyashita, S., Kawabata, K., 1994. Ridge collision and in situ greenstones: An example from the Late Cretaceous Ryuku Islands and southwest Japan margin. *The Island Arc, 3*, 103-111.

Kinoshita, O., **2002**. Possible manifestations of slab-window magmatisms in Cretaceous Southwest Japan. *Tectonophysics, 344 (1-2),* 1-13.

Kley, J., Monaldi, C.R., Salfity, J.A., 1999. Along-strike segmentation of the Andean foreland: causes and consequences. *Tectonophysics, 301 (1-2),* 75-94.

Kraemer, P.E., et Riccardi, A.C., 1997. Estratigrafia de la region comprendida entro los lagos Argentino y Viedma, Santa Cruz. *Revista de la Asociacion argentina, 52 (3),* 333-360.

Kusky, T.M., et Polat, A., 1999. Growth of granite-greenstone terranes at convergent margins, and stabilization of Archean cratons. *Tectonophysics, 305 (1-3)*, 43-73.

Kusky, T.M., Bradley, D., Rowley, D., haeussler, P.J., 2003. Controls on intrusion of near-trench magmas of the Sanak-Baranof belt, Alaska, during Paleogene ridge subduction, and consequences for forearc evolution. In Sisson, V.B., Roeske, S.M., and Palvis, T.L., eds., Geology of a transpressional orogen developed during ridge-trench interaction along the North pacific margin. Boulder, Colorado, *Geological Society of America Special paper 371*, 269-292.

Lagabrielle., Y., Le Moigne, J., Maury, R.C., Cotton, J., Bourgois, J., 1994. Volcanic record of the subduction of an active spreading ridge, Taitao Peninsula (southern Chile). *Geology, 22 (6)*, 515-518.

Lagabrielle, Y., Guivel, C., Maury, R.C., Bourgois, Y., Fourcade, S., Martin, H., 2000. Magmatic-tectonic effects of high thermal regime at the site of active spreading ridge subduction : the Chile Triple Junction model. *Tectonophysics 326 (3-4)*, 215-228.

Lagabrielle, Y., Suarez, M., Rossello, E.A., Hérail, G., Martinod, J., Régnier, M., de la Cruz, R., 2004. Neogene to Quaternary tectonic evolution of the Patagonian Andes at the latitude of the Chile Triple Junction. *Tectonophysics, 385*, 211-241.

Lagabrielle, Y., Godderis, Y., Donnadieu, Y., Malavieille, J., Suarez, M., 2009. The tectonic evolution of Drake Passage and its possible impacts on global climate. *Earth and Planetary Science Letters, 279 (3-4)*, 197-211.

Lagabrielle, Y., Scalabrino, B., Suarez, M., Ritz, J.F. Mio-Pliocene glaciations of Central Patagonia: New evidence and tectonic implications. Accepted to Andean Geology, special volume.

Lapierre, H., Dupuis, V., Bosch, D., Polvé, M., Maury, R.C., Hernandez, J., Monié, P., Yéghicheyan, D., Jaillard, E., Tardy, M., Mercier de Lépinay, B., Mamberti, M., Desnet, A., Keller, F., Sénebrier, F., 1999. Multiple plume évents in the genesis of the péri-Carribean Cretaceous Oceanic Plateau Province. *Journal of Geophysical Research*.

Lamb, D., Hoke, L., Kennan, L., Dewey, J., 1997. Cenozoic evolution of the central Andes in Bolivia and northern Chile. *In Burg, J.P., et Ford, M., (eds), Orogens Through Time. Geological Society Special Publications, 121*, 237-264.

Lamb, S., et Davies, P., 2003. Cenozoic climate change as a possible cause for the rise of the Andes. *Nature, 425*, 792-797.

Larter, R.D., et Barker, P.F., 1991. Effects of ridge crest-trench interaction on Antarctic-Phoenix spreading; forces on a young subducting plate. *Journal of Geophysical Research, 96 (B12)*, 19583-19607.

Lerch, D.W., Miller, E., McWilliams, M., Colgan, J., 2008. Tectonic and magmatic évolution of the northwestern Basin and Range and its transition to unextended volcanic plateaus : Black Rock Range, Nevada. *Geological Society of america Bulletin, 120 (3-4)*, 300-311.

Leuthold, J., Muntener, O., Baumgartner, L., Pitmitz, B., Jurgen, M., 2007. Petrology and structure of the Paine Mafic Complex (preliminary results). *5^e^ Swiss Geoscience Meeting*, Genève.

Levin, V., Park, J., Brandon, M., Less, J.M., Peyton, V., Gordeev, E., Ozerov, A., 2002. Crust and upper matle of Kamchatka from teleseismic receiver functions. *Tectonophysics, 358 (1-4)*, 233-265.

Levin, V., Shapiro, N.M., Park, J., Ritzwoller, M.H., 2005. Slab portal beneath the western Aleutians. *Geology, 33 (4)*, 253-256.

Liu, M., et Shen, Y., 1998. Crustal collapse, mantle upwelling, and Cenozoic extension in the North American Cordillera. *Tectonics, 17 (2)*, 311-321.

Londsale, P., 2005. Creation of the Cocos and Nazca plates by fission of the Farallon plate. *Tectonophysics, 404*, 237-264.

Long, M.D., Silver, P.G., 2008. The subduction zone flow field from seismic anisotropy : A global review. *Science, 319 (5861),* 315-318.

Madsen, J.K., Thorkelson, D.J., Friedman, R.M., Marshall, D.D., 2006. Cenozoic to Recent plate configurations in the Pacific Basin : ridge subduction and slab-window magmatism in the western North America. *Geoshere, 2 (1),* 11-34.

Malavieille, J., 1987. Les mécanismes d'amincissement d'une croûte épaissie : les Metamorphic Core Complexes du Basin and Range (USA). *Thèse d'Etat*, Université Montpellier 2, France, 333 p.

Mann, P., et Taira, A., 2004. Global tectonic significance of the Salomon Islands and Ontong Java Plateau convergent zone. *Tectonophysics, 389*, 137-190.

Marshak, R.S., et Karig, D.E., 1977. Triple junctions as a cause for anomalously near-trench igneous activity between trench and volcanic arc. *Geology, 5*, 233-236.

Martinez, M.P., Gimenez, M.E., Introcaso, A., Robles, J.A., 1997. Excesos de espesores corticales y acortamientos andinos en très secciones ubicadas en 36°, 37° y 39°S de latitud sur. 8° Congreso Geologico Chileno (Antofagasta). Actas, 1, 101-105.

Maury, R.C., Sajona, F.G., Pubellier, M., Bellon, H., Defant, M.J., 1996. Fusion de la croûte océanique dans les zones de subduction/collision récentes : l'exemple de Mindanao (Philippines). *Bulletin de la Société Géologique de France, 167 (5),* 579-595.

McKenzie, D.P., 1969, Speculations on the consequences and causes of plate motions: Geophysical. *Journal of the Royal Astronomical Society, 18*, 1-32.

Mégard, F., 1987. Cordilleran Andes and Marginal Andes : a review of Andean geology north of the Arica elbow (18°S). *In Monger, J.M.H., Francheteau, J., (eds). Circum-Pacific orogenic belts and évolution of the Pacific Ocean basin. International Lithosphere Program Contribution, Geodynamic Series, 18*, 71-96.

Menard, H.W., 1978. Fragmentation of the Farallon plate by pivoting subduction. *Journal of Geology, 86*, 99-110.

Mendez Fajury, R.A., 1989. *Catalogo de volcanes activos de Colombia. Boletin Geologico del Ingeominas 30 (3),* 1-75.

Michael, P.J., 1984. Chemical différenciation of the Cordillera Paine granite (southern Chile) by in situ fractional crystallization. *Contributions to Mineralogy and Petrology, 87,* 179-195.

Michaud, F., Royer, J.Y., Bourgois, J., Dyment, J., Calmus, T., Bandy, W., Sosson, M., Mortera-Gutierrez, C., Sichler, B., Rebolledo-Viera, M., Pontoise, B., 2006. Oceanic-ridge subduction vs. Slab break-off : Plate tectonic évolution along the Baja California Sur continental margin since 15 Ma. *Geology, 34 (1)*, 13-16.

Michel, J., Baumgartner, L., Cosca, M., Ovtcharova, M., Puliltz, B., Schaltegger, U., 2006. High précision ages from the Torres del Paine Intrusion, Chile. *American Geophysical Union Fall Meeting 2006*, abs. V11A-0550.

Michel, J., Baumgartner, L., Putlitz, B., Schaltegger, U., Ovtcharova, M., 2008. Incremental growth of the Patagonian Torres del Paine laccolith over 90 k.y. Geology, 36 (6), 459-462.

Miller, K.C., 2002. Geophysical évidence for Miocene extension and mafic magmatic addition in the California Continental Borderland. *Geological Society of America Bulletin, 114 (4)*, 497-512.

Montgomery, D.R., Balco, G., Willett, S.D., 2001. Climate, tectonics, and the morphology of the Andes. *Geology, 29 (7)*, 579-582.

Moore, J.C., Byrne, T., Plumley, P.W., reid, M., Gibbons, H., Coe, R.S., 1983. Paleogene évolution of the Kodiak Islands, Alaska : Consequences of ridge-trench interaction in a more southerly latitude. *Tectonics ; 2 (3),* 265-293.

Morata, D., Barbero, L., Suarez, M., de la Cruz, R., 2002. Early Pliocene magmatism and high exhumation rates in the Patagonian Cordillera (46°40'S) : K-Ar, and fission track data. ISAG.

Mortimer, E., Schoenbohm, L., Carrapa, B., Sobel, E.R., Sosa Gomez, J., Strecker, M.R., 2006. Compartmentalization of a foreland basin in response to plateau growth and diachronous thrusting : El Cajon-Campo Arenal basin, NW Argentina. *Geological Society of America Bulletin*.

Moucha, R., Forte, A.M., Rowley, D.B., Mitrovica, J.X., Simmons, N.A., Grand, S.P., 2008. Mantle convection and the récent évolution of the Colorado Plateau and the Rio Grande Rift valley. *Geology, 36 (6)*, 439-442.

Mpodozis, C., et Allmendinger, R.W., 1993. Extensional tectonics, Cretaceous Andes, northern Chile (27°S). *Geological Society of America Bulletin, 105*, 1462-1477.

Mpodozis, C., et Ramos, V.A., 1990. The Andes of Chile and Argentina. *In Ericksen, G.E., Canas Pinochet, M.T., Reinemund, J.A. (eds). Geology of the Andes and its relation to Hydrocarbon and Mineral Resources, Circum-Pacific Council for Energy and Mineral Resources, Earth Sciences Series, 11,* 59-90.

Munoz, J., Troncoso, R., Duhart, P., Crignola, P., Farmer, L., Stern, C., 2000. The Relationship of the mid-Tertiary coastal magmatic belt in south-central Chile to the late Oligocene increase in plate convergence rate. *Revista Geologica de Chile, 27*, 177-203.

Müller, R.D., Sdrolias, M., Gaina, C. Steinberger, B. and Heine, C., 2008. Long-Term Sea-Level Fluctuations Driven by Ocean Basin Dynamics. *Science, 319*, 1357-1362, DOI: 10.1126/science.115154.

Murdie, R.E., Pugh, D.T., Styles, P., 1999. A lightweight, portable, digital probe for measuring the thermal gradient in shallow water sediments, with examples from patagonia *Geo-Marine Letters, 18,* 315-320.

Murdie, R.E., Russo, R.M., 1999. Seismic anisotropy in the région of the Chile margin triple junction. *Journal of South American Earth Sciences, 12 (3),* 261-270.

Nakajima, J., Hasegawa, A., 2004. Shear-wave polarization anisotropy and subduction-induced flow in the mantle wedge of northeastern Japan. *Earth and Planetary Sciences Letters, 225 (3-4)*, 365-377.

Naranjo, J.A., Hervé., F., Prieto, X., Munizaga, F., 1984. Actividad cretacica de la falla de Atacama al este de Chanaral : milonizacion y plutonismo. *Comunicaciones, Santiago de Chile, 34*, 37-45.

Niemeyer, H., Skarmeta, J., Fuenzalida, R and Espinosa, W. 1984. Hojas Peninsula de Taitao y Puerto Aisen, Region de Aisen del General Carlos Ibanez del Campo. *Carta Geologica de Chile*, 60-61, 1:500.000. Sevicio Nacional de geololgia y Mineria, Chile

Nullo, F., Proserpio, C., Ramos, V.A., 1978. Estratigrafia y tectonica de la vertiente este del Hielo Continental patagonico, Argentina-Chile. *Actas, VII Congreso Geologico Argentino I*, 455-470.

Okada, T., Matsuzawa, T., Hasegawa, A., 1995. Shear-wave polarization anisotropy beneath the north-eastern part of Honshu, Japan. *Geophysical Journal International, 123 (3)*, 781-797.

O'Neill, R.L., Pavlis, T.L., 1988. Superposition of Cenozoic extension on Mesozoic compressional structures in the Pioneer Mountains metamorphic core complex, central Idaho. *Geological society of America Bulletin, 100 (11)*, 1833-1845.

Osozawa, S., 1992. Double ridge subduction recorded in the Shimanto accretionary complex, Japan, and plate reconstruction. *Geology, 20 (10),* 939-942.

Palvis, T.L., Sisson, V.B., 1995. Structural history of the Chugach metamorphic complex in the Tana River region, eastern Alaska. A record of Eocene ridge subduction. *Geological Society of American Bulletin, 107*, 1333-1355.

Pankhurst, R.J., Weaver, S., Hervé, F., Larrandon, P., 1999. Mesozoic-Cenozoic evolution of the North Patagonian Batholith in Aysen, southern Chile. *Journal of the Geological Society of London, 156*, 673-694.

Pankhurst, R.J., Riley, T.R., Fanning, C.M., Kelley, S.P., 2000. Episodic volcanism in Patagonia and the Antarctic Peninsula: Chronology of magmatism associated with the break-up of Gondwana. *Journal of Petrology, 41 (5),* 605-625.

Pankhurst, R.J., Rapela, C.W., Fanning, C.M., Marquez, M., 2006. Gondwanide continental collision and the origin of Patagonia. *Earth Science Reviews, 76,* 235-257.

Parada, M.A., Lahsen, A., Palacios, C., 2001. Ages and geochemistry of Mesozoic-Eocene back-arc volcanic rocks in the Aysen region of the Patagonian Andes, Chile. *International Geology Review, 43 (10),* 892-909.

Pardo, M., Comte, D., et Monfret, T., 2002. Seismotectonic and stress distribution in the central Chile subduction zone. *Journal of South American Earth Sciences, 15*, 11-22.

Pardo-Casas, F., et Molnar, P., 1987. Relative motion of the Nazca (Farallon) and South America plates since Late Cretaceous time. *Tectonics 6 (3)*, 233-248.

Parrish, R.R., Carr, S.D., Parkinson, D.L., 1988. Eocene extensional tectonics and geochronology of the southern Omineca belt, British Columbia and Washington. *Tectonics, 7 (2)*, 181-212.

Parsons, T., Thompson, G.A., Sleep, N.H., 1994. Mantle plume influence on the Neogene uplift and extension of the U.S. western Cordillera ? *Geology, 22 (1)*, 83-86.

Peacock, S.M., 1996. Thermal and petrologic structure of subduction zones. *In Subduction : Top to Bottom, Geophysical Monograph 1996*, 119-133.

Pennington, W.D., 1981. Subduction of the Eastern Panama Basin and seismotectonics of Northernwest South America. *Journal of Geophysical Research, 86*, 10753-10770.

Pedoja, K ., Dumont, J.F., Lamothe, M., Collot, J-Y., Ghaleb, B., Auclair, M., Alvarez, V., Labrousse, B. Plio Quaternary uplift of the Manta Peninsula and La Plata Island and the subduction of the Carnegie Ridge, central coast of Ecuador. 2006. *South American Earth Science Journal, 22(1-2)*, 1-21.

Peyton, V., Levin, V, Park, J., Brandon, M.T., Leea, J., Gordeev, E., Ozerov, A., 2001. Mantle flow at slab edge : Seismic anisotropy in the Kamchatka region. *Geophysical Research Letters, 28*, 379-382.

Pilger, R.H., 1984. Cenozoic plate kinematics, subduction and magmatism : Southern American Andes. *Journal Geological Society of London, 141*, 793-802.

Polet, J., Silver, P.G., Beck, S., Wallace, T., Xandt, G., Ruppert, S., Kind, R., Rudloff, A., 2000. Shear-wave anisotropy beneath the Andes from the BANJO, SEDA, and PISCO experiments. *Journal of Geophysical Research, 105 (B3),* 6287-6304.

Rahl, J.M., McGrew, A., Foland, K.A., 2002. Transition from contraction to extension in the northeastern Basin and Range : new évidence from the Copper Mountains, Nevada. *Journal of Geology, 110 (2),* 179-194.

Ramos, V.A., 1988. The Tectonics of the Central Andes: 30°S to 33°S latitude. In Clark, S., Burchfield, D., (Eds). Processes in Continental Lithospheric Deformation. *Geological Society of America Special Paper, 218*, 31-54.

Ramos, V.A., 1989. Andean foothills structures in the Northern magallanes Basin, Argentina. *American Association of Petroleum Geologists, 73 (7)*, 887-903.

Ramos, V., Kay, S.M., 1992. Southern Patagonian plateau basalts and déformation : backarc testimony of ridge collision. *Tectonophysics, 205*, 261-282.

Ramos, V.A., 1999. Plate tectonic setting of the Andean Cordillera. *Episodes, 22 (3),* 183-190.

Ramos, V.A., et Aguirre-Urreta, M.B., 2000. Tectonic evolution of South America. *In Cordani, U.J., Milani, E.J., Thomaz Filho, A., Campos, D.A, (eds), 31st International Geologic Congress*, 369-380.

Ramos, V.A., 2002. Evolucion tectonica. *In Haller, M.J., (ed.). Geologia y Recursos Naturales de Santa Cruz. Relatorio del XV Congreso Geologico Argentino (El Calafate), 1 (23)*, 365-387.

Ramos, V., Kay, S., Singer, B., 2004. Las adakitas de la Cordillera Patagónica: Nuevas evidencias geoquímicas y geocronológicas. *RAGA* 59, 693-706

Ramos, V.A., ET Folguera, A., 2005. Tectonic evolution of the Andes of Neuquen:constraints derived from the magmatic arc and foreland deformation. *Geological Society Special Publications, 252*, 15-35.

Restrepo, A.J.J., et Toussaint, J.F., 1973. Obduccion cretacea en el Occidente Colombiano, Cretaceous obduction in western Columbia. *Anales de la Facultad Nacional de Minas, 58*, 73-105.

Roeske, S.M., Dusel-Bacon, C., Aleinikoff, J.N., Snee, L.W., Lanphere, M.A., 1995. Metamorphic and structural history of continental crus tat a Mesozoic collisional margin, the Ruby Terrane, central Alaska. *Journal of Metamorphic Geology, 13 (1)*, 25-40.

Roseneau, M., Melnick, D., Echtler, H., 2006. Kinematic constraints on intra-arc shear and strain partitioning in the southern Andes between 38°S and 42°S latitude. *Tectonics, 25*, TC4013, doi:10.1029/2005TC001943.

Riddihough, R., 1984. Recent movements of the Juan de Fuca plate system. *Journal of Geophysical Research, 89 (B8),* 6980-6994.

Russo, R.M., Silver, P.G., 1994. Trench-parallel flow beneath the Nazca Plate from seismic anisotropy. *Science, 263 (5150)*, 1105-1111.

Salfity, J.A., 1984. Tectonic and sedimentary évolution of the Cretaceous-Eocene salta Group basin, Argentina. *In Salfity, J.A., (ed.), Cretaceous tectonics of the Andes, Earth Evolution Series, 266-315.*

Sanchez, A., Hervé, F., de Saint-Blanquat, M., 2008. Relations between plutonism in the barck-arc région in southern Patagonia and Chile Rise subduction : A geochronological review. *7th International Symposium on Andean geodynamics (ISAG, 2008, Nice), Extended Abstracts : 485-488.*

Sass, J.H., Lachenbruch, A.H., Galanis, S.P., Moragn, P., Priest, S.S., Moses, T.H., Munroe, R.J., 1994. Thermal régime of the southern Basin and Range Province. Heat flow data from Arizona and Mojave Desert of California and Nevada. *Journal of Geophysical Research, 99 (B11)*, 22093-22119.

Saunders, A.D., et Tarney, J., 1987. Ignoeius activity in the Southern Andes and northern Antarctic Peninsula : a review. *Journal of the Geological Society of London, 139 (6)*, 691-700.

Savage, M.K., 1999. Seismic anisotropy and mantle déformation : what have we learned from shear wave splitting. *Reveiws of Geophysics, 37 (1),* 65-106.

Schellart, W.P., Stegman, D.R., Freeman, J., 2008. Global trench migration velocities and slab migration induced upper mantle volume fluxes : Constraints to find an Earth reference frame based on minimizing viscous dissipation. *Earth –Sciences Reviews, 88*, 118-144.

Schubert, C., et Vivas, L., 1993. El Cuaternario de la Cordillera de Mérida, Andes Venezolanos. *Universidad de los Andes, Fundacion Polar, Mérida*, 1-345.

Sébrier, M., Mercier, J.L., Mégard, F., Laubacher, G., Carey-Gaihardis, E., 1985. Quaternary normal and reverse faulting and the state of stress in the central Andes of south Peru. *Tectonics, 7*, 739-780.

Sébrier, M., et Soler, P., 1991. Tectonics and magmatism in the Peruvian Andes from Late Oligocene time to the Present. *In Harmon, R.S., Rapela, C., (eds). Andean magmatism and its Tectonic Setting. Geological society of America Special Paper 265*, 259-276.

Sempere, T., Hérail, G., Oller, J., Bonhomme, M., 1990. Late Oligocene-early Miocene major tectonic crisis and related basins in Bolivia. *Geology, 18*, 946-949.

Severinghaus, J., et Atwater, T., 1990. Cenozoic geometry and thermal state of the subducting slabs beneath western North America. *Memoir-Geological Society of America, 176*, 1-22.

Silver, P.G., Russo, R.M., Lithgow-Bertelloni, C., 1998. Coupling of the South American and African Plate Motion. *Journal of Geophysical Research, 96*, 16429-16454.

Sisson, V.B., Poole, A.R., harris, N.R., Burner, H.C., Palvis, T.L., Copeland, P., Donelick, R.A., McLelland, W.C., 2003. Geochemical and geochronologc constraints for genesis of a tonalite-trondhjemite suite and associated mafic intrusive rocks in the eastern Chugach Mountains, Alaska : A record of ridge-transform subduction. In Sisson, V.B., Roeske, S.M., and Palvis, T.L., eds., Geology of a transpressional orogen developed during ridge-trench interaction along the North pacific margin. Boulder, Colorado, *Geological Society of America Special paper 371,* 293-326.

Sisson, V.B., et Palvis, T.L., 1993. Geologic consequences of plate reorganization: An example from the Eocene southern Alaska forearc. *Geology, .21*, 913-916.

Sisson, V.B., Poole, A.R., Harris, N.R, Burner, H.C. Palvis, T.L., Copeland, P., Donelick, R.A., McLellan

Smith, W.H.F., et sandwell, D.T., 1997. Global sea floor topography from satellite altimetry and ship deep soundings. *Science, 277 (5334)*, 1956-1962.

Somoza, R., 1998. Updated Nazca (Farallon)-South America relative motions during the last 40 Ma. Implications for mountain building in the central Andean regions. *Journal of South American Earth Sciences, 11,* 211-215.

Steinmann, M., Hungerbuhler, S., Winkler, W., 1999. Neogene tectonic évolution and exhumation of the southern Ecuadorian Andes : a combined stratigraphy and fission-track approach. *Tectonophysics, 307*, 255-276.

Stern, C.R., 1991. Role of subduction erosion in the génération of Andean Magmas. *Geology, 19 (1)*, 78-81.

Stern, C.R., et Kilian, R., 1996. Role of the subducté slab, mantle wedge and continental crust in the génération of adakites from the Andean austral volcanic zone. *Contributions to Mineralogy and Petrology, 123 (3)*, 263-281.

Stock, J.M., et Hodges, K.V., 1989. Pre-Pliocene extension around the Gulf of California, and the transfer of Baja California to the Pacific Plate. *Tectonics, 8 (1)*, 99-115.

Stock, J.M., 2007. Miocene to Recent volcanism in NE Baja California and its corrélation to adjacents regions. *American Geophysical Union, Fall Meeting 2007*, abstract #V23C-07.

Storey, M., Rogers, G., Saunders, A.D., Terrell, D.J., 1989. San Quintin volcanic field, Baja California, Mexico : 'within-plate' magmatism following ridge subduction. *Terra Nova, 1 (2)*, 195-202.

Strecker, M.R., Alonso, R.N., Bookhagen, B., carrapa, B., Hilley, G.E., Sobel, E.R., Trath, M.H., 2007. Tectonics and Climate of the Southern Central Andes. *Annual Review Earth Planetary Sciences, 35*, 747-787.

Suarez, M., de la Cruz, R., 1994. Estratigrafia y paleogeografia mesozoica de Aisen nororiental (45°S-46°S), Chile. *In Congreso Geologico Chileno,.7, Actas,.1*, 538-542. Concepcion.

Suarez, M., de la Cruz, R., 2000. Tectonics in the eastern central Patagonian Cordillera (45°30'-47°30'S). *Journal of the Geological Society (London) 157*, 995-1001.

Suarez, M., de la Cruz, R., 2001. Jurassic to Miocene K-Ar dates from eastern central Patagonian Cordillera plutons, Chile (45°-48°S). *Geological Magazine 138 (1),* 53-66.

Suarez, M., De la Cruz, R., Aguirre-Urreta, B., Fanning, M., 2009. Relationship between volcanism and marine sédimentation in the northern Austral (Aysen) Basin, central Patagonia : Stratigraphic, U-Pb SHRIMP and paleontologic evidence. *Journal of South American Earth Sciences*, doi : 10.1016/j.jsames.2008.11.2009.

Tamaki, K., 1985. Two modes of back-arc spreading. *Geology, 13 (7)*, 475-478.

Thorkelson, D., et Taylor, R.P., 1989. Cordilleran slab window. *Geology, 17 (9),* 833-836.

Thorkelson D.J.; 1996. Subduction of diverging plates and the principles of slab window formation, *Tectonophysics, 255*, 47–63.

Thorkelson, D.J., 2002. The Basin and Range Province as a composite extensional domain. *International Geology Review, 44 (1),* 1-38.

Thorkelson, D.J., et Breitsprecher, K., 2005. Partial melting of slab-window margins: genesis of adakitic and non-adakitic magmas. *Lithos, 79 (1-2),* 25-41.

Thorpe, R.S., Francis, P.W., Harmon, R.S., 1981. Andean andesites and crustal growth. *Philosophical transactions of the Royal Society of London, 301*, 305-320.

Tristan-Gonzalez, M., Aguirre-Diaz, G., Labarthe-Hernandez, G., Torres-Hernandez, J.R., Bellon, H., 2009. Post-Laramide and pre-Basin and Range deformation and implications for Paleogene (55-25 Ma) volcanism in central Mexico: A geological basis for a volcano-tectonic stress-model. *Tectonophysics, 471*, 136-152.

Underwood, M.B., Byrne, T., Hibbard, J.P., DiTullio, L., Laughland, M.M., 1993. The effects of ridge subduction on the thermal structure of accretionary prisms: A tertiary example from the Shimanto Belt of Japan. *Special Paper, Geological Society of America, 273*, 151-168.

Uyeda, S., Miyashiro, A., 1974. Plate tectonics and the Japanese Island: A synthesis. *Geological Society of America Bulletin, 85 (7),* 1159-1170.

Van den Beukel, J., et Wortel, R., 1988. Ridge-trench interaction: a possible mechanism for ophiolite emplacement. *Tectonics, 9 (4),* 825-844.

Vicente, J.C., Sequeiros F., Valdivia, M.A., Zavala, J., 1979. The Chincha-Lluta Overthrust: elements of a major Andean discontinuity in the Northwestern Arequipa. *Boletin de la Sociedad Geologica del Peru, 61*, 67-99.

Vicente, J.C., 1990. Early Cretaceous overthrusting in the Western Cordillera of Southern Peru. *In Ericksen, G.E., Canas Pinochet, M.T., Reinemund, J.A. (eds). Geology of the Andes and its relation to Hydrocarbon and Mineral Resources, Circum-Pacific Council for Energy and Mineral Resources, Earth Sciences Series, 11*, 91-117.

Wenzens, G., 2006. Terminal Moraines, Outwash Plains, and Lake Terraces in the Vicinity of Lago Cardiel (49°S; Patagonia, Argentina) :Evidence for Miocene Andean Foreland Glaciations. *Arctic, Antarctic, and Alpine Research, 276–291* DOI: 10.1657/1523-0430(2006)38[276:TMOPAL]2.0.CO;2

Wernicke. B.P., Christiansen, R.L., England, P.C., Sonder, L.J., 1987. Tectonomagmatic evolution of Cenozoic extension in the North American Cordillera. *In Coward, M.P., Dewey, J.F., Hancock, P.L., (eds), 1987, Continenetal Extensional Tectonics, Geological Society Special Publication, 28*, 203-221.

Whittaker, J.M., Muller, R.D., Sdrolias, M., Heine, C., 2007. Sunda-Java trench kinematics, slab window formation and overriding plate deformation since the Cretaceous. *Earth and Planetary Earth Sciences, 255 (3-4)*, 445-457.

Wiemer, S., Tytgat, G., Wyss, M., Duenkel, U., 1999. Evidence for shear-wave anisotropy in the mantle wedge beneath south central Alaska. *Bulletin of the Seismological Society of America, 89 (5)*, 1313-1322.

Witt, C., Bourgois, J., Michaud, F., Ordoñez, M., Jimenez, N., Sosson, M., 2006, Development of the Gulf of Guayaquil (Ecuador) during the Quaternary as an effect of the North Andean block tectonic escape. *Tectonics, 25,* TC3017, doi:10.1029/2004TC001723.

Yamamoto, T., et Hoang, N., 2009. Synchronous Japan Sea opening Miocene fore-arc volcanism in the Abukuma Mountains, NE Japan: An advancing hot asthenosphere flow versus Pacific slab melting. Lithos, doi:10.1016/j.lithos.2009.03.044.

Yamaoka, K., et Fukao, Y., 1986. Spherical shell tectonics: effects of sphericity and inextensibility on the geometry of the descending lithosphere. *Review of Geophysics, 24 (1),* 27-53.

Yang, X., Fischer, K.M., Abers, G.A., 1995. Seismic anisotropy beneath the Shumagin Islands segment of the Aleutian-Alaska subduction zone. *Journal of Geophysical Research, 100 (B9)*, 18165-18177.

Zandt, G., Velasco, A.A., Beck, S.L., 1994. Composition and thickness of the southern Altiplano crust, Bolivia. *Geology, 22 (11)*, 1003-1006.

Zandt, G., Humphreys, E., 2008. Toroidal mantle flow through the Western U.S. slab window. *Geology, 36 (4),* 295-298.

Zapata, T.R., et Allmendinger, R.W., 1996. The thrust front zone of the Precordillera thrust belt, Argentina : a thick-skinned triangle zone. *American Association of Petroleum Geologists Bulletin, 80 (3),* 359-381.

Résumé

Déformation d'un continent au-dessus d'une dorsale océanique active en subduction. La transversale du Point Triple du Chili, Patagonie Centrale (Chili-Argentine).

La subduction d'une dorsale active sous un continent est un processus inévitable dans l'évolution des chaînes de subduction. Le travail de cette thèse concerne l'évolution de la Cordillère de Patagonie Centrale, à la latitude du point triple du Chili, en relation avec la subduction de la dorsale active du Chili induisant le développement d'une fenêtre asthénosphérique sous la plaque sud-américaine. A l'aide d'une approche morphologique, structurale, couplée à l'analyse d'images satellites et topographiques, nous montrons l'influence de la fenêtre asthénosphérique depuis 3 Ma sur l'évolution morphostructurale de la Patagonie Centrale.

Au cours du Pliocène, la Cordillère de Patagonie Centrale est marquée par une phase d'extension majeure induisant la formation de dépressions transverses et internes à la chaîne. L'inversion négative du relief responsable de la topographie générale de type rift induit l'inversion du front morphotectonique et la déconnexion du piedmont volcano-sédimentaire du reste de la Cordillère à partir de 3 Ma. L'extension radiale dont l'amplitude est comprise entre 800 mètres et 3500 mètres, se localise dans la plupart des cas au niveau de failles polyphasées. L'évolution morphostructurale plio-quaternaire proposée est directement reliée à l'ouverture de la fenêtre asthénosphérique à 3 Ma sous la Patagonie et à la remontée de matériel asthénosphérique chaud induisant la collapse régionale de la Cordillère de Patagonie Centrale.

Mots clés : Subduction de dorsale active, fenêtre asthénosphérique, Cordillère de Patagonie Centrale, morphologie glaciaire, morphotectonique, inversion négative du relief.

Deformation of a continent above a subducting active spreading ridge. The Chile Triple Junction transversal, Central Patagonia (Chile-Argentina).

The spreading ridge subduction is an unavoidable process during the subduction-related belt elovution. The aim of this thesis concerns the evolution of the Central Patagonian Cordillera, at the latitude of the Chile triple junction, in relation with the Chile spreading ridge subduction inducing the opening of a slab-window beneath the South American plate. By a morphologic, and a structural analysis, coupled with the analysis of satelittes and topographic images, we show the influence of the slab-window development at 3 Ma on the morphostructural evolution of the Central Patagonia.

During the Pliocene, the Central Patagonian Cordillera experiences a major extensional phase inducing the formation of transverse and internal depressions. Negative tectonic inversion, responsible to the rift-type topography, induces the inversion of the morphotectonic front and the disruption of the volcano-sedimentary piedmont with the rest of the Cordillera at 3 Ma. Radial extensional regime is characterized by a magnitude comprises between 800 m and 3500 meters and vertical movements are localized along polyphazed faults. We suggest that the Plio-Quaternary morphostructural evolution is related to the opening of the slab-window at 3 Ma beneath the Central Patagonia. The upwelling of asthenospheric hot mantle through the slab window induces the regional collapse of the Central Patagonian Cordillera.

Key-words : active spreading ridge subduction, slab-window, Central Patagonian Cordillera, Glacial morphology, morphotectonic, negative tectonic inversion.

Laboratoire Géosciences Montpellier – UMR 5243 – Université de Montpellier II – CNRS. Cc060 Place Eugène Bataillon - 34095 Montpellier cedex 5, France.